

Energy, Environment, and Sustainability  
Series Editor: Avinash Kumar Agarwal

Avinash Kumar Agarwal  
Hardikk Valera *Editors*

# Greener and Scalable E-fuels for Decarbonization of Transport



 Springer

# **Energy, Environment, and Sustainability**

## **Series Editor**

Avinash Kumar Agarwal, Department of Mechanical Engineering,  
Indian Institute of Technology Kanpur, Kanpur, Uttar Pradesh, India

## **AIMS AND SCOPE**

This books series publishes cutting edge monographs and professional books focused on all aspects of energy and environmental sustainability, especially as it relates to energy concerns. The Series is published in partnership with the International Society for Energy, Environment, and Sustainability. The books in these series are edited or authored by top researchers and professional across the globe. The series aims at publishing state-of-the-art research and development in areas including, but not limited to:

- Renewable Energy
- Alternative Fuels
- Engines and Locomotives
- Combustion and Propulsion
- Fossil Fuels
- Carbon Capture
- Control and Automation for Energy
- Environmental Pollution
- Waste Management
- Transportation Sustainability

## **Review Process**

The proposal for each volume is reviewed by the main editor and/or the advisory board. The chapters in each volume are individually reviewed single blind by expert reviewers (at least four reviews per chapter) and the main editor.

**Ethics Statement** for this series can be found in the Springer standard guidelines here <https://www.springer.com/us/authors-editors/journal-author/journal-author-helpdesk/before-you-start/before-you-start/1330#c14214>

More information about this series at <https://link.springer.com/bookseries/15901>

Avinash Kumar Agarwal · Hardikk Valera  
Editors

# Greener and Scalable E-fuels for Decarbonization of Transport

 Springer

*Editors*

Avinash Kumar Agarwal  
Department of Mechanical Engineering  
Indian Institute of Technology Kanpur  
Kanpur, Uttar Pradesh, India

Hardikk Valera  
Department of Mechanical Engineering  
Indian Institute of Technology Kanpur  
Kanpur, Uttar Pradesh, India

ISSN 2522-8366

ISSN 2522-8374 (electronic)

Energy, Environment, and Sustainability

ISBN 978-981-16-8343-5

ISBN 978-981-16-8344-2 (eBook)

<https://doi.org/10.1007/978-981-16-8344-2>

© The Editor(s) (if applicable) and The Author(s), under exclusive license to Springer Nature Singapore Pte Ltd. 2022

This work is subject to copyright. All rights are solely and exclusively licensed by the Publisher, whether the whole or part of the material is concerned, specifically the rights of translation, reprinting, reuse of illustrations, recitation, broadcasting, reproduction on microfilms or in any other physical way, and transmission or information storage and retrieval, electronic adaptation, computer software, or by similar or dissimilar methodology now known or hereafter developed.

The use of general descriptive names, registered names, trademarks, service marks, etc. in this publication does not imply, even in the absence of a specific statement, that such names are exempt from the relevant protective laws and regulations and therefore free for general use.

The publisher, the authors and the editors are safe to assume that the advice and information in this book are believed to be true and accurate at the date of publication. Neither the publisher nor the authors or the editors give a warranty, expressed or implied, with respect to the material contained herein or for any errors or omissions that may have been made. The publisher remains neutral with regard to jurisdictional claims in published maps and institutional affiliations.

This Springer imprint is published by the registered company Springer Nature Singapore Pte Ltd. The registered company address is: 152 Beach Road, #21-01/04 Gateway East, Singapore 189721, Singapore

# Preface

Fuel requirement for the transport sector is a function of population growth. Currently, the automotive industry is powered extensively by fossil fuels. Diesel- and gasoline-powered vehicles contribute heavily to environmental pollution by emitting carbon dioxides (CO<sub>2</sub>) and other pollutant species. Greenhouse gas (GHG) emissions from fossil fuel combustion are significantly increasing since 1900. Fossil fuels depletion depends on discoveries of new petroleum reserves; however, the use of fossil fuels would not be feasible in the foreseeable future due to GHG emissions and other environmental concerns. To tackle these, several researchers have focused on developing alternative fuels.

The International Society for Energy, Environment and Sustainability (ISEES) was founded at the Indian Institute of Technology Kanpur (IIT Kanpur), India, in January 2014 to spread knowledge/awareness and catalyze research activities in the fields of energy, environment, sustainability, and combustion. Society's goal is to contribute to the development of clean, affordable, and secure energy resources and a sustainable environment for society and spread knowledge in the areas mentioned above and create awareness about the environmental challenges the world is facing today. The unique way adopted by ISEES was to break the conventional silos of specializations (engineering, science, environment, agriculture, biotechnology, materials, fuels, etc.) to tackle the problems related to energy, environment, and sustainability in a holistic manner. This is quite evident by the participation of experts from all fields to resolve these issues. ISEES is involved in various activities such as conducting workshops, seminars, and conferences in the domains of its interests. Society also recognizes the outstanding works of young scientists, professionals, and engineers for their contributions in these fields by conferring them awards under various categories.

Fifth International Conference on 'Sustainable Energy and Environmental Challenges' (V-SEEC) was organized under the auspices of ISEES from December 19 to 21, 2020, in virtual mode due to restrictions on travel because of the ongoing COVID-19 pandemic situation. This conference provided a platform for discussions between eminent scientists and engineers from various countries, including India, Spain, Austria, Bangladesh, Mexico, USA, Malaysia, China, UK, Netherlands, Germany,

Israel, and Saudi Arabia. At this conference, eminent international speakers presented their views on energy, combustion, emissions, and alternative energy resources for sustainable development and a cleaner environment. The conference presented two high-voltage plenary talks by Dr. V. K. Saraswat, Honorable Member, NITI Ayog, on ‘Technologies for Energy Security and Sustainability’ and Prof. Sandeep Verma, Secretary, SERB, on ‘New and Equitable R&D Funding Opportunities at SERB.’

The conference included nine technical sessions on topics related to energy and environmental sustainability. Each session had 6–7 eminent scientists from all over the world, who shared their opinion and discussed the trends for the future. The technical sessions in the conference included emerging contaminants: monitoring and degradation challenges; advanced engine technologies and alternative transportation fuels; future fuels for sustainable transport; sustainable bioprocessing for biofuel/non-biofuel production by carbon emission reduction; future of solar energy; desalination and wastewater treatment by membrane technology; biotechnology in sustainable development; emerging solutions for environmental applications’ and challenges and opportunities for electric vehicle adoption. Five hundred plus participants and speakers from all over the world attended this three days conference.

The conference concluded with a high-voltage panel discussion on ‘Challenges and Opportunities for Electric Vehicle Adoption,’ where the panelists were Prof. Gautam Kalghatgi (University of Oxford), Prof. Ashok Jhunjhunwala (IIT Madras), Dr. Kelly Senecal (Convergent Science), Dr. Amir Abdul Manan (Saudi Aramco), and Dr. Sayan Biswas (University of Minnesota, USA). Prof. Avinash Kumar Agarwal, ISEES, moderated the panel discussion. This conference laid out the roadmap for technology development, opportunities, and challenges in energy, environment, and sustainability domain. All these topics are very relevant for the country and the world in the present context. We acknowledge the support received from various agencies and organizations for the successful conduct of the Fifth ISEES Conference V-SEEC, where these books germinated. We want to acknowledge SERB (special thanks to Dr. Sandeep Verma, Secretary) and our publishing partner Springer (special thanks to Ms. Swati Meherishi).

The editors would like to express their sincere gratitude to a large number of authors from all over the world for submitting their high-quality work on time and revising it appropriately at short notice. We would like to express our special gratitude to our prolific set of reviewers, Dr. Ákos Bereczky, Dr. Harold Sun, Dr. Yuanxian Zhu, Dr. Song-Chang Kong, Dr. Apeng Zhou, Mr. Shubhanker Dev, Dr. Cheatn Patel, Dr. Cinzia Tornatore, Dr. Holubeck, Dr. Martin Pexa, Dr. Atul Dhar, Dr. Yanju Wei, Dr. Carlo Beatrice, Dr. Chunde Yao, Dr. Vipin Dhyani, Dr. Choongsik Bae, Dr. Miroslav Müller, Mr. Ajay Trehan, Dr. José R. Serrano, Dr. Jeevan Tirkey, Dr. Dilip Sharma, Dr. Sarbjot Singh Sandhu, Dr. Hua Zhao, Dr. Srinivasa Rao Sandepudi who reviewed various chapters of this monograph and provided their valuable suggestions to improve the manuscripts.

Electrofuels or e-fuels are produced using renewable electricity. They are an emerging class of carbon-neutral drop-in fuels for transport sector. E-fuels family is big and covers both gaseous and liquid fuels such as hydrogen ( $H_2$ ), methane ( $CH_4$ ), methanol ( $CH_3OH$ ), DME ( $CH_3-O-CH_3$ ), ammonia ( $NH_3$ ), synthetic petrol,

and diesel. These E-fuels powered vehicles are far better than battery electric vehicles (BEVs) in terms of overall greenhouse gases (GHGs) emissions. E-fuels can be delivered on existing fuel outlets without major modifications, which is not the case for BEVs. Development of infrastructure for charging the BEVs requires huge investment; therefore, policy makers of European Union (EU) have shown a great interest. Also, the major advantage of E-fuels is the energy efficiency of electricity used to power the battery electric vehicles (BEVs), and hydrogen fuel cells are ~4–6 times and 2 times higher than e-fuels used to power the internal combustion engines (ICEs), including grid integration. This book will provide the ways of using these fuels in existing engines and their effects on tailpipe emissions. Calibration and optimization procedure for adaptation of these fuels will be covered in this book. Also, economical perspective of these fuels will be covered. Chapters include recent results and are focused on current trends of automotive sector. We hope that the book would greatly interest the professionals and postgraduate students involved in fuels, IC engines, engine instrumentation, and environmental research.

Kanpur, India

Avinash Kumar Agarwal  
Hardikk Valera



# Contents

## Part I E-Fuels for Decarbonization of Transport Sector

- 1 Introduction of Greener and Scalable E-Fuels for Decarbonization of Transport** ..... 3  
Avinash Kumar Agarwal and Hardikk Valera
- 2 Potential of E-Fuels for Decarbonization of Transport Sector** ..... 9  
Sawan Bharti, Balendra V. S. Chauhan, Akshay Garg,  
Ajitanshu Vedrtam, and M. K. Shukla
- 3 A Historical Perspective on the Biofuel Policies in India** ..... 33  
Anuj Kumar and Anand B. Rao

## Part II Hydrogen as an E-Fuel

- 4 Hydrogen as Maritime Transportation Fuel: A Pathway for Decarbonization** ..... 67  
Omer Berkehan Inal, Burak Zincir, and Caglar Dere
- 5 Improving Cold Flow Properties of Biodiesel, and Hydrogen-Biodiesel Dual-Fuel Engine Aiming Near-Zero Emissions** ..... 111  
Murari Mohon Roy
- 6 Assessment of Hydrogen as an Alternative Fuel: Status, Prospects, Performance and Emission Characteristics** ..... 135  
Mohammad Towhidul Islam, Khodadad Mostakim,  
Nahid Imtiaz Masuk, Md. Hasan Ibna Islam, Fazlur Rashid,  
Md. Arman Arefin, and Md. Abid Hasan

<b>7</b>	<b>Effectiveness of Hydrogen and Nanoparticles Addition in Eucalyptus Biofuel for Improving the Performance and Reduction of Emission in CI Engine</b> .....	<b>173</b>
	P. V. Elumalai, N. S. Senthur, M. Parthasarathy, S. K. Dash, Olusegun D. Samuel, M. Sreenivasa Reddy, M. Murugan, PritamKumar Das, A. S. S. M. Sitaramamurty, S. Anjanidevi, and Selçuk Sarıkoç	
<b>8</b>	<b>The Roles of Hydrogen and Natural Gas as Biofuel Fuel-Additives Towards Attaining Low Carbon Fuel-Systems and High Performing ICEs</b> .....	<b>193</b>
	Samuel Eshorame Sanni and Babalola Aisosa Oni	
<b>Part III Dimethyl-Ether (DME) as an E-Fuel</b>		
<b>9</b>	<b>Prospects of Dual-Fuel Injection System in Compression Ignition (CI) Engines Using Di-Methyl Ether (DME)</b> .....	<b>223</b>
	Ayush Tripathi, Suhan Park, Sungwook Park, and Avinash Kumar Agarwal	
<b>10</b>	<b>Prospects and Challenges of DME Fueled Low-Temperature Combustion Engine Technology</b> .....	<b>261</b>
	Shanti Mehra and Avinash Kumar Agarwal	
<b>11</b>	<b>Optimization of Fuel Injection Strategies for Sustainability of DME in Combustion Engine</b> .....	<b>293</b>
	Anubhav, Niraj Kumar, and Rajesh Kumar Saluja	
<b>Part IV Application of Methanol and Ammonia as an E-Fuel</b>		
<b>12</b>	<b>ECU Calibration for Methanol Fuelled Spark Ignition Engines</b> ....	<b>317</b>
	Omkar Yadav, Hardikk Valera, and Avinash Kumar Agarwal	
<b>13</b>	<b>A Novel DoE Perspective for Robust Multi-objective Optimization in the Performance-Emission-Stability Response Realms of Methanol Induced RCCI Profiles of an Existing Diesel Engine</b> .....	<b>347</b>
	Dipankar Kakati, Srijit Biswas, and Rahul Banerjee	
<b>14</b>	<b>Scope and Limitations of Ammonia as Transport Fuel</b> .....	<b>391</b>
	Aaishi Ashirbad and Avinash Kumar Agarwal	

# Editors and Contributors

## About the Editors



**Prof. Avinash Kumar Agarwal** joined IIT Kanpur in 2001. He worked at the Engine Research Center, UW@Madison, the USA as a Post-Doctoral Fellow (1999–2001). His interests are IC engines, combustion, alternate and conventional fuels, lubricating oil tribology, optical diagnostics, laser ignition, HCCI, emissions, and particulate control, 1D and 3D Simulations of engine processes, and large-bore engines. Prof. Agarwal has published 435+ peer-reviewed international journal and conference papers, 70 edited books, 92 books chapters, and 12200+ Scopus and 19000+ Google Scholar citations. He is the associate principal editor of FUEL. He has edited “Handbook of Combustion” (5 Volumes; 3168 pages), published by Wiley VCH, Germany. Prof. Agarwal is a Fellow of SAE (2012), Fellow of ASME (2013), Fellow of ISEES (2015), Fellow of INAE (2015), Fellow of NASI (2018), Fellow of Royal Society of Chemistry (2018), and a Fellow of American Association of Advancement in Science (2020). He is the recipient of several prestigious awards such as Clarivate Analytics India Citation Award-2017 in Engineering and Technology, NASI-Reliance Industries Platinum Jubilee Award-2012; INAE Silver Jubilee Young Engineer Award-2012; Dr. C. V. Raman Young Teachers Award: 2011; SAE Ralph R. Teetor Educational Award-2008; INSA Young Scientist Award-2007; UICT Young Scientist Award-2007; INAE Young Engineer Award-2005. Prof. Agarwal received Prestigious

CSIR Shanti Swarup Bhatnagar Award-2016 in Engineering Sciences. Prof. Agarwal is conferred upon Sir J C Bose National Fellowship (2019) by SERB for his outstanding contributions. Prof. Agarwal was a highly cited researcher (2018) and was in the top ten HCR from India among 4000 HCR researchers globally in 22 fields of inquiry.



**Mr. Hardikk Valera** is pursuing Ph.D. from the Indian Institute of Technology Kanpur (IITK). He has completed his M.Tech. and B.Tech. from NIT Jalandhar (India) and Ganpat University, respectively. His research interests include methanol-fueled SI engines, methanol-fueled CI engines, optical diagnostics, fuel spray characterization and emission control from engines.

## Contributors

**Avinash Kumar Agarwal** Engine Research Laboratory, Department of Mechanical Engineering, Indian Institute of Technology Kanpur, Kanpur, India

**S. Anjanidevi** Department of Mechanical Engineering, Aditya Engineering College, Surampalem, Peddapuram, India

**Anubhav** Department of Mechanical Engineering, ASET, Amity University, Noida, India

**Md. Arman Arefin** Safe and Reliable Nuclear Applications, IMT Atlantique, Nantes, France

**Aaishi Ashirbad** Engine Research Laboratory, Department of Mechanical Engineering, Indian Institute of Technology Kanpur, Kanpur, India

**Rahul Banerjee** Department of Mechanical Engineering, NIT Agartala, Jirania, Tripura, India

**Sawan Bharti** Invertis University, Rajau Paraspur, India

**Srijit Biswas** Department of Mechanical Engineering, NIT Agartala, Jirania, Tripura, India

**Balendra V. S. Chauhan** Automotive Fuels and Lubricants Application Division, CSIR-Indian Institute of Petroleum, Dehradun, UK, India

**PritamKumar Das** Department of Mechanical Engineering, Aditya Engineering College, Surampalem, Peddapuram, India

**S. K. Dash** Department of Mechanical Engineering, Aditya Engineering College, Surampalem, Peddapuram, India

**Caglar Dere** Marine Engineering Department, Maritime Faculty, Istanbul Technical University, Istanbul, Turkey;  
Marine Engineering Department, Faculty of Naval Architecture and Ocean Engineering, Izmir Katip Celebi University, Izmir, Turkey

**P. V. Elumalai** Department of Mechanical Engineering, Aditya Engineering College, Surampalem, Peddapuram, India

**Akshay Garg** Department of Mechanical Engineering, College of Engineering Roorkee, Roorkee, India

**Md. Abid Hasan** American International University - Bangladesh, Dhaka, Bangladesh

**Omer Berkehan Inal** Marine Engineering Department, Maritime Faculty, Istanbul Technical University, Istanbul, Turkey

**Md. Hasan Ibna Islam** Department of Mechanical Engineering, Rajshahi University of Engineering & Technology, Rajshahi, Bangladesh

**Mohammad Towhidul Islam** Department of Mechanical Engineering, Rajshahi University of Engineering & Technology, Rajshahi, Bangladesh

**Dipankar Kakati** Department of Mechanical Engineering, NIT Agartala, Jirania, Tripura, India

**Anuj Kumar** Centre for Policy Studies (CPS), Indian Institute of Technology Bombay, Mumbai, India

**Niraj Kumar** Department of Mechanical Engineering, ASET, Amity University, Noida, India

**Nahid Imtiaz Masuk** Department of Mechanical Engineering, Rajshahi University of Engineering & Technology, Rajshahi, Bangladesh

**Shanti Mehra** Engine Research Laboratory, Department of Mechanical Engineering, Indian Institute of Technology Kanpur, Kanpur, India

**Khodadad Mostakim** Department of Mechanical Engineering, Rajshahi University of Engineering & Technology, Rajshahi, Bangladesh

**M. Murugan** Department of Mechanical Engineering, Aditya College of Engineering and Technology, Surampalem, India

**Babalola Aisosa Oni** Department of Chemical Engineering, Covenant University, Ota, Ogun State, Nigeria;

Department of Chemical Engineering, China University of Petroleum, Changping, Beijing, People's Republic of China

**Suhan Park** School of Mechanical and Aerospace Engineering, Konkuk University, Seoul, Republic of Korea

**Sungwook Park** School of Mechanical Engineering, Hanyang University, Seoul, Republic of Korea

**M. Parthasarathy** Department of Automobile Engineering, Vel Tech Rangarajan Dr, Sagunthala R&D Institute of Science and Technology, Chennai, India

**Fazlur Rashid** Department of Mechanical Engineering, Rajshahi University of Engineering & Technology, Rajshahi, Bangladesh

**M. Sreenivasa Reddy** Department of Mechanical Engineering, Aditya Engineering College, Surampalem, Peddapuram, India

**Anand B. Rao** Centre for Policy Studies (CPS), Indian Institute of Technology Bombay, Mumbai, India;

Centre for Technology Alternatives in Rural Areas (CTARA), Indian Institute of Technology Bombay, Mumbai, India

**Murari Mohon Roy** Mechanical Engineering Department, Lakehead University, Thunder Bay, ON, Canada

**Rajesh Kumar Saluja** Amity Institute of Aerospace Engineering, Amity University, Noida, India

**Olusegun D. Samuel** Department of Mechanical Engineering, Federal University of Petroleum, Effurun, Delta State, Nigeria;  
Department of Mechanical Engineering, University of South Africa, Science, Florida, South Africa

**Samuel Eshorame Sanni** Department of Chemical Engineering, Covenant University, Ota, Ogun State, Nigeria

**Selçuk Sarıkoç** Department of Motor Vehicles and Transportation Technologies, Tasova Yuksel Akin Vocational School, Amasya University, Amasya, Turkey

**N. S. Senthur** Department of Mechanical Engineering, Bharath Institute of Higher Education and Research, Chennai, India

**M. K. Shukla** Automotive Fuels and Lubricants Application Division, CSIR-Indian Institute of Petroleum, Dehradun, UK, India

**A. S. S. M. Sitaramamurty** Department of Mechanical Engineering, Aditya Engineering College, Surampalem, Peddapuram, India

**Ayush Tripathi** Engine Research Laboratory, Department of Mechanical Engineering, Indian Institute of Technology Kanpur, Kanpur, India

**Hardikk Valera** Engine Research Laboratory, Department of Mechanical Engineering, Indian Institute of Technology Kanpur, Kanpur, India

**Ajitanshu Vedrtam** Invertis University, Rajau Paraspur, India;  
Universidad de Alcalá, Alcalá de Henares, Spain

**Omkar Yadav** Engine Research Laboratory, Department of Mechanical Engineering, Indian Institute of Technology Kanpur, Kanpur, India

**Burak Zincir** Marine Engineering Department, Maritime Faculty, Istanbul Technical University, Istanbul, Turkey

**Part I**  
**E-Fuels for Decarbonization of Transport**  
**Sector**



# Chapter 1

## Introduction of Greener and Scalable E-Fuels for Decarbonization of Transport



Avinash Kumar Agarwal  and Hardikk Valera 

**Abstract** Electro fuels or e-fuels are produced by using renewable electricity. They are an emerging class of carbon-neutral drop-in fuels for the transport sector. E-fuels family is large and covers both gaseous and liquid fuels such as hydrogen ( $H_2$ ), methane ( $CH_4$ ), methanol ( $CH_3OH$ ), DME ( $CH_3-O-CH_3$ ), ammonia ( $NH_3$ ), synthetic petrol, diesel etc. These E-fuels powered vehicles are superior to battery electric vehicles (BEVs) in overall greenhouse gas (GHG) emissions. E-fuels can be delivered from existing fuel outlets without significant modifications, which is not the case for BEVs. Developing infrastructure for charging the BEVs requires huge investments; therefore, policymakers of the European Union (EU) have shown interest in the large-scale implementation of the E-fuels. Also, a significant advantage of E-fuels is their energy efficiency. The electricity used to power the battery electric vehicles (BEVs) and Hydrogen fuel cells is  $\sim 4$ – $6$  times and two times higher, respectively than the e-fuels used to power the internal combustion engines (ICEs). This book covers several ways to use these E-fuels in existing engines and their effects on tailpipe emissions. Calibration and optimisation procedures for the adaptation of these fuels are covered in this book. Also, the economics of these fuels is covered.

**Keywords** E-Fuels · Hydrogen · Dimethyl ether · Methanol · Ammonia

The rapid depletion of fossil fuels has prompted upcoming generations to adopt alternative resources, which are equally efficient and could meet the soaring energy demand. Furthermore, being non-renewable, harming the environment while burning and mining, replacing this outdated means of energy supplies will be a future challenge in sustaining the environmental and economic issues. However, among the practical alternative energy sources, the most popular ones are solar, wind, geothermal, biomass energy, and nuclear energy, or hybrid nuclear energy. Although the energy demand is getting fulfilled, these cannot contribute enough to fulfil energy demand

---

A. K. Agarwal (✉) · H. Valera

Engine Research Laboratory, Department of Mechanical Engineering,  
Indian Institute of Technology Kanpur, Kanpur 208016, India  
e-mail: [akag@iitk.ac.in](mailto:akag@iitk.ac.in)

© The Author(s), under exclusive license to Springer Nature Singapore Pte Ltd. 2022  
A. K. Agarwal and H. Valera (eds.), *Greener and Scalable E-fuels for Decarbonization of Transport*, Energy, Environment, and Sustainability,  
[https://doi.org/10.1007/978-981-16-8344-2\\_1](https://doi.org/10.1007/978-981-16-8344-2_1)

because of some drawbacks and inconsistencies. For instance, insufficient power generation capacity and relatively lower efficiency necessitate a huge upfront capital, and dependency on geographical conditions and locations impede their potential to cater to the energy demand on a large scale. Besides, nuclear energy poses a security risk and generates radioactive waste. Similarly, biomass energy sources can potentially lead to deforestation. However, hydrogen is becoming increasingly popular as an alternative fuel because of its cleaner production, non-toxic nature, economic feasibility, and excellent efficiency than most energy sources. Its non-polluting production from electrolysis and renewable sources and wide range of flammability indicate its scalability as a green solution for the transport sector. Hence, E-fuels may be a promising solution in the future.

The first section of the book has three chapters. The first chapter is the introduction chapter. The second chapter of this section focuses on the overview of alternate fuel utilisation and global efforts to decarbonise the transport sector by promoting e-fuels. This chapter briefly discusses the potential alternatives available to reduce GHG emissions for cleaner road transport. This chapter includes a brief discussion on fossil carbon energy carriers such as biofuels, e-fuels, and renewable electricity. Some barriers in implementing the renewable, greener scalable e-fuels for decarbonisation are reported as possible solutions. The third chapter provides a historical perspective on biofuel policies in India. The chapter analyses key factors that have played a significant role in shaping the biofuel policies in India after the independence. The timeline between 1947 and 2021 is analysed to understand events in the biofuel policy formulation landscape. This helps get a micro picture of why these policies have not been able to deploy biofuels as a substitute in the Indian automotive sector at a large scale. The chapter could help formulate a robust strategy for defining biofuel development pathways in the upcoming renewable boom, improving biofuels' share in the overall renewable energy sector.

The second section of the book focuses on hydrogen as an E-fuel. This section contains five chapters on hydrogen usage. The first chapter of this section is focused on hydrogen as a marine transportation fuel. Shipping is the most energy-efficient mode to transport goods, and it has a substantial role in the global economy. The vast majority of ships are operated on fossil fuels due to economic advantages, a strong bunkering network, and well-experienced operations of marine diesel engines. However, environmental concerns are driving the industry to reduce ship-sourced GHG emissions, and the International Maritime Organization (IMO), the controller of the maritime industry, is bringing stringent rules to regulate these emissions under The International Convention for the Prevention of Pollution from Ships—Annex VI (MARPOL). This chapter includes information on the status of maritime transport, current international maritime emission norms and regulations, and hydrogen's compliance with the International Code of Safety for Ships Using Gas or Other Low-flashpoint Fuels (IGF Code). Hydrogen production technologies, onboard hydrogen storage methods, hydrogen combustion concepts for marine diesel engines, and fuel cells are also reviewed. Last, the concluding section comprises the chapter discussions. The second chapter of this section focuses on improving the cold flow properties of biodiesel and hydrogen-biodiesel dual-fuel engines aiming at near-zero

emissions. A dual-fuel combustion system that burns hydrogen as a primary fuel and biodiesel as a pilot fuel is getting attention. The biggest challenges with a hydrogen-operated dual-fuel engine are the power output, almost similar to diesel engines, and sustaining stable engine operation at lean operating conditions (Verhelst and Wallner 2009; Verhelst 2014). Supercharging can address the power output issue, but it increases the likelihood of premature ignition and knock tendency unless the equivalence ratio and other parameters are appropriately adjusted. Hydrogen-diesel supercharged dual-fuel engine results are presented in this study. The charge dilution (by  $N_2$ ) that helps to reduce the  $NO_x$  emissions is also presented. Detailed engine conditions and parameters are suggested for near-zero emissions from the hydrogen-biodiesel dual-fuel engines. The third chapter of the section is focused on the assessment of hydrogen as an alternative fuel. In this chapter, hydrogen as a fuel over other alternative energy resources has been evaluated for their performance and emission characterisation. Economic assessment is also carried out in this chapter, which comprehensively demonstrates the feasibility and prospects of hydrogen over other sources. This study also identifies challenges, limitations and their possible solutions for the production and usage of hydrogen. The fourth chapter of this section focuses on the Effectiveness of hydrogen and nano-particle addition in eucalyptus biofuel to improve the performance and reduce emissions of a CI engine. The Eucalyptus biodiesel (EB) powered CI engine exhibits lower brake thermal efficiency (BTE) and higher smoke in this chapter. The inherent oxygen content of nano-particles could be added with EB, leading to improved hydrocarbon oxidation that results in low smoke emission. This study was initially carried out in a compression ignition engine powered by EB, considered a reference fuel. The higher energy density of hydrogen resulted in better combustion efficiency and drastically reduced global emissions. The last chapter of the section is focused on the role of hydrogen and natural gas as additives for attaining low carbon intensity and higher performance IC engines. The role of hydrogen and CNG in biofuels cannot be over-emphasised owing to a higher degree of spray atomisation, improved brake thermal efficiency, heat release rate, lower carbonaceous emissions, and moderate peak cylinder pressures. Hence, this chapter focuses on the role of hydrogen and natural gas in biofuels, the blending techniques adopted in mixing NG and  $H_2$  with biofuels, their compatibility/property variations and their spray characteristics.

The third section of the book is focused on Dimethyl-Ether (DME) as an E-fuel. This section has three chapters. The first chapter of the section is focused on the prospects of a dual-fuel injection system in CI engines using DME. The operating range of DME homogeneous charge compression ignition (HCCI) engines is limited due to knock intensity; however, it can be widened using dual-fuel mode. DME has ultra-low viscosity, higher vapour pressure, and negligible self-lubrication characteristics, which create difficulties in the conventional fuel injection systems to handle DME (Pal et al. 2021; Rai et al. 2021). These challenges can be overcome by using high octane number (ON) fuel as an ignition suppressor to reduce the chances of knocking and coefficient of variance (COV) of engine performance parameters with DME used in CI engines. This chapter explores different fuel injection strategies and fuels in dual-fuel mode by considering DME as an E-fuel. The combustion

and emission characteristics of the DME dual-fuel engine are also discussed. The second chapter of this section is focused on the prospects and challenges of DME fueled low-temperature combustion (LTC) engine technology. Engines with LTC concepts are highly efficient and environmentally friendly and offer a promising alternative to conventional combustion engine technologies (Benajes et al. 2015; Tormos et al. 2010). Homogeneous charge compression ignition (HCCI), partially premixed charge compression ignition (PCCI), Reactivity controlled compression ignition (RCCI), and gasoline compression ignition (GCI) are a few of the LTC variant technologies, which should be investigated for DME to combine both cleaner and efficient engine technology and environment-friendly alternative fuel. HCCI engine technology is a superior LTC engine technology with higher efficiency. However, there are limitations of HCCI engine technology, such as limited operational range. Hence, other LTC engine technologies are being widely explored. PCCI engine technology is one of them. Factors such as lean premixed charge, high compression ratio, and multi-point spontaneous ignition lead to excellent fuel economy and lower  $\text{NO}_x$  emissions. Another LTC engine technology is the RCCI, which uses two different fuel reactivities to achieve excellent engine efficiencies. Low reactivity fuels such as natural gas can be used along with high reactivity fuels such as DME, yielding lower  $\text{NO}_x$  and PM emissions, reducing heat transfer loss, and increasing engine efficiency. RCCI technology leads to an elimination of the need for expensive exhaust gas after-treatment systems. This chapter examines the concepts of various LTC engine technologies and their performance and emission characteristics, underlying challenges, and way forward for using DME. The last section of this chapter focuses on optimising fuel injection strategies for the sustainability of DME in a combustion engine. This chapter focuses on adopting suitable changes in fuel injection strategies to reduce emissions and improve the performance characteristics of DME fueled engines. Advance methods to sustain DME in the pre-existing diesel engine systems are also discussed by modifying the engine to extract the maximum output. Due to distinguished DME characteristics from the diesel, the effects of fuel compressibility on compression work spray pattern, and atomisation characteristics are also compared, which pave the way for the exploration of DME for combustion engines via manipulation of fuel injection strategies.

The last section of this book focuses on the application of methanol and ammonia as E-fuels. This section has three chapters. The first chapter of the section is focused on the ECU Calibration for methanol fuelled spark-ignition engines. Out of all the technologies, port fuel injection technology is one of the best ways for methanol utilisation in existing electronic fuel injection (EFI) engines with minimal structural changes. The specific properties of methanol, such as lower calorific value, higher latent heat of vaporisation, low volatility, higher laminar flame speed, and higher-octane number, warrant modifications in the conventional gasoline engines (Agarwal et al. 2021). For superior engine performance, these strategies must be optimised for corresponding engine operating conditions. The combustion of EFI engines is primarily governed by Electronic Control Unit (ECU), which contains pre-calibrated maps to decide optimum injection and ignition strategy. ECU calibration is the process of determining the optimal calibration tables for an engine.

In this chapter, the ECU calibration methodology for methanol-fueled SI engine equipped vehicles is discussed at length. The second chapter of this section focuses on a novel design of experiment (DoE) perspective for robust multi-objective optimization in the performance-emission-stability response realms of methanol induced RCCI engine. A constrained optimisation study was covered in this chapter based on the response surface methodology under the respective constraints of emission elements as per the EPA Tier-4 emission mandates and operational stability. The study also incorporated a novel customised DoE for the multivariate exploration of design space followed by a thorough analysis of the robustness of design space, which has been characterised through the measures of the fraction of design space (FDS) metric, D-optimality criteria, G-efficiency, and condition number (CoN). A desirability based multi-criteria decision-making approach was undertaken wherein the highest desirability was observed as 0.832. The last chapter of this section is focused on the scope and limitations of ammonia as a transport fuel. This chapter covers production methods, properties, environmental and health aspects, storage and transportation, and the potential of ammonia as a transport fuel in compression-ignition (CI) and spark-ignition (SI) engines. Pure Ammonia operation and dual-fuel modes are extensively discussed for both CI and SI engines. Hydrogen as a combustion improver is also covered towards the end of this chapter. However, to realise ammonia's potential as a fuel, it is essential to determine feasible ammonia induction and combustion techniques applicable to ICEs, which would enhance engine performance in the entire operating range.

This book is therefore divided into four different sections: (I) E-fuels for decarbonization of transport sector, (II) Hydrogen as an E-fuel, (III) Dimethyl-Ether (DME) as an E-fuel, and (IV) Application of methanol and ammonia as an E-fuel. Specific chapters covered in the manuscript include:

- Introduction of Greener and Scalable E-fuels for Decarbonization of Transport
- Potential of E-Fuels for Decarbonization of Transport Sector
- A Historical Perspective on the Biofuel Policies in India
- Hydrogen as Maritime Transportation Fuel: A Pathway for Decarbonization
- Improving Cold Flow Properties of Biodiesel, and Hydrogen-biodiesel Dual-fuel Engine Aiming Near-zero Emissions
- Assessment of Hydrogen as an alternative fuel: Status, prospects, performance, and emission characteristics
- Effectiveness of hydrogen and nano-particles addition in eucalyptus biofuel for improving the performance and reduction of emission in CI engine
- The Roles of Hydrogen and Natural Gas as Biofuel Fuel-Additives towards Attaining Low Carbon Fuel-Systems and High Performing ICEs
- Prospects of Dual-Fuel Injection System in Compression Ignition (CI) Engines Using Di-Methyl Ether (DME)
- Prospects and Challenges of DME Fueled Low-Temperature Combustion Engine Technology
- Optimisation of fuel injection strategies for sustainability of DME in combustion engine

- ECU Calibration for Methanol Fuelled Spark Ignition Engines
- A novel DoE perspective for robust multi-objective optimization in the performance-emission-stability response realms of methanol induced RCCI profiles of an existing diesel engine
- Scope and Limitations of Ammonia as Transport Fuel.

## References

- Agarwal AK, Valera H, Pexa M, Čedík J (2021) Introduction of methanol: a sustainable transport fuel for SI engines. In: Agarwal AK, Valera H, Pexa M, Čedík J (eds) Methanol. Energy, environment, and sustainability. Springer, Singapore. [https://doi.org/10.1007/978-981-16-1224-4\\_1](https://doi.org/10.1007/978-981-16-1224-4_1)
- Benajes J, Pastor JV, García A, Monsalve-Serrano J (2015) The potential of RCCI concept to meet EURO VI NOx limitation and ultra-low soot emissions in a heavy-duty engine over the whole engine map. Fuel 159:952–961. <https://doi.org/10.1016/J.FUEL.2015.07.064>
- Pal M, Kumar V, Kalwar A, Mukherjee NK, Agarwal AK, (2021) Prospects of fuel injection system for dimethyl ether applications in compression ignition engines. In: Singh AP, Kumar D, Agarwal AK (eds) Alternative fuels and advanced combustion techniques as sustainable solutions for internal combustion engines. Energy, environment, and sustainability. Springer, Singapore. [https://doi.org/10.1007/978-981-16-1513-9\\_2](https://doi.org/10.1007/978-981-16-1513-9_2)
- Rai A, Kumar D, Sonawane U, Agarwal AK (2021) Dimethyl ether spray characteristics for compression ignition engines. In: Singh AP, Agarwal AK (eds) Novel internal combustion engine technologies for performance improvement and emission reduction. Energy, environment, and sustainability. Springer, Singapore. [https://doi.org/10.1007/978-981-16-1582-5\\_4](https://doi.org/10.1007/978-981-16-1582-5_4)
- Tormos B, Novella R, García A, Gargar K (2010) Comprehensive study of biodiesel fuel for HSDI engines in conventional and low-temperature combustion conditions. Renew Energy 35(2):368–378. <https://doi.org/10.1016/J.RENENE.2009.07.001>
- Verhelst S (2014) Recent progress in the use of hydrogen as a fuel for internal combustion engines. Int J Hydrogen Energy 39(2):1071–1085. <https://doi.org/10.1016/J.IJHYDENE.2013.10.102>
- Verhelst S, Wallner T (2009) Hydrogen-fueled internal combustion engines. Prog Energy Combust Sci 35(6):490–527. <https://doi.org/10.1016/J.PECS.2009.08.001>

# Chapter 2

## Potential of E-Fuels for Decarbonization of Transport Sector



Sawan Bharti, Balendra V. S. Chauhan , Akshay Garg, Ajitanshu Vedrtnam , and M. K. Shukla

**Abstract** E-fuels are synthetic fuels, that can be considered greener as they are produced from green hydrogen. Green hydrogen is generally produced by sustainable process like gasification of biomass. The objective of the present chapter is to provide an overview of the alternate fuels utilization and global efforts towards decarbonization of the transport sector by promoting e-fuels. A detailed summary of articles including the gradual efforts for implementation of greener scalable E-fuels is reported. This chapter also discusses the potential alternatives available to decrease the greenhouse gas emissions for cleaner road transportation in brief. This chapter includes a brief discussion on fossil carbon energy carriers such as biofuels, e-fuels and renewable electricity. Further, some barriers in the way of implementation of renewable, greener scalable e-fuels for decarbonization are reported with the possible solutions. This chapter should provide a quick understanding of the present state of the art on E-Fuels.

**Keywords** E-fuel · Green fuel · Decarbonization · Global warming · Climate change

---

S. Bharti · A. Vedrtnam (✉)  
Invertis University, Rajau Paraspur, India  
e-mail: [ajitanshu.m@invertis.org](mailto:ajitanshu.m@invertis.org)

B. V. S. Chauhan · M. K. Shukla  
Automotive Fuels and Lubricants Application Division, CSIR-Indian Institute of Petroleum,  
Dehradun, UK, India

A. Garg  
Department of Mechanical Engineering, College of Engineering Roorkee, Roorkee, India

A. Vedrtnam  
Universidad de Alcalá, Alcalá de Henares, Spain

© The Author(s), under exclusive license to Springer Nature Singapore Pte Ltd. 2022  
A. K. Agarwal and H. Valera (eds.), *Greener and Scalable E-fuels for Decarbonization of Transport*, Energy, Environment, and Sustainability,  
[https://doi.org/10.1007/978-981-16-8344-2\\_2](https://doi.org/10.1007/978-981-16-8344-2_2)

## 2.1 Introduction

On 12 December 2015, 196 Parties at the Conference of Parties (COP 21) agreed in Paris. The goal of the agreement was to limit global warming underneath 2 °C, preferably 1.5 °C compared to the pre-industrial levels. The application of the Paris Agreement necessitates economic and social alteration which works on a 5-year cycle of increasingly determined climate change actions disbursed out by the countries. By 2020, countries submitted their plans for climate change actions known as Nationally Determined Contributions (NDCs) in which the plans of reducing the Greenhouse gas emissions were proposed. Long-term low greenhouse gas emission development strategies (LT-LEDs) provide a long-term horizon to the NDCs. It requires a framework for financial, technical, and capacity-building support from the developed countries. To accomplish these goals the European Union (EU) is exploring different mid-century setups that could lead to a low-carbon EU economy by 2050 (Rogelj et al. 2016; Wang et al. 2016).

We are currently well below the expected contributory measures that took place in the Paris Climate Agreement and require the greener means of transportations. For this application, Battery Electric Vehicles (EVs), Smart mobility impressions, biofuels and more efficient engines are been listed. For the solution of short-distance light vehicles like passenger cars and truck transportation, the EVs are well-thought-of (Woodburn and Whitening 2010; Bastani et al. 2011). The pros and cons of the e-fuels are discussed here for both the short and long-distance. It has also been emphasized previously that a greener mode for transport demands higher energy density (Van Kranenburg-Bruinsma et al. 2020). However, E-fuels are globally accepted as the future and to achieve the global goal of limiting the global temperature, these modes are considered as the potentially cost-effective technologies by the commission (Yugo and Soler 2019).

The Intergovernmental Panel on the Climate Change (IPCC) defined its fourth assessment report (AR4) on the sources of climatic sources of moisture. The report was an investigation report for the span of 1980–2012 and was divided into different sets and 21 reference regions (RRs) (refer Fig. 2.1) depending upon the climatic regions of different continents. The Lagrangian approach was implemented to investigate the transportation of moisture to continental regions from the major oceanic sources (Stohl and James 2005; Gimeno et al. 2010; Nieto et al. 2014).

The role of bioenergy can be foreseen as a more dependable mode for the time to come. According to the IEA's 2DS report, the biofuels will be utilized 10 times more than in 2020 worldwide by the year 2060, if more sustainable bioenergy is achieved. It is been estimated that around 30% of transport energy will be on biofuels which will be supplementary for the increase in electricity (Garg et al. 2021a, b). The World Energy Outlook New Policy Scenario (NPS) of IEA takes care of the policy measures of the current and the planned scenarios whereas the pathway for sustainability pathway is accounted by the Sustainability Development Scenario (SDS). Analysis shows around 70% of simulation of the deployment level as compared by both these



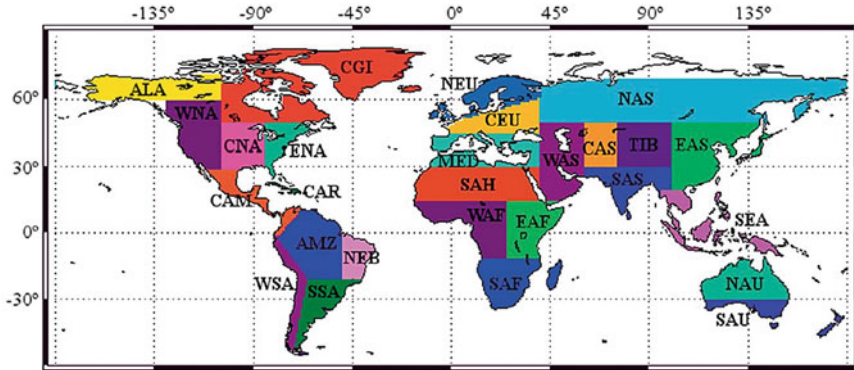


**Fig. 2.1** IPCC ARC defined continental RRs based on the geographical domains (Drumond et al. 2019)

scenarios are needed. To achieve the targets, set by the organizations, it is essential to set an ambitious approach towards the acceptance of biofuels. Ethanol production in 2019 was estimated to be around 114 billion liters or around 2.4 EJ. Different regions are dominating in production and use, for instance, the Corn in the USA and Sugarcane in Brazil is around 83% of the global production and also dominates in the usage. Production in China has risen quite rigorously for the last few years whereas India is overtaking Canada and Thailand in production and usage. EU is also emerging as the global production as per reports in 2019.

Figure 2.2 shows the Status of Global biofuel production in 2019 (Nystrom et al. 2019). Forty-one billion liters (about 1.4 EJ) of FAME biodiesel have been produced globally in 2019 and its production is comparatively less concentrated geographically

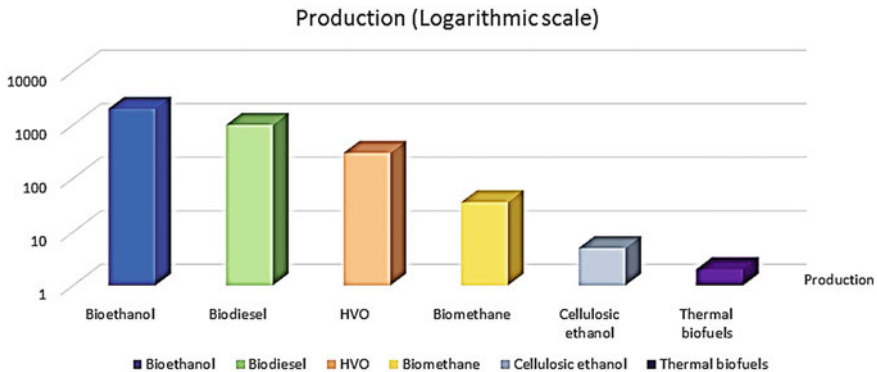


**Fig. 2.2** Status of global biofuel production in 2019. Data based on 2020 report of REN21, GSR (Nystrom et al. 2019)

as compared to ethanol. Production in Indonesia, the US, Brazil, Germany and France were estimated to be 17%, 14%, 12%, 8% and 6% respectively, contributing to about 60% of the global production. HVO production is expected to grow rapidly in the next 5 years as per the trend it has been following which suggests growth from 6 to 17 billion liters.

The majority of the production of electricity and heat is still been done by the direct usage of biogas and efforts are been made to refine the gas to biomethane. The USA, Europe and Sweden are some of the major biomethane markets in transportation whereas countries like China and India are among the rising nations in this field. Approximately 30 PJ of usage in the transportation of biogas has been estimated in 2018 but the level of cellulosic ethanol production is estimated to be very low and sufficient technical advancements are necessary for the satisfaction of global requirements. IEA is increasing its efforts in this direction and soon proposed to produce around 1.7 billion liters of cellulosic ethanol in the coming years (Bacovsky 2020). This chapter provides an overview of the e-fuels, their production technologies, the effects and the contribution of e-fuels in restricting the emissions of greenhouse gases.

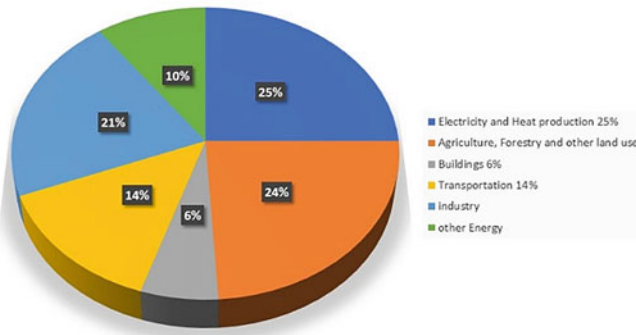
### ***2.1.1 The Concept of E-Fuels***

E-fuels are synthetic fuels that are a result of the combination of e-hydrogen or green hydrogen produced by the electrolysis of water with renewable electricity. The concentrated sources like flue gases from the industries or the air are considered to be the concentrated sources to capture the CO<sub>2</sub>. E-fuels also are described within the literature as electro-fuels, power-to-X (PtX), power-to-liquids (PtL), power-to-gas (PtG) and artificial fuels (Probstein and Hicks 2006; Ridjan et al. 2013).

Figure 2.3 suggests how the greenhouse gas emissions by economic affect the atmospheric temperature. The reports suggest approximately 29% of the greenhouse emissions were from the transport sector in 2019 in the context of the United States of America. Figure 2.4 shows that globally the transport sector contributes around 15% to the greenhouse effects. According to another report by the European Union (EU), around 74% of the emissions are from road transportation, 13% by Aviation, 11% maritime and the rest is others.

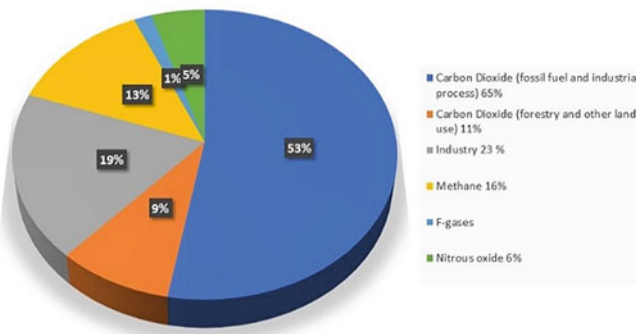
The summary of the primary use of e-fuels in different sectors of transportation is given in Table 2.1 where a comparison concerning gas and liquid modes of fuels according to the status is done. Along with this an overview of e-fuels as per their lower heating values and storage status is given in Table 2.2. Different alternatives are compared in Table 2.3 where a better understanding can be developed as per their characteristics (Espino et al. 2020; Capros et al. 2016; Hombach et al. 2019).

Global Greenhouse gas emissions by economic sector



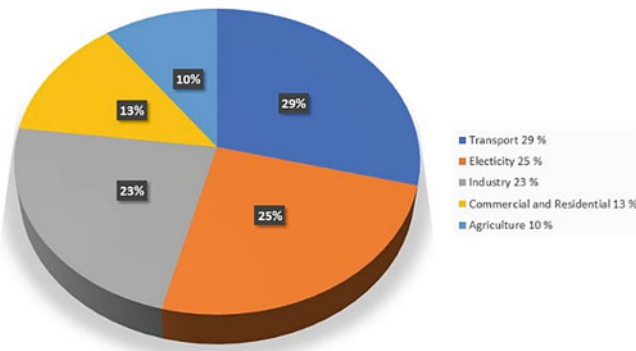
(a)

Global Greenhouse Gas Emissions by gas



(b)

Total U. S. Greenhouse gas emissions by economic sectors in 2019



(c)

Fig. 2.3 a global greenhouse emission by economic sectors, b global greenhouse emissions by gas, c U. S greenhouse emissions by economic sectors (Emissions 2014)

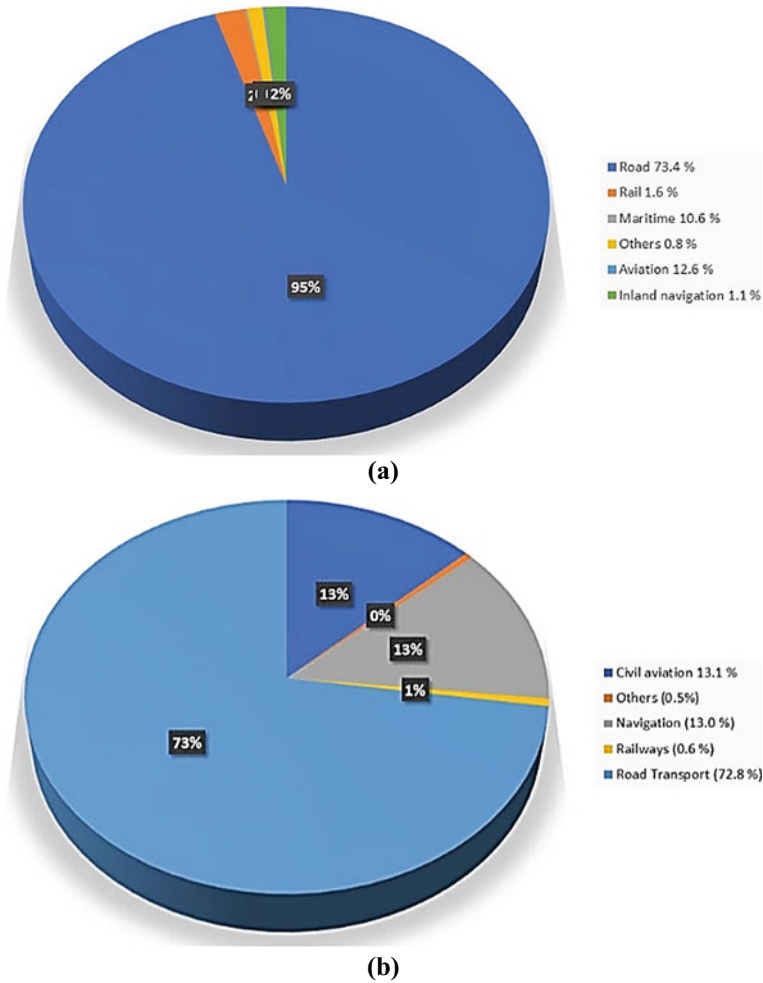


**Fig. 2.4** **a** Greenhouse gas emissions from transport by mode and **b** Share of transport energy demand by mode (Muller et al. 2017)

### 2.1.1.1 Technological Aspects of E-Fuels

E-hydrogen (also known as green hydrogen) is provided as a feedstock for producing e-fuels in hydrogen electrolysis. The e-fuel production technologies can be low-temperature (50–80 °C) technologies or high-temperature (700–1000 °C) processes. The production of e-fuels requires CO<sub>2</sub> (except e-ammonia) which is commonly obtainable from sources like biomass combustion, industrial processes, or can be captured from the air (Schulz 1999).

E-fuels production routes are demonstrated in Fig. 2.5. Steam reforming gasification partial oxidation of different elements i.e. natural gas, biomass, and coal is done

**Table 2.1** Potential primary uses of e-fuels

	E-fuels	Passenger cars	Heavy duty	Maritime	Aviation	Other sectors (non-transport)
Gas	e-methane (CH <sub>4</sub> )	x	xx	xx		xxx
	e-hydrogen (H <sub>2</sub> )	xx	xx	x		x
Liquid	e-ammonia (NH <sub>3</sub> )	x	x	xxx		
	e-methanol (CH <sub>3</sub> OH)	xx	x	x		
	e-DME/e-OME	x	xx	xx		
	e-gasoline	x				
	e-diesel	x	xxx	xx		
	e-jet					xxx

x-the relative potential role of e-fuel for the transport sector

Primary use, Secondary use, Minor usage

Other sector—industries, infrastructure, etc.

**Table 2.2** Qualitative overview of e-fuels

	E-fuels	Lower heating value (LHV), MJ/kg/MJ/l	Storage	Additional infrastructure	Powertrain development
Gas	e-methane	46.6/0.04	M	No	N
	e-hydrogen	120/0.01	D	Y	N
Liquid	e-ammonia	18.6/14.1	E	Y	Y
	e-methanol	19.9/15.8	E	N	Y
	e-DME	28.4/19.0	E	Y	Y
	e-OME	19.2/20.5	E	Y	Y
	e-gasoline	41.5/31.0	E	N	N
	e-diesel	44.0/34.3	E	N	N
	e-jet	44.1/33.3	E	N	N

<sup>a</sup>Most of the available logistics are applicable for E-methanol whereas storage is still an issue

<sup>b</sup>The applicability of FCEV is still not clear

N-No, Y-Yes

E-Easy, M-Medium, D-Difficult

Positive characteristics, Negative characteristics

in the primary stage which transforms the elements into Syngas comprise of CO and H<sub>2</sub>. Direct Fischer–Tropsch synthesis can be used to transform this syngas into liquid fuels whereas conversion of Syngas into traditional Fischer–Tropsch products

**Table 2.3** Different alternatives versus different key parameters

	Transport sectors	Infrastructure	Storage	Investment	Greenhouse gas reduction
Fossil fuels	All	Existing	E	L	L
Electricity	LDV/HDV	New	Difficult	H	H
Biofuels	All (limited by availability and cap in demand)	Existing	E	M	H
E-fuels	e-methanol (CH <sub>3</sub> OH)	Existing	E	H	H

<sup>a</sup>HDV-Heavy-duty vehicles, LDV-Light-duty vehicles

<sup>b</sup>Existing for liquid e-fuels, Not existing for gaseous e-fuels

E-Easy, L-Low, M-Medium, H-High

Most positive characteristics,  Nominal beneficial,  Negative characteristics

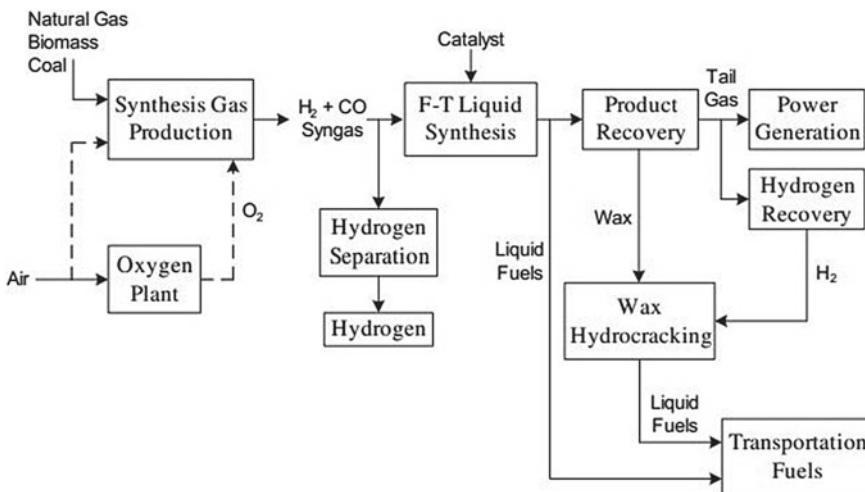


**Fig. 2.5** E-liquids production routes (Gill et al. 2011)

is performed using Fischer Tropsch synthesis. The traditional Fischer–Tropsch products process through hydro refining or hydrocracking to produce liquid fuels (Schulz 1999; Anderson 1984).

Gasoline, kerosene, and diesel are some of the fuels which are produced via Fischer–Tropsch synthesis whereas Water and Heat are dissipated in the final stage of the synthesis. Selectivity is also an important aspect in Fischer–Tropsch synthesis and Fig. 2.6 explains the selectivity of different liquid fuels according to the Fischer–Tropsch synthesis technique.

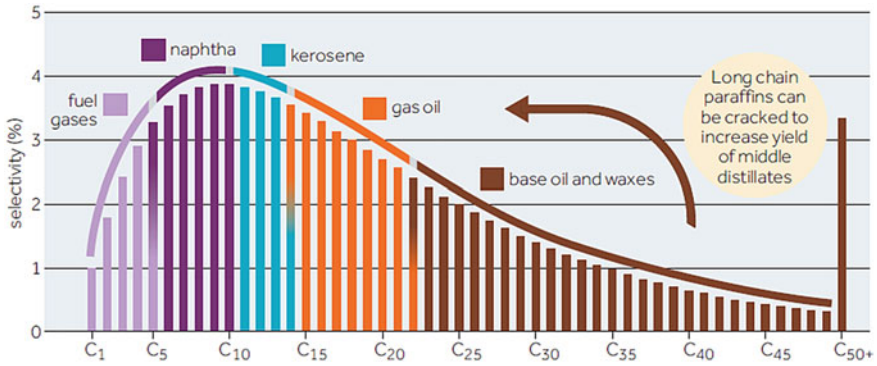


Fig. 2.6 Fischer-Tropsch liquid e-fuel products

### 2.1.1.2 Economic Aspects of E-Fuel

Figure 2.7 shows the resources required for e-fuel production. A gap is present while analyzing the economic efficiency of e-fuels even though it offers a long-term vision of renewable electricity if the transportation sector is considered. To efficiently counter this gap, wind energy is used in Germany to understand the economic and environmental effectiveness. Fischer-Tropsch synthesis is also performed which would be handy in the years to come. The cost of e-fuel is relatively on the higher side (about 7 euros/litre) but in time to come it is been expected that the cost decrease with the increase in adoption. As per the analysis, the costs of e-fuels could be 1–3 euros/litres in 2050 (Hombach et al. 2019).

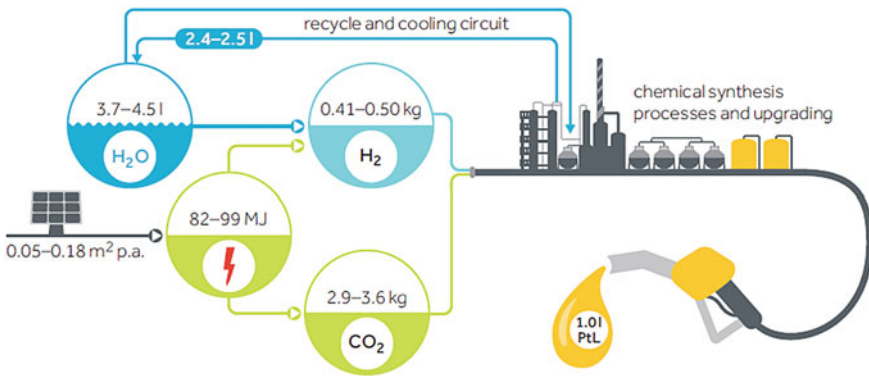


Fig. 2.7 Resources required for e-fuel production (Shell 2018)

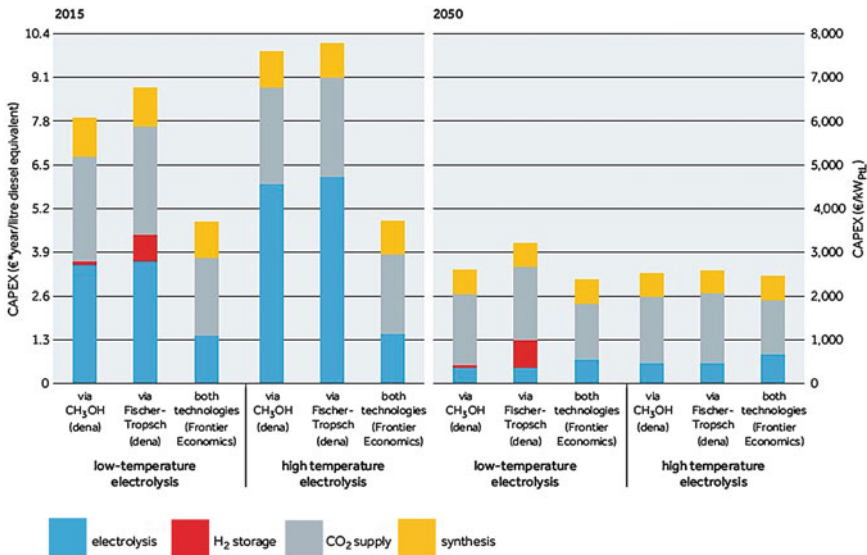


Fig. 2.8 E-fuels CAPEX (LBST and Dena 2017)

### 2.1.2 E-Fuel Investments

They're considered to be a progressive reduction as far as the investment cost with the technologies over the period. It may be due to the scale of the economy or the learning effects. Figure 2.8 shows the comparison of the Capital expenditure (CAPEX) which is associated with the different technologies for the production of e-fuels in 2015 and gives a forecasted cost in 2050. The production via different modes and expenditures is also justified to develop a better understanding of the present and future scenario.

### 2.1.3 Advantages of E-Fuels

Following are the main advantages of low-carbon fuels:

- E-fuels offer a significant degradation in the CO<sub>2</sub> emissions and as the reduction of greenhouse gases is the primary aim, it provides us an alternate for the future (Heyne et al. 2019).
- The life-cycle analysis suggests that the potential reduction of CO<sub>2</sub> will be about 70% which would be similar to that of DAC or from fossil sources (Liu et al. 2021).
- Higher energy density is achieved by e-fuels as compared to electricity and therefore it is considered suitable for the aviation and shipping sectors (Dahlgren et al. 2019).



- E-fuels are relatively cost-effective, they are easy to store and can be transported easily if compared to other modes like electricity. The fluctuation in seasonal demands can be easily compensated as storage (stationary as well as mobile) can be kept of e-fuels (Dahlgren et al. 2019)

### ***2.1.4 Disadvantages of E-Fuels***

Although the advantages of low carbon fuels overshadow the disadvantages, some of them are detailed as follows:

- It will require a substantial number of new plants for renewable generation of fuels to account for the losses which occur during the inherent thermodynamic conversions [30].
- The energy efficiency of e-fuels is significantly less than that of the efficiencies of vehicles running on electric batteries especially in combustion engines. From the point of view of power generation, the efficiency of Battery electric vehicles are estimated to be around 69% with comparison to the efficiency of 26–35% of those of vehicles running on fuel cell whereas the efficiency of e-fuel vehicles is in the range of 13–15% which are comparable to the conventional SI engines used as the efficiencies are in the range of 35–44% for the conventional engines (Economics 2018; Chauhan et al. 2021).

## **2.2 Opportunity to Reduce Carbon Emissions by E-Fuels**

The production of e-fuels is usually from water, electricity, and carbon dioxide or nitrogen. The net emissions are near zero when the biomass is directly captured from the air. There is very little difference between the e-fuels when analyzed concerning the cost of e-fuels whereas the most economical fuel comes out to be hydrogen. Variation in the cost of carbon dioxide directly affects the production costs of e-LNG, e-methanol, and e-diesel, and the cost of electricity affect all the e-fuels (Rameirez et al. 2020; Center 2017; Krol and Lenz 2020).

### ***2.2.1 Impact on the Transport Sector***

Currently, the transport sector accounts for approximately 23% of global Carbon Dioxide emissions (Schipper et al. 2020). Road transport is responsible for almost 75% of these emissions more than 10% are of aviation as well as deep-sea shipping each.

The CO<sub>2</sub> emissions are to be reduced by approximately 95% by the end of 2050 as compared to the level of emissions in 1990 to meet the proposed targets set in the

Paris Climate Agreement. Several strategies are available to somehow confine the emissions of CO<sub>2</sub>, i.e.:

- By restricting the traveling or emphasizing more on smart mobility or local sourcing.
- Opting fossil energy carriers to increase the energy efficiency of the vehicles
- By introducing some new carriers for energy could cause lower emissions of greenhouse gases as compared to the existing options.

The targets can be achieved even if the first two strategies are applied efficiently and a lot less (near zero) amount of emissions can be attained.

Because of higher energy efficiency, battery electric propulsion is considered the solution for short-distance and light vehicles. However liquid gaseous fuels have higher energy density and batteries are not suitable for high energy storage onboard so biofuels and e-fuels are considered for this (ICCT 2016).

The sustainability available for biofuels is assumed to be not sufficient meant for satisfying all the modes that required high energy densities (Espinoza et al. 2020; Capros et al. 2016). There is much to discuss the innovative approach in e-fuels. Some of the e-fuels are discussed here which would be potentially important in the time to come.

### 2.2.1.1 Green Hydrogen

Green hydrogen (H<sub>2</sub>) which uses renewable energy to produce hydrogen from water is made from H<sub>2</sub>O (water) using sustainable electricity. H<sub>2</sub> (hydrogen) and O<sub>2</sub> (oxygen) are split from water using an electrolyzer (Fig. 2.9) and can reach an efficiency of 64%. The electricity cost has to be utilized to minimize the production cost the production may also require buffering or storage (Ayodele and Munda 2019; Greentech media) (Geoupura).

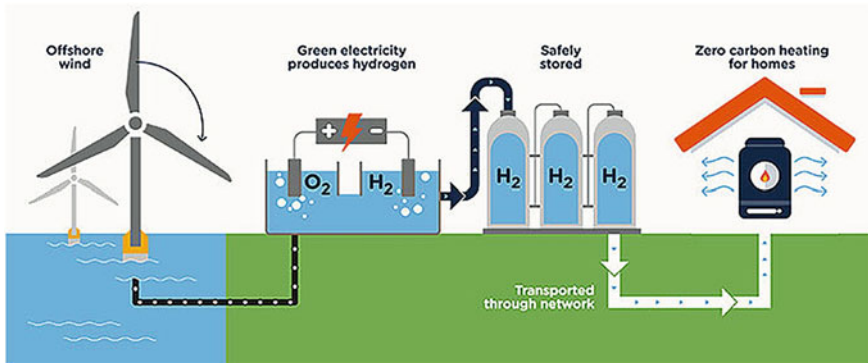
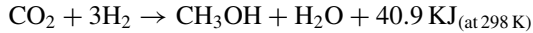


Fig. 2.9 Green hydrogen is produced using renewable energy (Muradov and Veziroglu 2008)

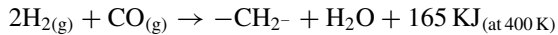
### 2.2.1.2 E-Methanol

Green hydrogen, electricity, and CO<sub>2</sub> are used for the production of E-methanol (CH<sub>3</sub>OH). To realize the circularity, the methanol is produced from hydro generation instead of the usual process which is from the syngas. Direct Air Capture (DAC) can be used to achieve by capturing CO<sub>2</sub> from biomass. The efforts for finding the fuels for tomorrow are underway and many places in the world are looking forward to large production plants of e-methanol (Nieminen et al. 2019; Wallenius 2020). The equation involved in methanol formation is:



### 2.2.1.3 E-Diesel

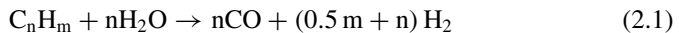
Green hydrogen is also used for the production of E-diesel and an efficiency of around 69% can be achieved by using the Fischer–Tropsch process (Brynnolf et al. 2018). The methanol-to-diesel synthesis can be an alternative to the Fischer–Tropsch process (Christensen and Petrenko 2017). The equation involved in diesel production is:



### 2.2.1.4 E-ammonia

With a yield of 70%, hydrogen and nitrogen can be synthesized using a Haber–Bosch reactor whereas e-ammonia produced by air separation consists of green hydrogen and nitrogen in the feedstock (Manna et al. 2021). The reactions include:

Steam Reforming process:



The Haber–Bosch process includes the reaction of atmospheric nitrogen (N<sub>2</sub>) with hydrogen (H<sub>2</sub>) in the presence of a metal catalyst under high temperature and high pressure (Fig. 2.10).



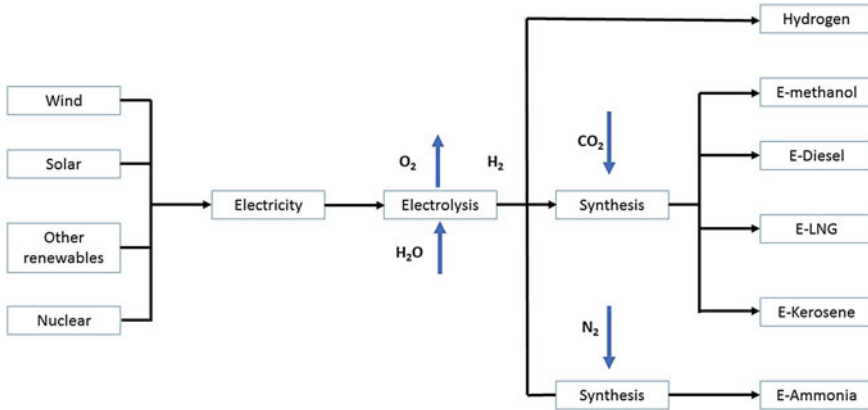


**Fig. 2.10** Ways of producing different e-fuels

### 2.2.1.5 E-LNG

Sabatier reaction can be used to produce E-LNG (Liquified Natural Gas), Predominantly  $\text{CH}_4$  (Nieto et al. 2014). For transport applications, the methane produced is usually liquified.

### 2.2.1.6 E-Kerosene

The green hydrogen,  $\text{CO}_2$ , and preferably Fischer–Tropsch synthesis can be used for the production of E-Kerosene ( $\text{C}_{12}\text{H}_{26}$ , ranging from  $\text{C}_{11}$  to  $\text{C}_{14}$ ). For the upgradation into kerosene, another way is to use e-methanol. Hydrogen can be bound in a chemical structure in liquids like liquid organic hydrogen carriers which can be used as the storage option for hydrogen.

A summary of different e-fuels is presented below which is based on KPIs (Key Performance indicators) and these KPIs can be used for the suitable e-fuel for transport.

### 2.2.1.7 Oxygenated Fuels

Dimethyl ether (DME) and Oxymethylene Dimethylethers (OME) are considered synthetic options for e-fuels that are produced by dehydration of methanol. Dimethyl also has favorable fuel properties as compared to methanol for both otto and diesel engines (Garg et al. 2021a, b). There found a reduction in emissions of  $\text{SO}_x$   $\text{NO}_x$  and PM while using DME and OME especially for marine applications so, they are considered cleaner because of their purity and chemical composition (Europa 2019).

**Table 2.4** KPIs to select the most suitable e-fuels

Practical application and safety	Environmental impact	Economics
<ul style="list-style-type: none"> <li>• Vehicle modifications</li> <li>• Impact on infrastructure</li> <li>• Impact on operations</li> <li>• Safety</li> </ul>	<ul style="list-style-type: none"> <li>• Emissions of pollutants: NOx, PM, SOx</li> <li>• CHG Emissions</li> </ul>	<ul style="list-style-type: none"> <li>• Cost of production</li> <li>• Storage cost and distribution costs</li> <li>• Vehicle costs</li> <li>• Powertrain efficiency</li> </ul>

### 2.2.1.8 Liquid Organic Hydrogen Carriers

Liquid organic hydrogen carriers (LOHC) are considered as a long-term option for higher energy density storage of greener hydrogen (Niermann et al. 2019; Aakko-Saksa et al. 2018). The storage of hydrogen at ambient conditions can be done using this technology. Hydrogeneration can be used for storage and dehydrogenations are applicable for hydrogen release of suitable molecules which are usually liquids. Several organic liquids including methanol, formic acid and M-Ethyl-carbazole come under the term LOHC. LOHC is inexpensive, it's comparatively easy to manage these substances and these are potentially secure. LOHC offers on-demand delivery and improved energy storage for the long term. One of the most important benefits of this technology is the SME Hydrogenous (Hydrogenous 2021). For the extraction of hydrogen from its carrier a reformer or a chemical plant is required on the vehicle if used for transportation.

Table 2.4 gives KPIs to select the most suitable e-fuels.

## 2.3 Safety and Practical Applications

A huge impact of transition from fossil fuels to e-fuel may be observed on vehicles, infrastructure, and logistics. The distribution technologies are not present for several e-fuels as well as there is a lack of new engines and tanks for the vehicles. The requirement of proper safety measures is prominent for the usage of hydrogen as an e-fuel. Therefore, for the practical application and KPI for safety, some elements are being considered:

- Impact of e-fuels technologies on vehicles (Maas et al. 2016)
- Impact on infrastructure for distribution and storage (Ramirez et al. 2020)
- Impact on operations
- Safety.

### 2.3.1 Impact of E-Fuels Technologies on Vehicles

Vehicles running on e-fuels may require larger and expensive storage. The existing IC engines (ICE) are quite efficient (40–50%) and feasible (between €200 and 500/kW). The Fuel cell electric vehicle (FCEV) powertrains prices are of range €2500–3500/kW (>200 kW size) and at present available only for the use of pure hydrogen. Existing engines whereas can be used for e-diesel and e-LNG. As the competitive existing technologies are available for the use of E-methanol, it is fairly easy for E-methanol to enter the market, whereas large development efforts are needed for e-ammonia and hydrogen to be used as e-fuels.

Table 2.5 explains the Different modalities available for e-fuels according to their form and suitability, where E-methanol and E-LNG are observed to be quite feasible for storage in vehicles. There are problems of storage in aviation and efforts are required to move forward in this direction. Table 2.6 shows the analysis of volume and space requirement of e-fuels onboard ships in comparison to the available standard diesel fuel. It is quite substantial that the storage of batteries would require a comparatively large volume and space and modification required in the existing engines can be understood by Table 2.7. Table 2.8 suggests the form and suitability of the transportation of different fuels for different modalities and different colors suggest the suitability status of e-fuels.

A whole new distribution system is required for Hydrogen which also includes the infrastructure. As there is a need for compression or liquefaction, the infrastructure will be more complex. The fuel distribution for road transport will require many fuel stations and this task is more of an extensive one. The quantity (tonnes of fuel) and energy (GJ) of fuel that are transportable by typical tanker trucks are given in

**Table 2.5** Different modalities available for e-fuels according to their form and suitability

Storage in vehicle	Green hydrogen	E-methanol	E-diesel (FT)	E-ammonia	E-kerosene	E-LNG
Distribution and long-haul trucks	Compressed or cryogen	Standard liquid	Standard liquid	Compressed (±10 bar)	Na	Compressed or cryogen
Inland shipping	Compressed or cryogen	Standard liquid	Standard liquid	Compressed (±10 bar) or cooled (– 33 °C)	Na	Cryogen
Short-sea shipping	Cryogen	Standard liquid	Standard liquid	Cooled (– 33 °C)	Na	Cryogen
Deep-sea shipping	–	Standard liquid	Standard liquid	Cooled (– 33 °C)	Na	Cryogen
Aviation	–	–	–	–	Standard	Cryogen

Easy, 
  Quite feasible, 
  Feasible, 
  Not impossible, 
  Impossible

**Table 2.6** Volume and space requirement of e-fuels onboard ships compared to the available standard diesel fuel

	Volume factor based on MJ/dm <sup>3</sup>	Packaging factor ship	Space requirement
E-diesel	1.0	1.0	1.0
E-methanol	2.3	1	2.3
E-LNG	1.6	2	3.2
E-ammonia (cooled)	3.1	1.1	3.4
E-ammonia (10 bar)	3.2	2	6.4
Hydrogen (cryogenic)	3.8	2	7.7
Hydrogen @700 bar	6.3	2.5	15.7
Battery	50	2	100

**Table 2.7** Impact of e-fuels on vehicle costs

Hydrogen	New modified engine and expensive tank
E-methanol	Requirement of modified engine and tank
E-diesel	No modification required
E-ammonia	Significant impact on the tank, the requirement of a new engine
E-LNG	Fair modification of engines, costly tank
E-kerosene	No modification required

No impact, 
  Small impact, 
  Medium-impact, 
  Significant impact

**Table 2.8** Form and suitability of the distribution of different fuels for different modalities

Distribution/transport via	Green hydrogen	E-methanol	D-diesel (FT)	E-ammonia	E-kerosene	E-LNG
Pipeline	Compressed			Compressed	Na	Compressed
Tanker truck	Compressed or cryogen	Standard liquid	Standard liquid	Compressed (±10 bar)	Na	Cryogen
Inland ship	Compressed or cryogen	Standard liquid	Standard liquid	Cooled (-33 °C)	Na	Cryogen
Short-sea ship	Cryogen	Standard liquid	Standard liquid	Cooled (-33 °C)	Na	Cryogen
Deep-sea ship	Cryogen	Standard liquid	Standard liquid	Cooled (-33 °C)	Na	Cryogen

Easy, 
  Quite feasible, 
  Feasible

Table 2.9. As a large quantity of fuel supply can take place with a comparatively small number of strategic locations, the distribution of fuels by aviation as well as shipping is way more efficient as compared to the road transport and the process can also be organized more efficiently for maximum results.

**Table 2.9** Typical volumes and energy contents of fuels transported by tanker trucks

	Tanker truck		The ratio of tanker trucks to diesel reference
	Tonnes	GJ	
E-diesel	16	683	1.0
Hydrogen (compressed)	1	120	5.7
Hydrogen (cryogenic)	4	480	1.4
E-methanol	16	315	2.2
E-ammonia (compressed)	16	298	2.3
E-LNG	16	784	0.9

### 2.3.2 Safety Issues

Some of the e-fuels for some ignitable mixture when comes in contact with air. As the e-fuels usually have comparatively low flash point temperatures and are toxic, it becomes more difficult to adopt several e-fuels. An example of such fuel is ammonia, which is a gas at environmental conditions and toxicity makes it unsafe for transportation via road. To apply it efficiently sufficient measures are to be taken (Vries 2019).

Methanol has been ingested with toxicity as gasoline (Klier 1982). Methanol also contains an invisible flame which is at times is advantageous but usually, considered as a disadvantage. California is among those regions where methanol has been applied in cars so, these have been at times called flexible-fuel vehicles which were then replaced by ethanol (Ott et al. 2000).

Similar to methanol, LNG and Hydrogen have ignition issues. LNG has the advantage of being lighter than air as well as it diffuses rapidly in the atmosphere whereas hydrogen is not advised to do so because of its combustibility.

### 2.3.3 Environmental Impacts

KPI, WTW (well-to-wheel), and TTW (Tank-to-wheel) analysis to examine the pollutants have been done in the literature, and significant results supporting the use of e-fuels are found in favor (Ramirez et al. 2020).

Combustion engines take reference to the vessel emissions for all the fuels (besides hydrogen). For the combustion engines, some of the latest pollutant emission requirement is taken. These are given as follows,

- Euro VI based Trucks
- Stage V inland vessels, and
- Maritime vessels (Tier III NO<sub>x</sub> (2021) and fuel Sulphur required).

Table 2.10 summarizes the projection of pollutant emissions. Zero pollutant emis-



**Table 2.10** Projection of emission for different fuels based on EURO VI for truck, stage V for inland ships Tier III for maritime vessels

	Emission	Current fossil diesel	Green hydrogen fuel cells	E-MeOH	E-Diesel (FT)	E-NH3	E-LNG
Trucks and inland ships	NOx	L	Z	L	L	L	L
	PM	L	Z	L	L	L	L
	SOx	L	Z	L	L	L	L
Maritime vessels	NOx	M	Z	M	M	M	M
	PM	M	Z	L	L	L	L
	SOx	M	Z	L	L	L	L

L-Low, M-Medium, Z-Zero

sions are only attained while using hydrogen in combination with fuel cells which are significant for urban areas. E-fuels (except H<sub>2</sub>) will not lead to significant reductions in pollutants as particulate filters are required in diesel engines. The absence of sulfur compounds can lead to reductions in SO<sub>x</sub> and PM emissions.

Due to IMO tier III legislation, the NO<sub>x</sub> emissions from the marine vessels are reducing. There will be an expected reduction in emissions and implementation of exhaust and the implementation of after treatment will be implemented. The zero pollutants are not anticipated because of the nature of combustion in ICEs so, emissions on some scale are expected. Further modifications are proposed and expected to be implemented post-2030 status.

Hydrogen and e-ammonia on the other hand are free of carbon and don't produce CO<sub>2</sub> emissions in combustion. Zero greenhouse emissions are attainable in case if the renewable source is used.

Table 2.11 represents the environmental impact of KPI scores for the different e-fuels.

Table 2.12 provides the barriers and potential remedies for the adoption of e-fuels.

Cooperation is the key, individual stakeholders or states may try their hardest but without the cooperation of states and stakeholders worldwide, the task seems humongous. There is a certain need of setting regional targets in the field of regulation

**Table 2.11** Environmental impact of KPI scores for the different e-fuels

	Pollutant emissions	CO <sub>2</sub> emissions
Hydrogen	Zero emission	No WTW & TTW CO <sub>2</sub> emissions
E-ammonia	Equal emission of all e-fuels in combustion engines	Zero WTW & TTW CO <sub>2</sub> emissions if all CO <sub>2</sub> is circular (under certain circumstances)
E-diesel (FT)		
E-methanol		
E-LNG		
E-kerosene (FT)		

**Table 2.12** Barriers for adoption of e-fuels (Ueckerdt et al. 2021)

	Barriers	How to overcome
Economic	<ul style="list-style-type: none"> <li>• Cost of e-fuels</li> <li>• Future development of renewable electricity is uncertain, so as the CO<sub>2</sub> feedstock costs</li> <li>• Advance infrastructure is required</li> </ul>	<ul style="list-style-type: none"> <li>• Investment required in R&amp;D for more effective routes of production</li> <li>• Acceptance of cost of sustainability of fuels over the current fossil fuel cost</li> <li>• Application of the financial model to meet the long-term requirement</li> <li>• Application of flexible hydrogen production to take advantage of current electricity costs</li> <li>• Apply the infrastructural concepts for the development of storage facilities</li> </ul>
Technical	<ul style="list-style-type: none"> <li>• Unclear feasibility of production routes</li> <li>• Not enough circular sources of CO<sub>2</sub> available</li> <li>• Requirement of development of engines and fuel cells</li> </ul>	<ul style="list-style-type: none"> <li>• Optimization of production routes</li> <li>• Development of DAC technologies for large scale applications</li> <li>• Investing in the development of engines and fuel cells</li> </ul>
Organizational	<ul style="list-style-type: none"> <li>• Need of a system perspective and stakeholders' cooperation</li> <li>• Electricity import dependency</li> <li>• Emphasis on advance policies for long route transportation</li> </ul>	<ul style="list-style-type: none"> <li>• Long term commitment from stakeholders</li> <li>• Extension of offshore wind capacity above 60 GW</li> <li>• Increasing awareness about e-fuels and making them applicable</li> </ul>
Regulatory	<ul style="list-style-type: none"> <li>• Costly fossil fuels preventing the investors from investing</li> <li>• No certification of e-fuels as of now</li> <li>• Uncertain future tax regimes for e-fuels vehicles</li> <li>• Goals needed worldwide</li> </ul>	<ul style="list-style-type: none"> <li>• E-fuels over fossil fuels approach</li> <li>• Sustainable initiative support</li> <li>• Arrangement of regulatory certainty</li> <li>• Base level creation of applicable field</li> </ul>

as well as emission and setting targets won't be enough, strict compilation rules are needed to be imposed.

## 2.4 The Climate Change Report Card

Figure 2.11 shows the climate change report card of the countries. Despite the 2015 agreement of reduction in carbon emission, it is estimated that many countries are not following the right track and it is quite substantial from the climate change report card. Even though the carbon emissions in The Gambia, Morocco and India are highly expected to rise, but they will fall short of exceeding the 1.5 °C limit and are among the countries which are taking the matter to priority and are listed as the top of the class. Norway, China, and the United Kingdom are among the countries which

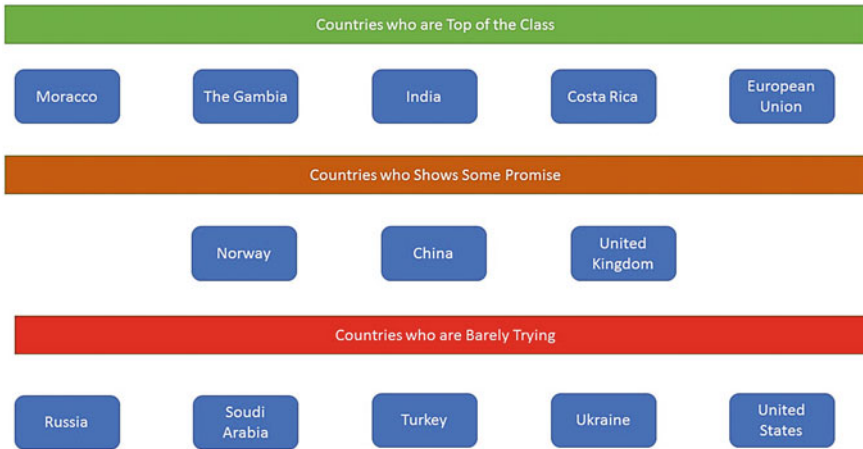


**Fig. 2.11** Climate change report card

are showing some promises although it will be a huge task and they might fall below but intent can be seen by their growth.

Russia is among the top for the emitter of greenhouse gases, and it is the only large emitter that has yet to endorse the Paris Agreement. Saudi Arabia on the other hand appears to be going backward their vision is yet to move on from oil dependency. Turkey, Ukraine, and the United States are considered to be critically insufficient (Mulvaney 2019).

## 2.5 Concluding Remarks

This chapter provides a statistical and technical overview of the e-fuels. The chapter also discusses the potential and challenges associated with the commercialization of the e-fuels to be used as transport fuels. There has been a significant increase in the development of e-fuels. Several conclusions can be drawn from the literature on e-fuels:

- Hydrogen as e-fuel does not apply to longer distances and is limited to shorter distances whereas it depends on the costs of electricity and of CO<sub>2</sub> as well as the nature of infrastructure and vehicles. All the other e-fuels i.e. e-methanol, e-diesel and e-LNG are considered as the options whereas E-ammonia is still not recommended for road transport.
- Depending upon the cost of CO<sub>2</sub>, Hydrogen for shipping can be an interesting option and still for the shorter distances. E-ammonia along with all the other alternates are applicable for the transport by shipping which again depends upon the cost fluctuation of CO<sub>2</sub>.

- In the case of aviation, E-kerosene is the only feasible option. A large investment is required for altering the engine design if the acceptance of alternate fuels takes place, which would again be dealing with the loss of passengers and the load capacity.

## References

- Aakko-Saksa PT, Cook C, Kiviaho J, Repo T (2018) Liquid organic hydrogen carriers for transportation and storing of renewable energy—review and discussion. *J Power Sources* 396:803–823. <https://www.hydrogenious.net/index.php/en/hydrogen-2-2/>
- Anderson RB (1984) Fischer-Tropsch synthesis
- Ayodele TR, Munda JL (2019) Potential and economic viability of green hydrogen production by water electrolysis using wind energy resources in South Africa. *Int J Hydrogen Energy* 44(33):17669–17687. <https://www.greentechmedia.com/articles/read/green-hydrogen-explained>. <https://www.geopura.com/blog/why-we-should-start-using-green-hydrogen-in-2019/>
- Bacovsky D (2020) The role of renewable transport fuels in decarbonizing road transport—deployment barriers and policy recommendations. IEA technology collaboration programmes advanced motor fuels annex, 58
- Baier J, Schneider G, Heel A (2018) A cost estimation for CO<sub>2</sub> reduction and reuse by methanation from cement industry sources in Switzerland. *Front Energy Res* 6, 5. <https://ec.europa.eu/environment/air/sources/road.htm>. <https://www.consilium.europa.eu/en/press/press-releases/2019/10/25/co2-emissions-fromships-council-agrees-its-position-on-a-revision-of-eu-rules/>
- Bastani F, Huang Y, Xie X, Powell JW (2011) A greener transportation mode: flexible routes discovery from GPS trajectory data. In: Proceedings of the 19th ACM SIGSPATIAL international conference on advances in geographic information systems, pp 405–408
- Brynnolf S, Taljegard M, Grahn M, Hansson J (2018) Electrofuels for the transport sector: a review of production costs. *Renew Sustain Energy Rev* 81:1887–1905
- Capros P, De Vita A, Tasios N, Siskos P, Kannavou M, Petropoulos A et al (2016) EU reference scenario 2016–energy, transport and GHG emissions trends to 2050
- Center AFD (2017) Emissions from hybrid and plugin electric vehicles
- Chauhan BV, Shukla MK, Dhar A (2021) Effect of n-butanol and gasoline blends on SI engine performance and emissions. In: Alcohol as an alternative fuel for internal combustion engines. Springer, Singapore, pp 175–190
- Christensen A, Petrenko C (2017) CO<sub>2</sub>-based synthetic fuel: assessment of potential European capacity and environmental performance. In: European climate foundation and the international council on clean transportation final, p 67
- Dahlgren S, Kanda W, Anderberg S (2019) Drivers for and barriers to biogas use in manufacturing, road transport and shipping: a demand-side perspective. *Biofuels*, 1–12. <https://windeurope.org/wpcontent/uploads/files/aboutwind/statistics/WindEuropeAnnual-Statistics-2018.pdf>
- De Vries N (2019) Safe and effective application of ammonia as a marine fuel
- Drumond A, Stojanovic M, Nieto R, Vicente-Serrano SM, Gimeno L (2019) Linking anomalous moisture transport and drought episodes in the IPCC reference regions. *Bull Am Meteor Soc* 100(8):1481–1498
- Economics F (2018) The future cost of electricity-based synthetic fuels. Extrait de [https://www.agoraenergiewende.de/fileadmin2/Projekte/2017/SynKost\\_2050/Agora\\_SynKost\\_S\\_tudy\\_EN\\_WEB.pdf](https://www.agoraenergiewende.de/fileadmin2/Projekte/2017/SynKost_2050/Agora_SynKost_S_tudy_EN_WEB.pdf), 64
- Emissions GG (2014) Iowa department of natural resources
- Espí E, Ribas Í, Díaz C, Sastrón Ó (2020) Feedstocks for advanced biofuels. *Sustain Mobil* 39

- Garg A, Dwivedi G, Baredar P, Jain S (2021a) Current status, synthesis, and characterization of biodiesel. *Biodiesel Technol Appl*, 167–194
- Garg A, Dwivedi G, Jain S, Behura AK (2021b) Impact of methanol on engine performance and emissions. In: *Methanol*. Springer, Singapore, pp 247–269
- Gill SS, Tsolakis A, Dearn KD, Rodríguez-Fernández J (2011) Combustion characteristics and emissions of Fischer-Tropsch diesel fuels in IC engines. *Prog Energy Combust Sci* 37:4 503–523
- Gimeno L, Drumond A, Nieto R, Trigo RM, Stohl A (2010) On the origin of continental precipitation. *Geophys Res Lett* 37(13)
- Heyne S, Bokinge P, Nyström I (2019) Global production of bio-methane and synthetic fuels-overview. CIT Industriell energi AB, Göteborg, Sweden
- Hombach LE, Doré L, Heidgen K, Maas H, Wallington TJ, Walther G (2019) Economic and environmental assessment of current (2015) and future (2030) use of E-fuels in light-duty vehicles in Germany. *J Clean Prod* 207:153–162
- ICCT (2016) <https://theicct.org/blogs/staff/a-world-of-thoughts-on-phase-2>
- Klier K (1982) Methanol synthesis. *Adv Catal* 31:243–313
- Krol T, Lenz C (2020) Can e-fuels close the renewables power gap? A review  
LBST and dena (2017)
- Liu X, Wahab S, Hussain M, Sun Y, Kirikkaleli D (2021) China carbon neutrality target: Revisiting FDI-trade-innovation nexus with carbon emissions. *J Environ Manage* 294:113043
- Maas H, Schamel A, Weber C, Kramer U (2016) Review of combustion engine efficiency improvements and the role of e-fuels. In *Internationaler motorenkongress 2016*. Springer Vieweg, Wiesbaden, pp 463–483
- Manna MV, Sabia P, Ragucci R, De Joannon M (2021) Thermokinetic instabilities for ammonia-hydrogen mixtures in a jet stirred flow reactor. *Chem Eng Trans* 86:697–702
- Müller B, Zachäus C, Meyer G (2017) European strategic processes towards competitive, sustainable and user-friendly electrified road transport. In: *30th international electric vehicle symposium, Stuttgart*, vol 10
- Mulvaney K (2019) Climate change report card: these countries are reaching targets. *Natl Geogr* 19(09):2019
- Muradov NZ, Veziroğlu TN (2008) “Green” path from fossil-based to hydrogen economy: an overview of carbon-neutral technologies. *Int J Hydrogen Energy* 33(23):6804–6839
- Nieminen H, Laari A, Koiranen T (2019) CO<sub>2</sub> hydrogenation to methanol by a liquid-phase process with alcoholic solvents: a techno-economic analysis. *Processes* 7(7):405. <https://wallenius-sol.com/en/e-methanol-future-fuel>
- Niermann M, Drünert S, Kaltschmitt M, Bonhoff K (2019) Liquid organic hydrogen carriers (LOHCs)—techno-economic analysis of LOHCs in a defined process chain. *Energy Environ Sci* 12(1):290–307
- Nieto A, Wahn U, Bufe A, Eigenmann P, Halken S, Hedlin G et al (2014) Allergy and asthma prevention 2014. *Pediatr Allergy Immunol* 25(6):516–533
- Nyström I, Bokinge P, Franck PÅ (2019) Production of liquid advanced biofuels-global status. CIT Industriell Energi AB
- Ott J, Gronemann V, Pontzen F, Fiedler E, Grossmann G, Kersebohm DB et al (2000) Methanol. Ullmann’s encyclopedia of industrial chemistry
- Probstein RF, Hicks RE (2006) Synthetic fuels. Courier Corporation
- Ramirez A, Sarathy SM, Gascon J (2020) CO<sub>2</sub> derived E-fuels: research trends, misconceptions, and future directions. *Trends in chemistry*
- Ridjan I, Mathiesen BV, Connolly D, Duić N (2013) The feasibility of synthetic fuels in renewable energy systems. *Energy* 57:76–84
- Rogelj J, Den Elzen M, Höhne N, Fransen T, Fekete H, Winkler H, Meinshausen M (2016) Paris agreement climate proposals need a boost to keep warming well below 2 C. *Nature* 534(7609):631–639
- Schipper C, Smokers R, Verbeek M, Verbeek R (2020) E-fuels: towards a

- Schulz H (1999) Short history and present trends of Fischer-Tropsch synthesis. *Appl Catal A* 186(1–2):3–12
- Shell RD (2018) Shell annual report and form 20-F 2017
- Stohl A, James P (2005) A Lagrangian analysis of the atmospheric branch of the global water cycle. Part II: moisture transports between Earth's ocean basins and river catchments. *J Hydrometeorol* 6(6):961–984
- Ueckerdt F, Bauer C, Dirnaichner A, Everall J, Sacchi R, Luderer G (2021) Potential and risks of hydrogen-based e-fuels in climate change mitigation. *Nat Clim Chang* 11(5):384–393
- van Kranenburg-Bruinsma KJ, van Delft YC, Gavrilova A, de Kler RFC, Schipper-Rodenburg CA, Smokers RTM et al (2020) E-fuels-Towards a more sustainable future for truck transport, shipping and aviation
- Wang H, Vicente-Serrano SM, Tao F, Zhang X, Wang P, Zhang C et al (2016) Monitoring winter wheat drought threat in Northern China using multiple climate-based drought indices and soil moisture during 2000–2013. *Agric For Meteorol* 228:1–12
- Woodburn A, Whiteing A (2010) Transferring freight to 'greener' transport modes. In: *Green logistics: improving the environmental sustainability of logistics*, Kogan Page, 124–139
- Yugo M, Soler A (2019) A look into the role of e-fuels in the transport system in Europe (2030–2050). *Concawe Rev* 28(1)

# Chapter 3

## A Historical Perspective on the Biofuel Policies in India



Anuj Kumar  and Anand B. Rao 

**Abstract** Despite having a valuable resource like biomass, India has constantly failed to tap its potential. For instance, out of a total annual potential of 29–48 billion m<sup>3</sup>, the Indian biogas sector only produces 2.07 billion m<sup>3</sup> per year. A similar situation has been there with the other biofuel sectors like bioethanol and biodiesel, where we have consistently failed to achieve the set blending targets. This points out the constant mismatch between the previous policies formed in the sector and the actual output received. The chapter analyzes the key factors that have played a major role in shaping the biofuel policies in India after independence. The timeline between 1947 and 2021 is analyzed to understand the processes that went through in the backdrop of biofuel policy formulation. This helps us in getting a micro picture of why these policies have not been able to deploy biofuels as a substitute in the Indian automobile sector at a mass scale. Majorly depending on limited number of first-generation feedstocks hindered the policies to achieve blending targets. It was found that issues like—opting for a top-down approach in initial policies, not scaling up the research and development in the initial stages, lack of coordination between stakeholders, etc., are also the main reasons for not achieving the expected goals. The work can potentially help to formulate a robust way of defining biofuel development pathways in the upcoming renewable boom, which can improve the share of biofuels in the overall renewable sector.

**Keywords** Biofuels · Policy issues · Historical analysis · Sustainable mobility

---

A. Kumar (✉) · A. B. Rao  
Centre for Policy Studies (CPS), Indian Institute of Technology Bombay, Mumbai 400076, India  
e-mail: [20f460006@iitb.ac.in](mailto:20f460006@iitb.ac.in)

A. B. Rao  
Centre for Technology Alternatives in Rural Areas (CTARA), Indian Institute of Technology  
Bombay, Mumbai 400076, India

© The Author(s), under exclusive license to Springer Nature Singapore Pte Ltd. 2022  
A. K. Agarwal and H. Valera (eds.), *Greener and Scalable E-fuels for Decarbonization of Transport*, Energy, Environment, and Sustainability,  
[https://doi.org/10.1007/978-981-16-8344-2\\_3](https://doi.org/10.1007/978-981-16-8344-2_3)

## 3.1 Introduction

### 3.1.1 Energy Security in India

Energy security is a major concern for all countries across the world. One of the main aims while designing the energy policies is to minimize imports which can help in ensuring energy security. In India, however, there is a constantly growing energy need that is majorly fulfilled by imports from other countries. Over the past ten years, crude oil import has increased from 163.60 MTs during 2010–11 to 226.95 MTs during 2019–20 at a compounded annual growth rate of 3.70% (Ministry of Statistics and Programme Implementation (MoSPI) 2021). This imposes serious concerns regarding the environmental health of the country.

India has aimed for various long- and short-term goals to reduce its dependence on external sources. For instance, the long-term goals include its commitment to reduce the emission intensity of its gross domestic product by 33–35% from the 2005 levels by the year 2030. The short-term goal includes reducing the country's dependence on imported crude oil by 10% in 2022 (International Energy Agency 2020). Hence, it becomes imperative to opt for energy policies that append the cause of smoother transition. Keeping these facts at the center, India is largely shifting its focus on renewable energy programs to become self-sufficient in the energy domain. It has set an ambitious target of achieving 450 GW renewable capacity by 2030 (Online 2021).

Renewable-based systems are the most promising and emerging technologies that can help in securing a sustainable future. For India, the most prominent renewable options include solar, wind, hydro, and biofuels. To deploy these technologies on a larger scale, many factors play a crucial role, which include—Research and Development, economic feasibility, social acceptance, stakeholder engagement, and most importantly the government policies being formed for that domain. In the present scenario, solar-based systems have been the primary focus for the past few years but are still under the development phase. To serve the large energy demand and collaterally ensure energy independence, it becomes essential to supplement solar energy with alternates like biofuels and hydropower. This can help us achieve our renewable targets and enhance the technologies in other renewable sectors.

### 3.1.2 The Untapped Potential of Biomass

Being the second-largest agricultural economy in the world (Countries by GDP Sector Composition 2017 2018), India has a high potential for energy generation from the organic waste generated from agricultural residues and other sources. An estimate suggests that around 17,500 MW power can be generated from the available 500 metric tons of biomass every year (Kumar et al. 2015). As shown in Fig. 3.1. In terms of state-wise per capita energy availability through crop residues, Punjab is



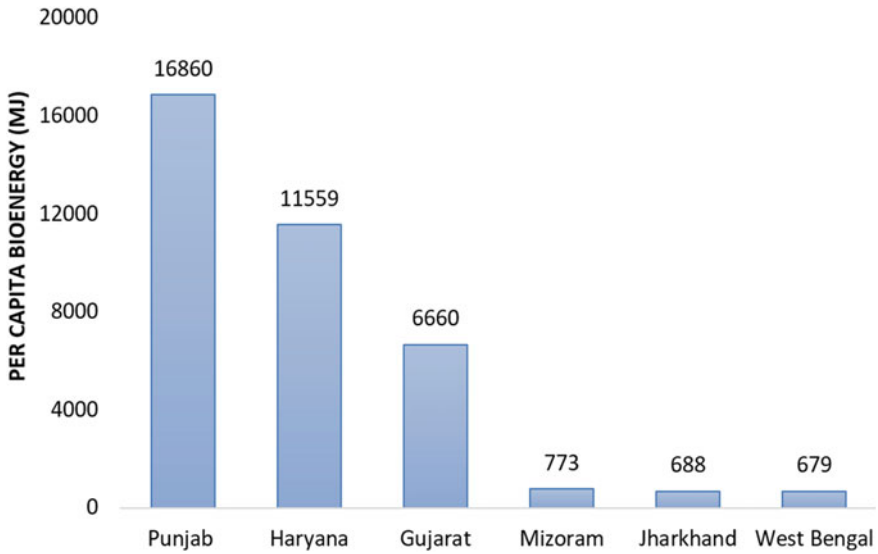


**Fig. 3.1** Per capita bioenergy availability in top three and bottom three states in India from crop residues

at the top with availability of 16,860 MJ bioenergy for every person in the state. It is followed by Haryana and Gujarat having a potential of 11,559 MJ and 6660 MJ respectively (Hiloidhari et al. 2014).

West Bengal on the other hand has the least bioenergy availability amongst all the Indian states. It is succeeded by Jharkhand and Mizoram having per capita availability at 688 MJ and 773 MJ, respectively. Further, research shows that the biofuel potential is in the range of 3–103 GGE/y from the energy crops being produced in India. This can meet upto 5–160% of India’s gasoline demand. Similarly, the agroforestry residues have a potential of 6–37 GGE/y, which can cover 10–56% of the country’s gasoline demand (Usmani 2020).

However, the present literature suggests that India has not utilized the potential of the biofuel sector to a larger extent. For instance, out of the estimated potential production of 29–48 billion m<sup>3</sup>/year in the biogas sector, only 2.07 billion m<sup>3</sup>/year biogas is being produced in India (Mittal et al. 2018). These figures also indicate that we have not achieved the expected goals from previously designed policies in the biofuel sector. Hence, there is a need to re-design these policies to fill the gaps which have been there in the earlier ones. A historical perspective on assessing the reasons behind this constant gap between the aimed objectives and the achieved targets in the previous biofuels policies can help in a meaningful manner.

### 3.1.3 *Scopes and Objectives*

Many researchers have studied and analyzed the biofuel policies in India. Ghosh and Roy (2018) in their work study the National Biodiesel Mission of 2003 using the Strategic Niche Management technique. The analysis pointed out various shortcomings related to *Jatropha* cultivation in the wastelands. The discrepancies in institutional mechanism and value chain of biodiesel were also elaborated in the study. Das (2020) studied the National Biofuel Policy 2018 with a particular focus on the Ethanol and Biodiesel blending programmes in India. The study raised concerns regarding hindrance to inter-state movements of feedstocks that were being transported for ethanol production purposes. The state taxes also raised the price of ethanol procurement that became a problem in implementation of NBPs in India. Similarly, Chandel et al. (2017) in their work studied that how these policies have affected the socio-economic indicators in rural areas in India. The work indicated that—use of advanced generation biofuels, efficient management of the effluents being generated after processing of first and second generation, can be the key factors in success of the biofuel policies in India.

Ebadian et al. (2020) analyzed the international biofuel policies including India and used a questionnaire survey approach for analysis. The work emphasized on the transportation sector specifically, and found that—relatively lower prices of petroleum products, issues related to the funding of advanced biofuels, etc. were the major factors that resulted in impediment of biofuel policies in India and across the world. It also pointed out that the Indian transportation sector is using 1.2% of biofuel share only.

Further, a study done by Baka and Bailis (2014) elaborated on the shortcomings of the Indian biodiesel policies specifically. The researchers performed a comparative analysis to study alternate options that can be opted in place of biodiesel and criticized the basic assumption of having ample amount of wasteland for feedstock production of biodiesel. Another research work done by Kumar et al. (2012) on the biodiesel policies in India pointed out the issue on availability of wasteland. Issue related to biodiesel engines where high sludge formation led to replacement of nozzles, leading to high maintenance cost, was also specified in this study. Kumar Biswas and Pohit (2013) particularly elaborated the role of state in improving the biofuel policies. The work suggested the state to act both as a facilitator and a regulator. Another recommendation done was regarding efficient institutional mechanism that can help in deploying the policies at ground level in a robust manner.

However, most of these studies have either been policy- or market-specific. Majority of them have focused on one biofuel policy, and none of them traced the status of policies after 1947 in India. The events that went through in forming these policies have also not been emphasized by these studies. It is evident that policies are not formed in isolation. It is a complex process, and a whole set of background events goes behind the formation of these policies. Hence, the chapter tries to analyze the policies on the timeline between 1947 and 2020. This study helps us understand

the nuances of all the simultaneous processes that helped in formulation these policies. The analysis also helps in establishing a cause-and-effect relation between the formation of the biofuel policies and the background events that went into before their formulation.

Further, a critical look into the literature gives an idea that the policies in the biofuel sector were formed in a cluster around the year 2000 and heavy investments were made around this period. Specific focus has been given on analysis of these policies, which were formed after the year 2000. While analyzing the biogas policies in India, it was observed (as explained under Sect. 3.2.3.2) that there was an exponential growth in the number of biogas digesters installed in the country during 1980–2000. The number of installed household digesters increased by around 40 times in 2000, with respect to the 1980 values.

Hence, the primary objectives of this chapter include:

- (i) To emphasize on the shifting policy processes by focusing on the three biofuel sectors in India
- (ii) To assess the issues related to the previous biofuel policies in India
- (iii) To identify the primary reasons that led to the clustering of policies near the year 2000 in the biofuel domain
- (iv) To identify the primary factors led to the exponential growth in the number of biogas digesters in the country between 1980 and 2000.

### ***3.1.4 Methodology***

A review of the timeline for biofuel policies in India is the central theme of this work. To study the timeline of biofuel policies after independence in India, the methodology mainly includes a thorough review of the available secondary sources. For this purpose, several published research articles and evaluation reports were analyzed. Analysis of evaluation reports on the state of biofuels, conducted by policy think tanks like Planning Commission, is done extensively to find the issues related to previous policies. A critical observation of the sources like reports on the status of biofuels in India carried out by various committees and institutes was carried out. This helped us scrutinize the gaps between recommendations and the actual policy outputs. Peruse of the news reports from sources like The Hindu, Economic Times, Financial Express, Down To Earth, etc. formed another important method to get a sedulous look into the policy outputs in the biofuel domain. Analysis of these news reports majorly helped in finding the status of the targets defined by the blending programs in India.

## 3.2 Historical Context of Biofuel Policies in India

### 3.2.1 Trends in the Energy Sector

Being the second-largest populous country in the world, India faces enormous resource constraints in various sectors. The energy sector has witnessed a constantly growing demand in India. The BP Energy Outlook Report (2014) points that India will surpass China and become the largest energy demand growth country by 2035.

#### 3.2.1.1 Increasing Energy Demand of India

The primary energy needs of the country tripled between 1990 and 2018 (International—U.S. Energy Information Administration (EIA) 2020). To serve these needs, we have mainly depended on unsustainable sources like fossil fuels. The import of crude oil, which was near 13 million metric tonnes (MMT) in 1972–73 (Ghosh and Roy 2018), grew to about 270.78 MMT by the end of financial year 2019–20 (News Express 2020).

The primary energy consumption (PEC) for India has been constantly growing. As evident from Fig. 3.2, the PEC increased by ~2.5 times between 2000 and 2018 (Statista 2021a). It accounted for around ~5.5% of global PEC and around 11% of global coal consumption in the year 2016 (Deloitte 2018). These figures put huge implications on the Indian energy policies to serve the energy needs in a sustainable

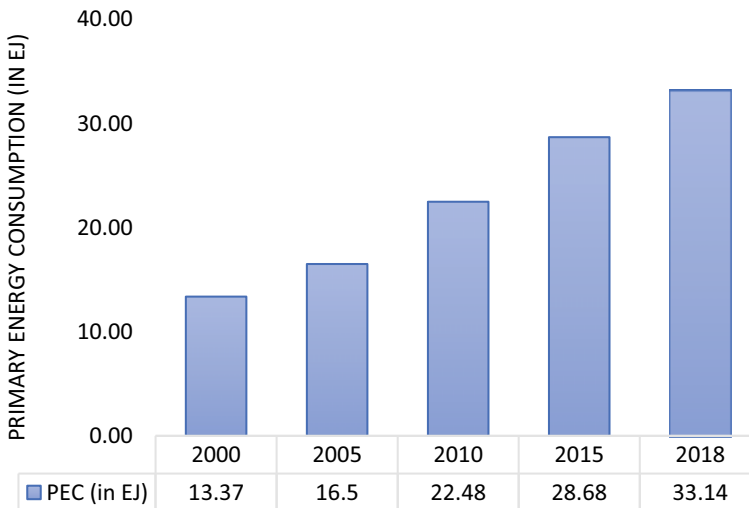


**Fig. 3.2** Primary energy consumption pattern of India between 2000 and 2018 (News Express 2020)

manner. To cater to these growing needs, it is a much necessary step that Indian policy makers explore all the possible sustainable options to the maximum extent possible. Renewable sector has emerged as the most promising alternate, that can fulfill the energy needs of our larger population.

### 3.2.1.2 Renewable Energy Share

As already stated, the major form of renewable energy for India comprises of- solar, wind, hydro and bioenergy. Out of these, solar energy has the maximum potential. The annual-report published by the MNRE stated the maximum solar potential to be around 750 Giga Watt-peak (GWp). Figure 3.3 shows the maximum peak potential distribution of solar energy across top five Indian states. The top five regions include—Rajasthan, Jammu & Kashmir, Maharashtra, Madhya Pradesh (MP), and Andhra Pradesh (AP). All together these states have a total solar potential of around 418 GWp. Out of these, Rajasthan has the maximum solar potential of 142.31 GWp, while Andhra Pradesh has a potential of 38.44 GWp (MNRE 2021a).

Similarly, the wind potential of top five states (above 120 m from the ground level) is around 568 GW, as shown in Fig. 3.4. These states are majorly situated at the western and eastern boundaries of India. At 120 m from ground, Gujarat has a maximum potential of 142.56 GW, while Andhra Pradesh is the fifth largest potential state for wind having 74.9 GW peak potential (MNRE 2021a).

The other two sources, i.e., small hydro and bioenergy have potential ~20 GW and 25 GW respectively. Jointly, these numbers indicate huge potential of renewables that can fulfil the energy security needs of the country. For India, the installed renewable capacity has constantly increased over the years. In March 2011, the share of renewables in the total installed capacity was 10.63%, which increased to 23.59% in May 2020. Figure 3.5 shows the continuously increasing share of renewables in

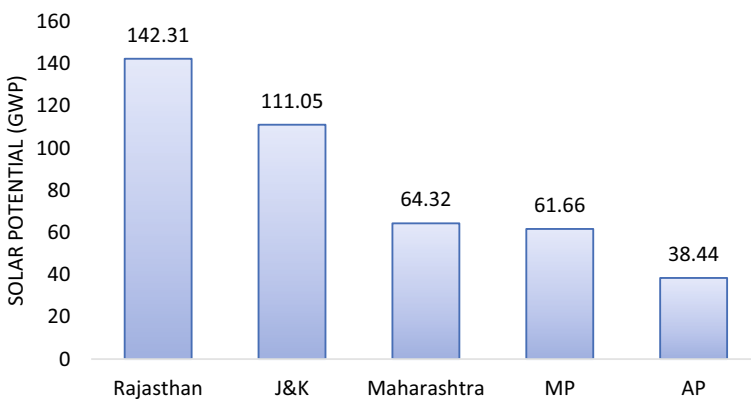
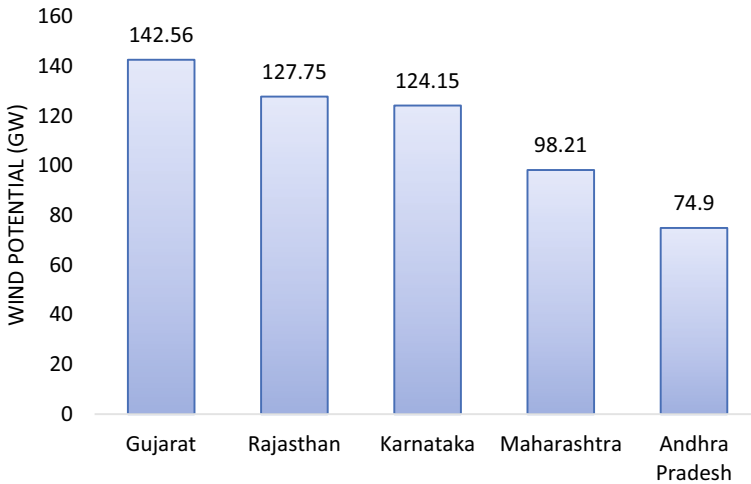
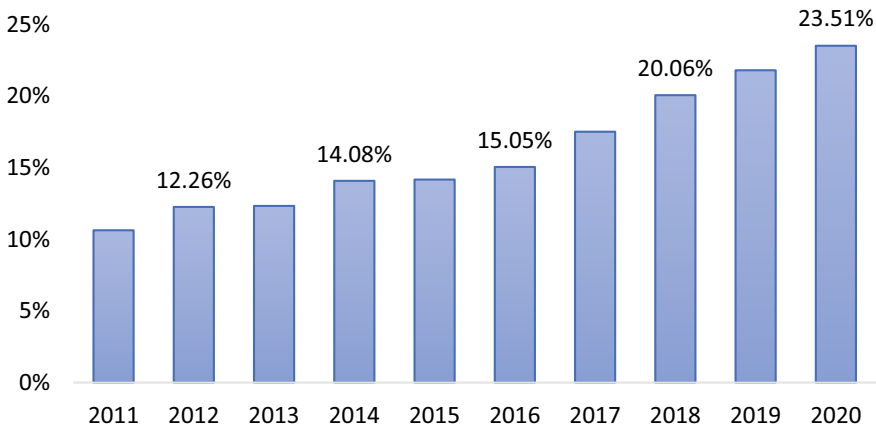


Fig. 3.3 Maximum solar potential of top five states in India



**Fig. 3.4** Wind energy potential of top five windy states in India (MNRE 2021a)

### Share of RE in total installed capacity



**Fig. 3.5** Share of renewable energy in total installed capacity (MNRE 2021b)

total installed capacity in India. In the past five years between 2015 and 20, it has increased at a CAGR of 9.33% (MNRE 2021b).

This growth can majorly be related to the commitment made through Paris Agreement of 2015, where India voluntarily agreed to reduce the greenhouse gas emission intensity of its GDP by 33–35% below the 2005 levels by 2030. Reports suggest that India is well on track to achieve our target of 175 GW of installed RE capacity by 2022 (Contributors 2021). However, to meet the target of 450 GW of installed RE

capacity by 2030, it becomes imperative to involve all the renewable resources. The solar capacity, which was near 0.065 GW in the year 2010, has now increased to 39.2 GW by the end of 2020 (Statista 2021b). But the bioenergy sector did not perform even near the growth rates of solar sector. Its capacity increased from 3 to 10.5 GW in past ten years (Statista 2021c). Many policies were formed for utilizing bioenergy but have not performed well enough to meet the expected objectives.

### ***3.2.2 International Status of Biofuel Policies***

Two most successful countries in implementing the biofuel policies include Brazil and USA. They have performed well to implement these biofuel policies on the ground level. These two countries dominate the global export of ethanol across the world.

Being the largest producer of corn, USA mainly uses it as a primary feedstock for bioethanol production. The Energy Policy Act (2005) of the country brought the mandate of using 4000 million gallons of biofuels with the petrol. The target was further increased to 7500 million gallons for the year 2012 and both the stated policy mandates came under the program—Renewable Fuel Standard (RFS). Further, under the Energy Independence and Security Act (2007), the RFS2 planned for 9000 million gallons ethanol blending by 2008 (Das 2020). Although the initial RFS programs mainly focused on the first-generation biofuels, now the attention is shifting on the alternates that mainly include the advanced feedstocks for bioethanol production. To reduce the dependence on corn for bioethanol production, the RFS now promotes lignocellulosic biomass as an alternate to the biofuels (MNRE 2021a).

Brazil, as a nation, was the amongst the first in the world to focus on its biofuel policies right after the fuel crisis of 1973. Through its ‘Proalcool’ program, Brazil was able to mix 15% ethanol in gasoline by 1979. By 2006, the nation became oil independent and around 83% of entire car fleet was working on the flex-fuel system (Sorda et al. 2010). Regarding recent advances, the country has launched the RenovaBio programme in 2020 that aims at decreasing the carbon emissions. Brazil is well on track to achieve these targets and meet the commitments done at Paris agreement (USDA 2021).

Table 3.1 shows the ethanol production rates, expected blending targets, and achieved target in Brazil, China, and India. If we look at the Asian counterpart of India- China, it has not performed well on biofuel policy front. The policies in China have mainly focused on the dissemination of technologies related to bioethanol only. The reason for this is because China is a vegetable-oil deficit country, which constrains it from making large scale policies in biodiesel. The bioethanol sector has been struggling to reach the set targets. Due to the fuel vs food conflict, the production as well as distribution of ethanol-based feedstocks was strictly monitored by the government during initial policies. In 2006, the National Development and Reform Commission had proposed a target of 6600 million litres of biofuel output. However, under the purview of rising food prices, the proposal was rejected by the Chinese

**Table 3.1** Status of ethanol blending in Brazil, China and India (Statista 2021d; USDA-GAIN 2019)

Country	Ethanol production in 2020 (in million gallons)	Ethanol blending target	Target achieved (in 2020) (%)
Brazil	7930	27% (in 2020)	27
China	880	10% (by 2020)	<4
India	480	20% (by 2025) <sup>a</sup>	7.93

<sup>a</sup>India's 2030 targets have been revised recently in July 2021

government (Sorda et al. 2010). A recent mandate of 2017 to achieve 10% blending rates by 2020 have also been put up on hold due to uncertainties. Although the capacity of production has increased since 2017 in China, the average blending rate are not expected to go above 4%. Above all, use of ethanol to make medicines during the COVID-19 pandemic also deviated the policy to achieve its blending targets (China: Biofuels Annual 2020).

### 3.2.3 Evolution in the Indian Biofuel Sector

In India, the biofuel policies have mainly evolved around three domains-Biogas, Bioethanol, and Biodiesel. It is imperative to emphasize that there has not been a clear legal definition of the term 'biofuels' (Saravanan et al. 2018), which sometimes creates ambiguities on the scope to use the term, as few works have only considered bioethanol and biodiesel as biofuels. However, biogas is also one of the gaseous biofuels and has been included in the chapter under the ambit of biofuels for our analysis.

#### 3.2.3.1 Timeline of Biofuel Policies and Programs in India

Regarding India's biofuel laws, the first in history was the Indian Power Alcohol Act of 1948, which came just after independence. The formulation of this law aimed to use the surplus molasse generated from sugarcane production. This, in turn, sought for a more energy secure India in the upcoming decades after independence. It also had the provision of determining the procurement price of power alcohol such that it can be blended with petrol for vehicular usage.

However, the law never made its presence on the ground and did not help in uplifting the biofuel sector. Along with various other acts, the P.C. Jain committee constituted by the government of India recommended to repeal the Power Alcohol Act 1948, as it failed to serve its intended purpose (Report of the Committee to identify ... 2014). The recommendation led to repealing of the act in the year 2000.



Due to the turbulence in the international oil market between 1970 and 80, countries worldwide started to form independent renewable energy units. India formed the Commission for Additional Sources of Energy (CASE) in 1981, which was made responsible for looking into the alternate energy sources for the nation. The CASE was further subsumed by the Department of Non-conventional Energy Sources (DNES) in 1982. As a result of the formation of the DNES, during the sixth five-year plan (1985–90), the biogas sector witnessed a significant push, which was the only developed technology in the biofuel domain. This led to installation of household biogas digesters all over the country in an exponential manner. As a result of these efforts, nearly 33.7 lakh household-level biogas digesters by the end of 2000 in India.

Table 3.2 elaborates on various key events and policies that have contributed in shaping up of the biofuel sector in India after independence.

Along with the biogas dissemination, the biodiesel and bioethanol sector witnessed a major push around 2000. First major policy on bioethanol came in 2002, when ethanol blending was made mandatory in nine states across the country. Regarding the biodiesel sector, the National Policy on Biodiesel also came in the year 2003 on the recommendation of Committee on Development of Biofuels in India. However, the targets set in both these policies were not achieved due to various reasons.

### **Reasons for heavy investments in biofuel sector near the year 2000**

During the formulation and push for any policy, a whole set of background actions take place. Multiple factors affected the investments in biofuel sector near the year 2000. Along with multiple geopolitical events, the intent of the government at centre was also a main reason for these huge investments in the biofuel sector around 2000. Following are the key points which led to analyze the events that affected these investments:

1. The dynamics of the global fuel market mainly regulates the investments in the alternate fuel options in any country. In the case of biofuels also, the geo-politics played a major role. The series of events started from the oil-shocks of 1973 and 1979 which alerted Indian policy makers to focus on energy security. Table 3.3 enlists the important global events which affected the oil prices across the globe (Holodny 2016).
2. Developmental organizations like the World Bank and the Asian Development Bank also had plans to promote agriculture in India, which could have helped in achieving sustainable development across the country (Ghosh and Roy 2018).
3. Other alternates like solar power were very expensive during that time. For instance, the solar PV module price was around USD 5 per Watt in the year 2000 (Evolution of solar PV module ... 2020) which was not affordable for large scale deployment in India. Also, the technology for these alternate sources of energy was not that developed around the year 2000.

**Table 3.2** Timeline of biofuel policies and programs in India (H. T. 2007; CSTEP, College of Legal Studies, PLR Chambers 2019)

Year	Specific policy changes and events	Key actors	Outcomes/consequences
1948	Power alcohol act	Government of India	<ul style="list-style-type: none"> <li>• No substantial on-ground implementation</li> <li>• The act was finally repealed in 2000</li> </ul>
1975	First feasibility check for blending ethanol with petrol in India	Government of India: 6 technical teams and 4 study groups	<ul style="list-style-type: none"> <li>• Marked the beginning of ethanol blending in India</li> <li>• However, no significant developments were made after this trial run</li> </ul>
1980	Trial tests on passenger cars and 3 wheelers using ethanol blends	Indian oil corporation limited and Indian institute of petroleum	<ul style="list-style-type: none"> <li>• No major initiatives were taken after these trial tests and India did not form any policy in the bioethanol sector for next 20 years till 2000</li> </ul>
1981	Formation of commission for additional sources of energy (CASE)	Ministry of energy	<ul style="list-style-type: none"> <li>• Laid the foundation for formation of renewable energy units in India</li> <li>• Got incorporated in the Department of Non-Conventional Energy Sources (DNES) in 1982</li> </ul>
1981	National project on biogas development	Planning commission	<ul style="list-style-type: none"> <li>• The program marked a very positive impact on installing household level biogas digesters</li> <li>• Installation witnessed an exponential growth in the number of plants across India</li> </ul>
2002	Ethanol blended petrol program made mandatory in nine states	Central government and committee on development of biofuels in India	<ul style="list-style-type: none"> <li>• Covered a wide range of states which promoted ethanol blending</li> <li>• As a nudge, many new renewable agencies started to form in various states</li> </ul>
2003	National Biodiesel mission	Committee on development of biofuels in India	<ul style="list-style-type: none"> <li>• First policy on blending biodiesels at national level</li> </ul>
2003	National auto fuel policy	Expert committee on auto fuel vision and policy 2025	<ul style="list-style-type: none"> <li>• Promoted the blending of ethanol</li> </ul>

(continued)

**Table 3.2** (continued)

Year	Specific policy changes and events	Key actors	Outcomes/consequences
2008	National policy on biofuels	Ministry of new and renewable energy	<ul style="list-style-type: none"> <li>Incorporated both the biodiesel and bioethanol into one policy document</li> </ul>
2018	New national policy on biofuels	Ministry of petroleum and natural gas	<ul style="list-style-type: none"> <li>First National Biofuel Coordination Committee (NBCC) was formed for effective implementation of the program</li> </ul>
Apr., 2018	GOBAR-dhan scheme	Ministry of drinking water and sanitation	<ul style="list-style-type: none"> <li>To be studied</li> </ul>
Oct., 2018	SATAT scheme	Ministry of petroleum and natural gas	<ul style="list-style-type: none"> <li>Sets an ambitious target of 5000 CBG plants by 2025</li> <li>Outcomes yet to be studied</li> </ul>

**Table 3.3** Important global events between 1970 and 2000

Year	Global event
<i>1974 and 1979</i>	<i>Two major oil crises across the globe</i>
1990	Invasion of Iraq on Kuwait
<i>1997</i>	<i>Asian financial crisis</i>
2001	September 11 attacks in the USA
<i>2002</i>	<i>Venezuelan oil workers' strike</i>

### 3.2.3.2 Policy Evolution in the Biogas Sector

Biogas has been one of the oldest technologies in the area of biofuels in India. The approach of policy formulation for the sector has witnessed a huge change over the years. The governments over time have shifted their focus from household-level digesters in 1980s to a more industry-based approach after 2015. In 1984–85, National Programme on Improved Chulhas (NPIC) was also launched to improve the condition of cooking in the rural areas. But now, more Compressed Biogas (CBG) plants are being promoted by the government through schemes like Sustainable Towards Affordable Transformation (SATAT) to enhance the idea of green transport fuel.

The following section discusses the changing approach of the governments after independence till 2020 in the biogas sector-

The period 1947–1980 was a nascent period for the development of biogas technology in India. Indian Agricultural Research Institute (IARI) conducted its first experiment on anaerobic digestion for biogas production in 1939 and subsequently

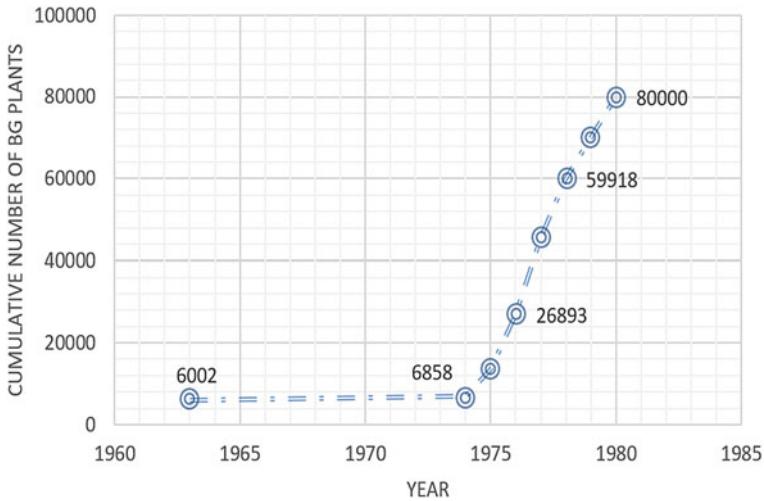


**Fig. 3.6** Number of installed biogas digesters in India between 1960 and 1980

developed the first biogas plant in 1946. An improved model of the reactor came in 1956, which worked on the principle of constant pressure and was easy to operate as compared to the earlier design.

The major aim of the Planning Commission was to improve the agricultural sector and enhance the rural economy during the third five-year plan of India. This helped in shifting the focus on technologies that may improve the state of economy in rural India. Khadi and Village Industries Commission (KVIC) took the responsibility of promotion and penetration of the biogas technology in mid 1960s (Kharbanda and Qureshi 1985). Their major focus was on the deployment of digesters in the rural areas.

Figure 3.6 indicates the number of biogas reactors in India between 1960 and 1980. During the initial ten years, no significant progress was made. From total 6002 digesters in 1963 across the country, we reached 6858 reactors by the year 1974 (Kharbanda and Qureshi 1985). But these numbers started to increase significantly after 1974.

After 1975, India added nearly 67,000 household biogas digesters in the rural areas in the next five years till 1980. Two major reasons for this steep rise in the number of digesters can be attributed to two simultaneous ongoing processes—one at the international and the other at the national level. The international phenomenon was related to the oil crisis of 1973, which nudged the nation to focus on energy security. At the national level, the most important push came from the Twenty-point programme (TPP), which was launched in 1975 by the Indian government. The programme aimed at installation of biogas plants in the rural areas at household level.

Although a dedicated executive agency, i.e., KVIC was appointed by the Planning Commission to improve biogas technology dissemination in rural areas, no specific

national level policy for promoting biogas in India was formulated until 1980. In the year 1981, the first national plan to improve the penetration of household level biogas plants in the rural areas was launched by the name—National Project on Biogas Development (NPBD). The NPBD programme helped in increasing the reactors at a much higher installation rate. This was a phase when India mainly focused on the Family Type Biogas Plants (FTBPs) and Community Based Biogas Plants. It involved a “multi-agency, multi-model” approach to promote the use of cooking stoves at the household level through these FTBPs. Along with KVIC, the Action for Food Production (AFPRO) and various other organisations also got involved to disseminate the biogas technology in the rural areas at a faster rate (Organization of the biogas sector 2021). KVIC mainly looked into the technical aspects of the programme, while AFPRO was given the responsibility to connect to ground-level NGOs that can help in capacity building of the local people for operating the digesters.

The second half of Fig. 3.7 gives an idea of the increase in the deployment rate of biogas digesters between 1980 and 2002. From nearly eighty thousand digesters by the end of 1980, the number grew to almost thirty lacs by the year 2000. These growth trends show the immense focus of the centre on the biogas sector at household level during 1980–2000.

By 2006, India was having around 38.37 lakh biogas plants, which further increased to 41.34 lakh plants by 2009, and to 45.45 lakh by the year 2012. These growth rates were relatively less as compared to the previous growth rates. If we look at the policies in past five years, the schemes are now trying to implement the advanced biogas technology at an industrial scale and also at the Community level after 2015. The government has brought in new schemes. For instance, the GOBAR-dhan scheme was rolled out in 2018 under the Swachh Bharat Mission- Gramin to promote cleanliness in rural areas. The idea was also to encourage entrepreneurship in villages through Community Based Biogas (CBG) plants. This mainly served the

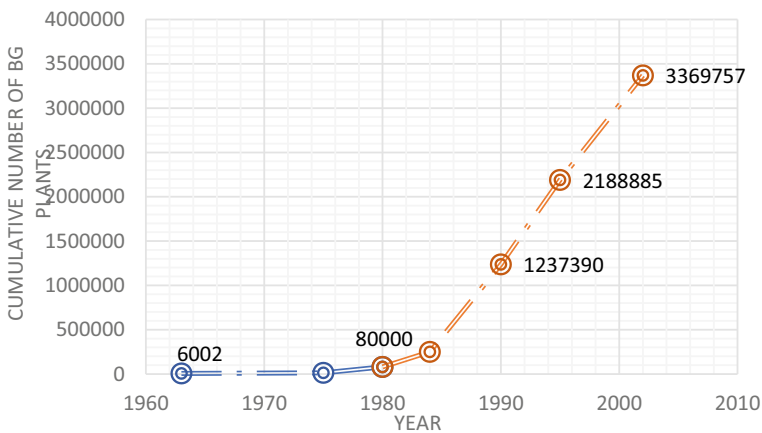


**Fig. 3.7** Number of installed biogas digesters in India between 1980 and 2002 (Kharbanda and Qureshi 1985; Lohan et al. 2015)

two prime purposes of the government—Promoting cleanliness in the rural areas and Promoting entrepreneurship. Cleanliness and Entrepreneurship have been the two primary motives of the current regime at the centre. The Sustainable Alternative towards Affordable Transportation (SATAT) scheme was also launched in October 2018, which directly involves the Oil Marketing Companies (OMCs) like the IOCL, BPCL, and HPCL to get involved in the process of production of Compressed Biogas (CBG). It also became the first biogas programme in the country to connect OMCs with the local entrepreneurs, Cooperative Societies etc. (Jayaswal 2020).

### **Reasons for the exponential growth of biogas digesters between 1980 and 2000 in India**

Through a critical comparison of the two biofuel sectors- bioethanol and biogas, it is evident that the focus of the policymakers was mainly on biogas between 1980 and 2000. On the one hand, there were no developments made in the bio-ethanol sector but on the other, the number of biogas digesters increased at a much faster rate all over the country (as shown in Figs. 3.6 and 3.7).

As already stated, the primary push in the sector came due to the Twenty-point programme which started in 1975. And this continued when the programme specifically included biogas in the year 1982. Also, the reason for this increase was because of the fact that the Planning Commission mainly focused on the already developed technologies across the nation which can help in energy security. The chapter on Energy of the sixth five-year plan stated explicitly that the need of mass-scale deployment of the technologies that already certain level of maturity across the nation (Planning Commission 1980). The document did not find any mention of the word bioethanol in the entire chapter on energy.

Unfortunately, these rising numbers just showed the growth in the number of installed digesters. An assessment report published by the Planning Commission (2002) suggested that although in terms of achieving the installation targets the programme was a great success, the plants under this scheme had much lower functionality rate. This indicated a flaw during the policy design of the programme. The programme never addressed the maintenance issue of these family biogas plants in a structured manner. No proper training was provided to the beneficiaries to look after the reactor independently, and they became non-functional after short usage.

#### **3.2.3.3 Policy Evolution in the Bioethanol Sector**

Bioethanol is a good source of alternate fuel which can be used with petrol to reduce pollution. Prior to the year 2000, the R&D in the bio-ethanol sector was slow, but after that, the government formed several policies. Although these policies helped in approaching the set targets, but unfortunately, due to various constraints, we have not been able to achieve most of the blending targets defined in these policies.

Due to the oil crisis of 1973, countries started to shift focus on energy security and become self-sufficient in their energy needs all over the world. It was during this time, when a minor focus on the biofuels took place in India. In India also, the first

test for mixing ethanol with petrol took place in the year 1975 (H. T. 2007). It is worth noting that Brazil, the largest producer of sugarcane, also started its National Alcohol Programme, “Proalcool” in the year 1975 and did exceptionally well in promoting the blending of ethanol to append petrol and diesel in their country (Stolf 2020). The country succeeded because of the strong legal provisions in biofuel sector.

The slight wave to start the ethanol blending program in India also came as a push from the Brazilian program but never got a major traction (Report of the Expert Committee on Auto Fuel Vision Policy 2025) in the initial years. Research and development in the bio-ethanol sector did not achieve the expected pace till the end of twentieth century. No major initiatives were taken between the twenty-year period from 1980 to 2000. Apart from the minor 1975 initiative to blend ethanol with gasoline, only one other instance can be traced. In 1980, the R&D section of Indian Oil Corporation Limited (IOCL) and the Indian Institute of Petroleum (IIP) conducted test on 13 passenger vehicles which also included the army vehicles (ENVIS centre-CPCB 2003). Although the test results favored ethanol blending, but these experiments did not come at a mass scale for vehicular use.

In the year 2001, India started to work on blending of ethanol with the gasoline at a larger scale. Three pilot projects were started in the states of Maharashtra and Uttar Pradesh. These pilot studies became successful, and also, the Research & Development in the area gave positive results. After discussions with expert committees, 5% ethanol blending in petrol was recommended for the first phase. Replicating the results of successful pilot study from two states, the Planning Commission decided to launch the Ethanol Blending Programme (EBP) in 2002 for nine states and three Union Territories. Blending of 5% ethanol in petrol was mandated for these states. But the policy didn't work well. Out of the total requirement of 363 million litres, only 196 L of ethanol were made available to the Oil Marketing Companies during 2003–04 (Ram Mohan et al. 2006). The issue of high procurement cost as compared to petrol also became one of the prominent reasons for the failure of the blending programme.

The National Biofuel Policy of 2008 had set an ambitious target of blending 20% bioethanol by 2017. Unfortunately, we were far behind the 2017 target, even till 2020. Figure 3.8 shows the percentage blending achieved in the respective years from 2010 till 2020 in India.

### **Major hurdles for bioethanol policies in India**

India had set a target of 5% ethanol blending through the Ethanol Blending Petrol Programme (EBPP) of 2002. However, the policy fell much behind in making ethanol available to the OMCs. The situation prevailed with the 2017 targets as well and only 1.9% of ethanol blending was done, contrary to the 20% blending expectations. The major issue faced during the production and procurement of molasses was due to the unavailability of sugarcane. Sugarcane is cyclic in its production, and most of the time, the policies failed due to a mismatch in demand and supply in the bioethanol sector. It shall be noted that the out of the total sugarcane produced, nearly 75% is used for production of sugar and the rest 25% is used for making jaggery and other

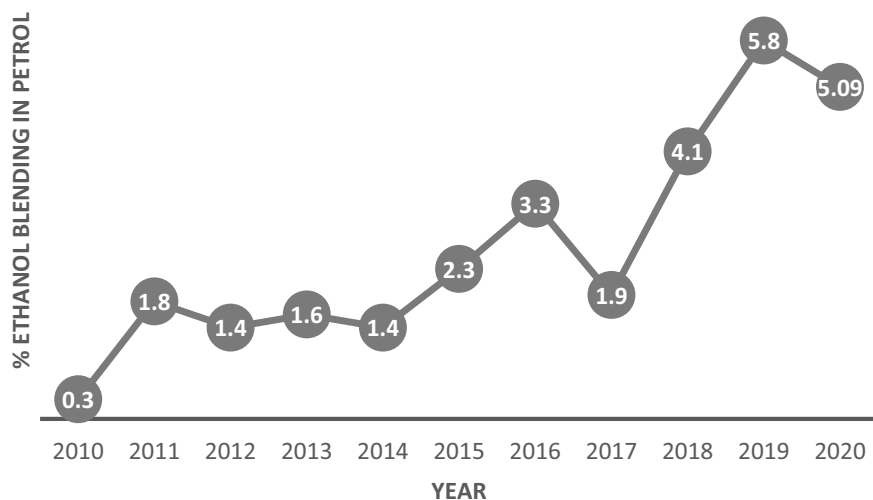


**Fig. 3.8** Ethanol blending percentage between 2010 and 2020 (Online 2019; Bhosale 2020)

**Table 3.4** Ethanol usage in different sectors (Kataki et al. 2017)

Sector	Percentages
Industrial use	~25
Drinking purposes	~35
Other usage	~5
Fuel	~35

products. Further, if we look at the bifurcation of the alcohol being produced, it is majorly divided in sections, as described in Table 3.4.

Hence, due to multi-sectoral usage of the alcohol being produced from sugarcane, the supply side got further constrained to meet the expected demands in previous bioethanol policies in the country. The other reason for improper working of these policies is related to the pricing mechanism, which again was dependent on cyclic nature of sugarcane (The Ethanol Blending Policy in India 2012). A SWOT analysis done by Dey et al. (2021) indicates three other issues that have been there with the Indian biofuel policies-

- Lack of proper infrastructure
- Issues in retrieval of agricultural residues
- Increasing ethanol deficit in the country (i.e., import increasing and export decreasing).

Also, one of the highly contested topics that comes inherently with the formation of any bioethanol-based policy is related to the ‘food versus fuel’ debate. Table 3.5 gives an overview of the primary feedstock used for bioethanol production across the world.



**Table 3.5** Primary feedstock used for ethanol production in different countries (Dey et al. 2021)

Country	Feedstock used for ethanol production
USA	Corn
Brazil	Sugarcane
China	Wheat and corn
Canada	Wheat
Thailand	Cassava and sugarcane
Argentina	Corn and sugarcane

In India, the main source of production of commercial scale bioethanol is molasses which comes from the sugarcane. This in turn gets dependent on the production of sugarcane and land usage in the country. Although the degree of contest between the land being diverted for biofuel production and rise in the food prices is complex, research suggests that whenever we produce biofuel from agricultural land, food price rises (Tomei and Helliwell 2016). Hence, it becomes imperative that the biofuel industry looks for sustainable alternates which can help in meeting the demand of ethanol blending.

Being an agriculture-based country, India has a huge availability of the alternate feed-stock option for the production of bioethanol. It has a huge potential, and can tap the advanced generation of the biofuels, that majorly consists of the lignocellulosic biomass. This mainly includes the lignocellulosic alternates like rice straw, wheat straw, legume stover, sugarcane tops, etc. The option will also help us in tackling the ‘food versus fuel’ debate, as these feedstocks are non-edible and come under the second-generation of biofuels. Along with the stated alternates, few other options are also available which can be used to meet the demand side of alternate feed. They are available in the North-Eastern and Himalyan region of India and can be used for bioethanol production. They include- Bamboo processing waste, Sweet sorghum, and pine (Singh et al. 2017).

However, as we advance to the future generation biofuel feedstocks, it is important to ensure robust technologies that can help in conversion of these feedstocks to bioethanol. The current government has planned out to setup 2G biorefineries that can help in achieving India’s ethanol blending targets (MoPNG 2019). Under the Pradhan Mantri Ji-Van Yojana, 12 commercial scale second generation bioethanol plants are proposed to be setup across India. This will potentially help in meeting the ethanol demand in the country and meet our long-term targets.

### 3.2.3.4 Policy Evolution in the Biodiesel Sector

In India, national-level policies to mix biodiesel with diesel came up around and after the year 2000. In the year 2002, a committee was formed by the central government to evaluate the state of biofuels in India. The final report (Planning Commission 2003) produced by the committee gave its recommendations on the state of bioethanol and biodiesel in India. For the biodiesel sector, various recommendations were made.

Main options related to the production of biodiesel were discussed extensively in the report. Tree-based oilseeds (TBOs) which includes plant species like *Jatropha Curcas* (Ratanjyot), *Pongamia Pinnata* (Karanj), *Calophyllum inophyllum* (Nagchampa), *Hevca brasiliensis* (Rubber) etc. were suggested to be the main source of biodiesel production in India. Out of all these species, *Jatropha Curcas* came up as the most important source for biodiesel production. The committee report stated a target of 5% blending by the end of 2006–07, which was supposed to be increased to 20% blending by the end of 2011–12.

Unfortunately, we were never able to reach even near to these targets set during the commencement of these schemes. By the end of 2010, the biodiesel blending rates were merely 0.09% (Abdi and ET EnergyWorld 2019). A comprehensive study conducted by the German Development Institute in 2008 also suggested that the purchase policies of the biodiesel program were economically infeasible. Although the yield of mature *Jatropha* was expected to be 3.5t/ha but that required severe inputs and intense care at the farmer's end. By applying those commensurate efforts, the farmers got a better opportunity cost in planting other seasonal food crops which gave much better returns (German Development Institute 2008). This resisted them from planting *Jatropha* in their fields.

This programme was promulgated with the National Biofuel Policies 2009, setting new targets for the year 2017. The National Biofuel Policy 2009 had set a target of achieving 20% blending of biodiesel with the diesel. India achieved only 0.13% of biodiesel blending by the end of 2017 (Abdi and EnergyWorld 2019). However, the new National Biofuel Policy 2018 sets a more realistic target of achieving a blending rate of 5% blending of the biodiesel with the conventional diesel by the end of 2030.

### Issues in implementing the biodiesel policies

Similar to the bioethanol programme, the policies for biodiesel also didn't work as per the expectations. There was a huge gap in the proposed policy and the actual on-ground outcomes after its implementation. Following points enlist few of the issues in biodiesel sector in India-

- Main issue was with the availability of *Jatropha* as a feed material for the biodiesel production. *Jatropha* has a gestation period of 3–5 years, making the simple payback period longer for the farmers. This made them to move away from the plantation of *Jatropha* in their fields, and hence prevented the large-scale production of *Jatropha* as per the national needs (Lahiry 2018).
- Research finds that *Jatropha Curcas* leaves are toxic in nature. And with a focus on plantation of *Jatropha curcas* in the common wastelands in India, there were chances that children may come in contact with the plant. There were number of cases reported in various parts of India (Gupta et al. 2016; Shah and Sanmukhani 2010), which left the farmers further skeptical regarding the plantation of *Jatropha* in the common places.

Along with this, some studies have even questioned the most basic assumption of the biodiesel policies in India, which is regarding availability of ample 'wasteland' for the purpose of feedstock production of these biofuels. A study conducted by

Baka (2014) stated that plantation of biodiesel on these lands can severely affect the agrarian livelihood, as the farmers already develop an energy economy around these lands. Although it is a fact that *Jatropha* plants grow well even in low water conditions and less fertile land, but the issue with the wastelands is that the farmers are using them as pastureland. Mostly it is being utilized by the animals like cow and buffalo for the feeding purpose in the rural areas. This has caused a conflict of interest among the farmers and the state governments (Ghosh and Roy 2018), leading to lower production of biodiesel.

### 3.3 Discussions

There are various biofuel options present that can help in serving the energy demand of India's transportation sector. It mainly includes- Bioethanol, Compressed Biogas (CBG), and Biodiesel. The number of vehicles for transportation has been continuously increasing in India. By 2030, it is expected that Indian roads will be having around 260 million vehicles, that need petrol as its fuel (Nouni et al. 2021). This shows huge opportunity for the ethanol industry (Singh et al. 2018), if it fixes its supply side issues mainly. Reaching the 20% ethanol blending rates with petrol will also decrease pollution levels significantly and increase the energy security in India. However, it shall be noted that there is no specific law or mandate that defines mixing targets for biofuels in the Indian transportation sector. At present, only around 1.2% biofuels are being used in the sector (Ebadian et al. 2020). This can cause deviations from achieving the emission reduction goals as well if we do not approach the mixing targets in a systematic manner in transport sector.

In the past few years, the ethanol blending rates are rising for India. This has been made possible because of the use of cereals along with sugarcane for bioethanol production. For the year 2019–20, cereals contributed to around 37.7% share in ethanol production, which is expected to grow to 50% in 2025–26 (Nouni et al. 2021). Although the increasing percentage of ethanol blending is a good sign, the policy makers have to be very cautious of the fact that this increase is based on a first-generation feedstock, i.e., cereals. This can potentially raise the conflict of 'food versus fuel' in the long term. However, the process also shows that opting for a multiple source feed input is going to be the key factor in achieving India's ethanol blending needs in the transportation sector.

For Compressed Biogas (CBG) systems to be efficiently employed in the transport sector, there are three basic requirements—availability of biogas energy, robust gas grid across the nation, and gas filling stations to fulfil the fuel needs of vehicles running on gas. In India, availability of energy through biogas is in abundance, which mainly comprises of the municipal solid waste and animal residues (IRENA 2017). As shown in Fig. 3.9, Indian biogas energy potential through MSW and animal by-products is around 125 PJ/year and 19.6 PJ/year respectively.

However, other factors required for scaling up of CBG have not worked well in the past. There is a huge investment cost that goes into setting up of the CBG plants

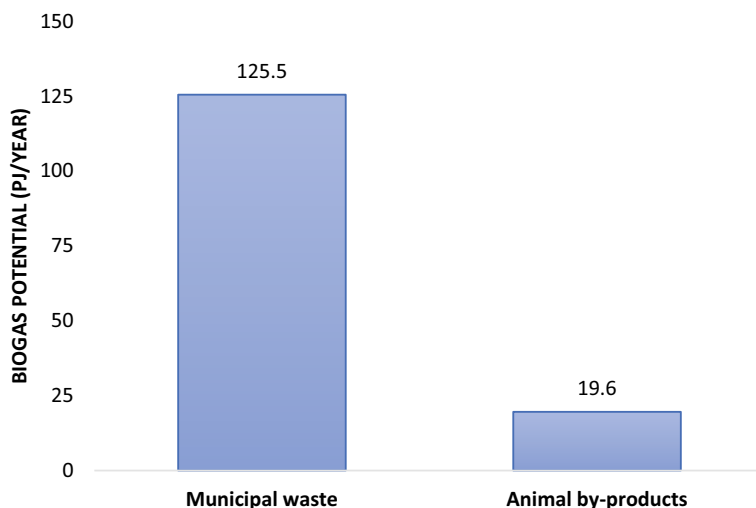


**Fig. 3.9** Indian biogas potential through MSW and animal by-products (in PJ) (IRENA 2017)

to pressurize and purify the raw biogas. It requires industry support for technology, and policy support for sustainability of these projects. Recently, the Sustainable Alternative Towards Affordable Transportation (SATAT) was launched by MoPNG to improve the production of CBG on a commercial scale in India. The scheme aims at setting up 1000 by 2022 and eventually 5000 CBG plants by 2025 across India. But reports suggest that the rate of installation has been very poor. Only seven plants have laid their foundation stone, out of which only two are working (India falls behind on biogas production plans 2021).

The other issue over which India is lagging is regarding average performance of nation-wide gas grid system. The ‘Vision 2030- Natural Gas infrastructure in India’ document, published by Petroleum and Natural Gas Regulatory board, also indicated that the country has an under-developed gas pipeline infrastructure (PNGRB 2013). There are technical issues related to use of CBG in vehicles as well, that stop the customer from opting to gas-based vehicles. For instance, the gas cylinders used to store the CBG inside the vehicles takes much space which puts technical limitation in driving these vehicles to longer distances. Hence, implementation of CBG on ground is still a mammoth task for the Indian policy makers to achieve, and concentrated efforts are needed to get to the national targets.

### ***3.3.1 Major Issues with the Previous Biofuel Policies in India***

Along with these above discussed issues related to the supply constraints, demand issues, feedstock quality, fuel pricing mechanism, technical issues etc., policies

formed in the past were also having various key design issues that need to be addressed. Following section elaborates on the major issues related in the Indian biofuel policy making-

### **3.3.1.1 Picking up Late in the Bioethanol Policy Formation**

During the initial phase of development, India mainly focused on its biogas program till the year 2000 after independence. After the oil-shocks of 1973 and 1979, various countries like Brazil, USA etc., started to take profound actions to enhance their biofuel technology. They started their large-scale biofuel programs and research to explore the feasibility of ethanol blending with diesel, and even succeeded in the process. For instance, the Proalcool program launched by Brazil in the year 1975 aimed at improving the state of ethanol production and blending all over the country. As a result, an exponential growth was observed, and the production capacity of 0.6 billion litres in 1975–76 increased to 12.3 billion litres in 1986–87 (Stolf 2020). By the end of 1980, the production of light vehicles that ran on ethanol reached 95% of all fleet produced in Brazil (Lopes et al. 2016).

However, the same was not true with India. The initial policies did not focus on the ethanol-based fuel development programmes in the initial days and mainly emphasized on our biogas program and its deployment in the rural areas. Our first large-scale blending program started around the year 2002. This clearly points out the need to speed up the research and development in bioethanol sector, that can help in filling earlier gap.

### **3.3.1.2 Disconnect Between the Policy Design and Ground Reality**

During our study, it was found that during the formation of initial programmes, there was a constant disconnect between the designed policies and the actual conditions on ground. This also showed the top-down approach of the policy makers where minor consultations were done with the major stakeholders like researchers, farmers etc., while designing the biofuel policies. This constant disconnect between the ground realities and designed policies never allowed to achieve the expected traction which were defined as the policy objectives.

Following instances can be cited to further augment the above argument of top-down approach opted by the policy makers.

- a. The report published by the commission on development of biodiesel in India (Planning Commission 2003) assumed that the *Jatropha* seeds proposed to be used for biodiesel production had production range between 0.4 and 1.2 tons/ha. However, this assumption was far from actual production rates, which were near to lower bound of the assumed limit, i.e., 0.4 tons/ha (German Development Institute 2008). As a result, the demand and supply synergy required to achieve 5% blending targets by the end of 2006–07 were also missed by a larger margin.

- b. Similarly, during the Ethanol Blending Program (2007) also, the Oil Manufacturing Companies (OMCs) contracted for 1.4 billion litres of ethanol between Nov 2006 and Nov 2009 but only 540 million liters were supplied till April 2009 due to lack of molasses. This pointed out the mismatch between the policy mandate and the actual procurement conditions on ground (Saravanan et al. 2018). However, despite the fact that the targets set in the EBP of 2007 were not met, the policy makers went ahead to set the targets to 10% in the revised policy mandate of October 2008, which unfortunately were again not achieved due to the unrealistic approach (Bandyopadhyay and Das 2014). It was in the year 2019, when we actually reached to 5% average blending rates across in the country.

### 3.3.1.3 Lack of Coordination Due to Complex Institutional Structure

The biofuel subsystem involves various policy areas such as renewable energy, rural development, fuel pricing, research and development, etc. This in turn engages range of complex actors who get involved in the policy-making process. Figure 3.10 gives an overview of various stakeholders involved in the policymaking process of biofuels in India.

The involvement of a range of actors has often brought inherent inefficiencies in policy formulation as well as implementation process. In our context, the Indian state

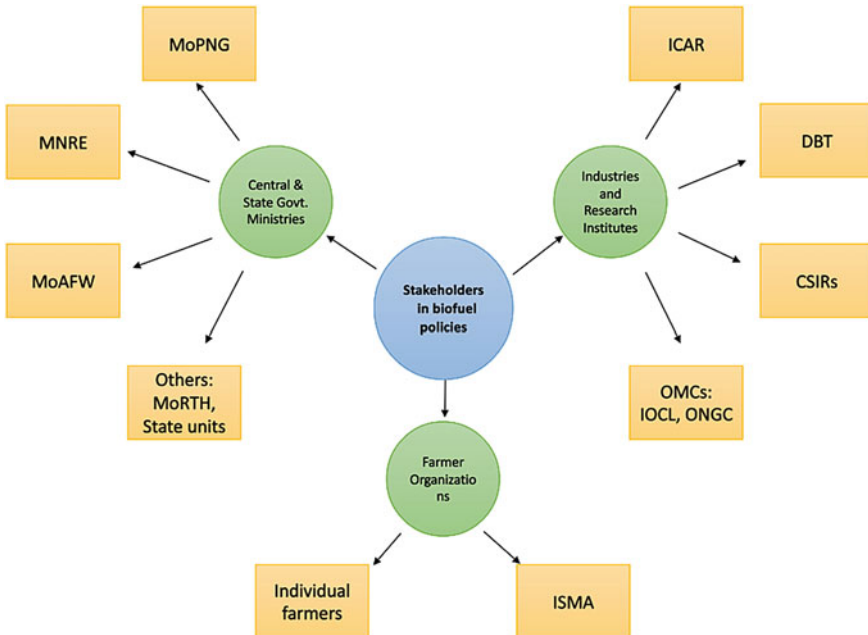


Fig. 3.10 An overview of various actors involved in the biofuel policymaking

follows a federal structure, where the central government and the state governments work in a compounded mode. Many times, the policies formed by the centre either clashes with the policies or interests of the state governments. This situation has also caused a significant impediment to the smoother functioning of biofuel policies in India. There are various examples where states put restrictions on free inter-state movement of raw materials like non-potable alcohol and molasses, leading to an increase in prices and restricting the free trade of these sources for blending (Das 2020).

### 3.3.2 *Changing Dimensions for Biofuel Policies in India*

Though there have been issues in designing previous biofuel policies, the space for biofuels has constantly been evolving over time. For instance, India is now shifting its focus on the industry scale digesters from a point in the 1980s, where we were only focusing on the household level biogas digesters. Energy access in rural areas has also been changing constantly in India. In 1993, the electricity access which was near about 40% of the rural population, has now increased to 96.67% in the year 2019 (Access to electricity, rural (% of rural population)—IndiaData 2021). Hence, compared to the earlier plans, where biogas plants were mainly used to provide clean fuel or electricity, a significant focus is now given to using this resource as a transportation fuel.

The data in seventeenth standing committee report (as shown in Fig. 3.11) on energy also depicts a decreasing trend in the number of reactors being installed under the New National Biogas and Organic Manure Programme (NNBOMP) all over the country. This constant decrease in the installation has also been due to the Ujjwala scheme launched by the Government of India, which has provided a greater penetration of cleaner cooking fuel options to the masses.

Therefore, on the one hand, there has been a decrease in the number of small plants being installed per year, while on the other, our biogas policies are now shifting to support the installation of large-scale Compressed Biogas (CBG) plants through schemes like Sustainable Alternative Towards Affordable Transportation (SATAT).

Similarly, in the biodiesel and bioethanol sector also, the focus is shifting towards future generation biofuels. For instance, keeping in mind the shortcomings of *Jatropha* cultivation, which was defined as the primary feedstock for biodiesel production in India, researchers are now shifting their focus to other feasible options like *Pongamia Pinnata* (Karanja), waste cooking oil, microalgae, etc. (Sharma and Singh 2017). The NBP of 2018 also mentions sources like—animal tallow, acid oil, used cooking oil, etc., for biodiesel production. The policy focuses on developing advanced biofuels and the drop-in-fuels, which can address the issue of ‘food versus fuel’ in an efficient manner, as these advanced biofuels are obtained from non-edible crops, agriculture residues, etc. Along with this, it opts for a more structured approach to address the issue of feed-stock management by proposing a ‘National Biomass Repository’.

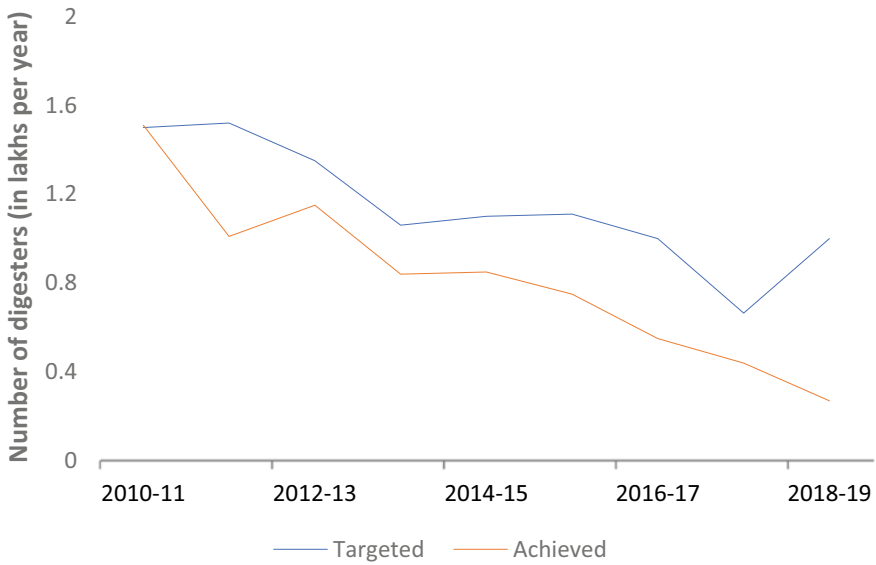


**Fig. 3.11** Trend of household digesters being installed after 2010 (MNRE 2021b)

### 3.3.3 Future Challenges for Advanced Biofuels

In biofuel domain, ethanol is considered as one of the best blending options with petrol due to its high-octane number. There are well established evidences which prove that blending of ethanol with petrol leads to reduction in air-pollution levels. However, due to huge dependence of almost all the major biofuel producing countries on first generation feedstocks, there is a constant mismatch between the demand and supply side for transport sector. In the current scenario, the focus is now shifting on advanced generations of biofuels. This mainly includes the lignocellulosic feedstocks present in the form of agricultural waste, municipal organic waste, forest wood residues, etc. However, there are many challenges related to the processing and commercialization of advanced biofuels which can hinder their full-fledged application in automotive sector. A review work done by Cheng and Timilsina (2011) specifically points out these overarching issues:

- The pre-treatment required to break the lignin, cellulose and hemicellulose layer over these feedstocks, makes it an energy intensive process. Hence, the cost of ethanol production after pre-treatment increases significantly.

As shown in Fig. 3.12 the cost of production of bioethanol from first-generation feedstock is around 0.44 USD/litre, which increases to around 1 USD/litre for the lignocellulosic feed, which are advanced generation feedstocks.



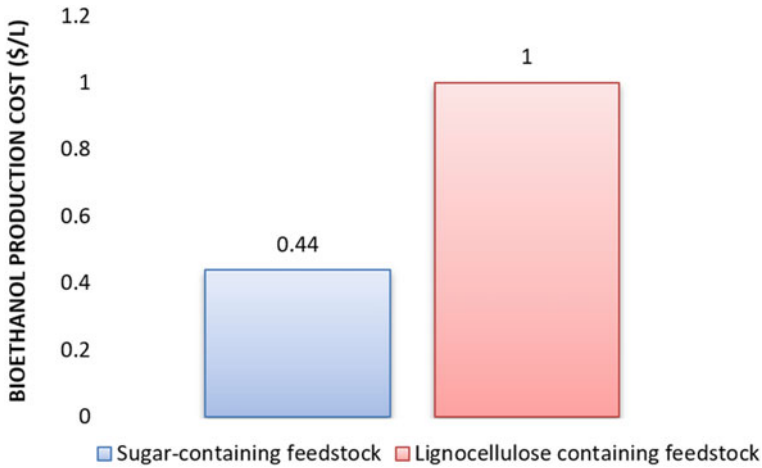


**Fig. 3.12** Cost of bioethanol production from different routes (Bušić et al. 2018)

- Most of the lignocellulosic materials have a lower bulk density. Due to this, it becomes very difficult to move larger quantities of lignocellulosic materials from one place to the other for processing purpose.
- The other important issue is related to the efficiency of processing the lignocellulosic materials. Generally, with the first-generation feedstocks the conversion efficiency is very high but when it comes to the 2G feedstocks, it reduces significantly and ranges between 30 and 60%.

Further, if we look at the major challenges for biodiesel to be utilized as a fuel in automobiles, again the cost of conversion of 2G feedstocks to biodiesel is quite high.

Figure 3.13 shows different costs for biodiesel production from various first-generation feedstocks which includes—soyabean, rapeseed, sunflower, palm, and castor. The cost of production for these feedstocks ranges between 0.53 and 1.24 USD/litre (average of the cost was taken in case range was provided for a particular feedstock). However, the cost of biodiesel production from microalgae is around 7.26 USD/litre, which makes the production of this advanced biofuel as a cost intensive one. Hence, a proper research and development is required in the biofuel domain, that can help in reducing the conversion cost of the feedstocks.

### 3.4 Conclusion

In India there is a huge food demand to serve the needs of its larger population. Depending only on the first-generation feedstock is not a sustainable option. It becomes essential that we extensively research on future generation biofuels and deploy these technologies at the national level. Biofuels can be a potential solution

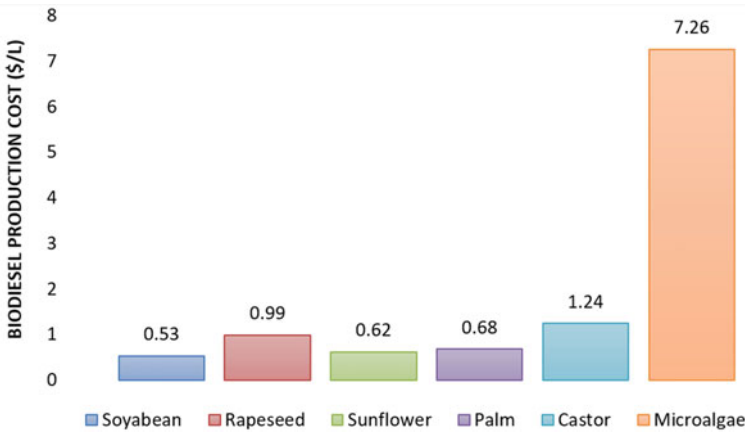


**Fig. 3.13** Cost of biodiesel production from different routes (Kumar et al. 2019)

to major problems like agriculture crop residue burning, organic waste management, increasing air pollution, etc. They can help in replacing traditional fuels used for transportation across the country. Opting for a multiple feedstock path for the production of biofuels can be a feasible option. This can help in improving the quality of future generation feedstocks and reduce their costs.

In the current scenario, when India is at the brink of transformation to renewable domain, it becomes very crucial to analyze the flaws made in the earlier policies in alternate fuel sector. In previous biofuel policies, many of our efforts were not planned, which became a cause of severe impediment in achieving the intended targets. The chapter traces the biofuel policies in India after its independence and attempts at addressing a few of these issues. Being one of the most dynamic sectors which is affected by various factors like—oil prices in the international market, involvement of multiple stakeholders, production and cyclicity of crops, etc., the policy formation process becomes even more difficult. However, the learnings from various policy design and implementation issues like—inefficient top-down approach in initial national level policies, lack of coordination with successful market players, etc., can be emphasized and rectified in the future policies to tap the potential of biofuels in India fully. An industry-level engagement is also required, which can support both research and development and help in scaling up the process at the national level to achieve our renewable targets of 2030.

## References

- Abdi B, ET EnergyWorld (2019) India's bio-diesel blending for road transport to remain muted in 2019: US department of agriculture. ETEnergyworld.Com. <https://energy.economictimes.indiatimes.com/news/oil-and-gas/indias-bio-diesel-blending-for-road-transport-to-remain-muted-in-2019-us-dept-of-agriculture/70868387>
- Access to electricity, rural (% of rural population)—IndiaData (n.d.) The World Bank. Retrieved July 16, 2021, from <https://data.worldbank.org/indicator/EG.ELC.ACCS.RU.ZS?end=2019&locations=IN&start=1993>
- Baka J (2014) What wastelands? A critique of biofuel policy discourse in South India. *Geoforum* 54:315–323. <https://doi.org/10.1016/j.geoforum.2013.08.007>
- Baka J, Bailis R (2014) Wasteland energy-escapes: A comparative energy flow analysis of India's biofuel and biomass economies. *Ecol Econ* 108:8–17. <https://doi.org/10.1016/j.ecolecon.2014.09.022>
- Bandyopadhyay K, Das K (2014) Biofuels in South Asia: connecting the dots. *Renew Energy Law Policy Rev* 5(2):150–166. Retrieved on 16 July 2021, from <http://www.jstor.org/stable/24324755>
- Bhosale J (2020) India achieved 5.09% ethanol blending from December 1 to June 22: ISMA. *The economic times*. <https://economictimes.indiatimes.com/industry/energy/oil-gas/india-achieves-5-09-ethanol-blending-from-december-1-to-june-22-says-isma/articleshow/76689086.cms?from=mdr>
- BP Energy Outlook (2014) BP energy outlook 2035. BP. <https://www.bp.com/content/dam/bp/business-sites/en/global/corporate/pdfs/energy-economics/energy-outlook/bp-energy-outlook-2014.pdf>
- Bušić A, Mardetko N, Kundas S, Morzak G, Belskaya H, Ivančić ŠAntek M, Komes D, Novak S, ŠAntek B (2018) Bioethanol production from renewable raw materials and its separation and purification: a review. *Food Technol Biotechnol* 56(3). <https://doi.org/10.17113/ftb.56.03.18.5546>
- Chandel AK, Bhatia L, Garlapati VK, Roy L, Arora A (2017) Biofuel policy in Indian perspective: socioeconomic indicators and sustainable rural development. *Sustain Biofuels Dev India*, 459–488. [https://doi.org/10.1007/978-3-319-50219-9\\_19](https://doi.org/10.1007/978-3-319-50219-9_19)
- Cheng JJ, Timilsina GR (2011) Status and barriers of advanced biofuel technologies: a review. *Renew Energy* 36(12):3541–3549. <https://doi.org/10.1016/j.renene.2011.04.031>
- China: Biofuels Annual (2020) USDA foreign agricultural service. <https://www.fas.usda.gov/data/china-biofuels-annual-6>
- Contributors ET (2021) India on track to meet 175 GW renewable energy targets by 2022: ETILC members. *The economic times*. <https://economictimes.indiatimes.com/industry/energy/power/india-on-track-to-meet-175-gw-renewable-energy-targets-by-2022-etilc-members/articleshow/80976846.cms?from=mdr>
- Countries by GDP Sector Composition 2017—StatisticsTimes.com. (2018) *Statistics times*. <https://statisticstimes.com/economy/countries-by-gdp-sector-composition.php>
- CSTEP, College of Legal Studies, & PLR Chambers (2019) Fuel blending in India: learnings and way forward. [https://cstep.in/drupal/sites/default/files/2019-02/Expert\\_Paper\\_on\\_Fuel\\_Blending\\_in\\_India\\_-\\_Final.pdf](https://cstep.in/drupal/sites/default/files/2019-02/Expert_Paper_on_Fuel_Blending_in_India_-_Final.pdf)
- Das S (2020) The national policy of biofuels of India—a perspective. *Energy Policy* 143:111595. <https://doi.org/10.1016/j.enpol.2020.111595>
- Deloitte (2018) The evolving energy landscape in India. <https://www2.deloitte.com/content/dam/Deloitte/in/Documents/energy-resources/in-enr-the-evolving-energy-landscape-india-april-2018-noexp.pdf>
- Dey B, Roy B, Datta S, Singh KG (2021) Comprehensive overview and proposal of strategies for the ethanol sector in India. *Biomass Conver Biorefinery*. Published <https://doi.org/10.1007/s13399-021-01546-2>

- Ebadian M, van Dyk S, McMillan JD, Saddler J (2020) Biofuels policies that have encouraged their production and use: an international perspective. *Energy Policy* 147:111906. <https://doi.org/10.1016/j.enpol.2020.111906>
- ENVIS centre-CPCB (2003) Alternative transport fuels: an overview. Central Pollution Control Board (CPCB). [https://www.cpcbenvnis.nic.in/cpcb\\_newsletter/Alternative%20Transport%20Fuels%20An%20Overview.pdf](https://www.cpcbenvnis.nic.in/cpcb_newsletter/Alternative%20Transport%20Fuels%20An%20Overview.pdf)
- Evolution of solar PV module cost by data source, 1970–2020—Charts—Data & Statistics (2020) IEA. <https://www.iea.org/data-and-statistics/charts/evolution-of-solar-pv-module-cost-by-data-source-1970-2020>
- German Development Institute (2008) Biodiesel policies for rural development in India. [http://www.compete-bioafrica.net/publications/publ/Endreport\\_final\\_India2008.pdf](http://www.compete-bioafrica.net/publications/publ/Endreport_final_India2008.pdf)
- Ghosh D, Roy J (2018) National mission on biodiesel in India (2003): an assessment based on strategic niche management. *Sustain Energy Technol Policies*, 229–255. [https://doi.org/10.1007/978-981-10-8393-8\\_10](https://doi.org/10.1007/978-981-10-8393-8_10)
- Gupta A, Kumar A, Agarwal A, Osawa M, Verma A (2016) Acute accidental mass poisoning by *Jatropha curcas* in Agra, North India. *Egypt J Forensic Sci* 6(4):496–500. <https://doi.org/10.1016/j.ejfs.2016.04.002>
- H. T. (2007) Evolution of Indian biofuels. *Hindustan times*. <https://www.hindustantimes.com/business/evolution-of-indian-biofuels/story-WAq1BJGVzMJq8lpaXPXJh.html>
- Hiloidhari M, Das D, Baruah D (2014) Bioenergy potential from crop residue biomass in India. *Renew Sustain Energy Rev* 32:504–512. <https://doi.org/10.1016/j.rser.2014.01.025>
- Holodny E (2016) TIMELINE: the tumultuous 155-year history of oil prices. *Business Insider*. <https://www.businessinsider.in/timeline-the-tumultuous-155-year-history-of-oil-prices/articleshow/56088176.cms>
- India falls behind on biogas production plans (2021) Argus Media. <https://www.argusmedia.com/en/news/2220706-india-falls-behind-on-biogas-production-plans>
- International—U.S. Energy Information Administration (EIA) (2020) Eia.Gov. <https://www.eia.gov/international/analysis/country/IND>
- International Energy Agency. (2020) India 2020—energy policy review. NITI Aayog. [https://niti.gov.in/sites/default/files/2020-01/IEA-India%202020-In-depth-EnergyPolicy\\_0.pdf](https://niti.gov.in/sites/default/files/2020-01/IEA-India%202020-In-depth-EnergyPolicy_0.pdf)
- IRENA (2017) Biogas for road vehicles—technology brief. [https://www.irena.org/-/media/files/irena/agency/publication/2017/mar/irena\\_biogas\\_for\\_road\\_vehicles\\_2017.pdf](https://www.irena.org/-/media/files/irena/agency/publication/2017/mar/irena_biogas_for_road_vehicles_2017.pdf)
- Jayaswal R (2020) UP leads in setting up compressed biogas plants, followed by Maharashtra and Haryana. *Hindustan Times*. <https://www.hindustantimes.com/india-news/up-leads-in-setting-up-compressed-bio-gas-plants-followed-by-maharashtra-and-haryana/story-k9ykwFZn7iBFKuM5BehwJM.html>
- Kataki R, Bordoloi N, Saikia R, Sut D, Narzari R, Gogoi L, Chutia RS (2017) An assessment on Indian government initiatives and policies for the promotion of biofuels implementation, and commercialization through private investments. *Sustain Biofuels Dev India*, 489–515. [https://doi.org/10.1007/978-3-319-50219-9\\_20](https://doi.org/10.1007/978-3-319-50219-9_20)
- Kharbanda VP, Qureshi MA (1985) Biogas development in India and the PRC. *Energy J* 6(3). <https://doi.org/10.5547/issn0195-6574-ej-vol6-no3-4>
- Kumar S, Chaube A, Jain SK (2012) Critical review of jatropha biodiesel promotion policies in India. *Energy Policy* 41:775–781. <https://doi.org/10.1016/j.enpol.2011.11.044>
- Kumar A, Kumar N, Baredar P, Shukla A (2015) A review on biomass energy resources, potential, conversion and policy in India. *Renew Sustain Energy Rev* 45:530–539. <https://doi.org/10.1016/j.rser.2015.02.007>
- Kumar Biswas P, Pohit S (2013) What ails India's biodiesel programme? *Energy Policy* 52:789–796. <https://doi.org/10.1016/j.enpol.2012.10.043>
- Kumar N, Sonthalia A, Pali HS, Sidharth (2019) Next-generation biofuels—opportunities and challenges. *Innov Sustain Energy Cleaner Environ*, 171–191. [https://doi.org/10.1007/978-981-13-9012-8\\_8](https://doi.org/10.1007/978-981-13-9012-8_8)

- Lahiry S (2018) Biodiesel in India: the Jatropha fiasco. Down to earth. <https://www.downtoearth.org.in/blog/energy/biodiesel-in-india-the-jatropha-fiasco-61321>
- Lohan SK, Dixit J, Kumar R, Pandey Y, Khan J, Ishaq M, Modasir S, Kumar D (2015) Biogas: a boon for sustainable energy development in India's cold climate. *Renew Sustain Energy Rev* 43:95–101. <https://doi.org/10.1016/j.rser.2014.11.028>
- Lopes ML, Paulillo SCDL, Godoy A, Cherubin RA, Lorenzi MS, Giometti FHC, Bernardino CD, Amorim Neto HBD, Amorim HVD (2016) Ethanol production in Brazil: a bridge between science and industry. *Braz J Microbiol* 47:64–76. <https://doi.org/10.1016/j.bjm.2016.10.003>
- Ministry of Statistics and Programme Implementation (MoSPI) (2021) Energy statistics India 2021. [https://www.mospi.nic.in/sites/default/files/reports\\_and\\_publication/ES/Energy%20Statistics%20India%202021.pdf](https://www.mospi.nic.in/sites/default/files/reports_and_publication/ES/Energy%20Statistics%20India%202021.pdf)
- Mittal S, Ahlgren EO, Shukla P (2018) Barriers to biogas dissemination in India: a review. *Energy Policy* 112:361–370. <https://doi.org/10.1016/j.enpol.2017.10.027>
- MNRE (2021a) Annual report 2020–21. [https://mnre.gov.in/img/documents/uploads/file\\_f-1618564141288.pdf](https://mnre.gov.in/img/documents/uploads/file_f-1618564141288.pdf)
- MNRE (2021b) Action plan for achievement of 175 gigawatt (GW) renewable energy target (No. 17). Lok Sabha Secretariat. [https://164.100.47.193/lssccommittee/Energy/17\\_Energy\\_17.pdf](https://164.100.47.193/lssccommittee/Energy/17_Energy_17.pdf)
- MoPNG (2019) Pradhan Mantri ji-van Yojana. MoPNG, GoI. [https://mopng.gov.in/files/uploads/PM\\_JI-VAN\\_YOJANA.pdf](https://mopng.gov.in/files/uploads/PM_JI-VAN_YOJANA.pdf)
- News Express (2020) Oil trade comes to a halt, but India's import bill gets cheaper. The new India express. <https://www.newindianexpress.com/business/2020/may/03/oil-trade-comes-to-a-halt-but-indias-import-bill-gets-cheaper-2138400.html>
- Nouni M, Jha P, Sarkhel R, Banerjee C, Tripathi AK, Manna J (2021) Alternative fuels for decarbonisation of road transport sector in India: options, present status, opportunities, and challenges. *Fuel* 305, 121583. <https://doi.org/10.1016/j.fuel.2021.121583>
- Online FE (2019) Renewable energy: Brazil to assist in India's alternative fuel ethanol programme. The financial express. <https://www.financialexpress.com/economy/renewable-energy-brazil-to-assist-in-indias-alternative-fuel-ethanol-programme/1807799/>
- Online FE (2021) Massive green push: reliance industries to invest Rs 75,000 crore in 3 years. The financial express. <https://www.financialexpress.com/industry/massive-green-push-reliance-industries-to-invest-rs-75000-crore-in-3-years/2278016/>
- Organization of the biogas sector (n.d.) FAO. Retrieved on 16 July 2021, from <http://www.fao.org/3/T0541E/T0541E0k.htm>
- Planning Commission (2002) Evaluation study of the national project on biogas development. <https://niti.gov.in/planningcommission.gov.in/docs/reports/peoreport/cmpdmpeo/volume1/185.pdf>
- Planning Commission (2003) Report of the committee on development of biofuel. [https://niti.gov.in/planningcommission.gov.in/docs/reports/genrep/cmtt\\_bio.pdf](https://niti.gov.in/planningcommission.gov.in/docs/reports/genrep/cmtt_bio.pdf)
- Planning Commission (1980) 6th five-year plan on energy. NITI Aayog. <https://niti.gov.in/planningcommission.gov.in/docs/plans/planrel/fiveyr/6th/6planch15.html>
- PNGRB (2013) "Vision 2030"—natural gas infrastructure in India. PNGRB-GoI. <https://www.pngrb.gov.in/Hindi-Website/pdf/vision-NGPV-2030-06092013.pdf>
- Ram Mohan MP, Phillippe G, Shiju M (2006) Biofuel laws in Asia: instruments for energy access, security, environmental protection and rural empowerment. *Asian Biotechnol Dev Rev* 8:51–75
- Report of the Committee to identify the Central Acts which are not relevant or no Longer Needed or Require Repeal/Re-Enactment In The Present Socio-Economic Context (2014) PMO. <https://www.pmindia.gov.in/wp-content/uploads/2015/01/Extracts-of-the-Committee-of-the-Report-Vol.I-.pdf?query>
- Report of the Expert Committee on Auto Fuel Vision & Policy 2025 (2014). GoI. <https://petroleum.nic.in/sites/default/files/autopol.pdf>
- Saravanan AP, Mathimani T, Deviram G, Rajendran K, Pugazhendhi A (2018) Biofuel policy in India: a review of policy barriers in sustainable marketing of biofuel. *J Clean Prod* 193:734–747. <https://doi.org/10.1016/j.jclepro.2018.05.033>

- Shah V, Sanmukhani J (2010) Five cases of *Jatropha curcas* poisoning. *J Assoc Physicians India* 58:245–246 (PMID: 21046881)
- Sharma YC, Singh V (2017) Microalgal biodiesel: a possible solution for India's energy security. *Renew Sustain Energy Rev* 67:72–88. <https://doi.org/10.1016/j.rser.2016.08.031>
- Singh S, Adak A, Saritha M, Sharma S, Tiwari R, Rana S, Arora A, Nain L (2017) Bioethanol production scenario in India: potential and policy perspective. *Sustain Biofuels Dev India*, 21–37. [https://doi.org/10.1007/978-3-319-50219-9\\_2](https://doi.org/10.1007/978-3-319-50219-9_2)
- Singh AP, Agarwal RA, Agarwal AK, Dhar A, Shukla MK (eds) (2018) Prospects of alternative transportation fuels. *Energy Environ Sustain*. Published. <https://doi.org/10.1007/978-981-10-7518-6>
- Sorda G, Banse M, Kemfert C (2010) An overview of biofuel policies across the world. *Energy Policy* 38(11):6977–6988. <https://doi.org/10.1016/j.enpol.2010.06.066>
- Statista (2021a) Primary energy consumption in India 1998–2020. <https://www.statista.com/statistics/265582/primary-energy-consumption-in-india/>
- Statista (2021b) Solar energy capacity in India 2009–2020. <https://www.statista.com/statistics/865760/india-solar-energy-capacity/>
- Statista (2021c) Bioenergy capacity in India 2009–2020. <https://www.statista.com/statistics/865793/india-bio-energy-capacity/>
- Statista (2021d) Ethanol fuel production in top countries 2020. <https://www.statista.com/statistics/281606/ethanol-production-in-selected-countries/>
- Stolf R (2020) The success of the Brazilian alcohol program (proálcool)—a decade-by-decade brief history of ethanol in Brazil. *SciELO*. <https://www.scielo.br/j/eagri/a/z8TkLPmKtJcVv3gHGvGdn4r/?lang=en>
- The Ethanol Blending Policy in India (2012) *Economic and political weekly*. <https://www.epw.in/journal/2012/01/commentary/ethanol-blending-policy-india.html>
- Tomei J, Helliwell R (2016) Food versus fuel? Going beyond biofuels. *Land Use Policy* 56:320–326. <https://doi.org/10.1016/j.landusepol.2015.11.015>
- USDA (2021) Implementation of RenovaBio—Brazil's national biofuels policy. [https://usdabrazil.org.br/wp-content/uploads/2021/05/Implementation-of-RenovaBio-Brazils-National-Biofuels-Policy\\_Sao-Paulo-ATO\\_Brazil\\_02-25-2021.pdf](https://usdabrazil.org.br/wp-content/uploads/2021/05/Implementation-of-RenovaBio-Brazils-National-Biofuels-Policy_Sao-Paulo-ATO_Brazil_02-25-2021.pdf)
- USDA-GAIN (2019) Brazil-biofuels annual. USDA. [https://apps.fas.usda.gov/newgainapi/api/report/downloadreportbyfilename?filename=Biofuels%20Annual\\_Sao%20Paulo%20ATO\\_Brazil\\_8-9-2019.pdf](https://apps.fas.usda.gov/newgainapi/api/report/downloadreportbyfilename?filename=Biofuels%20Annual_Sao%20Paulo%20ATO_Brazil_8-9-2019.pdf)
- Usmani RA (2020) Potential for energy and biofuel from biomass in India. *Renew Energy* 155:921–930. <https://doi.org/10.1016/j.renene.2020.03.146>

**Part II**  
**Hydrogen as an E-Fuel**

# Chapter 4

## Hydrogen as Maritime Transportation Fuel: A Pathway for Decarbonization



Omer Berkehan Inal , Burak Zincir , and Caglar Dere 

**Abstract** Shipping is the most energy-efficient way for the transportation of goods and it has a substantial role in the global economy. The vast majority of the ships are addicted to fossil fuels as an energy source due to economic advantages, strong bunkering nets, and well-experienced operations of marine diesel engines. However, environmental concerns drive the industry to take precautions on the ship-sourced greenhouse gas emissions, and the International Maritime Organization (IMO), the ruler of the maritime industry, is bringing strict rules to regulate the emissions under The International Convention for the Prevention of Pollution from Ships—Annex VI (MARPOL). On the way of decarbonization and emission-free shipping, marine alternative fuels may draw a framework for the future of the maritime industry. In this perspective, hydrogen is a promising alternative for maritime transportation with its carbon-free structure. Furthermore, green hydrogen is one of the electro-fuels for maritime transportation to solve the issue to achieve full decarbonization. The use of hydrogen for ships is still under investigation at the level of research projects. Therefore, elaboration of the feasibility from different points of view for the commercial fleet is necessary to enlighten the future of the industry. This chapter includes information about the status of maritime transportation, recent international maritime emission rules and regulations, and hydrogen compliance with the International Code of Safety for Ships Using Gas or Other Low-flashpoint Fuels (IGF Code). Furthermore, hydrogen production technologies, onboard hydrogen storage methods, hydrogen combustion concepts on marine diesel engines, and fuel cells are reviewed. Lastly, the conclusion section comprises the chapter discussion.

**Keywords** Hydrogen · Decarbonization · Maritime transportation · Zero-carbon

---

O. B. Inal (✉) · B. Zincir · C. Dere

Marine Engineering Department, Maritime Faculty, Istanbul Technical University, Istanbul, Turkey

e-mail: [inalo@itu.edu.tr](mailto:inalo@itu.edu.tr)

C. Dere

Marine Engineering Department, Faculty of Naval Architecture and Maritime, Izmir Katip Celebi University, Izmir, Turkey



## 4.1 Introduction

Global energy consumption has been continuously increasing year by year. It was 575 quadrillion BTU in 2015, and it is expected that the global energy consumption will be 663 quadrillion BTU in 2030 and 736 quadrillion BTU in 2040 (U. S. Energy Information Agency (EIA) 2017). Buildings, industry, and transportation are the end-users that consume energy worldwide. The transportation sector contains road, railway, aviation, and maritime, and it is an important energy-consuming share. According to the data of EIA, the transportation sector consumes 110 quadrillion BTU in 2015 and it is estimated that it will rise to 140 quadrillion BTU in 2040 (U. S. Energy Information Agency EIA (EIA) 2017).

Maritime transportation is the most important transportation type in the transportation sector. Ninety percent of global transportation (Deniz and Zincir 2016), 90% of outer freight, and 40% of inner freight of the European Union (EU) are done by maritime transportation (Fan et al. 2018). There are 98,140 commercial ships worldwide in 2020 which are 100 gross tons and above (United Nations Conference on Trade and Development (UNCTAD) 2020), and these ships consume approximately 300 million tons of fuel (International Maritime Organization (IMO) 2015). Furthermore, 72% of total fuel consumption was heavy fuel oil (HFO), while 26% is marine diesel oil (MDO), and 2% is liquefied natural gas (LNG) (International Maritime Organization (IMO) 2020). Some specifications of diesel fuel and marine low-grade fuels are shown in Table 4.1. The huge amount of fuel consumption results in a major amount of shipboard emissions. European Energy Agency (EEA) states that maritime transportation is responsible for 20.98% of the global  $\text{NO}_x$  emissions, 11.80% of the global  $\text{SO}_x$  emissions, 8.57 and 4.63% of the global  $\text{PM}_{2.5}$  and  $\text{PM}_{10}$  emissions, and 1.94% of the global  $\text{CO}$  emissions (European Energy Agency (EEA) 2019). Moreover, maritime transportation contributes to 3.1% of worldwide  $\text{CO}_2$  emissions (International Maritime Organization (IMO) 2015).

International Maritime Organization (IMO) has been working on controlling and mitigating shipboard emissions from the past until now. IMO put emission limitations for  $\text{NO}_x$  and  $\text{SO}_x$  and  $\text{PM}$  emissions under MARPOL Annex VI Regulation 13 and 14, respectively. Table 4.2 shows  $\text{NO}_x$  emission limits and Table 4.3 shows  $\text{SO}_x$  and

**Table 4.1** Specifications of diesel fuel and marine low-grade fuels (Yi et al. 2021)

	Diesel	LSHFO180	LSHFO380	HSFO380
Ash (% m/m)	–	0.03	0.05	0.07
Carbon residue (% m/m)	–	3.2	6.5	16.6
Sulfur (% m/m)	< 0.035	0.475	0.477	3.05
Density ( $\text{kg/m}^3$ ) at 20 °C	818	934.6	951.5	981.5
Kinematic viscosity (cSt) (°C)	3.35/20	180/50	380/50	380/50

*LSHFO* low sulfur heavy fuel oil

*HSFO* high sulfur fuel oil

**Table 4.2** NO<sub>x</sub> emission limits (International Maritime Organization (IMO) 2021a)

Tier	Ship construction date	Total weighted cycle emission limit (g/kWh) n = engine's rated speed (rpm)		
		n < 130	n = 130–1999	n ≥ 2000
I	1 January 2000	17.0	$45n^{(-0.2)}$	9.8
II	1 January 2011	14.4	$44n^{(-0.23)}$	7.7
III	1 January 2016	3.4	$9n^{(-0.2)}$	2.0

**Table 4.3** SO<sub>x</sub> and PM limits (International Maritime Organization (IMO) 2021b)

SO <sub>x</sub> and PM limits outside ECAs	SO <sub>x</sub> and PM limits inside ECAs
4.50% m/m prior to 1 January 2012	1.50% m/m prior to 1 July 2010
3.50% m/m on and after 1 January 2012	1.00% m/m on and after 1 July 2010
0.50% m/m on and after 1 January 2020	0.10% m/m on and after 1 January 2015

PM limits in the fuel inside and outside of the Emission Control Areas (ECAs).

IMO also pay attention to CO<sub>2</sub> emissions by more strict rules and regulations. The Regulations on Energy Efficiency for Ships entered into force on 1 January 2013 (International Maritime Organization (IMO) 2011). The mandatory terms Energy Efficiency Design Index (EEDI) and the Ship Energy Efficiency Management Plan (SEEMP), and voluntary term the Energy Efficiency Operational Indicator (EEOI) were described. The EEDI determines the energy efficiency index for new building ships and encourages the use of more efficient materials and systems on ships. On the other hand, the SEEMP aims to increase the operational efficiency of ships. And voluntary EEOI is for calculating the voyage-based efficiency of ships. Later then, IMO Data Collection System entered into force on 1 March 2018 (IMO data collection system 2021c). It aims to record and control the annual voyage-based CO<sub>2</sub> emissions of ships larger than 5000 GRT worldwide.

The latest action of IMO is the Initial Greenhouse Gas (GHG) Strategy that is announced in 2018. The Strategy aims to achieve two targets. The first target is to reduce CO<sub>2</sub> emissions per transport work at least 40% by 2030 and 70% by 2050, compared to 2008, and the second target is to decrease GHG emissions to 50% by 2050, compared to 2008 (International Maritime Organization (IMO) 2018). By this strategy, the short-term (2018–2023), mid-term (2023–2030), and long-term (2030–...) candidate measures were defined (Table 4.4). One candidate measure or combination of two or more candidate measures can be used and it is left up to ship owners/operators. The strategy includes various operational and technical measures, but the use of alternative fuels is a prominent candidate measure. From short-term candidate measures to long-term candidate measures, a transition from low-carbon alternative fuels to zero-carbon alternative fuels is observed. Alternative

**Table 4.4** Initial GHG strategy measures (International Maritime Organization (IMO) 2018)

Short-term measures (2018–2023)	Mid-term measures (2023–2030)	Long-term measures (2030+)
Improvement of the existing energy efficiency framework	Implementation programme for the effective uptake of alternative low-carbon and zero-carbon fuels	Pursue the development and provision of zero-carbon or fossil-free fuels
Development of technical and operational energy efficiency measures for both new and existing ships	Operational energy efficiency measures for both new and existing ships	Encourage and facilitate the general adoption of other possible new/innovative emission reduction mechanism(s)
Establishment of an Existing Fleet Improvement Programme	New/innovative emission reduction mechanism(s), market-based measures (MBMs)	
Speed optimization/speed reduction	Further continuation and enhancement of technical cooperation and capacity-building	
Measures for volatile organic compounds	Development of a feedback mechanism to enable lessons learned on implementation of measures	
Development and update of national action plans		
Continuing and enhancing technical cooperation and capacity-building		
Measures for port developments and activities		
Initiation of research and development activities on marine propulsion, alternative low-carbon and zero-carbon fuels, and innovative technologies		
Incentives for first movers of new technologies		
Development of a sufficient lifecycle GHG/carbon intensity guidelines for fuels		
Active promotion of the work of the IMO		
Undertake additional GHG emission studies		

fuels identified for maritime transportation are liquefied natural gas (LNG), liquefied petroleum gas (LPG), methanol, ethanol, ammonia, dimethyl ether (DME), ethane, biogas, biofuels, synthetic fuels, and hydrogen (Zincir and Deniz 2021). Among these alternative fuels, hydrogen is zero-carbon fuel that can meet the IMO Initial GHG Strategy reduction targets (American Bureau of Shipping (ABS) 2021). Moreover, if hydrogen is produced by water electrolysis which is powered by renewable energy, this type of hydrogen is named electrofuel. In general terms, electrofuels are hydrocarbon fuels that are produced from CO<sub>2</sub> and water while renewable electricity is the main source of production (Brynnolf et al. 2018). The renewable electricity is converted to hydrogen by the electrolysis process and the later step is to combine hydrogen with carbon atoms to form hydrocarbon fuels, for instance, ammonia, methane, methanol, etc. (Rixhon et al. 2021). Therefore hydrogen is an important alternative fuel to achieve full decarbonization at maritime transportation.

This chapter explains that the use of hydrogen as an alternative fuel can be a pathway for decarbonized maritime transportation. The chapter contains hydrogen fuel properties, hydrogen production methods, hydrogen storage methods, application of hydrogen fuel on fuel cells and diesel engines. Lastly, the chapter conclusion will discuss the role of hydrogen in maritime transportation.

## 4.2 Hydrogen Fuel Properties

International Energy Agency (IEA) states that hydrogen is a promising fuel to meet future energy demands (Qyyum et al. 2021) and will have an important role in sustainable energy systems by 2050 (Staffell et al. 2019). Hydrogen is the most available element in various feedstocks, but it is unusual to find solely (Inal et al. 2021a). Hydrogen is a carbon-free and clean alternative fuel for maritime transportation. Therefore the combustion of hydrogen results in water only as a by-product.

The properties of hydrogen are shown in Table 4.5. The remarkable fuel properties of hydrogen are high laminar flame speed, wide flammability limits, high diffusivity, smaller quenching distance, and low minimum ignition energy (Deniz and Zincir 2016). Hydrogen is a high octane fuel and the high auto-ignition temperature of hydrogen is an issue to overcome, especially combustion at diesel engines. On the other hand, low minimum ignition energy of hydrogen brings quick combustion of hydrogen by external sources such as spark plugs. The wide flammability limits provide using variable fuel–air ratios for the optimum combustion conditions for lower fuel consumption and lower emissions. The high laminar flame speed of hydrogen improves the spread of the flame in the cylinder and contributes to more complete burning. Due to the high diffusivity, hydrogen forms a more homogenous fuel–air charge in the cylinder that also leads to higher combustion efficiency.

Despite its high LHV than conventional marine fuels, the energy density of hydrogen is low. For this reason, the volumetric energy capacity of gaseous hydrogen is 3000 times lower than diesel oil (Inal et al. 2021a). And for instance, compressed hydrogen needs six to seven times more storage area than the same energy content of

**Table 4.5** Properties of hydrogen (Deniz and Zincir 2016; Inal et al. 2021a; Zincir and Deniz 2014, 2018)

Properties	Gaseous hydrogen	Liquid hydrogen
Auto-ignition temperature (°C)	571	571
Density (kg/m <sup>3</sup> )	17.50–20.54	70.85–71.10
Energy density (MJ/m <sup>3</sup> )	2101	8539
Diffusivity in air (cm <sup>2</sup> /s)	0.63	0.63
Laminar Flame speed (m/s)	3.51	3.51
Flame temperature (°C at 1 bar)	2045	2045
Flammability limits (Vol.%)	4–75	4–75
Flashpoint (°C)	–150	–150
Lower heating value (MJ/kg)	120.1	120.1
Minimum ignition energy (mJ)	0.02	0.02
Octane number	>130	>130
Stoichiometric air–fuel ratio on mass basis	34.3	34.3
<i>Storage type</i>	<i>Compressed gas</i>	<i>Cryogenic liquid</i>
Storage temperature (°C)	25	–253
Storage pressure (bar)	300	1
Onboard storage cost (€/kWh)	1.29–1.71	
Fuel cost (€/kWh)	153	153
Exposure limit (mg/m <sup>3</sup> —8 h)	336	336
Well to wheel life cycle emissions (g <sub>co2</sub> /MJ)	Grid electricity: 139 Wind electricity: 2.59–20.74 Solar PV electricity: 6.67–66.67	

HFO (Chryssakis et al. 2014). The energy densities without taking into account the container and insulation of gaseous and liquid hydrogen are shown in Table 4.5. The low energy density is the main disadvantage of hydrogen for being a maritime transportation fuel. The main storage options of hydrogen are as a compressed gas at 25 °C and 300 bar or as a cryogenic liquid at –253 °C and 1 bar. Detailed hydrogen storage techniques are explained in Sect. 4.4. Hydrogen is neither corrosive nor toxic which lowers operational procedures and costs. But the storage cost of cryogenic hydrogen storage is higher than the compressed hydrogen storage. The reasons for these are special insulation material for the cryogenic storage, cooling and pumping units to recover gasified hydrogen from the tank and transfer it again to the tank cryogenically. Although hydrogen is not a toxic substance, exposure to hydrogen in a place that contains more than 336 mg/m<sup>3</sup>—8 h results in asphyxiation.

Some main advantages of hydrogen are abundance, carbon-free structure, high energy conversion efficiency, variety of storage options, the possibility of long-distance transportation, higher LHV than the conventional marine fuels, and conversion options to other energy forms (Dincer and Acar 2015).

### 4.3 Hydrogen Production Methods

Hydrogen is an essential substance for various industries and 0.1 Gt of hydrogen is produced annually (Qyyum et al. 2021). Fifty-one percent of hydrogen production is for ammonia production, while 31% is for oil refining, 10% for methanol production, and 8% for other applications (Kannah et al. 2021). Hydrogen is produced from different feedstocks that 96% of them are fossil fuels (natural gas 48%, oil 30%, and coal 18%) and 4% from renewable resources (Taibi et al. 2018). The energy consumption of annual worldwide hydrogen production equals 2% of the global energy demand (American Bureau of Shipping (ABS) 2021).

Hydrogen production is determined in four different ways by their emitted GHG emissions during the process. These are brown hydrogen, grey hydrogen, blue hydrogen, and green hydrogen (American Bureau of Shipping (ABS) 2021). Brown hydrogen is the production way of using coal as feedstock, grey hydrogen is the production process of using other fossil fuels (natural gas, oil, etc.) as feedstock. Blue hydrogen is the process that uses fossil fuels as feedstock for hydrogen production, but the emitted carbon emissions are captured and stored by the carbon capture and storage (CCS) system. The emitted CO<sub>2</sub> emissions are approximately 90% lower than brown hydrogen and grey hydrogen. Lastly, green hydrogen is the production process that uses renewable energy sources (solar, wind) for electrolysis of water, or uses biomass or biological methods to produce hydrogen.

This section describes the hydrogen production methods based on feedstocks. The feedstocks are separated as hydrocarbon fuels, biomass, and water. The hydrogen production methods are also classified according to their production way color.

#### 4.3.1 Hydrogen Production from Hydrocarbon Fuels

Hydrogen production methods from hydrocarbon fuels are hydrocarbon reforming and pyrolysis. These two hydrogen production methods are the most mature and used methods that meet almost the total global hydrogen demand (Nikolaidis and Poullikkas 2017). Hydrogen production from hydrocarbon fuels can be done at high efficiencies and low costs (Baykara 2018).

##### 4.3.1.1 Hydrocarbon Reforming

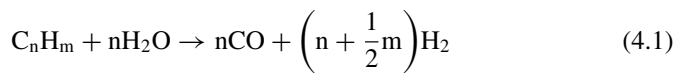
Hydrocarbon reforming is the conversion process of hydrocarbon fuels to hydrogen by chemical techniques. The hydrocarbon reforming process is named steam reforming, partial oxidation, or auto-thermal reforming, according to the reactant substance. If the reactant substance is steam, the process is named steam reforming, if the reactant substance is oxygen, the process is known as partial oxidation, and

if the hydrogen production process consists of these two reactions, the process is auto-thermal reforming (Chen et al. 2008).

### Steam Reforming

Steam reforming is a hydrogen production method that uses natural gas, liquefied petroleum gas (LPG), methanol, jet fuel, naphtha, and diesel fuel as feedstocks (Kannah et al. 2021). But natural gas is the major feedstock for steam reforming that has high process thermal efficiencies up to 85% (El-Shafie et al. 2019) and the lowest CO<sub>2</sub> emissions compared to all hydrogen production from hydrocarbon fuels (Qyyum et al. 2021). During the steam reforming process, hydrocarbon fuel reacts with steam at a high temperature (700–1000 °C) environment. The product of this reaction is carbon monoxide (CO), hydrogen, and unreacted natural gas mixture which is called syngas. After the syngas generation, the later step of the steam reforming is the water–gas shift (WGS) reaction that converts CO to CO<sub>2</sub>. The final step is methanation or gas purification to collect 99.99% purity of hydrogen from the process (Al-Qahtani et al. 2021). Equations (4.1)–(4.3) (Nikolaidis and Poullikkas 2017) and Fig. 4.1 show the main steps of steam reforming. If the hydrocarbon fuel contains sulfur compounds, the desulphurization process is done before the syngas generation step to prevent poisoning the reforming catalyst (Nikolaidis and Poullikkas 2017). Steam reforming is considered grey hydrogen production since the process uses fossil fuels. On the other hand, if the process contains CCS almost 90% of emitted CO<sub>2</sub> is captured. Thus the produced hydrogen is blue hydrogen.

Reforming step:



WGS step:



Methanation step:

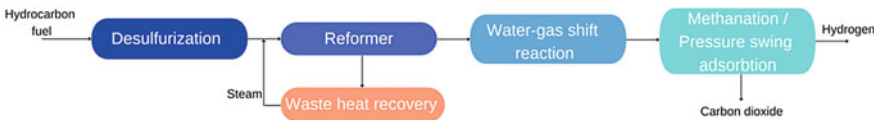
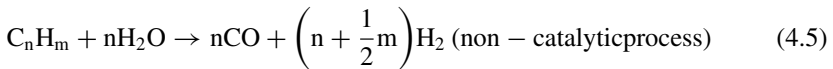
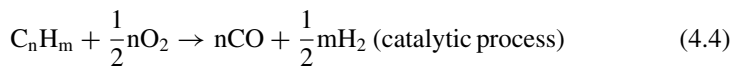


**Fig. 4.1** Steam reforming steps (figure reproduced and adapted) (Nikolaidis and Poullikkas 2017)

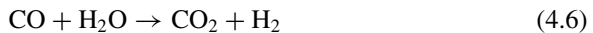
*Partial Oxidation*

Partial oxidation (POX) is the conversion process of hydrocarbon to hydrogen and carbon oxides by oxygen. The feedstocks for the POX are coal, heavy oil, methane, and naphtha (Nikolaidis and Poullikkas 2017). The POX with the feedstock of coal is also called gasification. After the desulphurization, the hydrocarbon feedstock is partially oxidized by oxygen to produce syngas. The further process is the same as steam reforming. Equations (4.4)–(4.7) and Fig. 4.2 show the main steps of the POX (Nikolaidis and Poullikkas 2017). POX is the most convenient hydrogen production method for using heavier hydrocarbon fuels, for instance, heavy fuel oil and coal (Chen et al. 2008). However, the hydrogen production by partial oxidation is more expensive due to the oxygen separation unit, and less energy efficient than the steam reforming (El-Shafie et al. 2019). Moreover, when the process uses heavier hydrocarbon fuels with lower carbon to hydrogen ratio, the POX results in higher CO<sub>2</sub> emissions (Al-Qahtani et al. 2021). The hydrogen production from the POX process is brown hydrogen when coal is used as feedstock; grey hydrogen when heavy fuel oil or methane is used as feedstock; and blue hydrogen when CCS is applied to capture CO<sub>2</sub> emissions during the hydrogen production process.

Reforming step:



WGS step:



Methanation step:

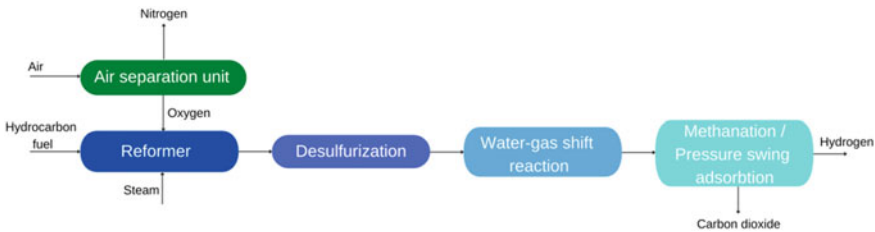
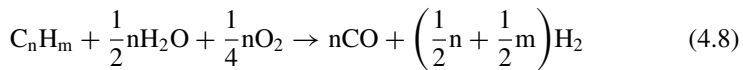


**Fig. 4.2** Partial oxidation steps (figure reproduced and adapted) (Nikolaidis and Poullikkas 2017)



### Auto-thermal Reforming

Auto-thermal reforming (ATR) is the hydrogen production process by the combination of steam reforming and partial oxidation (Zincir and Deniz 2016). The ATR includes the exothermic POX and endothermic steam reforming processes. The heat from the POX is used during the steam reforming process to increase the hydrogen production rate (Nikolaidis and Poullikkas 2017). The remaining steps of the process are the same as steam reforming and POX. Equation (4.8) shows the main step of the ATR (Nikolaidis and Poullikkas 2017), and the process steps are similar to Fig. 4.2. The ATR also requires pure oxygen that raises the complexity and cost of the system (Dincer and Acar 2015). Hydrogen is produced by the ATR is grey hydrogen since the process uses methane and if CCS is applied to capture CO<sub>2</sub> emissions the produced hydrogen is blue hydrogen.



#### 4.3.1.2 Pyrolysis

Pyrolysis is the decomposition of hydrocarbon fuels by heat. The decomposition reaction temperature is 350–400 °C for coal and 1400 °C and above for methane (El-Shafie et al. 2019). Products of the pyrolysis process are hydrogen-rich gas, gaseous hydrocarbon, and solid char (Kannah et al. 2021). Equation (4.9) (Nikolaidis and Poullikkas 2017) and Fig. 4.3 show the main chemical reaction of the pyrolysis process. Since there are no gaseous carbon emissions, the CCS is not needed. The pyrolysis process does not contain the WGS reaction and CO<sub>2</sub> capture process. Therefore, capital investments and hydrogen production costs are lower than steam reforming and partial oxidation (Muradov 1993). Despite its advantages, the pyrolysis process has a fouling issue due to the solid carbon product that reduces the effectiveness of the reactor (Guo et al. 2005). Although the pyrolysis process does not carbon oxide emissions, solid carbon is the product of the process and pollutes the environment. Hence, the produced hydrogen is either brown hydrogen or grey hydrogen when the feedstock is coal or other hydrocarbon fuels, respectively.

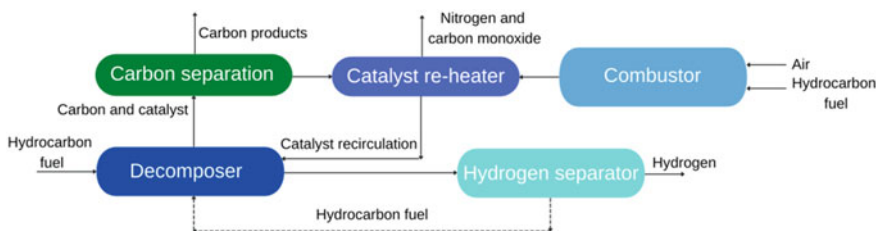


Fig. 4.3 Pyrolysis steps (figure reproduced and adapted) (Nikolaidis and Poullikkas 2017)



### 4.3.2 Hydrogen Production from Biomass

Hydrogen from biomass is the renewable production way. There are two main categories for hydrogen production from biomass. One of them is the thermochemical process and the other one is the biological process. The subcategories of the thermochemical process are pyrolysis and gasification. The biological process contains bi-photolysis, dark fermentation, and photo-fermentation. Although there are various ways of hydrogen production from biomass, most of the techniques are not mature enough, and the hydrogen production rate is not adequate to replace with fossil-based fuels (Qyyum et al. 2021).

#### 4.3.2.1 Thermochemical Process

Thermochemical processes are pyrolysis and gasification, and biomass is converted to hydrogen and hydrogen-rich gases (Nikolaidis and Poullikkas 2017). These methods are the same as the processes with hydrocarbon fuels. Biomass pyrolysis commenced at 650–800 K, 0.1–0.5 MPa, (Demirbaş 2001) and an oxygen-free environment. The products of the process are gaseous compounds, liquid oils, and solid charcoal. The reforming and WGS reactions follow the pyrolysis process. The main steps of the process are shown in Eqs. (4.10–4.12) (Nikolaidis and Poullikkas 2017) and Fig. 4.4.

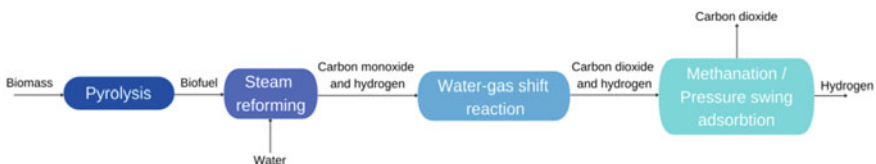
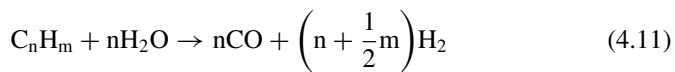
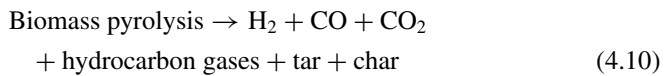


**Fig. 4.4** Biomass pyrolysis steps (figure reproduced and adapted) (Nikolaidis and Poullikkas 2017)

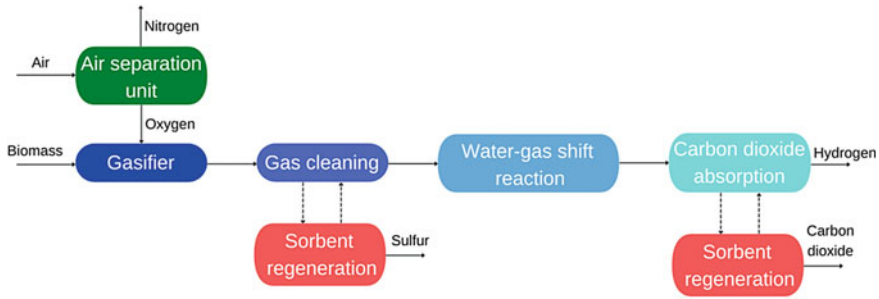
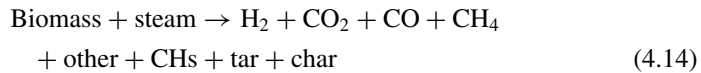
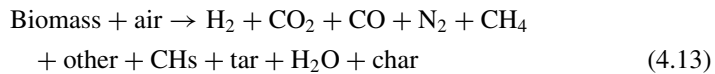


**Fig. 4.5** Biomass gasification steps (figure reproduced and adapted) (Nikolaidis and Poullikkas 2017)

Biomass gasification is the same process as coal gasification. It is the most well-known and promising hydrogen production method (Kannah et al. 2021). Biomass feedstock is partially oxidized by oxygen to form syngas. The operating conditions temperatures are between 500 and 1400 °C at 33 bar pressure (Iribarren et al. 2014). Equations (4.13) and (4.14) (Nikolaidis and Poullikkas 2017) and Fig. 4.5 show the main step of biomass gasification with air or steam respectively.



Biomass pyrolysis and biomass gasification processes are renewable processes and the produced hydrogen is green hydrogen. Moreover, if the CCS is applied to these processes the negative carbon balance is achieved (Al-Qahtani et al. 2021).

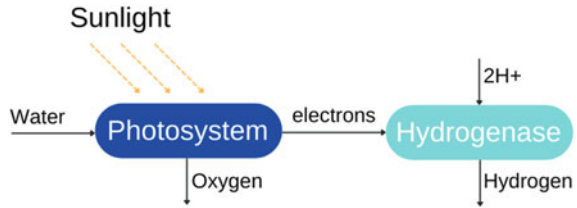
#### 4.3.2.2 Biological Process

The biological process uses biological technologies to produce hydrogen. The biological process commences at ambient temperature and pressure and the feedstocks are renewable and waste materials (Das and Veziroğlu 2001). The main methods of biological process are bio-photolysis, dark fermentation, and photo-fermentation. These hydrogen production methods are green production way of hydrogen.

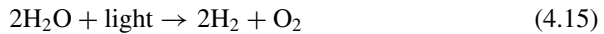
##### *Bio-photolysis*

Bio-photolysis is some kind of replica of photosynthesis but the product is hydrogen gas. Water is given to green and blue algae as a feedstock. They can split the water molecules into hydrogen ions and oxygen. Hydrogenase or nitrogenase enzymes of

**Fig. 4.6** Bio-photolysis steps (figure reproduced and adapted) (Nikolaidis and Poullikkas 2017)



algae convert hydrogen ions to hydrogen gas (Kapdan and Kargi 2006). It is not a mature and commercial technology (Dincer and Acar 2015) and has drawbacks of low hydrogen production rate and large surface area requirement to get satisfactory light (Holladay et al. 2009). The general formula for the bio-photolysis is shown in Eq. (4.15) (Nikolaidis and Poullikkas 2017) and the basic steps are shown in Fig. 4.6.



*Dark Fermentation*

Anaerobic bacteria digest carbohydrates in biomass feedstock to convert organic acids and then to hydrogen gas (Kapdan and Kargi 2006). This process is called dark fermentation. The process commences in oxygen-free and dark conditions. Dark fermentation is the most well-known and used method for hydrogen production from renewable biomass feedstock, for instance, lignocelluloses biomass, crop residues, organic waste, and algal biomass (Kannah et al. 2021). The hydrogen production rate depends on pH value (between 5 and 6) (Ni et al. 2006) and removal of produced hydrogen from the fermentation area since pressure rise decreases hydrogen production rate (Holladay et al. 2009). Despite dark fermentation has the advantage of continuous production of hydrogen day and night, the production capacity is low, the capital investment is high, and the process is on a laboratory scale (Dincer and Acar 2015; Kannah et al. 2021). The main chemical reaction of dark fermentation with acetate fermentation and butyrate fermentation is shown in Eqs. (4.16) and (4.17), respectively (Nikolaidis and Poullikkas 2017). Figure 4.7 shows the basic steps of the dark fermentation process.

Acetate fermentation:



**Fig. 4.7** Dark fermentation steps (figure reproduced and adapted) (Nikolaidis and Poullikkas 2017)

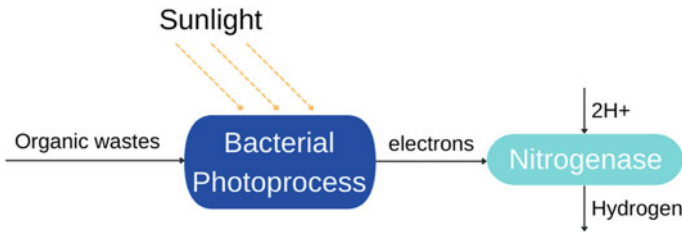


**Fig. 4.8** Photo-fermentation steps (figure reproduced and adapted) (Nikolaidis and Poullikkas 2017)

Butyrate fermentation:

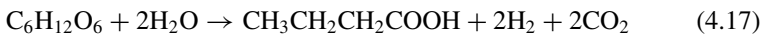
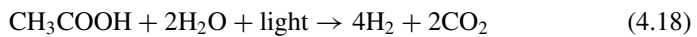


### *Photo-fermentation*

Photo-fermentation is a biological process that some photosynthetic bacteria that use solar power and organic acids to produce hydrogen and  $\text{CO}_2$  (Das and Veziroglu 2008). This hydrogen production method is on a laboratory scale and has challenges such as large surface area requirement and low light utilization efficiency (Zincir and Deniz 2016). The main chemical reaction of the process is shown in Eq. (4.18) (Nikolaidis and Poullikkas 2017) and Fig. 4.8.



## **4.3.3 Hydrogen Production from Water Splitting**

Water splitting is another hydrogen production way and it can be done by three methods. These methods are electrolysis, thermolysis, and photo-electrolysis. Hydrogen from water splitting is the cleanest energy when the energy for water splitting is provided from renewable energy sources (Nikolaidis and Poullikkas 2017).

### **4.3.3.1 Electrolysis**

Electrolysis is the most mature and well-known method for water splitting. The method is endothermic and requires high electric energy (Qyyum et al. 2021). The electrical current splits water at the anode and cathode of the electrolyzer unit.

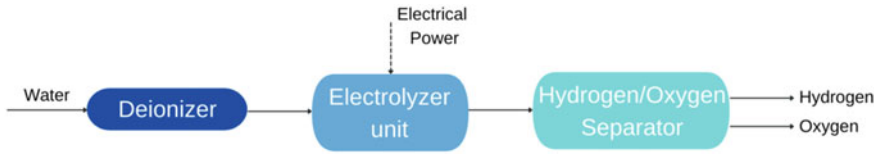


**Fig. 4.9** Electrolysis steps (figure reproduced and adapted) (Nikolaidis and Poullikkas 2017)

Hydrogen accumulates at the cathode and oxygen at the anode. The reaction for the water electrolysis is shown in Eq. (4.19) (Levene et al. 2007) and Fig. 4.9.

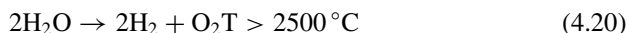


There are three types of water electrolysis methods for hydrogen production. These are alkaline, proton exchange membrane (PEM), and solid oxide electrolysis (SOE). Alkaline electrolysis has the lowest system efficiency, the lowest capital cost, and higher hydrogen production. On the other hand, the PEM has higher system efficiency than the alkaline electrolysis, no corrosion and sealing related issues, but the capital electrolyzer cost is higher than the alkaline electrolysis. Lastly, nevertheless, the SOE is the most efficient electrolysis system, it is still under development and there are corrosion and sealing issues that have to be solved (El-Shafie et al. 2019).

Water electrolysis is an intensive electricity-consuming process. Therefore, when the electricity production is from fossil fuels, the process emits a high amount of CO<sub>2</sub> emissions and the produced hydrogen is brown hydrogen if the electricity is generated from coal energy and grey hydrogen if the electricity is generated from oil and natural gas. Fossil power plants can use CCS to capture CO<sub>2</sub> emissions. Therefore, the produced hydrogen by using generated electricity from these power plants results in blue hydrogen production. When the electricity is produced from renewable energy sources (wind or solar), the produced hydrogen is green hydrogen. The green hydrogen is also named electrofuel which has a carbon-free lifecycle from well-to-wheel or well-to-propeller at maritime transportation.

#### 4.3.3.2 Thermolysis

Thermolysis is a water-splitting process that the water is decomposed to hydrogen and oxygen at a high temperature (Nikolaidis and Poullikkas 2017). The temperature has to be as high as more than 2500 °C to separate hydrogen (Funk 2001). The main chemical reaction of the process is shown in Eq. (4.20) (Steinfeld 2005) and Fig. 4.10.



The thermolysis process is under development since the compatible material to high thermal stress issue and the development of an effective technique has to be solved (El-Shafie et al. 2019). The required heat can be provided from fossil fuels or

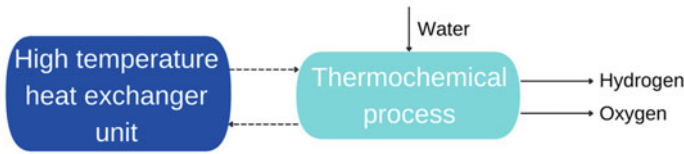


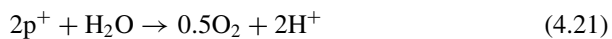
**Fig. 4.10** Thermochemical steps (figure reproduced and adapted) (Nikolaidis and Poullikkas 2017)

solar power, thus, the produced hydrogen will be brown or grey hydrogen and green hydrogen, respectively.

#### 4.3.3.3 Photo-Electrolysis

Photo-electrolysis is a water-splitting method that transforms the photonic energy of sunlight into chemical energy (Dincer and Acar 2015). Water is decomposed to hydrogen and oxygen by the photonic energy that is similar to electrolysis. The photo-electrolysis method is a more efficient water splitting method than electrolysis (Qyyum et al. 2021). The photo-electrolysis systems use semiconductor materials which is the same as the photovoltaic systems (El-Shafie et al. 2019). Equations (4.21)–(4.23) show the main chemical reactions of the photo-electrolysis method (Nikolaidis and Poullikkas 2017).

Anode:



Cathode:



Total reaction:



Photo-electrolysis hydrogen production is expected to be a promising long-term solution for carbon-free hydrogen production, but before it will happen, a more durable and inexpensive photocatalyst has to be developed for commercial hydrogen production (Maeda and Domen 2010). The photo-electrolysis method produces green hydrogen (Fig. 4.11).

Table 4.6 compares hydrogen production methods with their advantages and disadvantages. Technology readiness levels (TRL) of hydrogen production methods are compared. Steam reforming and electrolysis are the most mature methods

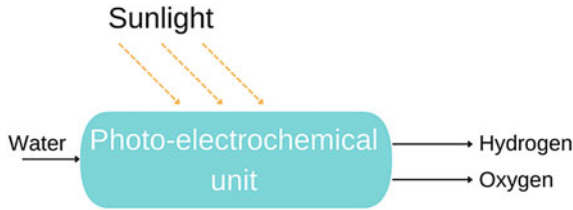


**Fig. 4.11** Photo-electrolysis process (figure reproduced and adapted) (Nikolaidis and Poullikkas 2017)

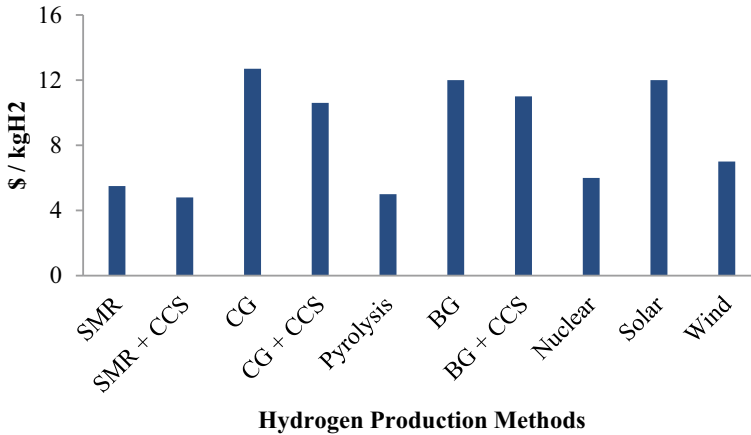
and bio-photolysis, dark fermentation, photo-fermentation, thermolysis, and photo-electrolysis are the least mature methods. The efficiencies are indicated in the table, of the hydrogen production methods represent energy conversion efficiency from the external energy sources to hydrogen production. Since steam reforming is the most mature and used hydrogen production method, the most developed technologies with higher efficiency have been used. On the other hand, the hydrogen production methods such as photo-fermentation and photo-electrolysis are on a laboratory scale and under development and the efficiencies are the lowest. The sunlight energy conversion efficiency of these methods is also effective on the efficiency. Steam reforming, partial oxidation, and auto-thermal reforming emit CO<sub>2</sub> emissions and hydrocarbon pyrolysis forms solid carbon. As a consequence, these hydrogen production methods are not able to produce hydrogen in a green way. The remaining methods have green production ways and the variety of hydrogen production is promising for future renewable hydrogen production pathways. It is known that steam reforming is the most used hydrogen production method recently. Thus, steam reforming with CCS (blue hydrogen) is a good option during the transition from brown/grey hydrogen to green hydrogen pathways. And in the future, green hydrogen production pathways will be used for achieving zero well-to-wake emissions in maritime transportation.

Figure 4.12 shows the hydrogen production lifecycle costs by considering human health, ecosystem, and resources. The data of the figure is derived from the study of Al-Qahtani et al. that is done in 2021 (Al-Qahtani et al. 2021). They assessed the hydrogen production methods by taking into account the effects of hydrogen production methods on human health, the environment, and resources. According to the results of the study, steam reforming with CCS has the lowest hydrogen production cost recently. Pyrolysis and steam reforming without CCS followed it. The highest production cost is for coal gasification since it has the highest effect on human health and the environment. Nuclear and wind energies can cope with steam reforming, but solar energy is not an effective way to produce hydrogen for now.



**Table 4.6** Comparison of hydrogen production methods (Qyyum et al. 2021; Dincer and Acar 2015; Kannah et al. 2021; Nikolaidis and Poullikkas 2017; Al-Qahtani et al. 2021)

Production methods	TRL Level	Efficiency	Advantages	Disadvantages	Produced hydrogen color
Steam reforming	9	74–85	Most mature and existing process	Emits CO <sub>2</sub> , fossil fuel depended	Brown Grey Blue
Partial Oxidation	8	60–75	Proven and existing process	Emits CO <sub>2</sub> , fossil fuel depended	Brown grey Blue
Auto-thermal reforming	8	60–75	Proven and existing process	Emits CO <sub>2</sub> , fossil fuel depended	Brown Grey Blue
Hydrocarbon pyrolysis	3–5	–	Emission-free, low process steps	Solid carbon formation, fossil fuel depended	Brown Grey
Biomass pyrolysis	3–5	35–50	CO <sub>2</sub> -neutral process, ample and cheap feedstock	Tar formation, unstable H <sub>2</sub> content	Green
Biomass gasification	5–6	40–50	CO <sub>2</sub> -neutral process, ample and cheap feedstock	Tar formation, unstable H <sub>2</sub> content	Green
Bio-photolysis	1–3	10	CO <sub>2</sub> -consuming process	Sunlight and large area requirement	Green
Dark fermentation	1–3	60–80	CO <sub>2</sub> -neutral process, waste recycling, O <sub>2</sub> -free process without light	Low H <sub>2</sub> production, low efficiency	Green
Photo-fermentation	1–3	0.1	CO <sub>2</sub> -neutral process, waste recycling	Sunlight and large area requirement, low efficiency	Green
Electrolysis	9	40–60	Proven and existing process, ample feedstock, zero-emission with renewable energy	High capital cost, low efficiency	Brown Grey Blue Green
Thermolysis	1–3	20–45	Clean and reliable process, ample feedstock	Toxicity, corrosion issues, high capital cost	Brown Grey Green
Photo-electrolysis	1–3	0.06	Ample feedstock, zero-emission process	Sunlight requirement, low efficiency	Green



**Fig. 4.12** Hydrogen production lifecycle assessment costs (data is derived and the graph is drawn) (Al-Qahtani et al. 2021)

#### 4.4 Hydrogen Storage Techniques for Maritime

The main objective on the use of hydrogen for ships is to eliminate greenhouse gas emissions. In this motivation, alternative fuels are gaining importance, however, the ultimate zero emission goal can be reached by hydrogen thanks to its carbon-free structure. Hence, onboard storage of the hydrogen receives attention and many industrial techniques have been tried to apply for ships. The major obstacle seems as the onboard storage of the hydrogen before using it for powering the ship's propulsion systems. From a wider perspective, several milestones need to be achieved in order to switch the fuel system to a newer and less experienced one. In this manner, there are several levels such as bunkering stations, refueling infrastructures (connections, production, and distributions), storage, and their safety aspects (Andersson and Grönkvist 2019). However, this chapter only focuses on the available and applicable onboard storage techniques and other requirements for the hydrogen use is out of the scope.

Hydrogen fuel has some advantageous properties compared to conventional marine fuels. For instance, lower heating value of the hydrogen is approximately 3 times higher than diesel oil, 33 kWh/kg and 11 kWh/kg, respectively (Inal et al. 2021b). However, being in gaseous form under atmospheric conditions and having roughly 3000 times lesser volumetric energy compared to diesel requires increased space onboard ship for long voyages. Therefore, substantial technological improvements may be needed for spreading the hydrogen fuel in shipping industry. As a nature of the marine environment, the use of hydrogen shows different challenges compared to land-based facilities and other transportation sectors. This section provides a general overview to onboard hydrogen storage techniques that can be applicable for ships.

### 4.4.1 Onboard Hydrogen Storage

In this section hydrogen storage techniques for the onboard ship are reviewed. The four main storage technologies compressed, liquid, solid-state, and alternative carriers are elaborated, respectively, and shown in Fig. 4.13. Additionally, alternative carriers are separated into three subtitles as  $N_2$  based,  $CO_2$  based, and organic liquids.

#### 4.4.1.1 Compressed Hydrogen Storage

The compressed hydrogen storage is the most developed and well-experienced method among different technologies. The hydrogen is kept under very high pressures around 350–700 bar which give a density of 23.3  $kg/m^3$  and 39.3  $kg/m^3$ , respectively (Raucci et al. 2015). Table 4.7 shows the four different pressurized vessel types with the used material, typical pressure in bar, and approximate cost in USD per kg.

The most well-known tank types to store the hydrogen are type I and II, all-metal, and mostly metal development types because of their somewhat lower costs. Additionally, since the material of type II is a combination of metal and composite parts it has a lower weight contrasted with the all-metal, type I tank. Be that as it may, the composite material diminishes the solidness of the vessel and it can simply go up to 200 bars. The primary issue is the significant expense because of the utilization of cutting edge materials like carbon fiber, for the third and fourth kinds of capacity tanks (O'Malley et al. 2015). On the other hand, high-pressure hydrogen storage

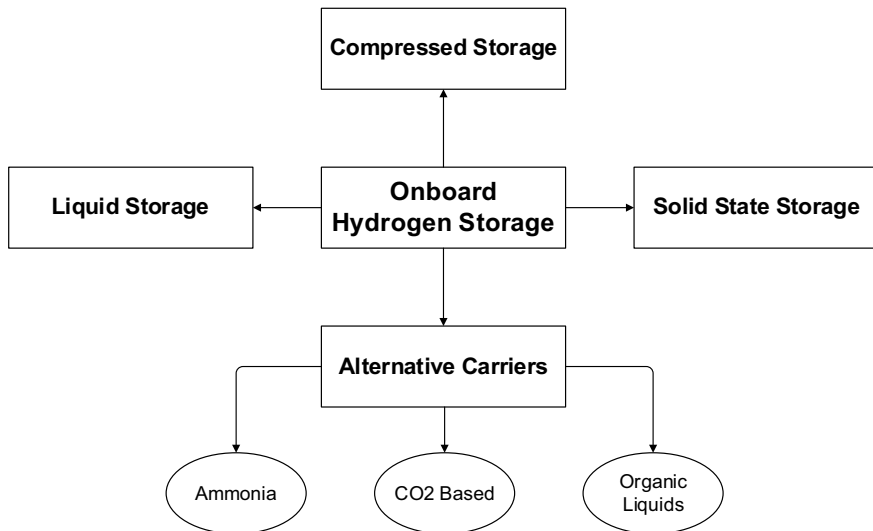


Fig. 4.13 Onboard hydrogen storage techniques (Inal et al. 2021b)

**Table 4.7** Storage tank types (Rivard et al. 2019)

Type	Material	Typical pressure (bar)	Cost (\$/kg)
I	All-metal construction	300	83
II	Mostly metal, composite overwrap in the hoop direction	200	86
III	Metal liner, full composite overwrap	700	700
IV	All-composite construction	700	633

tanks are in advantage with gravimetric density and well-proven by being used in fuel cell electric cars, Toyota Mirai, and Honda Clarity (Yamashita et al. 2015). This high gravimetric density serves to multiple times higher storage limit contrasted with low-pressure tanks (Rivard et al. 2019; Hoecke et al. 2021).

#### 4.4.1.2 Liquid Hydrogen Storage

The subsequent method to store hydrogen is by liquefaction. The central of putting away hydrogen in fluid structure is to lessen temperature to  $-253\text{ }^{\circ}\text{C}$  which is its bubbling temperature. The benefit of liquefaction is the capacity to arrive at high hydrogen densities at environmental pressing factors, which is  $70\text{ kg/m}^3$  and multiple times higher than the vaporous structure (Hoecke et al. 2021). The heat transfer should be limited to keep the temperature at the ideal level to store a cryogenic fluid. In the interim, cryogenic capacity is certifiably not a far idea for the maritime industry because of liquefied natural gas (LNG) transportation and boil-off gas use in marine diesel motors. Incidentally, LNG seems like another solid option through green shipping with its lesser carbon content contrasted with substantial fuel oil and marine diesel oil, additionally, with its free sulfur content.

The main piece of liquid hydrogen storage is to limit evaporation. Evaporation of hydrogen has two incidental effects; the first is the pressing factor increment within the tank and the second is the deficiency of the burned through effort during the liquefaction of the hydrogen. The decrease of heat transfer through the tank is the critical answer for stopping the evaporation. To fulfill this, the volume to surface proportion ought to be maximized, and this is reachable with circular tank shapes that have the biggest volume to surface proportion. In conclusion, the boil-off rates are below 0.1% per day with strongly insulated spherical tanks (Amos 1998).

#### 4.4.1.3 Solid-State Hydrogen Storage

There are various methods to store hydrogen in solid materials but the promising ones; metal hydride and boron-based storage have been reviewed. Firstly, metal hydrides were elaborated with magnesium hydrides. Secondly, the two most common boron-based storage materials  $\text{NaBH}_4$  and  $\text{NH}_3\text{BH}_3$  were summarized. There is a vast

number of researches are ongoing on putting hydrogen into a solid carrier, however, this scope is limited with the promising types for the marine environment.

The metal hydrides store hydrogen by synthetically holding the hydrogen to the metal as can be seen by the name. Hydrides have interesting properties for adsorbing and delivering hydrogen at various temperatures and pressing factors, in this way, each metal hydrides have various attributes. There two different ways of delivering hydrogen from metal hydrides; thermolysis and hydrolysis. Albeit the point is something very similar for both ways, they are genuinely unique. While thermolysis is a reversible endothermic cycle, hydrolysis is exothermic and irreversible. As a rule, metal hydride storage is primarily centered around the thermolysis-based activity. Notwithstanding there are different metal hydrides storage strategies, for instance, elemental, intermetallic, or complex, this paper mainly centered around elemental metal hydrides and boron-based (borohydrides) from complex metal hydrides.

The major solid-state elemental metal hydride is magnesium hydride since magnesium is widely available, magnesium hydrides are affordable and attractive hydrogen storage methods with a density of  $1.45 \text{ g/cm}^3$  and high hydrogen storage capacity of 7.6% (wt) (Yartys et al. 2019). Notwithstanding these benefits, the hydrogenation response energy of magnesium is moderate as a result of the framed  $\text{MgH}_2$  layer in the capacity vessel. This layer decreases the diffusion speed of hydrogen into further steps of metal along these lines the hydrogenation getting slower and slower (Webb 2015). To overcome this issue, the operation temperature transcends  $300 \text{ }^\circ\text{C}$  for adequate magnesium hydride formations.

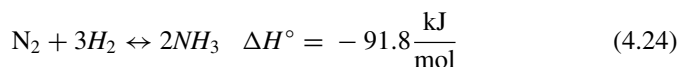
On the other hand, boron-based solid-state hydrogen storage is an alternative to metal hydrides. Boron is classified as a metalloid and involves both metallic and non-metallic properties. There are mainly two boron-based storage can be found in the literature;  $\text{NaBH}_4$  and  $\text{NH}_3\text{BH}_3$ . Both have bigger than 10% (wt) hydrogen capacity thanks to light boron with high storage capacity. Firstly,  $\text{NaBH}_4$  with a hydrogen storage capacity of 10.8% (wt) can be released from hydrogen at  $530 \text{ }^\circ\text{C}$  (Hoecke et al. 2021). The advantage of  $\text{NaBH}_4$  is the ability to give four moles hydrogen via reaction with water. Since the ships can produce pure water from the seawater thanks to evaporators, this reaction is beneficial. However, hydrogenate is not as simple as the dehydrogenation process, so the reverse reaction is hard. On the other hand,  $\text{NH}_3\text{BH}_3$  is another boron-based storage material for hydrogen. The gravimetric hydrogen capacity of this compound is higher than  $\text{NaBH}_4$  and it offers 19.4% (wt). One of the methods to release hydrogen from the compound is to apply heat, and above  $500 \text{ }^\circ\text{C}$  the process would be completed. The second is the hydrolysis reaction in an acidic solution at room temperature.

#### 4.4.1.4 Alternative Hydrogen Carriers

##### *Ammonia*

Ammonia is the key chemical in fertilizer production that forms 80% of the global consumption by combining hydrogen with nitrogen from the air (Hansson et al.

2020). Ammonia has a high gravimetric hydrogen storage capacity of 17.7% (wt) at a 10 bar liquid state (Zincir 2020). Ammonia-based storage of hydrogen is a good option for ships with its easy-to-handle properties, and its ability to be produced without carbon dioxide by the Haber–Bosch process (Foster et al. 2018). This process is an exothermic reaction that can be occurred at high temperature and high pressure, it can be expressed as the following Eq. (4.24):



The most common way to produce hydrogen from ammonia is thermolysis which needs very high temperatures typically above 650 °C (Mukherjee et al. 2018). At this point, catalyst gain importance but the need for temperature would have arisen if the catalyst getting cheaper.

#### *CO<sub>2</sub> based*

Methanol and formic acid are seen in this section as alternative hydrogen carriers for the shipping industry. Since both are viewed as elective hydrogen carriers, they differ from ammonia by their chemical properties.

Initially, formic acid has a gravimetric hydrogen storage limit of 4.4% (wt) and it is relatively low compared with different strategies. The main benefit of formic acid is the simple dehydrogenation measure at moderately lower temperatures compared to ammonia or methanol. However, it actually has a comparable issue as far as costly noble metal catalysts (Pérez-Fortes et al. 2016). Creation of formic acid from the hydrogenation of CO<sub>2</sub> is an uptrend as of late yet the high-pressure factor during the CO<sub>2</sub> separation is as yet an issue. Secondly, methanol is the simplest alcohol and it has a gravimetric hydrogen storage capacity of 12.5% (wt). Most commonly examined way of the renewable methanol is by hydrogenation of CO<sub>2</sub>. Dehydrogenation of methanol is realized mainly by steam reforming, oxidation, or thermolysis. The typical process occurs around 230 °C and up to 5 MPa. As an advantage, the relatively cheaper catalyst can be used during the synthesis of methanol.

#### *Organic Liquids*

Liquid organic hydrogen carriers (LOHCs) are based on the hydrogenation and dehydrogenation of the compounds to store hydrogen (Hu et al. 2015). The advantage of this method is easy handling compared to compression and appears like a promising method for ships.

The hydrogenations and dehydrogenation of LOHCs are exothermic and endothermic processes, respectively. Since the hydrogenation is an exothermic reaction, the generated heat should be removed to ensure the equilibrium. However, during dehydrogenation, heat energy should be supply for extraction of the hydrogen from the carrier. Therefore, using organic liquid for ships as a hydrogen carrier requires sustainable heat production and also a suitable heat management system to provide continuity and the efficiency of the hydrogen storage. Furthermore, LOHCs contain noble metal catalysts and this increases the cost. Although there are several types of

research on the use of non-noble metals, the lifetime of the catalyst is still a challenge to address (He et al. 2018). For instance, dodecahedron-N-ethyl carbazole is one the most investigated hydrogen carrier, and it needs costly materials like platinum or palladium as a catalyst.

Hydrogen has an extremely low ignition point and high combustibility, consequently, storage and use ought to be at the highest point of safety in a high-risk region like ships. Here the primary issue happens because of the poisonous properties of ammonia and explosion risk of high-pressure hydrogen tanks. Furthermore, bunkering framework and the worldwide spread of hydrogen bunkering stations are an outright requirement for the shipping industry in the meaning of applicability. However, it is likewise a typical issue for a wide range of storage techniques because of the usage frequency of hydrogen in the maritime industry. In this viewpoint, storage limit per weight and volume acquire significance for the ease of use onboard ships. The conspicuous techniques are compressed hydrogen in regards to its technological maturity and ammonia with relatively simpler storage conditions. Liquid hydrogen may be another solution in the next years if the onboard tank isolation and refrigeration system can be solved efficiently. The others are somewhat frail alternatives because of weighty ocean conditions and worldwide bunkering availabilities.

The efficiency is directly evaluated from the point of view of the energy need for hydrogen storage requirements. Van Hoecke et al. analyzed the total energy required to produce and store 1 kg hydrogen and the compressed hydrogen requirements seem like the optimum one among different methods (Hoecke et al. 2021).

Lastly, from the reliability perspective, ease of bunkering and onboard operational requirements are reviewed to evaluate the storage methods. The previous experiences in shipping industry are the key element to evaluate the reliability for bunkering and fuel operations. In this manner, liquid storage such as methanol, ammonia, liquid hydrogen, and also solid-state storage are the strong options. However, liquid hydrogen supply port still requires new and safe infrastructures and spread all over the world. Hence, methanol and ammonia are one step ahead of liquid hydrogen but formic acid has not been tested onboard ship yet and it reduces the advantage of methanol for CO<sub>2</sub> based storage in reliability.

## 4.5 Hydrogen Fuel Cells in Shipping

Fuel cells are electrochemical devices that can use hydrogen directly to generate electric power without any combustion process (Inal and Deniz 2018; Sharaf and Orhan 2014). There are many different application areas such as; fuel cell electric vehicles in the transportation sector, backup power sources for portable applications or energy, and heat generators for high power demands in stationary applications (Bassam 2017a; Ellamla et al. 2015; Hasani and Rahbar 2015; Inal and Deniz 2021; Ma et al. 2021; Sorlei et al. 2021; Abkenar et al. 2017; Wu and Bucknall 2020). Fuel cells play an important role during the transition to sustainable energy production with their fewer GHG emissions compared to fossil fuel using technologies like

internal combustion engines (Bicer and Dincer 2018). In this perspective, hydrogen fuel cells offer a great advantage for ships when the new emission regulations which are aiming to reduce GHG emissions of maritime transportation are considered (Bicer and Dincer 2018).

Fuel cells are formed from an electrolyte that is placed between a fuel electrode (anode) and an oxidant electrode (cathode). The hydrogen fed into the anode side releases its electrons to pass from an external circuit where the load is connected. Then, hydrogen atoms pass through the electrolyte to the cathode side and in presence of oxygen, they reunite with its electrons which are released at the anode side of the cell by producing water at the cathode side. The basic working equations can be seen in Eqs. (4.25) and (4.26).

Anode:



Cathode:



### 4.5.1 Fuel Cell Types

Fuel cells can be categorized according to their electrolyte types (Tronstad et al. 2017). There are mainly five types of commercial fuel cells; alkaline, proton exchange membrane, molten carbonate, solid oxide, and phosphoric acid. Alkaline fuel cell (AFC) is the first fuel cell type developed in 1939 (De-Troya et al. 2016). It works below 100 °C and uses relatively affordable alkaline electrolytes and this made it popular for a long time. AFCs are mostly used in NASA space shuttles to generate power during space missions. However, limited power capacity and requirements of pure hydrogen cause to lose its popularity compared to new fuel cell types. Proton exchange membrane fuel cells (PEMFC) are the most common and developed technology among different fuel cell types. It works at low temperatures and uses hydrogen in high purity as a fuel (Barbir 2005). In case of the need to use hydrocarbons as fuel, several methods of hydrogen extraction should be performed. PEMFC has two different working characteristics according to operating temperature; low and high. Low-temperature types (LT-PEMFC) are the most traditional ones compared to high-temperature working fuel cells (HT-PEMFC). As can be noticed from the classification, low-temperature types work below 100 °C, besides, high-temperature types work above 120 °C up to 200 °C (Rosli et al. 2017). The working temperature difference comes from the membrane material and its characteristics meanwhile the development of novel membranes and catalysts allows to work at higher temperatures. The higher temperatures offer an ability for reaching



higher efficiency and it reduces the sensitivity to impurities in the fuel, for example, HT-PEMFC is 3–5% less sensitive to CO compared to LT-PEMFC (Boaventura et al. 2011). The same approaches are valid for the three other high-temperature working fuel cells; solid oxide fuel cell (SOFC), phosphoric acid fuel cell (PAFC), and molten carbonate fuel cell (MCFC). Both can use hydrocarbons like natural gas as fuel thanks to high working temperature and internal reforming ability to produce hydrogen (Tronstad et al. 2017). However, it should be noted that, in the case of using hydrocarbons, the formation of CO<sub>2</sub> will be happened during the internal reforming to produce hydrogen. Therefore, not only power generation technology but also fuel type is also important in the aim of reaching zero-emission. While MCFC works around 600–800 °C, PAFC operates around 150–200 °C, and SOFC can reach to 1000 °C (Inal 2018; Marefati and Mehrpooya 2019). MCFC and SOFC have relatively higher energy output capacity (MW levels) and higher efficiency compared to low-temperature fuel cell types. They can be used with heat recovery systems, for instance, high-temperature fuel cells can be combined with steam and gas turbine systems by using flue gases to increase the total efficiency. In this case, the total efficiency can reach 85% (Tronstad et al. 2017). On the other hand, high-temperature fuel cells have slower start-up times, lower power density, and material corrosion disadvantages (Han et al. 2012). Due to the slow response time of fuel cells, an additional power source is required to supply peak power needs and store the excess energy for specific mission profiles (Garcia et al. 2009). Furthermore, since the researches on the extension of the fuel cell lifetime mostly focus on the PEMFC, the periodic change of electrolyte and components increase the operational cost for other types, especially for high-temperature types (Table 4.8).

Ship propulsion systems have high power requirements especially when they are compared with fuel cell cars. Therefore, it limits the range of fuel cell types as the main power unit. In this manner, MCFC and SOFC are the prominent types but PEMFC is also rapidly increasing the power capacity. Moreover, fuel cells are modular and it increases the flexibility of shipbuilding opportunities. So, fuel cells can be also an effective solution for electric production instead of the propulsion unit. But it should be noted that most of the ship-sourced emissions are coming from the main diesel engine which is used for powering the propeller.

**Table 4.8** Fuel cell types according to operation temperatures and efficiencies (Inal and Deniz 2020; Tronstad et al. 2017; Biert et al. 2016)

Type	Operation temperature (°C)	Efficiency (%)
AFC	50–90	50–60
LT-PEMFC	60–100	40–60
HT-PEMFC	120–200	40–80
PAFC	150–250	40–50
SOFC	800–1000	50–85
MCFC	600–700	40–85

## **4.5.2 Maritime Fuel Cell Projects**

Several fuel cell ship projects have been carried out for years and the most significant ones are briefly explained in this section.

### **4.5.2.1 FellowSHIP**

The FellowSHIP is one the most important fuel cell ship projects with the aim of demonstrating MCFC system onboard ship. The substantial side of the project is the use of a hydrocarbon fuel (LNG) instead of the pure hydrogen for a fuel cell system on an offshore supply vessel named “Viking Lady”. After an operation period of 18,500 h any  $\text{NO}_x$ ,  $\text{SO}_x$ , and PM emissions are observed (Ovrum and Dimopoulos 2012).

### **4.5.2.2 METHAPU**

The METHAPU project was aiming to develop and validate the successful application of methanol using SOFC system onboard ship. The tests were applied on a car carrier ship where the 20 kW SOFC is used which is developed by Wartsila (Bassam 2017b). The project has demonstrated the feasibility of methanol with fuel cell and assessed the environmental impact of this new fuel.

### **4.5.2.3 Nemo H2**

Nemo H2 program was a good demonstration of onboard hydrogen storage and PEMFC usage for powering a passenger ferry which operates in Amsterdam. Hybridization of 60 kW fuel cell system with lead acid battery packages shows a good performance, however, lack of hydrogen bunkering infrastructure causes not to enter into service (McConnell 2010).

### **4.5.2.4 ZEMSHIP**

The project is designed as an inland passenger ship equipped with PEMFC to serve in Hamburg, Germany. The ultimate goal was to demonstrate a zero-emission shipping using hydrogen fuel. In this perspective, installation of hybrid battery and fuel cell system successfully operated between 2006 and 2010.

#### 4.5.2.5 SchIBZ

This project is designed for the 500 kW diesel using SOFC system but only 27 kW is demonstrated on a multipurpose ship. Moreover, 50% electrical efficiency is reached for more than 1000 h by using low sulphur diesel oil by emitting lower pollutant emission compared to diesel engines at the 10 kW tests stands (Ma et al. [2021](#); Biert et al. [2016](#)).

#### 4.5.2.6 Pa-X-ell

The Pa-X-ell is the second project under SchIBZ program by focusing on the safety aspects of methanol fed HT-PEMFC powered ships. Rather than efficiency, emission or technical perspective, the project aims to find a suitable placement and management system for onboard alternative fuel and fuel cell applications (Table [4.9](#); Figs. [4.14](#) and [4.15](#)).

**Table 4.9** Examples of several fuel cell ship projects

Project	Time	FC type	Fuel type	Partners
FellowSHIP	2003–2013	MCFC	LNG	DNV&GL and Wartsila
METHAPU	2006–2009	SOFC	Methanol	Wartsila
Nemo H2	2008–2011	PEMFC	Hydrogen	Alewijnse
ZEMSHIP	2006–2010	PEMFC	Hydrogen	Proton motor
SchIBZ	2009–2016	SOFC	Diesel	Thyssen krupp
Pa-X-ell	2009–2016	HT-PEMFC	Methanol	Meyer werft

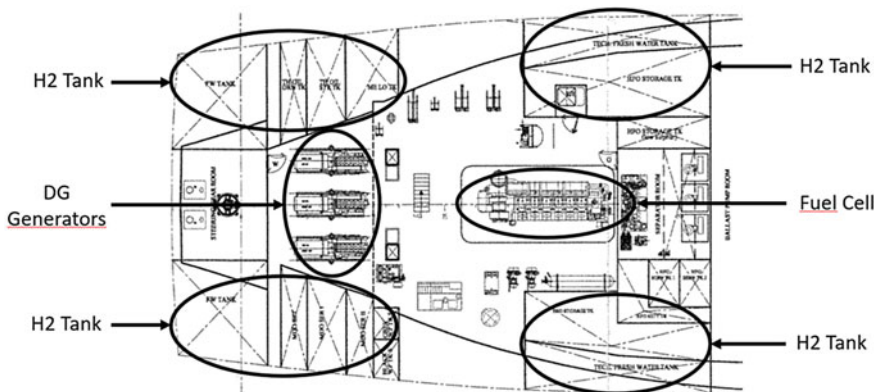


**Fig. 4.14** Possible placement of hydrogen tanks and fuel cell systems on the engine room plan of a chemical tanker ship (figure reproduced and adapted) (Inal [2018](#))

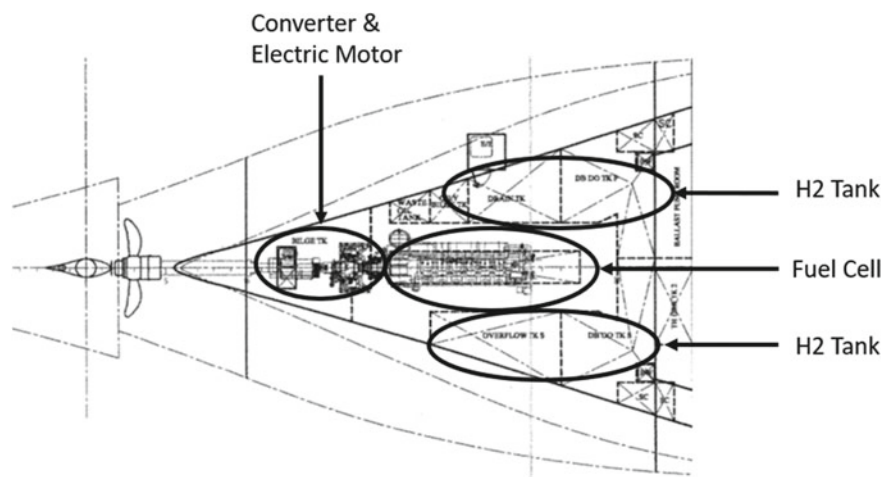


**Fig. 4.15** Possible placement of converter, electric motor, and hydrogen tanks on the engine room plan of a chemical tanker ship (figure reproduced and adapted) (Inal 2018)

## 4.6 Hydrogen Combustion in Marine Engines

Hydrogen is considered the most up-and-coming energy source because of its high heating value for unit mass, wide range of combustion limits, carbon-neutral content, and obtainability from renewable energy sources. This makes hydrogen as an attractive alternative fuel in the future. In this section, the potential usage of hydrogen in marine diesel engines will be examined.

### 4.6.1 Combustion of Hydrogen in Internal Combustion Engines

Carbon-free fuels are becoming significant topic in internal combustion engines. In order to decrease the harmful emissions of carbon-contained fuels, hydrogen is a prominent way for the transition of fuels into the environmentally friendly perspective.

There are significant breakthroughs at usage of hydrogen in the internal combustion engines. As a fuel, with zero-carbon content,  $H_2$  results in neither carbon emission nor soot, the water is produced as a combustion product. However, the pure  $H_2$  has technical drawbacks in combustion as well as in storage and transportation.

Hydrogen has higher heat value than other conventional fuels together with rapid burning and high reactivity specifications. Although intrinsic limitations of combustion of pure hydrogen in internal combustion engines owing to low ignition energy, there are many applications on both spark ignited and compression ignition engines.

The self-ignition of hydrogen and limited compression ratios in operation become more critical in high equivalence ratios. Therefore, applicable hydrogen combustion is generally limited to lean-combustion processes. The lean-combustion limitation enables low load operation with reduced peak power, can be eliminated by increased boost inlet pressures. Additionally,  $H_2$  can be advantageous to use with fuels that have relatively lower burning velocity and flammability. For instance, while the maximum burning velocity is 280 cm/s for hydrogen (Kwon and Faeth 2001), it is 6–8 cm/s and 40 cm/s for ammonia (Ronney 1988) and methane (Fells and Rutherford 1969), respectively. In the hydrogen-doped hydrocarbon fuels, the flame temperatures and flammability characteristics are increased. Therefore, the  $NO_x$  emissions increases together with increased  $H_2$  fraction in the mixture because of the elevated combustion temperatures (Li et al. 2014). On the other hand the  $H_2$  content in the fuel brings favourable effects on  $CO_2$  and soot emissions. The combustion concepts of hydrogen and subsequently marine engine applications are examined in the following parts.

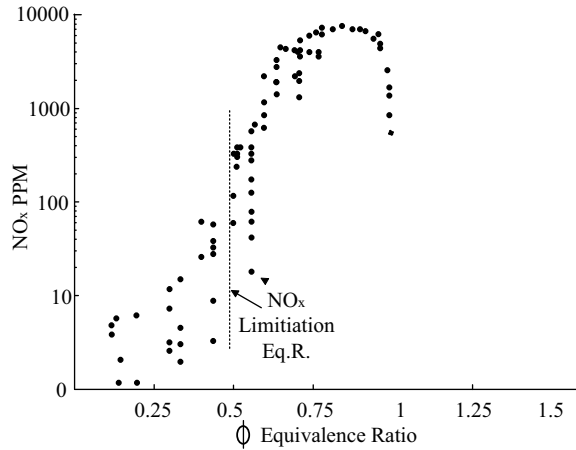
#### 4.6.1.1 Hydrogen as a Main Fuel for Internal Combustion Engines

Hydrogen fuel can be used in reciprocating engines with different cycles. The hydrogen combustion in the engines, as a main fuel, has been studied for premixed combustion applications for instance spark ignited engines and homogenous charge compression ignition engines generally. There are also some studies for compression ignition engines. Hydrogen has some intrinsic advantages and disadvantages for combustion in reciprocating engines where depends on characteristics of the engine and cycles.

Thanks to lean combustion capability of the hydrogen, the in-cylinder temperatures are not sufficient that to generate  $NO_x$  emissions at low load condition. That is a combustion characteristic of hydrogen, which allows low load operation. The capability of lean combustion characteristic enables  $NO_x$  emission reduction as an effective emission control strategy. The Fig. 4.16 represents the  $NO_x$  variation as a function of equivalence ration for hydrogen combustion (Tang et al. 2002). The compression ratios, in dataset, are between 12.5 and 15.3. It seems the limit for  $NO_x$  generation around 0.5 equivalence ration where a significant increment occurs above this value.

However in spite of high flammability temperature, low ignition energy of hydrogen causes unintended combustion timing near stoichiometric conditions, leads higher emissions levels (White et al. 2006). While auto ignition temperature is high for hydrogen, the activation energy quite low, comparing with the gasoline or methane (Lewis and Elbe 1962). Although the hydrogen has a wide operable equivalence ratio range, the limits, derived from increased  $NO_x$  levels and uncontrolled ignition, create a critical trade-off mechanism for combustion of hydrogen between power output and emissions. Hydrogen can be burned with spark plug in SI engines. Timing of ignition and injection has crucial role on combustion control (Hamada et al. 2013). Nevertheless, there are some issues to be solved in the engine design or operation basis

**Fig. 4.16** NO<sub>x</sub> generation as a function of equivalence ratio for H<sub>2</sub> combustion (figure reproduced and adapted) (Tang et al. 2002)

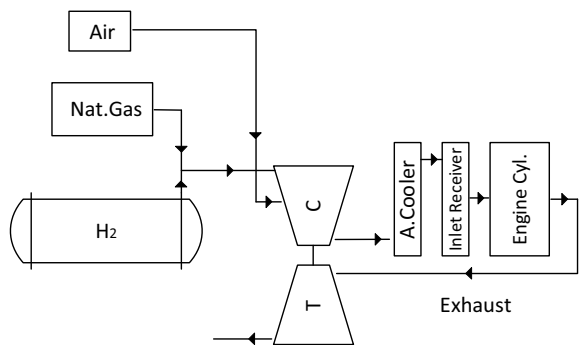


within the operation of the engine with hydrogen to inhibit knocking and nitrogen oxide emissions. NO<sub>x</sub> emission is derived from higher in-cylinder gas temperatures.

**4.6.1.2 Hydrogen-Natural Gas Combustion**

Natural gas has less carbon fraction than fuel oil by mass, thereby, the natural gas utilization is considered alternative fuel for carbon emission reduction. Particularly, lean-burn combustion of natural gas is highly attractive because of reduced NO<sub>x</sub> emissions and allowing high compression ratios. However, relatively low combustion speed and high ignition temperature gives disadvantage on natural gas combustion. In order to improve the combustion characteristics researchers show that, hydrogen addition can improve the flame speed (Ma and Wang 2008; Sapra et al. 2018). The schematic representation of H<sub>2</sub>-NG operation in a marine engine is demonstrated in Fig. 4.17.

**Fig. 4.17** The H<sub>2</sub> and Natural gas utilization in a marine SI engine



While the hydrogen addition can be carried out before TC together with natural gas, the NG can be injected to compressed air-H<sub>2</sub> mixture before cylinder inlet. The operation, performed in lean combustion with natural gas, the in-cylinder processes and the temperatures hence the NO<sub>x</sub> values can be diminished while the H<sub>2</sub> addition has contrary effect on all. However, by controlling the intake air amount, the temperatures and the NO<sub>x</sub> emissions could be achieved as the same amount which are under limitations.

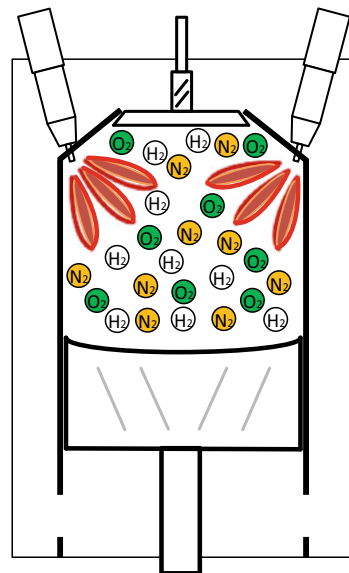
Together with NO<sub>x</sub> accomplishment the hydrogen provides more clean combustion with less carbon monoxide and complete combustion without hydrocarbon.

### 4.6.1.3 Hydrogen-Diesel Combustion

Combustion of hydrogen with diesel is carried out with diesel pilot fuel for the initiation of the combustion for the reason of high-self ignition temperature of hydrogen (Chintala and Subramanian 2016). Diesel combustion suffers from CO<sub>2</sub> and PM emissions because of the carbon mass fraction of the fuel. Altering the some part of diesel with the hydrogen by considering combustion energy equivalent of the diesel gives favourable effect on both carbon emissions and PM. Hydrogen addition can be conducted by two ways as intake port injection and injection at the beginning of compression stroke. A marine diesel scheme is demonstrated for the operation of the hydrogen in a two stroke marine diesel engine (Serrano et al. 2021) in Fig. 4.18.

The figure represents the engine that has uni-flow scavenging model. Hydrogen can be injected during induction via ports which are seen at the bottom of the liner or be injected after intake port and exhaust valve closes during compression. After the

**Fig. 4.18** Hydrogen mixture in a 2-stroke marine diesel engine (figure reproduced and adapted) (Serrano et al. 2021)



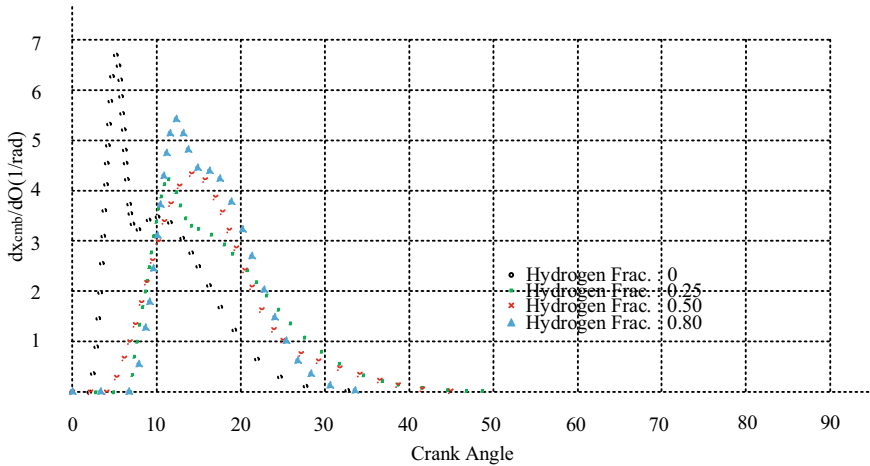


**Fig. 4.19** Parameterized heat release rate of fuel mixture for different  $H_2$  fractions (figure reproduced and adapted) (Serrano et al. 2021)

compression, the combustion is triggered by diesel injection around TDC. Hydrogen has an advantage to accelerate burning speed which causes different heat release rate during combustion process. The parametric heat release rate variation of fuel mixture (HFO- $H_2$ ) for different hydrogen fractions is given in Fig. 4.19 (Serrano et al. 2021).

It can be observed that two phase combustion (premixed and diffusive) becomes interpenetrated combustion phases with the addition of hydrogen. Also the study considers the water injection (WI) which causes ignition delay in  $H_2$  doped mixtures, however, WI has no significant effect on heat release rate shape.

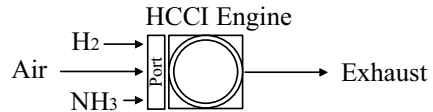
The rapid combustion of hydrogen could result in higher  $NO_x$  emission. As well as during diesel operation, the exhaust gas recirculation method (Wang et al. 2018) or water addition in the intake charge can be utilized to solve a high amount of  $NO_x$  generation in hydrogen-diesel combustion. The injection of the water in the air provide controlled combustion without self-ignition of hydrogen or knocking (Serrano et al. 2019). Addition of hydrogen in to the diesel combustion also increases the diesel combustion specific efficiency (Varde and Frame 1983).

#### 4.6.1.4 Hydrogen-Ammonia Combustion

Ammonia is considered as a clean energy carrier, compared with carbon contained fossil fuels with its carbon-free structure and obtainability from renewable energy sources as solar energy, wind energy or biomass. Both thanks to its energy density and easy storage capability, it can be used as a fuel in internal combustion engines, including marine engines (Zincir 2020). Ammonia is a significant hydrogen carrier with a capability of storage. It can be stored as liquefied phase in the room temperature which also allows an easy transportation. Howbeit there are favourable reasons to use,



**Fig. 4.20** H<sub>2</sub> and ammonia injection into the intake port for HCCI engine



the combustion properties as burning limitations (speed) and generation of nitrogen oxide emissions limit the operation of ammonia (Zhu et al. 2021). Therefore, it is a prevalent way that the ammonia is used with fuels, which have high reactivity. Diesel fuel, gasoline or natural gas improves the combustion performance of the ammonia as well as hydrogen (Feng et al. 2020; Yapicioglu and Dincer 2018). However, the high reactive fuels used with the ammonia, except hydrogen, contain carbon atoms, which prevent to achieve carbon dioxide neutral combustion. Hydrogen has an accelerant role on combustion, both increasing the reactivity and decreasing the time for ignition of the fuel. In order to increase the performance and practicality of ammonia, the hydrogen addition is a prominent way, which enables ammonia to use in internal combustion engines (Li et al. 2014; Lee et al. 2010) by injecting the ammonia and hydrogen in to the intake port. The representative scheme is shown in the Fig. 4.20 for the HCCI engine.

The combination of ammonia and hydrogen is regarded as ideal environmentally friendly fuel in the zero-carbon manner and has been studied by many researchers (Choi et al. 2015; Tang et al. 2021). The study (Wang et al. 2021) shows that even the addition of just 5% hydrogen improves combustion performance. By the addition of hydrogen the flame temperature increased 2080 K to ~2160 K and the laminar flame speed increased 13 m/s to 38 m/s around 1.1 equivalence ratio for 0% H<sub>2</sub> to 40% H<sub>2</sub> fraction, respectively in ammonia combustion. The doped hydrogen leads an increased propagation of combustion and also results in high NO<sub>x</sub> emissions (Rocha et al. 2019). Additionally, hydrogen addition helps to enhance the reactivity and the combustion rate of ammonia (Lee et al. 2010). On the other hand unburned ammonia can be used to decrease NO<sub>x</sub> emissions together with the high power output availability for the combustion (Valera-Medina et al. 2019).

#### 4.6.1.5 Hydrogen Usage for Heat Production

Boilers are used for heating purposes in the vessels. Oil tankers require heat and boiler operation during their voyages particularly (International Maritime Organization (IMO) 2020). The boilers also use conventional fuels which have carbon content. In the perspective of carbon-neutral operation, there are also some applications of hydrogen not in ships yet but industry exists. Catalytic combustion of hydrogen can be used for heat production purposes. Marine boilers, capable of producing steam for on-board usage, are convenient for the replacement of gas boilers for cleaner production. The mixture of methane and hydrogen can be used without major modification in burners, operated by natural gas (Ilbaş and Yilmaz 2012). The utilization of hydrogen together with ammonia and the hydrogen burners achieve

zero carbon emission mission (Hussein et al. 2019; Meraner et al. 2020). The studies mainly investigated the  $\text{NO}_x$  performance of the systems and a slight increase has been observed in hydrogen rich combustion (Pashchenko 2020).

### 4.6.2 Marine Engine Applications

To the best of author's knowledge, pure hydrogen combustion is not applicable yet, in marine engines. Due to the high power rates of marine engines and high temperatures through the components as exhaust valves, bring limitations for hydrogen combustion, while hydrogen requires high temperature for auto-ignition.

On the other hand, the injection of hydrogen in to the cylinder is another issue for marine engines which have two-stroke cycle and uniflow scavenging which allows bypass of hydrogen to the exhaust manifold without intervening the combustion process. Injection of  $\text{H}_2$  at the beginning of compression stroke is a solution which requires additional equipment, providing high pressure hydrogen in to the cylinder.

There are various studies about application of hydrogen combustion concept in marine engines.

An ammonia-hydrogen combustion is investigated for a marine engine theoretically in the research (Wang et al. 2021). The study carried for medium speed marine diesel engine (800 rpm) with homogenous charge combustion concept, for the ignition of the mixture for varying hydrogen fraction, intake temperature and pressure and for different fuel/air ratios. The study reveals that the flame propagation of ammonia enhanced with the addition of hydrogen. The equivalence ratio has an important effect on in-cylinder pressure, temperature and flame propagation. As the hydrogen concentration increases the strictness of initial condition of intake charge decreases. It is also stated that, in order to mitigate the  $\text{NO}_x$  emissions, additional treatment for reduce peak combustion temperature, as exhaust gas recirculation or after treatment are required.

In another study, the emission contribution of a ship to the environment during its lifetime was examined (Bicer and Dincer 2018). The study focussed on ocean going tanker and cargo vessel. The ships' environmental effects are revealed by comparing heavy fuel oil and other environmental friendly fuels as ammonia and hydrogen. Needless to say that production of hydrogen or ammonia costs  $\text{CO}_2$  equivalent that the most environmentally friendly sources used for the production are renewable energy sources. In the study, it was found that the  $\text{CO}_2$  equivalent of the heavy fuel oil is five times more than the hydrogen fuelled engines by considering hydrogen production with geothermal energy sources.

The combination of hydrogen and heavy fuel oil Combustion (HFO) in a marine diesel engine had been investigated in another research. In order to meet the emission requirements water injection was proposed as a  $\text{NO}_x$  emission reduction technology. The study comprises a modelling methodology for the prediction of combustion. The modelling study and the validation had been completed with the dataset of HFO combustion for two stroke low speed (125 rpm) marine diesel engine with 16 MW

power rate (Serrano et al. 2021). The study includes different hydrogen fractions in intake air for different engine loads to observe the effect on engine efficiency and the mean effective pressure. It is indicated that hydrogen can be supplied with two methods; (1) through port injection and (2) the injection after intake port closes. Since the two-stroke marine diesel engines have uniflow scavenging, some part of intake air passes the cylinder without any combustion process. In the port injection of hydrogen, significant amount of hydrogen bypasses the combustion zone which affects the efficiency of the engine. As a solution of problem, variable exhaust valve timing is applied to the engine operation in different loads. The exhaust valve timing advanced and the reduction of hydrogen bypass was achieved. The (2) second strategy is claimed as more effective than the (1) prior injection strategy without any excess leakage of hydrogen. However, additional modification is needed for injection after port closes. To sum up, hydrogen addition had increased the total efficiency by around 3.0% for max power of the marine diesel engine, and it has been indicated the high efficiency levels could be achieved with injection after the intake port closes. Another intake port injection study has been carried out for small sized two stroke marine diesel engines with 500 kW power (Pan et al. 2014). The hydrogen effect on the greenhouse gases for different fractions of hydrogen has been investigated. Noteworthy, reduction could be achieved in only idle speed of the engine, because of the limited flow amount of hydrogen into the intake air. It is obvious that the amount of hydrogen ratio highly affect the engine emissions. For the idle speed 20 to 37% of reduction of CO<sub>2</sub> emissions could be achieved. Study shows as the hydrogen contributes to the total energy input for the engine the emissions reduction can be achieved.

Natural gas combustion modelling with hydrogen has been investigated in marine spark ignited engine. The natural gas engine measurement were used to develop the engine combustion characteristics via modelling tool (Sapra et al. 2020). The cases are different mixtures' ratio of hydrogen and natural gas, different equivalence ratios with the engine load variation. The study shows Seilliger modelling has satisfied higher accuracy than Double-Wiebe function in the prediction of combustion process. In another experimental study, the hydrogen is used in 500 kW marine gas engine that performed with different engine loads and 2 different hydrogen fraction as 10–20% by volume (Sapra et al. 2018). The study shows that, the combustion duration has been reduced as a consequence of increased combustion speed by hydrogen. Additionally, the combustion could be controlled at lower equivalence ratios which also help to increase efficiency as providing complete combustion of carbon atoms. It seems 4% higher engine efficiency when compared to natural gas combustion. The few studies applied for marine engine purposes are given in this part. The application of hydrogen combustion will increase in the future of maritime sector.

## 4.7 Conclusion

Reducing the impact of shipping emissions on global warming is provided through carbon-free fuels. As a carbon-free fuel hydrogen is a promising alternative together with ammonia for the future of maritime transportation. Production of hydrogen need an energy source that can be provided by hydrocarbons, biomass, water-splitting, produce carbon emissions except using energy from renewable energy sources. While examining the favourable environmental impact of hydrogen, the emission costs in production process, must be taken into account. After production process, hydrogen storage is an important issue because of being gas phase in atmospheric conditions. While the volume required to store hydrogen at onshore facilities is not an issue, onboard storage is crucial due to the ship's limited gross tonnage. There are different ways to store hydrogen onboard as; liquid storage, compressed storage, solid-state storage, and alternative hydrogen carriers which have relative ease of storage capability. It is exceptionally evident that in not so distant future and with the present innovation, hydrogen can't be a solid option for ships yet, so the inventory network, bunkering, and capacity ought to be improved.

The hydrogen production lifecycle costs were examined in the study. According to the comparison of lifecycle costs of hydrogen production methods, steam reforming with CCS has the lowest hydrogen production cost recently. Pyrolysis and steam reforming without CCS followed it. The highest production cost is for coal gasification since it has the highest effect on human health and the environment. Nuclear and wind energies can cope with steam reforming, but solar energy is not an effective way to produce hydrogen for now.

The usage of hydrogen, to generate power in ships, performed by two main ways as fuel cells and internal combustion engines. Fuel cells are still expensive than conventional internal combustion engines. However, endeavours on emission mitigation drive the industry to alternative fuels and alternative energy producers. From this perspective, hydrogen fuel and fuel cells are promising technology with only water emissions. In the case of using hydrocarbons as fuel, fuel cells have still substantial advantages compared to marine diesel engines such as higher efficiency, lesser maintenance expenditures, lesser noise, and vibration onboard ships. Nevertheless, the first capital cost of fuel cells, limited lifetime, and difficulties onboard hydrogen storage of hydrogen are the major cost drivers and safety issues. For the maritime industry, hydrogen and fuel cells are still in early stages and immature technologies. As given before there are several problems to address. Whether these problems are resolved, it will be more realistic to expand fuel cell ships in commercial use.

The other way is combustion of hydrogen. Adding hydrogen to the intake air for the internal combustion engines both increasing the combustion efficiency and the engine total efficiency. The application reduces the emissions with the help of enhanced reaction capability and carbon-free content. While hydrogen can be burned in small spark-ignited engines directly, the knocking and self-ignition characteristics of hydrogen allow lean combustion and hinder usage in high power rated engines as marine engines. However, the addition of hydrogen into marine fuels as natural gas,

heavy fuel oil, or ammonia fuel gives significant advantages on emissions. Additionally, the dual-fuel concept significantly reduces the deficiencies of each individual fuel in combustion as low combustion speed, high soot emissions. The hydrogen utilization on ships initiated recently and it is expected to grow up in the near future of the shipping. To facilitate hydrogen usage at maritime transportation, bunkering infrastructures have to be spread worldwide, engine and fuel cell manufacturers have to speed up their development process, and safety procedures onboard have to be identified completely for hydrogen. Additional attention is needed for the adaptation of hydrogen based operation, during stricter emission regulations in maritime sector.

## References

- Abkenar T, Alireza AN, Gamin SD, Jayasinghe AK, Negnevitsky M (2017) Fuel cell power management using genetic expression programming in all-electric ships. *IEEE Trans Energy Convers* 32(2):779–787. <https://doi.org/10.1109/TEC.2017.2693275>
- Al-Qahtani A, Parkinson B, Hellgardt K, Shah N, Guillen-Gosalbez G (2021) Uncovering the true cost of hydrogen production routes using life cycle monetization. *Appl Energy* 281:115958. <https://doi.org/10.1016/j.apenergy.2020.115958>
- American Bureau of Shipping (ABS) (2021) Hydrogen as marine fuel. Sustainability Whitepaper. June 2021
- Amos WA (1998) Cost of storing and transporting hydrogen
- Andersson J, Grönkvist S (2019) Large-scale storage of hydrogen. *Int J Hydrogen Energy* 44(23):11901–11919. <https://doi.org/10.1016/j.ijhydene.2019.03.063>
- Barbir F (2005) PEM fuel cells theory and practice. Elsevier
- Bassam A (2017a) Use of voyage simulation to investigate hybrid fuel cell systems for marine propulsion. (June):275
- Bassam A (2017b) Use of voyage simulation to investigate hybrid fuel cell systems for marine propulsion. University of Southampton
- Baykara SZ (2018) Hydrogen: a brief overview on its sources, production and environmental impact. *Int J Hydrogen Energy* 43:10605–10614. <https://doi.org/10.1016/j.ijhydene.2018.02.022>
- Bicer Y, Dincer I (2018) Environmental impact categories of hydrogen and ammonia driven transoceanic maritime vehicles: a comparative evaluation. *Int J Hydrogen Energy* 43(9):4583–4596. <https://doi.org/10.1016/j.ijhydene.2017.07.110>
- Boaventura M, Sander H, Friedrich KA, Mendes A (2011) The Influence of CO on the current density distribution of high temperature polymer electrolyte membrane fuel cells. *Electrochim Acta* 56(25):9467–9475. <https://doi.org/10.1016/J.ELECTACTA.2011.08.039>
- Brynnolf S, Taljegard M, Grahn M, Hansson J (2018) Electrofuels for the transport sector: a review of production costs. *Renew Sustain Energy Rev* 81:1887–1905. <https://doi.org/10.1016/j.rser.2017.05.288>
- Chen HL, Lee HM, Chen SH, Chao Y, Chang MB (2008) Review of plasma catalysis on hydrocarbon reforming for hydrogen production—interaction, integration, and prospects. *Appl Catal B: Environmental* 85(1–2):1–9. <https://doi.org/10.1016/j.apcatb.2008.06.021>
- Chintala V, Subramanian KA (2016) Experimental investigation of hydrogen energy share improvement in a compression ignition engine using water injection and compression ratio reduction. *Energy Convers Manage*. <https://doi.org/10.1016/j.enconman.2015.10.069>
- Choi S, Lee S, Kwon OC (2015) Extinction limits and structure of counterflow nonpremixed hydrogen-doped ammonia/air flames at elevated temperatures. *Energy* 85:503–510. <https://doi.org/10.1016/j.energy.2015.03.061>

- Chryssakis C, Balland O, Tvette HA, Brandsæter A (2014) DNV GL strategic research & innovation position paper 1–2014, alternative fuels for shipping
- Das D, Veziroğlu TN (2001) Hydrogen production by biological processes: a survey of literature. *Int J Hydrogen Energy* 26(1):13–28. [https://doi.org/10.1016/S0360-3199\(00\)00058-6](https://doi.org/10.1016/S0360-3199(00)00058-6)
- Das D, Veziroğlu TN (2008) Advances in biological hydrogen production processes. *Int J Hydrogen Energy* 33(21):6046–6057. <https://doi.org/10.1016/j.ijhydene.2008.07.098>
- Demirbaş A (2001) Biomass resource facilities and biomass conversion processing for fuel and chemicals. *Energy Convers Manage* 42(11):1357–1378. [https://doi.org/10.1016/S0196-8904\(00\)00137-0](https://doi.org/10.1016/S0196-8904(00)00137-0)
- Deniz C, Zincir B (2016) Environmental and economical assessment of alternative marine fuels. *J Clean Prod* 113:438–449. <https://doi.org/10.1016/j.clepro.2015.11.089>
- De-Troya JJ, Álvarez C, Fernández-Garrido C, Carral L (2016) Analysing the possibilities of using fuel cells in ships. *Int J Hydrogen Energy* 41(4):2853–2866. <https://doi.org/10.1016/j.ijhydene.2015.11.145>
- Dincer I, Acar C (2015) Review and evaluation of hydrogen production methods for better sustainability. *Int J Hydrogen Energy* 40:11094–11111. <https://doi.org/10.1016/j.ijhydene.2014.12.035>
- Ellamla HR, Staffell I, Bujlo P, Pollet BG, Pasupathi S (2015) Current status of fuel cell based combined heat and power systems for residential sector. *J Power Sources* 293:312–328. <https://doi.org/10.1016/j.jpowsour.2015.05.050>
- El-Shafie M, Kambara S, Hayakawa Y (2019) Hydrogen production technologies overview. *J Power Energy Eng* 7:107–154. <https://doi.org/10.4236/jpee.2019.71007>
- European Energy Agency (EEA) (2019) Emissions of air pollutants from transport. <https://www.eea.europa.eu/data-and-maps/indicators/transport-emissions-of-air-pollutants-8/transport-emissions-of-air-pollutants-6#tab-related-briefings>
- Fan YV, Perry S, Klemes JJ, Lee CT (2018) A review on air emissions assessment: transportation. *J Clean Prod* 194:673–684
- Fells I, Rutherford AG (1969) Burning velocity of methane-air flames. *Combust Flame* 13(2):130–138. [https://doi.org/10.1016/0010-2180\(69\)90043-1](https://doi.org/10.1016/0010-2180(69)90043-1)
- Feng Y, Zhu J, Mao Y, Raza M, Qian Y, Yu L, Lu X (2020) Low-temperature auto-ignition characteristics of NH<sub>3</sub>/diesel binary fuel: Ignition delay time measurement and kinetic analysis. *Fuel*. <https://doi.org/10.1016/j.fuel.2020.118761>
- Foster SL, Pere SI, Bakovic RD, Duda SM, Milton RD, Minter SD, Janik MJ, Renner JN, Greenlee LF (2018) Catalysts for nitrogen reduction to ammonia. *Nat Catal* 1(7):490–500. <https://doi.org/10.1038/s41929-018-0092-7>
- Funk JE (2001) Thermochemical hydrogen production: past and present. *Int J Hydrogen Energy* 26(3):185–190. [https://doi.org/10.1016/S0360-3199\(00\)00062-8](https://doi.org/10.1016/S0360-3199(00)00062-8)
- Garcia P, Fernandez LM, Garcia CA, Jurado F (2009) Fuel cell-battery hybrid system for transport applications. In: International conference on electrical machines and systems ICEMS
- Guo YS, Fang WJ, Lin RS (2005) Coking-inhibition of pyrolysis-cracking of endothermic hydrocarbon fuel. *J Zhejiang Univ* 39:538–541
- Hamada KI, Rahman MM, Abdullah MA, Bakar RA, Aziz ARA (2013) Effect of mixture strength and injection timing on combustion characteristics of a direct injection hydrogen-fueled engine. *Int J Hydrogen Energy*. <https://doi.org/10.1016/j.ijhydene.2013.01.092>
- Han J, Charpentier JF, Tang T (2012) State of the art of fuel cells for ship applications. In: IEEE international symposium on industrial electronics (April):1456–1461. <https://doi.org/10.1109/ISIE.2012.6237306>
- Hansson J, Brynolf S, Fridell E, Lehtveer M (2020) The potential role of ammonia as marine fuel-based on energy systems modeling and multi-criteria decision analysis. *Sustainability (switzerland)* 12(8):10–14. <https://doi.org/10.3390/SU12083265>
- Hasani M, Rahbar N (2015) Application of thermoelectric cooler as a power generator in waste heat recovery from a PEM fuel cell—An experimental study. *Int J Hydrogen Energy* 40(43):15040–15051. <https://doi.org/10.1016/j.ijhydene.2015.09.023>

- He Y, Song Y, Cullen DA, Laursen S (2018) Selective and stable non-noble-metal intermetallic compound catalyst for the direct dehydrogenation of propane to propylene. *J Am Chem Soc* 140(43):14010–14014. <https://doi.org/10.1021/jacs.8b05060>
- Hoecke V, Laurens LL, Campe R, Perreault P, Verbruggen SW, Lenaerts S (2021) Challenges in the use of hydrogen for maritime applications. *Energy Environ Sci* (x). <https://doi.org/10.1039/d0ee01545h>
- Holladay JD, Hu J, King DL, Wang Y (2009) An overview of hydrogen production technologies. *Catal Today* 139(4):244–260. <https://doi.org/10.1016/j.cattod.2008.08.039>
- Hu P, Fogler E, Diskin-Posner Y, Iron MA, Milstein D (2015) A novel liquid organic hydrogen carrier system based on catalytic peptide formation and hydrogenation. *Nat Commun* 6. <https://doi.org/10.1038/ncomms7859>
- Hussein NA, Valera-Medina A, Alsaegh AS (2019) Ammonia- hydrogen combustion in a swirl burner with reduction of NO<sub>x</sub> emissions. *Energy Procedia*. <https://doi.org/10.1016/j.egypro.2019.01.265>
- Ilbaş M, Yilmaz I (2012) Experimental analysis of the effects of hydrogen addition on methane combustion. *Int J Energy Res*. <https://doi.org/10.1002/er.1822>
- International Maritime Organization (IMO) (2021c) IMO data collection system. <https://www.imo.org/en/ourwork/environment/pollutionprevention/airpollution/pages/data-collection-system.aspx>
- Inal, OB (2018) Analysis of the availability and applicability of fuel cell as a main power unit for a commercial ship. Istanbul Technical University
- Inal OB, Deniz C (2018) Fuel cell availability for merchant ships. In: 3rd international naval architecture and maritime symposium. Istanbul, pp 907–16
- Inal, OB, Deniz C (2020) Assessment of fuel cell types for ships: Based on multi-criteria decision analysis. *J Cleaner Produ* 265:121734. <https://doi.org/10.1016/j.jclepro.2020.121734>
- Inal OB, Deniz C (2021) Emission analysis of LNG Fuelled molten carbonate fuel cell system for a chemical tanker ship: a case study. *Mar Sci Technol Bulletin* 10:118–133. <https://doi.org/10.33714/masteb.827195>
- Inal OB, Zincir B, Deniz C (2021a) Comparison of hydrogen and ammonia for the decarbonization of shipping. In: 5th international hydrogen technologies congress (IHTEC-2021), May 26–28, 2021, Online
- Inal OB, Dere C, Deniz C (2021b) Onboard hydrogen storage for ships : An overview onboard hydrogen storage. In: in 5th international hydrogen technologies congress
- International Maritime Organization (IMO) (2011) Resolution MEPC.203(62), Annex 19, Adopted on 15 July 2011. Amendments to the annex of the protocol of 1997 to amend the international convention for the prevention of pollution from ships, 1973, as modified by the protocol of 1978 relating thereto (inclusion of regulations on energy efficiency for ships in MARPOL annex VI)
- International Maritime Organization (IMO) (2015) Third IMO greenhouse gas study
- International Maritime Organization (IMO) (2018) Adoption of the initial IMO strategy on reduction of GHG emissions from ships and existing IMO activity related to reducing GHG emissions in the shipping sector
- International Maritime Organization (IMO) (2020) The Fourth IMO GHG study -reduction of Ghg emissions from ships
- International Maritime Organization (IMO) (2021a) Nitrogen oxides. [https://www.imo.org/en/OurWork/Environment/PollutionPrevention/AirPollution/Pages/Nitrogen-oxides-\(NOx\)-%25E2%2580%2593-Regulation-13.aspx](https://www.imo.org/en/OurWork/Environment/PollutionPrevention/AirPollution/Pages/Nitrogen-oxides-(NOx)-%25E2%2580%2593-Regulation-13.aspx)
- International Maritime Organization (IMO) (2021b) Sulphur oxides. [https://www.imo.org/en/OurWork/Environment/PollutionPrevention/AirPollution/Pages/Sulphur-oxides-\(SOx\)-%25E2%2580%2593-Regulation-14.aspx](https://www.imo.org/en/OurWork/Environment/PollutionPrevention/AirPollution/Pages/Sulphur-oxides-(SOx)-%25E2%2580%2593-Regulation-14.aspx)
- Iribarren D, Susmozas A, Petrakopoulou F, Dufour J (2014) Environmental and exergetic evaluation of hydrogen production via lignocellulosic biomass gasification. *J Clean Prod* 69:165–175. <https://doi.org/10.1016/j.clepro.2014.01.068>

- Kannah RY, Kavitha S, Preethi, Karthikeyan OP, Kumar G, Dai-Viet NV, Banu JR (2021) Techno-economic assessment of various hydrogen production methods—a review. *Bioresour Technol* 319:124175. <https://doi.org/10.1016/j.biortech.2020.124175>
- Kapdan IK, Kargi F (2006) Bio-hydrogen production from waste materials. *Enzyme Microb Technol* 38(5):569–582. <https://doi.org/10.1016/j.enzmictec.2005.09.015>
- Kwon OC, Faeth GM (2001) Flame/stretch interactions of premixed hydrogen-fueled flames: measurements and predictions. *Combust Flame*. [https://doi.org/10.1016/S0010-2180\(00\)00229-7](https://doi.org/10.1016/S0010-2180(00)00229-7)
- Lee JH, Kim JH, Park JH, Kwon OC (2010) Studies on properties of laminar premixed hydrogen-added ammonia/air flames for hydrogen production. *Int J Hydrogen Energy* 35(3):1054–1064. <https://doi.org/10.1016/j.ijhydene.2009.11.071>
- Levene JI, Mann MK, Margolis RM, Millbrandt A (2007) An analysis of hydrogen production from renewable electricity sources. *Sol Energy* 81(6):773–780. <https://doi.org/10.1016/j.solener.2006.10.005>
- Lewis B, Von Elbe G (1962) Combustion, flames, and explosions of gases. *J Chem Educ*. <https://doi.org/10.1021/ed039pa312.2>
- Li J, Huang H, Kobayashi N, He Z, Nagai Y (2014) Study on using hydrogen and ammonia as fuels: combustion characteristics and NO<sub>x</sub> formation. *Int J Energy Res* 38:1214–1223. <https://doi.org/10.1002/er.3141>
- Ma S, Lin M, Lin TE, Lan T, Liao X, Maréchal, Van Herle J, Yang Y, Dong C, Wang L (2021) Fuel cell-battery hybrid systems for mobility and off-grid applications: a review. *Renew Sustain Energy Rev* 135(July 2020). <https://doi.org/10.1016/j.rser.2020.110119>
- Ma F, Wang Y (2008) Study on the extension of lean operation limit through hydrogen enrichment in a natural gas spark-ignition engine. *Int J Hydrogen Energy*. <https://doi.org/10.1016/j.ijhydene.2007.12.040>
- Maeda K, Domen K (2010) Photocatalytic water splitting: recent progress and future challenges. *J Phys Chem Lett* 1(18):2655–2661. <https://doi.org/10.1021/jz1007966>
- Marefati M, Mehrpooya M (2019) Introducing and investigation of a combined molten carbonate fuel cell, thermoelectric generator, linear fresnel solar reflector and power turbine combined heating and power process. *J Cleaner Prod* 240:118247. <https://doi.org/10.1016/j.jclepro.2019.118247>
- McConnell VP (2010) Now, voyager? The increasing marine use of fuel cells. *Fuel Cells Bull* 2010(5):12–17. [https://doi.org/10.1016/S1464-2859\(10\)70166-8](https://doi.org/10.1016/S1464-2859(10)70166-8)
- Meraner C, Li T, Ditaranto M, Løvås T (2020) Effects of scaling laws on the combustion and NO<sub>x</sub> characteristics of hydrogen burners. *Combust Flame*. <https://doi.org/10.1016/j.combustflame.2020.01.010>
- Mukherjee S, Devaguptapu SV, Sviripa A, Lund CRF, Wu G (2018) Low-temperature ammonia decomposition catalysts for hydrogen generation. *Appl Catal B: Environ* 226:162–181
- Muradov NZ (1993) How to produce hydrogen from fossil fuels without CO<sub>2</sub> emission. *Int J Hydrogen Energy* 18(3):211–215. [https://doi.org/10.1016/0360-3199\(93\)90021-2](https://doi.org/10.1016/0360-3199(93)90021-2)
- Ni M, Leung DYC, Leung MKH, Sumathy K (2006) An overview of hydrogen production from biomass. *Fuel Process Technol* 87(5):461–472. <https://doi.org/10.1016/j.fuproc.2005.11.003>
- Nikolaidis P, Poullikkas A (2017) A comparative overview of hydrogen production processes. *Renew Sustain Energy Rev* 67:597–611. <https://doi.org/10.1016/j.rser.2016.09.044>
- O'Malley K, Ordaz G, Adams J, Randolph K, Ahn CC, Stetson NT (2015) Applied hydrogen storage research and development: a perspective from the U.S. department of energy. *J Alloy Compd* 645(S1):S419–S422. <https://doi.org/10.1016/j.jallcom.2014.12.090>
- Ovrum E, Dimopoulos G (2012) A validated dynamic model of the first marine molten carbonate fuel cell. *Appl Therm Eng* 35:15–28. <https://doi.org/10.1016/j.applthermaleng.2011.09.023>
- Pan H, Pournazeri S, Princevac M, Miller JW, Mahalingam S, Khan MY, Jayaram V, Welch WA (2014) Effect of hydrogen addition on criteria and greenhouse gas emissions for a marine diesel engine. *Inter J Hydrogen Energy* 39(21):11336–11345. <https://doi.org/10.1016/j.ijhydene.2014.05.010>



- Pashchenko D (2020) Hydrogen-rich fuel combustion in a swirling flame: CFD-modeling with experimental verification. *Int J Hydrogen Energy*. <https://doi.org/10.1016/j.ijhydene.2020.05.113>
- Pérez-Fortes M, Schöneberger JC, Boulamanti A, Harrison G, Tzimas E (2016) Formic acid synthesis using CO<sub>2</sub> as raw material: Techno-economic and environmental evaluation and market potential. *Int J Hydrogen Energy* 41(37):16444–16462. <https://doi.org/10.1016/j.ijhydene.2016.05.199>
- Qyyum MA, Dickson R, Shah SFA, Niaz H, Khan A, Liu JJ, Lee M (2021) Availability, versatility, and viability of feedstocks for hydrogen production: product space perspective. *Renew Sustain Energy Rev* 145:110843. <https://doi.org/10.1016/j.rser.2021.110843>
- Rauci C, Calleya J, de la Fuente SS, Pawling R (2015) Hydrogen on board ship: A first analysis of key parameters and implications. In: International conference on shipping in changing climates 12
- Rivard E, Trudeau M, Zaghbi K (2019) Hydrogen storage for mobility: a review. *Materials* 12(12). <https://doi.org/10.3390/ma12121973>
- Rixhon X, Limpens G, Coppitters D, Jeanmart H, Contino F (2021) The role of electrofuels under uncertainties for the Belgian energy transition. *Energies* 14:4027. <https://doi.org/10.3390/en14134027>
- Rocha, R. C. da, Costa, M., & Bai, X. S. (2019). Chemical kinetic modelling of ammonia /hydrogen/air ignition, premixed flame propagation and NO emission. *Fuel*, 246(December 2018), 24–33. <https://doi.org/10.1016/j.fuel.2019.02.102>
- Ronney PD (1988) Effect of chemistry and transport properties on near-limit flames at microgravity. *Combust Sci Technol*. <https://doi.org/10.1080/00102208808947092>
- Rosli RE, Sulong AB, Daud WRW, Zulkifley MA, Husaini T, Rosli MI, Majlan EH, Haque MA (2017) A review of high-temperature proton exchange membrane fuel cell (HT-PEMFC) system. *Int J Hydrogen Energy* 42(14):9293–9314. <https://doi.org/10.1016/j.ijhydene.2016.06.211>
- Sapra HD, Linden Y, Van Sluijs W, Godjevac M, Visser K (2018) Experimental investigations of hydrogen-natural gas engines for maritime applications. In ASME 2018 internal combustion engine division fall technical conference, ICEF 2018. <https://doi.org/10.1115/ICEF2018-9615>
- Sapra H, Godjevac M, De Vos P, Van Sluijs W, Linden Y, Visser K (2020) Hydrogen-natural gas combustion in a marine lean-burn SI engine: a comparative analysis of Seiliger and double Wiebe function-based zero-dimensional modelling. *Energy Convers Manage* 207(February):112494. <https://doi.org/10.1016/j.enconman.2020.112494>
- Serrano J, Jiménez-Espadafor FJ, López A (2019) Analysis of the effect of different hydrogen/diesel ratios on the performance and emissions of a modified compression ignition engine under dual-fuel mode with water injection. *Hydrogen-diesel dual-fuel mode*. *Energy*. <https://doi.org/10.1016/j.energy.2019.02.027>
- Serrano J, Jiménez-Espadafor FJ, López A (2021) Prediction of hydrogen-heavy fuel combustion process with water addition in an adapted low speed two stroke diesel engine: performance improvement. *Appl Therm Eng* 195:117250. <https://doi.org/10.1016/j.applthermaleng.2021.117250>
- Sharaf OZ, Orhan MF (2014) An overview of fuel cell technology: fundamentals and applications. *Renew Sustain Energy Rev* 32:810–853. <https://doi.org/10.1016/j.rser.2014.01.012>
- Sorlei I-S, Bizon N, Thounthong P, Varlam M, Carcadea E, Culcer M, Iliescu M, Raceanu M (2021) Fuel cell electric vehicles—a brief review of current topologies and energy management strategies. *Energies* 14(1):252. <https://doi.org/10.3390/en14010252>
- Staffell I, Scamman D, Velazquez Abad A, Balcombe P, Dodds PE, Ekins P, Shah N, Ward KR (2019) The role of hydrogen and fuel cells in the global energy system. *Energy Environ Sci* 12:463–491
- Steinfeld A (2005) Solar thermochemical production of hydrogen—a review. *Sol Energy* 78(5):603–615. <https://doi.org/10.1016/j.solener.2003.12.012>
- Taibi E, Miranda R, Vanhoudt W, Winkel T, Lanoix JC, Barth F (2018) Hydrogen from renewable power: technology outlook for the energy transition

- Tang G, Jin P, Bao Y, Chai WS, Zhou L (2021) Experimental investigation of premixed combustion limits of hydrogen and methane additives in ammonia. *Int J Hydrogen Energy* 46(39):20765–20776. <https://doi.org/10.1016/j.ijhydene.2021.03.154>
- Tang X, Kabat DM, Natkin RJ, Stockhausen WF, Heffel J (2002) Ford P2000 hydrogen engine dynamometer development. In: SAE Tech Pap. <https://doi.org/10.4271/2002-01-0242>
- Tronstad T, Åstrand HH, Haugom GP, Langfeldt L (2017) Study on the use of fuel cells in shipping U. S. Energy Information Agency (EIA) (2017) International Energy Outlook 2017
- United Nations Conference on Trade and Development (UNCTAD) (2020) Review of maritime transport 2020
- Valera-Medina A, Gutesa M, Xiao H, Pugh D, Giles A, Goktepe B, Marsh R, Bowen P (2019) Premixed ammonia/hydrogen swirl combustion under rich fuel conditions for gas turbines operation. *Int J Hydrogen Energy* 44(16):8615–8626. <https://doi.org/10.1016/j.ijhydene.2019.02.041>
- van Biert L, Godjevac M, Visser K, Aravind PV (2016) A review of fuel cell systems for maritime applications. *J Power Sources* 327(X):345–364. <https://doi.org/10.1016/j.jpowsour.2016.07.007>
- Varde KS, Frame GA (1983) Hydrogen aspiration in a direct injection type diesel engine-its effects on smoke and other engine performance parameters. *Int J Hydrogen Energy*. [https://doi.org/10.1016/0360-3199\(83\)90007-1](https://doi.org/10.1016/0360-3199(83)90007-1)
- Wang L, Liu D, Yang Z, Li H, Wei L, Li Q (2018) Effect of H<sub>2</sub> addition on combustion and exhaust emissions in a heavy-duty diesel engine with EGR. *Int J Hydrogen Energy*. <https://doi.org/10.1016/j.ijhydene.2018.10.104>
- Wang Y, Zhou X, Liu L (2021) Theoretical investigation of the combustion performance of ammonia /hydrogen mixtures on a marine diesel engine. *Int J Hydrogen Energy* 46(27):14805–14812. <https://doi.org/10.1016/j.ijhydene.2021.01.233>
- Webb CJ (2015) A review of catalyst-enhanced magnesium hydride as a hydrogen storage material. *J Phys Chem Solids* 84(1):96–106. <https://doi.org/10.1016/j.jpcs.2014.06.014>
- White CM, Steeper RR, Lutz AE (2006) The hydrogen-fueled internal combustion engine: a technical review. *Int J Hydrogen Energy* 31(10):1292–1305. <https://doi.org/10.1016/j.ijhydene.2005.12.001>
- Wu P, Bucknall R (2020) Hybrid fuel cell and battery propulsion system modelling and multi-objective optimisation for a coastal ferry. *Int J Hydrogen Energy* 45(4):3193–3208. <https://doi.org/10.1016/j.ijhydene.2019.11.152>
- Yamashita A, Kondo M, Goto S, Ogami N (2015) Development of high-pressure hydrogen storage system for the Toyota ‘Mirai.’ SAE Tech Pap. <https://doi.org/10.4271/2015-01-1169>
- Yapicioglu A, Dincer I (2018) Performance assesment of hydrogen and ammonia combustion with various fuels for power generators. *Int J Hydrogen Energy*. <https://doi.org/10.1016/j.ijhydene.2018.08.198>
- Yartys VA, Lototskyy MV, Akiba E, Albert R, Antonov VE, Ares JR, Baricco M, Bourgeois N, Buckley CE, Bellosta von Colbe JM, Crivello JC, Cuevas F, Denys RV, Dornheim M, Felderhoff M, Grant DM, Hauback BC, Humphries TD, Jacob I, Jensen TR, de Jongh PE, Joubert JM, Kuzovnikov MA, Latroche M, Paskevicius M, Pasquini L, Popilevsky L, Skripnyuk VM, Rabkin E, Sofianos MV, Stuart A, Walker G, Wang H, Webb CJ, Zhu M (2019) Magnesium based materials for hydrogen based energy storage: past, present and future. *Int J Hydrogen Energy* 44(15):7809–7859. <https://doi.org/10.1016/j.ijhydene.2018.12.212>
- Yi P, Li T, Wei Y, Zhou X (2021) Experimental and numerical investigation of low sulfur heavy fuel oil spray characteristics under high temperature and pressure conditions. *Fuel* 286:119327. <https://doi.org/10.1016/j.fuel.2020.119327>
- Zhu X, Khateeb AA, Guiberti TF, Roberts WL (2021) NO and OH\* emission characteristics of very-lean to stoichiometric ammonia-hydrogen-air swirl flames. *Proc Combust Inst* 38(4):5155–5162. <https://doi.org/10.1016/j.proci.2020.06.275>
- Zincir B (2020) A short review of ammonia as an alternative marine fuel for decarbonised maritime transportation. In: Proceedings of ICEESEN2020

- Zincir B, Deniz C (2014) An investigation of hydrogen blend fuels applicability on ships. In: 2nd international symposium on naval architecture and maritime, Istanbul, 23–24 Oct 2014
- Zincir B, Deniz C (2016) Comparison of hydrogen production methods for shipboard usage. In: 10th symposium on high-performance marine vehicles (HIPER'16), Cortona, 17–19 Oct 2016
- Zincir B, Deniz C (2018) Assessment of alternative fuels from the aspect of shipboard safety. *J ETA Marit Sci* 6(3):199–214. <https://doi.org/10.5505/jems.2018.71676>
- Zincir B, Deniz C (2021) Methanol as a fuel for marine diesel engines. In: Shukla PC, Belgiorno G, Di Blasio G, Agarwal AK (eds) *Alcohol as an alternative fuel for internal combustion engines. Energy, Environment, and Sustainability*. Springer, Singapore, [https://doi.org/10.1007/978-981-16-0931-2\\_4](https://doi.org/10.1007/978-981-16-0931-2_4)

# Chapter 5

## Improving Cold Flow Properties of Biodiesel, and Hydrogen-Biodiesel Dual-Fuel Engine Aiming Near-Zero Emissions



Murari Mohon Roy 

**Abstract** Increasing concerns over environmental issues and traditional resource depletion have heightened the motivation to use clean and alternative fuels. Biodiesel is an alternate renewable fuel to be used in diesel engines. On the other hand, expert studies designate hydrogen as the fuel of the longer term. Ideally, it is possible to possess both zero-greenhouse gas (GHG) emissions, and zero regulated emissions, carbon monoxide (CO), particulate matter (PM), hydrocarbon (HC) and nitrogen oxides (NO<sub>x</sub>) from IC engines powered by hydrogen. A dual-fuel combustion system that burns hydrogen as the primary fuel and biodiesel as a pilot fuel is the main focus of this work. Use of diesel in dual-fuel combustion is typical. To completely replace diesel with biodiesel, improvement of cold flow properties (CFPs) of biodiesel is an absolute necessity. Cold flow properties indicate the low-temperature operation ability of any fuel. To render biodiesel usable during winter, biodiesel requires urea fractionation, which is discussed in this study. The most challenges with a hydrogen-operated dual-fuel engine are the power output almost like that of diesel engines, and to sustain stable engine operation at lean engine running conditions. Supercharging can address the power output issue, but it increases the likelihood of premature ignition and knock tendency unless the equivalence ratio and other parameters are properly adjusted. A hydrogen-diesel supercharged dual-fuel engine results are presented in this study. The charge dilution (by N<sub>2</sub>) that helps to lower NO<sub>x</sub> emissions is also presented. Furthermore, a detailed engine conditions and engine parameters are suggested to make near-zero emissions from hydrogen-biodiesel dual-fuel engine.

**Keywords** Biodiesel · Fractionation · Cold flow properties of biodiesel · Hydrogen · Supercharging · Hydrogen-biodiesel dual-fuel engine · Emissions

---

M. M. Roy (✉)

Mechanical Engineering Department, Lakehead University, Thunder Bay, ON P7B 51, Canada  
e-mail: [mmroy@lakeheadu.ca](mailto:mmroy@lakeheadu.ca)

## 5.1 Introduction

Gases that trap heat within the atmosphere are called greenhouse gases. There are four main greenhouse gases: carbon dioxide (CO<sub>2</sub>), methane (CH<sub>4</sub>), nitrous oxide (N<sub>2</sub>O) and fluorinated gases. CO<sub>2</sub> is the primary GHG emitted through human activities. In 2019, CO<sub>2</sub> accounted for about 76 percent globally (<https://www.epa.gov/ghg-emissions/global-greenhouse-gas-emissions-data>) and 80 percent of all U.S. GHG emissions from human activities (<https://www.epa.gov/ghgemissions/overview-greenhouse-gases>). The most act that emits CO<sub>2</sub> is the combustion of fossil fuels (coal, naturel gas, and oil) for energy and transportation. Internal combustion (IC) engines are serving mankind in transportation and stationary power generations over a century. Transport accounts for around one-fifth of worldwide CO<sub>2</sub> emissions. The worldwide transport sector was liable for approximately eight billion metric tons of CO<sub>2</sub> emissions in 2018 (<https://www.statista.com/statistics/1185535/transport-carbon-dioxide-emissions-breakdown/>). Undesirable emissions in combustion engines are of major concern due to their negative impact on air quality and human health. Undesirable emissions include unburned HC, CO, NO<sub>x</sub>, and PM. Therefore, emissions of CO, HC, NO<sub>x</sub> and PM also are a big concern for the continuation of the IC engines within the latter a part of this century. Due to the global warming of CO<sub>2</sub> from fuel combustion and related heating effect, and high emissions of air pollutants like CO, PM, HC and NO<sub>x</sub> some experts suspect that the traditional IC engine is entering its sunset era.

The Paris Agreement is a world treaty on global climate change. It had been adopted by 196 Parties in Paris, on 12 December 2015 and entered into force on 4 November 2016. Its goal is to limit temperature increase to well below 2, preferably to 1.5 degrees Celsius, compared to pre-industrial levels (reference period, 1850–1900). To satisfy the Paris Climate Agreement, many European countries (e.g., France and Britain) have already announced bans on new diesel and gasoline cars by 2040 (New York Times, July, 2017). Norway intends to sell only electric cars starting in 2025, and India wants to try to do so by 2030. We have quite few available options to scale back GHG emissions from transportation: (1) Use renewable energy, like biofuels in IC engines; (2) Reduce fuel use by incorporating hybrid cars; (3) Use electric cars; (4) Use a hydrogen IC engine (H<sub>2</sub>ICE); and (5) Use hydrogen fuel cell engines. This study focuses on (1) Use of renewable energy, biodiesel, and (4) Use of a hydrogen IC engine (H<sub>2</sub>ICE).

Climate change and mitigation of GHG emissions are the first motivators for biofuels research. Additionally, the growing concern on environmental pollution caused by extensive use of conventional fossil fuels has led to the search for more environmentally-friendly and renewable fuels. Biofuels like alcohols and biodiesel are proposed as alternatives for combustion engines (Agarwal 2007; Demirbas 2007). Although it is impossible for one alternative fuel to completely replace the diesel fuel, biodiesel can replace a big amount of diesel fuel in diesel engines. Biodiesel is a renewable and clean-burning diesel-like fuel that's produced from vegetable oils, animal fats, or used cooking oils. It's typically formed by the reaction of oils

and fats with alcohol that produce fatty acid esters. It is often utilized in pure form (B100), or blended with diesel in any proportion, for instance as B2 (2% biodiesel, 98% diesel), B5 (5% biodiesel, 95% diesel), B20 (20% biodiesel, 80% diesel) B50 (50% biodiesel, 50% diesel), etc. Biodiesel has received wide attention as a supplementary for diesel fuel because it emits less CO<sub>2</sub> and other pollutants. While the burning of biodiesel produces CO<sub>2</sub> emissions almost like that of ordinary fossil fuels, the plant feedstock used for its production absorbs CO<sub>2</sub> from the atmosphere when it grows. Biodiesel can reduce net CO<sub>2</sub> emissions by 78% on a lifecycle basis compared to standard diesel fuel (Sheehan et al. 1998). Biodiesel is additionally low in sulfur, but features a much higher cetane number than other lower sulfur diesel fuels. Canadian ultra-low sulfur diesel (ULSD), could have a cetane number as high as 50. Biodiesels from most oil sources are recorded as having a cetane number greater than 50, and animal-fat based biodiesels' cetane numbers range from 56 to 60 ([https://web.archive.org/web/20070714042908/http://www.biodiesel.org/resources/reportsdatabase/reports/gen/19940101\\_gen-297.pdf](https://web.archive.org/web/20070714042908/http://www.biodiesel.org/resources/reportsdatabase/reports/gen/19940101_gen-297.pdf)). The cetane number is an indicator of ignition quality of diesel-like fuel. The higher cetane number indicates the higher quality of the fuel. The addition of biodiesel reduces wear in fuel systems and increases the service lifetime of the fuel injection system equipment as a result of its high lubricity. Biodiesel is biodegradable, which suggests that it can be decomposed easily by bacteria. Consequently, any cleanup would be easier. As pure biodiesel doesn't leave deposits, it leads to increased engine life.

The US Environmental Protection Agency (US EPA) has conducted a comprehensive analysis of biodiesel impacts on exhaust emissions (US EPA 2002) mentioning that pure biodiesel can reduce HC as high as 70% and PM and CO about 50% compared with conventional diesel fuel. Several countries, including Canada, have already begun substituting conventional diesel by a particular amount of biodiesel. The utilization of biodiesel is being promoted by European Union (EU) countries to partially replace petroleum diesel so as to reduce the global warming and dependency on foreign oil. Meeting the targets established by the European Parliament for 2020 would have led to a biofuel market share of 10% (Directive 2009). The Canadian government announced a replacement biofuel strategy (2% biodiesel in diesel for ground transportation and heating by 2012 and 5% by 2015). Many investigations have indicated that the utilization of biodiesel may result in a substantial reduction in PM, HC and CO emissions (Ozsezen et al. 2009; Roy et al. 2013; Shahir et al. 2015). The performance and combustion characteristics of a direct injection (DI) diesel engine fueled with biodiesels like waste (frying) palm oil methyl ester (WPOME) and canola oil methyl ester (COME) were tested (Ozsezen et al. 2009). The experiments were conducted at the constant engine speed mode (1500 rpm) under the full load condition of the engine. The CO reductions by WPOME and COME were approximately 87% and 73%, respectively. The HC reductions by WPOME and COME were only about 14% and 10%, respectively. Finally, the smoke reductions by WPOME and COME were significant 68% and 48%, respectively. A DI diesel engine is tested with biodiesel–diesel and canola oil–diesel blends for performance and emissions at high idling operations (Roy et al. 2013). B20 or UCB20 shows average CO reduction of 13% than diesel. Similarly, B20 or UCB20 shows average

HC reduction of 22%. A review paper (Shahir et al. 2015) showed the results of CO, HC and PM emissions for various sorts of biodiesel blends. The utmost reduction of CO with 100% biodiesel was about 80% and maximum reduction in HC and PM with 100% biodiesel was about 55%. During a recent study (Sharma et al. 2020) of various biodiesel and diesel combustion, it had been found that with 10% and 20% microalgae, jatropha and polanga biodiesel reduced HC, CO and smoke emissions than diesel combustion. Furthermore, 20% microalgae biodiesel showed the very best reductions approximately 10% HC, 7% CO and 5% smoke. Therefore, biodiesel might be a far better substitute to diesel fuel in terms of lowering CO<sub>2</sub> emissions and pollutant emissions of HC, CO and PM. Although biodiesel has many advantages, its inferior CFPs compared to standard diesel makes it unusable in high percentages in colder climates. This study discusses the improvement of CFPs of biodiesel during a later section.

Now let's mention use of hydrogen IC engine (H<sub>2</sub>ICE). Within the coming decades, we'll see more and more diesel and gasoline vehicles being replaced by hybrid and electric vehicles. Several years ago, hydrogen car technology seemed to be promising, and government funding for hydrogen generation was flowing. Hydrogen is often generated using oil and gas. It can better be produced using wind energy, solar energy, or the other source of electricity that's available at that point, thus providing ultimate flexibility. When fueled by renewable hydrogen, H<sub>2</sub>ICE vehicles have near-zero lifecycle GHG emissions. Japan is betting heavily on hydrogen as an energy source to become a hydrogen society, despite the high cost and technical difficulties which have generally slowed its adoption as a carbon-free fuel. However, recently Toyota starts again developing a combustion engine that runs on hydrogen for racing ([https://www.greencarreports.com/news/1132023\\_toyota-is-developing-hydrogen-combustion-engines-for-racing](https://www.greencarreports.com/news/1132023_toyota-is-developing-hydrogen-combustion-engines-for-racing)). Ever since the EU initiated the "European Clean Hydrogen Alliance" in July 2020, the H<sub>2</sub>ICE has increasingly been within the spotlight within the mobility industry's debate on zero-emission drive solutions. Aachen-based FEV, a number one international vehicle and powertrain developer, welcomes this openness to technology regarding future mobility solutions and has nearly four decades of experience in hydrogen engine development. Therefore, there are new initiatives within the direction of H<sub>2</sub>ICE from different auto manufacturers. Hydrogen fuel cells are currently too cost-prohibitive to be competitive compared to electric cars. Additionally due to inadequate fueling station network, fuel cell cars are of low demand. The few models of fuel cell vehicles already available on the market cost around USD 80,000 for a mid- or upper-mid-range vehicle (<https://www.bmw.com/en/innovation/how-hydrogen-fuel-cell-cars-work.html#pwjt-3>). That's almost twice the maximum amount as comparable fully electric or hybrid vehicles. Additionally, to the value of purchase, operating costs also play a crucial role within the cost-effectiveness and acceptance of a propulsion technology. The value per km of running hydrogen fuel cell cars is currently almost twice as high as that of battery-powered vehicles. On the opposite hand, H<sub>2</sub>ICEs are less expensive than hydrogen fuel cell engines. This is due to the very fact that the hydrogen combustion engines are often manufactured using equipment from traditional engine manufacturing platform because the most components are very similar. Furthermore, the hydrogen

combustion engine features a longer expected lifetime than the fuel cell, which results in significantly lower operating costs (0.58 versus 2.62 €/h) (Handwerker et al. 2021). Therefore, H<sub>2</sub>ICEs are viewed by many experts as the means to supply power for transportation and stationary power generation within the near future. However, the hydrogen engine must overcome certain obstacles like fuel storage in small-to-medium vehicles to supply comparable mileage with diesel and gasoline cars. H<sub>2</sub>ICE's efficiency ( $\approx 45\%$ ) is less than that of the electrical motor (80% or more) or fuel cell vehicle (60% or more). To enhance the efficiency advantage of H<sub>2</sub>ICE, this might be utilized in a combined heat and power (CHP) system where engine exhaust heat is employed for heating purposes, which could end in a 70% efficiency or more. There are some areas (e.g., oil and gas sector, and world's marine diesel engine/cruise ships) where CHP plays an important role for power generation, also as heat or steam generation. H<sub>2</sub>ICE can play a big role in these sectors through high efficiency, and reduced GHG and other harmful emissions. Biodiesel and hydrogen-driven dual-fuel engine can play a really important role in these sectors. The transportation sector could also enjoy this engine once there are enough fueling infrastructures and the energy density (energy content per unit volume) of hydrogen can be significantly increased.

## 5.2 CFPs of Biodiesel

Biodiesel has inferior CFPs compared to conventional diesel, which is the main reason it is unusable in high percentages in colder climates (e.g., Canada). Cloud point (CP), pour point (PP) and cold filter plugging point (CFPP) represent the main CFPs of biodiesel.

**Cloud point**—the temperature at which a cloud of wax crystals first appears in a liquid fuel when it is cooled under specific testing conditions, ASTM Standard D-2500 (Kruka et al. 1995). It is important because the fuel line could get clogged if the fuel's cloud point is too high due to the presence of saturated esters in biodiesel. Biodiesel has a higher cloud point than diesel fuel.

**Pour point**—the lowest temperature at which a fuel ceases to flow. Pour point of a fuel is usually lower than cloud point.

**Cold filter plugging point**—the lowest temperature at which a given volume of a fuel still passes through a standardized filter in a specified time when cooled under certain conditions. It is also usually lower than cloud point, but higher than pour point.

Among those three cold flow properties, cloud point is usually the highest and thus, can be considered the safest cold flow property of a fuel; most fuels can be burned at the cloud point without problems.



### 5.2.1 Mechanism of CFPs Improvement

Fatty acids that include long carbon chains affect cold flow properties. Fatty acids are composed of a carboxyl and a hydrocarbon chain. This chain can differ in length from 4 to 24 carbon atoms. Generally, the fatty acids of biodiesel are divided into two categories: saturated and unsaturated. Unsaturated fatty acids are divided into monounsaturated and polyunsaturated fatty acids. Myristic, palmitic and stearic are saturated fatty acids with melting points (MPs) of 19 °C, 30 °C and 39 °C, respectively, whereas oleic (monounsaturated), linoleic and linolenic (polyunsaturated) are unsaturated acids with MPs −19.5 °C, −35 °C and −52 °C, respectively (Liu 2015; Yuan et al. 2017). Therefore, biodiesel with a better percentage of unsaturated fatty acids (especially polyunsaturated) shows a lower CP. Canola biodiesel contains the very best amount of polyunsaturated fatty acids (≈32%), whereas that of palm biodiesel contains only about 12%. This leads to an enormous difference in their CPs: canola biodiesel's CP is −2.6 °C, and palm biodiesel's CP is 16 °C (Roy et al. 2016; Hamdan et al. 2016; Sarin et al. 2010; Verma et al. 2016). A number of the prevailing approaches to enhance biodiesel's CFPs was achieved by simply modifying its fatty acid profile. Other techniques were followed by blending biodiesel with fuels that have low CFPs, and a few additives were proposed to enhance biodiesel CFPs. A quick review of the technology that were used is going to be discussed within the following sections.

**Modification of fatty acids profile**—The modification of fatty acids composition of biodiesel is often achieved mainly through fractionation. Fractionation is a process of separation of a mixture or chemical compound into components by fractional crystallization. Fractionation is often classified in three main groups: dry fractionation, solvent fractionation and urea fractionation. Dry fractionation is additionally called winterization. Winterization is essentially the method of preparing something for winter. For biodiesel, winterization may be a simple method to get rid of saturated fatty acid contents in biodiesel fuels for improving their CFPs. It's done by a process whereby biodiesel is cooled, thereby leading to the formation of crystals. Those crystals are then filtered to get a high level of unsaturated fatty acids (González Gómez et al. 2002). Nainwal et al. (2015) achieved a 3 °C reduction in biodiesel's CP through a four-stage winterization process. Pérez et al. (2010) increased the unsaturated level of peanut biodiesel from 84.45 to 88.21% using three-stage winterization, obtaining a CP reduction of roughly 12 °C. Solvent fractionation tackles winterization's disadvantages of long preparation time and low production efficiency. Through this method, solvents like methanol, acetone, chloroform, hexane, or isopropanol are blended with biodiesel to reduce its viscosity. The solvent fractionation process is characterized by shortened crystallization time and simple filterability, resulting in high separation efficiency and improved yield (O'Brien 2008). Urea fractionation is simply applied to alkyl ester, mixing methanol or ethanol with urea. Through this method, the biodiesel was separated into two or more portions (Knothe 2009; Dunn et al. 1996). The urea fractionation method significantly improved the biodiesel's

CFPs, and was reported to possess the power to lower the biodiesel's CP to  $-30\text{ }^{\circ}\text{C}$  (Dunn 2011).

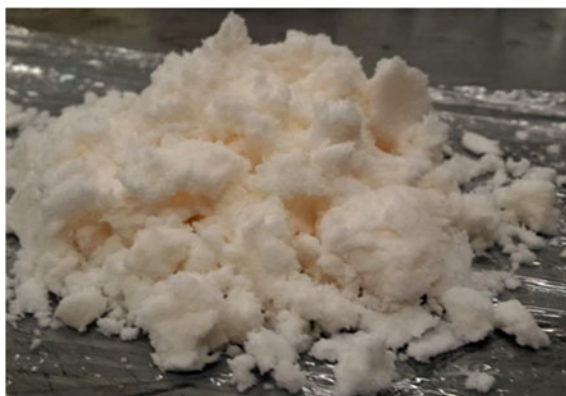
**Urea fractionation**—A detailed study of urea fractionation was performed by a grad student (Elsanusi 2017) under the supervision of the author of this chapter at Lakehead University. The materials utilized in this study include pure urea (44 gm), methanol (150 ml), and canola biodiesel (50 ml). The preparation procedure was as follows:

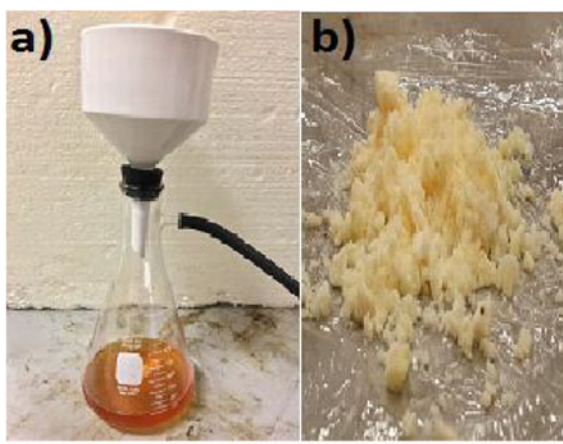
1. Mix the urea with biodiesel and methanol.
2. Heat the mixture to make a heterogeneous solution.
3. Cool the mixture to between  $15\text{ }^{\circ}\text{C}$  and  $30\text{ }^{\circ}\text{C}$ .
4. Separate the solid crystals (Fig. 5.1) from the liquid employing a Buchner funnel aspirator.
5. Collect the solid crystals.
6. Heat the remaining mixture until two distinct layers are formed (Fig. 5.2).
7. Cool the mixture to between  $15\text{ }^{\circ}\text{C}$  and  $30\text{ }^{\circ}\text{C}$ .
8. Separate the solids (recovered urea) from the liquid employing a Buchner funnel aspirator (Fig. 5.3a).
9. Collect the recovered urea (Fig. 5.3b).
10. Heat the remaining liquid (biodiesel) up to  $150\text{ }^{\circ}\text{C}$  to decompose the urea.

Although this method resulted in a significant reduction in the biodiesel's CP ( $-31.7\text{ }^{\circ}\text{C}$ ), it also caused lower production efficiency (33%).

**Crystal Fractionation Process**—In this study, the by-product (solid crystals and recovered urea) of urea fractionation is also used to produce fractionated biodiesel. The preparation steps are exactly the same as the urea fractionation steps, while the material compositions are different. This method is referred to as crystal fractionation. The material compositions, CP and production efficiency are listed in Table 5.1. Winter diesel in Canada has a CP of about  $-41\text{ }^{\circ}\text{C}$ . The goal was to make biodiesel with a CP of  $-41\text{ }^{\circ}\text{C}$  or lower. Transesterification was used to produce normal biodiesel from canola oil, and then urea fractionation was used in that normal

**Fig. 5.1** Solid crystals



**Fig. 5.2** Two-liquid phase**Fig. 5.3** a Buchner funnel aspirator; b Recovered urea

biodiesel to obtain fractionated biodiesel with CP of  $-31.7\text{ }^{\circ}\text{C}$ . Using the by-products of urea fractionation (solid crystals and recovered urea mixture) for crystal fractionated biodiesel resulted in significant improvements in production efficiency. Using 22.5 gm of solid crystals and 22.5 gm of recovered urea with 150 ml of methanol resulted in overall higher production efficiency, which reached 100 vol.%, and CP of  $-18\text{ }^{\circ}\text{C}$ , as seen in Table 5.1. The next step of this research could be to determine how to improve the CP while maintaining the production efficiency as high as possible. One possible route could be winterization of canola oil first to separate the high saturated fats, followed by using the remaining highly unsaturated oil to produce biodiesel, and finally using the urea fractionation to produce fractionated biodiesel. This might provide a fractionated biodiesel of CP of  $-41\text{ }^{\circ}\text{C}$  or lower.

**Table 5.1** CP and production efficiency of fractionated biodiesel prepared using different methods (Elsanusi 2017)

Material compositions				CP ( °C)	Production efficiency (vol.%)
Biodiesel				-2.6	80
Original urea fractionation					
<i>44 gm of urea + 150 ml methanol + 50 ml biodiesel</i>				-31.7	33
Recovered urea and crystal fractionation					
Solid crystals (gm)	Recovered urea (gm)	Methanol (ml)	Biodiesel (ml)	CP ( °C)	Production efficiency (vol.%)
22.5	22.5	150	50	-18	100
22.5	22.5	0	50	-9	87
50	-	150	75	-13.8	90
50	-	150	100	-11.1	92
50	-	150	125	-7.9	91
50	-	150	150	-9	95
66	-	150	200	-8.5	90
88	-	150	50	-14.8	95

**Additives**—Additives are usually used for improving biodiesel’s properties in order to reduce regulated emissions and to improve the fuel’s flow properties. Although the flow improvers do not change biodiesel’s CP, they inhibit the growth of wax crystals, which in turn improves the CFPP (Lanjekar and Deshmukh 2016; Mei et al. 2016). The additives used to improve biodiesel cold flow are usually known as wax crystallization modifiers. Roy et al. (2016) obtained CP reduction of 5.3 °C by adding 2% of Wintron Synergy to regular canola biodiesel. Using diethyl ether (DEE) as an additive of 15 vol. % to biodiesel, Roy et al. (2016) also improved the CP by 2.8 °C. Another study of urea fractionated biodiesel and biodiesel additive Wintron Synergy was performed by a graduate student (Mangad 2017) under the supervision of the author of this chapter. The CP of various fractionated biodiesel-winter diesel blends with the Wintron Synergy additive (2 vol.%) showed a remarkable reduction. FB20S2 (fractionated biodiesel 20% + winter diesel 80% with Synergy 2%) had the CP of as low as -48.2 °C. The other combination FB50S2 (fractionated biodiesel 50% + winter diesel 50% with Synergy 2%) showed the CP of -47.5 °C, both temperatures are lower than that of winter diesel (-41 °C) in Canada.

**Biodiesel blending**—Biodiesel is often blended and utilized in different concentrations with petroleum diesel or kerosene. Blends of 5% biodiesel with winter diesel have a little influence on CFPs (Verma et al. 2016). Ghanei (2015) studied the consequences of blending castor biodiesel with canola biodiesel, whereby significant improvements were obtained within the blends’ CFPs with the increased amount of castor biodiesel. Zhao et al. (2016) blended biodiesel with conventional diesel,

and reported that the CFPP and PP linearly decreased by increasing the diesel concentration within the blends.

### 5.3 Hydrogen as a Vehicular Fuel

Hydrogen is often used either in H<sub>2</sub>ICE or in fuel cell vehicles (FCVs). Hydrogen is abundant within the environment. The production of hydrogen at a low cost is the main challenge. It's stored in water (H<sub>2</sub>O), in hydrocarbons like methane (CH<sub>4</sub>), and in other organic matter. Currently, steam reforming that mixes high-temperature steam with natural gas to extract hydrogen accounts for the bulk of the hydrogen production. Hydrogen also can be produced from water through electrolysis. Although it's more energy-intensive, it is often achieved by using renewable energy, like wind or solar. Hydrogen fuel cells are currently too cost-prohibitive to be competitive. On the other hand, H<sub>2</sub>ICE is far cheaper than hydrogen fuel cell engines, and thus H<sub>2</sub>ICE is seen by many experts as the means to supply power for transportation and stationary power generation. It is often used to fuel IC engines with minimal emissions of pollutant gases. A hydrogen-operated engine produces water as its main combustion product. It doesn't produce significant amounts of CO, HC, smoke, sulfur oxides (SO<sub>x</sub>), leads or other toxic metals, sulfuric acid deposition, ozone and other oxidants, benzene and other carcinogenic compounds. Hydrogen combustion is free from CO<sub>2</sub>, the foremost important GHG. The sole undesirable emissions are nitric oxide (NO) and nitrogen dioxide (NO<sub>2</sub>), thus NO<sub>x</sub>. Because hydrogen features a wide flammability range compared to all or any other fuels, it is often combusted in an IC engine over a good range of fuel-air mixtures. Due to this significant advantage, hydrogen can run on a lean mixture. Generally, fuel economy is bigger and therefore the combustion reaction is more complete when an IC engine runs on a lean mixture. Additionally, the ultimate combustion temperature is typically lower, reducing the quantity of NO<sub>x</sub> emitted within the exhaust. Hydrogen has very low ignition energy, which enables hydrogen engines to ignite lean mixtures and ensures prompt ignition. A number of the important properties of hydrogen (H<sub>2</sub>) are given in Table 1.2 (Hord 1978).

The ratio of specific heat ( $\gamma$ ) plays an important role on thermal efficiency of IC engines; the higher the specific heat, the higher the thermal efficiency. Hydrogen's ratio of specific heat ( $\gamma = 1.4$ ) is higher than that of conventional petroleum fuels, for example gasoline's ( $\gamma = 1.1$ ). Therefore, H<sub>2</sub>ICE has higher thermal efficiency than traditional gasoline or diesel engines' efficiency.

### 5.4 Emissions from Hydrogen Combustion

The combustion of hydrogen with oxygen produces only water:

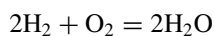


**Table 5.2** Important properties of hydrogen (Hord 1978)

Hydrogen property	Value
Limits of flammability in air, vol.%	4–75
Minimum energy for ignition, mJ	0.02
Quenching gap in NTP air, cm	0.064
Auto-ignition temperature, K	858
Burning velocity in NTP air, cm/s	265–325
Diffusion coefficient in NTP air, cm <sup>2</sup> /s	0.61
Heat of combustion (LCV), MJ/kg	119.93

However, the combustion of hydrogen with air also can produce NO<sub>x</sub>. Air contains nitrogen; most of it exits within the exhaust unreacted. Some nitrogen within the air reacting with oxygen at high temperature during combustion forms NO<sub>x</sub>. Additionally, to NO<sub>x</sub>, traces of CO, unburnt HC and CO<sub>2</sub> are often present within the exhaust gas due to engine oil burning within the combustion chamber. Depending on the condition of the engine (burning of engine oil) and the operating strategy used (rich or lean mixture), a hydrogen engine can produce from near-zero emissions (a few ppm) to high NO<sub>x</sub>, and emit significant CO (Table 5.2).

## 5.5 Hydrogen in a Dual-Fuel Engine

In an earlier study, Gopal et al. (1982) investigated the performance of a hydrogen dual-fuel engine under a good range of engine operation. The thermal efficiency obtained was like pure diesel operation, and up to half the engine's energy requirement might be derived from hydrogen. Mathur et al. (1992) found that hydrogen might be substituted for diesel fuel up to 85%, although with some penalty in engine performance. A big efficiency advantage was found when using hydrogen as against diesel fuel, with the hydrogen-fueled engine achieving efficiency of roughly 43% compared to 28% in the conventional, diesel-fueled mode (Antunes et al. 2009). Dual-fuel operation with hydrogen including exhaust gas recirculation (EGR) resulted in lowered emissions and improved performance compared to the case of neat diesel operation (Bose and Maji 2009). Early work testing a boosted hydrogen engine was administered by Nagalingam et al. (1983) with a single-cylinder research engine and simulated turbocharged operation by pressurizing inlet air to 2.6 bars. During the last decade of 2000, substantial advances were made by BMW (Berckmuller et al. 2003) and Ford (Gopal et al. 1982; Mathur et al. 1992). In (Berckmuller et al. 2003), Berckmuller et al. reported results from one cylinder engine supercharged to 1.8 bars that achieved a 30% increase in specific power output compared to a naturally-aspirated gasolines engine. Natkin et al. (2003) reported results for a supercharged 4-cylinder 2.0 l Ford Zetec engine and a 4-cylinder 2.3 l Ford Duratec engine that was utilized in conventional and hybrid vehicles (Jaura et al. 2004). Because boosting pressure

increases charge pressure and temperature, the issues of pre-ignition, knock and  $\text{NO}_x$  control were heightened during boosted operation. Additionally, Nagalingam et al. (1983) reported that the pre-ignition-limited equivalence ratio decreased from 1.0 to 0.5 once they increased the intake pressure from 1 bar to 2.6 bars. Berckmuller et al. reported a decrease in the pre-ignition-limited equivalence ratio from 1 to 0.6 when the inlet pressure was increased from 1 bar to 1.8 bars. To realize emissions of 3–4 ppm levels likely required to achieve super ultra-low emissions vehicle (SULEV), Ford's supercharged engine was run at a leaner fuel-air equivalence ratio of 0.23 (Natkin et al. 2003). To stop knock, diluents like nitrogen, helium or water are helpful. Sharma and Dhar during a recent publication (Sharma and Dhar 2018), expressed their thoughts on advances in hydrogen-fueled compression ignition engine. This work critically evaluated the amenities and shortcomings of the hydrogen as a fuel in compression ignition engines. Application of hydrogen in advanced compression ignition technologies like homogeneous charge compression ignition (HCCI) and premixed charge compression ignition (PCCI) was also explored. Hydrogen showed excellent combustion properties and enhanced the diesel combustion efficiency in dual-fuel mode. However, it required advance technologies to regulate the  $\text{H}_2$ –HCCI combustion, and if achieved, it not only offered excellent combustion efficiency but also reduced the emissions to negligible amounts.

Reference (Roy et al. 2010) is a publication by the author of this chapter and his group. In brief, the work investigated the engine performance and emissions of a supercharged dual-fuel engine fueled by hydrogen and ignited by a pilot amount of diesel fuel. The engine was tested first with hydrogen-operation condition up to the utmost possible fuel-air equivalence ratio of 0.3. Equivalence ratio couldn't be further increased because of engine knocking. The charge dilution (by  $\text{N}_2$ ) was then performed to lower  $\text{NO}_x$  emissions, thereby achieving zero  $\text{NO}_x$  emissions.

**Methodology**—Figure 5.4 shows the schematic diagram of the engine experiment, and Fig. 5.5 shows the single cylinder, water cooled, supercharged dual-fuel test engine. Table 5.3 shows the engine specifications.

This is a dual-fuel engine where the primary gaseous fuel source (hydrogen) is pre-mixed with air as it enters the combustion chamber. This homogenous air- $\text{H}_2$  mixture is ignited by a small quantity of diesel fuel injected towards the end of the compression stroke. Hydrogen is drawn from a high-pressure cylinder and moved through a mass flow controller, which is used to measure the flow of hydrogen. The intake pressure was kept constant at 200 kPa and the temperature was maintained at 30 °C throughout the study. The injection of pilot diesel fuel was controlled to a pressure of 80 MPa with a common rail system and introduced at a rate of 3 mg/cycle. In ref. (Roy et al. 2010), an in-depth description of engine control is provided. “The injection timing of the pilot diesel was adjusted counting on the equivalence ratio to get optimum timings for maximum engine power. The engine speed was 1000 rpm. The injection period/duration of the pilot diesel under these conditions was 3.5 °CA. The pilot injection signal was controlled by a computer. Therefore, the injection timing and injection duration are correctly controlled. The TDC signals and each half-degree crank angle were detected and used to control the injection timing and the diesel fuel period. The in-cylinder pressure was measured

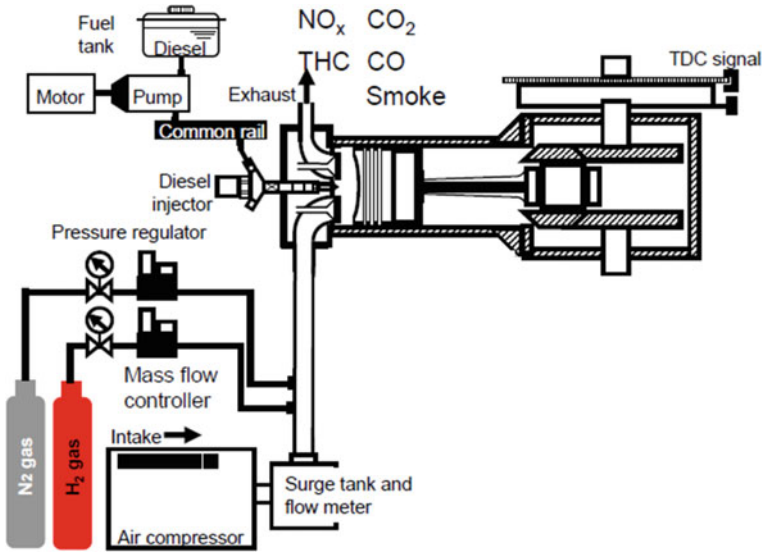


Fig. 5.4 Schematic diagram of the engine experiment (Roy et al. 2010)

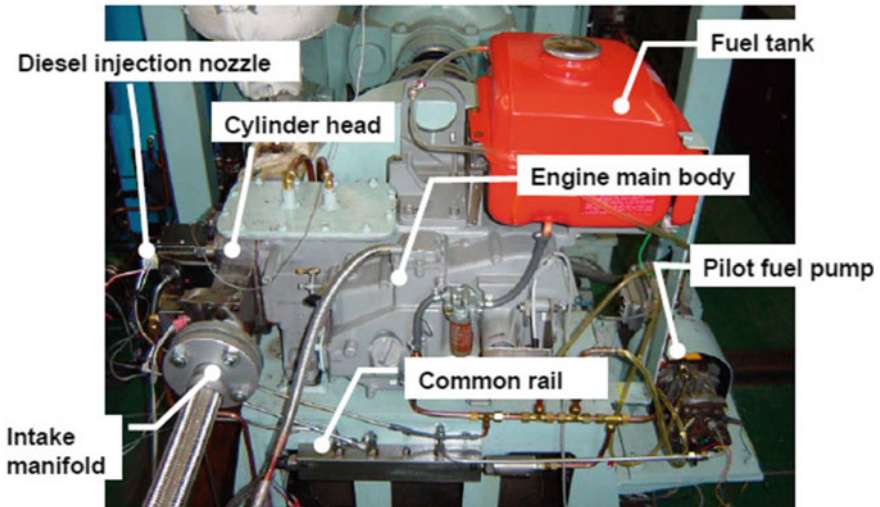


Fig. 5.5 Single cylinder water cooled supercharged dual-fuel test engine

with a piezoelectric pressure transducer (6052A, Kistler). The pressure history was analyzed to get the rate of heat release to research the combustion characteristics. The engine performance decided by the IMEP and the indicated thermal efficiency of the engine. The IMEP coefficient of variance (COV)<sub>imep</sub>, was measured to reflect the cycle-to-cycle variation of the engine.” Combustion pressure history and (COV)<sub>imep</sub>



**Table 5.3** Engine specifications (Roy et al. 2010)

Engine type	4-stroke, single cylinder, water cooled
Bore x stroke	96 × 108 mm
Swept volume	781.7 cm <sup>3</sup>
Compression ratio	16
Combustion system	Dual-fuel, direct injection
Combustion chamber type	Shallow-dish
Injection system type	Common-rail
Nozzle hole x diameter	4 × φ 0.10 mm
Engine speed	1000 rpm

were presented in Roy et al. (2010) intimately. To avoid repetition, those aren't shown here during this study. Data for every engine condition were captured when the engine was in equilibrium, where there was almost no change within the emission parameters and exhaust temperatures. For emission analysis, NO<sub>x</sub>, CO, HC, and smoke emissions were measured. Regarding to exhaust emissions, the NO<sub>x</sub> and CO concentrations were measured with a multi gas analyzer (Horiba, PG-240) and the HC concentration was measured with a hydrocarbon gas analyzer (Horiba, MEXA-1170 HFID). Smoke is additionally measured with an opacimeter (Horiba, MEXA-600S).

**Engine results**—Figure 5.6 illustrates energy supplied by the pilot diesel fuel, by the hydrogen, and therefore the total fuel energy per cycle. The pilot diesel fuel energy

**Fig. 5.6** Energy supplied by different fuels and percentage share at various equivalence ratios (Roy et al. 2010)

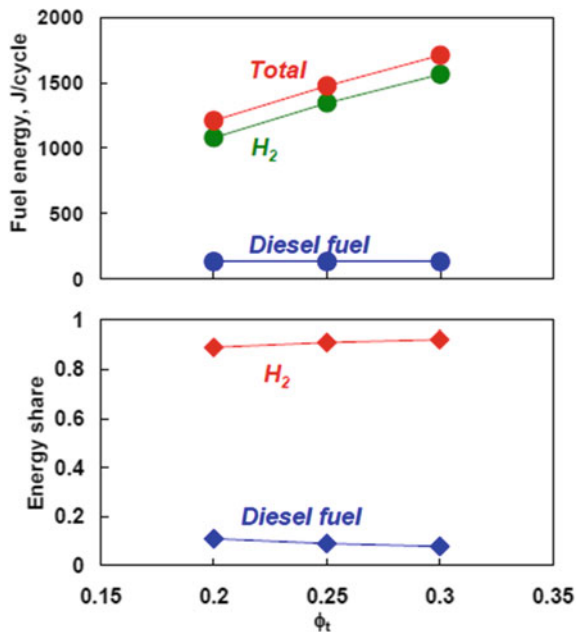
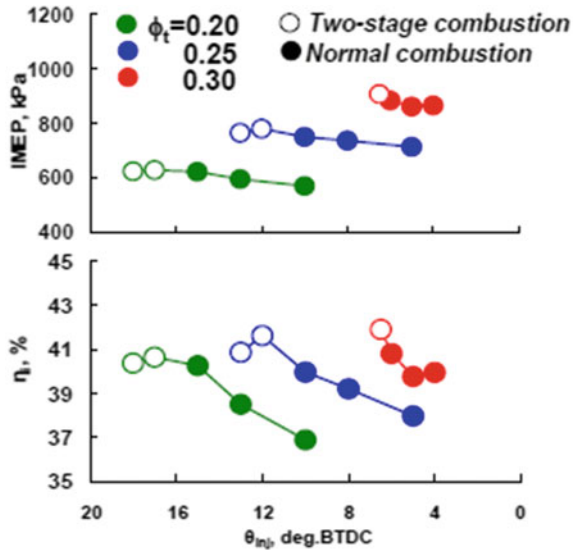


**Fig. 5.7** IMEP and  $\eta_i$  of hydrogen at various equivalence ratios (Roy et al. 2010)

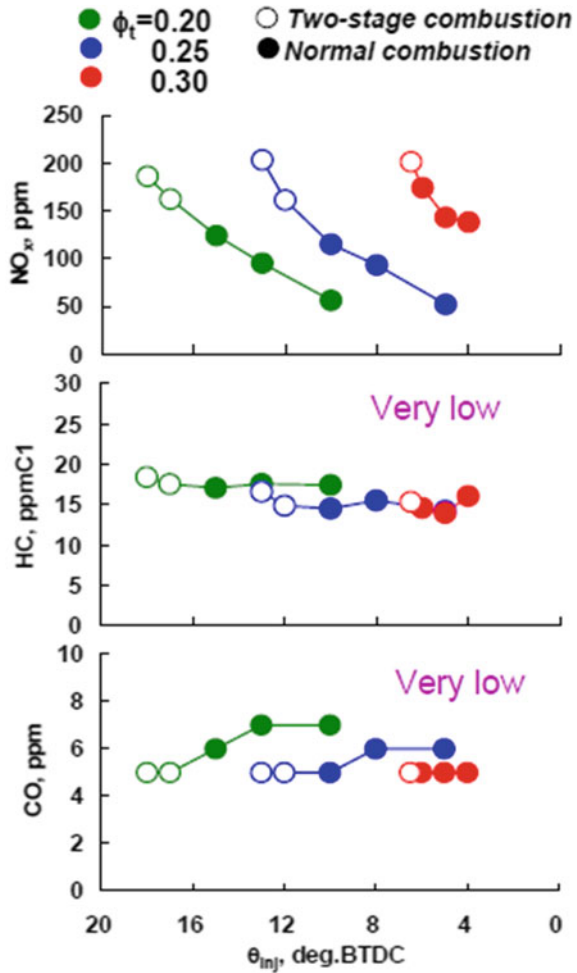


was constant (130 J/cycle), and energy from the hydrogen increased from 1080 to 1560 J/cycle, and therefore the total fuel energy increased from 1210 to 1690 J/cycle when the total fuel–air equivalence ratio was increased from 0.20 to 0.30. Figure 1.6 also shows diesel and hydrogen share in total energy for various fuel-air equivalence ratios. The share of diesel fuel changed from about 7.7 to 10.75%. The remaining 89.25–92.3% energy was supplied by the hydrogen.

Figure 5.7 present the IMEP and the indicated thermal efficiency of the hydrogen at various fuel-air equivalence ratios for various injection timings. The injection timings were varied to get maximum engine IMEP, i.e., maximum engine power, without knocking and within the safe limit of the utmost cylinder pressure of the engine. The safe maximum pressure of the tested engine was approximately 16 MPa. The IMEP increased with advanced injection timings at a constant equivalence ratio; it also increased as the equivalence ratio increased. The utmost IMEP level at the equivalence ratio of 0.20 was 630 kPa, and increased to the extent of 908 kPa when the equivalence ratio was increased to 0.30. The equivalence ratio of 0.30 was the utmost possible value for the tested engine with the hydrogen-operation, and will not be further increased due to knocking. Therefore, the utmost IMEP produced by the engine with the hydrogen was 908 kPa when there was no charge dilution. The thermal efficiency graph reveals that at a constant equivalence ratio, the indicated thermal efficiency increased with advanced injection timings, almost like the way the IMEP increased. The indicated thermal efficiency was as high as 42% for some best injection timings. Controlled two-stage combustion showed better IMEP and thermal efficiency.

Figure 5.8 indicates the  $\text{NO}_x$ , HC, and CO emissions at various equivalence ratios for various injection timings. At a constant equivalence ratio, the  $\text{NO}_x$  increased

**Fig. 5.8** Emissions of NO<sub>x</sub>, HC and CO of hydrogen at various equivalence ratios (Roy et al. 2010)



with advanced injection timings. Advancing the injection timing increased the peak cylinder pressure (figures aren't shown here); higher peak cylinder pressures resulted in higher peak burned gas temperatures, and hence more NO<sub>x</sub>. More NO<sub>x</sub> was produced when the equivalence ratio increased, although the injection timings were delayed. The utmost NO<sub>x</sub> level increased with the rise in the equivalence ratio, and the highest NO<sub>x</sub> emission level was about 200 ppm at an equivalence ratio of 0.25–0.30. The HC graph shows that the extent of HC emitted by the dual-fuel engine fueled by hydrogen varied only slightly (14–18 ppm). The CO graph reveals that the extent of CO emitted by the dual-fuel engine fueled by hydrogen was varied from only 5–7 ppm. The emissions of HC and CO were low enough to satisfy most of the future regulations. The NO<sub>x</sub> emissions in some cases were higher, and there's

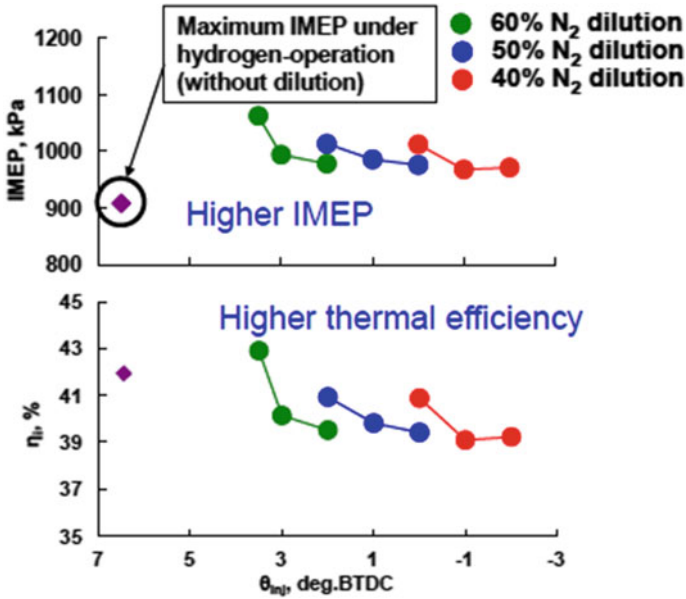


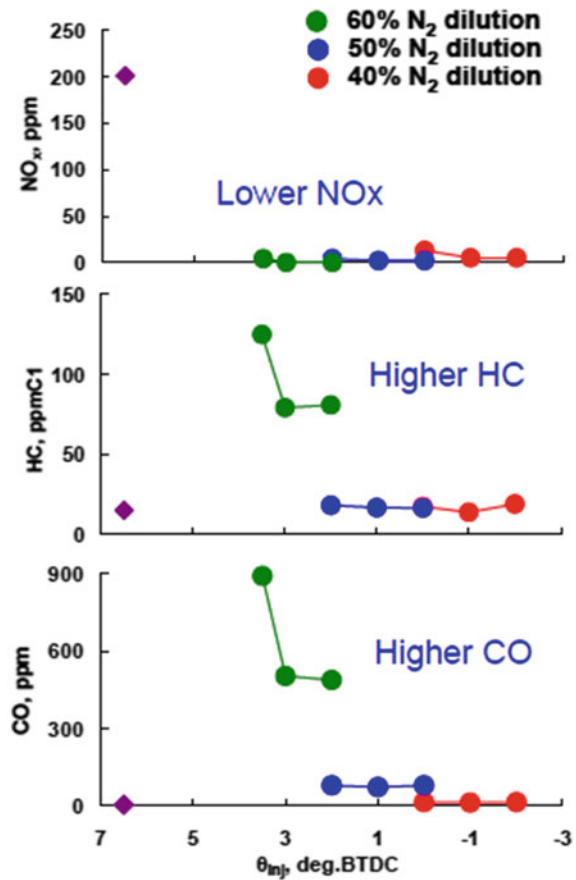
Fig. 5.9 IMEP and  $\eta_i$  at different N<sub>2</sub> dilution rates equivalence ratios

a requirement to further reduce the engine NO<sub>x</sub>, considering future stricter NO<sub>x</sub> regulations.

Figure 5.9 illustrates the IMEP and the indicated thermal efficiency at different percentages of N<sub>2</sub> dilution conditions for various injection timings. The IMEP increased with advanced injection timings similar to that with hydrogen-operation without charge dilution. The maximum IMEP of 1012–1013 kPa was obtained for 40 and 50% of N<sub>2</sub> dilution, which is about 13% higher than that of the highest possible IMEP obtained with hydrogen-operation only (908 kPa). With 60% N<sub>2</sub> dilution, it was more than 15% higher than that of hydrogen operation only. In the case of 40% N<sub>2</sub> dilution, the pilot injection timing could not be advanced before TDC due to knocking. However, for the N<sub>2</sub> dilution of 50% and 60%, the pilot injection timing was advanced to 2° and 3° BTDC, respectively, without knocking. The higher amount of N<sub>2</sub> in the inlet gases were believed to be responsible for the suppression of in-cylinder temperature, which made advancing injection timings possible. The maximum ignition delay without charge dilution was about 5° CA, whereas it was about 6–7° CA with charge dilution cases (not shown here). Longer ignition delay with charge dilution may be due to lower bulk gas temperatures. The thermal efficiency shows a very similar trend of results to that with the IMEP, i.e., the indicated thermal efficiency increased with advanced injection timings, and the highest thermal efficiency of 43% was obtained for 60% N<sub>2</sub> dilution.

Figure 5.10 shows the NO<sub>x</sub>, HC, and CO emissions at different percentage of N<sub>2</sub> dilution conditions for various injection timings by which a dramatic reduction of NO<sub>x</sub> was obtained. The level of NO<sub>x</sub> of 200 ppm with hydrogen-operation only was

**Fig. 5.10** Emissions of  $\text{NO}_x$ , HC and CO at different  $\text{N}_2$  dilution rates



reduced to 0 ppm level with 60%  $\text{N}_2$  dilution.  $\text{NO}_x$  was reduced by 98% and 99% for 40% and 50%  $\text{N}_2$  dilution, respectively. The maximum HC without  $\text{N}_2$  dilution was 18 ppm; this level was maintained for the 40% and 50%  $\text{N}_2$  dilution. However, HC increased to the level of about 120 ppm with 60%  $\text{N}_2$  dilution. The maximum CO without  $\text{N}_2$  dilution was only 7 ppm; this level was maintained for the 40%  $\text{N}_2$  dilution. However, CO was increased to the levels of about 80 ppm and 900 ppm with 50% and 60%  $\text{N}_2$  dilution, respectively. Without charge dilution,  $\phi$  value cannot be extended above 0.3 due to engine knocking. When nitrogen was added for dilution,  $\phi$  value became higher (up to 0.8 for 60% dilution). The heat value (input energy per cycle) in dilution conditions was also higher (1940 J/cycle) than that in non-dilution case of  $\phi$  0.3 (1690 J/cycle), which is a reason for higher IMEP in dilution cases. Moreover, energy supplied by the hydrogen in case of dilution tests is equivalent to the  $\phi$  value of 0.34 without dilution, for which higher IMEP could be obtained. Inert  $\text{N}_2$  molecules within fuel act as a sink of heat producing lower combustion temperatures. Lower combustion temperatures favored the suppression of autoignition of the end

gas. Thus, higher hydrogen energy substitution was possible with higher  $N_2$  dilution, which resulted in higher engine power as well as significant  $NO_x$  reduction.

## 5.6 Prospect of Biodiesel and Hydrogen in Dual-Fuel Engine

An experimental study was administered to evaluate the performance, combustion and emission characteristics of diesel operated in dual-fuel mode fueled with esters of honge (EHNO), honge (EHO) oils and hydrogen induction (Hosmath et al. 2015). The study revealed that the brake thermal efficiency increased up to 20% hydrogen energy ratio (HER); followed by a decrease. Emissions like HC, CO and smoke decreased together with HER, while  $NO_x$  increased. Combustion parameters like peak pressure, ignition delay and heat release rate (HRR) increased together with HER. A recent study investigated the results of co-combustion of biodiesel with hydrogen in a compression ignition (CI) combustion engine (Tutak et al. 2020). It had been determined that it's possible to exchange biodiesel with hydrogen to its energetic share of 38%. The rise in engine thermal efficiency was obtained with the rise of the hydrogen share. The share of hydrogen caused a big decrease in CO,  $CO_2$  and soot emissions. With the rise of hydrogen energy share, there was also a rise in specific HC emission. The very best increase in HC emissions was for 38%  $H_2$ , which was above that obtained for biodiesel fueled engine by 26%. Hydrogen contributed to a rise in  $NO_x$  emissions within the entire range of its share; for 38% hydrogen share a rise in specific  $NO_x$  emission of over 2.5 times was noted. Both studies used a naturally aspirated dual-fuel engine.

A modern dual-fuel engine (Fig. 5.4) might be far better fitted to a biodiesel and hydrogen-driven dual-fuel engine. Hydrogen is to be inducted, and biodiesel is to be injected within the engine cylinder. The engine operation parameters like compression ratio, intake pressure and temperature of the primary fuel (hydrogen), injection pressure and timing of the pilot fuel (biodiesel), amount of pilot fuel, EGR, equivalence ratio, and cooling water/oil temperature, engine speeds and others got to be varied so as to seek out their optimum values for minimum emissions and better output power. The experiments must be undertaken at a variable compression ratio (16–21) of the engine with differing types of combustion chamber (re-entrant, toroidal, etc.). Because intake pressure and temperature of primary fuel have a remarkable effect on engine performance and emissions, different intake pressures (1–4 atm) and temperatures (–40 to 60 °C) should be investigated to watch lean operation limit, output power and exhaust emissions.

The quantity of pilot fuel features a significant effect on power output and knocking of the engine. Therefore, pilot fuel rate shaping is extremely important for correct engine operation. The pilot amount should be varied between 5–10% of the entire energy supply to the engine. The lower end (5%) is better for minimal  $CO_2$  emission. Injection pressure and timing of the pilot fuel even have an excellent impact

on combustion and emissions. If the injection pressure is increased, very fine fuel droplets are often expected, thus creating a good fuel-air mixture within the combustion chamber, even within the remote part of the combustion chamber. This is often enhanced by the smaller orifice diameter of the injector. The above measure will increase the reaction rate and hence, the power output. Emissions also are expected to be lower at higher injection pressures. With advanced injection timing, the pressure peak could also be high, causing higher  $\text{NO}_x$ . However, with far advanced injection timing, the rate of heat release is predicted to be mild and therefore the pressure peak is reduced, leading to no knock or smoke, and reduced  $\text{NO}_x$ , HC and CO. A high cetane number of the pilot fuel may widen the knock-limited mixture strength within the weaker direction (leaner operation is possible). The injection timing could also be changed over a really wide selection from  $60^\circ$  BTDC up to TDC. Injection pressures of the pilot fuel are going to be varied from 20 to 300 MPa. Older diesel engine had fuel injection pressure of 20 MPa and modern diesel engine has fuel injection pressure as high as 300 MPa. A pressure transducer is required in the cylinder head to measure the cylinder pressure. The pressure signals within the cylinder, the TDC, and the degree of crank angle are going to be stored in a digital recorder. A multi-hole nozzle of the injector is required with a hole diameter from 0.1 to 0.26 mm (normal range of hole dia.). The spray angle is to be changed from  $130$  to  $160^\circ$  in some cases so as to research the effect of mixture formation on combustion. The overall equivalence ratio must be varied from 0.25 to 1.2 to investigate from very lean to rich combustions. The engine speed should be varied from 1000 to 3000 rpm (normal range of diesel engine speed). The temperatures of cooling water and engine oil are to be varied between 40 and  $90^\circ\text{C}$ . Higher cooling water/oil temperature is predicted to result in lower HC emissions. EGR features a marked effect on  $\text{NO}_x$  reduction. Different percentages of EGR 0–30% (usual range of EGR) are going to be investigated. Although external EGR helps to scale back  $\text{NO}_x$ , an internal EGR (by  $\text{N}_2$ , He,  $\text{H}_2\text{O}$ , etc.) must be considered to reduce  $\text{NO}_x$  to the zero level. Figure 5.10 shows nitrogen dilution. When charge diluents like He,  $\text{N}_2$  or  $\text{H}_2\text{O}$  in appropriate proportions is employed alongside the hydrogen fuel, the engine knocking tendency is suppressed and burning efficiency is improved. It's to explore more on charge diluents, especially on helium to work out its ability to reduce knock, to extend engine power and efficiency, and to scale back  $\text{NO}_x$  and smoke emissions. Exhaust emissions of HC, CO,  $\text{NO}_x$ , PM, aldehyde and  $\text{CO}_2$  must be determined with various gas analyzers. The right combination of the above-mentioned parameters, alongside employment of a catalyst system in a dual-fuel engine with proper strategy, renders the engine nearly emission-free. Ultimately, a near-zero emission hydrogen dual-fuel engine would evolve. Within the previous research work, the minimum diesel fuel used as a pilot fuel was 7.7% (Fig. 5.6). If the pilot amount was further reduced to 5% biodiesel as a pilot fuel, the  $\text{CO}_2$  emission is going to be on the brink of zero.

For the event of operational hydrogen engines, pre-ignition has been identified its most vital problems, which is due to hydrogen's lower ignition energy, wider flammability range, and shorter quenching gap. Premature ignition occurs when the fuel mixture within the combustion chamber pre-ignites, leading to an inefficient, rough-running engine. Variety of studies suggest that pre-ignition is caused by hot

spots within the combustion chamber, like on a sparking plug or exhaust valve, or on carbon deposits. Other research has revealed that backfire can occur when there's overlap between the openings of the intake and exhaust valves. Pre-ignition conditions are often reduced by EGR or water injection. EGR or water injection helps to reduce the temperature of hot spots, therefore reducing the likelihood of pre-ignition. The foremost effective means of controlling pre-ignition and knock is to re-design the engine for hydrogen use, specifically the combustion chamber and the cooling system. The combustion chamber should be such it generates low turbulence and swirl during compression. The cooling system must be designed to supply uniform flow to all or any locations that need cooling. Using multi-exhaust valves instead of bigger single-exhaust valves is useful to decrease pre-ignition. Cold-rated spark plugs are preferred over hot-rated types for hydrogen engines. A cold-rated plug is one that transfers heat from the plug tip to the cylinder head quicker than a hot-rated sparking plug. Hydrogen should be prevented from accumulating within the crankcase, and actually, just in case of accumulation, a correct pressure safety valve must be installed on the engine crankcase to avoid ignition inside the crankcase.

## 5.7 Conclusions

From the experimental results, the subsequent conclusions are drawn. A biodiesel is produced from urea fractionation with CP of  $-31.7^{\circ}\text{C}$ . However, the production efficiency was only 33%. To enhance the production efficiency, crystal fractionated by solid crystals and recovered urea mixture from the urea fractionation was attempted. This crystal fractionation resulted in significant improvements in production efficiency. Using 22.5 gm of solid crystals and 22.5 gm of recovered urea with 150 ml of methanol resulted in 100% production efficiency but CP was reduced to  $-18^{\circ}\text{C}$ . This biodiesel with CP of  $-18^{\circ}\text{C}$  may be a perfect one in mild winter in Canada. To form biodiesel with CP of  $-41^{\circ}\text{C}$  or lower, one possible method might be winterization of vegetable oil first to separate the high saturated fats, followed by using the remaining highly unsaturated oil to produce biodiesel, and eventually using the urea fractionation or crystal fractionation to produce fractionated biodiesel.

From hydrogen dual-fuel operation, a smooth and knock-free engine operation resulted from the utilization of hydrogen during a supercharged dual-fuel engine for leaner fuel-air equivalence ratios maintaining high thermal efficiency. It had been possible to achieve over 92% hydrogen energy substitution to the diesel fuel with zero smoke emissions. The hydrogen-operation produced the utmost IMEP of about 908 kPa and a thermal efficiency close to 42% with the very best fuel-air equivalence ratio of 0.3. CO and HC emissions were negligible. However, the  $\text{NO}_x$  emissions were high considering future regulations. Charge dilution by  $\text{N}_2$  was found as an efficient method of extending energy supplied by hydrogen to extend engine power. EGR in hydrogen engine seemed to be a superb method of reducing engine  $\text{NO}_x$  to the zero-ppm level, also as a practical method of suppressing engine knocking



and reducing the end gas temperature. The hydrogen with N<sub>2</sub> dilution 40% and 50% produced the very best IMEP of 1013 kPa, which was about 13% above that at hydrogen operation only. There was a dramatic reduction of NO<sub>x</sub> with different percentage of N<sub>2</sub> dilutions. The utmost NO<sub>x</sub> reduction of 100% was achieved with 60% N<sub>2</sub> dilution maintaining 15% higher IMEP than hydrogen operation.

To make a near-zero emissions from H<sub>2</sub>ICE, a dual-fuel engine operation with hydrogen as the primary fuel and biodiesel as a secondary fuel could be used. Although biodiesel's life cycle CO<sub>2</sub> emission is nearly 80% less than that of diesel, it still emits CO<sub>2</sub>. Therefore, the quantity of biodiesel use must keep as low as possible. From the hydrogen-diesel dual fuel operation, the minimum diesel was 7.7%. If the biodiesel amount is often brought right down to 5%, CO<sub>2</sub> emission would be 99% lower, as 95% primary hydrogen doesn't participate in CO<sub>2</sub> production. CP of biodiesel must be similar or less than winter diesel, in order that this engine is often used year-round with none problem of fuel gelling. This will be done by a method suggested before (winterization of vegetable oil first to separate the high saturated fats, followed by using the remaining highly unsaturated oil to produce biodiesel, and eventually using the urea fractionation to produce fractionated biodiesel) or some additives could also be necessary to decrease the CP of fractionated biodiesel. FB20S2 had the CP of as low as -48.2 °C and FB50S2 showed the CP of -47.5 °C, both temperatures are lower than winter diesel's CP (-41 °C). A neat H<sub>2</sub>ICE in dual fuel operation could also produce near-zero emissions of CO, HC, PM and NO<sub>x</sub>. Furthermore, this engine will help preserve petroleum fuels and can create a cleaner atmosphere and environment. From the economic point of view, H<sub>2</sub>ICE is going to be less expensive than hydrogen fuel cell vehicle, because H<sub>2</sub>ICE can use the prevailing IC engine infrastructure for its production, but hydrogen fuel cell vehicle must undergo an entire new costly infrastructure development.

The following outcomes are foreseen, if the aforementioned development of biodiesel and hydrogen-driven dual-fuel engines can be implemented.

- (1) Devise innovative methods or processes to enhance the CFPs of biodiesel.
- (2) Use hydrogen as the primary energy source in an IC engine aiming near-zero emissions.
- (3) Implement supercharging/turbocharging technology in hydrogen dual-fuel engine for higher power without knocking.
- (4) Bridge the gap between now and the time when fuel cell technology becomes a feasible option for everyday transportation.
- (5) Help the planet to meet the challenges of transitioning from a carbon economy to a hydrogen and bio-economy.

## References

- Agarwal AK (2007) Biofuels (alcohols and biodiesel) applications as fuels for internal combustion engines. *Prog Energy Combust Sci* 33:233–271
- Antunes JG, Mikalsen R, Roskilly AP (2009) An experimental study of a direct injection compression ignition hydrogen engine. *Int J Hydrogen Energy* 34:6516–6522
- Berckmuller M, Rottengruber H, Eder A, Brehm N, Elsasser G, Muller-Alander G et-al. (2003) Potentials of a charged SI-hydrogen engine. SAE paper 2003-01-3210

- Bose PK, Maji D (2009) An experimental investigation on engine performance and emissions of a single cylinder diesel engine using hydrogen as inducted fuel and diesel as injected fuel with exhaust gas recirculation. *Int J Hydrogen Energy* 34:4847–4854
- Demirbas A (2007) Progress and recent trends in biofuels. *Prog Energy Combust Sci* 33:1–18
- Directive 2009/28/EC. On the promotion of the use of energy from renewable sources and amending and subsequently repealing directives 2001/77/EC and 2003/30/EC. OJEU 2009; L 140:16–62
- Dunn RO, Shockley MW, Bagby MO (1996) Improving the low-temperature properties of alternative diesel fuels: vegetable oil-derived methyl esters. *J Am Oil Chem Soc* 73(12):1719–1728
- Dunn RO (2011) Improving the cold flow properties of biodiesel by fractionation. A book chapter by INTECH Open Access Publisher. <https://doi.org/10.5772/14624>
- Elsanusi O (2017) Cold flow improvement of biodiesel and investigation the effect of biodiesel emulsification on diesel engine performance and emissions. MSc Thesis, Mechanical Engineering Department, Lakehead University, Thunder Bay, Ontario, Canada
- Ghanei R (2015) Improving cold-flow properties of biodiesel through blending with nonedible castor oil methyl ester. *Environ Prog Sustain Energy* 34(3):897–902
- González Gómez ME, Howard-Hildige R, Leahy JJ, Rice B (2002) Winterization of waste cooking oil methyl ester to improve cold temperature fuel properties. *Fuel* 81(1):33–39
- Gopal G, Rao PS, Gopalakrishnan KV, Murthy BS (1982) Use of hydrogen in dual-fuel engines. *Int J Hydrogen Energy* 7:267–272
- Hamdan SH, Chong WWF, Ng JH, Ghazali MJ, Wood RJK (2016) Influence of fatty acid methyl ester composition on tribological properties of vegetable oils and duck fat derived biodiesel. *Tribol Int.* <https://doi.org/10.1016/j.triboint.2016.12.008>
- Handwerker M, Wellnitz J, Marzbani H (2021) Comparison of hydrogen powertrains with the battery powered electric vehicle and investigation of small-scale local hydrogen production using renewable energy. *Hydrogen* 2(1):76–100. <https://doi.org/10.3390/hydrogen2010005>
- Hord J (1978) Is hydrogen a safe fuel? *Int J Hydrogen Energy* 3:157–176
- Hosmath RS, Banapurmath NR, Bhovi M, Khandal SV, Madival AP, Dhannur SS, Gundalli V (2015) Performance, emission and combustion characteristics of dual fuel (DF) engine fuelled with hydrogen induction and injection of Honne and Honge methyl esters. *Energy Power Eng* 7:384–395
- Jaura AK, Ortmann W, Stuntz R, Natkin B, Grabowski T (2004) Ford's H2RV: an industry first HEV propelled with a H<sub>2</sub> fuelled engine—a fuel-efficient and clean solution for sustainable mobility. SAE paper 2004-01-0058
- Knothe G (2009) Improving biodiesel fuel properties by modifying fatty ester composition. *Energy Environ Sci* 2(7):759
- Kruka VR, Cadena ER, Long TE (1995) Cloud-point determination for crude oils. *J Pet Technol* 47(08):681–687. <https://doi.org/10.2118/31032-PA>
- Lanjekar RD, Deshmukh D (2016) A review of the effect of the composition of biodiesel on NO<sub>x</sub> emission, oxidative stability and cold flow properties. *Renew Sustain Energy Rev* 54:1401–1411
- Liu G (2015) Development of low-temperature properties on biodiesel fuel: a review: low-temperature properties of biodiesel fuel. *Int J Energy Res* 39:1295–1310
- Mangad A (2017) Year-round biodiesel use strategy in diesel engines in Canadian adverse cold weather conditions. MSc Thesis, Mechanical Engineering Department, Lakehead University, Thunder Bay, Ontario, Canada
- Mathur HB, Das LM, Patro TN (1992) Hydrogen fuel utilization in CI engine powered end utility system. *Int J Hydrogen Energy* 17:369–374
- Mei D, Luo Y, Tan W, Yuan Y (2016) Crystallization behavior of fatty acid methyl esters and biodiesel based on differential scanning calorimetry and thermodynamic model. *Energy Sources, Part A Recovery, Utilization, and Environmental Effects* 38(15):2312–2318
- Nagalingam B, Dübel M, Schmillen K (1983) Performance of the supercharged spark ignition hydrogen engine. SAE paper 831688

- Nainwal S, Sharma N, Sharma AS, Jain S, Jain S (2015) Cold flow properties improvement of *Jatropha curcas* biodiesel and waste cooking oil biodiesel using winterization and blending. *Energy* 89:702–707
- Natkin RJ, Tang X, Boyer B, Oltmans B, Denlinger A, Heffel JW (2003) Hydrogen IC engine boosting performance and NOx study. SAE paper 2003-01-0631
- O'Brien RD (2008) *Fats and oils: formulating and processing for applications*. CRC press
- Ozsezen AN, Canakci M, Turkcan A, Sayin C (2009) Performance and combustion characteristics of a DI diesel engine fueled with waste palm oil and canola oil methyl esters. *Fuel* 88:629–636
- Pérez A, Casas A, Fernández CM, Ramos MJ, Rodríguez L (2010) Winterization of peanut biodiesel to improve the cold flow properties. *Biores Technol* 101(19):7375–7381
- Roy MM, Calder J, Wang W, Mangad A, Diniz FCM (2016) Cold start idle emissions from a modern Tier-4 turbo-charged diesel engine fueled with diesel-biodiesel, diesel-biodiesel-ethanol, and diesel-biodiesel-diethyl ether blends. *Appl Energy* 180:52–65
- Roy MM, Calder J, Wang W, Mangad A, Diniz FCM (2016) Emission analysis of a modern Tier 4 DI diesel engine fueled by biodiesel–diesel blends with a cold flow improver (Wintron Synergy) at multiple idling conditions. *Appl Energy* 179: 45–54
- Roy MM, Tomita E, Kawahara N, Harada Y, Sakane A (2010) An experimental investigation on engine performance and emissions of a supercharged H<sub>2</sub>-diesel dual-fuel engine. *Int J Hydrogen Energy* 35:844–853
- Roy M, Wang W, Bujold J (2013) Biodiesel production and comparison of emissions of a DI diesel engine fueled by biodiesel–diesel and canola oil–diesel blends at high idling operations. *Appl Energy* 106:198–208. <https://doi.org/10.1016/j.apenergy.2013.01.057>
- Sarin A, Arora R, Singh NP, Sarin R, Malhotra RK, Sarin S (2010) Blends of biodiesels synthesized from non-edible and edible oils: effects on the cold filter plugging point. *Energy Fuels* 24(3):1996–2001
- Shahir VK, Jawahar CP, Suresh PR (2015) Comparative study of diesel and biodiesel on CI engine with emphasis to emissions—a review. *Renew Sustain Energy Rev* 45:686–697. <https://doi.org/10.1016/j.rser.2015.02.042>
- Sharma AK, Sharma PK, Chintala V, Khatri N, Patel A (2020) Environment-friendly biodiesel/diesel blends for improving the exhaust emission and engine performance to reduce the pollutants emitted from transportation fleets. *Int J Environ Res Public Health* 17:3896. <https://doi.org/10.3390/ijerph17113896>
- Sharma P, Dhar A (2018) *Advances in hydrogen-fuelled compression ignition engine*. Singh AP et al (eds) *Prospects of alternative transportation fuels, energy, environment, and sustainability*. Springer Nature Singapore Private Limited. [https://doi.org/10.1007/978-981-10-7518-6\\_5](https://doi.org/10.1007/978-981-10-7518-6_5)
- Sheehan J, Camobreco JD, Graboski M, Shapouri H (1998) Life cycle inventory of biodiesel and petroleum diesel for use in an urban bus. Final report for US department of energy's office of fuel development and the US department of agriculture's office of energy, by the national renewable energy laboratory. NERL/SR-580-24089
- Tutak W, Grab-Rogalinski K, Jamrozik A (2020) Combustion and emission characteristics of a biodiesel-hydrogen dual-fuel engine. *Appl Sci* 10:1082. <https://doi.org/10.3390/app10031082>
- US EPA (2002) A comprehensive analysis of biodiesel impacts on exhaust emissions. EPA420-P-02-001
- Verma P, Sharma MP, Dwivedi G (2016) Evaluation and enhancement of cold flow properties of palm oil and its biodiesel. *Energy Rep* 2:8–13
- Yuan MH, Chen YH, Chen JH, Luo YM (2017) Dependence of cold filter plugging point on saturated fatty acid profile of biodiesel blends derived from different feedstocks. *Fuel* 195:59–68
- Zhao W, Xue Y, Ma P, Ma W, Wang J, Lu D, Han S (2016) Improving the cold flow properties of high-proportional waste cooking oil biodiesel blends with mixed cold flow improvers. *RSC Adv* 6(16):13365–13370

# Chapter 6

## Assessment of Hydrogen as an Alternative Fuel: Status, Prospects, Performance and Emission Characteristics



**Mohammad Towhidul Islam, Khodadad Mostakim, Nahid Imtiaz Masuk,  
Md. Hasan Ibna Islam, Fazlur Rashid, Md. Arman Arefin,  
and Md. Abid Hasan**

**Abstract** The rapid depletion of fossil fuels has prompted the upcoming generations to adopt alternative resources which are similarly efficient and could meet the soaring energy demand. Furthermore, being non-renewable in nature, having an adverse effect on the environment while burning and mining, the replacement of this outdated means of energy supplies will be the future challenge in addressing the environmental and economic issues in a sustainable manner. However, among the practiced alternative sources, the most popular sources are renewable energy (solar, wind, geothermal, biomass energy), nuclear energy, or hybrid nuclear energy. Although the energy demand is somehow getting fulfilled, these are not able to contribute enough to fulfilling energy demand for having some drawbacks and inconsistencies. For instance, the insufficient power generation capacity, relatively lower efficiency, necessitating the huge upfront capital, and dependency on geographical conditions and locations impede their potential in covering the energy demand on a large scale. Besides, nuclear energy poses a security risk and generates radioactive waste. Similarly, biomass energy sources can lead to serious deforestation. On the contrary, hydrogen is getting popularity as an alternative fuel because of its cleaner production, non-toxicity, economic feasibility, and having a satisfactory efficiency than most other energy sources. It's nonpolluting production from electrolysis and renewable sources, and wide range of flammability implies its scalability and greener solution for transportation. Considering these aspects, hydrogen as fuel may be a promising solution in the future. In this study the evaluation of hydrogen as a

---

M. T. Islam (✉) · K. Mostakim · N. I. Masuk · Md. H. I. Islam · F. Rashid  
Department of Mechanical Engineering, Rajshahi University of Engineering & Technology,  
Rajshahi 6204, Bangladesh

Md. A. Arefin  
Safe and Reliable Nuclear Applications, IMT Atlantique, 44300 Nantes, France

Md. A. Hasan  
American International University - Bangladesh, Dhaka, Bangladesh

fuel over other alternative energy resources has been evaluated in terms of performance and emission characterization. Moreover, the economical assessment carried out in this chapter will make a comprehensive demonstration of the feasibility and prospect of hydrogen over the other sources. Further, this study also identifies some challenges and limitations and their possible solutions regarding the production and use of hydrogen.

**Keywords** Hydrogen · Alternative fuel · Emission control · Carbon reduction · Economical feasibility

## 6.1 Introduction

To keep pace with the soaring energy demand and rapid industrialization, global efforts are being enforced against the high fuel prices, environmental pollution, and energy insecurity. In this modern civilization, fossil fuels are the primary energy supplier for transportation and industrial application. Therefore, energy scarcity is now a serious concern for this overdependence on conventional fuels like diesel, gasoline, compressed natural gas, and liquefied petroleum gas. The limited reserves of this petroleum-based fuel lie only in certain regions in the world and their uses are on the verge of peak production. It is estimated that the reservation of current petroleum fuels will be depleted within 50 years if the rate of consumption remains like the present scenario (Demirbas 2017). However, significant attempts are being taken in order to introduce the alternative sources and adopt them efficiently. The uses of biomass sources becoming more attractive in terms of mitigating the emissions during the combustion due to the fossil-based fuels, increasing fuel costs, and scarcity of energy supplies (Şensöz et al. 2000). Growing trends are being noticed in developed countries to adopt modern technologies and advancements in order to produce different biofuels and use them cost-effectively and efficiently as compared to conventional fuels. Because of these laudable initiatives, different alternative fuels such as biodiesel, bioethanol, and hydrogen from biomass are being introduced which will hold sustainable energy security for the future (Demirbas 2007). However, among these alternative fuels hydrogen holds the most significant potential to be used as a fuel in the future because of its availability and environment-friendly production (Demirbas 2017). It is suggested that replacing the application of fossil resources by hydrogen energy system would be the prominent solution to the current global problems (Veziroglu 2007).

The by-products and the production of hydrogen fuel have made this more attractive because of its neutral impact on the environment and diversified application (Fig. 6.1). Though it is not the primary fuel, the production from using water can be done by electrolysis with the help of both renewable and non-renewable sources. Electrical energy can be produced by utilizing renewable sources like solar, wind, geothermal, or hydropower. All these sources can be used directly in the electrolysis process which eventually produces hydrogen fuel. Therefore, an important linkage

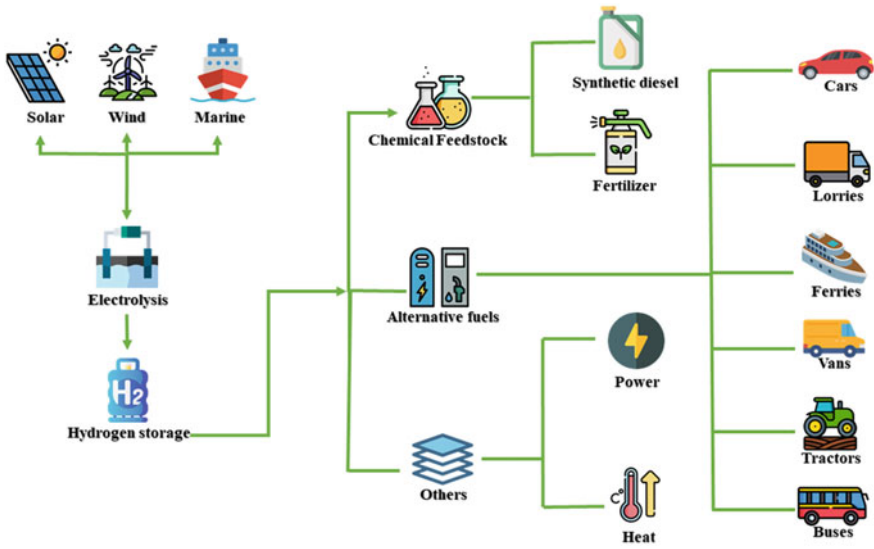


Fig. 6.1 Hydrogen production and its diversified uses

may be carried out between renewable energy and chemical energy because of hydrogen production.

Moreover, hydrogen holds some important properties as fuel which make it efficient economically and increasing the engine performance as compared to conventional fuel. From Table 6.1, it can be seen that hydrogen holds a wide range of flammability which implies that it can be combusted in an engine with the air–fuel mixture on a large scale. Another property of hydrogen is it can run on a lean mixture which effects positively fuel economy and complete combustion. Hydrogen has the highest flame propagation, widest lean-burn limit, highest diffusivity in air, smallest quenching gap, and lowest ignition energy (Duan et al. 2019; Verhelst et al. 2011). Hydrogen shortens combustion duration and advances combustion phasing. Thus, improving combustion and increasing thermal efficiency of engines can be done by hydrogen. Yu et al. (2017) conducted research on petrol engine to understand the lean

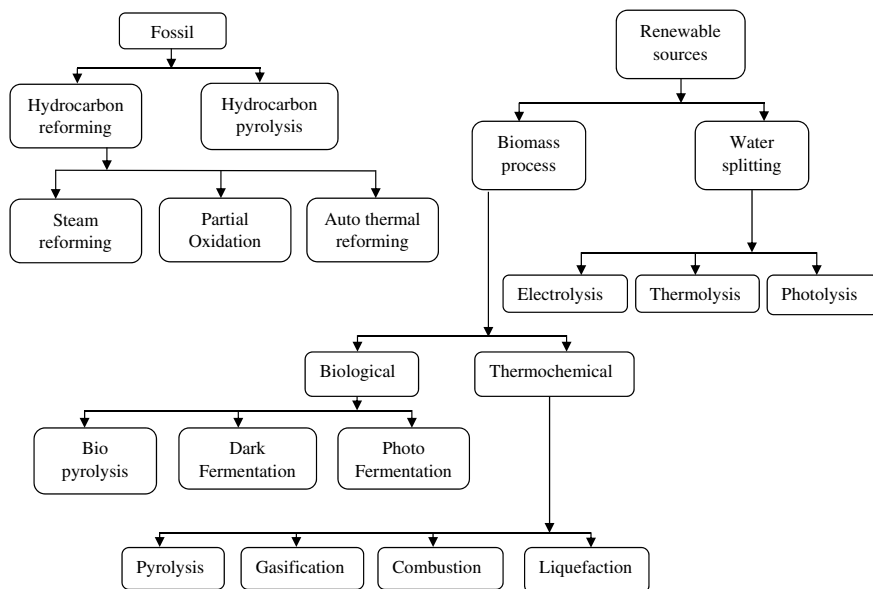
Table 6.1 Properties of hydrogen (Hord 1978)

Property	Value
Flammability in air (vol, %)	4–75
Autoignition temperature (k)	858
Lower calorific value (MJ/kg)	119.93
Burning Velocity in air (cm/s), NTP	265–325
Minimum Energy for ignition (mJ)	0.02
Diffusion coefficient in NTP air (cm <sup>2</sup> /s)	0.61
Quenching gap in NTP air (cm)	0.064

burn characteristics through direct injection of hydrogen. The study showed that at a constant heat released condition, 10% hydrogen fraction significantly improved the engines emission characteristics and performance. The direct injection of hydrogen significantly enhanced the combustion stability of lean-burn mixtures, and pointedly amended the thermal efficiency and mean effective pressure. The injection of hydrogen at optimum ignition timing suggestively shortens the rapid combustion duration and flame-development period. Li et al (2020) suggested that split hydrogen direct injection provides better fuel economy and performance. Authors reported that better performances, efficiency and emissions are obtained with split hydrogen direct injection. In such a case at the same time the mixture closer to the spark plug is denser and in other zone is more homogeneous. Study also reports that direct hydrogen injection removes the backfire issue, which is extremely helpful to reduce emission and enhance combustion. Also, the break power and break power efficiency of the engine improves with the direct injection of hydrogen (Meng 2018). Additionally, the in-cylinder temperature becomes lower which results in decreasing the NO<sub>x</sub> amount. The flame speed of hydrogen is also high which implies that the hydrogen-fueled engine is more identical to the ideal thermodynamic cycle. Also, the high diffusivity results in a uniformed air–fuel mixture. However, there can be a problem with storing to provide a sufficient driving range because of its lower density. Lower ignition energy could lead to premature ignition also.

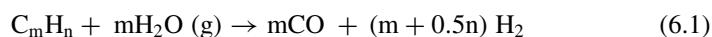
## 6.2 Worldwide Scenario of Hydrogen Production Technologies

Hydrogen is found to be the lightest chemical element in the periodic table having an atomic weight of 1.008 was discovered in 1766 by Cavendish (Szydło 2020). It is found abundantly in-universe constituting about 75% of all baryonic mass (Noorollahi and Yousefi 2010). A large amount of energy can be delivered by hydrogen (Manoharan, et al. 2019). Thus, the production of hydrogen has of great importance. There involve various methods of generating hydrogen involving different technologies. Hydrogen can mainly be generated using fossil fuels (FF) and renewable sources (RS). Producing hydrogen using fossil fuels further divided into the hydrogen reforming (HR) and hydrocarbon pyrolysis (HP) process. Hydrocarbon reforming further subdivided into steam reforming (SR), partial oxidation (PR), and auto thermal reforming (ATR). Hydrogen production regarding renewable sources can be divided into biomass process (BMP) and water splitting (WS). BMP is divided into biological processes (BP) and thermochemical processes (TP). WS is divided into electrolysis process (EP), thermolysis process (TP), and pyrolysis process (PP). BP is divided into bio-pyrolysis, dark fermentation, and photo fermentation. The thermochemical process is divided into pyrolysis, gasification, combustion, and liquefaction process (Nikolaidis and Poullikkas 2017). All these processes regarding hydrogen production are shown in Fig. 6.2.

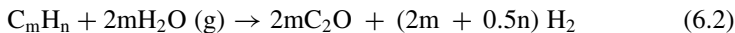


**Fig. 6.2** Different methods of hydrogen production (Nikolaidis 2017)

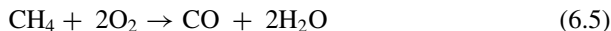
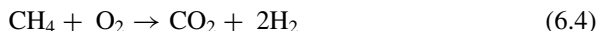
Generating hydrogen using fossil fuels constitutes the major portion of hydrogen production. Until 2016, Natural gas, heavy oil well as naphtha, and coal constitute 48%, 30%, and 18% of hydrogen production respectively (Nikolaidis and Poullikkas 2017). A major portion of hydrogen is generated using the steam reforming process from natural gas with or without Carbon Capture and Storage (CCS) (Noorollahi and Yousefi 2010). Steam reforming is an endothermic reaction process (Nikolaidis and Poullikkas 2017) and it can be accomplished using methane steam reforming (MSR), ethanol steam reforming (SRE) and methanol steam reforming (Mer) (Chen et al. 2019). Methane steam reforming is used in the production of 50% world hydrogen. Methanol steam reforming is used in 75% of hydrogen production. Due to less toxicity and easier storing benefit, ethanol steam reforming has more advantages in hydrogen production (Chen et al. 2019). Steam reforming is comprised of double stages. At the initial stage, the hydrocarbon is diluted with the steam and is passed into the tubular catalytic converter. At this stage, a syngas (mixture of carbon mono oxide and hydrogen) and a small amount of carbon dioxide is produced as shown in reaction (6.1) and (6.2). The desired temperature of the reaction is gained by introducing air or oxygen into the combustion part of the catalytic converter. At the second stage using CO (carbon monoxide) catalytic converter the carbon mono oxide is converted into carbon di oxide and hydrogen as shown in reaction (6.3). The raw material used in the steam reforming process need to be free of sulfur to avoid deactivation of catalysis used (Kalamaras and Efstathiou 2013a).







Partial oxidation is non-catalytic process where hydrocarbon is converted into hydrogen by reaction with oxygen as shown in reaction (6.4) and (6.5). In this process, more carbon mono oxide is produced compared to SR process which is further converted into Hydrogen and carbon di oxide (Kalamaras and Efstathiou 2013a).



Using partial oxidation the concentration of generated hydrogen from biodiesel (fatty acid methyl ester) and heavy fuel oil was found 18.80% and 17.67% respectively (Lin and Wu 2019). However partial oxidation has lower efficiency and higher production cost compare to the steam reforming process (El-Shafie et al. 2019). Steam reforming (SR) and partial oxidation's (PO) combined effect make the auto thermal reforming (ATR) process. Thus, the ATR has a combined effect of an exothermic and endothermic reaction. ATR is less expensive compared to SR of methane and does not require external heat. Along with this advantage, ATR has quick start-up and shut down characteristics and generates a large amount of hydrogen compared to partial oxidation (Kalamaras and Efstathiou 2013a). ATR truncates the requirement of hydrogen storage (Zhang et al. 2017). The catalytic and non-catalytic reaction makes a significant difference in the production of hydrogen in the ATR process. The catalytic reaction yields up to 29.4% of the molar fraction of hydrogen production while the non-catalytic one yields below half (12.2%) of the molar fraction of hydrogen production than of catalytic one (Zhang et al. 2017). ATR can produce 31% of hydrogen as compared to PO (Chen et al. 2021). Another method of hydrogen production is water splitting electrolysis. In water-splitting electrolysis, water is decomposed into hydrogen and oxygen with the aid of electricity. There exist electrolysis processes of three types such as Alkaline Electrolysis (AEL), Proton Exchange Membrane (PEM) electrolysis, and Solid Oxide Electrolysis (SOEL). SOEL is still in the progressive phase and yet to be developed. In the AEL two electrodes are dipped in the solution of 5–40% solution of sodium hydroxide (NaOH) or potassium hydroxide (KOH). External DC source is applied between electrodes. The water molecules are reduced to hydrogen gas ( $H_2$ ) and hydroxide ion ( $OH^-$ ) in the cathode. This  $OH^-$  ion is directed towards the anode and produce oxygen gas ( $O_2$ ) after giving up electrons to the anode (Burton 2021). In the case of PEM electrolysis, instead of electrolysis, a sulfonated polystyrene membrane is used. Here, hydrogen gives up electrons to produce  $O_2$  and hydrogen ions ( $H^+$ ) in the anode. This electron flows through the external circuit. The  $H^+$  is directed towards the cathode and reduced to form  $H_2$

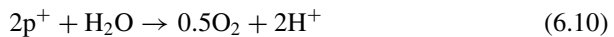
(Burton 2021). 4% of world total hydrogen is produced using electrolysis (Burton 2021).

Another form of water splitting sub type is thermolysis. In thermolysis the water molecule is divided into  $H_2$  and  $O_2$ . The following reaction takes place in a thermolysis process:



The temperature range for electrolysis can be of two types- low-temperature electrolysis (LTE) having a temperature range of 343–363 K and high-temperature electrolysis (HTE) having a temperature range of 973–1273 K. Among these two types, HTE is not industrially acceptable (Safari and Dincer 2020). Another form of water splitting type of hydrogen production is photolysis. In photolysis, sunlight is used to produce hydrogen. Sunlight is absorbed by the semiconducting material and an electron–hole pair is generated when the photon energy of sunlight is more than the bandgap energy of the semiconducting material. This electron–hole pair split the water into a hydrogen ion ( $H^+$ ) and  $O_2$  at the anode terminal. The  $H^+$  is directed to the cathode through the electrolyte and  $O_2$  is returned to the water. Electron is directed towards the cathode terminal by external circuit where they react with  $H^+$  and produce  $H_2$  (Nikolaidis and Poullikkas 2017). The following reaction takes place in a photolysis process:

Anode reaction:



Cathode reaction:

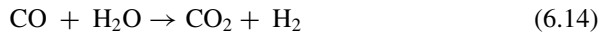
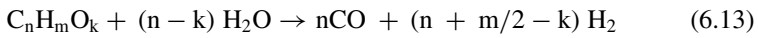


Overall reaction:

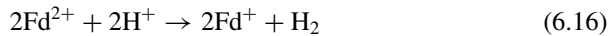
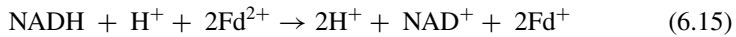


In the photolysis process, the hydrogen production cost is 10.26\$/kg (Nikolaidis and Poullikkas 2017). Hydrogen production from biomass can play a vital role in worldwide carbon dioxide ( $CO_2$ ) reduction. Bio pyrolysis, Dark fermentation, and

Photo fermentation are three types of biological processes to produce hydrogen from biomass sources. Pyrolysis is the process of biomass decomposition thermally without the presence of oxygen. The pyrolysis process gives rise to the fuel gas and bio-oil called pyrolytic oil, Pyrolytic oil has an energy density of ten times that biomass and it can be converted into bio-diesel and hydrogen (Soria et al. 2019). This pyrolytic oil is converted into syngas (mixture of carbon mono oxide and hydrogen) which is further converted to produce  $H_2$  using water gas shift reaction.



Hydrogen production from the rice was found to be 24.9% using pyrolysis from rice husk (bio mass) (Fu et al. 2020). Dark fermentation or heterotrophic fermentation is anaerobic fermentation where hydrogen is produced in anerobic condition without the presence of light and certain coenzyme. There are two ways of producing hydrogen in dark fermentation process. One is formic acid decomposition and another is reoxidation of nicotinamide adenine dinucleotide (NADH) with the presence of hydrogenase enzyme (Show et al. 2019). The reaction for the later one is:



In the dark fermentation process hydrogen is found below 70% (<70%) and other components found are  $CO_2$ , other gases such as  $H_2S$ ,  $CH_4$ , water vapor, and ammonia. Thus, the hydrogen used as fuel needs to be purified before using in any engine. The storage, purification, and transportation of hydrogen need to be considered before using the dark fermentation process (Show et al. 2019). Another form of the fermentation process is photo fermentation where the light source is needed to provide external energy to conduct a reaction and ultimately producing hydrogen gas (Argun and Kargi 2011). Production of hydrogen from acetic acid using photo fermentation is shown in Eq. (6.16).



A certain environmental condition such as  $p^H$  ranges from 6.8 to 7.5 and temperature ranges from 341 to 348 K is needed for photo fermentation (optimal condition) (Argun and Kargi 2011). Photo fermentation produces more  $H_2$  compared to the dark fermentation process. From photo fermentation,  $H_2$  yield is 80% (Argun and Kargi 2011).

### 6.3 Economically Feasible Hydrogen Production Processes

Hydrogen ( $H_2$ ) gas is a significant future fuel that can be utilized as an alternative to conventional fuel. The resources for conventional fuels (natural gas, coal, oil) are decreasing while energy demand is rising (Das et al. 2021; Hoque et al. 2021). On the other hand, hydrogen ( $H_2$ ) gas is the easiest, simpler, and abundant fuel source available globally. Hydrogen ( $H_2$ ) gas is possible to easily combine with different other elements. They are usually available with different other substances including alcohol, water, and so on. Additionally, they are even available in plants, biomass, and animals. Hence, this source of energy can be utilized to replace conventional fuels although it is usually assumed as a carrier of energy rather than a source of energy (Kalamaras and Efstathiou 2013b). However, in hydrogen fuelled engines, it is required to use natural gas to power them because hydrogen is very flammable than natural gas and even hard to carry than conventional fuel and natural gas. Therefore, hydrogen fuelled engines are powered using natural gas to make the system more safe and reliable.

Hydrogen ( $H_2$ ) gas is generally produced from different sources including nuclear, biomass, natural gas, renewable sources, coal, and so on. However, using fossil or conventional fuel, hydrogen can be generated and this method is one of the main options of hydrogen production. The other options for hydrogen generation are electrical, biochemical, thermal, and photonic. In the generation of hydrogen, plasma technology is used which is sensitive in nature, hence, a lower level of impacts on the environment is a major issue and so emissions generated during hydrogen production are processed to reduce the level of environmental pollutions (El-Shafie et al. 2019).

The normalized associated costs of different hydrogen generation processes such as electrolysis, plasma arc decomposition, splitting water thermally, and biomass gasification are 7.34, 9.18, 8.06, and 8.26 respectively. On the other hand, the normalized energy efficiency for these processes are 5.30 (electrolysis), 7.00 (plasma arc decomposition), 4.20 (splitting water thermally), and 6.50 (biomass gasification) (Kayfeci et al. 2019).

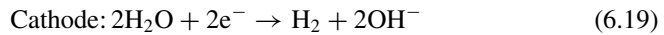
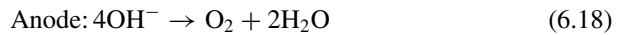
#### 6.3.1 Hydrogen Generation Through Electrolysis

The water electrolysis process for hydrogen generation is the fundamental method for the generation of hydrogen ( $H_2$ ) gas. In this process, electrons are transferred to generate hydrogen ( $H_2$ ) gas in an external electrical circuit. Among different available technologies for hydrogen ( $H_2$ ) generation, polymer membrane, alkaline, solid oxide electrolyzers are the most notable. The required cell temperatures for alkaline and polymer membrane process for hydrogen generation are lower usually than 353 K. While, the solid oxide electrolyzers method maintains a higher temperature for the generation of hydrogen ( $H_2$ ) gas. The rate of hydrogen generation is usually

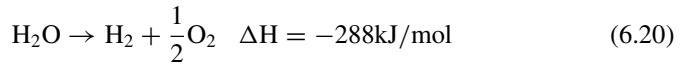
faster in the case of alkaline electrolyzers ( $<760 \text{ Nm}^3/\text{h}$ ) when compared to polymer membrane ( $<30 \text{ Nm}^3/\text{h}$ ) (Dincer and Acar 2015). The purity of hydrogen generated from alkaline electrolyzers was over 99.8% and in plasma membrane process, the purity was found 99.999% (Dincer and Acar 2015). The efficiency of each of the three hydrogen generation processes is dependent on the exact exergies required for driving the necessary reactions. However, the electrical efficiency of hydrogen generation through electrolysis is about 70–80%.

In the water electrolysis process, catalysts are usually used to raise the density of current and the reaction rate of electrolysis. Heterogeneous type material (Platinum) is usually used as one of the common catalysts in electrodes of the electrical circuits during hydrogen generation. Although the associated costs of homogeneous materials are low than heterogeneous materials (Karunadasa et al. 2010). Polymer membrane electrolyzers show a high level of sensitivity that is used for water purification and desalination purposes where brine solution is provided to at the electrolyzer.

In the alkaline electrolyzer process, a solution of alkaline is divided into two different types of electrolytes including Potassium hydroxide (KOH) and Sodium chloride (NaCl) with Sodium hydroxide (NaOH). In this process, hydroxide and hydrogen are produced in the cathode, and after that hydroxide is transferred to the anode to generate oxygen through the following two equations (Turner et al. 2008).



The overall anode and cathode reactions can be expressed through the Eq. (6.20).

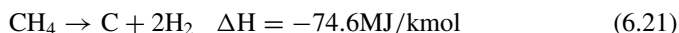


The associated costs of the alkaline process are low but the key challenge is the problems of corrosion. To overcome these challenges a proton exchange type membrane electrolyzer process is used although the production costs of hydrogen are much higher than alkaline electrolyzer.

### ***6.3.2 Hydrogen Generation Through Plasma Arc Decomposition***

Plasma is a state of ionization of material that includes exciting electrons and atoms. This method has the capacity to generate hydrogen ( $\text{H}_2$ ) by releasing medium to a high level of voltage and current. The reason for these high levels of voltages and currents is the presence of particles that are electrically excited.

By using plasma activity thermally, natural gas ( $\text{CH}_4$ ) is dissociated to hydrogen ( $\text{H}_2$ ) as well as black soot or carbon (C). In this process, the generated carbon or soot particles are solid in phase while hydrogen is obtained in the gaseous phase. In this reaction, an average of 74.6 MJ/kmol of heat is evolved as shown in the Eq. (6.21) (Fulcheri et al. 2002).

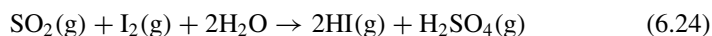
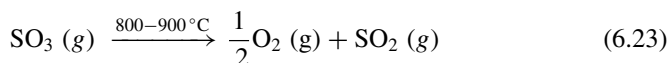
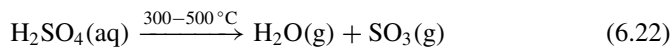


In this mechanism, gas of plasma is provided from 2 to 3 electrodes and natural gas ( $\text{CH}_4$ ) is supplied from the top of the system reactor. The main advantage of this method is the ability to generate pure hydrogen ( $\text{H}_2$ ) gas with less environmental emissions including carbon-dioxide ( $\text{CO}_2$ ), carbon-monoxide (CO), and so on. The costs of production of hydrogen ( $\text{H}_2$ ) gas are at least 5% lower in the plasma arc decomposition method than methane ( $\text{CH}_4$ ) reforming process (Gaudernack and Lynum 1998).

### 6.3.3 Hydrogen Generation Through Splitting Water Thermally

This method is economically viable as no catalysis is needed to operate or run chemical reactions. Additionally, all required materials for hydrogen generation through this process are recyclable except water ( $\text{H}_2$ ). In this method, no additional membrane separation for hydrogen–oxygen is needed and the full process can be performed with a reasonable level of temperatures in the range of 600–1200 K. The overall required amount of energy is zero that eventually decreases the overall costs of production.

Initially aqueous Sulphuric acid ( $\text{H}_2\text{SO}_4$ ) was heated up to a temperature of 773 K to generate water with  $\text{SO}_3$  in gaseous form. After that gaseous  $\text{SO}_3$  is subdivided into Sulphur-di-oxide ( $\text{SO}_2$ ) to make an exothermic reaction with iodine ( $\text{I}_2$ ) to produce hydrogen ( $\text{H}_2$ ) gas through the following equations (Balta et al. 2009).



Finally, hydrogen iodide (HI) is decomposed to hydrogen ( $\text{H}_2$ ) gas at a temperature of 698–723 K by using Eq. (6.25).



The full process of hydrogen generation through this mechanism is simple and straightforward. Also, there are no other side reactions required that helps to recycle all materials except water ( $H_2O$ ).

However, to reduce the overall hydrogen generation costs, solar, biomass and nuclear energy sources are used as possible thermal resources. These sources are considered renewable options that drastically reduce hydrogen generation costs.

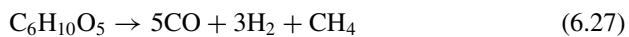
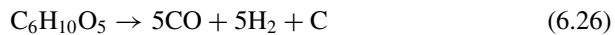
### 6.3.4 Hydrogen Generation Through Biomass Gasification

The gasification process is another economical process of hydrogen generation. This process is mainly incorporated for coal as well as biomass gasification method. The process is performed in absence of oxygen or partial supply of oxygen and mainly a partial process of oxidation. The product materials are natural gas ( $CH_4$ ), hydrogen ( $H_2$ ), and carbon monoxide ( $CO$ ) (Demirbas 2006).

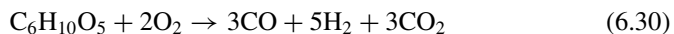
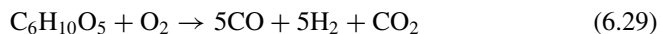
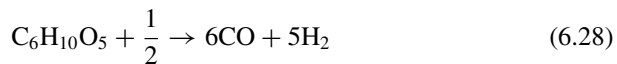
In this process, moisture is generated that needs to be vaporized to increase the overall efficiency. This mechanism can be performed without or with the use of catalysts in different types of reactors including fluidized, fixed bed type reactors where the performance and overall efficiency of the initial one are high when compared to the later one (Asadullah et al. 2002).

There are pyrolysis, partial oxidation, and steam reforming processes in the gasification method where hydrogen ( $H_2$ ) gas is produced through the following fundamental equations.

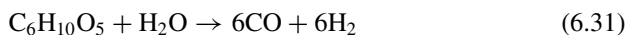
Pyrolysis process:



Partial oxidation process:



Steam reforming process:





The advantages of hydrogen gas generation from biomass gasification process are lower level of carbon-dioxide emissions, low cost of production, and reduction of cost of wastes, and increase usage of residues of crops of agriculture. The shortcomings of these processes are the generation of tars in higher quantities and corrosion.

## 6.4 Hydrogen as an Alternative Fuel

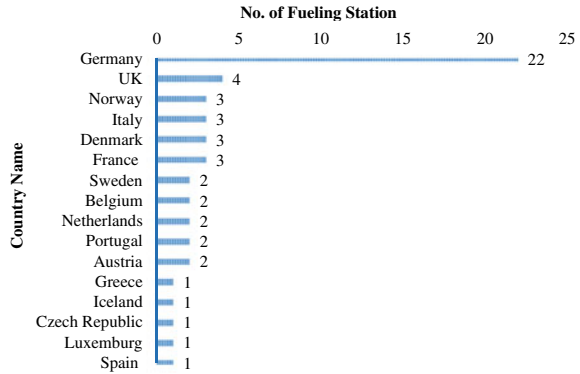
Hydrogen is a non-poisonous and non-toxic fuel. Hydrogen is 57 times the weight of gasoline and 14 times the weight of air. As a result, it will often increase and spread quickly. This is a secure benefit in a public setting. Hydrogen, on the other hand, has a large energy content by weight rather than volume. It's compressed and kept under extreme pressure. As a result, it may appear tough to store at first glance. The pressure relief mechanisms in hydrogen tanks, on the other hand, keep the pressure in the tanks from rising. In terms of accessibility, hydrogen is readily available, and there are various ways to obtain it in its purest form, which may then be utilized as a fuel. In terms of vehicle ignition temperature, hydrogen is hotter than other fuels, and its flammability range in the air is 4–75%, which is quite high when compared to other fuels. Hydrogen takes less energy to ignite than air under ideal combustion conditions (29% hydrogen to air volume ratio) (<https://h2tools.org/bestpractices/hydrogen-compared-other-fuels>).

### 6.4.1 *In Terms of Availability*

The need for natural gas is increasing more than any other fossil fuel alternatives available (Ogola 2012). The usable natural gas left up to 3rd July is  $1.088 \times 10^{12}$  in BOE (billions of Oil Equivalent). (Muffler 1978). According to the Global Energy Review 2021 (Ogola 2012), the demand for natural gas in 2021 has risen by 3.2% due to the incremental demand rise in the Middle East, Asia, and Russia which is visioned to be more than 1% global demand in 2019 (Ogola 2012). Most of the hydrogen is generated using natural gas involving different technologies. More than 50% of hydrogen is found using steam reforming of natural gas (Kaiwen et al. 2017). Figure 6.3 shows the total hydrogen fueling station in European Union that considers the hydrogen fueling station up to 2014. Referring to Fig. 6.3, it is seen that most numbers of the hydrogen fueling stations resides in Germany. The United Kingdom (UK) has 4 stations, Norway, Italy, Denmark and France have 3 stations each, Sweden, Belgium, Netherlands, Portugal, Austria, and Greece have 2 stations



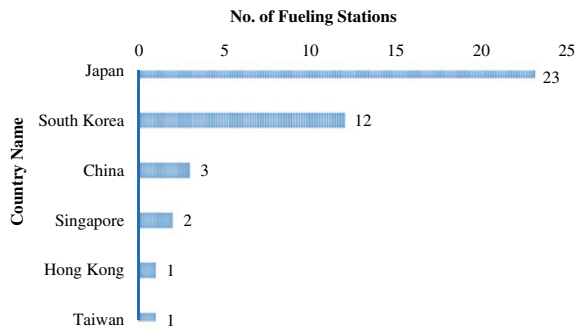
**Fig. 6.3** Hydrogen fueling station in European Union countries (Alazemi and Andrews 2015)



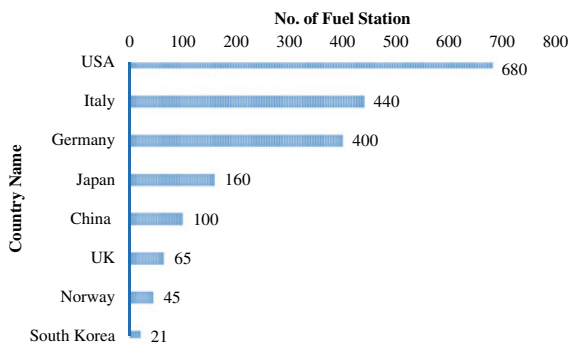
each, and Greece, Iceland, Czech Republic, Luxemburg, and Spain have 1 station each.

Figure 6.4 shows the hydrogen fueling stations in Asian countries up to 2014. Referring to Fig. 6.4, it is seen that Japan constitutes major numbers of hydrogen fueling stations while South Korea being the second-highest and Taiwan has only one fueling station. Comparing European and Asian overview, European Union countries cover more hydrogen fueling stations than in Asia. With the environmental concern and headache of reducing emissions of the greenhouse, the application of hydrogen as fuel is increasing day by day. Figure 6.5 shows the incremental condition of the hydrogen fueling station as stated by Apostolou and Xydis in 2018 (Apostolou and Xydis 2019).

**Fig. 6.4** Hydrogen fueling station in Asian countries (Alazemi and Andrews 2015)



**Fig. 6.5** Increased hydrogen fueling station (Apostolou and Xydis 2019)



### 6.4.2 In Terms of Characteristics (Octane Number, Density, Auto Ignition Temperature)

For an internal combustion (I.C) engine, octane number is an ideal characteristic to measure the compression capability of the fuel. A fuel containing a higher octane number has higher compression capability prior to detonation. Octane number is applied to indicate the knock property of any particular fuel. To measure the knock property, Cooperative Fuel Research (CFR) engine is used which makes the comparison between the testing fuel with the blend of normal iso-octane and normal heptane to determine its knocking resistance (Faizal et al. 2019). There are many ways of determining the knock properties of any fuel. Research Octane Number (RON) and Motor Octane Number (MON) are the two major standard procedures to detect the knocking properties of any fuel. In the case of values for the diesel oil, RON can be varied as RON is smaller than 88 to RON = 130, and in the case of lean mixture for the diesel engine RON varies as RON > 130 (Faizal et al. 2019). However, for the case of MON, it varies as  $115 < \text{MON} < 130$  (Faizal et al. 2019).

In terms of density, hydrogen contains lesser density than gasoline ( $0.0899 \text{ kg/m}^3 < 0.760 \text{ kg/m}^3$ ) (Masuk et al. 2021a). As a result, it contains more energy compared to other fuels and 1 kg of hydrogen carries the identical energy as 2.8 kg of gasoline (Lund 1997). Apart from it, due to lower density hydrogen is used mostly in its compressed form (Lund 1997). There is density variation when hydrogen is in compressed form compared to the liquid form. The hydrogen density is  $26 \text{ gL}^{-1}$  in compressed form as well as  $70.8 \text{ kg m}^{-3}$  when it is chilled to 20 K and it is the temperature at which hydrogen must be preserved when cooled (Hoecke et al. 2021).

In terms of auto ignition temperature, hydrogen contains greater auto ignition temperature compared to other fuels. Figure 6.6 shows the auto ignition temperature of different fuels along with hydrogen. From the figure, it is clear that hydrogen has higher auto ignition temperature than LNG, Formic acid, Methanol and Diesel.

Because of high auto-ignition temperature, proper combustion of hydrogen is hampered when compared to hydrocarbon fuels such as formic acid, methanol, or diesel as shown in Fig. 6.6. As a result, it is used in the dual-fuel mode for efficient

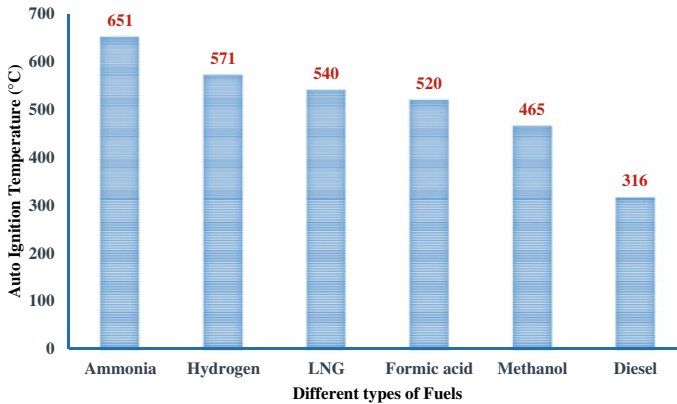


**Fig. 6.6** Auto ignition temperature of different fuels (Van Hoecke et al. 2021)

combustion in CI (Compression Ignition) engine. For the SI (Spark Ignition) engine, it is used as a mono-fuel mode where a high ignition temperature of the fuel is desired at the end of the compression stroke.

### 6.4.3 In Terms of Engine Performance

The application of hydrogen as a fuel additive has captivated the scientific community's curiosity, even though this is not a novel application, due to hydrogen's abundance (Dinga 1988). Several researchers have claimed that when hydrogen is used as an alternative fuel in an internal combustion engine, the engine's efficiency increases and toxic gas emissions diminish (Masuk et al. 2021b; Hacoheh and Sher 1989). Also, the rate of combustion of a fuel that is enriched with hydrogen is higher than the rate of combustion of pure fuel, so higher thermal efficiency is found. However, by utilizing hydrogen as a fuel, degradation in the heat efficiency of engine is observed; however, this does happen at the same time as increase in the consumption of energy. In the thermal efficiency of engine, it is raised by around 5% in Hoang and Pham (2020). This indicates that the energy efficiency of engines using a mixture of hydrogen with diesel fuel is substantially higher compared to pure diesel fuel. The results will be demonstrated in this section where the impacts of hydrogen as an alternative fuel in both CI and SI engines are investigated by employing measuring standards and design parameters.

Maximum engines are designed on the same principles, but only a few are simple in nature and require known and constant variables. Among internal combustion engine design parameters, compression ratio, swept length, power output, basic fuel consumption, effective pressure, and effective brake mean temperature, Brake power, specific fuel consumption, torque each are commonplace, but there is more variety in design.

The brake power (abbreviated as B.P.) of an internal combustion engine is the amount of power available at the crankshaft. Typically, an I.C. engine's brake power is determined using a brake mechanism. The ratio of an engine's braking power BP to the rate at which chemical energy is delivered to it in the form of fuel is referred to as brake thermal efficiency (BTE). The mean effective pressure (BMEP) is a quantity associated with the functioning of a reciprocating engine. It is a useful indicator of an engine's ability to perform work independently of its displacement ([https://www.wikiwand.com/en/Mean\\_effective\\_pressure](https://www.wikiwand.com/en/Mean_effective_pressure)) and maximum braking torque is achieved by optimizing ignition time in order to maximize the power and efficiency of an internal combustion engine ([https://www.wikiwand.com/en/Maximum\\_brake\\_torque](https://www.wikiwand.com/en/Maximum_brake_torque)). The brake thermal efficiency (BTE) ratio is the relationship between the brake power received from the engine and the fuel energy that was provided to the engine. The BTE is going to determine how effectively the heat is transformed into work. Again brake-specific fuel consumption (BSFC), which quantifies efficiency of fuel of a prime mover which inflames fuel and generates rotational, or shaft power. It is typically applied in situations where an internal combustion engine's performance needs to be compared to a shaft output. Here the alternative fuel is reviewed by these common parameters in SI and CI engine.

#### 6.4.3.1 In SI Engine

Figure 6.7 illustrates different performance measuring standards in a SI engine for using hydrogen as an alternative fuel. The difference is created by brake power (BP), brake mean effective pressure (BMEP), brake thermal efficiency (BTE), and brake torque (BT). Power available in the crankshaft is called the BP of an IC engine. In Fig. 6.7, it can be seen that by increasing speed, BP is increased using hydrogen. On the other hand, brake power is gradually decreased by increasing engine speed in case of gasoline. Figure 6.7 shows the representation of the experiment results for Brake power in KW and speed in rpm (Kahraman et al. 2007a).

#### Brake Power

Brake power assessment in the first one has shown between the two fuel options (hydrogen and gasoline) in Fig. 6.7a. From (Kahraman et al. 2007b), hydrogen can be defined as having a less specific amount of energy per unit volume, so it has lower power productivity than a higher starting speed compared to gasoline-fueled engines, but maximum BP can be seen here at approximately 3189 rpm. It can be seen that, at lower speeds, the output power of a hydrogen fuel engine appears to be less than that of a gasoline engine. However, as the load increases, the converse occurs. The brake power of a hydrogen-powered engine increased as the load increased, whereas the brake power of a gasoline-powered engine declined. For gasoline when the engine speed was approximately 3110 rpm then the BP was 6.81 kilowatts. But increasing the value to nearly 3700 the BP decreased to 4.13 kW. As long as the speed of the

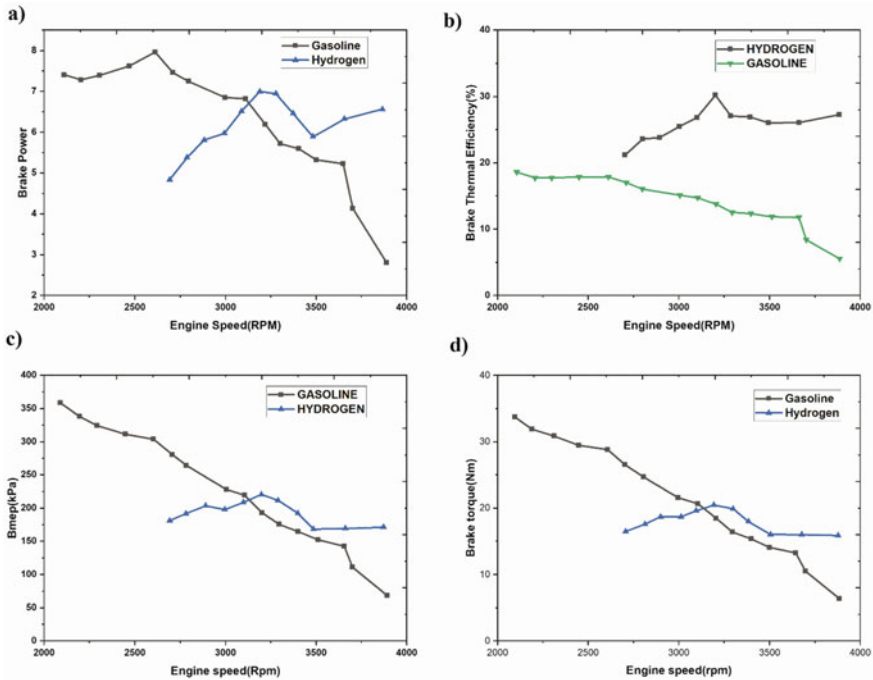


**Fig. 6.7** Variation of **a** BP, **b** BTE, **c** BMEP, **d** BT with respect to engine speed in a SI engine (Kahraman et al. 2007a; Masuk et al. 2021; Ayad et al. 2020)

engine increases the BP for gasoline fuel decreases proportionately. But a different phenomenon can be found for using hydrogen fuel. From Fig. 6.7a, the BP was seen to increase up to 3190 rpm for hydrogen and the value was nearly 7 kW at this speed. After reaching this, the value tends to decrease by a certain limit and then increases again. The highest brake power for gasoline fuel is was observed at nearly a value of 7.96 kW at 2611 rpm (approximately). In case of hydrogen, maximum BP is seen nearly a value of 7 kW at approximately 3189 rpm. Thus, it can be concluded from these findings that gasoline has a higher BP at smaller engine loads and a lower BP at greater engine loads, while hydrogen BP began at approximately 2692 rpm but has a higher BP at higher engine loads.

### Brake Thermal Efficiency

BTE is regarded as the thermal output of BP. This second graph (Fig. 6.7b) is an expanded graph of the BTE for the different fuel types (Hydrogen fuel and Gasoline fuel). With regard to fuel economy, a good efficiency is that it should be useful for supporting smaller loads while also enabling higher thermal efficiency. There is no problem with using higher engine speeds and fewer loads of hydrogen fuel at the

same time and in order to give the fuel additional efficiency. In case of gasoline, as the speed of engine increases, the BTE decreases. When it is examined closely, it can be found that BTE increase by 31% for the hydrogen-fueled engines than a gasoline-fueled engine (Masuk, et al. 2021). It is illustrated that as the speed of the engine increases, the BTE results in a decrease in the level of gasoline but the result is an increase in the amount of hydrogen. In case of gasoline BTE was found on nearby 2106 rpm and by increasing engine speed it went down gradually. At 3886 rpm, the BTE for gasoline was 5.54% while in case of hydrogen it was 27.28%. The maximum BTE achieved by hydrogen fuel is 30.22% in approximately 3201 rpm. So it can be said that, obtaining high engine speed increases BTE for hydrogen fuel and for gasoline it is opposite.

In order to improve the BTE of gasoline, the engine will produce a lot of toxic particles that are bad for the environment. However, while using hydrogen in this manner does not pollute the environment but it is quite expensive. This is because when gasoline is consumed, it converts into gaseous hydrocarbon particles that pollute the environment and the ozone layer. As a result of displacing polluting fuels by hydrogen will contribute to a cleaner environment.

### Brake Mean Effective Pressure

Another engine performance parameter is shown in the third graph which is brake mean effective pressure (BMEP). It can be seen from the graph that hydrogen shows a certain improvement after 3100 rpm engine speed relative to gasoline. But to achieve this higher BMEP for hydrogen, it needs higher engine speed. It can be seen clearly that, no BMEP was achieved for hydrogen in lower engine loads (Kahraman et al. 2007a). BMEP for hydrogen fuel starts at 2692 rpm and gradually increased by 3871 rpm. While in gasoline BMEP was achieved at lower engine load which is 2088 rpm and the respective BMEP was 358 kPa. While in hydrogen first BMEP achieved was 181.15 kPa and gradually it ended up in 171.25 kPa by increasing engine speed.

### Brake Torque

The variation of Brake Torque (BT) vs engine speed is also shown in Fig. 6.7. It shows almost the same result as BMEP. It can be seen that in lower engine load there is no BT for hydrogen fuel. On the other hand, for gasoline highest BT can be achieved in lower engine load. The highest BT for gasoline was 33.72 Nm in 2094 rpm engine speed. By increasing to 3884 rpm gradually its BT decreases to 6.39 Nm. While in the case of hydrogen the highest BT was seen 20.48 Nm in 3192 rpm engine speed value. It is obvious to show comparatively better results at higher engine loads as hydrogen has fast burning characteristics.

### 6.4.3.2 In CI Engine

Hydrogen can also be utilized as a substitution fuel in CI engines (Talibi et al. 2018; Boretti 2030). Figure 6.8 presents different performance characteristics for mixing hydrogen in diesel fuel. A set of measurements were recorded during the experiment. Brake specific energetic consumption (BSEC), brake energy consumption (BEC), brake efficiency (BE) can be shown for a CI engine in Fig. 6.8.

#### Brake Specific Energetic Consumption (BSEC)

The difference in Brake Specific Energetic Consumption (BSEC) versus xc substitute ratios at various engine loads is shown in Fig. 6.8a. The real energy consumption of each engine load decreased as xc increased, owing to an improved hydrogen-air mixing process and improved combustion. The BSEC fell by 8.16% and 4.16%, respectively, at partial loads of 40% and 55% correspondingly. For higher loads

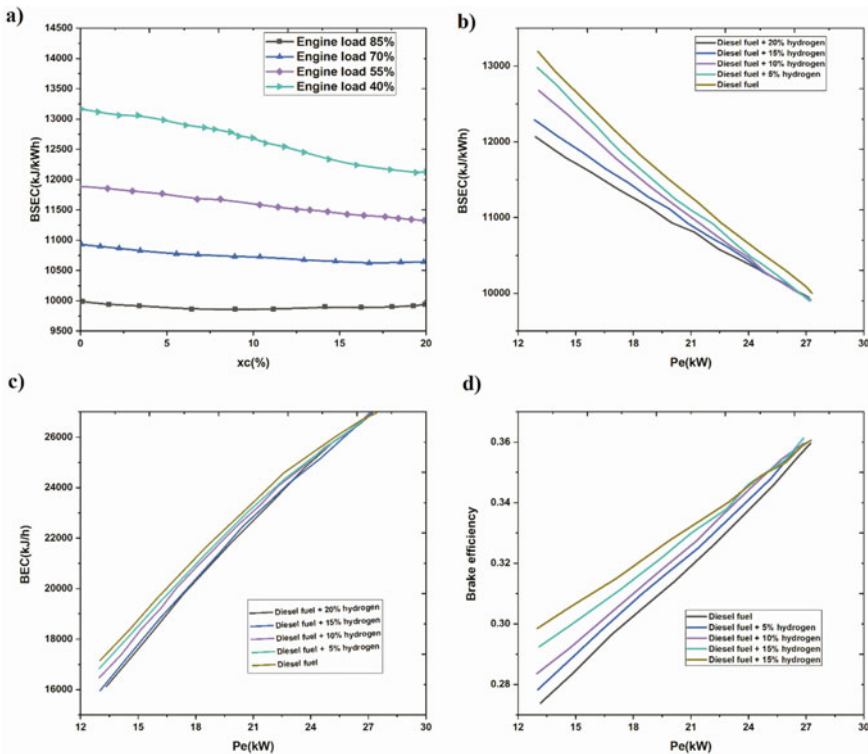


**Fig. 6.8** a BSEC versus substitute ratio (xc). b BMEP variation. c Variation of BEC. d Brake efficiency versus engine load variation at various engine loads  $2000 \text{ min}^{-1}$  speed and different substitute ratios (Cernat et al. 2020; Juknelevičius et al. 2019)

(85%), the BSEC gradually increased as the quantity of inlet air decreased. The highest BSEC is seen in engine load 40% and the lowest is seen in 85%.

Figure 6.8b also shows the BSEC difference versus engine load for  $2000 \text{ min}^{-1}$  and different replacement ratios (Fig. 6.8). As hydrogen fuel with flows is proved to be sufficient to maintain engine power at the same load and speed, substantial diesel fuel savings are achieved and energy consumption are reduced. The BSEC of diesel fuel is higher than the mixed fuels relatively. After mixing hydrogen in the fuel, BSEC decreased gradually. By mixing 5%, 10%, 15%, 20% hydrogen, BSEC is decreased respectively. The lowest BSEC is seen in the largest portion mixture of hydrogen with diesel fuel that is only 20%.

### Brake Energy Consumption (BEC)

Figure 6.8c shows the results for BEC vs engine load at  $2000 \text{ min}^{-1}$ . At an engine capacity of  $P_e = 18 \text{ kW}$ , diesel fuel consumed 1.32 kg of fuel per hour. Thus, it had an engine efficiency of 5.3% efficiency was achieved (Cernat et al. 2020). It can be seen that the BEC is decreasing by increasing the hydrogen percentage in the fuel. Hydrogen portion is added by 5, 10, 15, and 20% gradually in the percentage of diesel. By increasing the percentage, the BEC graph can be seen to downward and the highest BEC is seen in pure diesel fuel.

### Brake Thermal Efficiency (BTE)

BE results are illustrated in Fig. 6.8d It is observed that the BE graph shows the opposite results of BEC. Here, increasing the percentage of hydrogen in pure diesel fuel makes the line higher. Again, decreasing the percentage of hydrogen makes the line much lower. Pure diesel is seen in the lower line. 5, 10, 15, and 20% of the hydrogen is being added to the mixture as the process progresses to the solution with the incremental addition of the hydrogen.

## 6.4.4 In Terms of Emission

### 6.4.4.1 In Terms of NOx

Compression ignition engines are dominated in the automotive sector by higher torques and better fuel efficiency than spark ignition drivers. Nonetheless, nitrous oxides and particulate matter are the primary CI engine emissions. Hydrogen is utilized as an alternative fuel because of its high diffusion, high flame speed, and broad flammability (Syed and Renganathan 2019). But the main issue with using hydrogen as a fuel is the increased levels of nitric oxide emissions. It is possible to reduce NOx emissions through lean premixed combustion. When hydrogen is mixed



with inlet air, it reduces exhaust smoke, resulting in noxious emissions. Mohon Roy et al. (2011) mentioned that if the injection timing can be increased, then sometimes smoke and NO<sub>x</sub> emissions can come to zero. On the other hand, Lambe et al. (1993) claimed that by design optimization of diesel fuel engines, it is possible to reduce NO<sub>x</sub> emissions by 70%. Again, the amount of NO<sub>x</sub> increases and decreases with hydrogen content per ratio and equivalent ratio. When this aspect is examined, Roy et al. (2011) discover that the NO<sub>x</sub> level rises as the equivalent ratio rises. The NO<sub>x</sub> level increases a lot to the equivalent of 0.25–0.30 range.

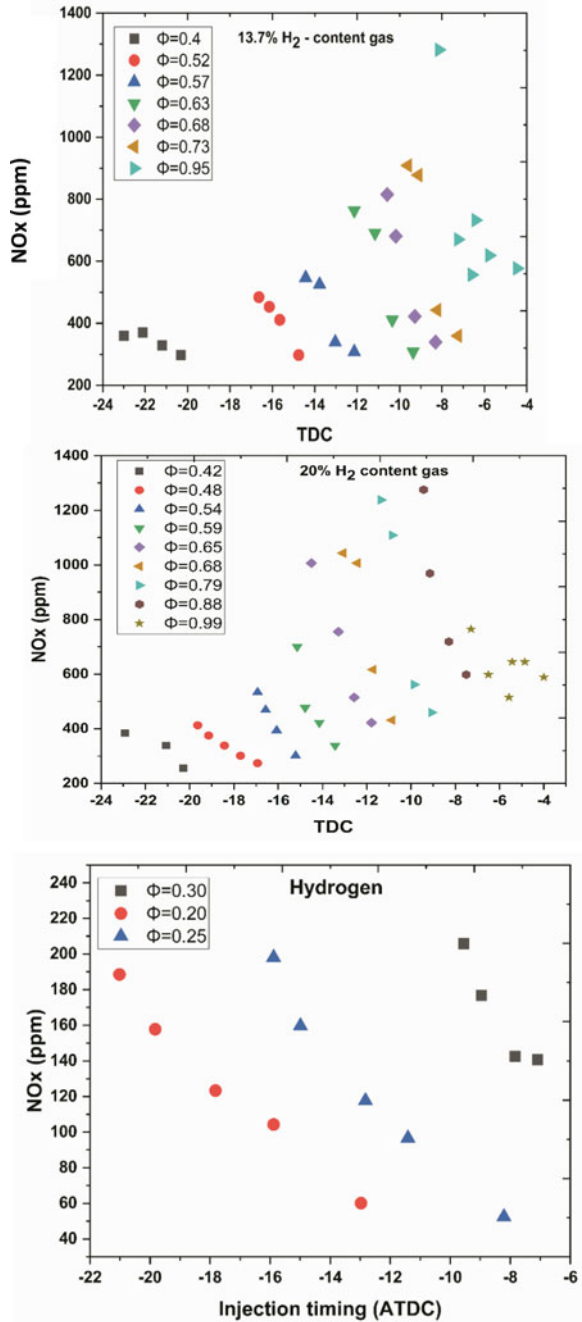
Based on an equivalent ratio, Fig. 6.9 depicts NO<sub>x</sub> emissions for various fuels at various injection timings. With injection timings at a constant equivalence ratio, the NO<sub>x</sub> accelerated. As the injection timing progressed, the peak cylinder pressure increased, resulting in higher peak burning gas temperatures and, as a result, more NO<sub>x</sub>. With a 0.85 equivalence ratio, the 13.7% H<sub>2</sub> gas level of NO<sub>x</sub> gradually increased to a maximum of 1255 ppm. The NO<sub>x</sub> level is lower (less than 50%) at the equivalent ratio of 0.95 than at the equivalent ratio of 0.85. With the 20% H<sub>2</sub>-content gas, the level of NO<sub>x</sub> gradually increased to an equivalence ratio of 0.76. However, due to the low cylinder temperature, the maximum NO<sub>x</sub> emission can be found at an equivalent ratio of 0.99. For pure H<sub>2</sub> as a fuel, the situation is completely different. With neat H<sub>2</sub> operation, NO<sub>x</sub> levels can be reduced by about 85–90%, indicating a significant reduction from other fuels due to very lean operation.

Figure 6.10 explains the emissions of nitrogen oxides with the engine that is hydrogen operated. These diagrams reveal variations in NO<sub>x</sub> levels of exhaust at different compression ratios with fuel–air equivalency. As can be seen from these figures, the maximum value for NO<sub>x</sub> emissions is around 0.8, where NO<sub>x</sub> concentration is negligibly small in the lower equivalence range. In addition to the fuel economy, lean mixtures in the hydrogen-driven SI engine open up the possibility of controlling the engine power supply by improving the fuel flow while maintaining unthrottled flow (Mathur and Khajuria 1984).

#### 6.4.4.2 In Terms of CO<sub>2</sub> and CO Emissions

Emission of CO exhaust means the chemical energy lost because of incomplete combustion. Emission of CO<sub>2</sub> leads by exact combustion and accurate combustion generates only water vapor and CO<sub>2</sub> (Sandalcı and Karagöz 2014). Emissions of CO exhaust increase according to fuel and engine loads. Koten (2018) mentioned that at a low engine load, this condition leads to lower CO emissions. As well, proved that in mixture formations, the addition of hydrogen to the diesel engine produces better results in CO exhaust emissions which is illustrated in Fig. 6.11. In comparison to a single combustion diesel fuel, hydrogen mixture cases also resulted in lower CO<sub>2</sub> emissions. In general, CO<sub>2</sub> emissions increase in proportion to the engine load as the combustion chamber injects higher fuel as well as higher temperature with exact combustion. The addition of hydrogen at 100% engine load contributed to a rise in CO emissions over other engine loads. CO emissions for 0.20, 0.40, 0.60, and 0.80 lpm H<sub>2</sub> addition decreased by 7.4, 12.7, 12.09, and 11.87% for all engine loads,

**Fig. 6.9** NO<sub>x</sub> emission level for different fuels based on equivalent ratio, adapted from Roy et al. (2011)



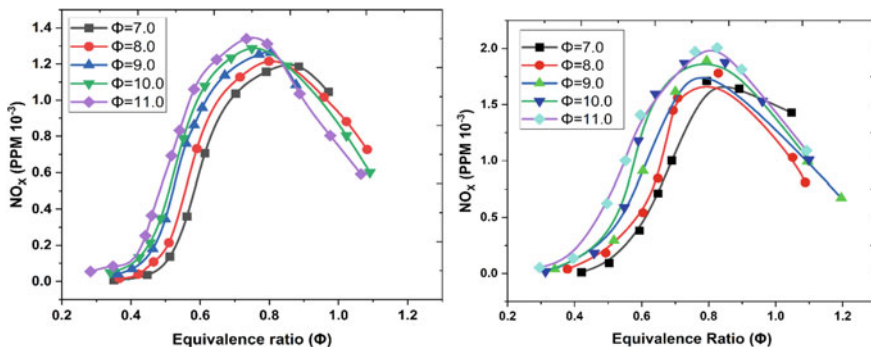


**Fig. 6.10** NO<sub>x</sub> emissions as a function of equivalence ratio for SI engine (Mathur and Khajuria 1984)

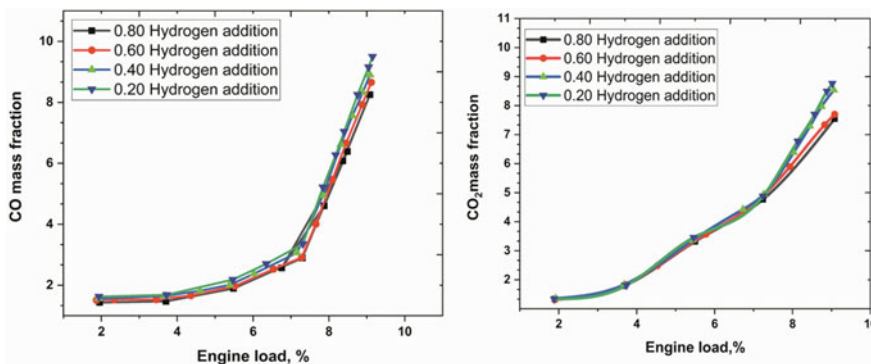
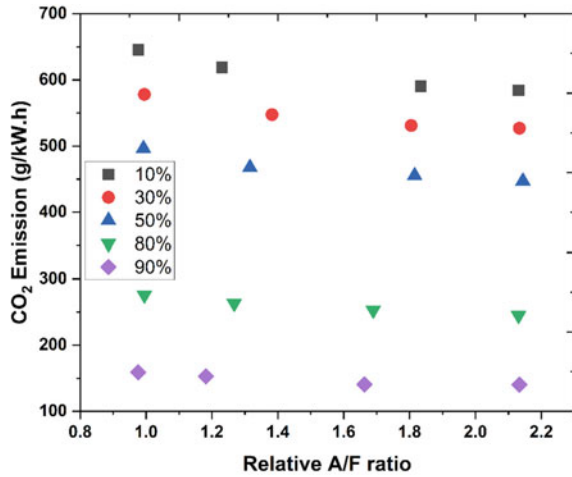


**Fig. 6.11** CO and CO<sub>2</sub> emission related to engine load with different amount of H<sub>2</sub> addition

respectively, when compared to single diesel fuel. Besides, CO<sub>2</sub> for the enrichment of 0.80 lpm H<sub>2</sub> is 9.22% by volume compared to 10.18% by volume with 100% load for diesel. CO<sub>2</sub> emissions have decreased in comparison with the single diesel fuel respectively by 6, 7.8, 11.45 and 10.78% for the addition of 0.20, 0.40, 0.60, and 0.80 lpm H<sub>2</sub> respectively. Hydrogen addition in fuel mixture at intake port is not a disadvantage it can be a better solution to reduce the emission of CO and CO<sub>2</sub> and can provide better thermal efficiency. Further, Fig. 6.12 (SI engine) shows that, as the air/fuel ratio increases, the latter offers more significant decreases as CO<sub>2</sub> emissions fall and eventually lead to a reduction in specific CO<sub>2</sub> emissions. Navarro et al. (2013) claimed that the gradually reducing carbon content can be attributed to a decrease in specific CO<sub>2</sub> emissions with increasing H<sub>2</sub> content of the fuel mixture.

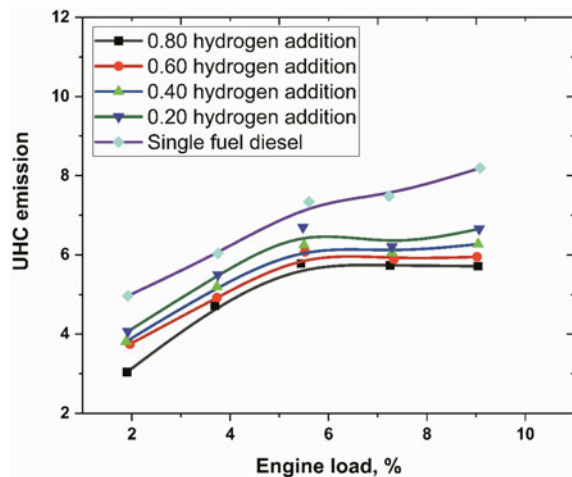
**Fig. 6.12** CO<sub>2</sub> emissions as a function of the relative air/fuel ratio for SI engine (Navarro et al. 2013)



### 6.4.4.3 In Terms of Unburnt Hydro-Carbon (UHC)

Hydrocarbons (HCs) are incomplete combustion products that may occur when internal combustion engines are used (Wallington et al. 2008). Unburned combustion affects both fuel consumption and engine performance (Rezai et al. 2014). However, for various operating conditions, UHC (Unburned Hydro Carbone) emissions have been shown in Fig. 6.13. An increase in hydrogen addition in the intake port of the engine causes a better result and decreases the emission proportionally which is mentioned by Shirneshan (Shirneshan 2013). Moreover, the addition of hydrogen to intake air produced mixing homogeneity and improved emissions of UHC (Laskowski et al. 2018). Also, it is clear from Fig. 6.13 that with an increase of

**Fig. 6.13** UHC emission related to engine load with different amount of H<sub>2</sub> addition



engine load, the UHC emission decreases. On average the UHC emissions decreased by 9.23, 17.6, 25.13, and 39.25% compared to single-diesel for all engine loads at 0.20, 0.40, 0.60, and 0.80 lpm H<sub>2</sub> respectively.

## 6.5 Advantages and Disadvantages

### 6.5.1 Advantages of Hydrogen as Fuel

Though the processes of hydrogen production might look simple, it is a costly process. At present, the steam methane reforming process is widely used for producing hydrogen as a large amount of hydrogen can be extracted. But this process emits a large amount of carbon-di-oxide and carbon monoxide. However, the advantages of using hydrogen as a fuel are huge. The major advantages are stated below:

1. Hydrogen is considered a renewable energy source. It's a very rich source of energy which is all around us. At present, photo electrocatalytic and photoelectrochemical water-splitting methods are considered quite effectual methods for the scalable production of hydrogen.
2. The burning of hydrogen produces zero harmful byproducts. However, the combustion of hydrogen may produce very small amounts of nitrogen oxides, along with the water vapor. Further, once it is used as fuel later it can be used for water production for astronauts.
3. Unlike nuclear and natural gas it does not cause damage to human and animal health. Moreover, Food and Drug Administration (FDA) has approved hydrogen water as safe (GRAS), meaning that the organization has approved the water for human consumption and not known to cause harm.
4. Hydrogen can provide a huge amount of power because of being very dense. Research suggests that it is three times more powerful than most fossil-based fuels. In comparison with all other fuels hydrogen has a wide flammability range. As a result, a wide range of fuel-air mixtures of hydrogen can be combusted in an internal combustion engine. A noteworthy benefit of hydrogen is that it can run on a lean mixture.

### 6.5.2 Disadvantages of Hydrogen as Fuel

Besides these advantages, hydrogen fuel also has some disadvantages. Those are stated as follows:

1. As a result of its high energy content, hydrogen gas is an exceptionally combustible and unpredictable substance which makes it a hazardous fuel to work with Both steam-methane transforming and electrolysis are costly cycles

that keep a ton of nations from resolving to large scale manufacturing. Exploration and preliminaries are in interaction to attempt to find a modest and feasible approach to deliver sufficient hydrogen without offering more carbon into the air.

2. Hydrogen is a lot lighter gas than gasoline which makes it hard to store and move. To have the option to store it we need to pack it's anything but fluid and store it's anything but a low temperature. There is likewise no smell to hydrogen so sensors are needed to recognize spills. Further, when H<sub>2</sub> and O<sub>2</sub> mixes they produce dihydrogen monoxide, which can kill a people instantly if they inhale one or two spoons in the liquid form.
3. Moreover, because of having very low molecular weight, the density of hydrogen is less than natural gas at atmospheric pressure and temperature of 273 K (Since we know density,  $\rho = (\text{weight}/\text{volume})$ ). In terms of storage facility, compressed hydrogen is the distinguished/suitable option due to its low boiling point. Due to the fact of confined vehicle space, implementation/accomplishment of hydrogen ICE in on-road vehicle is a vital challenge. Increment of hydrogen density and volumetric energy content require increment of hydrogen pressure. For example, increment of hydrogen density to 31 kg/m<sup>3</sup> or 3700 MJ/m<sup>3</sup> increment of volumetric energy content require hydrogen pressure of 350 bar (existent standard supply pressure for hydrogen refueling) (Yip 2019).
4. Hydrogen exhibits smaller quenching distance compared to traditional hydrocarbon fuels. As a result, increased temperature gradient close to the walls of combustion chamber can be anticipated which lead to incremental heat losses due to combustion. In case of using hydrogen in the applications of Port Fuel Injection (PFI) engine, elevated laminar flame speed along with short quenching distance impose a elevated tendency to flame backfiring into intake manifold. This problem can be neutralized by including modified engine geometry, reducing the crevice volume and returning of engine operating conditions and a complete removal of abnormal discharge and residual electric energy in the ignition system (Kondo 1997; Lee 2001). To avoid backfiring and pre-ignition in SI engine a non-platinum cold-rated spark plug should be utilized as well (Huyskens et al. 2011). This is due to the capability of platinum material of making undesired catalytic response with air and hydrogen. Engine knock and abnormal combustion which may be caused by hydrogen exposure to hot spots can be minimized using cold-facilitate quick heat transfer. This is the case where hydrogen DI exhibits a significant advantage since the backfiring can be totally neutralized the injection after the intake valve closing.

However, design of highly efficient ICE can be facilitated by the unique physical and thermo-chemical properties of hydrogen. For example, diffusion of hydrogen is four times faster than CNG which can be deduced by assimilating their diffusion coefficients for air. This phenomenon can enhance air and in-line cylinder fuel mixture in ICEs. The volume of fraction stoichiometric hydrogen is 29.53 vol%. Nevertheless, the comprehensive flammability limit ranging from 4 to 76 vol% hydrogen existing in air, along with high flame speed exhibits that hydrogen ICE can run with notably

lean while flourishing thermal efficiency (Yip 2019). NO<sub>x</sub> formation is promoted by relatively high adiabatic flame temperature of hydrogen at stoichiometry. However, lean operations or high level exhaust gas recirculation (EGR) can be utilized to lessen NO<sub>x</sub> emissions because of broaden/extensive flammability limits.

## 6.6 Prospective Challenges

Renewable energy sources are used as an alternative to traditional fuels. These sources solely depend on environmental and weather conditions. While hydrogen is one of the prospective options for future fuels that can be generated from different processes that are not solely dependent on environmental conditions. However, several kinds of challenges encounter to set hydrogen resources of energy in different practical applications including cooking, operating automobiles, and so on. Among these different challenges economic, policy, and regulatory-related challenges, environmental, technological, informational, and availability challenges are the most important.

- Policy and regulatory challenges include the problems associated to set the production methods for hydrogen generation as well as supply required raw materials. It mainly includes the construction of infrastructure, management to provide support to hydrogen production agents and make the hydrogen generation policy user-defined so that management for hydrogen generation can use these resources of energy. The managerial system and the agents who are engaged in hydrogen generation need to be supported and encouraged to focus on the hydrogen generation sources to generate hydrogen and make them available.
- Challenges of economics are the major concern for the setup of these resources of energy. As the associated cost with hydrogen generation methods is not negligible for a few cases such as hydrogen generated from biomass, fossil fuels, and thermal electrolysis sources. Usually, hydrogen generation sources of energy quantity are comparable with the value of traditional energy sources. While the cost of hydrogen generation sources of energy is compared with renewable sources of energy as well.
- Environmental challenge is an important challenge for hydrogen gas generation. Although hydrogen energy is considered a clean technology for future energy. However, generated tars during biomass gasification for hydrogen gas generation are a major issue. Proper environmental pollution management needs to be implemented before establishing hydrogen generation methods.
- Difficulties associated with technology are another shortcoming for the setup of processes for hydrogen gas generation. There are a number of technical difficulties including a mechanism for plasma arc decomposition, and splitting of water thermally for hydrogen generation. It is necessary to implement user-defined techniques to easily set those sources of energy.

- Technological support is one of the major requirements to implement the setup for hydrogen generation. Due to the lack of information on hydrogen generation, these sources are still not available globally. Additionally, lack of proper management for equipment and component suppliers, less availability of resources, and gap of information implements these sources difficult.
- Lack of available raw materials, a mechanism for biomass gasification, splitting water thermally are other drawback factors that affect the generation of hydrogen that will be suitable for future energy.
- The sustainability of materials must be checked before using hydrogen. Engine materials should be considered based on their sustainability to hydrogen and its burning. Hydrogen embrittlement susceptibility testing (e.g., ISO 11114-4) should be done in case of any doubt the material can be subjected. According to report presented in ISO/TR 15,916:2004, most of the materials show sensitivity to hydrogen embrittlement to some extent. However, brass and most of the copper alloys or aluminum and its alloys can be used without any specific precautions. On the opposite side, nickel and its alloys show high sensitivity to hydrogen embrittlement. Nevertheless, for steel, the sensitivity depends on many factors such as impurities, mechanical strength, heat treatment and so on. Some guidelines regarding the suitability of hydrogen can also be found in ISO/TR 15,916:2004.

## 6.7 European Union (EU) Hydrogen Strategy

The demand of hydrogen is growing rapidly due to its diverse applications in different fields. It can be used as an energy carrier or fuel, feedstock and storage and has many others applications including transport, industry, power and building sectors and so on. In terms of carbon di oxide (CO<sub>2</sub>) emission and air pollution, hydrogen provides the best possible solution. It does not eject any CO<sub>2</sub> and its air pollution tendency is very low. As a result, hydrogen is the best option in economic sectors and industrial processes where limitation of carbon emission is a vital issue and is difficult to accomplish (COMMISSION E 2020).

EU declared its hydrogen strategy in 2020 which is “A hydrogen strategy for a climate-neutral Europe”. The aim of their strategy is to increase the use of the hydrogen by 2050. European Commission has set the following goals focusing this strategy:

1. The goal of a carbon-neutral EU is to decarbonize sectors that are not directly electrifiable.
2. Improved wind and solar power integration with hydrogen as a storage medium.
3. Overcoming the economic damage caused by the Covid-19 lockout, in particular by allocating considerable EU Recovery Deal subsidies to the hydrogen economy.
4. In the hydrogen economy, new employment is being created.
5. Combating migration’s causes by establishing supply networks with nations outside the EU as part of the EU’s external energy strategy.



The EU hydrogen plan is divided into three parts and is part of the European Green Deal:

1. Green hydrogen generation is expected to reach one million tons per year by 2024.
2. Green hydrogen generation is expected to reach 10 million tons per year by 2030.
3. Green hydrogen is expected to be produced on a systemically relevant scale between 2030 and 2050.

By way of comparison, the EU now produces over 10 million tons of hydrogen per year from and with fossil fuels. The Netherlands, for example, which is looking for alternative uses for its existing natural gas infrastructure as a result of the end of natural gas production from the Groningen gas field, and Germany, which has already presented its national hydrogen strategy in June 2020, are both supporters of the EU hydrogen strategy (Röhm-Malcotti 2021).

## 6.8 Future Recommendation

It has been established that hydrogen has the potential to be a very eco-friendly fuel. On a weight-per-weight basis, hazardous emissions are nearly nil. Hydrogen is one of the most abundant elements in the universe. Extraction expenses are limiting efforts because of the energy density of the product and the high energy requirements. It looks intriguing, however it provides limited travel for a low cost. Hydrogen must have the same running costs, fill times, and range as gasoline to be considered a mass fuel. For the time being, gasoline will remain the primary fuel market. Hydrogen is certain to replace gasoline and traditional fossil fuels in the future. For this, important aspects of requirements need to be discerned and perfectly evaluated.

Most technologically sophisticated nations of the globe have focused on hydrogen storage for decades. Credence has been granted to the movement. Hydrogen is an effective energy storage method and it holds up global climate change (Sahaym and Norton 2008; Jia et al. 2015; Sakintuna et al. 2007; Ruse et al. 2018). All types of storage have their particular requirements and obstacles.

Stationary applications don't have as much serious weight and volume as mobile applications. The hydrogen storage system is stationary, functions at high temperatures, and has spare capacity to counteract sluggish kinetics. However, limited storage tank materials (Prabhukhot Prachi et al. 2016) hold the development of stationary hydrogen systems back. In comparison, the mobile application requirements for hydrogen storage are greatly extensive (Prabhukhot Prachi et al. 2016; Janot et al. 2005).

When storage becomes too heavy, the vehicle's range is reduced (Abe et al. 2019), and when storage becomes too voluminous, it reduces the amount of luggage space available (Durbin and Malardier-Jugroot 2013). In other words, it is necessary to maintain an effective equilibrium. The kinetics of hydrogen uptake and release are

extremely quick (Zhang et al. 2015). Low heat creation in order to reduce the amount of energy required for hydrogen release During the exothermic hydride formation, there is little heat dissipation (Ozturk and Demirbas 2007). Hydrogen charges and discharges with only a minimal loss in energy. Reversibility of hydrogen uptake and release throughout a number of cycles (Abe et al. 2019). For long cycle life, it is important to have strong stability against oxygen and moisture (Jia et al. 2015). The low cost of recycling and the availability of charging infrastructures should be taken into consideration (Mazzolai 2012). It is necessary to maintain high levels of safety under operational conditions, as well as public acceptance.

### 6.8.1 Performance

The type of fuel used has a direct impact on the performance and emission characteristics of the engine. These characteristics include, for example, power, torque, brake mean effective pressure, brake specific fuel consumption, brake power, and other similar properties.

Due to the fact that the self-ignition temperature of the hydrogen–air mixture is higher than that of the other fuels, a modest amount of hydrogen addition results in the production of a fuel with an antiknock characteristic (Al-Baghdadi 2003). Hydrogen has the highest energy-mass coefficient of the chemical fuel and the highest in terms of mass-energy consumption (Al-Baghdadi 2003). This confirms that supplementary hydrogen can improve engine efficiency and minimize specific fuel consumption (Petkov et al. 1989). Fuel coupled with a little amount of hydrogen and oxygen yields forms a flammable mixture that may be burned in a conventional spark-ignition engine at an equivalence ratio (Al-Baghdadi 2003).

The resulting ultra-lean combustion gives rise to better engine efficiency and lower emissions of CO and NO<sub>x</sub>. The hydrogen-air mixture ignites and burns about six times faster than a gasoline-air mixture. The indication diagram becomes closer to the ideal as the burning velocity rises by which a better thermodynamic efficiency can be conceivable (Al-Baghdadi 2003). When compared to the diesel fuel situations, the hydrogen mixture in the CI engine produced excellent results in all circumstances. With the addition of different nanoparticles to the fuel, the outcomes can be enhanced (Koten 2018).

### 6.8.2 Emissions

Because of growing environmental concerns, the world has seen an increase in the number of people concerned about emissions, which has resulted in stricter emission rules being implemented year after year. Vehicle emissions include hydrocarbons (HC), carbon monoxide, nitrogen oxides, particulate matter, volatile organic compounds, Sulphur oxides, and carbon dioxide. The understanding of these vehicle

emissions is important in conferences about air pollution issues and climate change challenges.

Alternate fuels, such as hydrogen are utilized in place of gasoline in SI engines if they are environmentally friendly and do not produce harmful compounds when the fuel is burned. By lowering the aromatic component of the fuel, each individual emission can be lessened (Al-Baghdadi 2004). The compression ratio and equivalence ratio of an engine has a considerable impact on both its performance and its emission characteristics, and they must be properly designed in order to get the highest engine performance characteristics possible (Masuk et al. 2021b). However, even though hydrogen is zero-carbon-emission energy at the point of use, the cleanness of the production pathway and the energy required to make it are dependent on the clean energy index (cleanness) of that pathway and the energy required to produce it (Dawood et al. 2020).

### **6.8.3 Production**

Hydrogen can be generated using renewable resources or fossil fuels. It can be also produced through steam reforming, partial oxidation, auto thermal oxidation, and gasification. Biomass gasification and water splitting by solar energy (Abdalla et al. 2018). The continual advancements in techniques and procedures of H<sub>2</sub> production, storage, and distribution are also challenged by some major issues. A significant improvement is required in the development of new technology, such as electrolysis and thermochemical biomass conversion, in order to be able to compete with the commonly used hydrogen generation techniques, such as steam methane reforming. In spite of a plentiful supply of feedstock materials, technological constraints during the manufacturing process result in higher production costs overall which need attention. The production of hydrogen is mostly fueled by nonrenewable resources, which contributes to an increase in the concentration of CO<sub>2</sub> in the atmosphere, which demands effort.

## **6.9 Conclusion**

It is proved beyond doubt that hydrogen holds significant potential in terms of ensuring a clean energy solution in transportation and industrial application. Attention is also being given for incorporating its increased utilization with sustainable production. The suitable properties for both steady and unsteady combustion processes make hydrogen more attractive in the automobile sector as a fuel. Additionally, hydrogen can be stored both in the gas and liquid phase for which it could be a favorable energy carrier for a wide range of applications and heat supply. The production of hydrogen from biomass is environmentally friendly and cost-efficient also. It is expected that hydrogen production will be accelerated after using renewable

sources for its production. It can also be stored easily with the help of some composite materials and compound metals which have moderate adsorption or desorption kinetics. By using Sabatier process  $\text{CO}_2$  can also be recycled with the help of storing the hydrogen as methane. Owing to this cleaner production potential and good properties as a fuel, hydrogen will play a significant role in energy security, stabilizing the foreign exchanges, climate-changing, and mitigating the socioeconomic issues remaining in the rural areas over the world. However, current policies working on using the energy more efficiently along with encouraging cleaner and sustainable production to reduce environmental issues like air pollution, global warming, greenhouse gases, and climate changes. Special policies should provide to encourage and support hydrogen production and utilization. Most importantly, public awareness should be raised to enhance the hydrogen utilization and safety issues related to this.

## References

- Abdalla AM et al (2018) Hydrogen production, storage, transportation and key challenges with applications: a review 165:602–627
- Abe JO et al (2019) Hydrogen energy, economy and storage: review and recommendation 44(29):15072–15086
- Alazemi J, Andrews J (2015) Automotive hydrogen fuelling stations: an international review. *Renew Sustain Energy Rev* 48:483–499
- Al-Baghdadi MJRE (2003) Hydrogen–ethanol blending as an alternative fuel of spark ignition engines 28(9):1471–1478
- Al-Baghdadi S, Maher AR (2004) Effect of compression ratio, equivalence ratio and engine speed on the performance and emission characteristics of a spark ignition engine using hydrogen as a fuel 29(15):2245–2260
- Apostolou D, Xydis G (2019) A literature review on hydrogen refuelling stations and infrastructure. Current status and future prospects. *Renew Sustain Energy Rev* 113
- Argun H, Kargi F (2011) Bio-hydrogen production by different operational modes of dark and photo-fermentation: an overview. *Int J Hydrogen Energy* 36(13):7443–7459
- Asadullah M et al (2002) Energy efficient production of hydrogen and syngas from biomass: development of low-temperature catalytic process for cellulose gasification. *Environ Sci Technol* 36(20):4476–4481
- Ayad SM et al (2020) Analysis of Performance Parameters of an Ethanol Fuelled Spark Ignition Engine Operating with Hydrogen Enrichment 45(8):5588–5606
- Balta MT, Dincer I, Hepbasli A (2009) Thermodynamic assessment of geothermal energy use in hydrogen production. *Int J Hydrogen Energy* 34(7):2925–2939
- Boretti AJ (2020) Hydrogen internal combustion engines to 2030 45(43):23692–23703
- Burton NA et al (2021) Increasing the efficiency of hydrogen production from solar powered water electrolysis. *Renew Sustain Energy Rev* 135
- Cernat A et al (2020) Hydrogen—an alternative fuel for automotive diesel engines used in transportation 12(22):9321
- Chen S, Pei C, Gong J (2019) Insights into interface engineering in steam reforming reactions for hydrogen production. *Energy Environ Sci* 12(12):3473–3495
- Chen W-H et al (2021) Hydrogen production from partial oxidation and autothermal reforming of methanol from a cold start in sprays 287:119638
- COMMISSION, E (2020) A hydrogen strategy for a climate-neutral Europe 1

- Das BK, Hasan M, Rashid F (2021) Optimal sizing of a grid-independent PV/diesel/pump-hydro hybrid system: a case study in Bangladesh. *Sustain Energy Technol Assess* 44:100997
- Dawood F, Anda M, Shafiullah GM (2020) Hydrogen production for energy: an overview 45(7):3847–3869
- Demirbas MF (2006) Hydrogen from various biomass species via pyrolysis and steam gasification processes. *Energy Sources Part A* 28(3):245–252
- Demirbas A (2007) Recent developments in biodiesel fuels. *Int J Green Energy* 4(1):15–26
- Demirbas A (2017) Future hydrogen economy and policy. *Energy Sources Part B Econ Plan Policy* 12(2):172–181
- Dincer I, Acar C (2015) Review and evaluation of hydrogen production methods for better sustainability. *Int J Hydrogen Energy* 40(34):11094–11111
- Dinga GP (1988) Hydrogen: the ultimate fuel and energy carrier 65(8):688
- Duan X et al (2019) Experimental Study the Effects of Various Compression Ratios and Spark Timing on Performance and Emission of a Lean-Burn Heavy-Duty Spark Ignition Engine Fueled with Methane Gas and Hydrogen Blends 169:558–571
- Durbin D, Malardier-Jugroot CJ Review of hydrogen storage techniques for on board vehicle applications 38(34):14595–14617
- El-Shafie M, Kambara S, Hayakawa Y (2019) Hydrogen production technologies overview. *J Power Energy Eng* 07(01):107–154
- Faizal M et al (2019) Review of hydrogen fuel for internal combustion engines review of hydrogen fuel for internal combustion engines. *J Mech Eng Res Develop* 42(3):35–46
- Fu P et al (2020) Comparative Study on the Catalytic Steam Reforming of Biomass Pyrolysis Oil and Its Derivatives for Hydrogen Production 10(22):12721–12729
- Fulcheri L et al (2002) Plasma processing: a step towards the production of new grades of carbon black. *Carbon* 40(2):169–176
- Gaudernack B, Lynum S (1998) Hydrogen from natural gas without release of CO<sub>2</sub> to the atmosphere. *Int J Hydrogen Energy* 23(12):1087–1093
- Hacohen Y, Sher E (1989) Fuel consumption and emission of SI engine fueled with H<sub>2</sub>-enriched gasoline. In: *Proceedings of the 24th intersociety energy conversion engineering conference*. IEEE
- Hoang AT, Pham VV (2020) A study on a solution to reduce emissions by using hydrogen as an alternative fuel for a diesel engine integrated exhaust gas recirculation. In: *AIP conference proceedings*. AIP Publishing LLC
- Hoque M, Rashid F, Aziz M (2021) Gasification and power generation characteristics of rice husk, sawdust, and coconut shell using a fixed-bed downdraft gasifier. *Sustainability* 13(4):2027
- Hord J (1978) Is hydrogen a safe fuel? *Int J Hydrogen Energy* 3(2):157–176
- Huyskens P, Van Oost S, Goemaere PJ, Bertels K, Pecqueur M (2011) The technical implementation of a retrofit hydrogen PFI system on a passenger car. *SAE Technical Paper*
- Janot R et al (2005) Development of a Hydrogen Absorbing Layer in the Outer Shell of High Pressure Hydrogen Tanks 123(3):187–193
- Jia Y et al (2015) Combination of Nanosizing and Interfacial Effect: Future Perspective for Designing Mg-Based Nanomaterials for Hydrogen Storage 44:289–303
- Juknelevičius R et al (2019) Research of Performance and Emission Indicators of the Compression-Ignition Engine Powered by Hydrogen-Diesel Mixtures 44(20):10129–10138
- Kahraman E, Ozcanlı SC, Ozerdem B (2007b) An experimental study on performance and emission characteristics of a hydrogen fuelled spark ignition engine. *Int J Hydrogen Energy* 32(12):2066–2072
- Kahraman E, Ozcanlı SC, Ozerdem BJ (2007) An experimental study on performance and emission characteristics of a hydrogen fuelled spark ignition engine 32(12):2066–2072
- Kaiwen L, Bin Y, Tao Z (2017) Economic analysis of hydrogen production from steam reforming process: a literature review. *Energy Sources Part B* 13(2):109–115
- Kalamaras CM, Efstathiou AM (2013) Hydrogen production technologies: current state and future developments. In: *Conference papers in science*. Hindawi

- Kalamaras CM, Efstathiou AM (2013a) Hydrogen production technologies: current state and future developments. *Conf Papers Energy* 2013:1–9
- Karunadasa HI, Chang CJ, Long JR (2010) A molecular molybdenum-oxo catalyst for generating hydrogen from water. *Nature* 464(7293):1329–1333
- Kayfeci M, Keçebaş A, Bayat M (2019) Hydrogen production. *Solar hydrogen production*. Elsevier, pp 45–83
- Kondo T, Iio S, Hiruma M (1997) A study on the mechanism of backfire in external mixture formation hydrogen engines-about backfire occurred by cause of the spark plug. *SAE Trans* 1953–1960
- Koten H (2018) Hydrogen effects on the diesel engine performance and emissions. *Int J Hydrogen Energy* 43(22):10511–10519
- Koten HJI (2018) Hydrogen effects on the diesel engine performance and emissions 43(22):10511–10519
- Lambe S, Watson H (1993) Optimizing the design of a hydrogen engine with pilot diesel fuel ignition. *Int J Veh Des* 14(4):370–389
- Laskowski P et al (2018) Vehicle hydrocarbons' emission characteristics determined using the Monte Carlo method. *Environ Model Assess* 24(3):311–318
- Lee JT, Kim YY, Lee CW, Caton JA (2001) An investigation of a cause of backfire and its control due to crevice volumes in a hydrogen fueled engine. *J Eng Gas Turbines Power* 123(1):204–210
- Li G, Yu X, Jin Z, Shang Z, Li D, Li Y, Zhao Z (2020) Study on effects of split injection proportion on hydrogen mixture distribution, combustion and emissions of a gasoline/hydrogen SI engine with split hydrogen direct injection under lean burn condition. *Fuel* 270:117488
- Lin K-W, Wu H-W (2019) Thermodynamic analysis and experimental study of partial oxidation reforming of biodiesel and hydrotreated vegetable oil for hydrogen-rich syngas production. *Fuel* 236:1146–1155
- Lund JW (1997) Direct heat utilization of geothermal resources. *Renew Energy* 10(2–3):403–408
- Manoharan Y et al (2019) Hydrogen fuel cell vehicles; current status and future prospect. *Appl Sci* 9(11)
- Masuk NI, Mostakim K, Kanka SD (2021a) Performance and emission characteristic analysis of a gasoline engine utilizing different types of alternative fuels: a comprehensive review. *Energy Fuels* 35(6):4644–4669
- Masuk NI et al (2021b) Performance and Emission Characteristic Analysis of a Gasoline Engine Utilizing Different Types of Alternative Fuels: a Comprehensive Review 35(6):4644–4669
- Masuk NI et al (2021) Performance and emission characteristic analysis of a gasoline engine utilizing different types of alternative fuels. *Comprehensive Rev*
- Mathur H, Khajuria P (1984) Performance and emission characteristics of hydrogen fueled spark ignition engine. *Int J Hydrogen Energy* 9(8):729–735
- Mazzolai GJ (2012) Perspectives and challenges for solid state hydrogen storage in automotive applications 5(2):137–148
- Meng F, Yu X, He L, Liu Y, Wang Y (2018) Study on combustion and emission characteristics of a n-butanol engine with hydrogen direct injection under lean burn conditions. *Int J Hydrogen Energy* 43(15):7550–7561
- Muffler P, Cataldi R (1978) Methods for regional assessment of geothermal resources. *Geothermics* 7(2–4):53–89
- Navarro E, Leo TJ, Corral R (2013) CO<sub>2</sub> emissions from a spark ignition engine operating on natural gas–hydrogen blends (HCNG). *Appl Energy* 101:112–120
- Nikolaidis P, Poullikkas A (2017) A comparative overview of hydrogen production processes. *Renew Sustain Energy Rev* 67:597–611
- Nikolaidis P, Poullikkas A (2017) A comparative overview of hydrogen production processes. *Renew Sustain Energy Rev* 67:597–611
- Noorollahi Y, Yousefi H (2010) Geothermal energy resources and applications in Iran. In: *Proceedings world geothermal congress*. Bali, Indonesia

- Ogola PF (2012) The power to change: creating lifeline and mitigation-adaptation opportunities through geothermal energy utilisation, in School of Engineering and Natural Science. University of Iceland, Iceland
- Ozturk T, Demirbas AJES (2007) Part A, Boron compounds as hydrogen storage materials 29(15):1415–1423
- Petkov T, Veziroğlu T, Sheffield HE (1989) An outlook of hydrogen as an automotive fuel 14(7):449–474
- Prabhukhot Prachi R, Wagh Mahesh M, Aneesh G A review on solid state hydrogen storage material 4(2):11–22
- Rezai A, Keshavarzi P, Mahdiye R (2014) A novel MLP network implementation in CMOL technology. Eng Sci Technol Int J 17(3):165–172
- Röhm-Malcotti E (2021) EU hydrogen strategy
- Roy MM et al (2011) Comparison of performance and emissions of a supercharged dual-fuel engine fueled by hydrogen and hydrogen-containing gaseous fuels. Int J Hydrogen Energy 36(12):7339–7352
- Ruse E et al (2018) Hydrogen Storage Kinetics: the Graphene Nanoplatelet Size Effect 130:369–376
- Safari F, Dincer I (2020) A review and comparative evaluation of thermochemical water splitting cycles for hydrogen production. Energy Conv Manage 205
- Sahaym U, Norton MG Advances in the application of nanotechnology in enabling a ‘hydrogen economy’ 43(16):5395–5429
- Sakintuna B, Lamari-Darkrim F, Hirscher MJ Metal hydride materials for solid hydrogen storage: a review 32(9):1121–1140
- Sandalcı T, Karagöz Y (2014) Experimental investigation of the combustion characteristics, emissions and performance of hydrogen port fuel injection in a diesel engine. Int J Hydrogen Energy 39(32):18480–18489
- Şensöz SA, Yorgun D (2000) Influence of particle size on the pyrolysis of rapeseed (*Brassica napus* L.): fuel properties of bio-oil. Biomass Bioenergy 19(4):271–279
- Shirmeshan A (2013) HC, CO, CO<sub>2</sub> and NO<sub>x</sub> emission evaluation of a diesel engine fueled with waste frying oil methyl ester. Procedia Soc Behav Sci 75:292–297
- Show K-Y, Yan Y-G, Lee D-J (2019) Biohydrogen production from algae: perspectives, challenges, and prospects. In: Biofuels from algae, pp 325–343
- Soria MA, Barros D, Madeira LM (2019) Hydrogen production through steam reforming of bio-oils derived from biomass pyrolysis: thermodynamic analysis including in situ CO<sub>2</sub> and/or H<sub>2</sub> separation. Fuel 244:184–195
- Syed S, Renganathan M (2019) NO<sub>x</sub> emission control strategies in hydrogen fuelled automobile engines. Australian J Mech Eng 1–23
- Szydio ZA (2020) Hydrogen—some historical highlights. Chem Didactics-Ecol Metrol 25(1–2):5–34
- Talibi M et al (2018) Hydrogen-Diesel Fuel Co-Combustion Strategies in Light Duty and Heavy Duty CI Engines 43(18):9046–9058
- Tools, H. Hydrogen compared with other fuels. Available from: <https://h2tools.org/bestpractices/hydrogen-compared-other-fuels>
- Turner J et al (2008) Renewable hydrogen production. Int J Energy Res 32(5):379–407
- Van Hoecke L et al (2021) Challenges in the use of hydrogen for maritime applications. Energy Environ Sci 14(2):815–843
- Verhelst S, T’Joel C, Vancoillie J, Demuyneck J (2011) A correlation for the laminar burning velocity for use in hydrogen spark ignition engine simulation 36(1):957–974
- Veziroglu TN (2007) 21st century’s energy: hydrogen energy system. Assessment of hydrogen energy for sustainable development. Springer, pp 9–31
- Wallington T, Sullivan J, Hurley M (2008) Emissions of CO {sub 2}, CO, NO {sub x}, HC, PM, HFC-134a, N {sub 2} O and CH {sub 4} from the global light duty vehicle fleet. Meteorologische Zeitschrift (Berlin) 17












- Wikiwand (2021) Maximum brake torque Available from: [https://www.wikiwand.com/en/Maximum\\_brake\\_torque](https://www.wikiwand.com/en/Maximum_brake_torque)
- Wikiwand (2021) Mean effective pressure. Available from: [https://www.wikiwand.com/en/Mean\\_effective\\_pressure](https://www.wikiwand.com/en/Mean_effective_pressure)
- Yip HL, Srna A, Yuen ACY, Kook, Sanghoon T, Robert A, Yeoh GH, Medwell, Paul R, Chan, QN A review of hydrogen direct injection for internal combustion engines: towards carbon-free combustion. *Appl Sci* 9(22):4842
- Yu X, Du Y, Sun P, Liu L, Wu H, Zuo X (2017) Effects of hydrogen direct injection strategy on characteristics of lean-burn hydrogen-gasoline engines. *Fuel* 208:602–611
- Zhang Y-H et al (2015) Development and Application of Hydrogen Storage 22(9):757–770
- Zhang S et al (2017) Hydrogen production via catalytic autothermal reforming of desulfurized Jet-A fuel. *Int J Hydrogen Energy* 42(4):1932–1941



# Chapter 7

## Effectiveness of Hydrogen and Nanoparticles Addition in Eucalyptus Biofuel for Improving the Performance and Reduction of Emission in CI Engine



P. V. Elumalai , N. S. Senthur , M. Parthasarathy , S. K. Dash , Olusegun D. Samuel , M. Sreenivasa Reddy , M. Murugan , PritamKumar Das , A. S. S. M. Sitaramamurty , S. Anjanidevi , and Selçuk Sarıkoç 

**Abstract** Eucalyptus biodiesel (EB) powered CI engine was characterized by low brake thermal efficiency (BTE) and more smoke emission. The inherent oxygen content of nanoparticles could be added with EB leading to improve the oxidation of hydrocarbon that results in low smoke emission. The present study was initially carried out on a compression ignition engine powered by EB considered as reference fuel. Further, this experiment was assessed with the same modified CI engine fuelled

---

P. V. Elumalai (✉) · S. K. Dash · M. S. Reddy · PK. Das · A. S. S. M. Sitaramamurty · S. Anjanidevi

Department of Mechanical Engineering, Aditya Engineering College, Surampalem, India  
e-mail: [elumalai@aec.edu.in](mailto:elumalai@aec.edu.in)

N. S. Senthur

Department of Mechanical Engineering, Bharath Institute of Higher Education and Research, Chennai, India

M. Parthasarathy

Department of Automobile Engineering, Vel Tech Rangarajan Dr, Sagunthala R&D Institute of Science and Technology, Chennai, India

O. D. Samuel

Department of Mechanical Engineering, Federal University of Petroleum, Resources, P.M.B 1221, Effurun, Delta State, Nigeria

Department of Mechanical Engineering, University of South Africa, Science, Campus, Private Bag X6, Florida 1709, South Africa

S. Sarıkoç

Department of Motor Vehicles and Transportation Technologies, Tasova Yuksel Akin Vocational School, Amasya University, Amasya, Turkey

M. Murugan

Department of Mechanical Engineering, Aditya College of Engineering and Technology, Surampalem, India

with hydrogen enrichment in EB blends. The high energy density of hydrogen may results better combustion efficiency and drastically reduce global emissions. The hydrogen flow rate was fixed at 5 lpm throughout engine operation for enrichment of air. In this experiment, the different combination of fuel blends were used such as Eucalyptus biodiesel 15% + diesel 85% (EB15), neat Eucalyptus biodiesel 100% (EB100), Eucalyptus biodiesel 15% + diesel 85% + Alumina nanoparticle 50 ppm (EB15-A), Eucalyptus biodiesel 15% + diesel 85% + Alumina nanoparticle ( $\text{Al}_2\text{O}_3$ ) 50 ppm + hydrogen enrichment (EB15-A-H), neat Eucalyptus biodiesel 100% +  $\text{Al}_2\text{O}_3$  50 ppm (EB100-A), neat Eucalyptus biodiesel 100% +  $\text{Al}_2\text{O}_3$  50 ppm + hydrogen enrichment (EB100-A-H). The results indicated that EB15-A-H showed 6.6% increase in the thermal efficiency whereas it was 2.5% lower fuel consumption as compared to diesel operation. EB100 powered CI engine indicated 17% lower combustion efficiency as compared to diesel in CI mode. The results also showed that the emission value of CO, HC, and smoke for fuel EB15-A-H were 9.5%, 12.6%, and 15.9% lower when compared to neat diesel in CI mode operation. However, the emission of NO<sub>x</sub> was slightly higher for the fuel EB15-A-H than other blends. Overall, it was concluded that EB15-A-H as a potential alternative fuel for CI engine application.

**Keywords** Eucalyptus biofuel · Aluminium oxide · Hydrogen · CI engine · Emission

## Abbreviations

BTE	Brake Thermal Efficiency
CN	Cetane Number
CO	Carbon monoxide
DI	Direct Ignition
E15	85% Diesel + 15% of Biodieesl
E100	100% Of Biodiesel
E100-A	100% Of Biodiesel + 50 ppm of nannoparticle
E100-A-H	100% Of Biodiesel + 50 ppm of nanoparticle + 5 lpm H <sub>2</sub>
E15-A	85% Diesel + 15% of Biodieesl + 50 ppm of nanoparticle
E15-A-H	85% Diesel + 15% of Biodieesl + 50 ppm of nanoparticle + 5 lpm H <sub>2</sub>
HC	Hydrocarbon
ID	Ignition Delay
NO <sub>x</sub>	Oxides of Nitrogen

## 7.1 Introduction

Sustainable energy source and clean energy technologies are the major researched area in this century. Due to the ever-increasing need for energy, which is mostly reliant on the imperilled and dwindling fossil fuel stocks, the demand for renewable energy or fuel sources is expanding. To address this major problem of pollution and fuel scarcity, it is critical to establish alternative renewable energy sources that can be used as a clean fuel. The internal combustion engine run by petrol and diesel find huge application in the entire world (Dash et al. 2020). However, the primary fuel for IC engine is changed to more sustainable and cleaner fuel biodiesel. From the last couple of decades, many improvements have been made by various researchers regarding engine modification technology, fuel modification technology, fuel blending by mixing various fuels and additives and dual fuel engine technology incorporating gaseous fuel for better performance and lower exhaust pollution. Biodiesel is produced by chemically reacting oils and fats with suitable alcohol (Dash et al. 2018). It has been established that biodiesel is far from superior compared to conventional diesel in terms of physicochemical properties (Dash and Lingfa 2018). Nanoparticles have become increasingly important because of the advancement of nanotechnology. Many researchers reported that the use of nanoparticles as an additive in the engine cylinder reduces pollutions by greater margin (Elumalai 2021). The main advantage of nano additive in liquid fuel is that it reduces hazardous pollutants and imparts more heat transfer area for better distributions of flame front in the combustion chamber (Manigandan 2020). Another sought out advantage is micro explosion which supports better combustion. An excellent comprehensive review has been carried out by Yusof et al. (2020) on the nanoparticle as fuel performance enhancer for internal combustion engine. Various types of nanoparticles have been explored such as  $\text{CeO}_2$ ,  $\text{TiO}_2$ ,  $\text{Al}_2\text{O}_3$ ,  $\text{ZnO}$ , Carbon nanotubes,  $\text{ZrO}_2$  etc. (Soudagar 2020).

In addition to Nano additives, supplement of hydrogen as a clean burning combustion engine fuel has attracted the attention of scientific community. Hydrogen has long been recognised as a fuel with several distinct and desired characteristics for use in engines (Akar et al. 2018). It is the only fuel that can be made totally from the abundant renewable resource water, but at a high cost in terms of energy input (Karim 2003). The impact of additives on the key physicochemical characteristics and performance test in a DI diesel engine were investigated by Javed et al. (2016). At 100 ppm, zinc oxide ( $\text{ZnO}$ ) nanoparticles with sizes of 20 and 40 nm in JME biodiesel. Nanoparticles in the fuel blends helped to minimise  $\text{NO}_x$  emissions. Hydrocarbon (HC) emissions reduced as the  $\text{H}_2$  flow rate increased for nanoparticles with a diameter of 20 nm. (Kanth et al. 2020) studied the performance of a diesel engine powered by hydrogen enriched honge biodiesel diesel blend. The engine running on honge biodiesel blend improved the thermodynamic efficiency. In comparison to diesel, the BTE increased by 2.2%, while the  $\text{H}_2$  enriched blend consumed 6% less fuel. Further, the emission of exhaust gases such as CO and HC is reduced by 21% and 24%, respectively. (Tosun and Özcanlı 2021) studied on the use of diesel-soybean

biodiesel-hydrogen fuels and aluminium oxide ( $\text{Al}_2\text{O}_3$ ) nanoparticle additives were used in a diesel engine. Engine tests were conducted at full load at 400 rpm intervals between 1200 and 2800 rpm engine speeds. Unfortunately, when compared to diesel fuel, all test fuels produce greater  $\text{NO}_x$ . When compared to diesel fuel, H-B20-A performed well with a 6.64% increase in power and a 2.72% reduction in BSFC. H-B100-A achieved the greatest reduction in CO (15.91%). In terms of  $\text{NO}_x$  emissions, all fuels released higher than diesel. In comparison to diesel fuel, the smallest increase was seen with B20, at 6.73%. It was observed that the studies related to nano additive blended biodiesel enriched with hydrogen have been scantily reported. Thus, it is imperative more investigations are necessary in this area of research. From above literature survey it was clearly found using biodiesel as fuel in engine to increase the emission characteristics and reduced the performance characteristics. To adding the aluminium nanoparticles to reduce the emission characteristics except oxides of nitrogen. To overcomes this problem, some amount of hydrogen induced into the fuel to reduce the oxides of nitrogen. After adding the nanoparticles and hydrogen to get the better performance and emission characterises. Table 7.1 show that different nanoparticles mixed with biodiesel.

**Table 7.1** Show that different nanoparticles mixed with biodiesel

Fuels used	Nanoparticle	Performance		Emissions					References
		BTE	BSFC	HC	CO	$\text{CO}_2$	$\text{NO}_x$	PM	
E20	$\text{CeO}_2$ and CNT	↑	NA	↓	↑	NA	NA	–	(Selvan et al. 2014)
Biodiesel	$\text{Al}_2\text{O}_3$ CNT	↑	NA	↓	↓	↓	↓	↓	(Basha and Anand 2013)
DB-10 DB10E4 DB10E4NP	Al-C	↑	↓	↑	↓	NA	↓	NA	(Wu et al. 2018)
Biodiesel	AIO (OH)	↑	NA	↓	↓	NA	↓	NA	(Srinivasa and Anand 2016)
BD-5 BD-10	CNT	↑	↓	↓	↓	NA	↑	NA	(Hosseini et al. 2017)
MOME	$\text{TiO}_2$	NA	NA	↓	↓	NA	↓	NA	(Yuvarajan et al. 2018)
DBE n butanol ( $\text{C}_4\text{H}_9\text{O H}$ )	$\text{TiO}_2$	↑	↓	↓	↓	↑	↑	NA	(Örs et al. 2018)
Diesel	$\text{TiO}_2$	↑	↓	↓	↓	NA	NA	NA	(D'Silva et al. 2015)
JME	Graphene oxide (GO)	↑	↓	↓	↓	NA	↓	NA	(El-Seesy et al. 2018a)
B20	Grapene oxide (GO)	↑	↓	↓	↓	NA	↓	NA	(El-Seesy et al. 2018b)

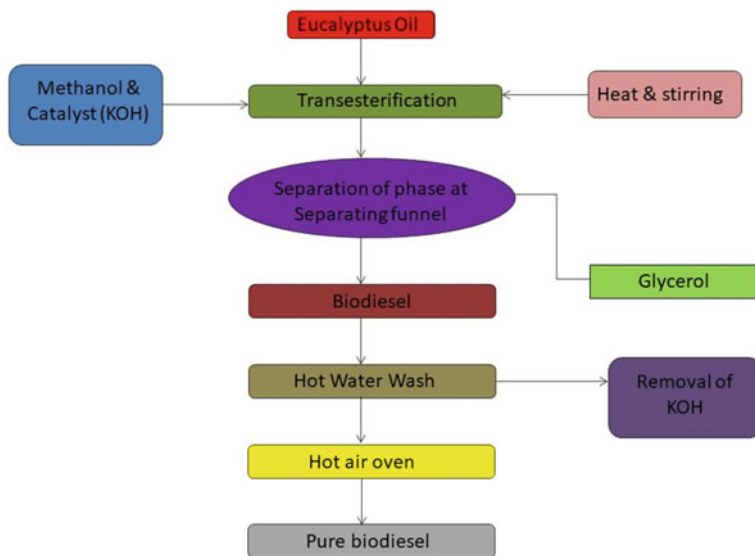


Fig. 7.1 Transesterification Process

## 7.2 Materials and Methods

### 7.2.1 Biodiesel Production

Sodium hydroxide (NaOH) as catalyst and methanol as alcohol ( $\text{CH}_3\text{OH}$ ) were chosen for the transesterification reaction.. To make a homogeneous mixture for neat biofuel and alcohol, NaOH was dissolved in the mixture. In a flask, neat biofuel was heated to  $80^\circ\text{C}$  with the presence of alcohol-catalyst mixture. A magnetic stirrer was used to mix the blend continually for about 2 h at a temperature of  $60\text{--}80^\circ\text{C}$ . Biodiesel was left in a separation funnel for 8 h at the end of the reaction to collect glycerine from the bottom of the funnel using phase difference principle. Finally, Eucalyptus biodiesel was derived through transesterification operation. Biodiesel properties were observed to be superior than neat biofuel. Figure 7.1 show that transesterification process.

Table 7.2 shows the properties of test fuel.

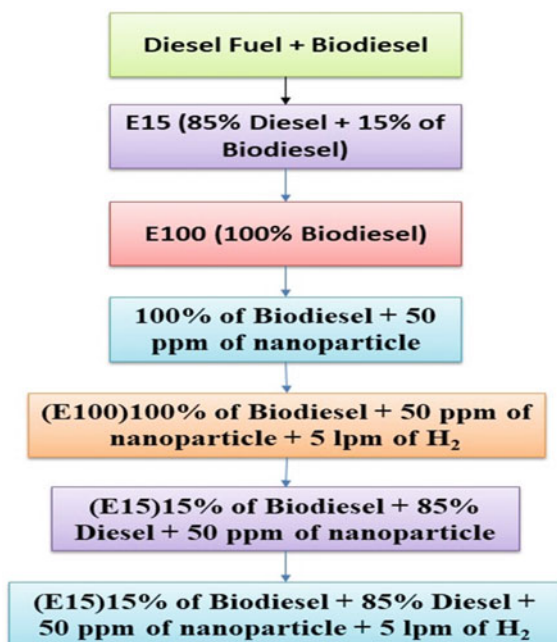
### 7.2.2 Test Fuel Preparation and Determination of Physicochemical Properties

The diesel fuel was chosen as reference fuel. A commercial firm provided  $\text{Al}_2\text{O}_3$  as an additive in powder form. To investigate the effects on engine performance, a

**Table 7.2** Properties of test fuel

Fuel used	Cetane number	Density (kg/m <sup>3</sup> )	Heating value (MJ/kg)	Viscosity (mm <sup>2</sup> /s)	Flash point (°C)
Diesel	54.2	836	44.7	2.68	66
EB-15	48	847	41.9	3.16	80
EB-100	45.3	887	40.1	4.28	162
EB-15-A	49	849	42.6	3.2	78
Hydrogen	–	0.0836	119.86	–	–
EB-100-A	46.2	889	40.2	4.38	179

50-ppm dose of Al<sub>2</sub>O<sub>3</sub> nanoparticle was added to base fuel and biodiesel. To achieve homogeneous dispersion of nanoparticles in fuels, ultrasonic processor was used. In regards, at a flow rate of 6 L/min, blends were enhanced with hydrogen supplement. Furthermore, determining fuel characteristics is critical for both fuel usability and the interpretation of performance and emission results. The various fuel properties such as cetane number, calorific value, density, viscosity and flash point have been evaluated by using different types of instruments. Figure 7.2 shows the flow chart for fuel preparation.

**Fig. 7.2** Flow chart for fuel preparation

### 7.3 Experimental Test Rig and Procedure

Experimentation have been carried out with the help of a hydraulic dynamometer and a normally aspirated, four-stroke, four-cylinder direct injection diesel engine. Before each experiment, the test engine was run for 15 min to ensure stable operation and to clear any residual fuel from the end of the experiment from the fuel system. Engine testing were conducted three times for each fuel, with the average of the results recorded under identical conditions. At full load condition, test fuels were run at 400 rpm intervals between 1200 and 2800 rpm engine loads. Multi-gas analyzer with the AVL-444 type that can measure CO, HC, CO<sub>2</sub>, O<sub>2</sub>, and NO<sub>x</sub> concentrations in exhaust. The AVL-437 model smoke metre (with a measuring range of 0 to 100 percent, a resolution of 0.1%, and an uncertainty of 1.2) is used to determine smoke opacity. For cylinder pressure and combustion temperature, the uncertainty analysis is 1.2 and 64.78 K, respectively. Using numerous sensors, a computerised data acquisition system is employed to gather, store, and evaluate data during the experiment. Before each emission test, the gas analyser was calibrated to verify the accuracy of the measurements. Figure 7.3 shows the experimental setup diagram. Table 7.3 shows the specification of the engine.

#### 7.3.1 Uncertainty Analysis

Depending upon the manufacturing of the instruments, the degrees of reliability may be varied. The prediction of an uncertainty analysis has been performed with

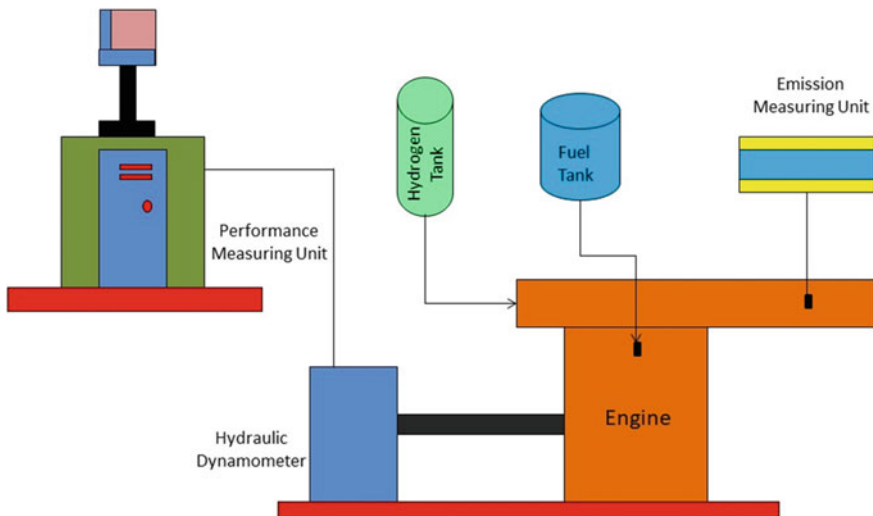


Fig. 7.3 Experimental setup

**Table 7.3** Specification of engine

Engine model	4D34-2A
Bore (mm)	104
Stroke (mm)	115
Compression ratio	17:1
Maximum torque	295 Nm
Maximum power	89 kW
Displacement	7.5 L
Connecting rod	150 mm
Injection pressure	200 bar
Injection timing	23 deg bTDC

the estimated measurements and measured values during this study to ensure the precision level of the data obtained from the devices (Tüccar and Uludamar 2018). Errors and uncertainties in a product cause several environmental variables that focus on the system being tested, calibrated, operational state, and reliability. The analyses have been carried out in five cycles, and the moderate values were used to quantify uncertainty in this study (Gumus et al. 2016; Soudagar et al. 2020). During the investigation, the researchers and scientists have used multifactorial approach to perform an uncertainty analysis, which would have been a popular as shown in Table 7.4.

**Table 7.4** Uncertainty analysis

S. No.	Parameters	Systematic Errors ( $\pm$ )
1	Load indicator	$\pm 0.2$
2	Speed sensor	$\pm 1.0$
3	Temperature sensor	$\pm 0.15$
4	Pressure sensor	$\pm 0.5$
5	Crank angle encoder	$\pm 0.2$
6	Smoke meter	$\pm 1.0$
7	Eddy current dynamometer	$\pm 0.15$
8	Fuel burette	$\pm 1.0$
9	Manometer	$\pm 1.0$
10	Load indicator	$\pm 0.2$
11	Smoke, HSU	$\pm 3$
12	CO <sub>2</sub>	$\pm 1$
13	NOx	$\pm 0.4$
14	CO	$\pm 0.2$
15	HC	$\pm 1.0$



## 7.4 Results and Discussions

### 7.4.1 Power

Figure 7.4 depicts power variations with respect to various engine speed for different test fuel. The performance parameter of B100 were inferior than other test fuel at standard operating condition. Poor spray characteristics caused by biodiesel's increased viscosity and lower energy content could be resulted in poor efficiency. A Low energy rating of biodiesels could be another possible explanation for inferior engine performance (Uludamar 2018). The above reason could be responsible for power reductions when engine operated with EB15 and EB100 instead of diesel fuel. Experiment shows that adopting nanoparticles into the fuel would boost the power output because of the catalytic activity on chemical reaction. The usage of hydrogen-enriched fuels resulted in a significant increase in power due to enriched the heating value of mixture. Due to increase in oxidation rate and the catalytic action of nanoparticles, power output could be improved for EB15-A-H (Serin and Yıldızhan 2018; Ozcanli et al. 2017). Results was seen that combustion efficiency was exhibited reasonable improvement for fuel EB15-A-H owing to hydrogen energy contribution and faster flame speed which enhance combustion (Rocha et al. 2017) In terms of power output, both EB15-A and EB15-A-H was found close to similar performance at all speed condition.

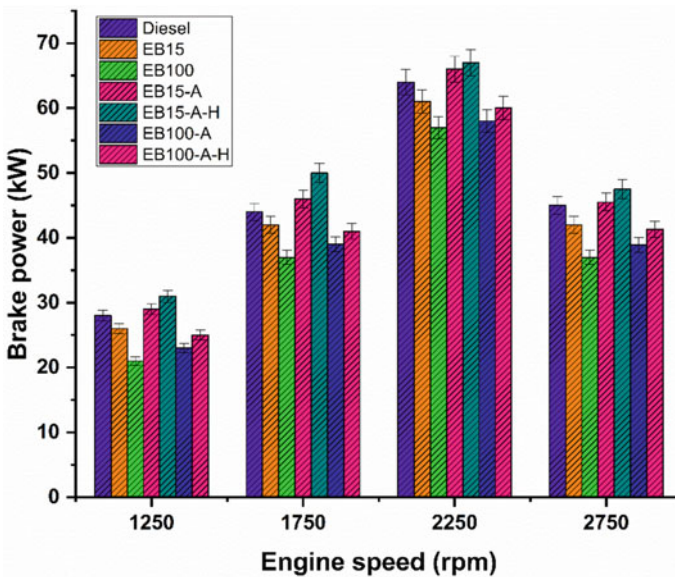


Fig. 7.4 Power versus speed

### 7.4.2 BSFC

Figure 7.5 depicts BSFC fluctuations as a function of engine speed. The quantity of fuel consumed by an engine to produce unit power is known as the BSFC. The nominal amount of fuel consumed by engine to generate the same power output is called as fuel economy. EB100 and EB15 raised the BSFC when compared to diesel fuel owing to the low CV of biodiesel (Keskin et al. 2015). BSFC could be reduced by using nanoparticles with blend and further it dropped for hydrogen enriched with air. BSFC value of nano additive and hydrogen enriched blends EB15 and EB100 operated engine showed slightly lower than without fuel modification. EB15-A and EB15-A-H have found lower BSFC values at rated power output condition. On the other hand, BSFC of EB100-A and EB100-A-H fuels was outperformed at all speed condition. The use of nanoparticles with biodiesel could have reduced the BSFC value due to slightly increase in the calorific value of biodiesel. The inherent oxygen of biodiesel and combustion-catalysing actions of nanoparticles leads to achieve the high temperatures and pressures in the chamber which exhibits lower fuel consumption rate (Shahir et al. 2015). Hydrogen was added because it has superior properties such as a high heating value (HHV), a fast flame speed (FFS), a short quenching distance (SQD), and a larger flammability range (LFR) which contribute more fuels burns completely during combustion (Ozcanli et al. 2017). The high heating value of hydrogen raises the cylinder gases temperature which speeds up the

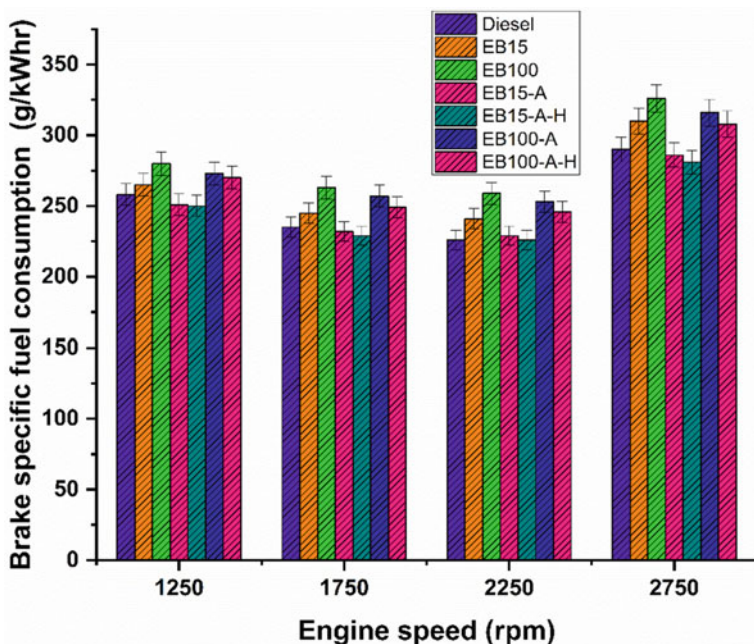


Fig. 7.5 Speed versus BSFC

combustion process therefore resulting in higher mean indicated pressure and lower BSFC (Channappagoudra 2019).

### 7.4.3 CO

Figure 7.6 represent CO variation with different speed condition for various test fuel.. A significant reason for CO formation is incomplete combustion of fuel. When inhaled CO causes series injurious to human health. Because of its colourless and odourless features, it is crucial to find its existence in the environment (Jhang et al. 2016). The EB100 and blend EB15 was noticed reduction in CO emissions when compared with base fuel. It was because of biodiesel contains inbuilt oxygen in the structure which helps oxidation for CO emission (Seraç et al. 2020). When compared to diesel fuel, EB15-A, EB15-A-H, EB100-A, and EB100-A-H was emitted lesser CO at all speed condition. As previously stated, the presence of O<sub>2</sub> in the biodiesel blend and sufficient temperature are the primary reason for lower CO formation. The addition of nanoparticles with strong catalytic activity and high surface/volume ratio leads to increase combustion efficiency that turn in higher CO<sub>2</sub> formation (Vellaiyan et al. 2018). Due to hydrogen enrichment, it encourages more homogeneous mixture

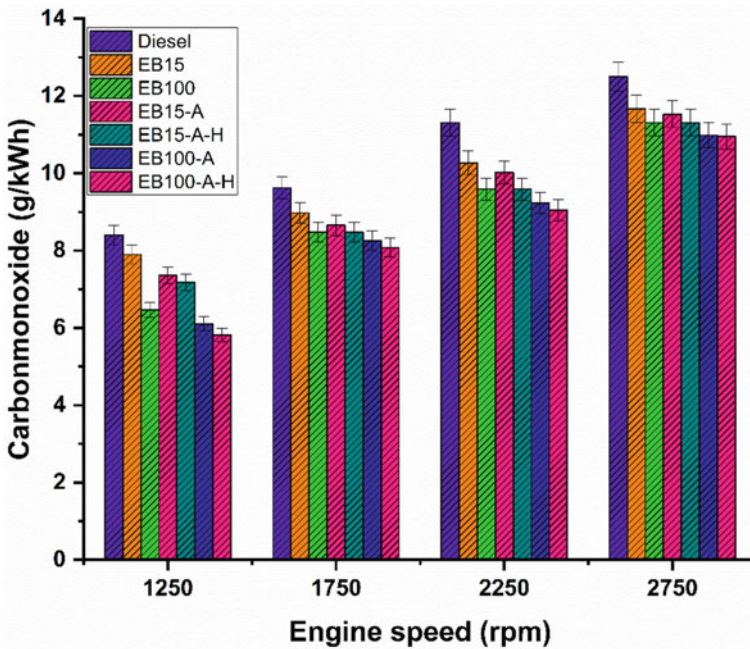


Fig. 7.6 Speed versus CO

preparation and shorter combustion time that results in more CO into CO<sub>2</sub> conversion (Manigandan et al. 2020).

### 7.4.4 CO<sub>2</sub>

Figure 7.7 illustrates the difference in CO<sub>2</sub> emission with various speed condition for hydrogen and nanoadditive blend biodiesel. CO<sub>2</sub> is one of the most common greenhouse gas compounds, and it has a detrimental impact on climate change. In contrast to CO emission, CO<sub>2</sub> production often increases when biodiesel was used (Baltacioglu et al. 2016). EB15 and EB100 produced more CO<sub>2</sub> than diesel resulting in greater combustion afforded by the higher oxygen component in their structure (Pattanaik et al. 2013). To adding the nanoparticles in EB15-A and EB100-A has enhanced CO<sub>2</sub> levels owing to the presence of nanoparticles leads to improved combustion process that results in increased CO<sub>2</sub> generation. However, hydrogen utilization may somewhat compensate for this increment of CO emission (Sezer 2020). EB15-A-H and EB100-A-H was shown reasonable reduction in CO<sub>2</sub> emission than EB15-A and EB100-A. Lower CO<sub>2</sub> levels achieved as a result of higher hydrogen/carbon ratio, shorter combustion duration, and improved combustion efficiency (Pattanaik et al. 2013). In other words, utilization of hydrogen could be

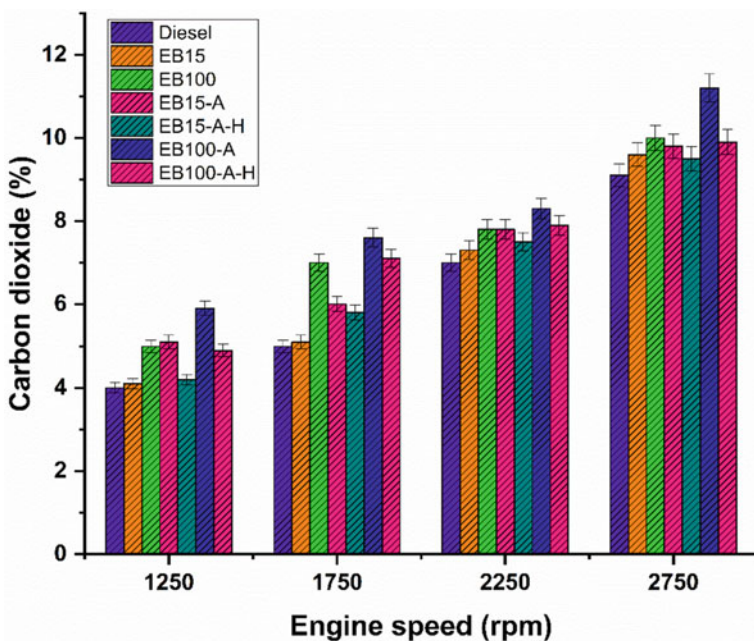


Fig. 7.7 Speed versus CO<sub>2</sub>

increased the cylinder temperature that helps to CO conversion rate. Using biodiesel in CI engine, it was found to be more CO<sub>2</sub> emissions during combustion. Moreover, during photosynthesis, its closed carbon life cycle shows that net CO<sub>2</sub> emissions are reduced (Sezer 2020).

### 7.4.5 NO<sub>x</sub>

Figure 7.8 portrays the NO<sub>x</sub> formation with a respect to different engine speed. CI engines emits more NO<sub>x</sub> which is one of the combustion-related emissions. It has severe negative consequences for both human health and the environment. The temperature of combustion, high pressure in the cylinder, air/fuel ratio, the period of combustion, moisture, and the oxygen concentration of the fuel have influence on NO<sub>x</sub> emissions formation (Sezer 2020). The blend EB15 and EB100 was exhibited in an increase in NOx when compared with base fuel. Based on the previous study (Baltacioglu et al. 2016), addition of oxygen in the biodiesel structure promotes more nitrogen oxidation along with greater cylinder temperatures. In comparison to diesel fuel, adoption of nanoparticle and hydrogen was increased the NOx generation for EB15-A, EB15-A-H, EB100-A, and EB100-A-H fuels. This result was reasonable for higher hydrogen flammable temperatures in the combustion chamber and catalytic

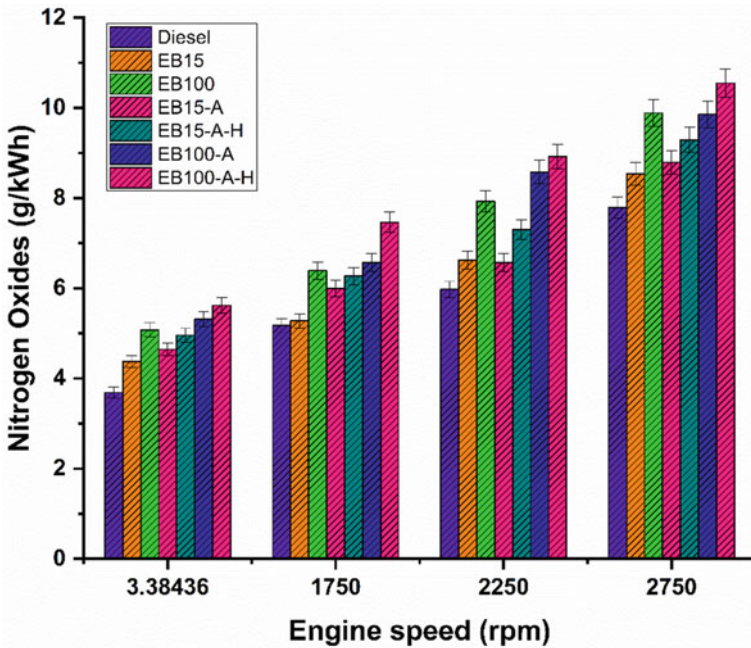


Fig. 7.8 Speed versus NO<sub>x</sub>

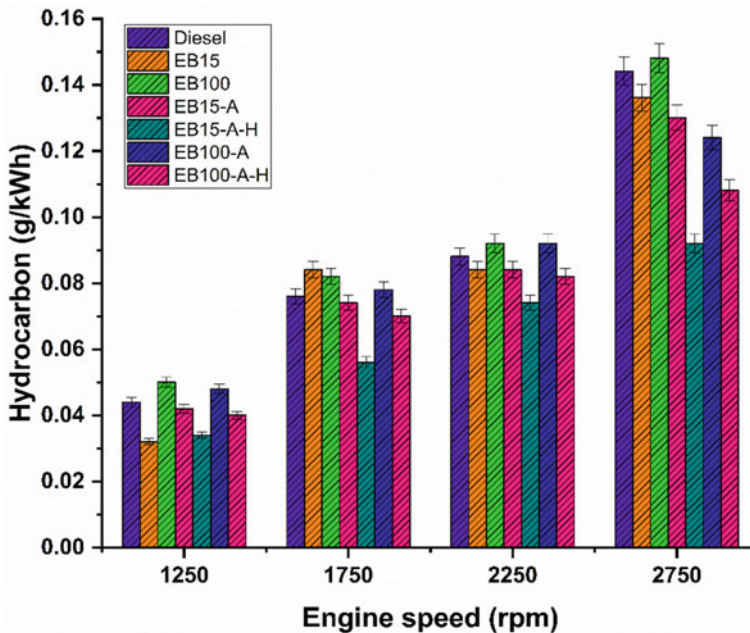


Fig. 7.9 Speed versus HC

properties of nanoparticles, which generate higher peak cylinder temperatures that result in an increased  $\text{NO}_x$  (Hamdan et al. 2015).

Figure 7.9 exhibits that variations of engine speed and HC emission for adoption of hydrogen and nanoparticle with biodiesel. The formation of HC engine in diesel engine is mainly depends on the unburnt fuel and fuel quenching during the process of combustion. Normally, conventional CI engine emitted lower HC when compared with the SI engines. The HC emission of blend E100 emitted at higher 2.7% when correlated with neat fuel. Because of the poor secondary stage of combustion of the fuel which results in lower combustion temperature that results in more unburnt hydrocarbon. When addition of the hydrogen and nanoparticle in the fuel there is drastically reduced HC emission in the conventional fuel (Perumal et al. 2021). the HC emission of the blends EB-15, EB15-A, EB15 A-H, EB 100-A, EB 100-A-H was decreased by 5.5%, 9.7%, 45%, 16.12% and 27.7% respectively when compared with the diesel fuel. The HC emission of blend EB15-A-H was decreased by 45% when correlated with base fuel, because of the addition of hydrogen into fuel and proper atomization takes place during the combustion.

Figure 7.10 shows that variations of smoke emission with respect to engine speed for different test fuel. Formation of smoke opacity is mainly depending up on the fuel droplet size and improper atomization of fuel (Shurpali et al. 2019) In the graph, it was clearly showed that highest smoke opacity emission was achieved for diesel due to high C/H ratio of diesel and lack of  $\text{O}_2$  in chamber which leads to partial burn the

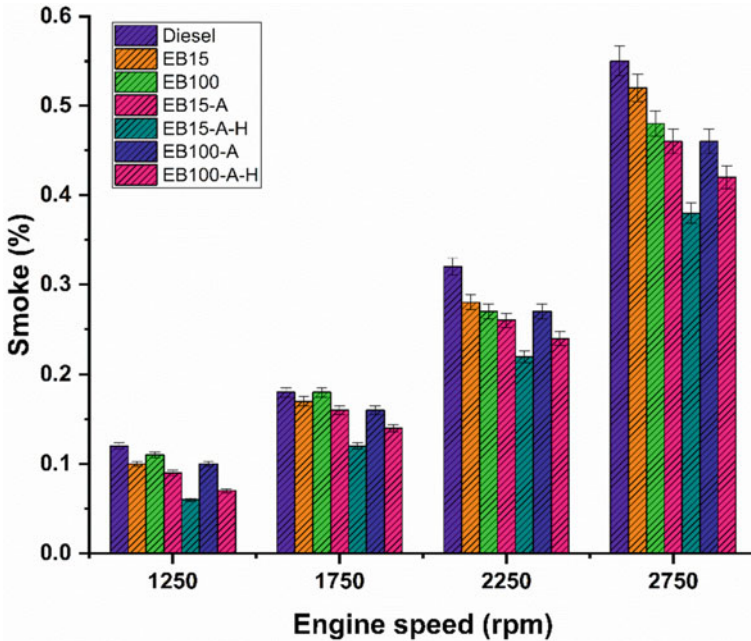


Fig. 7.10 Speed versus smoke opacity

diesel that results in higher CO formation. When addition of the nanoparticles and hydrogen into the fuels, it was exhibited drastic decrement in the smoke emission. The smoke emission of the blends EB-15, EB15-A, EB15 A-H, EB 100-A, EB 100-AH was decreased by 5.4%, 16.36%, 30.90%, 46.12% and 23.7% respectively when compared with the diesel fuel. The EB15 A-H was achieved lower smoke opacity emission when compared with other fuel blends. It could be attributed to the enough oxygen in the fuel and air mixture and elevated energy value which enhance the combustion process. The smoke opacity was decreased for the blend EB15-A-H by 28.90% when compared with neat biodiesel. This was mainly due to the hydrogen induced into the fuels that promote the volatility of mixture therefore produce lesser soot particles (Shukla et al. 2018; Murugesan et al. 2021; Elumalai et al. 2021).

### 7.5 Conclusions

Based on the experimental study, EB15-A-H has been showed 6.64% increase in power as well as 2.72% decrease in BSFC. Unfavourable engine operation occurred on utilizing EB100 exhibited 17% decrease in power as well as 11.8% increase in BSFC as related to diesel. Apart from that, EB100-A-H showed high reduction in global emissions (HC and CO). In contrast to neat biodiesel, it has resulted inferior

performance characteristics. Minimum CO<sub>2</sub> release was observed by diesel fuel at standard condition. Moreover, EB100-A emitted 34.92% more CO<sub>2</sub> contrasting to diesel. Diesel fuel indicated nominal NO<sub>x</sub> emission when compared to other test fuels. Other side, EB100-A-H indicated slightly increase NO<sub>x</sub> whereas the same fuel without modification of hydrogen and nanoparticle adoption was 37.68% higher than diesel. Hydrogen addition showed high power output but it could be emitted more NO<sub>x</sub> emission owing to high flame speed and propagation period which enhanced the cylinder temperature. Utilization of neat eucalyptus biodiesel in CI engine was not suitable for long term operation due to lower calorific value and higher viscosity. This could be resolved by induction of hydrogen with atmospheric air. Furthermore, doping of nanoparticle with biodiesel blends noticed improvement in performance characteristics and reasonable reduction in emission. The result of CO was more for diesel fuel but it was contrast to biodiesel. Dosage of nanoparticles with biodiesel showed lower CO emission than conventional fuel. This might be lower C/H ratio of fuel and inherent O<sub>2</sub> in both biodiesel and nanoparticle which promote the oxidation of CO. The HC emission of EB15-A-H was 45% lesser than diesel owing to addition hydrogen and catalytic effect of nanoparticles that helps in complete combustion. The result of smoke opacity for EB15-A-H was 28.9% lower than B100 because of hydrogen enrichment and proper atomization take place during the combustion process. On the whole, it was concluded that EB15-A-H was chosen as a potential alternative energy sources for CI engine application.

**Declaration of Competing Interest** The authors declare that they have no known competing financial interests or personal relationships that could have appeared to influence the work reported in this paper.

## References

- Akar MA, Kekilli E, Bas O, Yildizhan S, Serin HM, Ozcanli M (2018) Hydrogen enriched waste oil biodiesel usage in compression ignition engine. *Int J Hydrogen Energy* 43(38):18046–18052, <https://doi.org/10.1016/j.ijhydene.2018.02.045>
- Baltacioglu MK, Arat HT, Özcanli M, Aydin K (2016) Experimental comparison of pure hydrogen and HHO (hydroxy) enriched biodiesel (B10) fuel in a commercial diesel engine. *Int J Hydrogen Energy* 41(2016):8347–8353. <https://doi.org/10.1016/j.ijhydene.2015.11.185>
- Basha JS, Anand RB (2013) The influence of nano additive blended biodiesel fuels on the working characteristics of a diesel engine. *J Braz Soc Mech Sci Eng* 35:257–264. <https://doi.org/10.1007/s40430-013-0023-0>
- Channappagoudra M (2019) Influence of the aluminium oxide (Al<sub>2</sub>O<sub>3</sub>) nanoparticle additive with biodiesel on the modified diesel engine performance. *Int J Ambient Energy* 2019:1–9. <https://doi.org/10.1080/01430750.2019.1614992>
- Dash SK, Lingfa P, Chavan SB (2018) An experimental investigation on the application potential of heterogeneous catalyzed Nahar biodiesel and its diesel blends as diesel engine fuels. *Energy Sources Part A Recover Util Environ Eff* 40(24):2923–2932. <https://doi.org/10.1080/15567036.2018.1514433>
- Dash SK, Lingfa P (2018) An overview of biodiesel production and its utilization in diesel engines. *IOP Conf Ser Mater Sci Eng* 377:012006. <https://doi.org/10.1088/1757-899X/377/1/012006>



- Dash SK, Lingfa P, Barik D (2020) Combined adjustment of injection timing and compression ratio for an agricultural diesel engine fuelled with Nahar methyl ester. *Int J Ambient Energy* 0(0): 1–13. <https://doi.org/10.1080/01430750.2020.1712250>
- D'Silva R, Binu K.G, Bhat T (2015) Performance and emission characteristics of a C.I. Engine fuelled with diesel and TiO<sub>2</sub> nanoparticles as fuel additive. *Mater Today Proc* 2:3728–3735. <https://doi.org/10.1016/j.matpr.2015.07.162>
- EL-Seesy AI, Hassan H, Ookawara S (2018a) Performance, combustion, and emission characteristics of a diesel engine fueled with jatropa methyl ester and graphene oxide additives. *Energy Convers Manag* 166:674–686. <https://doi.org/10.1016/j.enconman.2018.04.049>
- El-Seesy AI, Hassan H, Ookawara S (2018b) Effects of graphene nanoplatelet addition to jatropa biodiesel–diesel mixture on the performance and emission characteristics of a diesel engine. *Energy* 147:1129–1152. <https://doi.org/10.1016/j.energy.2018.01.108>
- Elumalai PV (2021) An experimental study on harmful pollution reduction technique in low heat rejection engine fuelled with blends of pre-heated linseed oil and nano additive. *J Clean Prod* 283:124617 <https://doi.org/10.1016/j.jclepro.2020.124617>
- Elumalai PV, Nambiraj M, Parthasarathy M, Balasubramanian D, Hariharan V, Jayakar J (2021) Experimental investigation to reduce environmental pollutants using biofuel nano-water emulsion in thermal barrier coated engine. *Fuel* 285:119200
- Gumus S, Ozcan H, Ozbey M, Topaloglu B (2016) Aluminum oxide and copper oxide nanodiesel fuel properties and usage in a compression ignition engine. *Fuel* 163:80–87. <https://doi.org/10.1016/j.fuel.2015.09.048>
- Hamdan MO, Selim MYE, Al-Omari SAB, Elnajjar E (2015) Hydrogen supplement co-combustion with diesel in compression ignition engine. *Renew Energy* 82(2015):54–60. <https://doi.org/10.1016/j.renene.2014.08.019>
- Hosseini SH, Taghizadeh-Alisaraei A, Ghobadian B, Abbaszadeh-Mayvan A (2017) Performance and emission characteristics of a CI engine fuelled with carbon nanotubes and diesel-biodiesel blends
- Javed S, Satyanarayana Murthy YVVC, Satyanarayana MRC, Rajeswara Reddy R, Rajagopal K (2016) Effect of a zinc oxide nanoparticle fuel additive on the emission reduction of a hydrogen dual-fuelled engine with jatropa methyl ester biodiesel blends. *J Clean Prod* 137:490–506. <https://doi.org/10.1016/j.jclepro.2016.07.125>
- Jhang SR, Chen KS, Lin SL, Lin YC, Cheng WL (2016) Reducing pollutant emissions from a heavy-duty diesel engine by using hydrogen additions. *Fuel* 172(2016):89–95. <https://doi.org/10.1016/j.fuel.2016.01.032>
- Kanth S, Debbarma S, Das B (2020) Effect of hydrogen enrichment in the intake air of diesel engine fuelled with honge biodiesel blend and diesel. *Int J Hydrogen Energy* 45(56):32521–32533. <https://doi.org/10.1016/j.ijhydene.2020.08.152>
- Karim G (2003) Hydrogen as a spark ignition engine fuel. *Int J Hydrogen Energy* 28:569–577. <https://doi.org/10.2298/HEMIND0206256K>
- Keskin A, Ocakoglu K, Resitoglu IA, Avsar G, Emen FM, Buldum B (2015) Using Pd (II) and Ni(II) complexes with N, N-dimethyl-N0-2-chlorobenzoylthiourea ligand as fuel additives in diesel engine. *Fuel* 162(2015):202–206. <https://doi.org/10.1016/j.fuel.2015.09.023>
- Manigandan S (2020) Effect of nanoparticles and hydrogen on combustion performance and exhaust emission of corn blended biodiesel in compression ignition engine with advanced timing. *Int J Hydrogen Energy* 45(4):3327–3339. <https://doi.org/10.1016/j.ijhydene.2019.11.172>
- Manigandan S, Sarweswaran R, Booma Devi P, Sohret Y, Kondratiev A, Venkatesh S, Rakesh Vimal M, Jensin Joshua (2020) Comparative study of nanoadditives TiO<sub>2</sub>, CNT, Al<sub>2</sub>O<sub>3</sub>, CuO and CeO<sub>2</sub> on reduction of diesel engine emission operating on hydrogen fuel blends. *Fuel* 262:116336. <https://doi.org/10.1016/j.fuel.2019.116336>
- Murugesan P et al (2021) Role of hydrogen in improving performance and emission characteristics of homogeneous charge compression ignition engine fueled with graphite oxide nanoparticle-added microalgae biodiesel/diesel blends. *Int J Hydrogen Energy*. <https://doi.org/10.1016/j.ijhydene.2021.08.107>

- Ozcanli M, Akar MA, Calik A, Serin H (2017) Using HHO (Hydroxy) and hydrogen enriched castor oil biodiesel in compression ignition engine. *Int J Hydrogen Energy* 42(2017):23366–23372. <https://doi.org/10.1016/j.ijhydene.2017.01.091>
- Örs I, Sarıkoç S, Atabani AE, Ünalan S, Akansu SO (2018) The effects on performance, combustion and emission characteristics of DICI engine fuelled with TiO<sub>2</sub> nanoparticles addition in diesel/biodiesel/n-butanol blends. *Fuel* 234:177–188. <https://doi.org/10.1016/J.FUEL.2018.07.024>
- Pattanaik BP, Nayak C, Nanda BK (2013) Investigation on utilization of biogas & Karanja oil biodiesel in dual fuel mode in a single cylinder DI diesel engine. 4(2013):279–290
- Perumal Venkatesan E, Balasubramanian D, Samuel OD, Kaisan MU, Murugesan P (2021) Effect of hybrid nanoparticle on DI diesel engine performance, combustion, and emission studies. In: Singh AP, Agarwal AK (eds) *Novel internal combustion engine technologies for performance improvement and emission reduction. Energy, environment, and sustainability*. Springer, Singapore. [https://doi.org/10.1007/978-981-16-1582-5\\_10](https://doi.org/10.1007/978-981-16-1582-5_10)
- Rocha HMZ, Das Pereira M, Nogueira MFM, Belchior CRP, de L.Tostes ME (2017) Experimental investigation of hydrogen addition in the intake air of compressed ignition engines running on biodiesel blend, *Int J Hydrogen Energy* 42(2017):4530–4539. <https://doi.org/10.1016/j.ijhydene.2016.11.032>
- Selvan VAM, Anand RB, Udayakumar M (2014) Effect of cerium oxide nanoparticles and carbon nanotubes as fuel-borne additives in diesterol blends on the performance, combustion and emission characteristics of a variable compression ratio engine. *Fuel* 130:160–167. <https://doi.org/10.1016/j.fuel.2014.04.034>
- Seraç MR, Aydın S, Yılmaz A, Sevik S (2020) Evaluation of comparative combustion, performance, and emission of soybean-based alternative biodiesel fuel blends in a CI engine. *Renew Energy* 148(2020):1065–1073. <https://doi.org/10.1016/j.renene.2019.10.090>
- Serin H, Yıldızhan S (2018) Hydrogen addition to tea seed oil biodiesel: performance and emission characteristics. *Int J Hydrogen Energy* 43:18020–18027. <https://doi.org/10.1016/j.ijhydene.2017.12.085>
- Sezer I (2020) A review study on using diethyl ether in diesel engines: effects on fuel properties, injection, and combustion characteristics. *Energy Environ* 31(2020):179–214. <https://doi.org/10.1177/0958305X19856751>
- Shahir SA, Masjuki HH, Kalam MA, Imran A, Ashrafal AM (2015) Performance and emission assessment of diesel-biodiesel-ethanol/bioethanol blend as a fuel in diesel engines: a review. *Renew Sustain Energy Rev* 48(2015):62–78. <https://doi.org/10.1016/j.rser.2015.03.049>
- Shukla PC, Gupta T, Agarwal AK (2018) Techniques to control emissions from a diesel engine. In: Sharma N, Agarwal A, Eastwood P, Gupta T, Singh A (eds) *Air pollution and control. Energy, environment, and sustainability*. Springer, Singapore. [https://doi.org/10.1007/978-981-10-7185-0\\_4](https://doi.org/10.1007/978-981-10-7185-0_4)
- Shurpali N, Agarwal AK, Srivastava VK (2019) Introduction to greenhouse gas emissions. In: Shurpali N, Agarwal A, Srivastava V (eds) *Greenhouse gas emissions. Energy, environment, and sustainability*. Springer, Singapore. [https://doi.org/10.1007/978-981-13-3272-2\\_1](https://doi.org/10.1007/978-981-13-3272-2_1)
- Soudagar MEM (2020) The potential of nanoparticle additives in biodiesel: a fundamental outset. *AIP Conference Proceedings* 2247. <https://doi.org/10.1063/5.0003775>
- Soudagar MEM, Nik-Ghazali NN, Kalam MA, Badruddin, LA Banapurmath NR, Bin Ali MA, Kamangar S, Cho HM, Akram N (2020) An investigation on the influence of aluminium oxide nano-additive and honge oil methyl ester on engine performance, combustion and emission characteristics. *Renew Enrgy* 146 2291–2307. <https://doi.org/10.1016/j.renene.2019.08.025>
- Srinivasa Rao M, Anand RB (2016) Performance and emission characteristics improvement studies on a biodiesel fuelled DICI engine using water and AlO(OH) nanoparticles. *Appl Therm Eng* 98:636–645. <https://doi.org/10.1016/j.applthermaleng.2015.12.090>
- Tosun E, Özcanlı M (2021) Hydrogen enrichment effects on performance and emission characteristics of a diesel engine operated with diesel-soybean biodiesel blends with nanoparticle addition. *Eng Sci Technol Int J* 24(3):648–654. <https://doi.org/10.1016/j.jestch.2020.12.022>

- Tüccar G, Uludamar E (2018) Emission and engine performance analysis of a diesel engine using hydrogen enriched pomegranate seed oil biodiesel. *Int J Hydrogen Energy* 43:18014–18019. <https://doi.org/10.1016/j.ijhydene.2017.11.124>
- Uludamar E (2018) Effect of hydroxy and hydrogen gas addition on diesel engine fuelled with microalgae biodiesel. *Int J Hydrogen Energy* 43:18028–18036. <https://doi.org/10.1016/j.ijhydene.2018.01.075>
- Vellaiyan S, Subbiah A, Chockalingam P (2018) Combustion, performance, and emission analysis of diesel engine fueled with water-biodiesel emulsion fuel and nanoadditive. *Environ Sci Pollut Res* 25(2018):33478–33489. <https://doi.org/10.1007/s11356-018-3216-3>
- Wu Q, Xie X, Wang Y, Roskilly T (2018) Effect of carbon coated aluminum nanoparticles as additive to biodiesel-diesel blends on performance and emission characteristics of diesel engine. *Appl Energy* 221:597–604. <https://doi.org/10.1016/j.apenergy.2018.03.157>
- Yusof SNA, Sidik NAC, Asako Y, Japar WMAA, Mohamed S, Muhammad NM (2020) A comprehensive review of the influences of nanoparticles as a fuel additive in an internal combustion engine (ICE). *Nanotechnol Rev* 9(1):1326–1349. <https://doi.org/10.1515/ntrev-2020-0104>
- Yuvarajan D, Dinesh Babu M, BeemKumar P, (2018) Experimental investigation on the influence of titanium dioxide nanofluid on emission pattern of biodiesel in a diesel engine. *Atmos Pollut Res* 9:47–52. <https://doi.org/10.1016/j.apr.2017.06.003>

# Chapter 8

## The Roles of Hydrogen and Natural Gas as Biofuel Fuel-Additives Towards Attaining Low Carbon Fuel-Systems and High Performing ICEs



Samuel Eshorame Sanni and Babalola Aisosa Oni

**Abstract** The continuous depletion of the earth's natural reserves has spurred recent research towards searching for alternative fuels. In addition, it is common knowledge that the conventional gasoline from fossils is associated with high gaseous emissions owing to its hydrocarbon content and high flammability when in contact with air in automobile engines. In recent times, fuels sourced from other sources/biomass such as hydrogen and natural gas have also gained considerable attention as alternative fuels. This has also led to the era of electro/e-fuels which are an emerging class of **carbon neutral replacement fuels** that have the ability to store electrical energy from renewable sources in inherent chemical bonds of liquid/gaseous fuels. However, the major problem associated with their being commercialized for use in their unblended forms is that of high relative volatilities, very low viscosities, high oxidative instabilities, low engine compatibilities etc. hence, the reason they are adopted as additives in gasoline, also it is important to note that biofuels are currently being exploited for use in diesel engines whereas, their use in spark ignition engines is still currently being exploited due to the fact that they also lack some basic properties listed for hydrogen and natural gas but have higher viscosities and give low carbon emissions. This then implies that the world can begin to look towards adopting biofuels in modified forms by blending them with gasoline/natural gas and hydrogen as done for diesel engines so as to further reduce the carbon emissions, as well as improve the ignition potentials, oxidative stability, viscosities etc. of the fuels towards improving the tendencies for their application in compression ignition engines (ICEs). In modern-day research, the role of hydrogen and compressed natural gas in biofuel cannot be over emphasized owing to the high degree of atomization, improved break thermal efficiency, heat release rate, low carbon emissions as well as moderate peak pressures induced in the fuels. Hence, this chapter will focus on the role of hydrogen and natural gas in biofuels, the blending techniques adopted in

---

S. E. Sanni (✉) · B. A. Oni

Department of Chemical Engineering, Covenant University, Ota, Ogun State, Nigeria  
e-mail: [samuel.sanni@covenantuniversity.edu.ng](mailto:samuel.sanni@covenantuniversity.edu.ng)

B. A. Oni

Department of Chemical Engineering, China University of Petroleum, Changping, Beijing, People's Republic of China

© The Author(s), under exclusive license to Springer Nature Singapore Pte Ltd. 2022  
A. K. Agarwal and H. Valera (eds.), *Greener and Scalable E-fuels for Decarbonization of Transport, Energy, Environment, and Sustainability*,  
[https://doi.org/10.1007/978-981-16-8344-2\\_8](https://doi.org/10.1007/978-981-16-8344-2_8)

193

mixing NG and H<sub>2</sub> with biofuels, their measures of compatibility/property-variations as well as their spray characteristics, and how they related to the carbon contents of these fuel-blends when used in ICEs.

**Keywords** Alternative fuels · Natural gas · Hydrogen · Internal combustion engine · Biofuel

## 8.1 Introduction

Fossil fuels provide the majority of the global energy supplies. The combustion of fossil fuels produces waste materials, primarily emissions to the atmosphere in the form of combustion fuel gases/dust, as well as some ash and/or clinker (Weaver 1989). These waste materials have hazardous environmental effects, some of which are localized, while others have a more widespread or even global impact. Alternative fuels such as CH<sub>4</sub>, H<sub>2</sub>, and mixtures of H<sub>2</sub> and CH<sub>4</sub> are being considered to reduce these pollutions. Natural gas (NG) is a mixture of various gases (Arat et al. 2013). The concentration of these gases can vary from one source to the next. CH<sub>4</sub> is one of the components of NG, accounting for up to 99% of the total volume. The composition of NG is never constant. Non-methane hydrocarbons (NMHCs) such as C<sub>2</sub>H<sub>6</sub>, C<sub>3</sub>H<sub>8</sub>, and C<sub>4</sub>H<sub>10</sub>, as well as traces of higher hydrocarbons and inert gases such as nitrogen, He, CO<sub>2</sub>, H<sub>2</sub>S, and H<sub>2</sub>O, may also be present. As a fuel, NG performs admirably. It is the cleanest fossil fuel, with reserves of up to 5288.5 trillion cubic feet, which is larger than that of crude oil (Park et al. 2012a). It is readily available, is convenient to transport, store, produce and is less expensive relative to gasoline and diesel. It is inexpensive and widely available in most parts of the world with a high-octane number, and is thus suitable for engines with high compression ratios, with the potential to enhance both engine power output and efficiency (Yusuf 1993). NG has comparative properties with hydrogen, hence the reason both gases are considered as additives in ICEs (Table 8.1).

Hydrogen has long been considered as a fuel additive owing to its distinctive and extremely valuable properties it offers when used in engines. H<sub>2</sub> is now used in a variety of applications. H<sub>2</sub> has a number of characteristics that make it an appealing alternative (Ogden et al. 1995). Hydrogen has been used as a fuel in ICEs and fuel cells as well as an additive to conventional fuels like CH<sub>4</sub> or gasoline. Compared to HC fuels, H<sub>2</sub> has a higher diffusivity which improves its mixing potential, turbulence and charge homogeneity (Oni et al. 2021). The lower ignition energy requirement ensures prompt ignition and reduces cold starts. The quenching distance is the largest passage through which a flame can be extinguished and since hydrogen has a smaller quenching distance than gasoline, its flame can travel closer to the cylinder wall and deeper into crevices, which results in more complete combustion (Malogorzata 2014).

The use of H<sub>2</sub> as an additive to HC fuels is one method of introducing H<sub>2</sub> into the energy sector. The addition of H<sub>2</sub> to natural gas heralds the dawn of the age

**Table 8.1** Properties of hydrogen and natural gas

Property	Hydrogen	Methane
Heat of combustion (low) MJ/m <sup>3</sup>	10.8	39.7
Gas density (kg/m <sup>3</sup> )	0.084	0.65
Heat of combustion (high) MJ/m <sup>3</sup>	12.8	35.8
Flammability range (limits) in air %	4.1–75	5.2–15
Stoichiometric composition in air %	29.5	9.5
Minimum ignition energy (mJ)	0.02	0.3
Burning velocity cm/s	237	42
Energy of explosion of gaseous fuel (MJ/m <sup>3</sup> )	9.9	32.3
Deniability range in air (%)	18–59	6.3–13.5
Adiabatic flame temperature in air (K)	2318	2158
Minimum self-ignition temperature (K)	858	813

Adapted from Hoekstra et al. (1994)

of hydrogen as an energy carrier. Another application for hydrogen as an additive could be in fuels for internal combustion engines (Adamson and Pearson 2000). The addition of H<sub>2</sub> to natural gas engines has been shown to improve combustion properties and reduce emissions, particularly for lean-burn operations. Automobiles fueled with this mixture are expected to emit significantly less NO<sub>x</sub>, CO and HCs (Carlucci et al. 2008). A transportation system based on natural gas containing H<sub>2</sub> would be an efficient way of addressing urban environmental issues while also introducing H<sub>2</sub> into energy supply infrastructures (Ghazal 2013).

Adt and Swain (1974) investigated the emissions and efficiency levels of a multi-cylinder automobile engine running on H<sub>2</sub> and methanol at part load. They discovered that the BTE of the hydrogen-fueled engine was higher than that of a methanol-fueled engine, and that the NO<sub>x</sub> emissions of the hydrogen-fueled engine were lower than those of the methanol-fueled engine. Bauer and Forest (2001) studied the use of H<sub>2</sub> with methanol to support fuel in a SI engine and to enhance its combustion characteristics. They discovered that adding a small amount of hydrogen to a methanol–air mixture increased the flame propagation rate, decreased the ignition delay period, reduced combustion time loss, and improved the engine’s performance.

In the work of Ihracska et al. (2013), it was mentioned that the absence of carbon in hydrogen makes it a reliable candidate for future energy carriers and use as transport fuel. H<sub>2</sub>-/dual fueled engine are fast becoming viable alternatives to pure hydrocarbon fueled engines but, there is need for some modifications in the design of current/existing engines. In their study, they investigated the properties of premixed propagated H<sub>2</sub>-flame in a single-cylinder four-stroke optically accessible spark ignition engine. They adopted the concept of ellipse-fitting on flame contours during the test as a way of determining the flame speed and centre of motion. Engine speeds in the range of 1000–2000 rpm were adopted with a lean mixture equivalent of 0.67.

Based on their findings, fine temporal resolutions gave room for timed measurements which showed the periodic effects of the parameters that influenced the spark governed kernel formation. Figure 8.1 is an illustration of the variation of engine speed with time for the operation.

Despite all the giant strides and achievements in researches conducted on the use of  $H_2$  and NG as additives in natural gas, only a very few concerted efforts are channeled towards the consideration of these additives as blends for biofuels for use in gasoline engines whereas, the bulk volume of literature has only been dedicated to the use of NG/ $H_2$  or their combinations as additives for use in gasoline/spark ignition engines. This then goes further to imply that this chapter is aimed at discussing the previous and recent advances made in the use of  $H_2$  and NG as additives in gasoline fueled engines and the prospects that underly their considerations for use as biofuel additives in spark ignition engines/ICES; this is one of the basic objectives this chapter intends to project. This chapter unveils some of the prospects that underly this area of consideration although it may require some engine modifications as well as apt techniques for producing synthetic fuels (biofuel +  $H_2$ /NG mixtures) that are

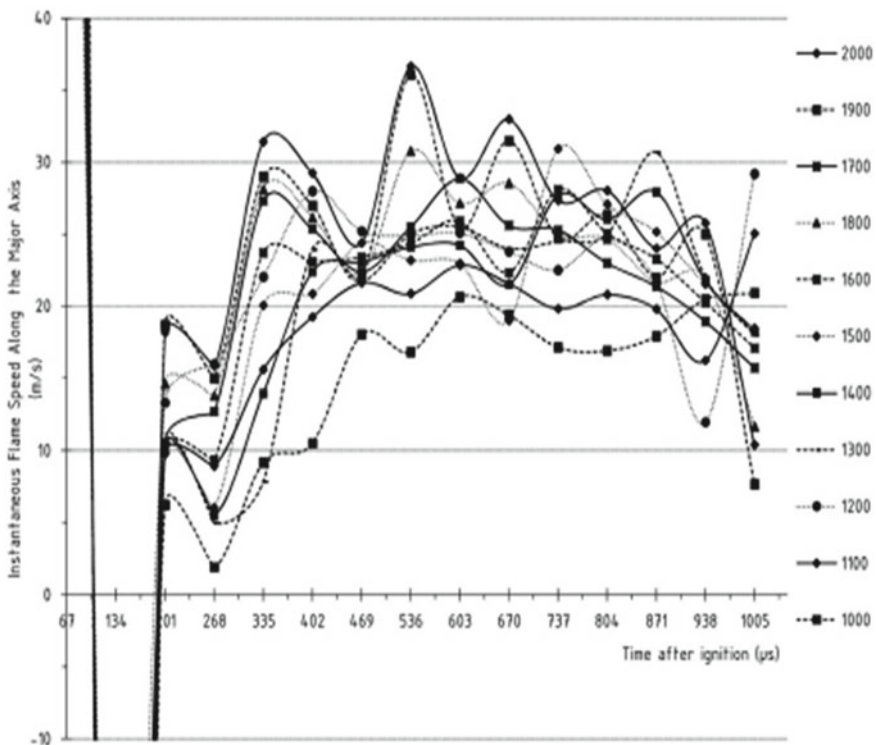


**Fig. 8.1** Instantaneous flame speed variation with time and engine speed. Adopted from Ihracska et al. (2013) with preprint permission obtained from Elsevier

compatible with ICEs or better still, slight engine modifications might be feasible as highlighted in some studies in later sections.

Based on literature, improved fuel economy in SI-engines can be achieved by operating these engines with dilute mixtures by adding extra air or via exhaust gas recirculation (EGR) owing to low combustion temperature, and lower heat transfer/pumping losses at part loads. This led to the advent of DI-SI engines which have significantly reduced the inherent pumping/heat transfer losses and fuel consumption associated with such engines. Similarly, Homogenous charge compression ignition (HCCI) gasoline engines fueled with dilute mixtures of NG and biofuels can also improve the fuel economy of these engines when the apt stoichiometric amounts of the fuel mix are ignited with air. The use of NG is one promising alternative fuel due to its inherent properties such as high H/C ratio and RON which is about 130. The beauty of NG when used as fuel is the ability to tweak its H/C in different ratios ranging from 1.8 to 3.7 to 4.0. Other important properties of NG include its wide flammability limits, low peak temperature of combustion and lean conditions relative to its stoichiometric conditions (King 1992) which reduces the tendency for engine knocks of NG-engines thus resulting in higher power at constant engine displacement caused by a pressure-boost (Borges et al. 1996). Wang et al. (2017) studied the effect of hydrogen injection parameters on the properties of H<sub>2</sub>-air mixture formation for a port fuel injector (PFI) hydrogen-fueled internal combustion engine.

## 8.2 EU Policy Considerations for Environmental Protection

Owing to the ratification of the Paris agreement in 2016, there is the imposition of a mandate to maintain the average global temperature surge at less than 2 °C with consistent efforts to limit its increase to 1.5 °C above preindustrial level (Rogelj et al. 2016), which will in turn reduce the emission of GHGs. Compared to the Kyoto Protocol of 1997, this agreement only regulated the climate of 37 advanced countries, whereas, the Paris Agreement is more expansive and binds on about 195 countries. Thus, as a way of responding to the change in global policy, considerations for alternative fuels have led to the need to look into renewable energy as a possible way to remedy the situation.

The use of biogas as alternative fuel for power generation will help to mitigate global warming by reducing the consumption of fossil fuels and rather encourage the use of bio-CH<sub>4</sub> as fuel since it is also regarded as a greenhouse gas pollutant. Biogas is the product of anaerobic digestion of biomasses which are largely distributed (Lim et al. 2015). It comprises mainly of 50–70 vol% CH<sub>4</sub>, 25–50 vol% CO<sub>2</sub>, 1–5 vol% H<sub>2</sub>, 0.3–3 vol% N<sub>2</sub> and other minor impurities such as H<sub>2</sub>S (Bari 1996). Biogas mixes easily with air to give a uniform air-fuel mix. Well-modified biogas fueled IC-engines may be the future prospect of the future generation as a way of ensuring high engine compatibilities for improved engine performance since biofuel-based fuels still experience compatibility issues when it comes to them being applied in ICEs (Bora et al. 2014), hence adequate power can be generated. Some studies that



have also encouraged the use of biogas powered IC engines have been documented (Ahmed et al. 2013; Arroyo et al. 2013; Barik and Murugan 2014; Byun and Park 2015; Cardozo and Cifuentes 2009; Lee et al. 2014; Mustafi et al. 2006; Park et al. 2011, 2012b; Porpatham et al. 2012; Singh 2016; Subramanian et al. 2013). In China, based on World Bank statistics, the yearly economic loss resulting from air pollution is about 1.2% of her GDP (Zheng et al. 2015). This informs the need to give the production and consumption of energy from clean sources high priority towards ensuring a safe environment with improved quality of life for her citizens. Hence, the need to begin to look towards the development of biofuel-based spark ignition engines for transport.

### **8.3 Biofuels, Hydrogen and Natural Gas: Their Origins, Sources, Compositions and Their Synthetic Pathways**

#### ***8.3.1 Synthetic Pathways for Biofuels/Methane/Ethanol***

The most widely used gas/alcohol for SI engines is biomethane/bioethanol which can be sourced from fossils of biomass. CH<sub>4</sub> can be found in coal mines, petroleum reservoirs and can be produced via gasification of biomass. Whereas ethanol is obtained via fermentation or transesterification of reducing sugars produced from lignocellulosic biomass.

#### ***8.3.2 Synthetic Pathways for H<sub>2</sub>***

According to Sanni et al. (2021) hydrogen can be synthesized via various pathways including formic acid, steam reforming reactions of alkanes, electrolysis of water, thermochemical conversion of biomass, fermentation and photolysis of water molecules by *Scenedesmus*/green algae; *Cyanobacteria-Spirulina* species split water molecules into H<sub>2</sub> and O<sub>2</sub>.

H<sub>2</sub> can be obtained from different variety of materials, such as biomass and fossils. The price of manufacturing H<sub>2</sub> is still high in lieu of the technically associated problems yet to be resolved i.e., an engine that solely uses H<sub>2</sub> as fuel is not yet on the road. Usage of H<sub>2</sub> from well to wheel, is a very important issue. The hydrogen—carbon ratio of natural gas is about 3.7 to 4.0, which is very high when compared to those of gasoline and diesel (Demirbas 2002). H<sub>2</sub> is the main supplement to compressed natural gas as a result of its properties. Most researches have shown that natural gas and hydrogen mixtures have several advantages, such as high-calorific values, rapid flame speeds, renewability, large flammability limits, and less CH<sub>4</sub> emissions, etc. (Dulger 1991).

## 8.4 The Use of Natural Gas–Hydrogen Mixture in Internal Combustion Engines

The origin of combustion engines started decades ago. Natural gas and  $H_2$  are well-known as clean energy; since they are abundant and easy to collect. CNG production is accomplished by compressing the natural gas (majorly  $CH_4$ ) at high pressure and are distributed in a vessel of cylindrical shape under a pressure of 210–250 bars (2900–3600 psi) (Das 1996). There are about 23.305 million natural gas vehicles (NGVs) running in about 85 nations where China, Pakistan, Argentina, India, Brazil, and Iran are the leading countries amongst the 85 nations (Das 2002). Research has shown that  $H_2$  is a promising alternative fuel for ICEs.

It has been proven by researchers that HCNG is an ecofriendly global fuel for ICEs, and the potential for HCNG-ICE's is promising if there are available infrastructures for the production of  $H_2$  at low costs such that the supply system is as easy as that available for fossil-based fuel/gasoline (Ghazal 2013). This lays emphasis on the technical aspects of the HCNG-ICE's, as to what are the turnouts of HCNG fuel on an engine's overall performance. The method of producing hydrogen is a key factor that determines the properties of hydrogen. Hydrogen can be produced from renewable energy sources, with great concern for its delivery and storage systems. A comparative experimental research study of literature on HCNG fuels for adopting the optimal parameters of various types of operating conditions of ICE is also considered (Heffel 2003b).

Conservatively, to improve CNG performance under lean burn condition, there is a need to explore what improves its slow flame burning velocity. There is a remarkable way to admix compressed natural gas (CNG) with the fuel that has a fast burning velocity (Huang et al. 2006).  $H_2$  is a best selection for compressed natural gas as per its broad range of flammability limits in air and high flame velocity (Jian et al. 2010). The blends are expected to improve the lean burn properties and low tail pipe emissions (Konoplev et al. 2018a). All the characteristics of  $H_2$ , gasoline, and compressed natural gas are based on the normal temperature and pressure or standard temperature and pressure conditions. Based on reports, it has been noticed that  $H_2$  and CNG have almost the same combustion properties (Lather and Das 2019).

Hydrogen-fueled SI engines deliver noticeable improvements in their overall engine performance. The self-ignition temperature of  $H_2$ —air mixture is very high when compared with those of other fuels (Luo et al. 2019). Therefore, combining  $H_2$  with other fuels improves the antiknock property of fuels with resultant lower flame luminosity.

In terms of combustion quality,  $H_2$  gives no emission as compared to gasoline and diesel fuels (Mehra et al. 2017). The laminar burning velocity of the hydrogen-air mix is about 6 times higher than that of gasoline-air mixtures (Nwafor 2003).

$H_2$ -addition to NG reduces  $CO_2$ , CO, and total hydrocarbon (HC) emissions caused by NG combustion. In fact,  $H_2$  addition to natural gas produces exhaust emissions which contain very little amount of HC,  $CO_2$ , CO and  $NO_x$ . The combination of hydrogen and natural gas is known as hythane. Natural gas and  $H_2$  engines

have been investigated in terms of their mixtures and percentages. The majority of these studies can be found in literature (Bauer and Forest 2001; Das 2002). Das (1996) tested a SI engine with CNG and an 18% HCNG blend for a three-wheeler application. It was equipped with an oxygen catalytic convertor and an EGR system. The engine was put through its paces using the Indian driving cycle. CNG fuel consumption increased by 18% when 18% HCNG fuel was used without adjusting the ignition timing. It decreased slightly with the addition of EGR and improved with HCNG when used with a catalytic converter. HCNG significantly lowers CH<sub>4</sub> and HC emissions slightly, while engine modifications, helps to reduce them (i.e., with maximum EGR and catalytic converter). EGR was found to reduce NO<sub>x</sub> emissions. It was also discovered that CNG emits a high level of formaldehydes which were reduced after enhancement with H<sub>2</sub> (Boretti 2020).

Konoplev et al. (2018b) tested an AVL engine with 100/0, 80/20, 50/50, 0/100, and CNG/H<sub>2</sub> mixtures in a SI engine. They discovered that the maximum engine output was lost by about 23% when using H<sub>2</sub> while the maximum percentage reduction in the thermal efficiency was about 12%. Power loss can be compensated for by increasing the size of the H<sub>2</sub> engine for stationary applications. For H<sub>2</sub> mixtures, optimal spark timing decreased by up to 20 BTDC, thus indicating increased flame speed. Due to the higher combustion temperature, NO<sub>x</sub> emissions for pure H<sub>2</sub> also increased. The direct displacement of a carbon-based fuel with H<sub>2</sub> reduced the unburned HC and CO emissions. For 0.8–0.9 equivalence ratios of H<sub>2</sub> supplementation, the performance of a H<sub>2</sub>-supplemented natural gas engine was found to be in between natural gas and H<sub>2</sub> engine performances (Aslan et al. 1991).

Yusuf (1993) tested a mixture of CH<sub>4</sub> and H<sub>2</sub> in a SI engine with a Toyota 2TC type 4-cylinder engine with a maximum HP of 88 and 6000 rpm and a CR of 9.0:1. The engine was modified to use a single cylinder rather than four cylinders. The measured HC, CO and NO<sub>x</sub> concentrations, as well as the spark advance and thermal increased efficiencies while varying the equivalence ratio. The engine was run at 1000 rpm with the best efficiency spark advance and a light load. When compared to pure CH<sub>4</sub> operation at the same equivalence ratio, the CH<sub>4</sub>–H<sub>2</sub> mixture increased the BTE and NO<sub>x</sub> emissions while decreasing the best efficiency spark advantage, unburned HCs, and CO. Furthermore, the lean limit of natural gas combustion was reduced from 0.61–0.54.

Ovsyannikov et al. (2016) adopted natural gas and 15% H<sub>2</sub> by volume in a 4-stroke cycle, water cooled, 3:135 l, and CR of 8.8:1 SI Chevrolet Lumina with 6-cylinder engine. In this study, BSFC for both CNG and CNG-H<sub>2</sub> mixtures decreased compared to that obtained for pure gasoline fuel, while the spark timing (BTDC) values increased. CNG had a higher HC than the fuel mixture. However, the NO<sub>x</sub> emissions of the CNG/H<sub>2</sub> mixture were higher than those of CNG.

Hoekstra et al. (1995) tested different ERs on different fuels: 100/0, 89/11, 80/20, 72/28, and 64/36 CH<sub>4</sub>/H<sub>2</sub>% mixtures in a SI engine running at 1700 rpm. They took NO<sub>x</sub>/HC readings and discovered that as the ER increased, the NO<sub>x</sub> emissions increased while the HC emissions decreased.

Jorach et al. (1997) evaluated the knock properties in CH<sub>4</sub>–H<sub>2</sub> proportions of 100/0, 90/10, 70/30, 50/50, 30/70, and 0/100. They ran simulations and compared

their findings with those of previous works on knock characteristics. They stated that when the intake temperature of  $H_2$  and methane is high, the knocking regions obtained from simulations corresponded to the experimental results. However, because of the high energy release, the theoretical  $H_2$  deviates significantly from experimental data at low intake temperatures. Karim (2003) studied the knock limits in mixtures with varying percentages of  $H_2$  and  $CH_4$ , ERs and intake temperatures. According to Karim, when hydrogen and methane are blended in relatively small amounts, the excellent knock resistance properties of methane are not compromised. Konoplev et al. (2018a) investigated  $CH_4$ - $H_2$  proportions of 100/0, 90/10, 80/20, 70/30, 60/40, 50/50, 40/60, 30/70, and 20/80 at varying ERs. They investigated the average power output difference, average indicated output efficiency, average ignition lag, average combustion duration (CA), average maximum cylinder pressure, knocking regions in different percentages of  $H_2$  and  $CH_4$ , different ER, and different BTDC (10, 20, 30). With increasing concentrations of  $H_2$  for 10° BTDC and 20° BTDC in the engine, there was an increase in the power output, however, the power output decreased at 30° BTDC. At 20° BTDC, the maximum power output was obtained. At this point, when  $H_2$  was added to  $CH_4$  as fuel in the spark ignition engine, there was drastic increase in the engine's performance characteristics (Kahraman et al. 2009).

Konoplev et al. (2018a) studied the efficiency and emissions of a turbocharged lean natural gas and  $H_2$  admix in a SI engine. The turbocharged 6-cylinder, 4-stroke SI engine was used to compare the efficiency and emissions of the 85/-/15 CNG- $H_2$  admix fuel by volume to those of pure methane at different loads, speeds and ERs for HC, CO,  $NO_x$  and  $CO_2$ , engine performance and exhaust gas temperatures. The results clearly confirmed that  $H_2$  and  $CH_4$  mixtures can reduce the concentrations of the exhaust gases and also increase the performance/efficiency of spark ignition engines. The emissions of primary concern in a lean-fueled engine were hydrocarbons and  $NO_x$ . Subsequently, the discovery that lower levels of  $NO_x$  and HC emissions can be attained with  $CH_4$  and  $H_2$  mixture-fueling had important implications (Sierens and Rosseel 2000).

Steinberg and Cheng (1989) studied several compositions including 100–0, 70–30 and 0–100% methane-hydrogen mixtures. They conducted computational and experimental studies using a 3-D computational fluid dynamic (CFD) code. Their objective was to compare the BTE, ER,  $NO_x$ , and BTDC in the different proportions of Hydrogen and methane mixtures. The results showed high efficiency and zero equivalent emissions for the auxiliary powered unit of the hybrid vehicles fueled by pure  $H_2$  or 30%  $H_2$  /70% natural gas blends.

Shrestha and Karim (1999) investigated the effects of the occurrence of some gaseous fuels and pre-ignition reaction products with  $H_2$  in spark ignition engines with 100–0, 90–10, 80–20, 70–30, 20–80 and 10–90% methane-hydrogen in varying compression rates by changing the ERs. They reported that  $H_2$ - $CH_4$  addition in the SI engine improved the engine's performance at low ERs. The optimal concentration of  $H_2$  in the mixture for avoiding knock was about 20–25% vol.

Sierens and Rosseel (2001) examined a 100–0, 90–10 and 80–20 compressed natural gas-hydrogen mixtures. They studied a V-8 Crusader T 7600 SI engine operating at a speed of 3800 rpm and a compression ratio 8.5:1. They considered a

fuel-supply system and applied a device that delivers  $H_2$ – $CH_4$  mixture in different proportions to the engine. The composition of this mixture can be set independently of the engine's operation. According to their report,  $CH_4$ – $H_2$  mixture with low  $H_2$  content (about 20%), a low advancement in emissions could be achieved due to the conflicting requirements for low  $NO_x$  and HCs. To reduce HC emissions, compression ratio must be less than 1.3, while for low  $NO_x$ , it must be less than 1.5 (Montoya et al. 2016).

Das et al. (2000) studied the BTE and BSFC of  $H_2$  and CNG as fuels in an ICE. They noticed that the BSFC was low with improved BTE in the  $H_2$  operated engine compared to CNG's. The brake thermal efficiency was as high as 31.82% for  $H_2$  operation compared to that of 27.97% for compressed natural gas (CNG) (Konoplev et al. 2018a).

In Brazil, the cumulative of all motorized trips informs that over 60% is based on public mode, with buses (comprising of CI-engines) conveying about 94% of that number. However, the country has a high biofuel production potential owing to her vast landfills as well as hydroelectric plants; the country has an extensive biogas/hydrogen production history that can be used as fuel in Spark Ignition (SI) engines in lieu of the fact that SI engines experience lower efficiencies compared to CI engines. Partial loading of SI engines is achieved conventionally by means of a throttle device which helps to regulate the airflow/air–fuel mix which transits into the engine. This results in exergy losses that in turn decrease the performance/engine efficiency. The study by Nadaleti et al. (2018) examined the pollutants/emissions and conversion efficiency of fuel chemical energy for different fuel-blends of  $H_2$ , biogas (BIO60) and methane (BIO95) as fuel in a SI engine operated on part load. The inclusion of  $H_2$  was aimed at increasing the efficiency via cutting down on the pumping work via throttling thus increasing the lambda value. During the test, several ignition angles and air–fuel ratios were tried. Their findings revealed that the adjustment of the ignition advance angle helped to maximize the engine's brake thermal efficiency (BTE). Also,  $H_2$ -addition extended the combustion limits over the usual range with significant reduction in the resulting CO and  $NO_x$  emissions.

## 8.5 Hydrogen and Natural Gas as Additives in Low-Carbon Biofuels Used in ICEs

Natural gas is a fossil fuel found in nature's reserves which can either be associated or not associated with crude oil. Natural gas contains approximately 90%  $CH_4$ , 3%  $C_2H_6$ , 3% nitrogen, 2%  $C_3H_8$  and other gases. Since it has a high hydrogen/carbon ratio, natural gas is one of the cleanest fuels (Orhan et al. 2004). Furthermore, city buses run with natural gas engines in most countries. Consequently, most countries encourage the use of natural gas as a substitute for gasoline and diesel fuel in vehicles. Since natural gas blends perfectly with air, it can be easily ignitable, thus providing a clean combustion and with high heat. Natural gas' engine thermal efficiency is

higher than that of gasoline engines due to their relative compression ratios (Oni et al. 2021; Montoya et al. 2016; Moore and Raman 1996).

Unlike diesel engines and gasoline, natural gas-powered ICEs do not involve fuel enrichment in cold-starts, and they are not affected by exhaust emissions at low temperatures. Natural gas vehicles (NGV) produce lower emissions than those of the EURO-6 standard based on vehicles using fossil fuel (Boretti 2020; Liu and Karim 1995).

Based on NGV worlds report, the number of fuel filling stations (Fig. 8.2) and NGVs in the world is growing speedily (Fig. 8.3). China is the first country in the NGV Park with about 6,090,000 automobiles and 8500 service stations, according to the data generated in 2018. Pakistan, Iran, and India are countries that follow after China. The overall total of NGVs is about 26,130,000 as of July 2018 (Konoplev et al. 2018a; Luo et al. 2019; Global 2019). One of the disadvantages of the NGV transportation sector arises from the storage of natural gas. Natural gas is lighter than air with a density of about 0.71 kg/m<sup>3</sup>. As natural gas is a light gas, the energy density per unit volume is low and in order to ensure a reasonable driving distance, the storage volume should be large. Luckily, technology has developed and the natural gas can be stored in steel or carbon-tubes at 200 bars with high pressure compressors. Storing NGV in an enclosed space is unsafe for safety reasons. Today, cars with natural gas engines have a range greater than 300 miles with a single filling (Oni et al. 2021; MacLean and Lave 2003; Papagiannakis et al. 2010).

Hydrogen is an alternative fuel for ICEs. Hydrogen has some problems associated with liquid fuels, such as cold wall quenching, inadequate vaporization, vapor lock, and lean mixing. Hydrogen burns clean in nature. As hydrogen is burned, its product is majorly water. When H<sub>2</sub> combusts, its products are nontoxic (water) or harmful

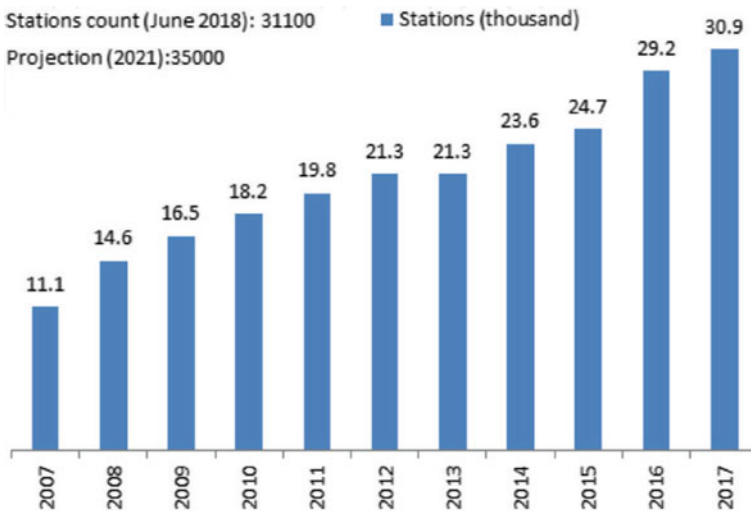
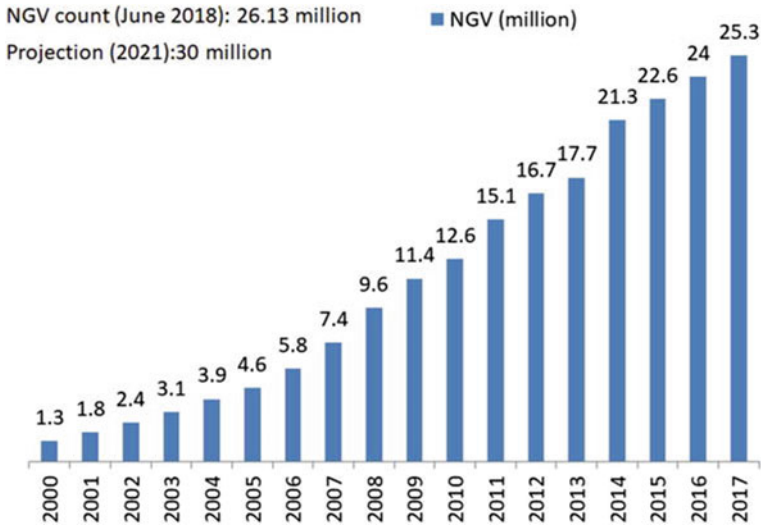


Fig. 8.2 Number of natural gas fueling stations worldwide by years. Source NGV Global (2019)



**Fig. 8.3** Number of natural gas vehicles (NGV) worldwide by years. *Source* NGV Global (2019)

(HCs, CO and CO<sub>2</sub>) (Yousufuddin 2017; Wallace and Cattelan 1994). Furthermore, H<sub>2</sub> has a wide flammability range than diesel, natural gas and gasoline fuels (Renny and Janardan 2008). Hydrogen has high self-ignition temperature and flame speed (Shrestha and Karim 1999). Also, hydrogen can easily burn in ultra-lean mixtures. The energy needed to ignite H<sub>2</sub> in air is just 0.02 MJ (Oni et al. 2021). Also, H<sub>2</sub> can be used at wide compression rates in ICEs because the self-ignition temperature of H<sub>2</sub> is too high (Raman et al. 1994). As a result of these, most studies have been carried out on the potential use of H<sub>2</sub> as fuel in ICEs (Ji and Wang 2009; Konoplev 2008). One disadvantage of hydrogen is its low energy density (Akansu et al. 2007; Karim and Wierzbka 1992). Furthermore, NO<sub>x</sub> formations from hydrogen are increased by H<sub>2</sub> combustion as a result of high flame temperature (Orhan et al. 2004).

Since H<sub>2</sub> has some negative impacts on ICEs, it is often blended with other fuels. The most common is with CNG. The mixture can be formed by the blending of natural gas (Blarigan and Keller 1998). HCNG is considered as an alternative fuel for ICE engines, it is blended with hydrogen to form a superior property of hythane (Renny and Janardan 2008). Researches are ongoing on the use of HCNG as an alternative fuel (Tiashen et al. 1985; Tangoz et al. 2015). As observed, the addition of H<sub>2</sub> causes an increase in thermal efficiency which results in an expansion of the flammability limits. Hydrogen addition increases combustion stability and brake power and decreases the specific fuel consumption of an ICE (Shioji et al. 2001). Figure 8.4 shows the torque measured at different mass air flow rates, fixed mass fuel flow (1.97 kg/h) and equivalence ratios in an ICE.

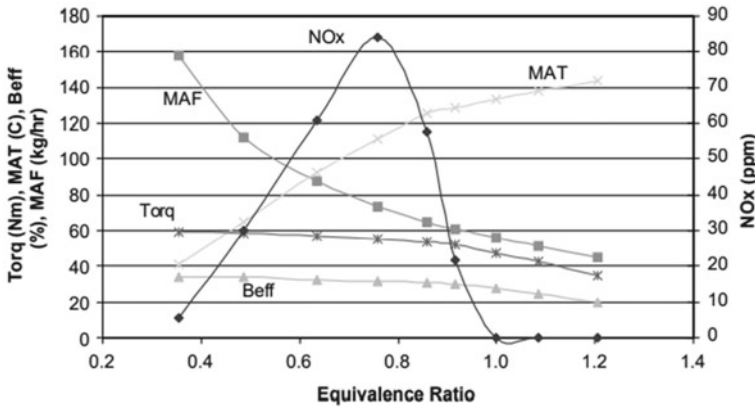


**Fig. 8.4** The torque measured at different mass air flow rates, fixed mass fuel flow (1.97 kg/h) and equivalence ratios in an ICE. Adopted from Heffel (2003b) with reprint permission obtained from Elsevier

### 8.5.1 *The Mechanisms of the Performance of Hydrogen and Natural Gas as Additives for Low Carbon Biofuels Used in Diesel Engines/ICEs*



The combination of hydrogen and natural gas gives hythane or compressed natural gas which is a suitable mixture or fuel for ICEs. The process conditions under which this can occur can be at a pressure of about 0.1–1.4 MPa, injection duration of 4.2–10 ms, poppet valve diameter of 6 mm and temperature of 288 K (near ambient condition) in consonance with the study by Choi et al. (2016).

### 8.5.2 *Recent Works on Hydrogen and Natural Gas Additives/their Hybrids in Fuels/Biofuels for Improved Engine Performance*

When HCNG is used in an internal combustion engine, the addition of small amount of hydrogen to NG (5–30% by volume) can offer several advantages, owing to the alteration in the physicochemical properties of the mix (Bysveen 2007). Park et al. (2012b) adopted a premixed HCNG fuel-system which was blended with the desired amount of hydrogen in CNG. According to Dalton's law, the partial pressure of  $\text{H}_2$  in the mix is determined by the nature of the individual partial pressures of the two components in the HCNG fuel-tank. One major parameter for ascertaining the impact on engine behavior by gas composition is the Wobbe index (Dhyani and Subramanian



2019). At constant Wobbe index, any change in gas composition does affect the air–fuel ratio and combustion rate. The properties of HCNG lie in its inherent constituents i.e., between hydrogen and the CNG. There are a myriad of distinct features that are associated with HCNG which in turn renders the fuel remarkably suitable for engine applications (Ceper et al. 2009).

Morones et al. (2014) adopted a Kiloskars AV1 engine in their investigation in which the CR was 10:1 at an engine speed of 2000 rpm, where fuels of different proportions (100% CNG, 90% CNG + 10% H<sub>2</sub>, 80% CNG + 20% H<sub>2</sub>, 70% CNG + 30% H<sub>2</sub>) or blends were tested. The engine was operated at full and 65% load conditions at varying  $\lambda$ . They asserted that mixing H<sub>2</sub> with CH<sub>4</sub> significantly improved the engine's BTE.

Hydrogen mixed with NG brings about improved combustion stability with reduced hydrocarbon emissions, however, there are higher NO<sub>x</sub> emissions. The effects of several CNG-hydrogen or blends on the combustion traits of a direct injection SI engine have also been investigated by Wang et al. (2007) and Wang et al. (2010). Based on the results obtained, the authors proposed optimum hydrogen volumetric fractions and CNG-hydrogen blends that resulted in a balanced compromise as regards the resulting emissions and engine performance. The burning of NG with hydrogen improves the lean-burn traits with resultant reductions in the engine emissions, particularly CO, HC, and CO<sub>2</sub>, however, the main concern is the probable rise in NO<sub>x</sub> emissions (Ma et al. 2008; Navarro et al. 2013). The added hydrogen influences/speeds up the combustion process with the added possibility of developing engines with lower environmental impacts and high performances.

Since the year 2000, NG, C<sub>3</sub>H<sub>8</sub>, and CH<sub>3</sub>OH have been used as alternative fuels in vehicles. Also, hydrogen, NG and mixtures of both are currently being considered as alternative fuels in recent years as possible options for reducing emissions from vehicles. The addition of H<sub>2</sub> to NG increases the H/C ratio of their mixed fuel. A higher H/C ratio gives rise to less CO<sub>2</sub> emissions per unit of energy produced which also translates to reduced greenhouse gas emissions. NG has low flame speed which is about one-eighth that of hydrogen. Therefore, when the excess air–fuel ratio is much higher than the stoichiometric air–fuel requirement, the combustion of NG becomes less stable relative to HCNG (Patil et al. 2009). The problem usually associated with using NG only as fuel is that the engine will experience incomplete combustion/misfire which is also complemented by sufficient NO<sub>x</sub> reduction. Thus, adding hydrogen to NG extends the amount of charge dilution that is achievable while still maintaining efficient combustion (Sorrell et al. 2010; Xu et al. 2015).

Blends of HCNG in the range of 15–30% extend the lean operating limits while ensuring complete combustion which in turn reduces the resulting HC and CO emissions. The laminar burning speed of hydrogen is about eight times that of NG, hence the presence of hydrogen in the fuel has the potential to increase the burning velocity of the mixture, thus giving rise to shorter combustion durations, high measures of constant volume combustion rates as well as improved thermal efficiencies (Sorrell et al. 2010). Ouellette and Hill (2000) investigated the turbulent transient injection of CH<sub>4</sub> and air into a constant volume chamber. The effects of the geometry of the subsonic/sonic jets emanating from the single-injection nozzle were also studied.

The work of Choi et al. (2016) involves modelling the gaseous fuel injection process in a CNG-DI engine. The simulations were done using KIVA-3 V Release 2 code by modifying the liquid fuel injection system to mimic a gaseous fuel injection system. Gaseous spheres were injected as liquid molecules evaporated together without considerations for their latent heat of evaporation. Experiments involving the gas-jet visualization were carried out using planar laser induced fluorescence (PLIF) method. However, compressed  $N_2$  was used to simulate the behaviour of CNG. Other engine experiments were performed using a single cylinder CNG DI engine. The results showed comparative in-cylinder pressures for the fuel injection and combustion processes which were simulated by considering a 3D engine-mesh with 4 valves from intake to exhaust (i.e., from intake valve open—IVO to exhaust valve open- EVO).

The work of Park et al. (2010) bothers on the evaluation and visualization of the stratified ultra-lean combustion features exhibited by the spray-guided gaseous fuel mix in a DI-gasoline engine. A similar investigation was also conducted by Choi et al. (2015) where the combustion characteristics and performance of a CNG fueled DI-engine was considered. Chitzas et al. (2013) carried out an experimental and numerical study on the characteristics/properties of the fuel-jets released from a gaseous-direct injector into a spark ignition engine.

Kwon et al. (2017) investigated the performance of biogas-fueled ICE of less than 5 kW power rating by monitoring the effect of compression ratio on the engine's characteristics. A decrease in the volume of the combustion chamber from 19.3 to 16.6 cc, and compression ratio from 8.01:1 to 9.22:1 was done to improve the brake power output from 2.2 to 2.68 kW, the engine BTE from 22.0 to 29.8% and the brake specific fuel consumption (BSFC) from 290.6 to 218.6 ghps. Also, they examined the effect of the biogas composition on the engine's performance by adopting varying  $CO_2$ -dilution ratios in the range of 0–50%. However, it was observed that the best engine performance was obtained at the lowest  $CO_2$ -diluted fuel.

### ***8.5.3 Some Advantages of HCNG and Challenges Associated with their Use in ICEs***

#### **8.5.3.1 Advantages**

- It is compatible with the existing CNG infrastructure and requires only small hydrogen in storage and a column for blending hydrogen with NG (Bielaczyc et al. 2014).
- It has similar safety properties with CNG. HCNG is safer to handle than hydrogen, because of lower risk due to very low energy content from hydrogen (only up to 30 vol.%) (Verma et al. 2016).
- It extends the lean misfire limit of CNG (Thipse et al. 2009).

- Minor modifications are required for engines fueled with HCNG owing to the moderate concentration of hydrogen in the fuel mix; also, the excellent anti-knock properties of CNG are not undermined (Arat et al. 2013).
- Hydrogen embrittlement does not occur with respect to the engine's components; hence, no major change is anticipated in the fuel system/engine components (Helmut et al. 2009).
- Hydrogen addition to NG can decrease the engine's unburnt HCs and NO<sub>x</sub> emissions owing to the existence of lean burn rates which may in turn speed up the combustion process (Helmut et al. 2009).
- It improves the engine efficiency and lowers fuel consumption (Arat et al. 2013).

### 8.5.3.2 Challenges of HCNG

- HCNG storage and supply infrastructures are not readily available (Sorrell et al. 2010).
- Efforts have been channeled on responding aptly to the fuel's system performance and material compatibility. Emission of NO<sub>x</sub> gases is usually high for higher than moderate amounts of hydrogen in HCNG blends (Belchior et al. 2001).
- Continuous availability of HCNG needs be assured before embarking on its major use in IC engines (Kavathekar et al. 2007).
- Continuous engine performance/routine checks, emissions and durability tests in engine of different types and sizes need be conducted in order to increase consumer and manufacturer confidence (Chugh et al. 2016).
- The need to develop less expensive quality tests for the blends.
- The occurrence of three dimensional compressible turbulent reacting flows in ICEs is also a complex problem to resolve especially for situations of direct injection of the fuels.
- There is the tendency for backfiring in the engine owing to the presence of hydrogen.
- Formation of the apt fuel mixture with good combustion properties is more difficult and critical for natural gas entrained fuels due to its lower density compared to liquid fuels. Hence, very high injection velocities give low fuel penetration, which then result in poor mixing of the fuel. This can be resolved by improving on the in-cylinder charge motion of the fuel in the gasoline engines (Chiodi et al. 2006). To enhance NG penetration in the cylinder, fuel rail pressures as high as 200 bar can be adopted; this brings about sonic flow at the nozzle exit with the occurrence of a complex shock pattern of expansion waves downstream from the nozzle exit (Li et al. 2004).

## 8.5.4 Effects of HCNG on the Emissions from a SI Engine

### 8.5.4.1 Hydrocarbon Emissions (HC)

Unburned HC can be produced as a result of incomplete combustion.  $\text{CH}_4$  is the source of total hydrocarbon content (THC) emission for the HCNG engine due to a large valve overlap angle. Furthermore, hydrocarbon emissions can result from both misfire and abnormal combustion. The main sources of HC emission for combustion procedures are the wall quenching influence and incomplete combustion (Belyi and Teregulov 2016). The addition of  $\text{H}_2$  reduces unburned HC emissions, indicating enhanced combustion efficiency. The decrease in heat transfer caused by the fast burn speed can be eliminated by increasing the in-cylinder temperature, which, together with the shorter quenching distance caused by adding  $\text{H}_2$ , may be the causes of this phenomenon (Akansu et al. 2007). Karim (1996) did a comparison between CNG and HCNG 30 with two compression ratios to test the emissions of THC and  $\text{CH}_4$ . The study from Arat et al. (2013), indicated that the emission of HC with HCNG 30 and a CR of 11.5 is reduced when compared to 10.5 CR and HCNG 30 in a lean combustion condition. The high efficiency combustion reduces THC emissions with a high temperature of combustion. According to Carlucci et al. (2008), the compression ratio (CR) in the CNG case had no effect on the HC emission. Basye et al. (1997), demonstrated that increasing the CR at the same air ratio reduces  $\text{CH}_4$  emissions while HCNG-30, and CNG exhibit the same trend. Nonetheless, the reduction in  $\text{CH}_4$  emissions was greater than the reduction in HC emissions, with 11.5 CR. Sagar et al. (2018) discovered a similar result in lean premixed  $\text{CH}_4\text{-H}_2\text{-air}$  flames at higher pressures and temperatures.

### 8.5.4.2 Carbon Monoxide Emissions (CO)

CO is produced as a result of the incomplete combustion of the fuel in the engine. Incomplete combustion occurs when the combustion cannot be completed due to a lack of oxygen. According to the Moore and Raman (1996), decreasing the ER reduces CO emission, which then begins to rapidly increase after a minimum value as a result of a misfire in the large lean mixture. The presence of  $\text{H}_2$  had no substantial effect on the formation of CO prior to the misfiring limitation for pure CNG (0.6); however, after this, introducing  $\text{H}_2$  resulted in a greater decrease in CO, and misfiring was delayed based on estimated outcomes. By increasing the percentage of hydrogen, the engine's operating range could be extended to that of a leaner mixture while having no effect on CO concentration. Ji et al. (2009) investigated the differences in CO emissions from engines at various engine speeds and fuel mixtures. Even though there is enough air in the cylinder for complete combustion, the engine cannot burn the entire amount of fuel. The hydrogen-powered engine was expected to emit no  $\text{CO}_2$ . A trace of CO may still be found in the results. This was caused by the combustion of the lubricating oil film inside the engine cylinder (Shrestha and Karim

1999). The amount of CO emitted decreases as engine speed increases. When the excess air ratio is nearly the stoichiometric requirement, the addition of H<sub>2</sub> increases CO emission; however, it decreases when H<sub>2</sub> is added under lean conditions. The increased in-cylinder temperature after the addition of H<sub>2</sub> promotes the oxidation of CO into CO<sub>2</sub>. CO is emitted as a result of incomplete combustion of the fuel within the combustion chamber. The incomplete combustion is highly dependent on the combustion temperature of the blend. According to Allenby et al. (2001), the CO emissions produced by 30% and 50% hydrogen fractions were insignificant in comparison to that of pure natural gas fuel combustion.

#### 8.5.4.3 Nitrogen Oxide Emissions (NO<sub>x</sub>)

The combustion of coal produces nitrogen oxides (NO<sub>x</sub>), which are essentially (NO<sub>2</sub>) or (NO) and are commonly referred to as NO<sub>x</sub>. NO<sub>x</sub> is produced by ignition and is composed primarily of NO (90–95%) and a trace amount of NO<sub>2</sub> (5–10%). The arrangement of nitric oxide in the burning zone is determined by two factors: the prompt system (Fenimore system) and the thermal system (Tanoue et al. 2000). High-temperature ignition, i.e., when the burning temperature exceeds 1400 K, initiates the formation of thermal NO. The development rate of the NO increases rapidly as the burning temperature rises, and as the burning temperature falls, the development rate of this component decreases (Banapurmath and Tewari 2009). The rapid formation of NO occurs in the rich, low-temperature burning zones where sufficient amount of dynamic radicals can be accessed (Verhelst 2014). Because of the dominant influence of temperature, fuel-rich mixtures (with low values of  $\lambda$ ) favor the formation of NO<sub>x</sub>. Moreover, by controlling the spark advance temperature, the combustion temperature that is reached within the cylinders can be altered. Banapurmath and Tewari (2009) investigated the effect of ignition timing on the lean combustion limit when natural/hydrogen gas is used as a fuel. Chintala and Subramanian (2017) conducted a study to investigate the spark advance and mole fraction of CH<sub>4</sub> ( $\eta$ ) in the HCNG mixture as a function of specific NO<sub>x</sub> emissions at full load,  $\lambda$  of 1.6 and speed of 3400 rpm. Spark advance increases particulate NO<sub>x</sub> emissions, whereas methane content significantly reduces them due to a decrease in combustion temperature. This is one advantage of adding CH<sub>4</sub> to H<sub>2</sub> fuel. When the spark advance is optimal, only the air/fuel ratio governs the specific emission which is not affected by fuel composition at a specific value of  $\lambda$  in the limits set by their study. At the required stoichiometric conditions ( $\lambda = 1$ ), only the fuel mixture that has the maximum CH<sub>4</sub> content ( $\eta = 0.20$ ) can be combusted. However, pure H<sub>2</sub>, displayed a tendency to knock which disallowed the use of a  $\lambda$  value less than 1.6.

### 8.5.4.4 Effects of Combustion

In an effort to convert a 4-cylinder gasoline multi-point port fuel injection (PFI) engine to a CNG direct injection engine, Yadollahi and Boroommand (2013) developed a numerical model to investigate the effects of the fuel combustion chamber geometry in such engines. Two phases were considered, in the first phase, the investigation of fuel mixing properties and flow field was done via multi-dimensional numerical modelling of the transient gas injection. In all cases, the experimental and numerical results were found to be in agreement. In the other phase, a moving mesh was adopted to include the direct injection of  $\text{CH}_4$  in a DI engine-cylinder for different combustion chamber geometries. 5 piston heads of different geometries with two different injectors (a single hole and multi hole type which were centrally mounted) were considered. The effects of injection parameters/type, cylinder head/shape and the combustion chamber geometry were studied on the mixing of air and fuel inside the cylinder. Based on the results, a stratified in-cylinder charge and a narrow bowl configuration gave better engine performance due to higher mixture distribution near the ignition timing. Also, the multi hole injector produced richer fuel composition with slightly improved flame properties relative to that obtained for the single hole injector. Figure 8.5 is an illustration of the variation of mass fraction with crank angle as obtained for the fuel mixture.

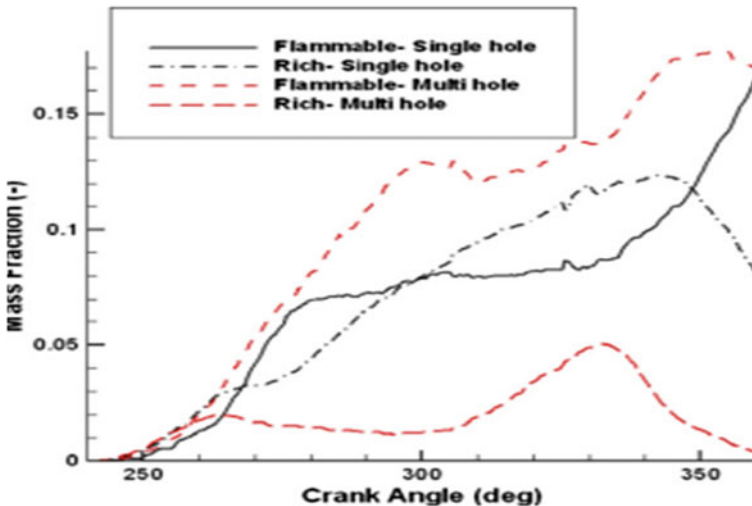


**Fig. 8.5** Mass fraction of fuel-mixture variation with crank angle. Adopted from Yadollahi et al. (2013)

## 8.6 The Future of ICEs Fueled with Hydrogen and Natural Gas as Additives

HCNG is a well-known technology that originated from the widespread use of CNG in engines and its existing manufacturing facilities. The benefits of HCNG that make it a viable alternative fuel for the future have been discussed (Wimmer et al. 2005). Before it is consumed by hydrogen fuel cells for use in hydrogen fuel infrastructures, HCNG technology explores the hydrogen market. As the H<sub>2</sub> concentration in HCNG increases, so does the fuel storage density, allowing for greater onboard energy storage density (Tinaut et al. 2011). In comparison to hydrogen fuel cells, this advantage broadens the HCNG on-board energy storage applications for IC engine vehicles and small fueling infrastructures such as local transportation facilities. Conversely, at larger scales, such as airport shuttles and local delivery trucks, HCNG storage has limitations for fuel cell powertrains and short-range IC powertrains (Tinaut et al. 2011). The second advantage is the overall cost effectiveness of HCNG. The optimal H<sub>2</sub> value to deploy for maximum usage in terms of both range and emissions is 30% H<sub>2</sub>.

Using this value, the CH<sub>4</sub> combustion will be nearly complete, implying that the after-combustion exhaust emissions will be close to zero (Jian et al. 2010). This not only reduces the costs of after-treatment exhaust equipment, but it also reduces space and design complexity, as well as weight considerations. Because of the lower H<sub>2</sub> content, the H<sub>2</sub> energy content is equal to 11 percent, making it easier for renewable sources to meet the emerging HCNG market demands. As the applications of fuel cell vehicles expand and the price of H<sub>2</sub> falls, the benefits of HCNG improve (Zareei et al. 2014; Åhman 2010).

A number of issues can be raised in relation to the difficulties that HCNG is experiencing. In terms of greenhouse gas emissions, another H<sub>2</sub> alternative could be biogas. It is possible that adding locally derived biogas to CNG will improve its performance to the point where it will be considered a better treatment than adding H<sub>2</sub> (Yousufuddin 2017). As for the engine's compatibility, the engine should be designed in such a way as to operate on both HCNG and CNG as per the expected necessity in the case of HCNG fueling system breakdown. HCNG-fueling stations are much more expensive than CNG or H<sub>2</sub> fueling stations, developing an HCNG flex-fuel system is more affordable based on current prices and availability, as it will allow the combustion of any mixture of any of the named gases, even on a random basis (Shudo et al. 2000). Such flexi-fuel equipment will therefore make it possible to utilize hydrogen from all sources, thus expanding the hydrogen market. From the other side, any expansion of HCNG relies on the expansion of current international standards for receptacle and nozzle design for more HCNG blends. The standards would consist of different mixing ratios of HCNG blends such as 20% and 30% or any other percent. Promoting such standards will motivate manufacturers to produce dispensing products to match the requirements of HCNG engines (Yusuf 1993; Oni et al. 2021; Lather and Das 2019). Yadollahi and Broommand (2013) proposed the

connection of a 4-cylinder gasoline multi-point port fuel injection (PFI) engine to a CNG direct injection engine for improved fuel combustion.

Despite the role of hydrogen in ICEs, engines fueled with NG exhibit lean burn and stoichiometric conditions which also influences their combustion and emission characteristics. The study by Cho and He (2007) bothers on the maximization and importance of maintaining a good fuel economy, the operating envelope, low emissions, cycle-to-cycle variations and the need to attain mean effective pressures and strategic approaches that can help achieve stable combustion in lean burning NG fuel in NG-engines. The relevance of stoichiometric air-NG ratio in NG-fueled engines was mentioned as a way of improving the output power and torque relative to their gasoline or diesel counterparts. Hence, for GN-biofuel mixtures, high boost in pressure should be maintained. Furthermore, highly reactive catalysts/a 3-way catalyst for CH<sub>4</sub>-oxidation and lean deNO<sub>x</sub> systems or three-way with precise air-fuel ratios are good control strategies for meeting stringent emission standards.

### **Concluding Remarks**

The potential of hydrogen and natural gas as additives in fuels for high engine performance is quite achievable by ensuring that the required proportions of hydrogen and natural gas are mixed in order to ensure lower carbon emissions at moderate engine speeds. Based on related studies, it is clear that using the separate fuels in ICEs is not only expensive but renders the service-life of the engine at stake. No doubt hydrogen is the fuel of the future however, owing to issues associated with its low density, its backfiring tendency and storage, it is rather used with natural gas in compressed form (CNG) for improved fuel economy, performance, and ignition. Biofuels are prospective renewable energy sources that exhibit enormous potentials that can be tapped for the transportation industry which when maximized by adopting equilibrium concentrations alongside the compatible additive compositions, will render the environment and humans safe owing to their lower potential emissions relative to fossils. The use of PFI and DIs in ICEs are indicative of ways by which spark ignition engines can be modified to suit the different stoichiometric air to fuel measurements required for efficient mixing of the fuels so as to achieve the desired ignition potential for complete combustion. Although, the issue of 3D compressible turbulent reacting flows in ICEs is also a complex problem to resolve especially for situations of direct injection of the fuels, efficient throttling and cylinder pressure adjustments can moderate these effects. Since the formation of apt fuel mixtures with good combustible properties is somewhat herculean and critical for natural gas entrained fuels owing to their low density compared to liquid fuels, very high injection velocities give rise to low fuel penetration and poor mixing of the fuel. However, this can be resolved by improving on the in-cylinder charge motion of the fuel in the ICE. To enhance NG penetration in the cylinder, fuel rail pressures as high as 200 bar can be adopted which then brings about sonic flow at the nozzle exit with the occurrence of a complex shock pattern of expansion waves downstream from the nozzle exit. Furthermore, the world can begin to think biofuel-HCNG fueled SI-engines with the proposed modification as one of the very fast measures of abating the current situation bedeviling the transport industry, especially with regards to the use of gasoline or fossil-based fuels as



transport fuels. The viability of the proposed hybrid mix is its propensity to induce low carbonization in ICEs when used as fuel.

## References

- Adamson KA, Pearson P (2000) Hydrogen and methanol: a comparison of safety, economics, efficiency and emissions. *J Power Source* 86:548–555
- Adt RR, Swain MR (1974) The hydrogen/methanol–air breathing automobile engine. In: *The hydrogen economy Miami Energy Conference*, 18–20 March, Miami Beach, USA, 1974, p S10-38–48
- Åhman M (2010) Biomethane in the transport sector—an appraisal of the forgotten option. *Energy Policy* 38(1):208–217. <https://doi.org/10.1016/j.enpol.2009.09.007>
- Ahmed K, Amare B, Ramayya AV (2013) Experimental investigation on thermal efficiency of diesel Engine with jatropha-diesel blend with biogas. *IJERT*
- Akansu SO, Kahraman N, Ceper B (2007) Experimental study on spark ignition engine fuelled by methane-hydrogen mixtures. *Int J Hydrogen Energy* 32:4279–4284
- Allenby S, Chang W-C, Megaritis A, Wyszynski ML (2001) Hydrogen enrichment: a way to maintain combustion stability in a natural gas fueled engine with exhaust gas recirculation the potential of fuel reforming. *Proc Instr Mech Eng Part D* 215:405–418
- Arat HT, Aydin K, Baltacioğlu E, Yaşar E, Kaan MB, Conker C, Burga A (2013) A review of hydrogen-enriched compressed natural gas (HCNG)-fuel in 44 44 diesel engines. *J Macro Trends Energy Sustain* 1(1):115–122
- Arroyo J, Moreno F, Munoz M, Monne C (2013) Efficiency and emissions of a spark ignition engine fuelled with synthetic gases obtained from catalytic decomposition of biogas. *Int J Hydrogen Energy* 38:3784–3792
- Aslan E, Ergeneman M, Sorousbay C (1991) Use of hydrogen in internal combustion engine as fuel. Istanbul Technical University, Istanbul
- Banapurmath NR, Tewari PG (2009) Comparative performance studies of a 4-stroke CI engine operated on dual fuel mode with producer gas and honge oil and its methyl ester (HOME) with and without carburettor. *Renew Energy* 34:1009–1015
- Bari S (1996) Effect of carbon dioxide on the performance of biogas/diesel dual-fuel engine. *Renew Energy* 9:1007–1010
- Barik D, Murugan S (2014) Investigation on combustion performance and emission characteristics of a DI (direct injection) diesel engine fuelled with biogas-diesel in dual fuel mode. *Energy* 72:760–771
- Basye L, Swaminathan S (1997) Hydrogen production costs—a survey. Sentech, Inc., Report, DOE/GD/10170/778, US
- Bauer CG, Forest TW (2001) Effect of hydrogen addition on performance of methane-fueled vehicles. Part I: effect on S.I. engine performance. *Int J Hydrogen Energy* 26:55–70
- Belchior CR, Barcellos WM, Pimentel VSDB, Pereira PP (2001) Analysis of vehicles converted from gasoline to CNG using conversion devises (kits). SAE 2001-01-3883
- Belyi YuI, Teregulov TR (2016) Hydrogen energy: advantages and disadvantages. *J Sci Educ* 12:8–10
- Bielaczyc P, Woodburn J, Szczotka A (2014) An assessment of regulated emissions and CO<sub>2</sub> emissions from a European light-duty CNG-fueled vehicle in the context of Euro 6 emissions regulations. *Appl Energy* 117:134–141
- Blarigan PV, Keller JO (1998) A hydrogen fueled internal combustion engine designed for single speed/power operation. *Int J Hydrogen Energy* 23:603–609

- Bora BJ, Saha UK, Chatterjee S, Veer V (2014) Effect of compression ratio on performance, combustion and emission characteristics of a dual fuel diesel engine run on raw biogas. *Energy Convers Manage* 87:1000–1009
- Boretti A (2020) Advances in diesel-LNG internal combustion engines. *Appl Sci* 10(4):1296. <https://doi.org/10.3390/app10041296>
- Borges LH, Hollnagel C, Muraro W (1996) Development of a Mercedes Benz natural gas engine M366LAG with a lean-burn combustion system. SAE Paper 962378
- Bysveen M (2007) Engine characteristics of emissions and performance using mixtures of natural gas and hydrogen. *Energy* 32:482–489
- Byun JS, Park J (2015) Predicting the performance and exhaust NO<sub>x</sub> emissions of a spark-ignition engine generator fueled with methane-based biogases containing various amounts of CO<sub>2</sub>. *J Nat Gas Sci Eng* 22:196–202
- Cardozo JIH, Cifuentes SI (2009) H<sub>2</sub>S and CO<sub>2</sub> filtration of biogas used in internal combustion engines for power generation. In: ASME international mechanical engineering Congress and exposition
- Carlucci AP, de Risi A, Laforgia D, Naccarato F (2008) Experimental investigation and combustion analysis of a direct injection dual-fuel diesel-natural gas engine. *Energy* 33:256–263
- Ceper BA, Akansu SO, Kahraman N (2009) Investigation of cylinder pressure for H<sub>2</sub>/CH<sub>4</sub> mixtures at different loads. *Int J Hydrogen Energy* 34:4855–4861
- Chintala V, Subramanian KA (2017) A comprehensive review on utilization of hydrogen in a compression ignition engine under dual fuel mode. *Renew Sustain Energy Rev* 70:472–491
- Chiodi M, Berner HJ, Bargende M (2006) Investigation on different injection strategies in a direct-injected turbocharged CNG-engine. SAE paper 2006-01-3000
- Chitsaz I, Saidi MH, Mozafari AA, Hajjalimohammadi A (2013) Experimental and numerical investigation on the jet characteristics of spark ignition direct injection gaseous injector. *Appl Energy* 105:8–16
- Cho HM, He BQ (2007) Spark ignition natural gas engines—a review. *Energy Convers Manage* 48:608–618. <https://doi.org/10.1016/j.enconman.2006.05.023>
- Choi M, Lee S, Park S (2015) Numerical and experimental study of gaseous fuel injection for CNG direct injection. *Fuel* 140:693–700
- Choi M, Song J, Park S (2016) Modeling of the fuel injection and combustion process in a CNG direct injection engine. *Fuel* 179:168–178. <https://doi.org/10.1016/j.fuel.2016.03.099>
- Chugh S, Posina VA, Sonkar K, Srivatsava U, Sharma A, Acharya GK (2016) Modeling & simulation study to assess the effect of CO<sub>2</sub> on performance and emissions characteristics of 18% HCNG blend on a light duty SI engine. *Int J Hydrogen Energy* 41:6155–6161
- Das LM (1996) Utilization of hydrogen e CNG blends in an internal combustion engine. In: 11th World hydrogen energy conference, Stuttgart, Germany, pp 1513–1535
- Das LM (2002) Hydrogen engine: research and development (R&D) programmes in Indian Institute of Technology (IIT), Delhi. *Int J Hydrogen Energy* 27:953–965
- Das LM, Gulati R, Gupta PK (2000) A comparative evaluation of the performance characteristics of a spark ignition engine using hydrogen and compressed natural gas as alternative fuels. *Int J Hydrogen Energy* 25:783–793
- Demirbas A (2002) Fuel properties of hydrogen, liquiled petroleum gas (lpg), and compressed natural gas (CNG) for transportation. *Energy Sources* 24:601–610
- Dhyani V, Subramanian KA (2019) Control of backfire and NO<sub>x</sub> emission reduction in a hydrogen fueled multi-cylinder spark ignition engine using cooled EGR and water injection strategies. *Int J Hydrogen Energy* 44:6287–6298
- Dulger Z (1991) Numerical modeling of heat release and flame propagation for methane fueled internal combustion engines with hydrogen addition. PhD thesis, University of Miami
- Ghazal OH (2013) Performance and combustion characteristic of CI engine fueled with hydrogen enriched diesel. *Int J Hydrogen Energy* 38:15469–15476
- Heffel JW (2003a) NO<sub>x</sub> emission and performance data for a hydrogen fueled internal combustion engine at 1500 rpm using exhaust gas recirculation. *Int J Hydrogen Energy* 28:901–908

- Heffel JW (2003b) NO<sub>x</sub> Emission reduction in a hydrogen fueled internal combustion engine at 3000 rpm using exhaust gas recirculation. *Int J Hydrogen Energy* 28:1285–1292
- Helmut E, Klaus S, Daniel L, Manfred K, Markus S (2009) Potential of synergies in a vehicle for variable mixtures of CNG and hydrogen. SAE 2009-01-1420
- Hoekstra RL, Collier K, Mulligan N, Chew L (1995) Experimental study of clean burning vehicle fuel. *Int J Hydrogen Energy* 20:737–745
- Hoekstra RL, Collier K, Mulligan N (1994) Demonstration of hydrogen mixed gas vehicles. In 10th World hydrogen Energy Conference, Cocoa Beach, USA, June 20–24, 1994
- Huang Z, Wang J, Liu B, Zeng K, Yu J, Jiang D (2006) Combustion characteristics of a direct-injection engine fueled with natural gas/hydrogen blends under different ignition timings. *Fuel* 86:381–387
- Ihracska B, Wen D, Imran S, Emberson DR, Ruiz LM, Crookes RJ, Korakianitis T (2013) Assessment of elliptic flame front propagation characteristics of hydrogen in an optically accessible spark ignition engine. *Int J Hydr Energy* 38:15452–15468
- Ji C, Wang S (2009) Effect of hydrogen addition on combustion and emissions performance of a spark ignition gasoline engine at lean conditions. *Int J Hydrogen Energy* 34:7823–7834
- Jian X, Xin Z, Jianhua L, Longfei F (2010) Experimental study of a single cylinder engine fuelled with natural gas- hydrogen mixtures. *Int J Hydrogen Energy* 35(2010):2909–2914
- Jorach R, Enderle C, Decker R (1997) Development of a low-NO<sub>x</sub> truck hydrogen engine with high specific power output. *Int J Hydrogen Energy* 22:423–427
- Kahraman N, Ceper B, Akansu SO, Aydin K (2009) Investigation of combustion characteristics and emissions in a spark-ignited engine fuelled with natural gas and hydrogen blends. *Int J Hydrogen Energy* 34:1026–1034
- Karim GA (2003) Hydrogen as a spark ignition engine fuel. *Int J Hydrogen Energy* 28:569–577
- Karim GA, Wierzbza I (1992) Safety measures associated with the operation of engines on various alternative fuels. *Reliab Eng System Safety* 37:93–98
- Kavathekar K, Rairikar S, Thipse S (2007) Development of a CNG injection engine compliant to Euro-IV norms and development strategy for HCNG operation. SAE 2007-26-029
- King SR (1992) The impact of natural gas composition on fuel metering and engine operational characteristics. SAE Paper 920593
- Konoplev VN (2008) Scientific basis for the design of motor vehicles operating on gas-engine fuels. Dissertation, Moscow
- Konoplev VN, Melnikov ZG, Sarbaev V (2018a) The main aspects of safety of hydrogen energy in relation to the motor transport process on gas engine fuels. *Transp Res Arch Proc* 36:295–302
- Konoplev VN, Korzin AS, Melnikov ZG, Belitsky GV (2018b) Hydrogen energy in the strategy of international energy consumption and its relationship with the perspective of the development of transport technologies. In: IAA SciTech Forum, pp 58–63
- Kwon E-C, Song K, Kim M, Shin Y, Choi S (2017) Performance of small spark ignition engine fueled with biogas at different compression ratio and various carbon dioxide dilution. *Fuel* 196:217–224
- Lather RS, Das LM (2019) Performance and emission assessment of a multi-cylinder SI engine using CNG & HCNG as fuels. *Int J Hydrogen Energy* 44(38):21181–21192
- Lee S, Park C, Park S, Kim C (2014) Comparison of the effects of EGR and lean burn on an SI engine fueled by hydrogen-enriched low calorific gas. *Int J Hydrogen Energy* 39:1086–1095
- Li Y, Kirkpatrick A, Mitchell C, Willson B (2004) Characteristic and computational fluid dynamics modeling of high-pressure gas jet injection. *ASME Trans J Eng Gas Turb Power* 126:192–197
- Lim C, Kim D, Song C, Kim J, Han J, Cha JS (2015) Performance and emission characteristics of a vehicle fueled with enriched biogas and natural gases. *Appl Energy* 139:17–29
- Liu Z, Karim GA (1995) Knock characteristics of dual-fuel engines fueled with hydrogen fuel. *Int J Hydrogen Energy* 20:919–924
- Luo S, Ma F, Mehra RK, Huang Z (2019) Deep insights of HCNG engine research in China. *Fuels*
- Ma F, Liu H, Wang Y, Li Y, Wang J, Zhao S (2008) Combustion and emission characteristics of a port-injection HCNG engine under various ignition timings. *Int J Hydrogen Energy* 33:816–822

- MacLean HL, Lave LB (2003) Evaluating automobile fuel/propulsion system technologies. *Prog Energy Combust Sci* 29:1–69
- Malogorzata P (2014) Mitigation of landfill gas emissions. Taylor and Francis, ISBN: 0415630770
- Mehra RK, Duan H, Juknelevicius R, Ma F, Li J (2017) Progress in hydrogen enriched compressed natural gas (HCNG) internal combustion engines e a comprehensive review. *Renew Sustain Energy Rev* 80:1458–1498
- Montoya JPG, Amell AA, Olsen BD (2016) Prediction and measurement of the critical compression ratio of methane number for blends of biogas with methane, propane, and hydrogen. *Fuel* 186:168–175
- Moore RB, Raman V (1996) Hydrogen infrastructure for fuel cell transportation. In: 11th World hydrogen energy conference, Stuttgart, Germany, June 23–28, pp 133–142
- Morones A, Ravi S, Plichta D, Petersen EL, Donohoe N, Heufer A et al (2014) Laminar and turbulent flame speeds for natural gas/hydrogen blends. In: Turbine Technical Conference and Exposition. ASME, V04BT04A039
- Mustafi NN, Raine RR, Bansal PK (2006) The use of biogas in internal combustion engines: a review. In: ASME internal combustion engine division spring technical conference
- Nadaleti WC, Przybyla G, Vieira B, Leandro D, Gadotti G, Quadro M, Kunde E, Correa L, Andrezza R, Castro A (2018) Efficiency and pollutant emissions of an SI engine using biogas-hydrogen fuel blends: BIO60, BIO95, H20BIO60 and H20BIO95. *Int J Hydr Energy* 43:7190–7200. <https://doi.org/10.1016/j.ijhydene.2018.02.133>
- Navarro E, Leo TJ, Corral R (2013) CO2 emissions from a spark ignition engine operating on natural gas/hydrogen blends (HCNG). *Appl Energy* 101:112–120
- NGV Global (2019) Current natural gas vehicle statistics. Available online: [www.iangv.org/current-ngvstats](http://www.iangv.org/current-ngvstats). Accessed on 16 Dec 2019
- Nwafor OMI (2003) Combustion characteristics of dual-fuel diesel engine using pilot injection ignition. *Inst Eng (India) J* 84:22–25
- Ogden J, Steinbugler M, Kreutz T (1995) Hydrogen as a fuel for fuel cell vehicles: a technical and economic comparison. PU/SEES
- Oni BA, Sanni SE, Ibegbu AJ, Adujo AA (2021) Experimental optimization of engine performance of a dual-fuel compression-ignition engine operating on hydrogen-compressed natural gas and Moringa biodiesel. *Energy Rep* 7(2021):607–619
- Orhan A, Zafer D, Nafiz K, Veziroglu T (2004) Internal combustion engines fueled by natural gas hydrogen mixtures. *Int J Hydrogen Energy* 29(14):1527–1539
- Ouellette P, Hill PG (2000) Turbulent transient gas injections. *ASME Trans J Fl Eng* 122:743–753
- Ovsyannikov E, Gaitova T, Klyukin P, Poliakova V (2016) Device for producing and addition of hydrogen into fuel-air mixture for internal combustion engine. *Alternative Fuel Transp* 6(54):85–92
- Papagiannakis RG, Rakopoulos CD, Hountalas DT, Rakopoulos DC (2010) Emission characteristics of high speed, dual fuel, compression ignition engine operating in a wide range of natural gas/diesel fuel proportions. *Fuel* 89:1397–1406
- Park C, Choi Y, Kim C, Oh S, Lim G, Moriyoshi Y (2010) Performance and exhaust emission characteristics of a spark ignition engine using ethanol and ethanol-reformed gas. *Fuel* 89:2118–2125
- Park C, Park S, Lee Y, Kim C, Lee S, Moriyoshi Y (2011) Performance and emission characteristics of a SI engine fueled by low calorific biogas blended with hydrogen. *Int J Hydrogen Energy* 36:10080–10088
- Park C, Kim C, Choi Y (2012a) Power output characteristics of hydrogen-natural gas blend fuel engine at different compression ratios. *Int J Hydrogen Energy* 37:8681–8687
- Park C, Park S, Kim C, Lee S (2012b) Effects of EGR on performance of engines with spark gap projection and fueled by biogas-hydrogen blends. *Int J Hydrogen Energy* 37:14640–14648
- Patil KR, Khanwalkar PM, Thipse SS, Kavathekar KP, Rairikar SD (2009) Development of HCNG blended fuel engine with control of NO<sub>x</sub> emissions. In: Second International conference of Engineering Trends in Engineering and Technology (ICETET). IEEE, New York, pp 1068–1074

- Porpatham E, Ramesh A, Nagalingam B (2012) Effect of compression ratio on the performance and combustion of a biogas fuelled spark ignition engine. *Fuel* 95:247–256
- Raman V, Hansel J, Fulton J, Brudery D (1994) Hythane—an ultraclean transport fuel. In: *Proceedings, 10th World hydrogen Energy Conference, Cocoa Beach, USA, June 20–24*, pp 1797–1806
- Renny A, Janardan S (2008) Hydrogen CNG blend performance in a three-wheeler. *SAE*, 28-0119
- Rogelj J, den Elzen M, Höhne N, Fransen T, Fekete H, Winkler H et al (2016) Paris agreement climate proposals need a boost to keep warming well below 2 C. *Nature* 534:631–639
- Sagar SMV, Agarwal AK (2018) Knocking behavior and emission characteristics of a port fuel injected hydrogen enriched compressed natural gas fueled spark ignition engine. *Appl Therm Eng* 141:42–50
- Sanni, SE, Alaba PA, Okoro E, Emetere M, Oni B, Agboola O, Ndubuisi OA (2021) Strategic examination of the classical catalysis of formic acid decomposition for intermittent hydrogen production, storage and supply: a review. *Sustain Energy Technol Assessments* 45:101078. <https://doi.org/10.1016/j.seta.2021.101078>
- Shioji M, Ishiyama T, Ikegami M, Mitani S, Shibata H (2001) Performance and exhaust emissions in a natural-gas fueled dual-fuel engine. *JSME Int J* 44:641–648
- Shrestha SO, Karim GA (1999) hydrogen as an additive to methane for spark ignition engine applications. *Int J Hydrogen Energy* 24:577–586
- Shudo T, Shimamura K, Nakajima Y (2000) Combustion and emissions in a methane DI stratified charge engine with hydrogen pre-mixing. *JSAE Rev* 21:3–7
- Sierens R, Rosseel E (2000) Variable composition hydrogen/natural gas mixtures for increased engine efficiency and decreased emissions. *J Eng Gas Turbines Power* 122:135–140
- Sierens R, Verhelst S (2001) Hydrogen fuelled V-8 engine for city bus application. *Int J Hydrogen Energy* 2:39–45
- Singh S (2016) Performance analysis of (hydrogen+biogas) as fuel for SI engine. *IJIR*
- Sorrell S, Speirs J, Bentley R, Brandt A, Miller R (2010) Global oil depletion: a review of the evidence. *Energy Policy* 38:5290–5295
- Steinberg M, Cheng HC (1989) Modern and prospective technologies for hydrogen production from fossil fuels. *Int J Hydrogen Energy* 14(11):797–820
- Subramanian KA, Mathad VC, Vijay VK, Subbarao PMV (2013) Comparative evaluation of emission and fuel economy of an automotive spark ignition vehicle fuelled with methane enriched biogas and CNG using chassis dynamometer. *Appl Energy* 105:17–29
- Swain MR, Yusuf MJ, Dulger Z, Swain MN (1993) The effects of hydrogen addition on natural gas engine operation. *SAE paper* 932775
- Tangoz S, Akansu SO, Kahraman N, Malkoc Y (2015) Effects of compression ratio on performance and emissions of a modified diesel engine fueled by HCNG. *Int J Hydrogen Energy* 44:15374–15380
- Tanoue K, Kido H, Hamatake T, Shimada F (2000) Improving the turbulent combustion performance of lean methane mixture by hydrogen addition. In: *Proceedings of the FISITA world automotive Congress, Seoul–Korea, F2000A115*
- Thipse S, Rairikar S, Kavathekar K, Chitnis P (2009) Development of a six-cylinder HCNG engine using an optimized lean burn concept. *SAE* 2009-26-0031
- Tiashen D, Jingding L, Yingqing L (1985) Combustion-supporting fuel for methanol engines: hydrogen. In: *The International symposium on hydrogen systems, Beijing, China, 7–11 May, 1985*, pp 105–113
- Tinaut F, Melgar A, Gimenez B, Reyes M (2011) Prediction of performance and emissions of an engine fuelled with natural gas/hydrogen blends. *Int J Hydrogen Energy* 36:947–956
- Verhelst S (2014) Recent progress in the use of hydrogen as a fuel for internal combustion engines. *Int J Hydrogen Energy* 39:1071–1085
- Verma G, Prasad RK, Agarwal RA, Jain S, Agarwal AK (2016) Experimental investigations of combustion, performance and emission characteristics of a hydrogen enriched natural gas fuelled prototype spark ignition engine. *Fuel* 178:209–217

- Wallace JS, Cattelan AI (1994) Hythane and CNG fueled engine exhaust emission comparison. In: Proceedings 10th World hydrogen Energy Conference, Cocoa Beach, USA, June 20–24, pp 1761–1770
- Wang J, Huang Z, Fang Y, Liu B, Zeng K, Miao H et al (2007) Combustion behaviors of a direct-injection engine operating on various fractions of natural gas/hydrogen blends. *Int J Hydrogen Energy* 32:3555–3564
- Wang L, Yang Z, Huang Y, Liu D, Duan J, Guo S, Qin Z (2017) The effect of hydrogen injection parameters on the quality of hydrogen-air mixture formation for a PFI hydrogen internal combustion engine. *Int J Hydr Energy* 42:23832–23845
- Wang J, Huang Z, Tang C, Zheng J (2010) Effect of hydrogen addition on early flame growth of lean burn natural gas/air mixtures. *Int J Hydrogen Energy* 35:7246e52
- Weaver CS (1989) Natural gas vehicles—a part of the state of art sierra research inc. Sacramento, CA, USA, SAE paper 892133
- Wimmer A, Wallner T, Ringler J, Gerbig F (2005) H<sub>2</sub>-Direct injection—a highly promising combustion concept. SAE Paper 2005-01-0108; SAE International: Warrendale, PA, USA
- Xu Y, Gbolagah FE, Lee D, Liu H, Rodgers MO, Guensler RL (2015) Assessment of alternative fuel and powertrain transit bus options using real-world operations data: life-cycle fuel and emissions modeling. *Appl Energy* 154:143–159
- Yadollahi B, Boroomand M (2013) The effect of combustion chamber geometry on injection and mixture preparation in a CNG direct injection SI engine. *Fuel* 107:52–62. <https://doi.org/10.1016/j.fuel.2013.01.004>
- Yousufuddin S (2017) Effect of combustion duration on the operating and performance characteristics of a hydrogen-ethanol dual fueled engine: an experimental analysis. *Int J Adv Automot Technol* 1:36–45
- Yusuf MJ (1993) Lean Burn natural gas fueled engines: engine modification versus hydrogen blending. PhD thesis, University of Miami
- Zareei J, Mahmood FW, Abdullah S, Ali Y, Mohamad TI (2014) Prediction of performance a direct injection engine fueled with natural gas/hydrogen blends. *Int J Mech Mechatron Eng* 14(3):149–156
- Zheng S, Yi W, Li W (2015) The impacts of provincial energy and environmental policies on air pollution control in China. *Renew Sustain Energy Rev* 49:386–394

**Part III**  
**Dimethyl-Ether (DME) as an E-Fuel**

# Chapter 9

## Prospects of Dual-Fuel Injection System in Compression Ignition (CI) Engines Using Di-Methyl Ether (DME)



Ayush Tripathi , Suhan Park , Sungwook Park,  
and Avinash Kumar Agarwal 

**Abstract** Governments worldwide have imposed strict emission regulations to control GHG emissions from the road transport sector. The industry is under stress to find alternative fuels and technologies to cope with these stringent emission regulations. E-Fuels are the kind of alternative fuels whose production aim towards storing electrical energy from renewable energy sources in the form of chemical bonds of fuels. Soot and NO<sub>x</sub> emissions are the main problems in diesel-fuelled compression ignition (CI) engines. Using alternative fuels alone can solve the issues related to conventional Fuel, but it has its challenges. Optimization of fuel injection strategies along with the use of alternative fuels has been explored as a solution. The dual-fuel mode has shown superior control over the combustion and simultaneous reduction of soot-NO<sub>x</sub> in several studies. DME is one of the most promising ultra-clean, alternate CI engine fuels. DME is considered as an e-fuel if production occurs from renewable energy sources. Its superior atomization characteristics result in the homogeneous fuel-air mixture formation. Its higher cetane number (CN) and oxygenated nature help to achieve efficient in-cylinder combustion. This results in lower PM, soot, hydrocarbons (HC), and carbon monoxide (CO) emissions than baseline diesel. However, nitrogen oxides (NO<sub>x</sub>) and unregulated emissions are higher in DME direct injection (DI) engines. The operating range of DME homogeneous charge compression ignition (HCCI) engines is limited due to knock intensity; however, it can be widened using the dual-fuel mode. DME has ultra-low viscosity, high vapour pressure, and negligible self-lubrication characteristics, which create difficulties in the conventional fuel injection systems to handle the DME. These challenges can be

---

A. Tripathi · A. K. Agarwal (✉)  
Engine Research Laboratory, Department of Mechanical Engineering,  
Indian Institute of Technology Kanpur, Kanpur 208016, India  
e-mail: [akag@iitk.ac.in](mailto:akag@iitk.ac.in)

S. Park  
School of Mechanical and Aerospace Engineering, Konkuk University,  
120 Neungdong-ro, Gwangjin-gu, Seoul 05029, Republic of Korea

S. Park  
School of Mechanical Engineering, Hanyang University, 222 Wangsimni-ro,  
Seongdong-gu, Seoul 04763, Republic of Korea



overcome by using high octane number (ON) fuel as an ignition suppressor to reduce the chances of knocking and coefficient of variance (COV) of engine performance parameters with DME used in CI engines. This chapter explores different injection strategies and fuels in dual-fuel mode by considering DME as an E-Fuel. The combustion and emission characteristics of the DME dual-fuel engine are discussed.

**Keywords** Alternative fuels · DME · Dual-fuel · CI engines · HCCI · PCCI

## 9.1 Introduction

Rapid depletion of fossil fuel reserves due to increased energy demand has emerged as a significant global challenge in the twenty-first century. These reserves are limited and are expected to exhaust in the next 45 years at the current consumption rate (World Oil Reserve 2021). A higher consumption rate also causes alarm because fossil fuels emit GHG emissions. GHG emissions are the main contributors to global warming. According to National Oceanic and Atmospheric Administration (NOAA), this has led to an  $\sim 0.8$  °C rise in the earth's average temperature over the past 100 years. According to the Environmental Protection Agency (EPA), there has been a  $\sim 20$ -cm rise in the sea level since 1870 (Effects of Global Warming 2021). Many weather forecast models predicted a 2 °C rise in the average earth temperature and  $\sim 3$  feet rise in the sea level by the end of this century at the current rate of GHG emissions, which would lead to rapid melting of polar ice (Effects of Global Warming 2021; Climate Change Over the Next 100 Years 2021). This can completely wash off major coastal cities and island nations such as the Maldives and submerge vast swaths of land globally. The temperature rise would lead to extreme weather events such as hurricanes, droughts, and flooding (Effects of Global Warming 2021). The timely globalization of carbon-neutral fuels and sustainable approaches could help bring down the temperature rise by 0.5 °C (What is carbon neutrality, and how it can be achieved 2021). Therefore, the production of carbon-neutral alternative fuels should also be carbon-neutral for sustainable development.

Today, the world is in the middle of a crucial energy transition since the industrial revolution. Many governments are making policies to become carbon neutral before 2050. Many European countries like Norway and the UK plan to ban all fossil fuel-powered cars by 2035 (European countries banning fossil fuel cars and switching to electric cars 2021). There is a drive to cut net GHG emissions to at least 55% by 2030 to reach the goal of carbon-neutrality before 2050 (Proposal for a “Regulation of the European parliament and of the council” 2021). One solution to attain these goals is to use cleaner alternative fuels, resulting in lesser GHG emissions than conventional fuels. The transport sector constitutes a large amount of GHG emissions (Fig. 9.1). Worldwide, many governments are imposing stringent emission regulations to control GHG emissions from the road transport sector. Europe has imposed EURO emission regulations on IC engine-powered vehicles to cut down GHG emissions. New vehicles have to follow EURO-VI emission regulations in

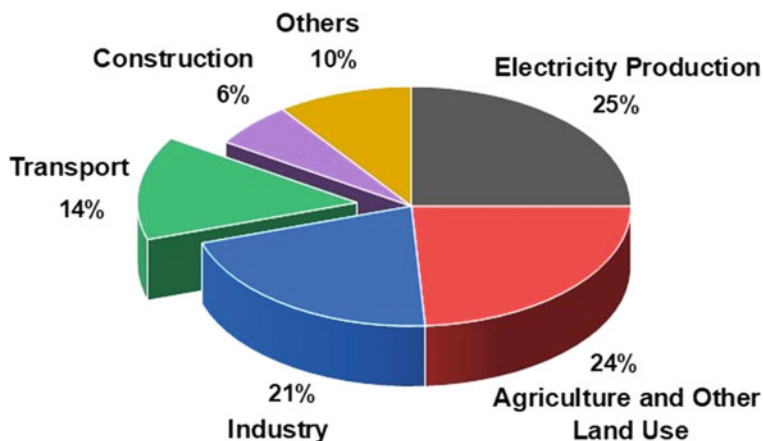


**Fig. 9.1** Share of the transport sector in global GHG emissions (Adapted from Global Greenhouse Gas Emissions Data 2021)

Europe (Proposal for a “Regulation of the European parliament and of the council” 2021). India also imposed Bharat stage-VI emission regulations to control emissions from the IC engine-powered vehicles. The transport industry needs to explore novel alternative fuels, advanced combustion, and injection strategies to survive with the rejuvenation of the electric mobility industry. The dual-fuel injection strategy is one of the fuel injection strategies to introduce alternative fuels into the IC engines to improve their performance and reduce harmful emissions.

**Dual-Fuel Injection Strategies:** Fuel properties of directly injected and premixed fuels tend to affect the emissions and the performance characteristics of dual-fuel engines (Cha et al. 2012). The fuel reactivity plays a vital role in advanced low-temperature combustion (LTC) control. Using two different fuels with substantially different cetane numbers (CN) helps control ignition timing and combustion stability in dual-fuel mode. A greater reduction in NO<sub>x</sub> and soot can be achieved by increasing the premixed ratio of the low cetane fuels (Cha et al. 2012). Combustion phasing can be retarded by injecting low CN fuels such as liquefied petroleum gas (LPG) with cleaner diesel alternatives such as DME (Jamsran and Lim 2016). At higher loads, higher brake thermal efficiency (BTE), lower engine knock, lesser combustion noise, and lower NO<sub>x</sub> emissions can be achieved by dual-fuel RCCI mode over the other LTC modes (e.g., HCCI, PCCI) (Singh et al. 2020a, b). Despite the advantages of RCCI combustion technology, no study has been carried out to use this technology in DME fueled dual-fuel engines. These dual-fuel strategies combine DI and PFI fuel injection strategies and use HCCI, PCCI combustion technology. In the DI method, a heterogeneous mixture forms inside the combustion chamber (CC). In-cylinder temperature reduction occurs because directly injected fuel vaporizes and absorbs the surrounding heat equivalent to its latent heat of vaporization. Auto-ignition timing can be retarded by direct fuel injection because of the heterogeneous mixture and reduced temperatures (Jang et al. 2009).

## 9.2 Di-Methyl Ether (DME)

Alternative fuelled vehicles have shown promising performance and emission characteristics than the vehicle powered by conventional fuels. Production of alternative fuels from renewable sources, their compatibility with engine components, economic viability, lesser overall carbon footprint, and higher H/C ratio than conventional fuels are essential parameters for sustainable alternative fuels (Valera and Agarwal 2019). Other properties such as fuel-bound oxygen, absence of a C–C bond make them more attractive. DME is one such fuel, the simplest of all ethers, having fuel-bound oxygen and absence of C–C bond (Fig. 9.2).

**DME Properties:** Among all alternative fuels, DME is gaining interest among researchers as an ultra-clean, renewable CI engine fuel. DME has superior atomization characteristics at relatively lower fuel injection pressure (FIP). It has higher CN, oxygen content, high latent heat (LH), and lower self-ignition temperature than baseline diesel. There is no direct C–C bond in the molecular structure of DME (Fig. 9.2); hence the possibility of C≡C bond formation is negligible. C≡C bond is the leading cause for forming polycyclic aromatic hydrocarbons (PAHs) and, ultimately, the soot. DME is a non-toxic fuel, which easily degrades in the troposphere upon accidental release. DME contains the C–O bonds, and due to the smaller bond energy of the C–O bond than the C–H bond, the C–O bond breaks much easier than the C–H bond. Therefore, the pyrolysis mechanism can start the chain reactions at relatively low temperatures, resulting in a lower auto-ignition temperature for DME (Park and Lee 2014; Arcoumanis et al. 2007; Agarwal et al. 2017). Existing infrastructure for storage and transportation of propane can be used for the DME, with slight modifications (Morsy et al. 2006).

There are several drawbacks of DME for the utilization of fuel in engines. Ultra-low viscosity, negligible self-lubrication characteristics, high vapour pressure, and low critical point pose challenges for conventional fuel injection systems handling DME (Agarwal et al. 2017). DME has a lower heating value and bulk modulus (one-third of mineral diesel) (Agarwal et al. 2017). The diesel fuel injection system requires special sealing materials while using DME due to its ultra-low viscosity and corrosive nature. Inferior self-lubrication characteristics lead to corrosion of many Fuel Injection Equipments (FIE) components. Therefore, the same sealing materials cannot be used for DME as conventional diesel fuel injection systems. DME has a compatibility issue with polymeric compounds (Kumar and Agarwal 2021). For fuel blends having 25% DME, the viscosity remains below the American Society for Testing and Materials (ASTM) diesel fuel specifications (Fig. 9.3). This can, however, be overcome by adding viscosity improvers and lubricity additives to the

**Fig. 9.2** Molecular structure of DME

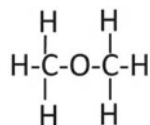
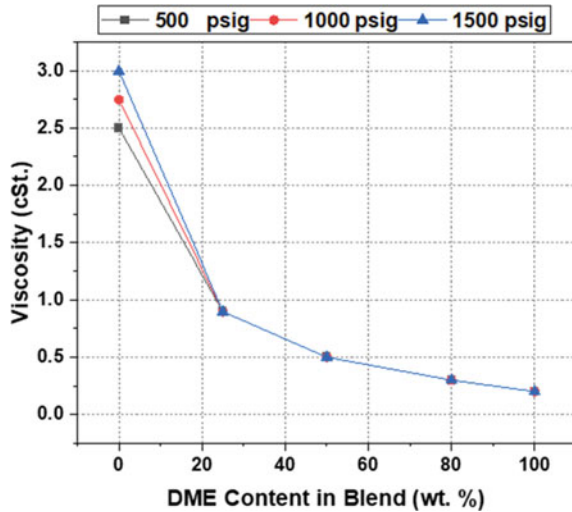


**Fig. 9.3** Effect of blending ratio of DME on viscosity of DME-diesel blend (Adapted from Chapman et al. (2003))



DME/ blends. Additives alone cannot increase the DME viscosity to the level of conventional fuels. Studies have shown that none of the additives developed so far has resolved lubricity issues faced by higher blends (50% or higher DME) (Chapman et al. 2003). DME does not form a hydrodynamic fluid layer due to its low viscosity and ensures metal-to-metal contact, which ultimately causes wear. This problem can be resolved by designing a dedicated DME fuel injection system rather than adding different additives to DME to make it compatible with conventional diesel FIE (Pal et al. 2021). DME has a lower modulus of elasticity, therefore, has five times higher compressibility than baseline diesel. This leads to higher compression work by the fuel pump for DME (Park and Lee 2014; Arcoumanis et al. 2007). DME has lower combustion enthalpy than diesel as well.

There are several renewable and non-renewable methods for the production of DME (Kumar and Agarwal 2021). DME can be produced from fossil sources such as coal and natural gas using suitable catalysts (Jang et al. 2009). Moreover, DME can be produced from renewable energy sources such as biomass (via methanol route), solar, and wind. That’s why DME is a renewable energy storage medium (<http://www.oilgasportal.com/dimethyl-ether-dme-production-2>). Table 9.1 shows a comparison of physical- and chemical properties of commonly used fuels and DME (Valera and Agarwal 2019; Agarwal et al. 2017; Kalwar et al. 2020; Temwutthikun et al. 2018; Zhao et al. 2014; Theinnoi et al. 2017; Yao et al. 2006; Lee and Lim 2016; Oh et al. 2010; Engineering Toolbox 2021; Mahla et al. 2010).

**Table 9.1** Comparison of properties of various fuel

Properties	DME	Diesel	Gasoline	Methanol	LPG		CNG
					Propane	n-Butane	
Chemical structure	CH <sub>3</sub> OCH <sub>3</sub>	C <sub>8</sub> -C <sub>25</sub>	C <sub>4</sub> -C <sub>12</sub>	CH <sub>3</sub> OH	C <sub>3</sub> H <sub>8</sub>	C <sub>4</sub> H <sub>10</sub>	CH <sub>4</sub> (>95%)
Molecular weight (g/mol)	46.07	190-220	95-120	32.026	44	58	17.19
Density (liquid) (kg/m <sup>3</sup> ) @25 °C	668	856	732	790	503	580	715
Density (gaseous) (kg/m <sup>3</sup> ) @25 °C	1.918	-	-	1.11	1.53	2	-
Flammability range in air (% vol)	(3.4-18)	(1-6)	(1.4-7.6)	(5.5-26)	(2.1-9.4)	(1.86-8.41)	(5-15)
Boiling Point (°C)	-23.6	180-370	230	65	-42	-0.5	-162
Autoignition temperature (°C)	235	250	257	465	504	430	813
CN	55-62	40-55	-	<15	5	≤10	06
ON	-	-	86-94	111	125	91	105
Lower heating value (LHV) (MJ/Kg)	27.6-28.8	42.5-43.2	43.8	19.9	46.4	45.6	48
Latent heat of vaporization (kJ/kg)	460-470	270	289-305	1110	370	-	509
Stoichiometric A/F ratio	8.9	14.3	14.7	6.5	15.6	-	17
Oxygen (% w/w)	34.8	0	0	50	0	0	0.4
Flash point (°C)	-41	>55	-43	11.1	-104	-60	124
Kinematic viscosity (liquid) cSt @30 °C	<0.1	3.0-7.5	0.6-0.9	0.69	4.5	3.11	-
Minimum ignition energy (mJ)	0.29	20	0.80	0.14	0.25	0.25	0.28
Vapour pressure (kPa) @20 °C	516.76	1-10	48-103	13	215.1	858.7	-

### 9.3 DME Dual-Fuel Engines

DME can be used with conventional hydrocarbon fuels as well as alternative fuels in dual-fuel mode. Several studies have reported emission benefits by pairing DME with conventional fuels. However, low-carbon alternative fuels are superior options for further reduction in emissions. Methanol has several desirable properties: higher latent heat of vaporization, oxygen content, and high autoignition temperature. It has been possible to achieve simultaneous soot-NO<sub>x</sub> reduction with methanol (Valera and Agarwal 2019; Kalwar et al. 2020; Yao et al. 2006). However, low reactivity and lubricity restrict methanol usage in the CI engines. High reactivity fuels such as diesel and DME can be used with methanol to improve their combustion characteristics. Complex hydrocarbons in diesel may reduce the benefit of soot emissions associated with methanol. Therefore, a low sooting fuel such as DME can be a good option for methanol adaption in CI engines in dual-fuel mode (Lee and Lim 2016; Kozole and Wallace 1988).

LPG is widely considered a cleaner fuel due to its low sulfur content and sootless combustion (Oh et al. 2010). The low carbon content of LPG helps to reduce CO<sub>2</sub> emissions from conventional engines. LPG has a lower flame speed than conventional hydrocarbon fuels. LPG-diesel dual-fuel engines have been successfully operating on the roads for several decades now. Their emissions can be further minimized by replacing diesel with DME.

Natural gas (NG) is another alternative gaseous fuel for dual-fuel DME engines. The main constituent of NG is methane (CH<sub>4</sub>). A small proportion of ethane, propane, nitrogen is also present in natural gas. Natural gas can be stored in both gaseous and liquified forms. The advantage of using NG in diesel engines is its ability to better mix with air than diesel. The main disadvantage of NG is its ultra-low CN.

### 9.4 Dual-Fuel Injection Strategies

There are different strategies to inject two different fuels in the dual-fuel mode (Fig. 9.4). These strategies will be discussed in this section, along with their advantages and drawbacks. Dual-Fuel injection strategies with premixed fuel in the port, premixed chamber, and torch injection chamber show lower particulate matter, nitrogen oxide emissions, and improved brake thermal efficiency (Lim et al. 2010; Wang et al. 2019). Research shows that using two fuels in IC engines is one of the most feasible approaches to controlling ignition timing over a wide range of engine loads (Wang et al. 2019). Higher CN fuels such as DME also accelerate the combustion (Yeom and Bae 2009). Among conventional HCCI engines, low-temperature combustion, dual-fuel combustion, and dual-fuel strategy are gaining interest from developers in the automotive industry because of their superior fuel economy and lower CO<sub>2</sub> emissions (Cha et al. 2012). DME can be used as an ignition improver

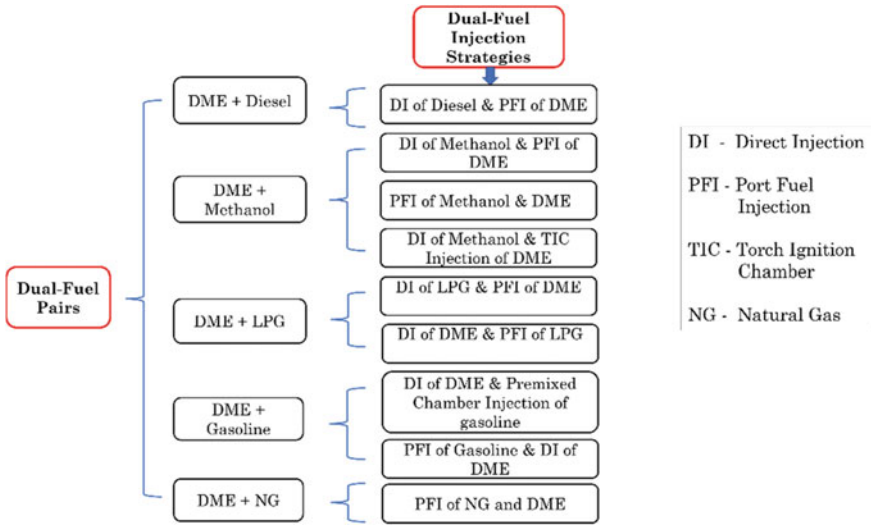


**Fig. 9.4** Overview of different dual-fuel injection strategies

for the low CN fuels used in CI engines and injected using different fuel injection strategies, as discussed below.

**DI of Diesel and PFI of DME:** In this method, DME is injected into the intake port and mixed with the intake air to form a homogeneous mixture before being inducted by the engine. Diesel is directly injected into the combustion chamber, as shown in Fig. 9.5. Port injection of DME leads to an advanced start of combustion than diesel-fueling alone, resulting in efficient combustion and lesser PM emissions (Sittichompoo et al. 2016). NO<sub>x</sub> and smoke emissions get significantly reduced with 30% port-injected DME. Diesel consumption was reduced by 22%, leading to an increase in BTE (Theinnoi et al. 2017). Port injection quantity of DME needs to be optimized. Increasing DME quantity leads to higher CO and HC emissions than baseline diesel engines (Theinnoi et al. 2017). Direct injection of DME is also an option. However, the PFI method requires fewer modifications in the fuel injection equipment (FIE) (Sittichompoo et al. 2016). PFI mode resolves the issue of fuel lubricity because of the gaseous injection of DME (Sittichompoo et al. 2016).

**DI of Methanol and PFI of DME:** Methanol alleviates the cold starting issue of CI engines due to low reactivity and high evaporative cooling effect (Yao et al. 2006). DME can be used as the ignition improver in methanol-fueled CI engines. Combustion and emission characteristics of methanol-fueled CI engines improve with the introduction of DME than the conventional glow plug heating method (Chen et al. 2009). The combustion is initiated by the premixed DME fraction, which increases the in-cylinder temperature to the level required for auto-ignition of directly injected methanol. The injection timing of methanol has a significant impact on the heat release rate (HRR) of the dual-fuel mode operation (Green et al. 1990).

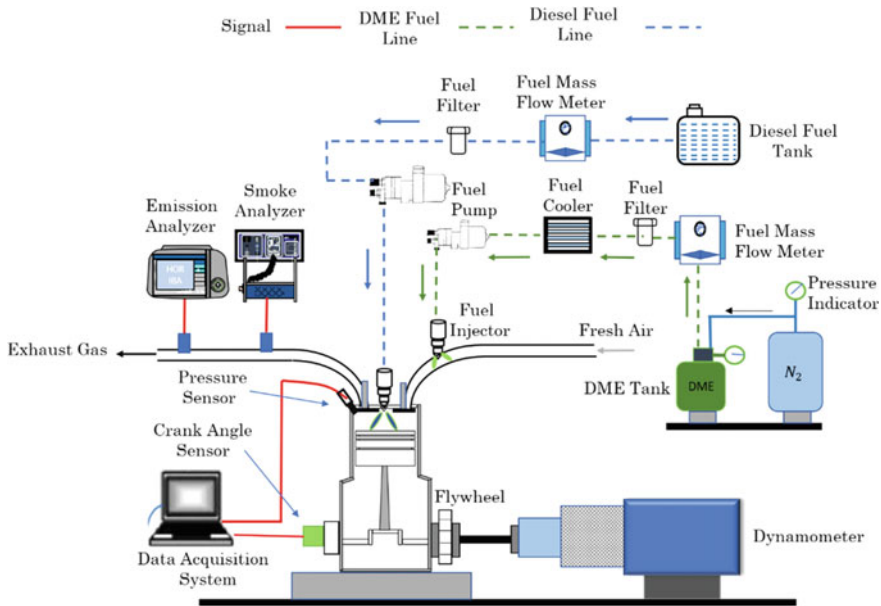
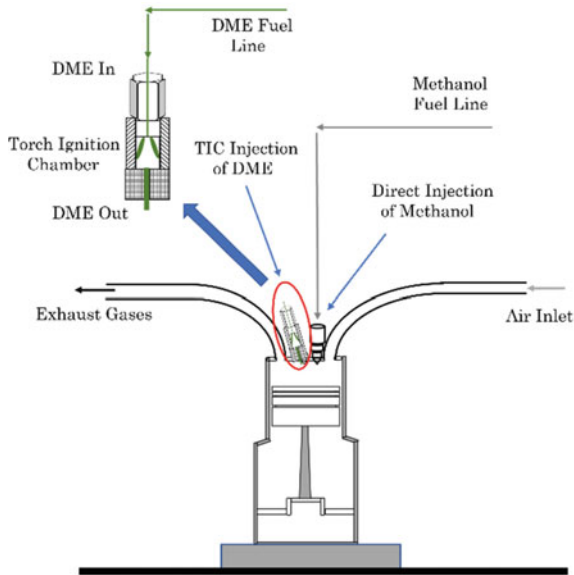


Fig. 9.5 Schematic of DME-Diesel dual-fuel operated CI engine

**HCCI of Methanol and DME mixture:** In this method, both fuels are introduced into the intake port of the CI engine (Yao et al. 2006). The knock-limited load range is one of the major hurdles in HCCI commercialization. Methanol premixing fraction can be optimized to control the overall mixture reactivity and temperature. Therefore, the rate of pressure rise (ROPR) and knocking can be controlled at higher loads (Zheng et al. 2004). Higher ON and higher latent heat of vaporization of methanol inhibits too advanced ignition of DME, and the operation range is also enlarged (Zheng et al. 2004).

**DI of Methanol and TIC of DME:** In this method, a torch ignition chamber (TIC) is used to inject DME during an intake stroke, as shown in Fig. 9.6 (Murayama et al. 1992). The torch ignition chamber is placed inside the hole made for the pressure transducer. DME is introduced into this chamber for premixing. PFI of DME emits large amounts of unburned hydrocarbons, formaldehyde, unburned DME, especially at low loads, even for smooth engine operations delivering high BTE. A large amount of PFI of DME is required to sustain the ignition. The torch ignition method is used to inject DME to overcome these difficulties with the PFI. TIC controls DME diffusion during the compression stroke in this method, resulting in lower HC emissions and a lower DME injection rate. TIC method consumes nearly 30% lesser DME with a 10% increase in thermal efficiency than the PFI at a given load range (Murayama et al. 1992). Although, NO<sub>x</sub> emissions are slightly higher in the case of the TIC method. Emission characteristics and fuel economy can be further increased with





**Fig. 9.6** Schematic of TIC injected DME and DI of methanol operated CI engine (Adapted from Murayama et al. (1992))

the TIC method by optimizing the DME quantity, location, and geometry of the TIC. The TIC acts as a premixing chamber in this fuel injection strategy.

**Dual-fuel HCCI using LPG and DME:** LPG is a suitable alternative fuel to displace gasoline in SI engines. However, it has been investigated as a potential fuel for HCCI engines as well. HCCI is a hybrid technology of CI and SI (Yeom and Bae 2009, 2007a). It can be used with DME as a low CN fuel to control combustion. There is no direct control over the ignition timings in conventional single fuel HCCI engines operated using high CN fuel. In dual-fuel mode, one can inject a low CN fuel due to its properties of self-ignition suppression and the resulting delay in the ignition timings (Oh et al. 2010). DME and LPG are gaseous fuels under ambient conditions, and it is convenient to inject the gaseous fuels through the PFI method. High compression ratio and residual gases from the previous combustion event provide sufficient heat to ignite LPG with low CN in the HCCI mode. This leads to the rapid pressure rise in the combustion chamber, high engine noise, and possible damage to the engine components (Oh et al. 2010; Yeom and Bae 2009). Researchers use many fuel injection strategies for the introduction of LPG and DME.

Yeom and Bae (2009), Oh et al. (2010), and Jang et al. (2009) used PFI of LPG and direct injection of DME to achieve HCCI combustion. Jamsran and Lim (2016) used PFI of LPG and DME for realizing HCCI combustion. Autoignition timing of charge retarded and combustion duration increased with increased quantity of PFI of LPG. Autoignition generally occurred when the directly injected DME mixed with the LPG-air mixture. A large quantity of low CN fuel (i.e., LPG) suppressed

the autoignition of DME (Jang et al. 2009). Researchers have explored several other injection strategies to achieve desired control over the combustion phasing (Jamsran and Lim 2016; Jang et al. 2009; Oh et al. 2010). Low-temperature reactions decreased after the increased LPG injection quantity because radicals from the cool flames of DME were released and transferred to ignite LPG.

**PFI of LPG and Gasoline with DI of DME:** In this method, LPG and gasoline are introduced into the intake port and DI of DME in HCCI mode. PFI of one fuel occurs at any time, but the arrangement is given at the port to introduce both fuels at different locations. In a study by Yeom and Bae (2009), gasoline and LPG injectors were placed 10 cm and 30 cm upstream from the intake valve, respectively. The LPG-DME HCCI engines improved the operating range compared to gasoline-DME HCCI engines because of the higher octane number and higher latent heat of vaporization of LPG compared to gasoline. The knocking intensity of LPG-DME dual-fuel mode was lower than gasoline-DME due to lower self-ignition characteristics and higher latent heat of vaporization of the LPG-DME dual-fuel pair.

**DI of DME and Premixed Chamber Injection of Gasoline:** In a study, gasoline was injected into a premixed chamber at 3 MPa pressure (Fig. 9.7).

DME was directly injected into the combustion chamber at 50 MPa pressure to control the combustion phasing, which was done through variations in the DME injection timings from  $-20^\circ$  to  $+2^\circ$  crank angle (Cha et al. 2012). Higher volatility and shorter ignition delay are the essential properties of directly injected fuel to control combustion phasing. The split injection strategy promoted a more homogeneous fuel-air mixture and showed further reduction in exhaust emissions. In this

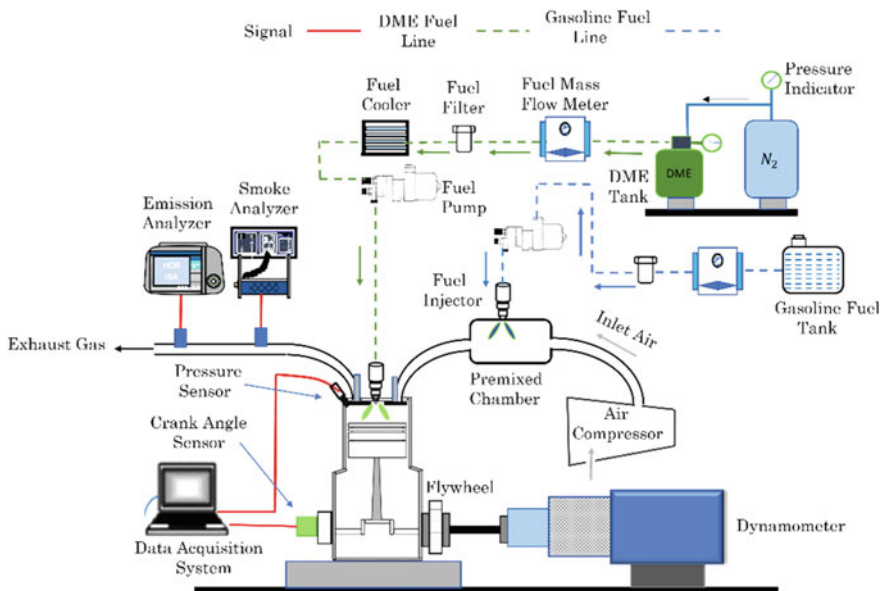


Fig. 9.7 Schematic of DME-gasoline dual-fuel HCCI engine

strategy, the total injected mass of DME was split between two consecutive injections. Secondary injection of DME improved the late-cycle combustion, which increased the combustion efficiency.

**PFI of Gasoline and DI of DME in HCCI Mode:** Knocking is a big challenge in the HCCI engines. Hence, various intake valve opening timings and fuel quantities must be tested to identify the knock limits of the HCCI dual-fuel engine to eliminate knocking (Yeom and Bae 2007b). HCCI mode cannot operate at every load and cause noise/knocking in the engine. Therefore, the peak combustion pressure, rate of combustion pressure rise, and IMEP must be correlated with the knocking probability and knock intensity to characterize the high load operation limit of the engine (Yeom and Bae 2007b).

**PFI of NG and DME in HCCI Combustion:** Simultaneous reduction in NO<sub>x</sub> and soot emissions is challenging in the CI engines (Mahla et al. 2010). NO<sub>x</sub> emissions can be reduced to nearly zero, and thermal efficiency improves in the NG-air operated CI engines. However, NG alone is not good for CI engines due to its high autoignition temperature and low CN. A small amount of port injected DME can trigger the ignition of the NG-air mixture and control the ignition timing. The addition, optimum DME quantity also leads to an increase in the operating load range of the engine (Fig. 9.8).

Chen et al. (2000) observed the effect of DME injection quantity on the NG-DME fueled CI engine by changing the excess air ratio of NG, DME, and total fuel.

$$\lambda_{NG} = G_{air} / (G_{NG} * AF_{NG\ th.})$$

$$\lambda_{DME} = G_{air} / (G_{DME} * AF_{DME\ th.})$$

$$\lambda_{total} = G_{air} / (G_{total} * AF_{total\ th.})$$

where  $\lambda$  = excess air ratio,  $G$  = flow rate,  $AF_{fuel\ th}$  = theoretical air–fuel ratio.

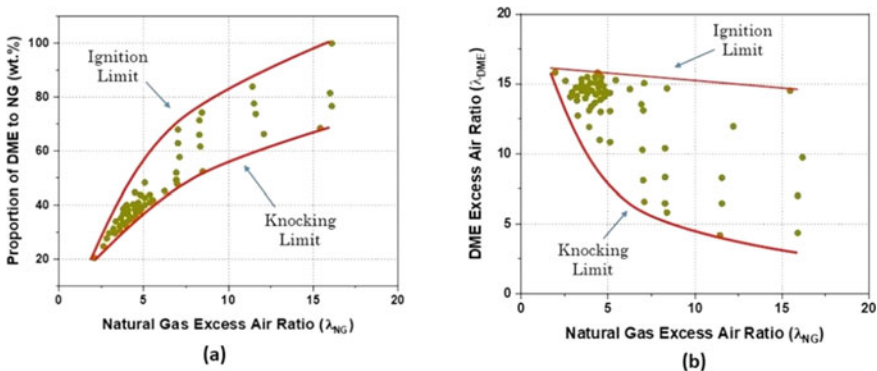


**Fig. 9.8** Effect of (a) DME proportion and (b) DME excess air ratio on operating range of DME-NG dual-fuel engine (Adapted from Chen et al. (2000))

The results suggested that the requirement of the minimum DME quantity to ignite the NG-air mixture is dependent only on the equivalence ratio of DME and not a function of the total equivalence ratio. The engine’s operating range widens with increasing DME proportion and narrows with increasing NG proportion in DME-NG dual-fuel engine (Chen et al. 2000).

## 9.5 Effect of Dual-Fuel Strategies on Engine Combustion and Performance Characteristics

### 9.5.1 Combustion Characteristics

**In-cylinder Pressure and Temperature:** In-cylinder pressure and temperature are highly sensitive to the premixing fraction of DME (Zhao et al. 2014). The shorter ignition delay of DME leads to the advanced combustion and higher pressure peak (Figs. 9.9 and 9.10) (Zhao et al. 2021). The onset of the maximum pressure and temperature also moved closer to the TDC. The combustion of the premixed DME fraction improved the in-cylinder ambient, which helped in a higher mixing rate of the DI diesel. Therefore, diesel’s combustion efficiency improved, leading to higher peak pressure and temperature (Wang et al. 2014). H<sub>2</sub>O and CO<sub>2</sub> present in the cooled EGR improved the heat capacity of the in-cylinder charge, leading to lower P<sub>max</sub> and T<sub>max</sub> (Zhao et al. 2014).

In the PFI of methanol and DME strategy, with increased port-injected methanol, the in-cylinder temperature reduced due to its higher latent heat of vaporization and adverse effects on the low-temperature reactions (LTR) (Zheng et al. 2004).

Jamsran and Lim (2016) showed that both in-cylinder pressure and temperature reduced dramatically with a reduction in DME quantity in the PFI of LPG-DME HCCI mode. Peak combustion pressure decreased with retarded inlet valve open

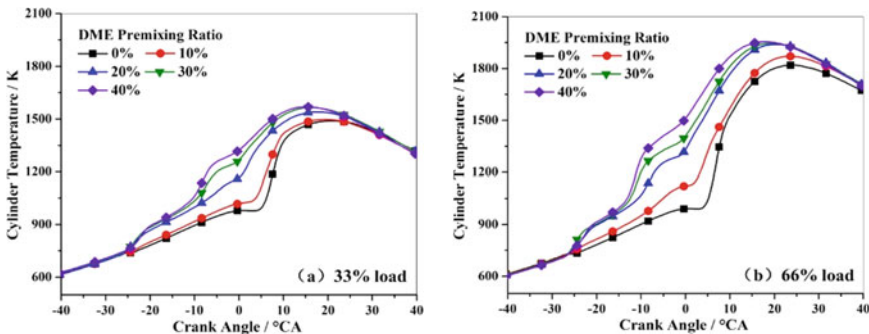


**Fig. 9.9** Variations in the in-cylinder pressure at constant load with different DME premixing ratios in DME-diesel dual-fuel engine (Zhao et al. 2021)

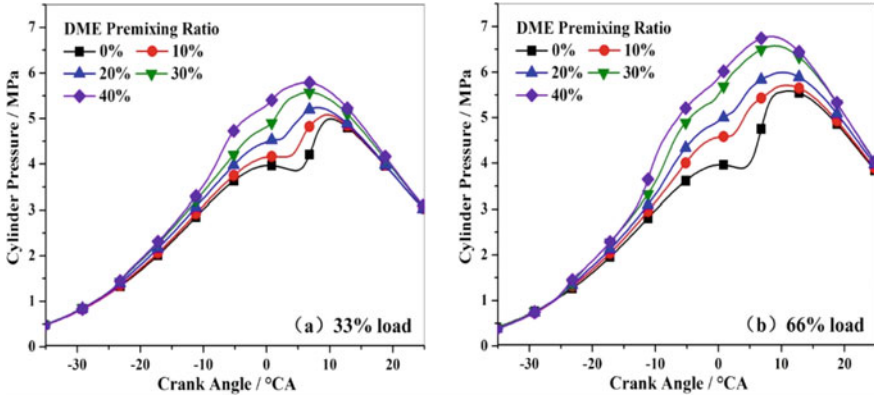


**Fig. 9.10** Variations in the in-cylinder temperature at constant load under various DME premixing ratios in DME-diesel dual-fuel engine (Zhao et al. 2021)

(IVO) timings due to reductions in volumetric efficiency and hot residual gases (Yeom and Bae 2007a). Volumetric efficiency was reduced due to a reduction in valve overlap and late intake valve closing, so the combustion starting point was retarded. This reduced overall combustion temperature, resulting in a large unburned fuel due to the weaker fuel oxidation reactions.

Chen et al. (2000) reported decreased in-cylinder pressure and mean temperature at reduced DME supply in the DME-NG dual-fuel engine.

**Heat Release Rate (HRR):** Large part of the heat release is concentrated around  $CA_{50}$  timing (Lee and Lim 2016). At lower DME premixing ratio and low load operation, DME Low-Temperature Reactions (LTR) and diffusion combustion of diesel are responsible for two peaks in the HRR curve for DI of diesel and PFI of DME strategy. At low DME premixing ratios, the high-temperature reactions (HTR) phase reactivity is less due to a relatively lean mixture (Wang et al. 2014). Thus, at higher DME premixing ratios, DME LTR, DME HTR, and diesel diffusion combustion are responsible for three peaks in the HRR curve (Figs. 9.11 and 9.12) (Zhao et al. 2014). HCCI LTR and HTR of DME are chemical kinetics controlled combustion, and diesel mainly burns in the diffusion combustion (Yeom and Bae 2007b). The peak of the HRR curve increased for HCCI (LTR and HTR) combustion and decreased for the diesel diffusion combustion stage for higher DME premixed ratios. HRR for diffusion combustion stage reduces because of the increased quantity of port injected DME and reduced quantity of diesel, leading to deteriorated mixing of diesel and air (Wang et al. 2014). CAD for maximum HRR in HCCI HTR combustion and diesel diffusion combustion advanced by increasing DME premixed ratios due to shortening of the ignition delay. Maximum HRR decreased, and the corresponding CAD retarded with the introduction of EGR and an increased EGR rate. This happens because the dilution effect and higher specific heat capacity of inert exhaust gases inhibited the HRR.

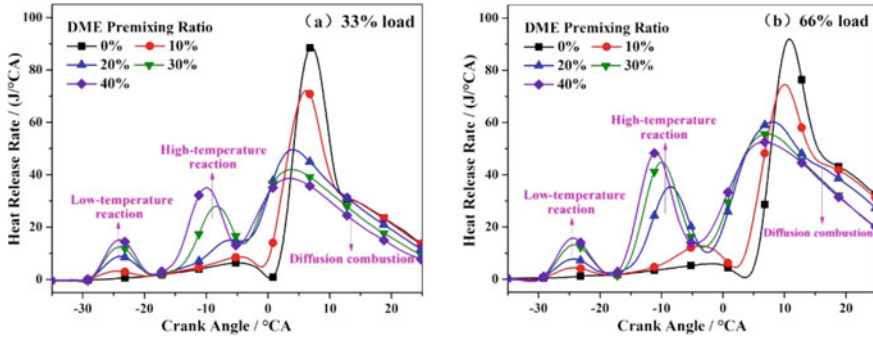


**Fig. 9.11** Variations in HRR under various DME premixing ratios in DME-diesel operated engines (Zhao et al. 2021)

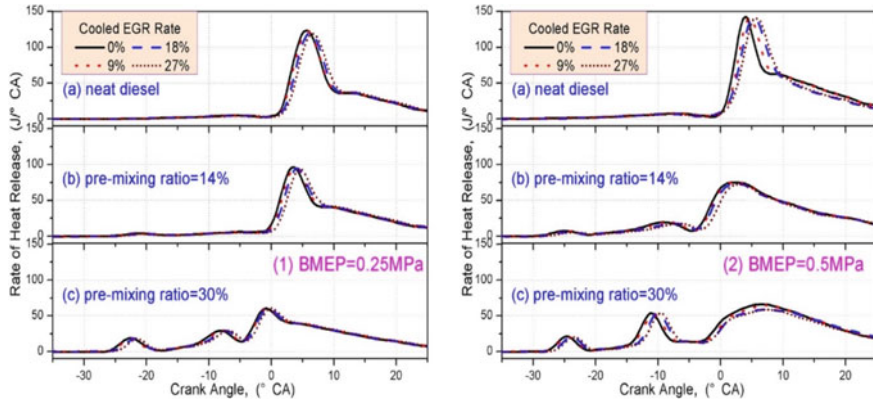


**Fig. 9.12** Variations in HRR under different EGR rates and DME premixing ratios in DME-diesel operated engines (Zhao et al. 2014)

Zheng et al. (2004) reported that HRR of LTR reduced with increased port-injected methanol quantity with the amount of port injected DME maintained constant. Moreover, the HRR of LTR is completely inhibited at a large methanol quantity. There were two main reasons for this trend. First is the higher latent heat of vaporization of methanol, which led to a reduction in the in-cylinder temperature inhibiting the LTR of DME. The second is the formation of OH radicals during LTR of DME and their consumption during their reactions with methanol.

Jang et al. (2009) showed that the peak of LTR decreased with increasing port injection of LPG in DME-DI and LPG-PFI mode. At a higher LPG fraction, the radicals formed during the LTR of DME were consumed by the LPG combustion. The peak of HTR also decreased due to an increased ignition delay and reduced heat release of the LTR (Oh et al. 2010). HRR is delayed with an increasing proportion of propane in the LPG due to better antiknock quality and higher ON of propane

than butane (Oh et al. 2010). The peak of HTR was advanced, and the peak of HRR increased with increasing DME quantity in this mode. Cha et al. (2012) demonstrated that the  $HRR_{max}$  in premixed gasoline dual-fuel engines was comparatively higher than DME fuelled engines even if the combustion duration was shorter because DME elevated the ignition of the gasoline-air mixture, hence promoted localized combustion. The peak of HRR decreased significantly by decreasing the port-injected DME in DME-NG dual-fuel engines (Chen et al. 2000).

**Combustion Duration and Combustion Phasing:** Combustion duration can be defined as the CAD between 10% (SOC) and 90% (EOC) accumulated heat release (Zhao et al. 2014, 2021). The start of combustion (SOC) and combustion duration widened with an increased premixed DME quantity because DME HCCI combustion occurred before the direct injection of diesel.

Shorter ignition delay, higher CN of DME led to the observed trend in Fig. 9.13 (Zhao et al. 2014, 2021). Using a PCCI strategy, exhaust gas recirculation (EGR) prolongs the combustion duration of a DME-diesel dual-fuel engine.

Combustion duration prolonged with increasing LPG quantity in DME-DI and LPG-PFI mode (Jang et al. 2009). The increased quantity of directly injected LPG had an insignificant effect on the combustion phasing in LPG-DI and DME-PFI mode. This was because DME injection took place before the LPG injection in the CC formed a homogeneous DME-air mixture, which was auto-ignited. But in this mode, the combustion phasing advanced upon increasing the DME quantity. Combustion efficiency decreased with an increasing proportion of LPG in the DME-LPG dual-fuel mode. Jamsran and Lim (2016) reported that combustion phasing retarded and

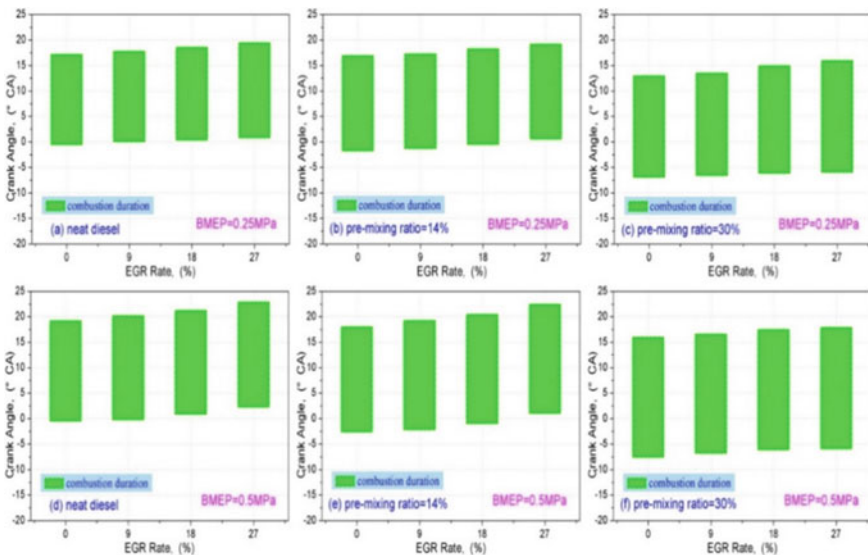


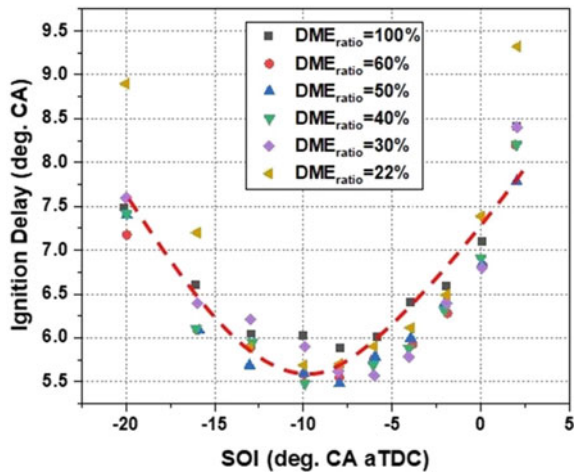
**Fig. 9.13** Variation in the combustion duration at different EGR rates and DME premixed ratio in DME-diesel operated engines (Zhao et al. 2014)

combustion duration reduced with an increasing the port-injected LPG quantity in PFI of LPG and DME HCCI combustion mode because the energy density of LPG was higher than DME. In LPG-DME dual-fuel HCCI combustion mode, the SOC retarded with a reduction in  $\lambda_{total}$ . Yeom and Bae (2007b) reported that the start of combustion is not dependent on the quantity of premixed gasoline. The higher reactivity of DME played a dominant role in triggering the combustion in gasoline-DME dual-fuel HCCI engines. Combustion duration increased by decreasing the amount of port injected DME in DME-NG engines (Chen et al. 2000). Higher combustion efficiency was observed at leaner DME concentrations in DME-NG dual-fuel engines.

**Ignition Delay:** Ignition delay is the interval between the start of fuel injection and the point where cumulative heat release becomes positive. High CN fuels have lower ignition delay. Ignition delay decreased with an increasing load and engine speed due to superior air–fuel mixing in higher in-cylinder turbulence. The addition of DME in dual-fuel engines leads to shorter ignition delay (Karpuk et al. 1991). Methanol-DME dual-fuel engines have shorter ignition delays than diesel-fueled engines. Ignition delay determines mainly two parameters: (i)  $P_{max}$  of the cycle and (ii) ROPR. Suppose any dual-fuel injection strategy needs to be implemented in the existing diesel engines. In that case, the  $P_{max}$  of the cycle and ROPR of the corresponding dual-fuel strategy must be less than the  $P_{max}$  of the cycle and ROPR of the diesel-fueled engines. Jang et al. (2009) reported that auto-ignition timing retarded with increased LPG quantity in DME-DI and LPG-PFI mode because LPG with low CN prevented the DME-air mixture from auto-ignition. Kim et al. (2004) stated that ignition timing advanced with an increased premixed ratio of gasoline.

Cha et al. (2012) observed that ignition delay could be reduced by optimizing the start of injection (SOI) timing of DME (i.e., 10° CAD bTDC) from the excessive advanced/ retarded timings (Fig. 9.14).

**Fig. 9.14** Variations in ignition delay at different SOI timings by varying DME premixed ratios in DME-gasoline operated engines (Adapted from Cha et al. (2012))





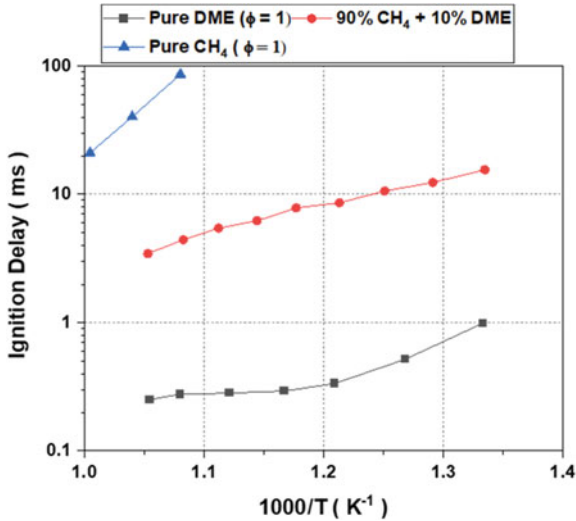


**Fig. 9.15** Ignition delay for DME, methane, and mixture of both fuels (Adapted from Morsy et al. (2006))

Morsy et al. (2006) observed a significant reduction in the ignition delay by adding a small amount of DME in the NG. Injection of liquid DME took place to ignite the NG (Fig. 9.15).

**Indicated Mean Effective Pressure (IMEP):** DME's injection timing influences the IMEP (Jang et al. 2009). IMEP generally decreases with early combustion of the fuel–air mixture due to negative work during compression (Yeom and Bae 2007a). Jamsran and Lim (2016) reported that IMEP and indicated thermal efficiency (ITE) increased with an increasing DME mixing ratio up to 0.6 in LPG-DI and DME-PFI mode. At lower DME mixing ratios, retardation in combustion phasing caused misfire due to the large LPG proportion in the overall mixture. This is reflected in lower IMEP (Fig. 9.16).

Yeom and Bae (2007a) explained the effect of IVO timings on the IMEP. Negative work caused the reduction in IMEP at early IVO timings, and IMEP also decreased by too late IVO timings due to incomplete combustion in the LPG-DME HCCI engine. Jang et al. (2009) demonstrated that IMEP increased for delayed fuel injection timing up to 260° CA due to reduced compression work but started to decrease with further delayed fuel injection timing. This happens because lower fuel–air mixing duration led to localized fuel-rich regions in DME-DI and LPG-PFI mode (Fig. 9.17). In LPG-DI and DME-PFI mode, IMEP variations were lower because the effect of LPG on the autoignition of DME was lesser (Jang et al. 2009). Cha et al. (2012) explained that IMEP deteriorated with increased premixed gasoline quantity in the DME-gasoline dual-fuel injection strategy. IMEP increased with advanced fuel injection timings in DME-gasoline dual-fuel engines than DME fueled engines. IMEP decreased with too advanced fuel injection timing due to the premixing of low CN fuel (i.e., gasoline)

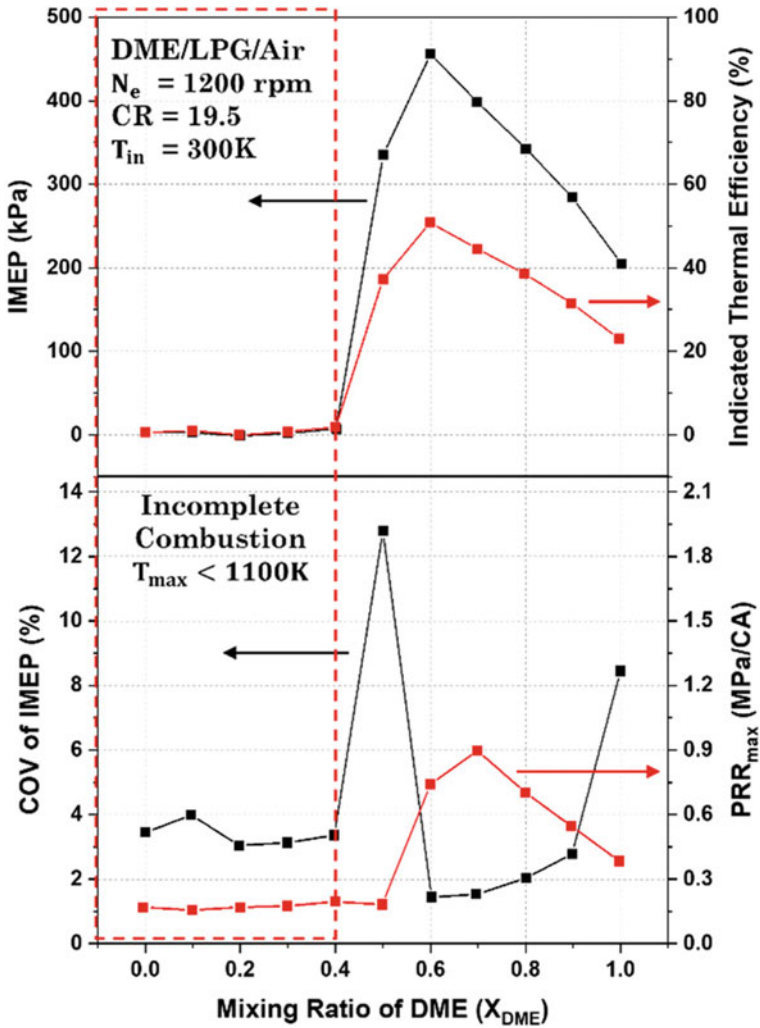


Fig. 9.16 Variations in IMEP indicated thermal efficiency, COV of IMEP, and maximum PRR by changing the DME mixing ratio (Adapted from Jamsran and Lim (2016))

and reduced combustion efficiency. Higher brake mean effective pressure (BMEP) was achieved at a higher injection quantity of NG in NG-DME dual-fuel engine (Chen et al. 2000).

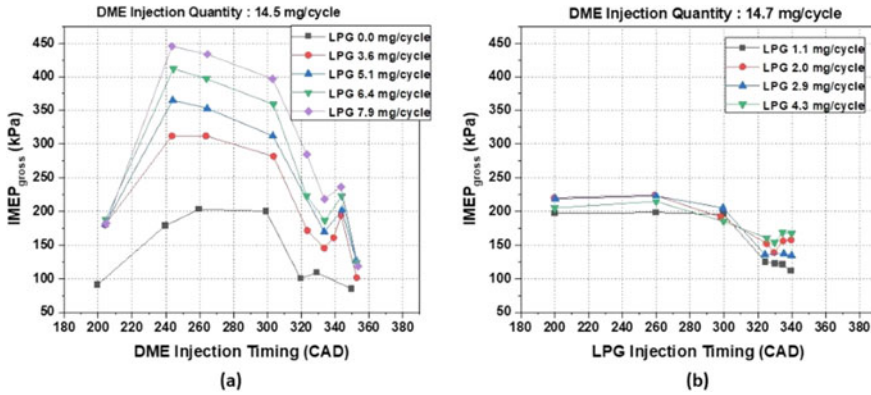


Fig. 9.17 Variations in IMEP for (a) DI of DME and PFI of LPG, and (b) DI of LPG and PFI of DME (Adapted from Jang et al. (2009))

### 9.5.2 Performance Characteristics

**Brake Thermal Efficiency (BTE):** Several investigators reported higher BTE for DME dual-fuel engines than conventional diesel-fueled engines. Zhao et al. (2021) reported that HCCI combustion with the port injection of DME elevated the in-cylinder temperature, promoting superior charge reactivity and improved fuel conversion efficiency. This is reflected in increased BTE and reduced fuel consumption in the PCCI DME engines (Zhao et al. 2014). Combustion efficiency improved because increased port-injected DME quantity increased the HCCI DME (LTR + HTR) combustion, resulting in an earlier start of combustion, shorter ignition delay, and CA<sub>50</sub> closer to the TDC, and complete combustion (Theinnoi et al. 2017; Wang et al. 2014). BTE decreased with a reduction in BMEP. BTE also decreased with increasing EGR since oxygen availability decreased with an increasing EGR rate and less efficient combustion. BTE decreased with an increasing premixing ratio of DME after the optimum ratio (>30%) due to the lower heating value of DME than diesel and the increased cooling losses caused by the extensive DME combustion at earlier timings (Fig. 9.18) (Theinnoi et al. 2017; Murayama et al. 1992). BTE also reduces at lower DME premixed ratios due to unstable combustion with misfiring (Murayama et al. 1992). DME quantity could be optimized by considering the combustion stability of the engine (Murayama et al. 1992). An optimum DME quantity was injected for every load for achieving the maximum BTE at corresponding loads (Fig. 9.19).

Zheng et al. (2004) concluded that in the HCCI combustion of methanol-DME, ITE dropped with high methanol quantity at low loads. However, ITE increased to peak and dropped at medium and high loads. An adequate methanol supply can ensure the best possible combustion phasing. A significantly higher fraction of DME participates in the combustion reactions at low methanol proportions, leading to advanced combustion and knocking (Zheng et al. 2004). At higher methanol injection

**Fig. 9.18** Variations in the BTE of DME-diesel dual-fuel engines at different DME premixing ratios at 1500 rpm and 50% load (Adapted from Theinnoi et al. (2017))

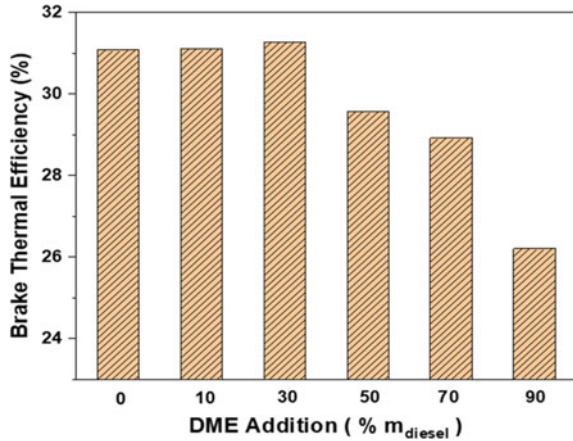
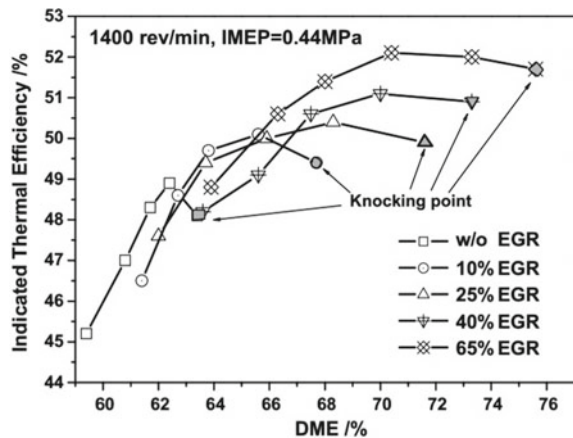


**Fig. 9.19** Variations in ITE at different percentages of DME and EGR rate in DME-methanol operated engines (Yao et al. 2006)



quantities, delayed ignition timing and unfavourable combustion phasing cause a reduction in the BTE.

Higher heat transfer and higher mechanical losses were observed in the rich DME mixture. Lean DME causes elongated combustion duration. Both too rich and too lean DME have an adverse impact on the BTE; hence, there should be optimum DME excess air ratio at maximum BTE in DME-NG dual-fuel engines (Chen et al. 2000). High BTE was observed for DME-NG than the diesel-fueled engine (Fig. 9.20).

**Brake Specific Fuel Consumption (BSFC) and Break Specific Energy Consumption (BSEC):** Zhao et al. (2014) showed that BSFC for PCCI DME-diesel dual-fuel engines was lower than conventional DI CI diesel engines and is further reduced with higher DME quantity injected for a fixed load. BSFC increased with a reduction in BMEP. BSFC also increased with an increasing EGR because the air–fuel ratio reduced (Theinnoi et al. 2017). Wang et al. (2014) showed that BSFC

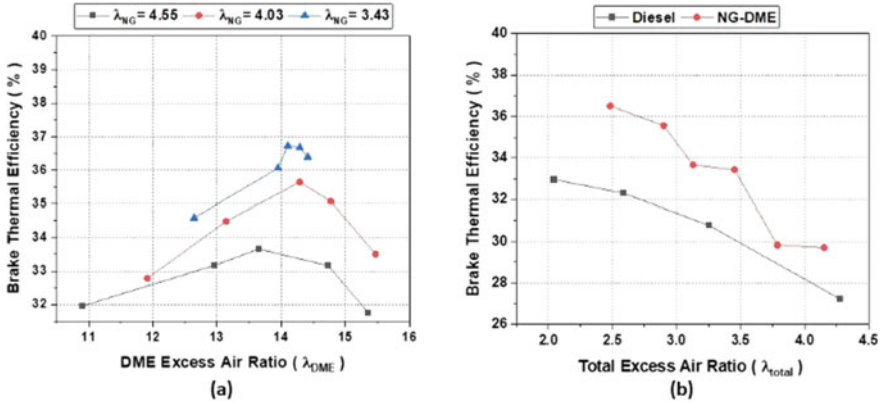
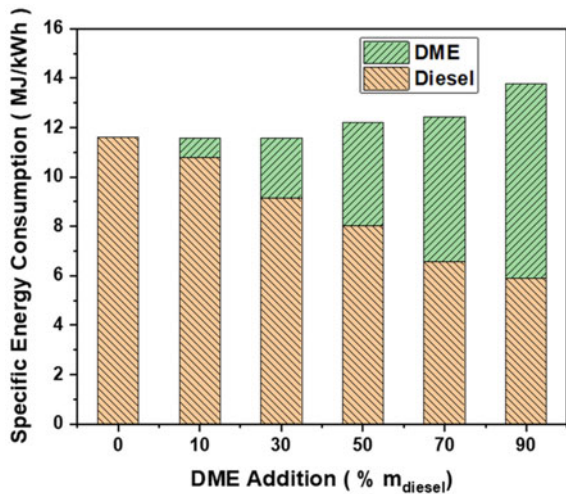


Fig. 9.20 Variations in the BTE by changing (a)  $\lambda_{DME}$  (b)  $\lambda_{total}$  (Adapted from Chen et al. (2000))

decreased with an increased port-injected DME quantity because improved combustion efficiency and superior fuel conversion efficiency led to lower fuel consumption. BSFC decreased with advanced fuel injection timing due to superior fuel–air mixing and improved combustion.

BSEC is a parameter considered for assessing the fuel economy for dual-fuel engines. BSEC increased upon increasing the port-injected DME quantity in the DME-diesel dual-fuel injection strategy under the same load operation due to lower LHV of DME (Fig. 9.21) (Theinnoi et al. 2017). 30% port fuel injection of DME was the optimum quantity of DME for the best BSEC.

Fig. 9.21 Variations in the specific energy consumption of DME-diesel operated engines at 1500 rpm and 50% load (Adapted from Theinnoi et al. (2017))

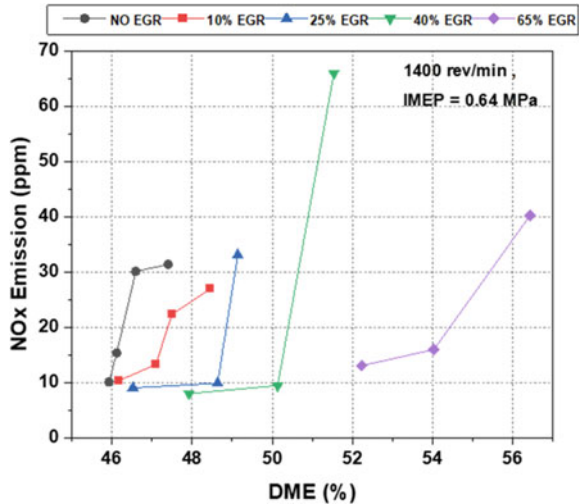


### 9.6 Effect of Injection Strategies on Emission Characteristics

**NOx Emissions:** Availability of oxygen, in-cylinder temperature, and residence time are the factors responsible for NOx formation (Zhao et al. 2014). NOx emissions increase in the regions of large oxygen availability in high-temperature zones in the CC. Zhao et al. (2014) reported a marginal drop in NOx emissions in dual-fuel engines than diesel-fueled engines. This happens because the ignition delay is shorter in the DME-diesel dual-fuel engines, leading to faster diffusion combustion reactions of diesel. This reduced the localized zones of elevated temperatures. The formation of NOx also reduces by increasing the port-fueled premixed DME quantity. A more homogeneous mixture is introduced into the CC, suppressing the localized high temperature, oxygen-rich zones. NOx also showed a decreasing trend after the introduction of EGR. EGR dilutes the fuel–air mixture. EGR deteriorates the combustion to some extent, helping in reducing the flame temperatures and oxygen-rich zones (Fig. 9.22) (Zhao et al. 2014; Wang et al. 2014). Wang et al. (2014) demonstrated that reduction in NOx ceased after optimizing the premixed DME quantity in every cycle because higher DME injection quantity promoted rapid HTRs leading to rapid HRR inside the CC. This increased the overall charge temperature. Lim et al. (2010) showed that NOx emissions depend on the quantity of DME injected in the port and engine load.

Yao et al. (2006) showed that for DME-methanol dual-fuel injection strategy, NOx emission is constant till the threshold percentage of DME injection and suddenly increases with further increment in DME percentage. This threshold percentage changes for different EGR rates. Figure 9.23 shows that the threshold limit extended with an increase of the EGR rate. Zheng et al. (2004) showed that NOx emission

**Fig. 9.22** Variation in NOx emission and smoke opacity for DME-diesel dual-fuel engines at a different premixed ratio of DME and cooled EGR rate (Adapted from Zhao et al. (2014))



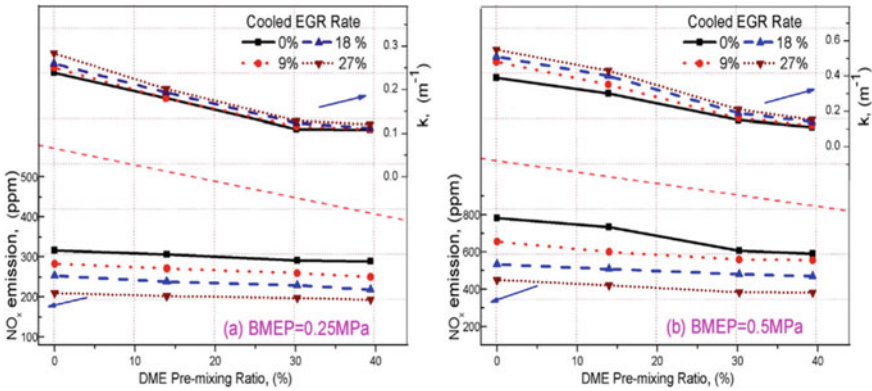


**Fig. 9.23** Variation in NO<sub>x</sub> emission for DME-Methanol dual-fuel engines at a different premixed ratio of DME and EGR rate [24]

rises with IMEP because a richer mixture at high IMEP causes temperature rise with IMEP. At constant IMEP, NO<sub>x</sub> increases with the decrement in the proportion of methanol for high load operation. An adverse effect of Methanol on LTR becomes weaker with a rise in the proportion of methanol. So these reactions contribute significantly to HRR and temperature rise inside CC. NO<sub>x</sub> is almost constant for every proportion of methanol for low load operation (Zheng et al. 2004).

Oh et al. (2010) showed that NO<sub>x</sub> emissions worsened with an increased DME quantity and retarded injection timing for fixed LPG injection quantity. The authors used a dual-fuel injection strategy where DI of DME and PFI of LPG was used. NO<sub>x</sub> emissions approached zero at excessively advanced fuel injection timings (i.e., more than 200 CAD) irrespective of DME and LPG injection quantities. NO<sub>x</sub> emissions showed an increasing trend after increasing the propane portion of LPG because higher ON of propane suppressed the self-ignition of DME higher more than butane. NO<sub>x</sub> emissions in LPG DI engine were higher than DME DI engine because the mixture of port injected LPG and air resisted DME from ignition in DI of DME and PFI of LPG engine (Fig. 9.24) (Jang et al. 2009). NO<sub>x</sub> increased in the DI of LPG and PFI of DME engine because premixed DME-air mixture created fuel-rich mixture locally with favourable conditions for ignition of charge in the engine CC, leading to an increased combustion temperature. Jamsran and Lim (2016) showed that the in-cylinder temperature was increased upon increasing the DME mixing ratios. This led to the oxidation of HC and CO emissions. NO<sub>x</sub> emissions were also reduced because the temperature was lower (i.e., ~2100 K) than required for NO<sub>x</sub> formation (i.e., ~2200 K).

In the DME-gasoline dual-fuel injection strategy, self-ignition of directly injected DME spray caused the combustion of premixed gasoline. The size of DME spray in the CC was reduced when the gasoline addition was increased. This helped reduce NO<sub>x</sub> formation due to reduction in the diffusion flame zones and ultimately reducing the high-temperature zones (Cha et al. 2012). The split injection strategy of directly

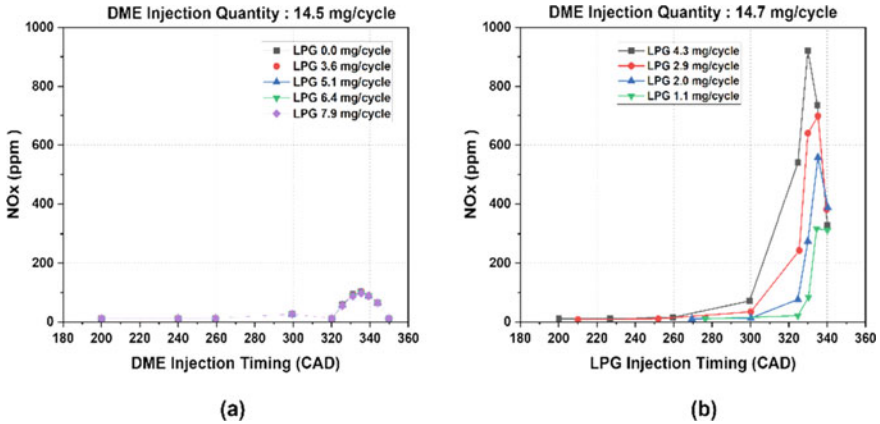


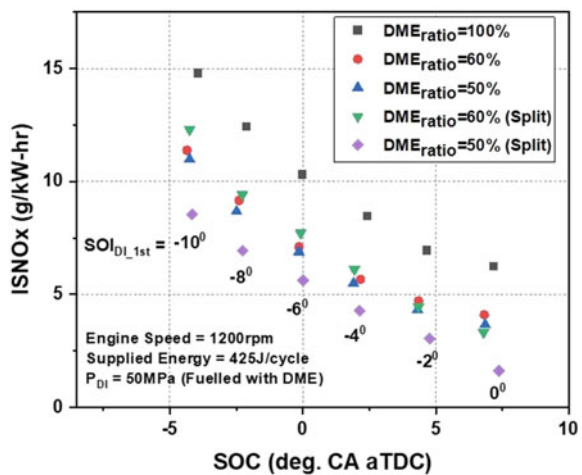
Fig. 9.24 Variations in NOx emissions for (a) DI of DME and PFI of LPG, and (b) DI of LPG and PFI of DME engines (Adapted from Jang et al. (2009))

injected DME had very little impact on the NOx emissions in the DME-gasoline dual-fuel injection strategy (Fig. 9.25) (Cha et al. 2012).

At lower DME injection quantity, NOx emissions reduced drastically because delayed combustion events caused a reduction in the in-cylinder temperatures. NOx emissions are also reduced with the use of a diluted NG-air mixture. In the case of NG-DME operated HCCI mode combustion, NOx emissions were reduced to negligible levels with a simultaneous increase in the BTE (Fig. 9.26) (Chen et al. 2000).

**HC and CO Emissions:** HC and CO emissions are intermediates in the combustion reactions of complex hydrocarbons, further oxidizing to CO<sub>2</sub> and H<sub>2</sub>O in favourable

Fig. 9.25 Variations in ISNOx at different SOI and SOI<sub>Dl\_1st</sub> timings from 100° to 0° CA bTDC in DME-gasoline dual-fuel engines (Adapted from Cha et al. (2012))





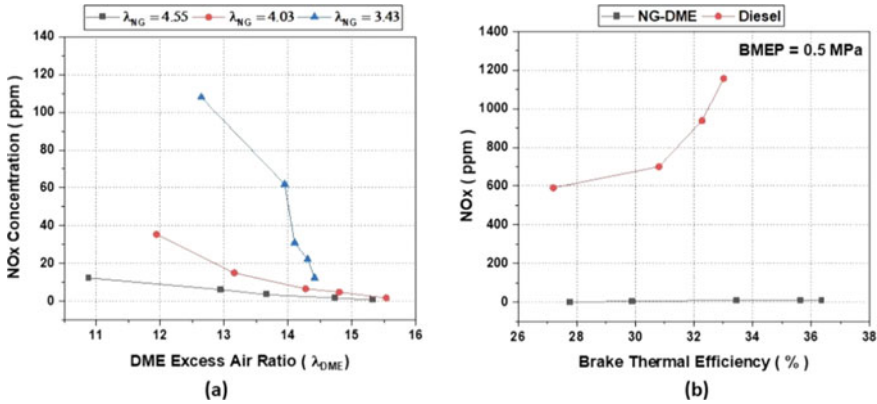


**Fig. 9.26** Variations in NOx emission by changing (a)  $\lambda_{DME}$  (b) BTE (Adapted from Chen et al. (2000))

conditions (Oh et al. 2010). HC emissions occur due to the termination of hydrocarbons oxidation reactions (Jang et al. 2009; Oh et al. 2010). HC emissions can be reduced by lean-burn combustion (Jang et al. 2009). CO is a product of partial (incomplete) combustion and forms when there are insufficient combustion reactions (Karpuk et al. 1991). Lim et al. (2010) showed that DME exhibits lower HC and CO emissions than diesel at all loads. Port injection of DME further reduces CO emission due to premixed compression ignition. HC and CO emissions reduce with the increasing temperature in the engine CC because high temperature promotes HC and CO oxidation reactions (Wang et al. 2014). Advanced fuel injection promotes complete combustion and temperature rise in the CC, leading to lower HC and CO emissions (Yeom and Bae 2007b). Wang et al. (2014) showed that CO and HC emissions increased with increasing port-injected DME quantity at fixed injection timing. Crevice region, quenching zone, piston ring and cylinder walls (where the temperature is lower due to heat transfer), and compression clearance are responsible for the emission of unburned hydrocarbons (Zhao et al. 2014; Yao et al. 2006). Zhao et al. (2014) showed that diesel-DME dual-fuel engines emit higher HC emissions than DI diesel engines because, in the HCCI mode, HC formation was more in the engine (Fig. 9.27). HCCI is a low-temperature combustion mode. There are two contradictory effects of EGR on HC emissions. HC and CO emissions increase with the introduction of EGR and further increased with the increasing EGR rate due to a reduction in the in-cylinder temperature. This happens because oxygen concentration decreases, and charge composition changes by supplying exhaust gases to the CC. However, the consumption of unburnt HC with the exhaust gas into the next engine cycle reduced overall HC emissions (Yao et al. 2006). Yao et al. (2006) showed that HC and CO emissions decreased with increased DME quantity at the same EGR rate due to the increased in-cylinder temperature. A high EGR rate requires a larger quantity of DME to reduce HC emissions. CO and HC emissions decreased with increasing IMEP (Oh et al. 2010). HC and CO emissions can be further reduced

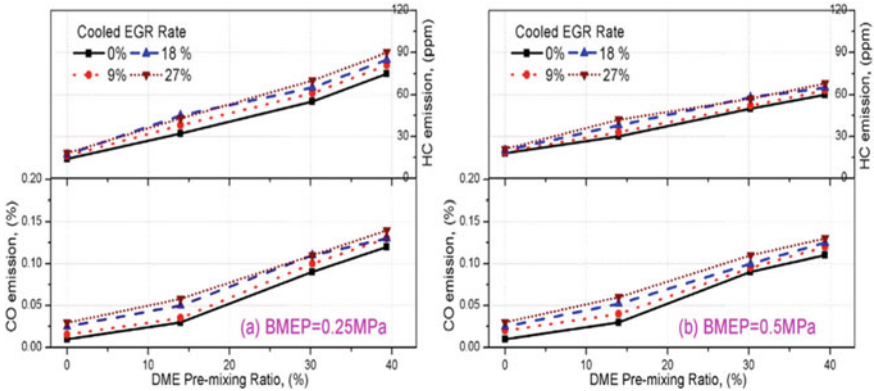


**Fig. 9.27** Variations in CO and HC emissions for DME-diesel dual-fuel engine at different premixed ratios of DME and cooled EGR rate (Zhao et al. 2014)

by introducing a larger amount of air (i.e., by turbocharging) because it promotes the oxidation of HC and CO (Zhao et al. 2014; Karpuk et al. 1991). HC emissions decreased at high load operation due to a rise in HRR and temperature, making it possible for the flame front to reach the cylinder wall and shrink the quenching zone (Yao et al. 2006; Murayama et al. 1992; Karpuk et al. 1991).

In DME-methanol dual-fuel injection strategy, a well-mixed DME-air charge permeates through the entire CC along with quench and crevice zones. Low temperature and higher heat loss in these regions increase the chain termination reactions. CO emission from DME-methanol dual-fueled engines was 30% higher than baseline diesel-fueled engines. This can be attributed to mixing some unburned charge with the hot residual gases (leftover from the combustion event) late in the expansion, exhaust, and engine strokes. The intake manifold does not have adequate time to complete the oxidation reactions (Karpuk et al. 1991). CO emission increased with too retarded DME injection timing due to incomplete combustion (Oh et al. 2010). HC emissions from DME-diesel dual-fuel engines were lower than methanol-fueled engines (Kozole and Wallace 1988). HC and CO emissions reduced drastically at higher DME percentages in the DME-methanol fueled engines (Fig. 9.28) (Yao et al. 2006).

Oh et al. (2010) showed that with too advanced DME injection timing in LPG-DME HCCI engines, the in-cylinder temperature decreased due to overall lean premixed charge, leading to higher CO emission. An increase in the HC emissions and reduction in CO emission was observed with an increased quantity of LPG while fixing all other variables. The same trend was observed with an increasing proportion of propane in the LPG. The main reason for this trend is that HC is a function of the molecular ratio of high ON fuel and high CN fuel, and CO emission is mainly affected by the combustion temperature. Large LPG quantity (i.e., higher ON fuel) increased the high ON to high CN fuel ratio, which increased HC emissions because low-temperature oxidation of high CN fuel (i.e., DME) is responsible for

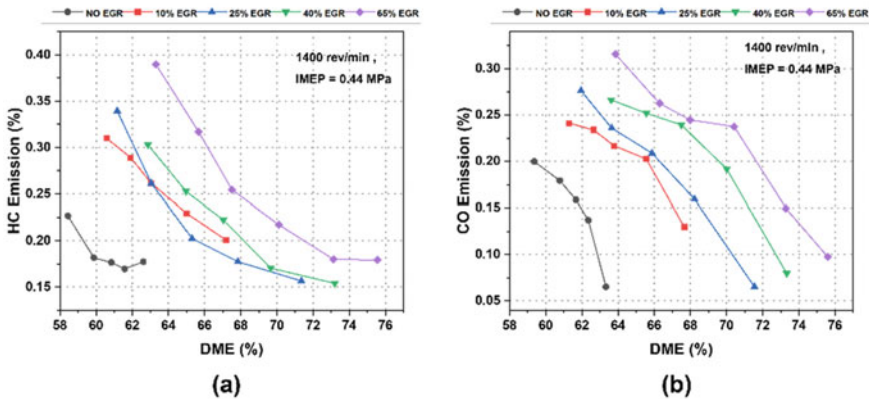


**Fig. 9.28** Variations in HC and CO emissions at different premixed ratios of DME and EGR rate in DME-methanol dual-fuel engines (Adapted from Yao et al. (2006))

rapid hydrocarbon chain termination. Higher chain termination generates more active intermediate species with a higher propane ratio due to its higher ON. CO and HC emissions in the LPG-DME HCCI engine showed an increasing trend with retarded IVO timing due to incomplete combustion (Yeom and Bae 2007a). Jang et al. (2009) showed that at too early and too late DME DI timing, HC emissions were more due to lower combustion temperature and incomplete combustion, respectively. Still, at moderate injection timing up to  $300^\circ$  CA, HC emissions were lower because the fuel oxidized more efficiently at higher combustion temperatures caused by DME fuel-rich zones inside the CC. HC emissions also increased with increased LPG quantity in the previous case. But in the LPG DI case, HC emissions were lower for all LPG injection timings because port-injected DME fuel formed a homogeneous mixture of DME-air and was self-ignited easily during the compression stroke. This caused an increase in the temperature inside the CC in the LPG DI case and allowed HC to oxidize (Fig. 9.29) (Jang et al. 2009). The CO emission followed a different trend than HC emissions in the DME DI case due to deteriorated combustion in the DME-LPG dual-fuel engine.

A higher quantity of premixed gasoline fuel was responsible for higher HC and CO emissions in DME-gasoline dual-fuel engines (Cha et al. 2012). A large amount of gasoline led to unstable combustion. HC and CO emissions were reduced with a split injection strategy by providing additional DME to reduce incomplete combustion (Fig. 9.30).

**Soot, Smoke, Particle Number (PN) & Particle Mass Emissions:** A fuel can be potentially sootless if it does not contain a C–C bond in its molecular structure. DME and methanol are such fuels. Combining such fuels doesn't produce the basic materials required to form aromatic rings and acetylenic species. Soot formation occurs from these aromatic rings, and soot grows with the help of acetylenic species (Karpuk et al. 1991).

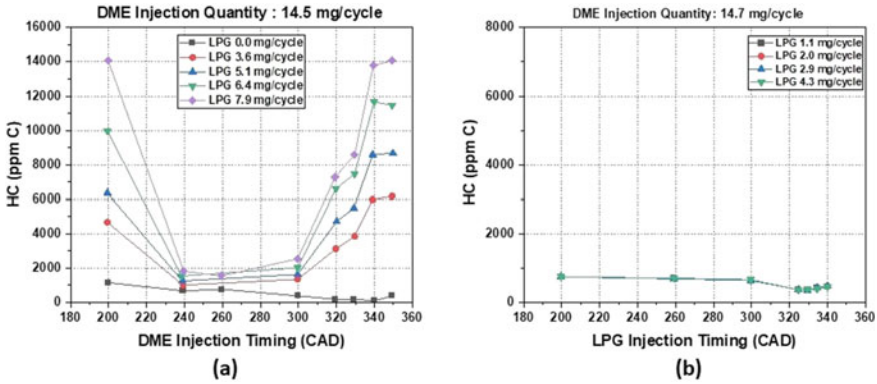
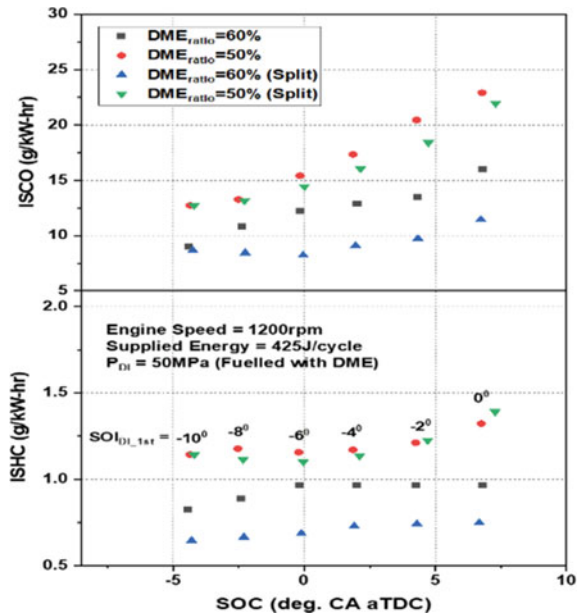


**Fig. 9.29** Variations in the HC emissions for (a) DI of DME and PFI of LPG and (b) DI of LPG and PFI of DME cases (Adapted from Jang et al. (2009))

**Fig. 9.30** Impact of split-injection strategy on CO and HC emissions at different  $SOI_{DI\_1st}$  timing varying from  $10^\circ$  to  $0^\circ$  CA bTDC (Adapted from Cha et al. (2012))



High concentrations of free radicals promote the oxidation of carbon after adding oxygenated fuel (DME), limiting carbon availability for the formation of soot precursors. Favourable conditions for soot formation are fuel-rich and high-temperature zones (Zhao et al. 2014). Smoke is also produced in the fuel-rich and high-temperature regions (Zhao et al. 2014). Black smoke showed a decreasing trend with increasing premixed DME (Theinnoi et al. 2017). Smoke showed an increasing trend with increasing EGR rate due to reduced oxygen concentration and incomplete combustion. Near zero soot emissions were observed with >20% port fuel injected

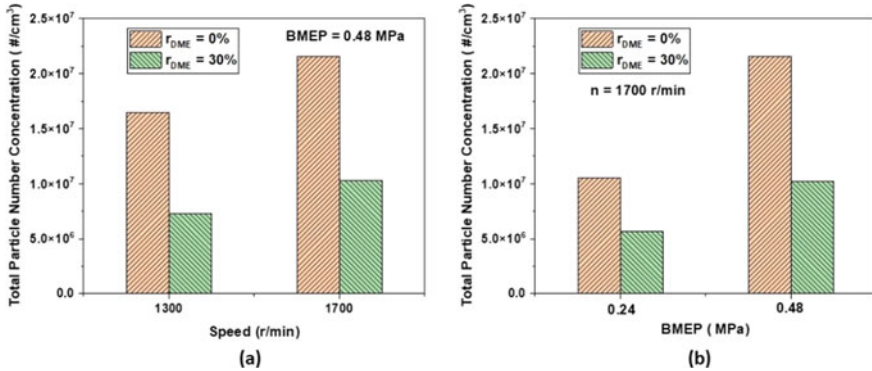


**Fig. 9.31** Effect of (a) engine speed and (b) BMEP on particulate number concentrations (Adapted from Wang et al. (2016))

DME in DME-diesel dual-fuel injection strategy (Lim et al. 2010). Early injection decreased soot emission due to homogeneous mixture formation and prolonged soot oxidation phase (Wang et al. 2014). The lower C-H ratio of DME led to complete combustion and reduction in smoke (Temwutthikun et al. 2018).

PN reduces in DME-diesel dual-fuel engines than DI CI diesel engines due to soot suppression characteristics of DME (Wang et al. 2016). Particle number concentration increases substantially with engine load at a constant speed. A higher quantity of injected fuel at a higher engine load creates fuel-rich regions, promoting higher PN due to inadequate oxygen availability. PN concentration increases slightly with increasing engine speed at constant load because lesser time is available for combustion at higher engine speeds, resulting in a larger amount of unburned fuel. This unburnt fuel is responsible for the formation of particulates (Fig. 9.31). Delayed injection timing leads to an increase in particle numbers due to a reduction in time available for fuel vaporization and consequent reduction in fuel–air mixing, which causes fuel impingement on the piston head and cylinder walls (Wang et al. 2016). The peak of the aerodynamic diameter of particulates shifts towards slightly smaller sizes in the case of DME-diesel dual-fuel engine compared to baseline DI CI diesel engine. The PM and PN concentrations reduce with increased DME injection quantity (Fig. 9.32) (Wang et al. 2016). The PM and PN reduce upon using alcohols in the dual-fuel mode.

## 9.7 Cyclic Variations in Combustion Parameters of DME Engine

HCCI combustion is dominated by chemical kinetics. A rapid charge consumption rate and earlier start of combustion cause high-pressure oscillations and knocking at higher engine loads. At lower loads, lower in-cylinder temperature and leaner

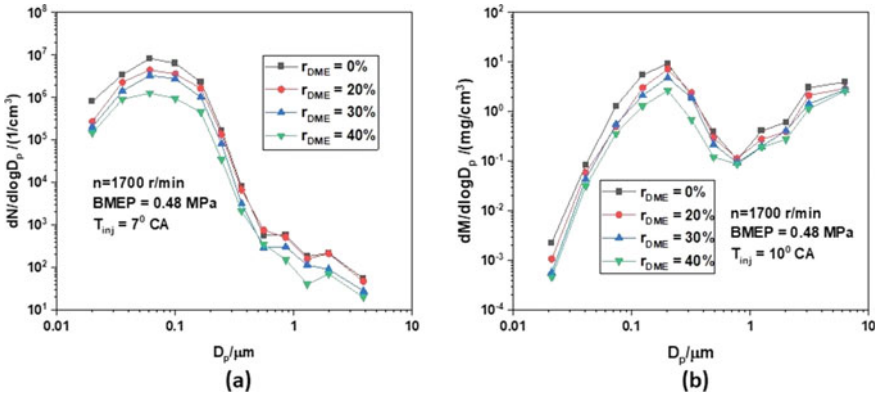


**Fig. 9.32** Variations in (a) particle number and (b) particle mass versus particulate size for varying DME premixed ratios (Adapted from Wang et al. (2016))

fuel–air mixture in the CC usually lead to engine misfire and cyclic variations. DME-diesel dual-fuel HCCI engines exhibit higher cyclic variations than the baseline DICI diesel engines (Wang et al. 2015). High cyclic variations adversely affect engine performance, reduce combustion efficiency, power output, and increase engine-out emissions. These variations are due to combustion variations and are influenced by several parameters such as in-cylinder charge motion, the composition of fuel–air mixture, cyclic cylinder charging, etc.

**Variations in in-cylinder Temperature and Pressure:** With reduced DME quantity, COV of maximum pressure ( $P_{max}$ ) and maximum temperature ( $T_{max}$ ) decreases as the quantity of port injected DME reduces due to a reduction in the knocking tendency. Cyclic variations in  $P_{max}$  are crucial for the dynamic loading of engine components. The cyclic variations of  $T_{max}$  are directly related to emissions and heat transfer from the cylinder liner, thereby controlling the  $T_{max}$  is essential for controlling all dependent parameters. Heat transfer from the liner increases with an increase in COV of  $P_{max}$ .

$P_{max}$  and  $T_{max}$  show scattered frequency distribution of cyclic variations with an increased DME quantity. The location of  $P_{max}$  and  $T_{max}$  was more distributed for the DME-dual-fuel engines compared to DI diesel engines. Crank angle corresponding to  $T_{max}$  advanced with increasing DME quantity (Fig. 9.33).

**Variations in ROHR:** Power and efficiency of an engine are a function of ROHR and its timing. The share of HCCI combustion increases, and diesel diffusion combustion decreases in DME-diesel PCCI combustion as one increases the DME quantity, reducing the maximum ROHR ( $ROHR_{max}$ ). Cyclic variations in  $ROHR_{max}$  decrease with increasing temperature and pressure due to diesel’s more complete and faster diffusion combustion. Higher DME quantity also showed similar characteristics for DME-diesel dual-fuel engines. However, cyclic variations in  $ROHR_{max}$  increased with a further increase in DME quantity after the optimum limit. HCCI combustion

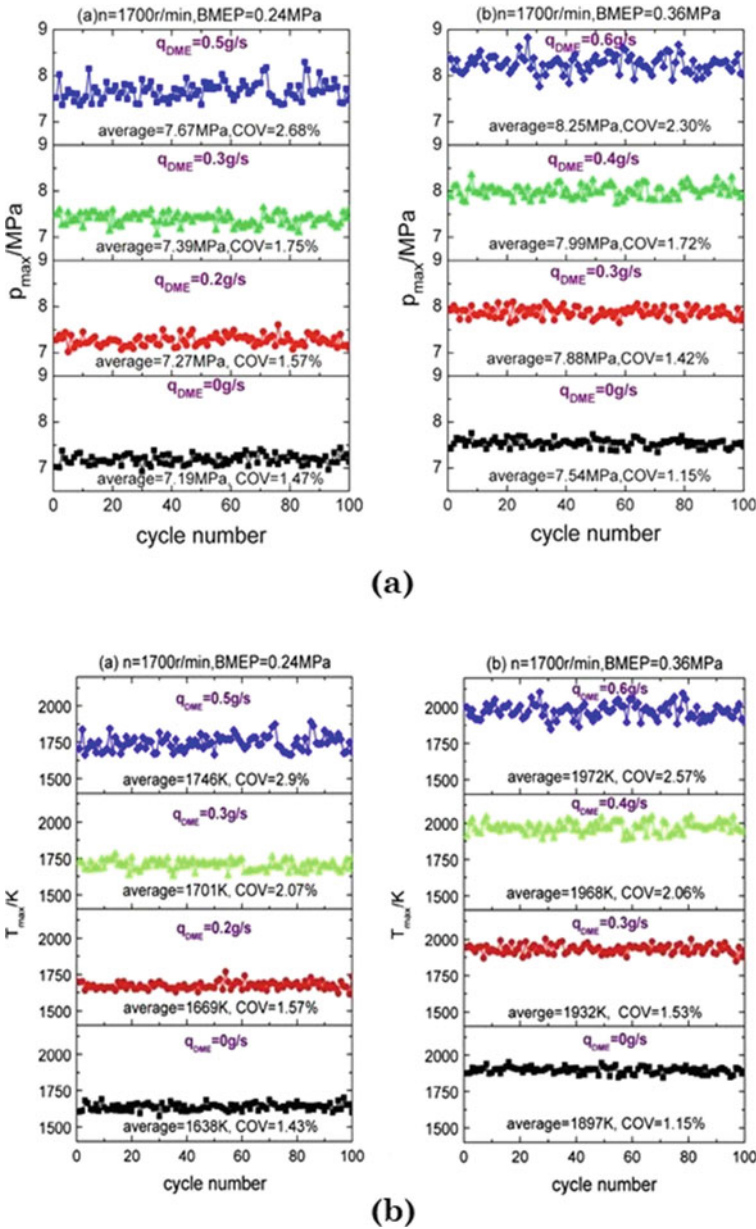


Fig. 9.33 Cyclic variations of (a)  $P_{\text{max}}$  (b)  $T_{\text{max}}$  by varying port-injected DME quantity (Wang et al. 2015)

started to govern the overall combustion, and heat release during the HCCI combustion possibly exceeded the heat released by DIC diesel combustion.  $ROHR_{max}$  appeared in the HCCI HTR zone after the optimum limit.

The frequency distribution of cyclic variations of  $ROHR_{max}$  was concentrated for the higher DME fractions but started to scatter beyond the optimum value. Crank angles corresponding to  $ROHR_{max}$  advanced with an increasing DME quantity. Crank angles for  $ROHR_{max}$  were concentrated around their average value in DIC diesel engines. However, a wider distribution was observed with the introduction of DME into the port.

**Variation in ROPR:** Maximum ROPR ( $ROPR_{max}$ ) was mainly responsible for combustion noise. The trends of variations in  $ROPR_{max}$  were similar to the variations in  $ROHR_{max}$ . COV of  $ROPR_{max}$  first decreased with an increasing DME injection quantity but increased after optimal injection quantity of DME.

Similar to  $ROHR_{max}$ , the distribution of frequency of cyclic variations of  $ROPR_{max}$  got concentrated for an increased DME quantity. A similar trend of  $ROHR_{max}$  for the variations of crank angle was seen in  $ROPR_{max}$ , as well.

**Variations in IMEP:** COV of IMEP increased with increasing DME injection quantity because, at higher DME injection quantity, DME HCCI combustion started to become a significant factor in the overall combustion process, increasing the cyclic variations in the burn rate and ignition timing (Wang et al. 2015). The frequency of cyclic variations in the IMEP was concentrated for the diesel-operated engines and scattered for the DME fueled engines.

## 9.8 Future Scope

HC and CO emissions from diesel-DME dual-fuel PCCI engines were higher than DIC diesel engines. Further research is required to reduce these emissions without compromising the advantages of diesel-DME dual-fuel engines. PFI of Diesel and DI of DME injection strategy is yet to be explored by researchers. The effect of IVO timing on various engine parameters was discussed only in some studies related to LPG-DME and gasoline-DME dual-fuel engines. The impact of IVO timing should also be analyzed for other dual-fuel pairs in the future for assessing the potential of improvement in engine performance. The effect of change in the composition of propane and butane in the LPG on various engine parameters in DME-LPG dual-fuel mode is scarcely studied.

Further research is required to cover these aspects of engine research. Less research focus has been given to DME-gasoline dual fuel operation despite several advantages. Several other fuels could be used with DME in the dual-fuel modes, such as di-ethyl ether, Biogas, CNG, and hydrogen, which need to be explored. The study of unregulated emissions is almost absent; therefore, future research should also explore unregulated emissions from various dual-fuel mode-operated engines. Very few researches have focused on dual-fuel RCCI mode combustion using DME as a high reactivity fuel. No study has been done to use dual-fuel mode operation in split



injection strategy and variations in IVO timings in conventional CI engines. There are several challenges in handling multiple fuels having different physical properties. Significant research efforts are required to bring this technology to on-road vehicles.

## 9.9 Summary

This chapter discussed various dual-fuel injection strategies for introducing DME into the engine CC along with other fuels. The effect of these strategies on various engine parameters is explored in this chapter. Diesel-fuelled CI engine emits higher PM and soot emissions. DME is one of the best alternatives to diesel in CI engines due to its high CN, absence of C–C bond that suppresses the formation of soot, and lower CO, HC, PM emissions. Some properties of DME are not favourable, which make its implementation in CI engines challenging, such as lower viscosity and inferior self-lubrication characteristics. Any fuel with high ON (low CN) can be used along with DME in dual-fuel mode. Higher ON fuel is difficult to auto-ignite; hence DME acts as an ignition promoter.

Using this method, one can expand the operating range of a single fuel DME HCCI engine by extending its knock limit via suppressing the auto-ignition characteristics of DME. There are several advantages of using different dual-fuel injection strategies. Using port injection of DME and DI of higher ON fuel helps start combustion reactions by injecting homogeneous DME-air mixture. Combustion of charge helps build perfect conditions in the engine CC to ignite directly injected high ON fuel. By varying the premixing ratio of port injected DME, many combustion parameters such as in-cylinder pressure and temperature, rate of pressure rise, HRR (LTR + HTR + diffusion), and ignition delay can be controlled. Fewer modifications are required in the existing diesel injection system while the PFI of DME can be undertaken. Combustion duration increases, and ignition timings retard with increased port-injected quantity of high ON fuel (LPG) due to decreased combustion efficiency. The effect of LPG injection becomes insignificant in LPG-DI and DME-PFI engines due to dominant self-ignition characteristics of the premixed DME-air mixture inside the CC. NO<sub>x</sub> emission reduces with an increasing DME premixed ratio till the optimum quantity of DME; however, NO<sub>x</sub> emissions increase with further increasing DME quantity because DME promotes high-temperature reactions. NO<sub>x</sub> also decreases with an increasing EGR rate. HC and CO emissions decrease with an increasing DME injection quantity and advanced fuel injection timing because complete combustion in the CC increases the in-cylinder temperature. This helps oxidize HC, and CO. HC emissions generally increase with an increasing ON/CN ratio in dual-fuel mode. Soot emission decreases with DME use. Dual-fuel combustion can be used to reduce NO<sub>x</sub> and PM emissions from existing diesel engines. These benefits come at the cost of slight modifications in the current CI engine design. Cyclic variations of different parameters such as  $P_{\max}$ ,  $T_{\max}$ , and IMEP increase, but ROHR decreases, ROPR first decreases, and then increases with an increasing DME port injection quantity in HCCI DME-diesel dual-fuel engine.

## References

- Agarwal AK, Sharma N, Singh AP (2017) Potential of DME and methanol for locomotive traction in India: opportunities, technology options, and challenges. In: Agarwal A, Dhar A, Gautam A, Pandey A (eds) *Locomotives and rail road transportation*. Springer, Singapore. [https://doi.org/10.1007/978-981-10-3788-7\\_7](https://doi.org/10.1007/978-981-10-3788-7_7)
- Arcoumanis C, Bae C, Crookes R, Kinoshita E (2007) The potential of di-methyl ether (DME) as an alternative fuel for compression-ignition engines: a review. *Fuel* 87(07):1014–1030. <https://doi.org/10.1016/j.fuel.2007.06.007>
- Cha J, Kwon S, Kwon S, Park S (2012) Combustion and emission characteristics of gasoline–dimethyl ether dual-fuel engine. *J Automobile Eng* 226(12):1667–1677. <https://doi.org/10.1177/0954407012450122>
- Chapman EM, Boehman A, Wain K, Lloyd W, Perez JM, Stiver D, Conway J (2003) Annual technical progress report for project entitled “Impact of DME-diesel fuel blend properties on diesel fuel injection systems.” The Pennsylvania state university, DOE Award Number: DE-FC26-01NT41115
- Chen Z, Yao M, Zheng Z, Zhang Q (2009) Experimental and numerical study of methanol/dimethyl ether dual-fuel compound combustion. *Energy Fuels* 23:2719–2730. <https://doi.org/10.1021/ef8010542>
- Chen Z, Konno M, Oguma M, Yanai T (2000) Experimental study of CI natural-gas/DME homogeneous charge engine.: SAE Technical Paper No. 2000-01-0329. <https://doi.org/10.4271/2000-01-0329>
- Climate Change Over the Next 100 Years. <https://clintonwhitehouse5.archives.gov/Initiatives/Climate/next100.html>. Accessed on (8 May 2021)
- Effects of Global Warming. <https://www.livescience.com/37057-global-warming-effects.html>. Accessed on (7 May 2021)
- Engineering Toolbox <https://www.engineeringtoolbox.com/>. Accessed on (21 May 2021)
- European countries banning fossil fuel cars and switching to electric cars. <https://www.roadtraffic-technology.com/features/european-countries-banning-fossil-fuel-cars/>. Accessed on (15 May 2021)
- Falco, M.D., Dimethyl Ether (DME) Production. Journal: Univ UCBM nd <http://www.oilgasportal.com/dimethyl-ether-dme-production-2>
- Global Greenhouse Gas Emissions Data. <https://www.epa.gov/ghgemissions/global-greenhouse-gas-emissions-data>. Accessed on (14 May 2021)
- Green CJ, Cockshutt NA, King L (1990) Dimethyl ether as a methanol ignition improver: substitution requirements and exhaust emissions impact. SAE Technical Paper No. 902155. <https://doi.org/10.4271/902155>
- Jamsran N, Lim O (2016) A study on the autoignition characteristics of DME-LPG dual fuel in HCCI engine. *Heat Transf Eng* ISSN: 0145-7632. <https://doi.org/10.1080/01457632.2016.1142816>
- Jang J, Yang K, Bae C (2009) The effect of injection location of DME and LPG in a dual fuel HCCI engine. SAE Technical Paper No. 2009-01-1847. <https://doi.org/10.4271/2009-01-1847>
- Kalwar A, Singh AP, Agarwal AK (2020) Utilization of primary alcohols in dual-fuel injection mode in a gasoline direct injection engine. *Fuel* 276(2020):118068. <https://doi.org/10.1016/j.fuel.2020.118068>
- Karpuk ME, Wright JD, Dippe JL (1991) Jantzen, D.E. dimethyl ether as an ignition enhancer for methanol-fueled diesel engines, SAE Technical Paper No. 912420. <https://doi.org/10.4271/912420>
- Kim DS, Kim MY, Lee CS (2004) Effect of premixed gasoline fuel on the combustion characteristics of compression ignition engine. *Energy Fuels* 18:1213–1219. <https://doi.org/10.1021/ef049971g>
- Kozole KH, Wallace JS (1988) The use of di-methyl ether as a starting aid for methanol-fueled SI engines at low temperatures. SAE Technical Paper No. 881677. <https://doi.org/10.4271/881677>

- Kumar V, Agarwal AK (2021) Material compatibility, technical challenges and modifications required for DME adaptation in compression ignition engines. In: Singh AP, Kumar D, Agarwal AK (eds) *Alternative fuels and advanced combustion techniques as sustainable solutions for internal combustion engines*. Energy, environment, and sustainability. Springer, Singapore. [https://doi.org/10.1007/978-981-16-1513-9\\_3](https://doi.org/10.1007/978-981-16-1513-9_3)
- Lee H, Lim O (2016) A computational study of DME-methanol fractions with controlling several factors on HCCI combustion. Springer. *J Mech Sci Technol* 30(4):1931–1941. <https://doi.org/10.1007/s12206-016-0352-x>
- Lim OT, Park KY, Pyo YD, Lee YJ (2010) Research on the combustion and emission characteristics of the DME/diesel dual-fuel engine. SAE Technical Paper No. 2010-32-0096. <https://doi.org/10.4271/2010-32-0096>
- Mahla SK, Das LM, Babu MKG (2010) Effect of EGR on performance and emission characteristics of natural gas fueled diesel engine. *Jordan J Mech Ind Eng*. ISSN 1995-6665. 523–530
- Morsy MH, Ahn DH, Chung SH (2006) Pilot injection of DME for ignition of natural gas at dual-fuel engine like conditions. *Int J Automot Technol*. 7(1):(1–7), 2009. 1229-9138/2006/025-01
- Murayama T, Chikahisa T, Guo J, Miyano M (1992) A study of a compression ignition methanol engine with converted dimethyl ether as an ignition improver. SAE Technical Paper No. 922212. <https://doi.org/10.4271/922212>
- Oh C, Jang J, Bae C (2010) The effect of LPG composition on combustion and performance in a DME-LPG dual-fuel HCCI engine. SAE Technical Paper No. 2010-01-0336. <https://doi.org/10.4271/2010-01-0336>
- Pal M, Kumar V, Kalwar A, Mukherjee NK, Agarwal AK (2021) Prospects of fuel injection system for dimethyl ether applications in compression ignition engines. In: Singh AP, Kumar D, Agarwal AK (eds) *Alternative fuels and advanced combustion techniques as sustainable solutions for internal combustion engines*. Energy, environment, and sustainability. Springer, Singapore. pp 11–36. [https://doi.org/10.1007/978-981-16-1513-9\\_2](https://doi.org/10.1007/978-981-16-1513-9_2)
- Park SH, Lee CS (2014) Applicability of di-methyl ether (DME) in a compression ignition engine as an alternative fuel. *Energy Convers Manage* 86:848–863. <https://doi.org/10.1016/j.enconman.2014.06.051>
- Proposal for a “Regulation of the European parliament and of the council” on the deployment of alternative fuel fuels infrastructure and repealing directive 2014/94/EU of the European parliament and the council. [https://ec.europa.eu/info/sites/default/files/revision\\_of\\_the\\_directive\\_on\\_deployment\\_of\\_the\\_alternative\\_fuels\\_infrastructure\\_with\\_annex\\_0.pdf](https://ec.europa.eu/info/sites/default/files/revision_of_the_directive_on_deployment_of_the_alternative_fuels_infrastructure_with_annex_0.pdf). Accessed on (20 Sep 2021)
- Singh AP, Kumar V, Agarwal AK (2020a) Evaluation of comparative engine combustion, performance and emission characteristics of low-temperature combustion (PCCI and RCCI) modes. *Appl Energy* 278:115644. <https://doi.org/10.1016/j.apenergy.2020.115644>
- Singh AP, Sharma N, Kumar V, Agarwal AK (2020b) Experimental investigations of mineral diesel/methanol-fueled reactivity controlled compression ignition engine operated at variable engine loads and premixed ratios. *Int J Engine Res* 1–15, SAGE. <https://doi.org/10.1177/1468087420923451>
- Sittichompoo S, Pridoung P, Sriphumma P, Songklod R, Theinnoi K (2016) Effects of DME port-injection on performances of a single-cylinder diesel engine in dual-fuel mode. The 2nd international conference on engineering science and innovative technology. Bangkok: King Mongkut’s University of Technology North Bangkok, pp 19–24
- Temwutthikun W, Suksompong P, Sridech W, Theinnoi K, Sriumpunuk P (2018) Experimental study on the behavior of a common rail diesel engine fueled with diesel—dimethyl ether dual fuel on engine performance. Third international conference on engineering science and innovative technology (ESIT). <https://doi.org/10.1109/ESIT.2018.8665332>
- Theinnoi K, Suksompong P, Temwutthikun W (2017) Engine performance of dual fuel operation with in-cylinder injected diesel fuels and in-port injected DME. *Energy* 142(2017):461–467. <https://doi.org/10.1016/j.egypro.2017.12.072>

- Valera H, Agarwal AK (2019) Methanol as an alternative fuel for diesel engines. In: Agarwal A, Gautam A, Sharma N, Singh A (eds) Methanol and the alternate fuel economy. Energy, environment, and sustainability. Springer, Singapore, pp. 9–33. [https://doi.org/10.1007/978-981-13-3287-6\\_2](https://doi.org/10.1007/978-981-13-3287-6_2)
- Wang Y, Zhao Y, Xiao F, Li D (2014) Combustion and emission characteristics of a diesel engine with DME as port premixing fuel under different injection timing. *Energy Convers Manage* 77(2014):52–60. <https://doi.org/10.1016/j.enconman.2013.09.011>
- Wang Y, Xiao F, Zhao Y, Li D, Lei X (2015) Study on cycle-by-cycle variations in a diesel engine with di-methyl ether as port premixing fuel. *Appl Energy* 143(2015):58–70. <https://doi.org/10.1016/j.apenergy.2014.12.079>
- Wang Y, Guo C, Wang P, Wang D (2019) Numerical investigation on knock combustion in a diesel–dimethyl ether dual-fuel engine. *Energy Fuels* 33:5710–5718. <https://doi.org/10.1021/acs.energyfuels.9b00695>
- Wang Y, Liu H, Huang H, Ke X (2016) Particulate size distribution from diesel–dimethyl ether dual fuel premixed compression ignition combustion engine. *J Energy Eng* 142(4). [https://doi.org/10.1061/\(ASCE\)EY.1943-7897.0000351](https://doi.org/10.1061/(ASCE)EY.1943-7897.0000351)
- What is carbon neutrality, and how it can be achieved by 2050? <https://www.europarl.europa.eu/news/en/headlines/society/20190926STO62270/what-is-carbon-neutrality-and-how-can-it-be-achieved-by-2050>. Accessed on (14 May 2021)
- World Oil Reserve. <https://www.worldometers.info/oil/html>. Accessed on (2 May 2021)
- Yao M, Chen Z, Zheng Z, Zhang B, Xing Y (2006) Study on the controlling strategies of homogeneous charge compression ignition combustion with fuel of di-methyl ether and methanol. *Fuel* 85(2006):2046–2056. <https://doi.org/10.1016/j.fuel.2006.03.016>
- Yeom K, Bae C (2007) The dual-fueled homogeneous charge compression ignition engine using liquefied petroleum gas and di-methyl ether. SAE Technical Paper No. 2007-01-3619. <https://doi.org/10.4271/2007-01-3619>
- Yeom K, Bae C (2007b) Gasoline-di-methyl ether homogeneous charge compression ignition engine. *Energy Fuels* 21:1942–1949. <https://doi.org/10.1021/ef070076h>
- Yeom K, Bae C (2009) Knock characteristics in liquefied petroleum gas (LPG)-dimethyl ether (DME) and gasoline-DME homogeneous charge compression ignition engines. *Energy Fuels* 23:1956–1964. <https://doi.org/10.1021/ef800846u>
- Zhao Y, Wang Y, Li D, Lei X, Liu S (2014) Combustion and emission characteristics of a DME (di-methyl ether)—diesel dual fuel premixed charge compression ignition engine with EGR (exhaust gas recirculation). *Energy* 72:608–617. <https://doi.org/10.1016/j.energy.2014.05.086>
- Zhao Y, Weibo E, Niu T, He J (2021) Study on combustion processes of a premixed charge compression ignition (PCCI) engine fueled with DME/diesel. *J Phys: Conf Ser* 1732:012154. <https://doi.org/10.1088/1742-6596/1732/1/012154>
- Zheng Z, Yao M, Chen Z, Zhang B (2004) Experimental study on HCCI combustion of dimethyl ether (DME)/methanol dual fuel. SAE Technical Paper No. 2004-01-2993. <https://doi.org/10.4271/2004-01-2993>

# Chapter 10

## Prospects and Challenges of DME Fueled Low-Temperature Combustion Engine Technology



Shanti Mehra and Avinash Kumar Agarwal

**Abstract** The ever-increasing demand for energy, the exhaustible nature of conventional fuels, and increasing pollution have led to an immediate search for clean, sustainable, and renewable alternative energy sources. DME is one such alternative fuel that is quite promising for internal combustion (IC) engines because of several advantages over conventional fuels. DME is the ultimate next-generation e-fuel since it can be produced from renewable feedstocks such as agricultural, municipal sewage waste, and many kinds of biomass fuels by direct and indirect synthesis. However, DME-fueled IC engines have few limitations, e.g., high  $\text{NO}_x$  emissions, which need to be overcome to expand their usage in production-grade engines. In addition to environment-friendly fuel, there is also a need to investigate emerging, innovative combustion technologies capable of meeting fuel economy targets and complying with the prevailing stringent emission norms. Engines with low-temperature combustion (LTC) concepts are highly efficient and environmentally friendly and offer promising alternatives to conventional combustion engine technologies. Homogeneous charge compression ignition (HCCI), partially premixed charge compression ignition (PCCI), Reactivity controlled compression ignition (RCCI), and gasoline compression ignition (GCI) are a few of the LTC variant technologies, which should be investigated for DME to combine both cleaner and efficient engine technology and environment-friendly alternative fuel. HCCI engine technology is an ideal LTC engine technology with higher efficiency. However, there are some limitations of HCCI engine technology, such as limited operational range. Hence, other LTC engine technologies are being widely investigated. PCCI engine technology is one of them. Factors such as lean premixed charge, high compression ratio, and multi-point spontaneous ignition lead to excellent fuel economy and low  $\text{NO}_x$  emissions. Another LTC engine technology is the RCCI, which uses two different fuel reactivities to achieve excellent engine efficiencies. Low reactivity fuels such as natural gas can be used along with high reactivity fuels such as DME, yielding lower  $\text{NO}_x$  and

---

S. Mehra · A. K. Agarwal (✉)

Engine Research Laboratory, Department of Mechanical Engineering,  
Indian Institute of Technology Kanpur, Kanpur 208016, India  
e-mail: [akag@iitk.ac.in](mailto:akag@iitk.ac.in)

PM emissions, reducing heat transfer loss, and increasing engine efficiency. Moreover, the RCCI technology leads to an elimination of the need for expensive exhaust gas after-treatment systems. This chapter examines the concepts of various LTC engine technologies and their performance and emission characteristics, underlying challenges, and way forward for using DME as a fuel in IC engines.

**Keywords** Dimethyl Ether · Low-temperature combustion · Homogeneous charge compression ignition · Partially premixed charge compression ignition · Reactivity controlled compression ignition · Exhaust gas recirculation

## Abbreviations

CI	Compression ignition
CIDI	Compression ignition direct injection
DI	Direct injection
DME	Dimethyl ether
EGR	Exhaust gas recirculation
HCCI	Homogeneous charge compression ignition
HRF	High reactivity fuel
HRR	Heat release rate
LRF	Low reactivity fuel
LTC	Low-temperature combustion
PCCI	Premixed charge compression ignition
PFI	Port fuel injection
RCCI	Reactivity controlled compression ignition
RoPR	Rate of pressure rise
SI	Spark ignition
UHC	Unburned hydro carbon

## 10.1 Introduction

The usage of DME as fuel in low-temperature combustion (LTC) engines is a significant area of research since it can lead to efficient and very clean combustion delivering an excellent fuel economy.

### 10.1.1 Properties, Advantages, and Use of DME in IC Engine

#### DME Properties

DME is the simplest ether compound with a chemical formula  $\text{CH}_3\text{-O-CH}_3$ . DME is a highly flammable gas under normal ambient conditions (temperature 298 K and pressure 0.1 Mpa). However, at standard atmospheric temperature and when pressure is increased above 0.5 MPa, it gets liquified (Park and Lee 2013). It is colourless but burns with a visible blue flame, therefore inherently safe during combustion. DME is quite similar to LPG in storage, handling, distribution, and safety aspects. It has a higher cetane number (55–60) than diesel (40–55). Therefore, it has emerged as a good alternative for CI Engines. DME, due to its very low freezing point ( $-141\text{ }^\circ\text{C}$ ), has excellent cold-working characteristics. DME is more compressible than other hydrocarbons since its bulk modulus is lower than other hydrocarbon fuels (Park and Lee 2014) (Table 10.1).

#### Advantages of DME Fueled Vehicles

DME is a non-toxic and environmentally benign compound. The majority of hydrocarbon fuels can be mixed with DME. It can be produced from various feedstocks such as coal, natural gas, and renewable feedstocks such as many kinds of biomass fuels (Huang et al. 2009) (Fig. 10.1).

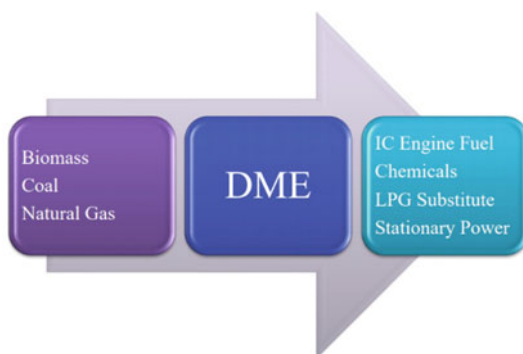
DME has no C–C bonds in its molecular structure, leading to an almost smoke-free combustion. Also, each molecule of DME has an oxygen atom, which leads to superior and complete burning with ultra-low soot emission. The DME combustion

**Table 10.1** Physical and chemical properties of DME and diesel fuel (Park and Lee 2014)

Property	DME	Diesel
Chemical formula	$\text{CH}_3\text{OCH}_3$	$\text{C}_8\text{-C}_{25}$
Molecular weight	46.07	96~
Vapor pressure at 20 °C (bar)	5.1	<0.01
Boiling temperature (°C)	- 25	≈150–380
Liquid density at 20 °C (kg/m <sup>3</sup> )	660	800–840
Liquid viscosity at 25 °C (kg/ms)	0.12–0.15	2–4
Gas specific gravity (vs air)	1.59	–
Lower heating value (MJ/kg)	28.43	42.5
Cetane number	55–60	40–55
Stoichiometric A/F ratio (kg/kg)	9.0	14.6
Enthalpy of vaporization at NTP <sup>a</sup> (kJ/kg)	460 ( $-20\text{ }^\circ\text{C}$ )	250

<sup>a</sup>Normal temperature and pressure

**Fig. 10.1** A schematic of a future fuel supply chain, DME plays a central role in deriving fuel from different feedstocks for various applications. Adapted from Sorenson (2001)



has no significant emissions of polycyclic aromatic hydrocarbons (PAHs), benzene, and toluene. The  $\text{SO}_2$  formation is nearly zero because of the absence of sulfur in DME. The higher latent heat of DME reduces the  $\text{NO}_x$  concentration because the injected liquid DME spray absorbs heat during evaporation (Park and Lee 2014). DME has considerably lower initial rates of pressure rise and maximum pressure than baseline diesel. Therefore, DME engines/ vehicles exhibit significantly lower combustion noise and are quieter than diesel engines/ vehicles. DME is non-corrosive to metals and does not require special materials for its tank and fueling system designs.

### Safety Aspects of DME

For decades, DME has been used as propellants in aerosol cans, as cooking fuel, solvent, and medical treatment (Park and Lee 2014). In addition, DME is an environmentally benign compound. It doesn't have any carcinogenic, teratogenic, or mutagenic effects upon exposure; however, it has a slight narcotic effect. It is not only a non-greenhouse gas but also degrades easily in the troposphere. DME's handling and storage are similar to LPG since DME is a gas at atmospheric temperature and pressure conditions and is a liquid when pressurized above 0.5 MPa. DME is susceptible to leakage at normal temperature because of its high vapour pressure. Also, DME has a higher density than air which poses further safety challenges. DME tends to dissolve elastomers. Therefore, most sealing materials used in conventional fuel pumps and high-pressure injection pumps dissolve and swell when exposed to DME, resulting in leakages from the high-pressure DME fuel supply system. Therefore, the selection of DME-compatible materials is of prime importance for designing leakage arrestors for DME injection systems.

Moreover, level sensors that are used for safety monitoring have a reduced lifetime with DME. Frequent inspections and replacements of fuel components, if required, are necessary for DME fueled engines. The lubricity of DME can be increased with surface film-forming additives. DME's viscosity must also be increased to prevent premature frictional wear of the injection system and internal leakage problems. Additives such as Lubrizol, Hitec, Infinium R655, etc., can be added to improve the viscosity and lubricity of DME. Careful attention needs to be given to the lubricity



additives mixed with DME as they can adversely affect the generation of oxygen-based compounds. DME tanks are pressure vessels that are more rugged than conventional diesel tanks; thus, the risk of tank failure is relatively low. However, potentially more severe consequences may occur in case of tank failure. Firefighters will be required to receive special training on extinguishing a DME-fed fire since the improper technique can lead to explosions.

### **Use of DME in Engines/Vehicles**

Development and usage of DME trucks are being done across the world currently (Park and Lee 2014). Various DME-fueled vehicles such as mini-buses and light, medium, and heavy-duty trucks have been developed in Sweden, Denmark, Japan, China, USA, and Korea. Many countries have successfully tested the vehicles on the roads under actual driving conditions. In Europe, DME-fueled vehicles were first developed by Haldor Topsoe (Denmark) in 1996. By the year 1998, DME-fueled engines complying with EURO-4 emission standards were developed. In 1999, Volvo developed the first DME-fueled bus in Sweden. Between 1999 and 2001, in North America, a consortium of Pennsylvania State University, Air Products and Chemicals, Inc., Department of Energy (DOE), Navistar International, and Caterpillar developed a project to operate diesel buses on DME. They used a shuttle bus with a displacement volume of 7.1 L and a turbocharged intake system (Eirich et al. 2003). In Asia, between 1998 and 2001, a consortium led by the National Traffic Safety and Environment Laboratory (NTSEL) with Nissan diesel motors and Bosch Japan developed a heavy-duty DME bus with a mechanical fuel injection system. In China, in 2005, a consortium of Shanghai Motor Company, Shanghai Jiao Tong University (SJTU), and Shanghai Coking & Chemical Corporation developed a DME filling station and 10 DME-fueled buses. A DME engine research project was started by the Korea Institute of Energy Research (KIER) in 2000. In three years, they developed a prototype DME truck with a displacement volume of 3 L. In addition, they developed a prototype DME bus for 33 passengers with 8.071 L displacement in 2005. This bus was successfully driven on the road in 2010. In India, a pilot plant has been set up to produce DME from methanol dehydration in National Chemical Laboratory, Pune. Bureau of Indian Standards has notified 20% DME blending with LPG. According to NITI Ayog, Rs. 6000 Crore can be saved annually by blending 20% DME in LPG. This would result in a saving of Rs. 50 to 100 per cylinder to the consumer.

The latest policy drafted by the European Union (EU) in the Renewable Energy Directive (REDII), targets nearly 32% usage of renewable energy by the year 2030 (<https://eur-lex.europa.eu/legal-content/EN/TXT/PDF/?uri=CELEX:32018L2001&from=fr>). However, a proposal of the European Parliament and the council states that this target is insufficient and needs to be increased to 38–40% for meeting the Climate Target Plan (CTP) ([https://ec.europa.eu/info/sites/default/files/amendment-renewable-energy-directive-2030-climate-target-with-annexes\\_en.pdf](https://ec.europa.eu/info/sites/default/files/amendment-renewable-energy-directive-2030-climate-target-with-annexes_en.pdf)). The proposal for the revision of REDII is consistent with the energy efficiency directives, which contribute to the efficient use of renewable energy in end-use sectors. It is also consistent with the fuel quality directive, which supports renewable and low-carbon



**Fig. 10.2** A DME-powered mack truck. Adapted from ([https://www.greencarmjm.p;\[‘congress.com/](https://www.greencarmjm.p;[‘congress.com/”))

fuels in transport. This policy and revised proposal are important for developing low-carbon fuels like DME and DME fueled vehicles. With the development of adequate infrastructure for DME’s supply and distribution system, DME-fueled vehicles have the potential to become a suitable and sustainable replacement for conventional CI engine-powered vehicles (Singh et al. 2018) (Fig. 10.2).

### ***10.1.2 DME Spray Characterization***

DME develops a highly evaporating spray upon injection into the combustion chamber due to its very low boiling point. This results in good atomization and rapid fuel–air mixing. The formation of a homogenous mixture leads to complete combustion (Yu and Bae 2003). The microscopic and macroscopic spray characteristics of DME are studied to understand its spray morphology and spray characterization.

## Macroscopic Spray Characteristics

### *Spray Tip Penetration*

Spray penetration length is the maximum length from the nozzle tip to the farthest point on the spray plume, where the spray diminishes. It should be of optimum value since a longer penetration length leads to spray plume hitting the wall resulting in a breakup of lubrication oil layer resulting in higher engine wear and soot formation. In contrast, a shorter penetration length leads to an inefficient air–fuel mixture formation resulting in improper combustion. Spray tip penetration of DME increases with an increase in fuel injection pressure (FIP) due to the rise in inertia or momentum of fuel. Spray tip penetration of DME is lesser than diesel because of the low viscosity and low density of DME. Spray tip penetration reduces with an increase in ambient chamber pressure (Lee et al. 2001). On increasing the injection angle, spray tip penetration decreases. A narrow injection angle accumulates the fuel near the piston bowl, which results in the complete combustion of DME and the production of more power output.

### *Spray Cone Angle*

Spray Cone angle is a measure of the extent of dispersion of the spray cone. DME is a highly dispersive fuel and therefore has a large cone angle. The spray cone angle increases with an increase in the ambient pressure. In the experiment on DME spray characteristics in a common-rail fuel injection system, the spray angle is obtained by calculating the mean of all the spray cone angles created from the five nozzle holes. During atmospheric chamber conditions, the spray cone angle decreases with an increase in the injection pressure (Yu et al. 2002).

### *Spray Area*

The spray area is calculated by post-processing the spray image captured by a high-speed camera. It is defined as the area covered by spray droplets within the spray regime. With an increase in the injection pressure, the vaporizing region of the DME spray increases regardless of the chamber pressure conditions. At higher chamber pressures, the area of the vapour phase decreases (Hwang et al. 2003).

## Microscopic Spray Characteristics

### *Spray Droplet Size*

Droplet is assumed to be spherical, and its size is measured by various diameters such as arithmetic mean diameter, volume mean diameter, and Sauter mean diameter (SMD). On increasing the ambient pressure, the droplet size decreases due to the higher drag offered by ambient air. Small size droplet promotes the formation of the homogeneous fuel–air mixture. At any instant, the overall SMD is calculated by taking the mean of all measuring droplets. The smaller-sized droplets of DME evaporate quickly and mix with ambient air, leaving the larger droplets to be included in the calculations resulting in large SMD values for DME. This shows that the fuel

temperature and ambient gas temperature affect the increase in the overall SMD (Lee et al. 2001). For the comparison of diesel and DME fuels, spray characteristics were performed under the test conditions of 70 MPa (injection pressure), 1 MPa (ambient pressure), and 1.0 ms (energizing duration). The average SMD values for DME and diesel were 16.9  $\mu\text{m}$  and 28.9  $\mu\text{m}$ , respectively (Park et al. 2011a).

### *Spray Droplet Velocity*

Droplet velocity increases with an increase in FIP because of an increase in driving force. Droplet velocity increases to a maximum value due to momentum, then decreases due to evaporation and destabilizing force in the high-pressure chamber. Higher droplet velocity will lead to higher drag force resulting in droplets of small size. Droplet velocity reduces with an increase in ambient pressure. Suh and Lee (2008) performed an experimental and analytical study on the spray characteristics of DME and diesel. They found that around 20 mm downstream of the nozzle exit, diesel droplets have under 17 m/s droplet velocity. For DME, the distribution of droplets velocity was over 10 m/s. 40 mm downstream of the nozzle exit, the droplet velocity distributions increased for diesel to over 20 m/s. Whereas for DME, the droplet velocity decreased slightly due to greater fuel atomization. The comparison results between diesel and DME showed that diesel exhibited a faster spray droplet velocity than DME.

## **10.1.3 LTC Engine Concept**

Once an alternative fuel is chosen, there is a need to investigate innovative combustion technologies capable of delivering fuel economy and meeting prevailing stringent emission norms. Various LTC engine technologies have proven to be highly efficient, environmentally friendly, and promising alternatives to conventional combustion modes (Singh and Agarwal 2018). HCCI, PCCI, and RCCI are examples from many, which will be explored further in this chapter. We will explore these concepts one by one, including the advantages and challenges they face.

### **Homogeneous Charge Compression Ignition (HCCI)**

HCCI combustion is a noble LTC engine technology in which a well-mixed charge of fuel and air is compressed to auto-ignite, resulting in lower  $\text{NO}_x$  and PM emissions (Gowthaman and Sathiyagnanam 2017). In addition, HCCI engine technology offers very low cyclic variations and good fuel economy. However, there is a need for ignition timing control since the operational range of HCCI mode is rather limited. In addition, HC and CO emissions are quite high, and there are no direct means to initiate the ignition. Once the ignition starts, there is a very rapid rise in the heat release rate.

### **Premixed Charge Compression Ignition (PCCI)**

The combustion phasing in HCCI engine technology cannot be adequately controlled, leading to newer LTC concepts. The fuel is directly injected into the engine cylinder in the PCCI concept to form a homogeneous premixed charge. Parameters such as pilot injection, fuel injection pressure, and temperature inside the cylinder predominantly determine the ignition characteristics of this premixed charge (Singh et al. 2020). In PCCI, the premixed combustion is more important than the mixing-controlled combustion. PCCI engine technology has relatively better combustion control than the HCCI engine technology. The engine performance is also superior. However, the  $\text{NO}_x$  and soot emissions are higher than the HCCI engine technology at high loads. At low and medium engine loads, the PCCI engine technology offers superior emission characteristics, though. Still, a high rate of pressure rise (RoPR) at higher engine loads leads to severe knocking. This knocking severely limits the application of PCCI engine technology in production-grade engines.

### **Reactivity Controlled Compression Ignition (RCCI)**

To control the limitations of HCCI and PCCI engine technologies, yet another advanced variation of LTC, i.e., RCCI combustion, was developed. RCCI is a dual fuel combustion engine technology, using two fuels of different reactivities known as low reactivity fuel (LRF) and high reactivity fuel (HRF). The principle of RCCI engine technology is based on direct injection of the HRF into the cylinder while the LRF is inducted into the intake manifold (Maurya et al. 2018). The high reactivity fuels such as DME control the ignition and combustion characteristics of LRF, such as natural gas. The brake thermal efficiency (BTE) is higher in RCCI combustion than in HCCI combustion.

## **10.2 DME Fueled LTC Engine Technologies**

### ***10.2.1 DME Fueled HCCI Combustion***

HCCI engine technology is a promising alternative to conventional engine technologies since it combines the principles of both spark ignition (SI) and compression ignition (CI) engines. In an SI engine, the premixed fuel–air mixture is directly injected into the cylinder, after which it auto-ignites, similar to a CI engine. The HCCI engines have higher thermal efficiency than a traditional SI engine and a lower  $\text{NO}_x$ , PM, and soot than a traditional CI engine. The excess air in the HCCI engine technology leads to a low combustion temperature, consequently reducing  $\text{NO}_x$  emissions. Due to the homogeneously lean charge, particulate emissions are low. Also, the flame temperature is relatively low, which lowers the soot formation (Jang et al. 2013). However, due to homogenous charge and simultaneous auto-ignition at numerous sites within the cylinder, there is an excessive RoPR and heat release rate (HRR). This leads to pressure ringing and even knocking in the engine at times (Luong et al. 2015). In

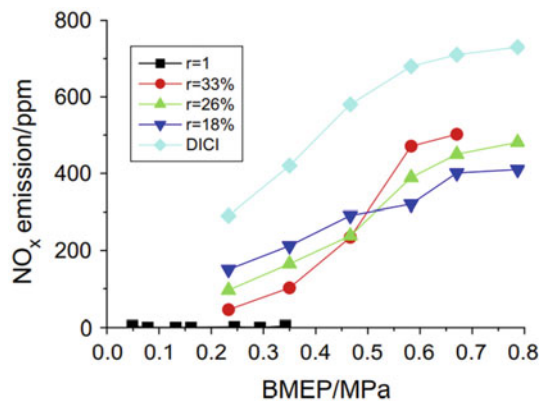
addition, the HCCI engine technology has a narrow operating range and therefore, cannot be used reliably over the full engine load spectrum. There are problems with HCCI in both high and low load conditions. The combustion efficiency is relatively low at low load, leading to improper combustion and misfire, leading to a significant increase in the HC and CO emissions (Putrasari et al. 2017).

Another technical challenge for HCCI is its inability to control the auto-ignition timing, a crucial parameter for engine performance. There is no precise control on the start of combustion and HRR. With all these challenges, investigations are on for using DME in HCCI combustion engines. DME has good ignitability and can prevent fuel adhesion to the cylinder surface while maintaining a stable ignition in the HCCI engine (Ogawa et al. 2003a).

### DME Fueled HCCI-DI Combustion

The main challenge with DME fueled engines is to reduce the  $\text{NO}_x$  emissions to comply with the most stringent emission norm. Other challenges are to control the start of combustion and the HRR. Unburned HC and CO emissions are also high from the DME fueled engines (Ying et al. 2009). One approach to overcome these limitations is combining HCCI engine technology and conventional DI engine technology to use the DME, which is referred to as the ‘HCCI-DI engine technology.’ HCCI-DI engine technology adds the benefits of the HCCI engine and expands its operational range by using DI. Different premixed ratios can be obtained by adjusting the amount of fuel directly injected into the cylinder and the amount injected in the port. When the equivalence ratio is kept high in a DME fueled HCCI engine, it reduces local temperature and overall temperature, which then suppresses the formation of thermal  $\text{NO}_x$ . Thus,  $\text{NO}_x$  emissions over the whole load range are negligible from a DME HCCI engine. However, a narrow range exists for the HCCI engine technology. Therefore, to increase the load range, the HCCI-DI engine technology can be used. With HCCI-DI mode, the  $\text{NO}_x$  emissions are more than HCCI mode but lower than the conventional CIDI mode. With increased DME in port aspiration,  $\text{NO}_x$  emissions decrease substantially at low loads while increasing at high loads (Fig. 10.3). The

**Fig. 10.3**  $\text{NO}_x$  emissions for HCCI mode and HCCI-DI mode operation with different premixed ratios ( $r$ ) (Ying et al. 2009)



reason is the trade-off between  $\text{NO}_x$  reduction during HCCI engine technology and  $\text{NO}_x$  increase during DICI engine technology.

The CO emission from HCCI-DI engine technology is lower than HCCI engine technology. However, with an increased port aspirated quantity of DME, CO emission also increased. This happened because for the HCCI-DI engine, the equivalence fuel-air ratio has a much wider range than the HCCI engine technology (Chapman and Boehman 2008) (Fig. 10.4).

The HC emissions for the HCCI-DI engine were much lower than the HCCI engine technology. Therefore, HCCI engine technology can prove efficient in further oxidation of unburnt HC molecules produced at the premixed homogenous charge combustion stage (Amann et al. 2006) (Fig. 10.5).

*Effect of Cooled EGR on HCCI-DI Combustion*

EGR reduces the  $\text{NO}_x$  emissions from traditional CI engines. EGR also helps in controlling the rate of combustion and ignition timing in the HCCI engines. Moreover, EGR affects the combustion and emission characteristics of an engine

**Fig. 10.4** CO emission for HCCI and HCCI-DI mode operation with different premixed ratios ( $r$ ) (Ying et al. 2009)

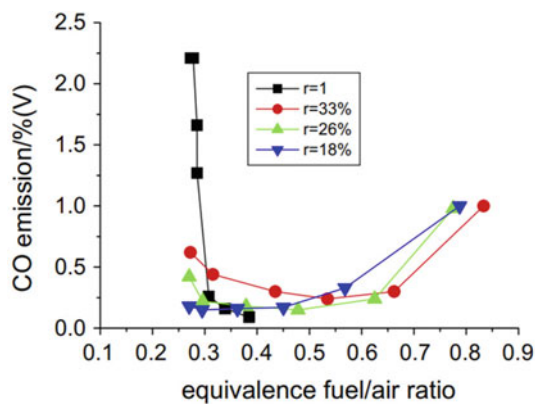
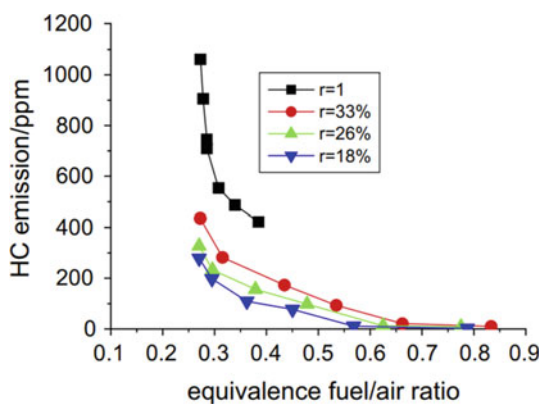


**Fig. 10.5** HC emissions for HCCI and HCCI-DI mode operation with different premixed ratios ( $r$ ) (Ying et al. 2009)



(Zhao et al. 2001). It is seen that the heat capacity of the fuel–air mixture increases with an increasing EGR rate. Consequently, the RoPR during the compression stroke decreases. The fuel concentration gets reduced to show a dilution effect. The quantity of various gases such as CO<sub>2</sub>, CO, NO, and H<sub>2</sub>O present in the EGR increases the final product concentrations, preventing oxidation reactions (Ying et al. 2009).

On the other hand, reverse reactions are promoted. Because of all these effects in the HCCI-DI engine technology, overall combustion duration gets delayed since combustion is initially postponed. Thus, with the help of low-temperature reactions in the HCCI-DI engine technology, EGR suppresses the highly advanced start of combustion (SoC). The knocking, which limits the operating range of HCCI due to excessively advanced and rapid combustion, can also be overcome. Therefore, EGR can successfully expand the operational range of HCCI-DI engines (Fig. 10.6).

With EGR, the emissions of NO<sub>x</sub> decrease while the emissions of HC and CO increase slightly in the HCCI engines (Fig. 10.7).

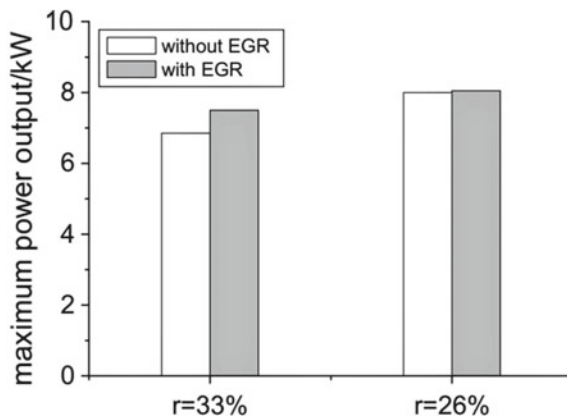


**Fig. 10.6** Effect of EGR on the maximum power output of the HCCI-DI combustion engine (Ying et al. 2009)

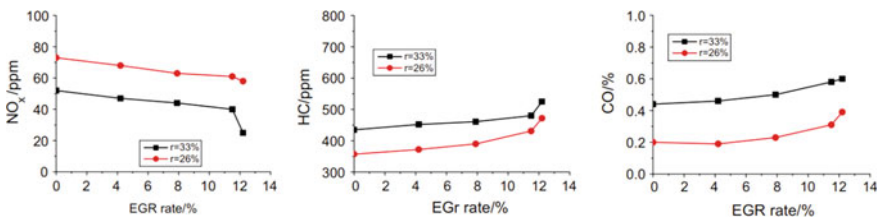


**Fig. 10.7** Effect of EGR on the emissions of HCCI-DI engine technology with different premixed ratios (r) (Ying et al. 2009)



### **Advantages of DME Fueled HCCI Combustion**

DME as a fuel is used in HCCI engines because it has a high cetane rating, no C–C bond, an ‘O’ atom in each molecule, and it evaporates easily and mixes well with the air. Therefore, it leads to negligible soot formation in the engine combustion chamber since the formation of fuel-rich zones gets prevented.

Under the same operating conditions, the ignition delay is shorter for DME-fueled HCCI engine technology than diesel-fueled HCCI engine technology since DME evaporates more quickly than diesel. The benefit of a shorter ignition delay of DME is that ignition timing can be easily controlled with the help of various schemes such as fuel–air mixing, exhaust gas recirculation, and the use of additives (Jang et al. 2013).

### **Challenges of DME Fueled HCCI Combustion**

Some operational issues with DME-fueled HCCI combustion inhibit the widespread implementation of this LTC engine technology. First, the limited power output is a serious challenge with DME-fueled HCCI engines. Second, the combustion rate is controlled by parameters such as temperature and pressure in the cylinder, the ratio of air and fuel, and the dilution level. The rate of the maximum pressure rise increases with the fueling rate, which limits the load. The HCCI engine encounters knocking upon the occurrence of explosive combustion.

Consequently, knocking leads to engine damage and excessive noise. Also, using EGR with HCCI has disadvantages, such as the rapid burning rate of EGR forming constituents like CO<sub>2</sub> and H<sub>2</sub>O, thus increasing the unburned HC and CO emissions, subsequently lowering the power output. If the intake pressure is boosted for increasing the load range, the fuel autoignition reactivity gets intensified.

## ***10.2.2 DME Fueled PCCI Combustion***

HCCI engine technology with EGR can be superior; however, it is complex, expensive, and restrictive in use. In addition, there are some operational challenges, such as the inability to control the HRR and relatively higher HC and CO emissions. As discussed previously, these issues motivate exploring another LTC engine technology, namely premixed charge compression ignition (PCCI), which is an intermediate between the HCCI engine technology and the conventional CI engine technology. A partially homogenous fuel–air mixture is prepared in the PCCI engine by injecting the fuel early during the compression stroke (Agarwal et al. 2021a). The PCCI engine technology exhibited superior combustion control than conventional CI combustion but has a limitation of emitting slightly higher NO<sub>x</sub> and PM emissions. With the help of a high EGR rate, multiple injections and additives, optimization of fuel injection parameters such as the start of injection timing and FIP, this limitation of PCCI engine technology can be overcome (Singh et al. 2021a).

### DME Fueled PCCI-DI Combustion

Using DME as a fuel in PCCI-DI engines leads to a wider range of engine speeds and loads (<https://worldwidescience.org/>). Moreover, the BTE also increases than the baseline DME fueled CI engine. Also, DME fueled PCCI-DI combustion lowers the NO<sub>x</sub> emissions effectively for all loads. In PCCI-DI engine technology, fuel injection is divided into pilot fuel injection and main fuel injection. The pilot DME fuel forms a partially homogenous mixture with air and is injected into the cylinder via the intake port. The ignition of the charge takes place simultaneously at multiple sites at suitable fuel–air ratios and in-cylinder temperatures. Experiments were performed on the DME-fueled PCCI-DI engine using part DME as the primary fuel and other part DME as the pilot fuel (Ying et al. 2010). In these experiments, it is seen that the increase in the pilot DME fuel quantity leads to the following effects:

1. At low loads, NO<sub>x</sub> emissions decrease, while at high loads, they increase.
2. The HC and CO emissions show an increasing trend irrespective of load.
3. The maximum pressure and highest heat release rate were also observed.
4. The combustion duration was shortened.
5. Maximum power output was achieved without knocking.
6. At low and medium loads, the brake thermal efficiency was comparable to DME CIDI, and at high loads, it was higher than DME CIDI (Figs. 10.8, 10.9 and 10.10).

### DME Fueled Port PCCI

Port PCCI combustion mode is yet another possible approach to achieve cleaner combustion and higher efficiency. The reasons for choosing gaseous DME as fuel are its low boiling point and excellent ignition delay characteristics (Wang et al. 2013).

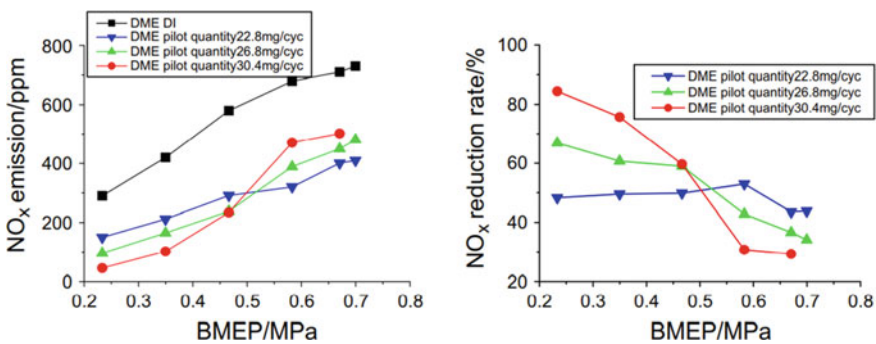


**Fig. 10.8** Effects of pilot fuel quantities on NO<sub>x</sub> emissions of PCCI-DI engine at n = 1400 rpm (Ying et al. 2010)

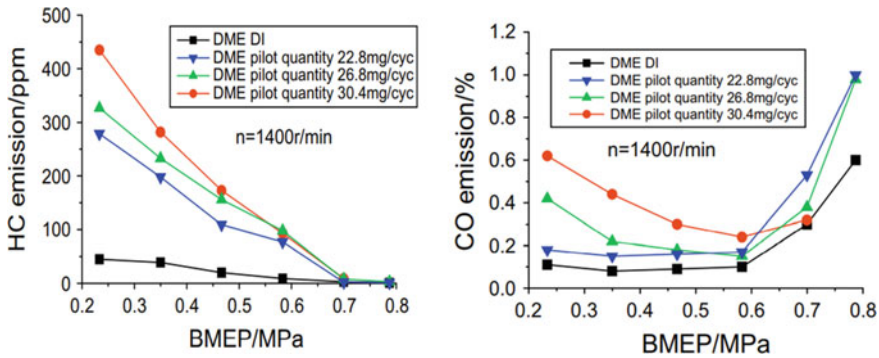
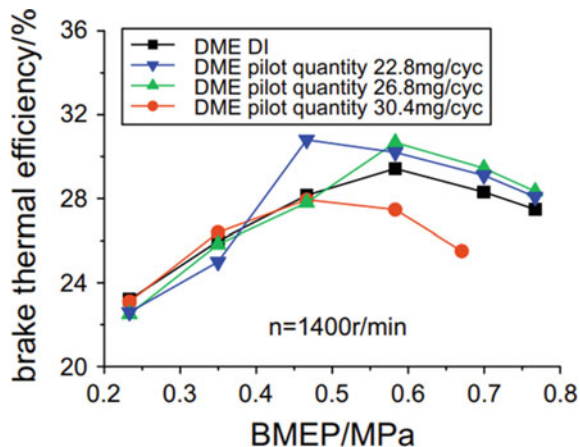


**Fig. 10.9** Effects of pilot fuel quantities on a HC and b CO emissions of PCCI-DI engine (Ying et al. 2010)

**Fig. 10.10** Effects of pilot fuel quantities on the brake thermal efficiency of PCCI-DI engine (Ying et al. 2010)



**Advantages of DME Fueled PCCI Combustion**

As the premixing ratio increases in the PCCI engine technology, there is a substantial reduction in NO<sub>x</sub> and smoke emissions. On heating to a high temperature, DME produces enough hydrogen, leading to reduced brake-specific fuel consumption. DME has a high latent heat of vaporization; therefore, it absorbs comparatively more heat than diesel in the gaseous form (Laguitton et al. 2007). Experiments were performed in a DME-diesel dual fuel PCCI engine with EGR, and this emerged as an excellent strategy to control the combustion and reduce the NO<sub>x</sub> emissions (Zhao et al. 2014) (Fig. 10.11).

The temperature inside the cylinder is one of the key parameters for controlling the auto-ignition process. With EGR, auto-ignition timing gets delayed, leading to a lower peak charge temperature, reducing the NO<sub>x</sub> emissions (Kiplimo et al. 2012). Since combustion noise is proportional to the maximum temperature, the noise also

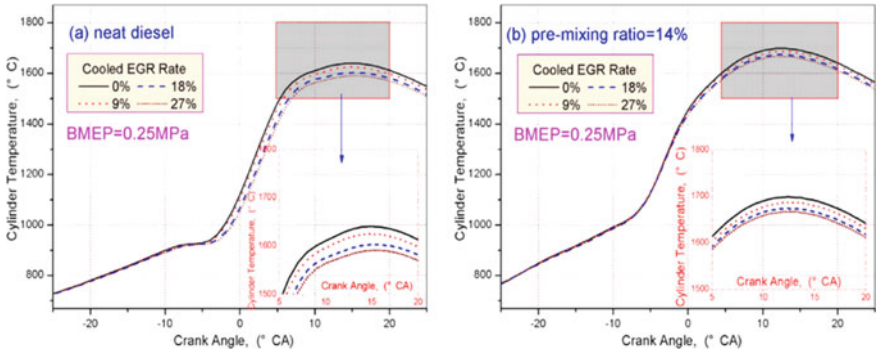


Fig. 10.11 Effects of premixing ratio and EGR rate on the calculated mean charge temperature (Zhao et al. 2014)

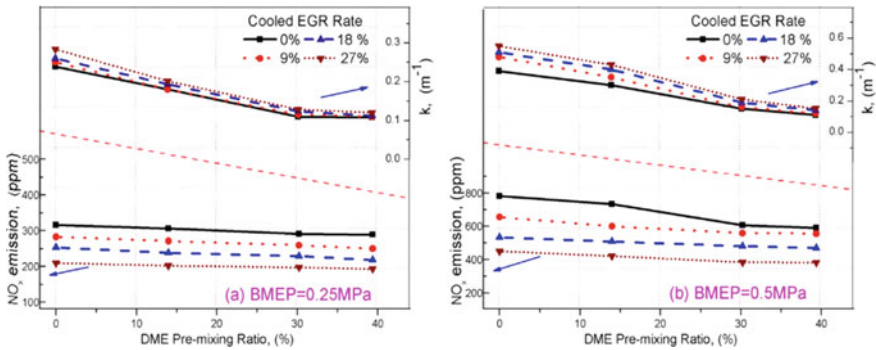


Fig. 10.12 NO<sub>x</sub> emissions and smoke opacity for different operating modes (Zhao et al. 2014)

gets reduced with a reduction in the peak temperature and pressure (Torregrosa et al. 2011) (Fig. 10.12).

The emission of NO<sub>x</sub> decreased since the oxygen concentration decreased, leading to a lower flame temperature (Lee et al. 2003). With an increasing DME premixing ratio, the NO<sub>x</sub> reduction rate slowed down, and the EGR rate was increased for achieving high premixing ratios to overcome this. The smoke was mainly observed at higher temperatures and fuel-rich regions. Therefore, with an increasing DME premixing ratio, it decreased. However, the smoke increased with an increasing EGR rate since oxygen concentration decreased, leading to incomplete combustion.

### Challenges of DME Fueled PCCI Combustion

There is only limited knowledge regarding the combustion and emission characteristics of EGR in the DME-fueled PCCI engine. Also, it is seen that with EGR in a DME-diesel dual-fuel PCCI engine, the brake thermal efficiency was reduced while the equivalent brake-specific fuel consumption increased (Fig. 10.13).

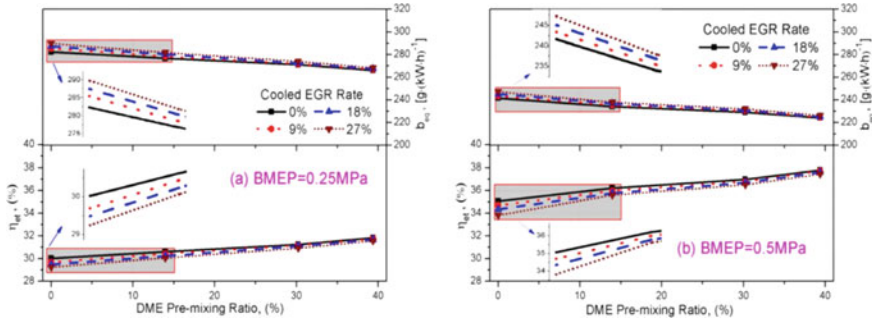


**Fig. 10.13** Equivalent brake-specific fuel consumption and brake thermal efficiency for different operating modes (Zhao et al. 2014)

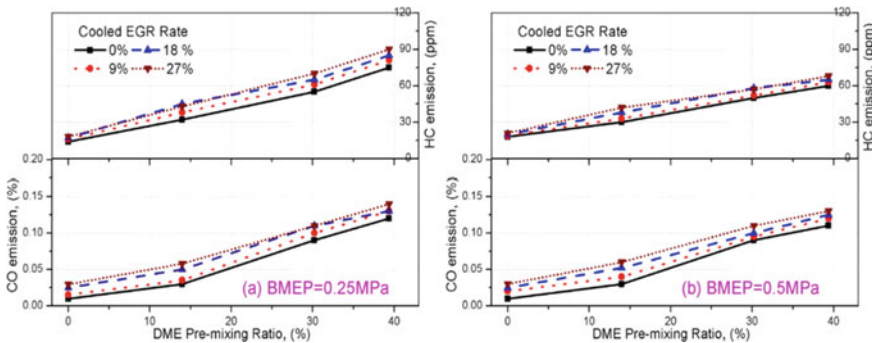


**Fig. 10.14** HC and CO emissions for different operating modes (Zhao et al. 2014)

Moreover, with increasing EGR rate,  $NO_x$  reduced, but smoke and unburnt CO and HC emissions increased (Fig. 10.14).

Therefore, further investigation using the DME fueled PCCI engine technology experiments would help develop a superior understanding of this LTC engine technology.

### 10.2.3 DME Fueled RCCI Combustion

Due to the existing challenges of HCCI and PCCI engine technologies, a new LTC engine technology, namely reactivity-controlled compression ignition (RCCI), was developed for application in commercial engines. The RCCI engine creates a reactivity gradient and a suitable global reactivity in the engine combustion chamber. The reactivity gradient is created by using two fuels of different reactivities, known as low reactivity fuel (LRF) and high reactivity fuel (HRF). LRF, such as natural gas, gasoline, methanol, etc., is port-injected, while the HRF (DME) is injected directly

into the engine combustion chamber (Agarwal et al. 2021b). Once the direct injection of HRF is completed, RCCI combustion is started. This dual-fuel LTC engine technology uses two fuels inside the cylinder to control the combustion phasing and HRR (Singh et al. 2021b).

RCCI engine technology offers an advantage over other LTC technologies. It is capable of being used at low as well as high engine loads. Fuels with different cetane numbers regulate combustion. Additives such as hydrogen can change the heating value of the fuel–air mixture.

### **DME-CH<sub>4</sub> Fueled RCCI Combustion**

Methane as an alternative fuel is of prime importance for reducing smoke from IC engines since it is a highly clean-burning fuel. It can be produced from eco-friendly renewable energy sources. Generally, for hydrocarbon fuels such as methane, the combustion process occurs in two stages. The low-temperature chemical reactions control the first stage, whereas the high-temperature reactions govern the second stage (Jin et al. 2019). Methane has comparatively lower Reactivity than DME; therefore, DME is added to methane. The reactivity is increased because of higher radical production by the chain branching pathway of DME at low temperatures and by fast rate constants of hydrogen atom abstraction and unimolecular decomposition at high temperatures.

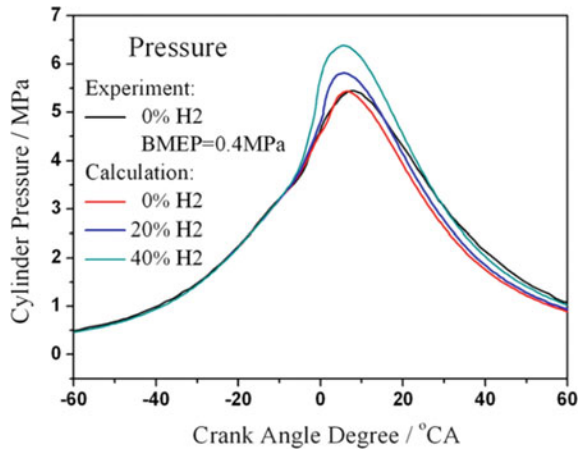
Consequently, with increased DME concentration, the ignition delay is reduced. With the RCCI engine technology, NO<sub>x</sub> and soot emissions can be easily reduced without the need for any exhaust gas after-treatment devices. Smoke and PM emissions of this dual-fuel engine are almost negligible. However, at part loads, the unburned HC and CO emissions are comparatively higher than CI engines, whereas they are comparable at high engine loads. The addition of hydrogen to the DME-CH<sub>4</sub> RCCI engine has the following effects (Liu et al. 2012):

- (a) The maximum pressure in the cylinder increases, leading to advanced ignition timing (Fig. 10.15).
- (b) The initial stages of combustion are affected more than the later stages.
- (c) There is a reduction in the unburnt CH<sub>4</sub> emission (Fig. 10.16).
- (d) CO emission is also reduced. However, the little amount of CO produced is only because of the premixed combustion of methane (Fig. 10.17).
- (e) The emission of NO is increased. However, the final NO<sub>x</sub> emissions in the exhaust are predominantly controlled by the mode of injection and the amount of pilot fuel (Fig. 10.18).

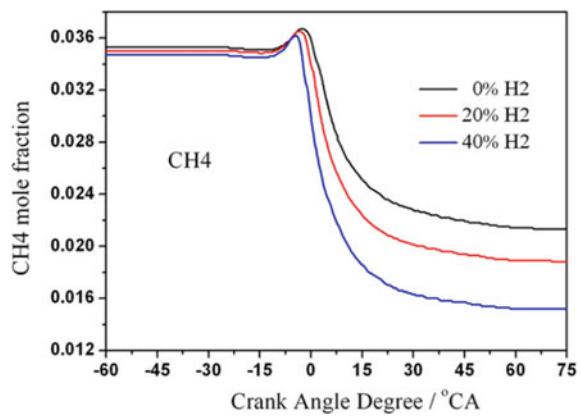
### **DME/Methanol Fueled Unconventional RCCI**

The disadvantage with conventional RCCI engine technology is that at high loads, it is obstructed by the RoPR due to the quicker combustion of port fuel injected (PFI) fuel (80%). Also, emissions of unburnt HC and CO are observed. In DME/Methanol fueled unconventional RCCI engine, the DI and PFI fuels are exchanged, i.e., the HRF (here DME) is port injected, and the LRF (here methanol) is direct-injected (Maes and Borosan 2021). This unconventional engine technology reduces

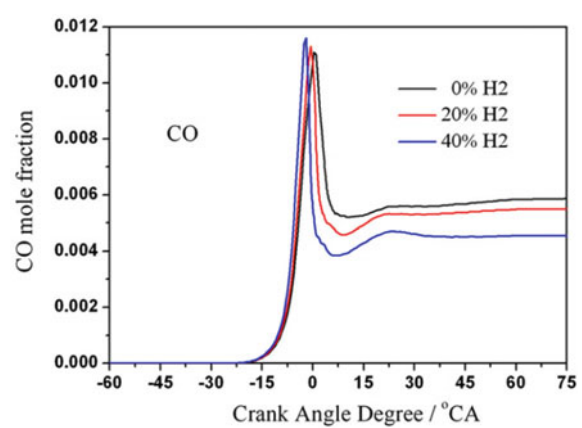
**Fig. 10.15** Calculated in-cylinder pressures for varying H<sub>2</sub> addition to DME-CH<sub>4</sub> RCCI engine (Liu et al. 2012)



**Fig. 10.16** Calculated CH<sub>4</sub> mole fractions with varying H<sub>2</sub> addition to DME-CH<sub>4</sub> RCCI engine (Liu et al. 2012)



**Fig. 10.17** Calculated CO mole fractions with varying H<sub>2</sub> addition to DME-CH<sub>4</sub> RCCI engine (Liu et al. 2012)



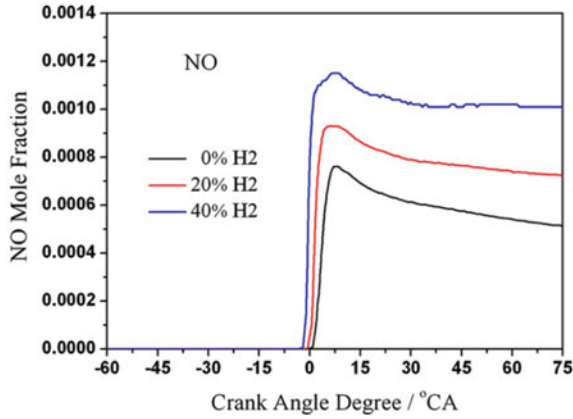


**Fig. 10.18** Calculated NO mole fractions with varying H<sub>2</sub> addition to DME-CH<sub>4</sub> RCCI engine (Liu et al. 2012)

NO<sub>x</sub> emissions. Also, it reduces the engine operating cost by reducing the usage of aqueous urea solution in the after-treatment systems (Singh et al. 2019) (Fig. 10.19).

Since the combustion in this unconventional RCCI engine is lean and homogeneous, the local high-temperature gradient was not observed. This lowered the formation of NO<sub>x</sub>. However, the emissions of HC and CO slightly increased, but they were still lower than the EURO VI limits.

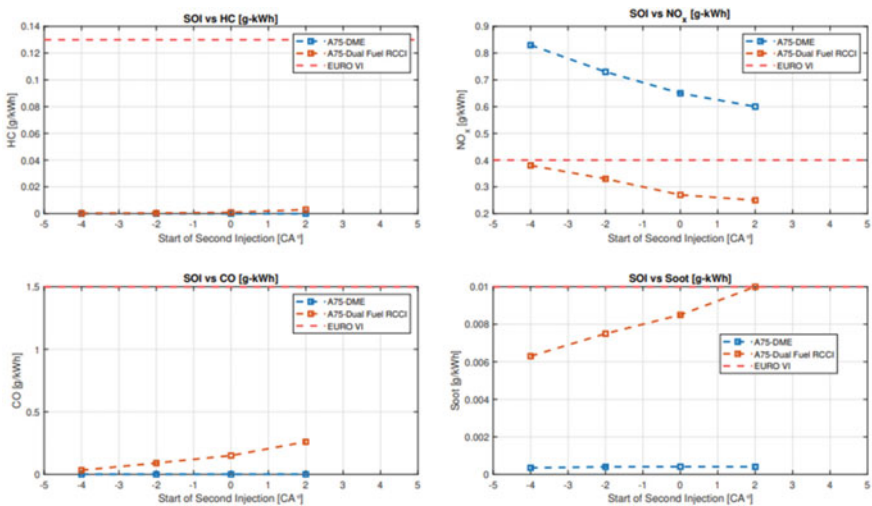


**Fig. 10.19** Comparison of emission characteristics of conventional DME engine and Dual fuel RCCI engine (Maes and Borosan 2021)



### Advantages of DME Fueled RCCI Engine Technology

The RCCI engine technology has the advantage of lower  $\text{NO}_x$ , smoke, and PM emissions than other LTC engine technologies (Agarwal et al. 2021a). Other benefits include stable combustion and wider load limits. The RCCI combustion mode achieves comparatively higher net indicated thermal efficiency. The unburned HC and CO emissions were comparable to those from the CI engine at high engine loads. With hydrogen addition to the DME- $\text{CH}_4$  fueled RCCI engine, ignition timing advanced, increasing the peak cylinder pressure. Also, it reduced the emissions of unburnt  $\text{CH}_4$  and CO (Liu et al. 2012). In the RCCI engine, the final  $\text{NO}_x$  emissions in the exhaust were determined by the injection mode and the pilot fuel quantity. Therefore, with appropriate strategies and calculations,  $\text{NO}_x$  emissions can be controlled efficiently.

### Challenges of DME Fueled RCCI Combustion

There is a good understanding of the RCCI engine technology at the laboratory scale, and the benefits are also known. However, at a practical level, DME-fueled RCCI combustion mode still has a long way to go since it hasn't made its way to production yet. The dual-fuel RCCI engine technology still struggles with higher emissions of unburnt HC and CO at high loads. It was found that for a traditional dual-fuel engine, operation at higher loads was limited because of the instant combustion of the LRF. DME-fueled RCCI engine technology is technically feasible and has the potential to meet the EURO VI emission norms. Another challenge is that the DME combustion also suffers from the soot- $\text{NO}_x$  trade-off (Table 10.2).

**Table 10.2.** Overall comparison of DME fueled HCCI, PCCI, RCCI engine technologies based on combustion, performance, and emission characteristics

S. No.	Combustion, performance and emission characteristics	HCCI	PCCI	RCCI
1	HRR	Very High	High	High
2	RoPR	Very High	High	High
3	Ignition delay	Short	Short	Short
4	Output power	Limited	Higher than HCCI	Higher than HCCI
5	Brake thermal efficiency	Relatively low	Better than HCCI	Better than HCCI
6	$\text{NO}_x$ emission	Low	Higher	Lowest
7	Particulate emission	Low	Higher	Negligible
8	HC emission	High	Higher than HCCI	High
9	CO emission	High	Higher than HCCI	High
10	Soot emission	Low	Higher	Low

## 10.3 Emission Characteristics of DME Fueled LTC Engines

### 10.3.1 Regulated Gaseous Emissions

#### Oxides of Nitrogen (NO<sub>x</sub>)

NO<sub>x</sub> emissions show variations in DME fueled CI engines, depending on the engine condition and the fuel supply system. DME has a shorter ignition delay than diesel, leading to the burning of lesser fuel during the premixed combustion phase (Kapus 1995; Fleisch 1995). Thus, the NO<sub>x</sub> emissions are lower. However, higher NO<sub>x</sub> is observed if the start of injection is advanced (Kajitani et al. 1997). For optimized injection retardation, the NO<sub>x</sub> emissions are lower for DME than diesel (Kajitani et al. 1997; Longbao et al. 1999). The higher latent heat of DME reduces the NO<sub>x</sub> emission formation because the injected liquid DME spray absorbs the heat during evaporation (Park and Lee 2014). Kim et al. (Kim et al. 2008) compared the emission characteristics of a CI engine fueled with DME and diesel. They reported that the NO<sub>x</sub> emissions were higher for DME because of faster ignition, leading to higher charge temperature. Park et al. (Park and Yoon 2015) also studied the effect of injection timing on the DME-fueled engine emissions. They used a two-stage injection strategy consisting of pilot injection with advanced main injection and reported that this strategy resulted in the lowest NO<sub>x</sub>, CO, and HC emissions. Suh et al. (Suh et al. 2010) also investigated the effect of multiple injection strategies on the emission characteristics of a DME fueled CI engine and observed that the NO<sub>x</sub> emissions were reduced by advancing the first injecting timing without any increase in the soot emissions. NO<sub>x</sub> emissions are negligible from a DME fueled HCCI engine. In the HCCI-DI engine, NO<sub>x</sub> emissions are higher than HCCI but lower than conventional compression ignition direct injection (CIDI) engine (Park et al. 2011b). EGR can be used to reduce NO<sub>x</sub> emissions. In the PCCI engine, NO<sub>x</sub> emissions were slightly higher than the conventional engine. DI combustion mode was combined with the PCCI mode to form PCCI-DI combustion mode, which effectively reduced NO<sub>x</sub> emissions at all loads. The DME fueled RCCI engine reduced NO<sub>x</sub> emissions without exhaust gas after-treatment. DME-methanol-fueled unconventional RCCI also reduced NO<sub>x</sub> emissions effectively.

#### Carbon Monoxide (CO)

DME has a low C/H ratio, lack of C–C bonds, and high oxygen content, leading to rapid combustion and preventing incomplete combustion. Thus, ideally, the CO emission decreases in a DME fueled CI engine. However, CO in the exhaust gas is relatively higher in almost all LTC engine technologies, i.e., HCCI, HCCI-DI, PCCI, and RCCI w.r.t. conventional diesel and SI engine. When EGR was used with the LTC engine technology to reduce NO<sub>x</sub> emissions, there was a further increase in CO emissions. One way to reduce CO emission was by adding hydrogen, as in the DME-CH<sub>4</sub> RCCI engine. CO emission was comparatively higher at low loads, and

upon increasing the equivalence ratio, it slowly approached the levels of conventional diesel engines (Junjun et al. 2009).

### Unburned Hydrocarbon (UHC)

UHC emission is caused by the partial burning of a fuel-rich mixture. In DME, no significant fuel-rich zone is formed due to an oxygen atom in each molecule. In addition, DME has a shorter spray tip penetration; consequently, UHC emission due to wall-wetting is also reduced. Hence, UHC emission in DME fueled vehicle is lesser as compared to diesel. THC emissions are lesser for DME fueled engines than that of diesel at all operating conditions. However, for LTC engine technologies, UHC emission followed a similar trend as the CO emission. They were observed to be relatively higher in LTC engines compared to conventional engines. At part loads, UHC emissions were higher in DME fueled LTC engine than baseline CI engine, whereas, at low load, UHC emissions were similar to CI engine operation. The reason is incomplete combustion in the bowl and crevice regions in the engine cylinder (Kim et al. 2011). As shown in Fig. 10.20, with an increase in the DME fuel addition, the composition of the lighter HC emissions (C1–C6) shows an increasing trend.

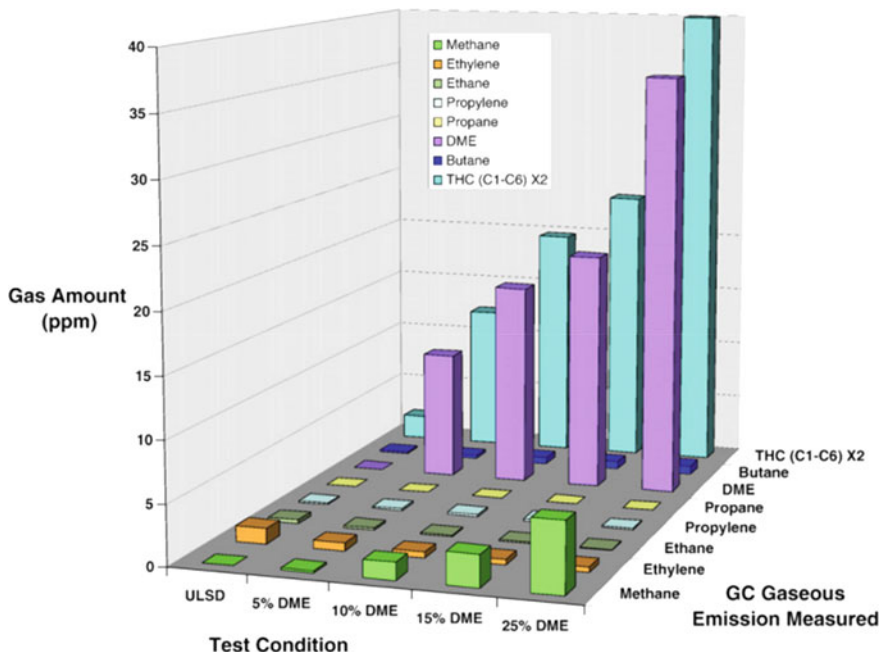


**Fig. 10.20** Hydrocarbon emissions (C<sub>1</sub>–C<sub>6</sub>) with increasing energy equivalent percent in DME concentration in a dual-fuel engine (Chapman and Boehman 2008)

## Particulate Emission

The particulate emissions were lower for HCCI engines compared to conventional engines. The PCCI combustion mode showed slightly higher particulate emissions than the conventional CI engines. On the other hand, RCCI engines notably emitted lesser particulates as compared to other LTC engines. A new engine technology, namely, controllable premixed combustion with DME as fuel, can lead to negligible PM emissions (Liu et al. 2012). It was also seen that while EGR is an excellent method for reducing  $\text{NO}_x$  emissions, increasing the EGR rate beyond a certain level can cause an increase in the PM emissions (Maes and Borosan 2021).

### 10.3.2 Unregulated Emissions

Incomplete combustion of hydrocarbon fuels produces various unregulated emission species as a byproduct, such as polycyclic aromatic hydrocarbons (PAHs), Benzene Toluene, Xylene (BTX),  $\text{CH}_2\text{O}$ . There is an emission of unburnt DME due to fuel-rich regions in the cylinder, either too lean or too rich (wivedi et al. 2019). As DME injection is retarded,  $\text{CH}_2\text{O}$  emission from the engine increases. Retarding injection timing, especially at lower engine speeds, causes a slight increase in DME emission. From Fig. 10.20, it can be seen that with an increase in the DME fuel addition, the light olefin emissions show a decreasing trend. With the absence of sulfur in DME, DME-fueled engines emit zero  $\text{SO}_x$  (Fischer et al. 2000).

### Oxygen Compound Emissions

Emissions of oxygen compounds such as acetaldehyde ( $\text{CH}_3\text{CHO}$ ), formic acid ( $\text{HCOOH}$ ), and a major fraction of formaldehyde ( $\text{HCHO}$ ) are seen during the combustion of DME because of the presence of additives and higher oxygen content (Jie et al. 2010). The formaldehyde concentration increases at low-temperature reactions and then gradually decreases at high-temperature reactions (Azimov et al. 2012). Formaldehyde concentration can be reduced to almost zero by the usage of an oxidation catalyst (Jie et al. 2010; Oguma et al. 2005; Zhang et al. 2008). As DME injection is retarded,  $\text{HCHO}$  emission from the engine increases. Zhu et al. (Zhu et al. 2012) investigated a DME engine's regulated and unregulated emissions under different injection timings. They revealed that as the injection timing is delayed, the  $\text{HCHO}$  emission increases. Incomplete combustion of HC produces  $\text{HCHO}$  emissions. The  $\beta$ -scission of the methoxy-methyl radicals determines the concentration of  $\text{HCHO}$  in exhaust emission (Curran et al. 1998).  $\text{HCHO}$  emission of DME fueled engine is almost the same as that of diesel.

### DME Emission

DME emission results from the unburnt DME fuel because of rich or lean mixtures. Zhu et al. (Zhu et al. 2012) revealed that the DME emission slightly increased with the retardation of injection timing at lower engine speed. However, they decreased

with an increase in load. However, there is an increase in DME emissions when the injection timing of DME fuel is retarded.

### **Smoke Emission**

DME has no C–C bond, an oxygen content of 35%, and a low C/H ratio, leading to complete combustion and negligible smoke emission (Arcoumanis et al. 2008). If any smoke is observed, it is because of the lubricating oil and not DME (Zhu et al. 2012; Arcoumanis et al. 2008). Moreover, the molecular structure of DME consists of a C–O–C bond, because of which the formation of C≡C radicals is improbable (Westbrook 1999; Ogawa et al. 2003b). Therefore, as per the acetylene mechanism, no smoke will be formed during the combustion process of DME (Frenklach and Wang 1991). Therefore, it can be said that the combustion of DME is almost smoke-free under all operating conditions (Longbao et al. 1999; Zhu et al. 2012). There is no need for any particulate filter in the after-treatment systems for DME fueled vehicles.

## **10.4 Future Prospects of DME**

### ***10.4.1 DME Production and Usage***

China is the leading producer of DME with a record production of 3.8 MT of DME in 2015, the highest in the world. China has the third-largest coal reserves and produces ~70% of its DME from coal, while countries like the US, South America, and Iran mainly use natural gas for DME production (Agarwal et al. 2021c). Like China, India also has an abundant reserve of coal and has 5<sup>th</sup> position in having the largest coal reserves in the world. Therefore, efficient use of these coal reserves can significantly produce DME at a very low price. DME and its blends with gasoline or diesel can be used as a transport fuel in road transport, railways, and ships. DME has a vast potential to replace diesel in telecom towers.

Further research and development on DME are the need of the hour. Sufficient DME production and adequate distribution infrastructure are required in India to accept DME as a replacement for conventional fuels without any hesitation. There should be the development of indigenous flex-fuel vehicles operating on DME/blends. With the help of a suitable development program, railway locomotives currently running on diesel can also be converted to operate on DME. India should leap forward in DME adaptation, which will reduce its import dependence and carbon footprint simultaneously (Saraswat and Bansal 2017; Agarwal et al. 2019).

### ***10.4.2 Path Forward for DME Fueled LTC Engines***

With some modifications, DME-fueled LTC engine technologies can offer a promising future to IC engines. Using suitable EGR and boosting, the operational range of HCCI engines can be extended to cater to higher loads efficiently. The control mechanism of boosting with EGR in the HCCI engine is an area that needs to be researched further (Putrasari et al. 2017). Since there isn't much information about the combustion and emission characteristics of DME-diesel dual fuel PCCI engines using EGR, it is also important to assess the prospects of PCCI engine technology.

RCCI engine combustion also needs to be investigated for the low and part load conditions for adopting different proportions of DME and other LRFs. There is a need to assess intake temperature sensitivity to understand the ignition delay behaviour of DME at low loads. Various studies involving pre-, main- and post-injection, and injection pressure variations could be performed to understand the mixture formation process. Further research is needed to understand the effects of key parameters such as composition and temperature stratification, mixing layer thickness, and shear-layer turbulence on the cool flames formed in RCCI combustion mode (Jin et al. 2019). Investigations of the turbulent flame speeds, flame propagation, and emission characteristics of natural gas in a dual-fuel engine need to be carried out (Liu et al. 2012). Also, experimental and computational studies of natural gas and DME dual-fuel RCCI engine technology will be of great significance. The effects of various additives such as hydrogen on the natural gas combustion with EGR should also be studied.

## **10.5 Conclusions**

DME as fuel has vast potential to replace the existing conventional fuels and overcome their shortcomings. DME has numerous favourable properties such as high cetane rating, no C–C bond, an oxygen atom in each molecule, easier evaporation, good mixing tendency with air, excellent cold working characteristics, making it highly compatible with IC engines. When used with the innovative LTC engine technologies, DME enhances the engine performance. LTC engine technology, such as RCCI, eliminates the need for expensive exhaust gas after-treatment, consequently lowering the operating cost of the engine. Moreover, the combination of conventional engine technologies and LTC engine technologies such as HCCI-DI can coalesce the benefits, leading to a cleaner combustion, excellent fuel economy, and wider operational range. DME has some challenges as a fuel, such as its lower energy content due to oxygen in its molecular structure. Therefore, the range of a DME fueled vehicle is lower compared to a diesel fueled vehicle. The size of the DME fuel tank needs to be increased to compensate for the reduced range, making the vehicle bulkier. DME combustion also suffers from a soot-NO<sub>x</sub> trade-off. Also, different LTC engine technologies have limitations concerning emissions and fuel economy. HCCI engine

technology has a limited operating range. Using EGR in the HCCI engine has disadvantages, such as the rapid HRR leading to higher unburned HC and CO emissions and reduced power output.

Also, brake thermal efficiency reduces, and an equivalent brake-specific fuel consumption increases with EGR in a DME-diesel dual fuel PCCI engine. Presently, the research for the development of DME-fueled LTC engines is limited. However, it can replace conventional fuels and adapt DME in modern engines to comply with stringent emission norms while delivering excellent thermal efficiency. More research and development of DME-fueled low-temperature combustion engine technologies with DME and DME fuel blends or the use of dual-fuel modes is essential. DME's production and distribution infrastructure must be developed simultaneously to transform DME fueled engine technologies into completely reliable systems.

## References

- Agarwal AK, Gautam A, Sharma N, Singh AP (2019) Introduction of methanol and alternate fuel economy. In: Methanol and the alternate fuel economy. Springer, Singapore, pp 3–6. [https://doi.org/10.1007/978-981-13-3287-6\\_1](https://doi.org/10.1007/978-981-13-3287-6_1)
- Agarwal AK, Singh AP and Kumar V (2021a) Particulate characteristics of low-temperature combustion (PCCI and RCCI) strategies in single cylinder research engine for developing sustainable and cleaner transportation Solution. In: Environmental pollution, p 117375. <https://doi.org/10.1016/j.envpol.2021.117375>
- Agarwal AK, Singh AP, Kumar V (2021b) Particulate characteristics of low-temperature combustion (PCCI and RCCI) strategies in single cylinder research engine for developing sustainable and cleaner transportation solution. In: Environmental pollution, p 117375. <https://doi.org/10.1016/j.envpol.2021.117375>
- Agarwal AK, Valera H, Pexa M, Cedik J (2021c) Methanol. Springer Science and Business Media LLC
- Amann M, Buckingham J, Kono N (2006) Evaluation of HCCI engine potentials in comparison to advanced gasoline and diesel engines. SAE Technical Paper No. 2006-01-3249. <https://doi.org/10.4271/2006-01-3249>
- Arcoumanis C, Bae C, Crookes R, Kinoshita E (2008) The potential of dimethyl ether (DME) as an alternative fuel for compression-ignition engines: a review. Fuel 87(7):1014–1030. <https://doi.org/10.1016/j.fuel.2007.06.007>
- Azimov U, Kawahara N, Tomita E (2012) UV-visible light absorption by hydroxyl and formaldehyde and knocking combustion in a DME-HCCI engine. Fuel 98:164e75. <https://doi.org/10.1016/j.fuel.2012.03.033>
- Chapman EM, Boehman AL (2008) Pilot ignited premixed combustion of dimethyl ether in a turbodiesel engine. Fuel Process Technol 89(12):1262–1271. <https://doi.org/10.1016/j.fuproc.2008.08.010>
- Curran HJ, Pitz WJ, Westbrook CK, Dagaut P, Boettner JC, Cathonnet M (1998) A wide range modelling study of dimethyl ether oxidation. Int J Chem Kinet 30(3):229–241. [https://doi.org/10.1002/\(SICI\)1097-4601\(1998\)30:3<229::AID-KIN9%3e3.0.CO;2-U](https://doi.org/10.1002/(SICI)1097-4601(1998)30:3<229::AID-KIN9%3e3.0.CO;2-U)
- wivedi G, Pillai S, Shukla AK (2019) Study of performance and emissions of engines fueled by biofuels and its blends. In: Methanol and the alternate fuel economy. Springer, Singapore, pp 77–106. [https://doi.org/10.1007/978-981-13-3287-6\\_5](https://doi.org/10.1007/978-981-13-3287-6_5)

- Eirich J, Chapman E, Glunt H, Klinikowski D, Boehman AL, Hansel JG, (2003) Development of a dimethyl ether (DME)-fueled shuttle bus. SAE Technical Paper No. 2003-01-0756. <https://doi.org/10.4271/2003-01-0756>
- Fischer SL, Dryer FL, Curran HJ (2000) The reaction kinetics of dimethyl ether. I: High-temperature pyrolysis and oxidation in flow reactors. *Int J Chem Kinet* 32(12):713–740. [https://doi.org/10.1002/1097-4601\(2000\)32:12<713::AID-KINI>3.0.CO;2-9](https://doi.org/10.1002/1097-4601(2000)32:12<713::AID-KINI>3.0.CO;2-9)
- Fleisch TH (1995) DME: the Diesel fuel for the 21st Century? In: Proceedings of conference program International congress engine and the environment, Graz, Austria
- Frenklach M, Wang H (1991) Detailed modelling of soot particle nucleation and growth. In: Symposium (international) on combustion, vol 23, no 1. Elsevier, pp 1559–1566. [https://doi.org/10.1016/S0082-0784\(06\)80426-1](https://doi.org/10.1016/S0082-0784(06)80426-1)
- Gowthaman S, Sathiyagnanam AP (2017) performance and emission characteristics of homogeneous charge compression ignition engine—a review. *Int J Ambient Energy* 38(7):672–684. <https://doi.org/10.1080/01430750.2016.1155491>
- Huang Z, Qiao X, Zhang W, Wu J, Zhang J (2009) Dimethyl ether as alternative fuel for CI engine and vehicle. *Front Energy Power Eng Chin* 3(1):99–108. <https://doi.org/10.1007/S11708-009-0013-1>
- Hwang JS, Ha JS, No SY (2003) Spray characteristics of DME in conditions of common rail injection system (II). *Int J Automot Technol* 4(3):119–124
- Jang J, Lee Y, Cho C, Woo Y, Bae C (2013) Improvement of DME HCCI engine combustion by direct injection and EGR. *Fuel* 113:617–624. <https://doi.org/10.1016/j.fuel.2013.06.001>
- Jie L, Shenghua L, Yi L, Yanju W, Guangle L, Zan Z (2010) Regulated and nonregulated emission from a dimethyl ether powered compression ignition engine. *Energy Fuel* 24:2465e9. <https://doi.org/10.1021/ef9016043>
- Jin T, Wu Y, Wang X, Luo KH, Lu T, Luo K, Fan J (2019) Ignition dynamics of DME/methane-air reactive mixing layer under reactivity-controlled compression ignition conditions: Effects of cool flames. *Appl Energy* 249:343–354. <https://doi.org/10.1016/j.apenergy.2019.04.161>
- Junjun Z, Xinqi Q, Zhen W, Bin G, Zhen H (2009) Experimental investigation of low-temperature combustion (LTC) in an engine fueled with dimethyl ether (DME). *Energy Fuels* 23(1):170–174. <https://doi.org/10.1021/ef800674s>
- Kajitani S, Chen ZL, Konno M, Rhee KT (1997) Engine performance and exhaust characteristics of direct-injection diesel engine operated with DME. SAE Trans, pp 1568–1577
- Kapus P (1995) Development of fuel injection equipment and combustion system of DI diesel engine using a new alternative fuel. SAE Paper 950062
- Kim MY, Yoon SH, Ryu BW, Lee CS (2008) Combustion and emission characteristics of DME as an alternative fuel for compression ignition engines with a high-pressure injection system. *Fuel* 87(12):2779–2786. <https://doi.org/10.1016/j.fuel.2008.01.032>
- Kim HJ, Park SH, Lee KS, Lee CS (2011) A study of spray strategies on improvement of engine performance and emissions reduction characteristics in a DME fueled diesel engine. *Energy* 36(3):1802–1813. <https://doi.org/10.1016/j.energy.2010.12.026>
- Kiplimo R, Tomita E, Kawahara N, Yokobe S (2012) Effects of spray impingement, injection parameters, and EGR on the combustion and emission characteristics of a PCCI diesel engine. *Appl Therm Eng* 37:165–175. <https://doi.org/10.1016/j.applthermaleng.2011.11.011>
- Laguitton O, Crua C, Cowell T, Heikal MR, Gold MR (2007) The effect of compression ratio on exhaust emissions from a PCCI diesel engine. *Energy Convers Manage* 48(11):2918–2924. <https://doi.org/10.1016/j.enconman.2007.07.016>
- Lee SW, Kusaka J, Daisho Y (2001) Spray characteristics of alternative fuels in constant volume chamber (comparison of the spray characteristics of LPG, DME, and n-dodecane). *JSAE Rev* 22(3):271–276. [https://doi.org/10.1016/S0389-4304\(01\)00117-5](https://doi.org/10.1016/S0389-4304(01)00117-5)



- Lee CS, Lee KH, Kim DS (2003) Experimental and numerical study on the combustion characteristics of partially premixed charge compression ignition engine with dual fuel. *Fuel* 82(5):553–560. [https://doi.org/10.1016/S0016-2361\(02\)00319-8](https://doi.org/10.1016/S0016-2361(02)00319-8)
- Liu J, Yang F, Wang H, Ouyang M (2012) Numerical study of hydrogen addition to DME/CH<sub>4</sub> dual-fuel RCCI engine. *Int J Hydrogen Energy* 37(10):8688–8697. <https://doi.org/10.1016/j.ijhydene.2012.02.055>
- Longbao Z, Hewu W, Deming J, Zuohua H (1999) Study of performance and combustion characteristics of a DME-fueled light-duty direct-injection diesel. SAE Technical Paper engine No. 1999-01-3669. <https://doi.org/10.4271/1999-01-3669>
- Luong MB, Yu GH, Lu T, Chung SH, Yoo CS (2015) Direct numerical simulations of ignition of a lean n-heptane/air mixture with temperature and composition inhomogeneities relevant to HCCI and SCCI combustion. *Combust Flame* 162(12):4566–4585. <https://doi.org/10.1016/j.combustflame.2015.09.015>
- Maes IN and Borosan II (2021) A CFD study on DME/Methanol fuelled unconventional RCCI. M. Tech Thesis, Department of Mechanical Engineering, Eindhoven University of Technology
- Maurya RK, Maurya RK, Luby (2018) Characteristics and control of low-temperature combustion engines. Springer, Cham
- Ogawa H, Miyamoto N, Kaneko N, Ando H (2003a) Combustion control and operating range expansion with direct injection of reaction suppressors in a premixed DME HCCI engine. SAE Technical Paper No. 2003-01-0746. <https://doi.org/10.4271/2003-01-0746>
- Ogawa H, Miyamoto N, Yagi M (2003b) Chemical-kinetic analysis on PAH formation mechanisms of oxygenated fuels. SAE Technical Paper. No. 2003-01-3190. <https://doi.org/10.4271/2003-01-3190>
- Oguma M, Shiotani H, Goto S, Suzuki S (2005) Measurement of trace levels of harmful substances emitted from a DME DI diesel engine. SAE tech paper; SAE Technical Paper No. 2005-01-2202. <https://doi.org/10.4271/2005-01-2202>
- Park SH, Kim HJ, Lee CS (2011a) Study on the dimethyl ether spray characteristics according to the diesel blending ratio and the variations in the ambient pressure, energizing duration, and fuel temperature. *Energy & Fuels* 25(4):1772–1780. <https://doi.org/10.1021/ef101562b>
- Park S, Choi B, Oh BS (2011b) A combined system of dimethyl ether (DME) steam reforming and lean NO<sub>x</sub> trap catalysts to improve NO<sub>x</sub> reduction in DME engines. *Int J Hydrogen Energy* 36(11):6422–6432. <https://doi.org/10.1016/j.ijhydene.2011.02.124>
- Park SH, Lee CS (2013) Combustion performance and emission reduction characteristics of automotive DME engine system. *Prog Energy Combust Sci* 39(1):147–168. <https://doi.org/10.1016/j.peccs.2012.10.002>
- Park SH, Lee CS (2014) Applicability of dimethyl ether (DME) in a compression ignition engine as an alternative fuel. *Energy Convers Manage* 86:848–863. <https://doi.org/10.1016/j.enconman.2014.06.051>
- Park SH, Yoon SH (2015) Injection strategy for simultaneous reduction of NO<sub>x</sub> and soot emissions using two-stage injection in DME fueled engine. *Appl Energy* 143:262–270. <https://doi.org/10.1016/j.apenergy.2015.01.049>
- Putrasari Y, Jamsran N, Lim O (2017) An investigation on the DME HCCI autoignition under EGR and boosted operation. *Fuel* 200:447–457. <https://doi.org/10.1016/j.fuel.2017.03.074>
- Saraswat VK and Bansal R (2017) India's leapfrog to methanol economy. NITI AAYOG
- Singh AP, Kumar V, Agarwal AK (2020) Evaluation of comparative engine combustion, performance and emission characteristics of low-temperature combustion (PCCI and RCCI) modes. *Appl Energy* 278:115644. <https://doi.org/10.1016/j.apenergy.2020.115644>
- Singh AP, Agarwal AK (2018) Low-temperature combustion: an advanced technology for internal combustion engines. In: *Advances in internal combustion engine research*, pp 9–41. [https://doi.org/10.1007/978-981-10-7575-9\\_2](https://doi.org/10.1007/978-981-10-7575-9_2)

- Singh AP, Dhar A, Agarwal AK (2018) Evolving energy scenario: role and scope for alternative fuels in transport sector. In: *Prospects of alternative transportation fuels*. Springer, Singapore, pp. 7–19. [https://doi.org/10.1007/978-981-10-7518-6\\_2](https://doi.org/10.1007/978-981-10-7518-6_2)
- Singh AP, Sharma N, Satsangi DP, Kumar V, Agarwal AK (2019) Reactivity-controlled compression ignition combustion using alcohols. In: *Advanced engine diagnostics*, pp 9–28. [https://doi.org/10.1007/978-981-13-3275-3\\_2](https://doi.org/10.1007/978-981-13-3275-3_2)
- Singh AP, Kumar D, Agarwal AK (2021a) *Alternative fuels and advanced combustion techniques as sustainable solutions for internal combustion engine*. Springer Science and Business Media LLC
- Singh AP, Kumar V, Agarwal AK (2021b) Evaluation of reactivity-controlled compression ignition mode combustion engine using mineral diesel/gasoline fuel pair. *Fuel* 301:120986. <https://doi.org/10.1016/j.fuel.2021.120986>
- Sorenson SC (2001) Dimethyl ether in diesel engines: progress and perspectives. *J Eng Gas Turbines Power* 123(3):652–658. <https://doi.org/10.1115/1.1370373>
- Suh HK, Lee CS (2008) Experimental and analytical study on the spray characteristics of dimethyl ether (DME) and diesel fuels within a common-rail injection system in a diesel engine. *Fuel* 87(6):925–932. <https://doi.org/10.1016/j.fuel.2007.05.051>
- Suh HK, Yoon SH, Lee CS (2010) Effect of multiple injection strategies on the spray atomization and reduction of exhaust emissions in a compression ignition engine fueled with dimethyl ether (DME). *Energy Fuels* 24(2):1323–1332. <https://doi.org/10.1021/ef9010143>
- Torregrosa AJ, Broatch A, Novella R, Mónico LF (2011) Suitability analysis of advanced diesel combustion concepts for emissions and noise control. *Energy* 36(2):825–838. <https://doi.org/10.1016/j.energy.2010.12.032>
- Wang Y, Zhao Y, Yang Z (2013) Dimethyl ether energy ratio effects in a dimethyl ether-diesel dual fuel premixed charge compression ignition engine. *Appl Therm Eng* 54(2):481–487. <https://doi.org/10.1016/j.applthermaleng.2013.02.005>
- Web Source: <https://worldwidescience.org/>. Accessed on 6 June 2021
- Web Source: [https://www.greencarmjm.p;\[congress.com/](https://www.greencarmjm.p;[congress.com/). Accessed on 3 June 2021
- Web source: <https://eur-lex.europa.eu/legal-content/EN/TXT/PDF/?uri=CELEX:32018L2001&from=fr>. Accessed on 26 Sept 2021
- Web source: [https://ec.europa.eu/info/sites/default/files/amendment-renewable-energy-directive-2030-climate-target-with-annexes\\_en.pdf](https://ec.europa.eu/info/sites/default/files/amendment-renewable-energy-directive-2030-climate-target-with-annexes_en.pdf). Accessed on 26 Sept 2021
- Westbrook CK (1999) *Chemical kinetic modelling of oxygenated diesel fuels in advanced petroleum-based and alternative fuels*. DOE report
- Ying W, Li H, Jie Z, Longbao Z (2009) Study of HCCI-DI combustion and emissions in a DME engine. *Fuel* 88(11):2255–2261. <https://doi.org/10.1016/j.fuel.2009.05.008>
- Ying W, Longbao Z, Wei L (2010) Effects of DME pilot quantity on the performance of a DME PCCI-DI engine. *Energy Convers Manage* 51(4):648–654. <https://doi.org/10.1016/j.enconman.2009.10.023>
- Yu J, Bae C (2003) Dimethyl ether (DME) spray characteristics in a common-rail fuel injection system. *Proc Inst Mech Eng Part D J Automob Eng* 217(12):1135–1144. <https://doi.org/10.1243/09544070360729473>
- Yu J, Lee J, Bae C (2002) Dimethyl ether (DME) spray characteristics compared to diesel in a common-rail fuel injection system. SAE Technical Paper No. 2002-01-2898. <https://doi.org/10.4271/2002-01-2898>
- Zhang Y, Yu J, Mo C, Zhou S (2008) A study on combustion and emission characteristics of small DI diesel engine fuelled with dimethyl ether. SAE technical paper no. SAE2008-32-0025. <https://doi.org/10.4271/2008-32-0025>

- Zhao H, Peng Z, Ladommatos N (2001) Understanding of controlled autoignition combustion in a four-stroke gasoline engine. *Proc Inst Mech Eng Part D J Automob Eng* 215(12):1297–1310. <https://doi.org/10.1243/0954407011528824>
- Zhao Y, Wang Y, Li D, Lei X, Liu S (2014) Combustion and emission characteristics of a DME (dimethyl ether)-diesel dual fuel premixed charge compression ignition engine with EGR (exhaust gas recirculation). *Energy* 72:608–617. <https://doi.org/10.1016/j.energy.2014.05.086>
- Zhu Z, Li DK, Liu J, Wei YJ, Liu SH (2012) investigation on the regulated and unregulated emissions of a DME engine under different injection timing. *Appl Therm Eng* 35:9–14. <https://doi.org/10.1016/j.applthermaleng.2011.08.015>

# Chapter 11

## Optimization of Fuel Injection Strategies for Sustainability of DME in Combustion Engine



Anubhav, Niraj Kumar, and Rajesh Kumar Saluja

**Abstract** Fossil fuels are seized or stored underground for millions of years and are all non-sustainable resources. They are derived from non-renewable resources that cause irreversible degradation to the environment. Fossil fuel related prominent drawback of limited petroleum reserves, the concentration of global warming, harmful emissions and stores in specific areas. This has led to a situation where the use of alternative fuels such as natural gas, biodiesel, hydrogen, alcohol and dimethyl ether is under intense scrutiny. Compared to other candidates, DME ( $\text{CH}_3\text{--O--CH}_3$ ) appears to have great potential and should be examined as fuel of choice for eliminating the dependency on petroleum. In particular, DME can be used as a clean, high-efficiency fuel for the diesel engines and exhibits minimum environmental impact due to its molecular structure which has no carbon-carbon bonds and much oxygen with respect to diesel fuel. Good burning characteristics, high thermal efficiency, non-toxicity, renewability and high cetane content make it a superior clean, green and scalable fuel as compare to that of fossil fuel. Sustainable application of DMEs requires critical evaluation of performance, efficiency, fuel injection characteristics, combustion and exhaust emission characteristics. Both pure and blended DME fuel is tested in combustion engine to acquire the optimal conditions of various parameters for extracting out maximum and efficient output. Hence, to maximize the sustainability of DMEs, the effects of fuel injection parameters and in-cylinder air motion, such as the pump plunger diameter, nozzle type, fuel injection timing, nozzle tip protrusion, nozzle opening pressure, fuel delivery angle, vapor pressure and swirl ratio on emissions and performance of the DME engine must be critically evaluated and compared with those of diesel engine. The present chapter focuses on adopting suitable changes in fuel injection strategies to enhance the emission and performance characteristics of DMEs fueled engine. Advance methods to sustain DME in the preexisting diesel engine system are discussed by modifying some effective

---

Anubhav · N. Kumar (✉)

Department of Mechanical Engineering, ASET, Amity University, Noida, India

R. K. Saluja

Amity Institute of Aerospace Engineering, Amity University, Noida, India

improvements in the engine for getting maximum optimal output. Due to distinguished characteristics of DME from the diesel, the effects of fuel compressibility on compression work spray pattern, atomization characteristics are also compared, which may pave way for maximum exploration of DME as fuel for combustion engine through manipulation of fuel injection strategies.

**Keywords** Di-methyl ether · Fuel injection · Emission characteristics · Biofuels · Fuel injection parameters

## 11.1 Introduction

Despite the advantage in fuel economy and better power output than gasoline fuel, diesel engine emissions presents a greater concern. The emissions of diesel engine especially CO, NO<sub>x</sub>, HC and smoke create much panic about public health and environmental degradation (Kumar 2019; Nautiyal et al. 2015; Saxena et al. 2021). To match with the regulating norms, various complicated post-combustion treatment systems have been proposed and tested. A study held on diesel SUVs by Centre for Science and Environment summarized that the quantity of toxicity in exhaust gases are much higher for diesel operated vehicles than those of petrol cars. In fact, the addition of one diesel SUV in city is like adding 25 to 65 small petrol cars in terms of NO<sub>x</sub> emissions. The ‘NGO Transport and Environment’ concludes that overall pollution of diesel engines are more than gasoline engines in terms of CO<sub>2</sub> emitted during their whole life cycle. Instead of forcing manufactures to make harsh changes in engine design and adding complicated exhaust after treatment devices, moving towards some alternative oxygenated fuel that fits conventional diesel engine with minimal changes is much better option. To eliminate the problems with diesel fuel various oxygenated fuels like biodiesel, dimethyl ether, ethanol etc. are introduced by different researchers as in Fig. 11.1.

In this context, DME (Dimethyl ether) is one of the major promising fuels and can become a preferable fuel in near future as it is highly oxygenated, non-toxic, noncorrosive, and environmentally benign in nature. DME is a clean burning, energy efficient and renewable alternative fuel compared to diesel. As renewability of Dimethyl ether is discussed, it has also produced from renewable source of origin and contributes to a green and scalable e-fuel for transportation. Syngas can be generated as biomass or renewable electricity from fossil fuels (coal, methane) or from renewable sources. In this there are two modes for extracting DME from the syngas named as direct process and indirect process. Direct process use single reactor with bifunctional catalyst to propel the following reactions (Peral and Martín 2015; Liuzzi et al. 2020).

Formation of Methanol:  $\text{CO} + \text{H}_2 \leftrightarrow \text{CH}_3\text{OH} \quad \Delta\text{H} = -90.4 \text{ KJ/mol}$

Water-gas shift:  $\text{CO} + \text{H}_2\text{O} \leftrightarrow \text{CO}_2 + \text{H}_2 \quad \Delta\text{H} = -41 \text{ KJ/mol}$

Dehydration of Methanol:  $2\text{CH}_3\text{OH} \leftrightarrow \text{CH}_3\text{OCH}_3 + \text{H}_2\text{O} \quad \Delta\text{H} = -23 \text{ KJ/mol}$

Overall reaction:  $3\text{CO} + 3\text{H}_2 \leftrightarrow \text{CH}_3\text{OCH}_3 + \text{CO}_2 \quad \Delta\text{H} = -258.3 \text{ KJ/mol}$

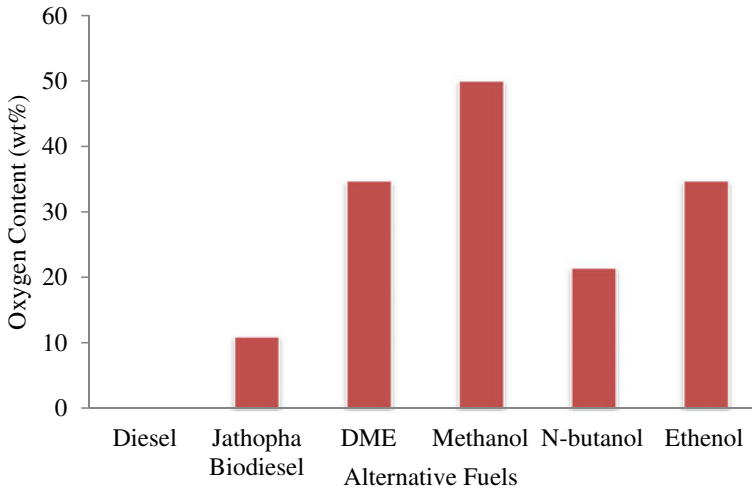


**Fig. 11.1** Presence of oxygen contents of different fuels (Rao et al. 2009; Song et al. 2009; Kamil and Nazzal 2016; Rakopoulos et al. 2011)

After this, distillation of the product is taken place to get pure dimethyl ether. Other than this, in indirect production syngas is used to form methanol and DME is extracted from this in separate reactors in the presence of précised catalysts. (Pontzen et al. 2011; Perathoner and Centi 2014; Iliuta et al. 2010) Other than this, under the pure renewable source of production agro-residue, energy-crops, forest residue, organic manure etc. are user to get syngas via gasification or anaerobic digestion and then further DME is produced from snygas as usual. As same solar energy and biomass is used to produce hydrogen and syngas respectively to produce DME.

DME powered CI engines have almost negligible soot, sulfur and aromatic emissions, while CO and HC emissions are significantly lower than diesel powered engines. Furthermore, the trend of  $\text{NO}_x$  emission varies with the variation of injection strategies. Despite of these favorable characteristics, some properties of DME like boiling point, kinematic viscosity, calorific value, density and vapor pressure create a concern in terms of high wear in fuel system, vapor lock, low lubricity, reduced energy conversion, and more fuel consumption when fueled in diesel engine. For this, some suggested modification given by researchers is to store dimethyl ether in high pressurized tank i.e., over 0.5 MPa pressure, to resist vapor formation due to the high vaporization characteristics of DME (Li 2010). Wattanavichien (Wattanavichien 2009) confirms no modification in the fuel system material is necessary while operating same engine with DME fuel due to its non-corrosive nature.

Various literatures pointed out that several complications arose in injection strategies when DME is used in compression ignition engine. Longbao et al. (Longbao et al. 1999) reported longer injection delay for DME than diesel because of low acoustic velocity in liquid DME and Kim et al. (Kim et al. 2007) reported shorter injection rate of DME by 0.03 ms than that of diesel. These associated problems

with DME, require some changes in conventional fuel injection strategies for efficient performance of engine. This paper covers the same, the study requirements in fuel injection strategies with DME application in compression ignition engine and focusses on optimization of all the important factors related to fuel strategies in DME fueled engine to move as much closer towards ideal sustainability of DME in compression ignition engine. Although Dimethyl Ether fuel is in devolving phase and different research papers are available on various fuel injection systems, yet the optimization of fuel injection strategies is least explored area. This study investigates the parameters and factors effecting DME fuel injection and analyses the optimization of the fuel-injection strategies to enhance performance, efficiency, and emissions characteristics of compression ignition engine.

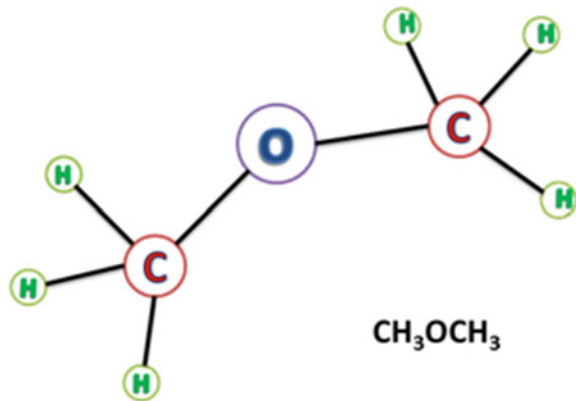
## 11.2 Physicochemical Properties of Fuel

The properties of DME are comparatively different from diesel fuel that are analyze and shown in Table 11.1, and some of these properties have great influence on the fuel injection in combustion engines. DME comes from the group of ethers, and is also known as methoxy methane, that is an organic compound with chemical

**Table 11.1** Physicochemical properties of DME and diesel (Roh and Lee 2017; Zhang et al. 2008; Wakai et al. 1999)

S. No.	Property	Units	DME	Diesel
1	Chemical Formula	–	CH <sub>3</sub> –O–CH <sub>3</sub>	C <sub>x</sub> H <sub>y</sub>
2	Boiling point	°C	–24.9	180–360
3	Molecular weight	g/mol	46.07	180–360
4	Liquid viscosity	cP	0.15	4.4–5.4
5	Liquid density	g/cm <sup>3</sup>	0.668	0.84
6	Auto ignition temperature	°C	235	250
7	Cetane number	–	55–60	40–55
8	Carbon content	wt%	52.2	86
9	Hydrogen content	wt%	13	14
10	Oxygen content	wt%	34.8	0
11	Enthalpy of vaporization	KJ/Kg	460	290
12	Vapor Pressure at 20 °C	Bar	5.1	<0.01
13	Bulk modulus of elasticity at 20 °C and 2MP	N/mm <sup>2</sup>	553	1549
14	Lower heating value	MJ/Kg	28.43	42.5
15	Stoichiometric air–fuel ratio	–	9	14.6
16	Critical temperature	K	400	708
17	Explosive limit in air	Volume %	3.4–17	0.6–6.5

**Fig. 11.2** Structural representation of Dimethyl ether



formula of  $\text{CH}_3\text{-O-CH}_3$  or  $\text{C}_2\text{H}_6\text{O}$ . The chemical structure of DME has been shown in Fig. 11.2 (Khunaphan et al. 2013). It is highly oxygenated fuel as it contains 34.8% more oxygen than that of diesel and which plays a significant role for proper combustion of DME fuel. However, the oxygen content replaces the hydrogen and carbon from the chemical structure of dimethyl ether, which leads to reduction in calorific value of DME. Presence of additional oxygen content and absence of carbon-carbon bonds in the fuel structure promotes the reduction of CO and maintains smoke emissions from the exhaust nearly zero. Cetane number of DME lies between 55 and 60 which is higher than diesel fuel, having cetane value 40–55, this is the key condition which considers DME fuel suitable for diesel engines. Further, higher cetane value is responsible for shorter ignition delay and premixed combustion period, which results in reduction of  $\text{NO}_x$  emissions and combustion noises.

IARC (International Agency of Research on Cancer) declared many of the diesel engine exhaust as carcinogenic (Thomas et al. 2014), but on other hand DME is chemically free from sulfur and also have no other pollutants such as phosphorus and cancerous aromatic compounds like benzene and toluene, hence considered as almost non-toxic fuel for combustion engine (Wattanavichien 2009). Besides advantageous properties of DME over diesel, some properties such as low auto-ignition temperature, viscosity, density, and bulk modulus have unfavorable effects on fuel injection strategies. Hence, it requires some optimization to make DME fuel more suitable and efficient for diesel engine. Low viscosity induces fuel leakage and surface wear in the moving parts of fuel injection system. Low heating value demands for more fuel injection per cycle for getting same output power as by the diesel engine and responsible for injection delay.

Since the boiling point of DME is much lower than that of diesel fuel, phase change always comes first in DME. Hence greater heat dissipation is observed during its latent phase change. This is the reason why dimethyl ether has a large enthalpy of vaporization. As the bulk modulus of elasticity is also one third of that of diesel fuel which is related to producing a significant effect on the fuel property. It is also responsible for the undesirable characteristics of fuel injection and speed of



pressure wave propagation (Sato et al. 2004). Lower bulk modulus cause higher compressibility of DME, means large amount of energy is being stored in compressed DME and with the increase in temperature, modulus of elasticity of fuel also increased and compression work reduced (Roh and Lee 2017). Auto ignition temperature of DME is 15 °C lower than diesel because of extra oxygen content in DME results in higher low-temperature reactivity than that of diesel fuel and reduces with rise in pressure (Longbao et al. 1999). In particular, the vapor pressure of pure DME is very high, so a two-phase flow occurs at room conditions. Hence diesel is preferred to reduce the vapor pressure of the charge (Saxena et al. 2021).

### 11.3 Factors Affecting Fuel Injection

The injection strategies by DME fueled system, under same operated engine conditions, are quite different from diesel due to some distinction in the properties of both fuels, shown in Table 1. The factors that affect the fuel injection strategies of Dimethyl ether are discussed individually below.

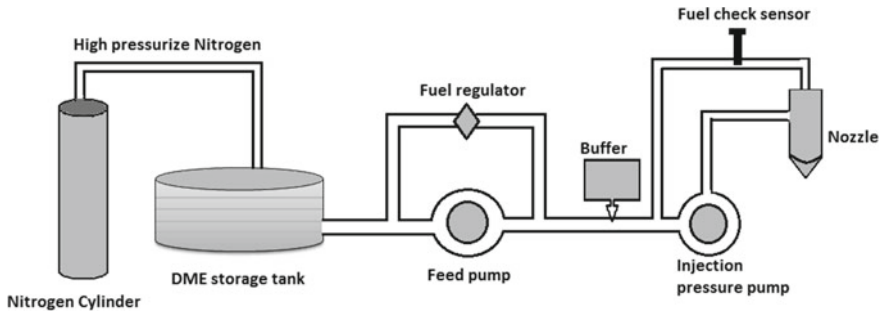
#### 11.3.1 Vapor Lock

The boiling point of DME is  $-24.9$  °C and has high vapor pressure of 5.1 bar. Fuel starts changing phase as it reaches at  $-20$  °C. So, at atmospheric conditions, dimethyl ether is in fully vaporized form. This phase change problem leads to bubble formation and cavitations in fuel system which means uneven fuel injection operation, known as vapor lock. Some problems that arise due to vapor lock are feed obstacle in fuel supply system and incomplete force feeding, difficulty in fuel measurement, variation in theoretical and actual amount of fuel injected, poor spray penetration and increase CO and HC emissions (Thomas et al. 2014; Roh and Lee 2017). Therefore, to avoid vapor lock and proper mixing of DME-Diesel blend in the fuel system, it is desirable to keep DME in pure liquid form. With the increase of pressure, boiling point of the fuel rises and hence it requires more temperature for vaporization of same fuel, therefore DME is needed to be pressurized above atmospheric pressure inside the fuel storage tank to minimize vapor lock. The temperature of the fuel tank is approximately equal to atmospheric temperature, but the fuel line is relatively at higher temperature (40–50 °C) due to its proximity to the engine. This also enhances the tendency of creating gas phase bubble in fuel delivery pipe. Required feed supply pressure suggested by different researchers to prevent vapor lock in fuel line are shown in Table 11.2.

Increasing the pressure inside fuel system can be achieved by installing components like fuel pressure regulator, low-pressure pump and buffer in conventional fuel supply system (Longbao et al. 1999) as seen in Fig. 11.3. It helps to precisely control the fuel quantity to the nozzle and DME flows continuously without any

**Table 11.2** Different fuel-line pressure suggested by different research papers:

S. No.	Fuel	References	Fuel-line pressure (MPa)
1	Dimethyl ether	Wattanavichien (2009)	3
2	Dimethyl ether	Arcoumanis et al. (2008)	1.2–3
3	Dimethyl ether	Zhang et al. (2008), Wang et al. (2000)	1.7–2
4	Dimethyl ether	Sorenson et al. (1998)	2

**Fig. 11.3** Schematic diagram of fuel system used for DME fueled engine (Longbao et al. 1999; Zhang et al. 2008)

delay. As shown in Fig. 11.3, DME fuel storage tank is pressurized by nitrogen gas to avoid leakage and vapor lock of the fuel system (Alam and Kajitani 2001). Alternatively, vapor lock may also be reduced by increasing the ratio of diesel fuel in blend, however, it may increase tail pipe emission.

In order to deliver liquid DME to the high pressure injection pump, the low pressure primary pump in the storage tank maintains a constant flow rate of the liquefied DME fuel to the high injection pump. This complication is needed in the fuel system because if the dimethyl-ether is discharged at a pressure lower than its sub-cooling pressure, the fuel forms radiant vapor and partial gas bubbles in the fuel system. So to avoid feed bottlenecks, the fuel in the storage tank and fuel line must be in a compressed liquid state (Longbao et al. 1999). Furthermore, it undergoes continuous phase shift and cavitation due to poor spray penetration under high speed and load conditions. To prevent this therefore high speed vehicles use a feed pump, which maintains the DME pressure at injection to approximately 20 bar, to counteract the formation of vapor before it enters the injection pump (Wu et al. 2021; Failed 1995). Another way to reduce the possibility of vapor lock in the fuel system is by proper mixing of diesel with it in the storage area, as diesel increases in the mixture, the vapor-locking tendency of the fuel decreases. In addition, vapor locking is minimized by keeping the fuel lines away from exhaust sections, heater hoses, and other heat suppressor components.

### 11.3.2 Injection Timing

The total time taken for complete injection by the fuel for one cycle after entering the combustion chamber is called injection time. The carbon and hydrogen content in DME is lesser than in diesel and hence DME has low calorific value. As a result, a higher volume i.e., 1.9 times volume of DME is required to be injected into cylinder for getting comparable output as from diesel fueled engine. For injection of such high volume of DME fuel, longer injection duration and advanced injection timing is necessary (Arcoumanis et al. 2008). Time interval taken by the fuel from start of energizing to the start of injection is known as Injection delay, which is longer for DME fuel than diesel under same fuel injection conditions (Longbao et al. 1999; Zhang et al. 2008; Huang et al. 2009). Table 11.1 also shows that bulk modulus of DME is approximately one-third of the diesel fuel, which reflects higher compressibility of DME than diesel oil. This concludes lower acoustic velocity for dimethyl ether as also shown in Fig. 11.4 (Huang et al. 2009), which takes more time to reach the injector opening which as results in a longer injection delay as compared to diesel. Zhang et al. 2008 (Wattanavichien 2009) analyzed the needle lift behavior and the fuel line pressure in DI diesel engine and concluded that due to the high compressibility of the DME, the delay in needle lift occurs, that postpones the injection timing by 8 °CA than diesel oil for same operating conditions.

Kajitani et al. 2000 (Egnell 2001) conducted experiment in which DME flowed at higher pressure than diesel in fuel line to resist vapor lock. Due to higher feed pressure, nozzle opening is supposed to be earlier for DME than that of diesel. Hence, the injection delay for DME is found shorter than that of diesel. In context

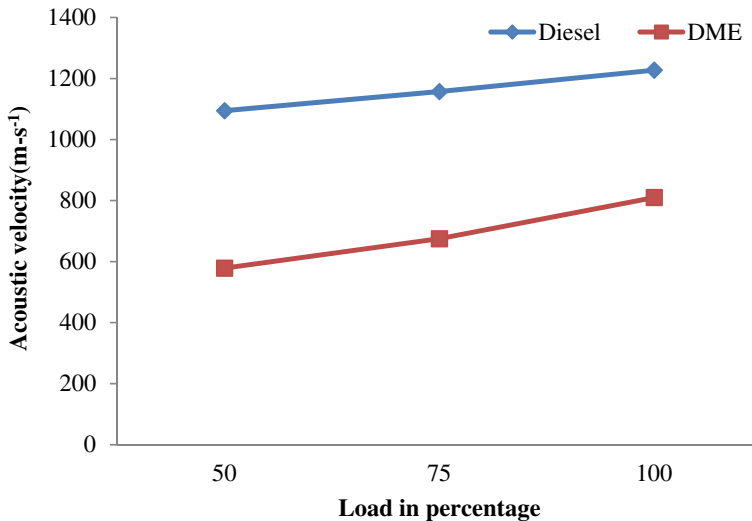


Fig. 11.4 Acoustic velocity of fuels at different engine load conditions (Huang et al. 2009)

to the injection timing, Xinling and Zhen (2009) reported that injection duration increased with enhancing engine speed or load due to injection of more fuel to produce more power. Increased quantity of fuel required more time to inject fuel resulting in increased injection duration. Further, advancing the fuel injection may lead to decrease in  $\text{NO}_x$  and PM emissions due to reduction of peak combustion temperature inside combustion chamber. But excess advancement of injection leads to improper combustion due to lack of oxygen in engine cylinder and increase the possibility of fuel to occupy piston crevice volume which is responsible for unburned HC and CO emissions. On the contrary, if fuel injecting is delayed beyond a certain limit, it causes several problems like misfire, non-uniform power production, increment in CO, formaldehyde, and hydrocarbon emissions. Therefore it is essential to optimize this factor to a certain value of crank angle at which engine acquires boosted performance and decreased emissions simultaneously (Thomas et al. 2014).

### ***11.3.3 Injection Pressure***

The evaporation rate for DME is quite higher than diesel fuel. Therefore, the necessity of high injection pressure is not required in DME fueled engine for fuel atomization and mixing, which ultimately reduces the power occupied for driving the fuel pump and so this contributes to the enhancement of thermal efficiency also. In addition to this, by increasing injection pressure however a reduced ignition delay can result in earlier start of combustion. Therefore, less time will be available for premixing of charge which may cause lesser rise in peak pressure. But in contrast, due to decrease in injection pressure, injection delay will increase which is undesirable from performance perspective (Zhang et al. 2008; Wang et al. 2000). Hence, the injection pressure is needed to be optimized to keep the favorable combustion conditions to attain maximum peak pressure and reduced injection delay value.

### ***11.3.4 Needle Lift Behavior***

Needle lift defines as the upward lifting of needle from the base needle seat against the spring action present inside injector and this can occur when pressure force exerted by the fuel on the needle overcomes the spring forces. Needle lift behavior is affected by the needle opening height, time duration for needle opening and bouncing of needle due to feed pressure and other properties of fuel. It has high influence on injection strategies in engine cylinder that affects performance and emissions of CI engine.

Bulk modulus of elasticity of dimethyl ether is lesser than diesel fuel that causes change in needle lift behavior compared to that of diesel. The nozzle opening for DME is much slower than diesel due to high compressibility of DME fuel. It has been shown that increase in feed pressure of the fuel leads to advance opening of needle. However,

Arcoumanis et al. (2008) have highlighted the problem of needle bouncing during the needle lift that arises when DME is injected at low opening pressure (6.68 MPa). Because at the lower nozzle opening pressure, the maximum displacement of needle is not much, so spring force easily overcomes opening pressure and causes the needle to close at very early stages. Then the needle after striking with the needle seat, bounces back and opens the injection path again. Due to early needle bouncing, a large part of injected fuel burns in secondary combustion phase instead of premix combustion phase which results in decreased power output and increased emissions. Thus, high needle opening pressure, in the range of 8.82 MPa, is required for well-defined injection behavior and to reduce the needle bouncing which facilitates larger portion of the fuel to combust during pre-mix combustion phase (Arcoumanis et al. 2008; Lee et al. 2002).

### ***11.3.5 Plunger Diameter***

Fore cited discussion highlighted the importance of fuel injection strategies, which also include the modification in plunger diameter for DME fuel system. The modification in plunger diameter is mandatory to produce comparable power output as in diesel fueled engine. Hence, by increasing the diameter, problems like longer injection duration, emissions, unburned fuel can be resolved when DME is used instead of diesel for the same CI engine. The reason behind this is that more fuel is allowed to come at one go into the engine cylinder with the increment of plunger diameter and this leads to the fuel spray jet gets bulkiness which further reduces the contact of surface area between DME droplets and surrounding pressurized air. So, it is difficult to atomize fuel droplets at initial stage, near the fuel injector, which results in more penetration, and hence promotes more homogeneous air–fuel mixing in combustion chamber. Thus, by increasing the plunger diameter for DME fueled engine, the injection strategies can be improved which may result in enhancement in combustion as well as thermal efficiency of the engine. Second motive for enlarging plunger diameter is to reduce injection duration (Zhang et al. 2008). For DME fuel, due to low calorific value, approximately 1.9 times more fuel required to be injected compare to diesel and this increase injection duration. With longer inject duration, more fuel take part in later stages of combustion that leads to improper combustion and partially or unburned DME, which expels as it is during exhaust stroke and raise HC and CO emissions. Hence, enlarging plunger diameter can solve this problem to some extent.

### ***11.3.6 Number of Nozzles and Nozzle Diameter***

Number of nozzles and the nozzle diameter are two areas that largely affect the injection strategies of dimethyl ether. In general, increasing the number of nozzles

ensures the effective air–fuel mixing in engine cylinder (Zhang et al. 2008) and considered a perfect alternative to single injection. Multiple nozzle holes increase the total spray width than single injection and facilitate homogeneity in chamber. This strategy further contributes to complete combustion of charge with almost negligible CO and HC emissions. (Thomas et al. 2014).

Wang et al. (2000) experimentally demonstrated that by increasing the number of nozzles and orifice area two benefits can be achieved. Firstly, the fuel delivery per cycle increases and the secondly it decreases swirl ratio. Both these modifications are in the favor of DME fuel injection strategies for granting better mixture formation and combustion efficiency. Sato et al. (2001) worked on common rail fuel injector system with two nozzles ( $0.55 \times 5$  holes) and ( $0.70 \times 3$  holes) separately. Numerous studies concluded that fuel injected in 5 hole injector nozzle vaporizes and atomizes more rapidly than fuel injected in 3 hole injector nozzle because of less fuel quantity per jet spray and more surface contact of fuel in 5 hole injector that easily entertains fuel molecules with surrounding air. It can also be noticed that with the increase of number of injector holes from 3 to 5 for same nozzle orifice area, the participation of fuel percentage in pre-mix combustion phase increases that enhances the maximum heat release value and  $\text{NO}_x$  emission along with decrease in CO and HC emissions. However, this trend is valid till certain optimum number of nozzle holes. Thereafter, if nozzle holes are increased further, then counter outcomes emerge, because of too much rapid atomization of fuel molecules which forms rich and lean pockets that cause improper combustion and higher CO and HC emissions. Hence, optimization of nozzle characteristics is required for balanced output.

### 11.3.7 Ignition Timing

Fuel ignition timing has a major influence on performance of diesel. With injection closer to TDC, the ignition delay reduces due to higher pressure and temperature of in-cylinder air resulting in quicker start of combustion of DME charge (Zhu et al. 2012). Ignition delay (ID) is the time lag between the start of fuel injection and the start of combustion. The ID for dimethyl ether is found to be shorter than that of diesel fuel under same operating conditions as in Fig. 11.5 due to its superior atomization characteristics, higher cetane number and low auto-ignition temperature of DME (Saxena et al. 2021). The combined result of these dealings is the early start of combustion for DME, which decreases the time for mixing of air–fuel and less combustible mixture is formed during premix combustion phase. This may decrease the maximum combustion pressure, combustion noise and  $\text{NO}_x$  formation. In comparison, due to short ignition delay, the maximum pressure of DME is only 82.8% of the value that comes with diesel (Xinling and Zhen 2009). Hence, DME is used as blend fuels with various other fuels having larger ignition delay to mitigate the early start combustion and greater emission of  $\text{NO}_x$ .

In a study, Wattanavichien (2009) used dimethyl ether as an additive in alcohol fueled engine for improving ignition difficulties. In another study, Wakai et al. (1999)

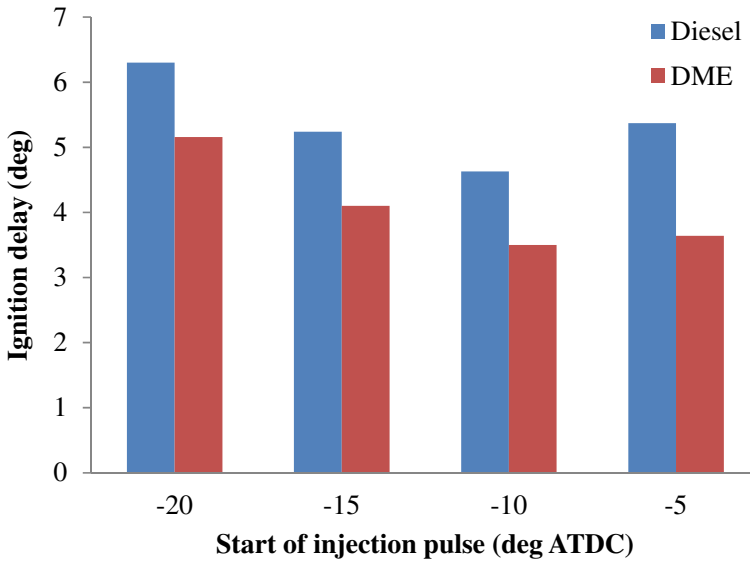


**Fig. 11.5** Comparison of ignition delay between diesel and DME (Park and Chang 2014)

researched on variation in ignition delay of DME with the variation of oxygen concentration in air present in combustion chamber during fuel injection. The authors observed that at lower oxygen concentration in air, the ignition delay of DME fuel is longer as compared to fuel spray in ordinary air. In addition, at low oxygen concentrated air, the ignition delay of DME decreases quickly with the rise of ambient pressure but it is not much affected by the variation in ambient air pressure at ordinary oxygen concentrated air. Further if the ignition delay of dimethyl ether and diesel fuel are compared, irrespective to oxygen concentrated air and ambient air pressure, ignition delay of dimethyl ether is always be lesser.

### 11.3.8 Fuel Property

Bulk modulus of elasticity is one of the important properties of DME fuel that affects the fuel injection. For DME, the modulus of elasticity is about one-third of the diesel fuel. The lower bulk modulus of DME affects the propagation of pressure wave and development of injection pressures which results in lower injection delay and poor injection quality (Roh and Lee 2017).

Vapor pressure of the DME is high as compared to diesel fuel and while its propagation through fuel-line, it further elevated which may create the problem of vapor lock. This opposes the forward movement of DME towards fuel injector and undesirable affects are observed in injection process. To get rid from this, the back pressure of the fuel supply system is setup to 0.8 MPa (Li 2010). In addition to

increasing the diesel percentage in DME-diesel blend, vapor pressure of fuel can also be decreased.

The calorific value of dimethyl ether is 35.3% less than that of diesel. Therefore, for getting equivalent power output, much higher fuel is required and that forced the researchers to manipulate the injection strategies of DME fueled engine. For better performance, 90% more volume of fuel in comparison to diesel should be injected in each injection (Huang et al. 2009). Due to this, the injection timing will increase and to compensate this, modifications in fuel injection system like plunger diameter, number of nozzles, start of injection timing, injection pressure, etc. become inevitable.

The viscosity of DME is much lesser than the diesel as shown in Table 11.1. This is responsible for problems like lubrication and leakage in injection system (Fleisch et al. 1995). Due to this, there is always a requirement of mixing lubricants with pure DME oil for minimizing excessive wear. For this, researchers suggested like lubricants, biodiesel and other hydrocarbons for attaining satisfactory injection performance (Wattanavichien 2009). Wang et al. (2000) reported that mixing of 2% of castor oil to neat DME is required to achieve desire injection strategies. On the other hand, the fuel leakage from DME operation along the plunger has been observed up to 40–50% (Makoś et al. 2019) that is also responsible for inferior injection quality.

## 11.4 Alteration in Spray Characteristics with DME as Fuel

Application of DME as fuel for CI engine has shown alteration in spray characteristics like the shape of injection, penetration length, area of spray and pattern of atomization of DME fuel molecules in cylinder chamber in comparison to diesel spray under the same engine operational conditions. The molecules of both the fuels DME and diesel, gesture differently in spray injection due to variations in their existing properties, which may be responsible for such behavior. This variation in spray characteristics are observed in detail by considering individual parameter separately in the following section.

### 11.4.1 *Spray Shape*

Spray shape is the pattern of the outer locus of the fuel droplets that arranged in the cylinder after the injection of fuel. It is deviated as the injection phase passes on. In the early stage of injection, the nozzle is partially open, due to which less fuel is injected and hence, development in spray structure is not much. This rate of spray development increases with increase in nozzle opening. Further, the spray structure of injected fuel is described by illustrating the parts of jet spray and for this, the spray is divided in two parts: jet core region and mixed-flow region. Jet core portion consists of large fuel droplets having velocity almost similar as that of inside



orifice and surrounded by mixed-flow section that formed due to involvement of high pressurized cylinder air at spray boundaries. Beyond the length of jet core in axial direction, the portion of mixed-flow region is called spray tip. Teng and McCandless (2005) described that at initial injection period, the length of the core is much larger than the length of spray tip but at later stage opposite trend is observed. As the spray tip or mixed-flow region is increased, the periphery of the spray become more rugged and irregular.

In addition, shape of spray influenced by spray cross-section area and axial direction centroid that indicates spray distribution about the spray-center. As the temperature inside the cylinder rises, there is an increase in spray area which shifts the axial centroid far from the nozzle tip (Suh et al. 2006). Park et al. (2010) compared spray shape of DME with diesel fuel and clarify that diesel injection guides long-narrow spray jet but DME injection leads to broad and short spray structure. In their experimentation, the shape of DME spray tip was observed to be rounder than diesel that causes quick loss in momentum for droplets interacting with neighboring air and generates a vortex at spray tip. Another factor is axial to radial ratio of spray that demonstrates its shape. As the injection is held into atmospheric pressure (0.1 MPa) the transfer of spray momentum in radial direction is larger and more rapid for DME than diesel spray till 0.2 ms after SOI (start of injection). Afterward axial to radial ratio becomes constant for both the fuels. As the ambient pressure is increased to 0.3 MPa, the axial to radial ratio decreased for DME spray because with the increasing temperature, density of surrounding air increases which resists the forward axial motion of spray (Park et al. 2010).

### ***11.4.2 Spray Tip Penetration***

Spray tip penetration is farthest fuel periphery from the orifice exit and for DME it is lesser than that of diesel operation for same injection conditions. This shorter penetration is due to quick atomization of DME molecules because of their low kinetic viscosity and higher evaporation rate. Same trend is observed with the DME-diesel blend. However, with increasing percentage of diesel in blend, the spray penetration length increases with respect to penetration of pure DME spray. Kim et al. 2007 (Ying et al. 2008) reported that this variation is due to higher volatile nature and compressibility of DME fuel. Further, the deceleration of DME droplets is more in direction of nozzle axis and results in shorter penetration under same injection conditions and fuel quantity (Kim et al. 2007). With the fact that more DME fuel is requires to be injected per cycle, the need for longer injection duration and larger nozzle injection area are inevitable. With these modifications, a similar spray penetration for both DME and diesel can be achieved. Teng and Mccandless (2005) reported that at full load condition, a longer DME penetration length than diesel can be achieved as a consequence of improved injection strategies like increased nozzle hole diameter, number of nozzles and injection timing etc.

Suh et al. (2006) claimed that spray tip penetration increased with the rise of injection pressure. This is because the force generated to push the spray downstream dominates the loss of spray momentum due to decreased breakup timing of fuel molecules with increase in injection pressure. Glensvig et al. (1997) also confirmed this result but observed much increased penetration with respect to high rise in injection pressure. The higher penetration may be the result of the increase of injection pressure due to which the leakage about the plunger also increases that compensates most of the variation in spray penetration.

### 11.4.3 Spray Cone Angle

Spray cone angle is defined as the angle between two straight lines that were created by joining the nozzle tip and two maximum radial points of spray separately as shown in Fig. 11.6. The active air–fuel mixing is superior with DME spray as compared to diesel spray due to better vaporization properties, atomization and improved flash

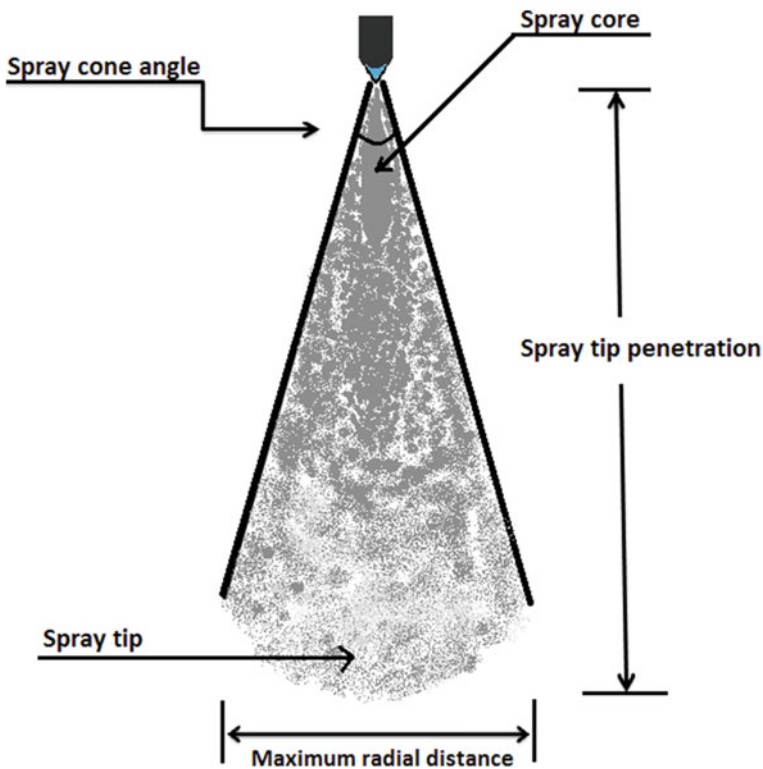


Fig. 11.6 Schematic fuel-spray structure

boiling effect that widen the spray angle of DME (Park et al. 2010). Under similar injection condition, the spray cone angle of the DME is wider than that of diesel by 15–20% (Teng and Mccandless 2005). Spray cone angle for dimethyl ether is also drastically influenced by injection pressure. It has been noticed that the cone angle enhances with increasing injection pressure. Ambient pressure and temperature conditions also affect the spray cone angle. With increase in ambient pressure, the cone angle increases while increase of ambient temperature results in decrease in cone angle.

#### ***11.4.4 Tip Velocity***

Tip velocity of DME spray has a swift rise in initial injection stage and after attaining a peak level, it constantly decreases. This trend is observed due to high momentum in initial phase owing to the higher injection pressure and large droplet particles in initial phase. The regular decrement in tip velocity may be due to sudden vaporization of spray molecules. But as the injection is done at higher pressure, there is extra resistance on tip spray droplets as compared to that offered by cylinder air. Hence, the vaporization occurs in very initial phase and there is no initial rise in tip velocity, unlike in case with diesel spray, thus only continuous decrease in tip velocity for DME is noticed. In addition, overall tip velocity at atmospheric condition is higher than pressurized ambient condition. The momentum of the spray plays an important role for defining tip velocity of spray. Hence, the maximum momentum of the spray is observed in jet core part, and the velocity of spray is also governed by it. Further, the density of DME is much lesser than that of diesel. Due to this, the retardation of tip velocity increases as spray droplets move downstream. Another factor for slower tip velocity is proposed to be the fast breakup time in DME spray after injection, which is calculated 0.198 ms earlier than diesel spray (Suh et al. 2006).

Surface tension is also an important factor that cuts down the tip velocity of the DME as compared to that of diesel. At critical point, the surface tension is zero which means it is the major barrier to vaporization of liquid droplets. Due to the very high surface tension of diesel, its critical temperature is three times that of the dimethyl ether. So, under ambient temperature and pressure of 500 °C and 40 bar respectively; and initial fuel temperature of 20 °C, DME fuel droplets evaporate much quickly, as shown in Table 11.3, that increases momentum loss in spray and simultaneously decrease the tip velocity of DME fuel (Teng and Mccandless 2005).

#### ***11.4.5 Atomization***

*Atomization* is the method of breaking down of liquid fuel into small droplets or mist and can further be mixed more effectively or rapidly with air. DME has full-size fuel droplets near the injector nozzle as in Fig. 11.7 and as it goes downstream,

**Table 11.3** Vaporization duration of different droplet sized fuel spray (Teng and Mccandless 2005)

Fuel	Droplet size (um)	Vaporization duration (ms)
DME	<5	Instantly
DME	10	0.076
Diesel	10	0.78
DME	>20	1.14
Diesel	>20	3.10

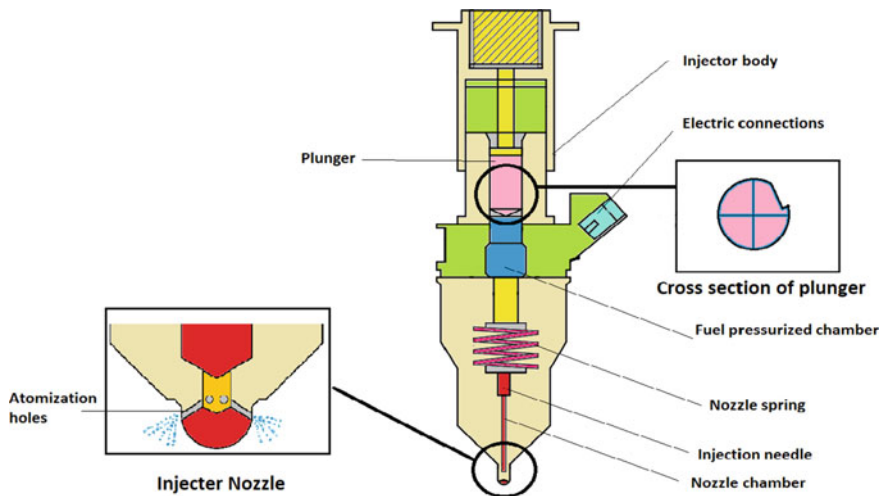


**Fig. 11.7** Fuel injector with injector nozzle and plunger

droplets start degrading in size due to the atomization. Better the atomization, more effective is the air fuel mixing in chamber. As mentioned earlier, increase in number of nozzle holes, swirl intensity, injection pressure, and ambient pressure enhanced atomization in DME spray. During the injection, the rapid pressure drop is held below the saturated vapor pressure of the fuel which helps in achieving better atomization of spray. This phenomenon is called flash boiling effect that assists to get homogeneity of charge. The outer and tip portion of DME spray is very blurred and of less intensity as compare with central core as observed in Fig. 11.5, due to high atomization due to presence of friction between outer periphery droplets and the surrounding air (Kim et al. 2010).

Suh et al. (2006) examined the pattern of atomization of spray droplets and found that many diesel droplets were spotted all over the time after SOI but in case of DME spray, most of the droplets collapsed after 3 ms of start of injection. This result may be due to lower surface tension of the DME fuel droplets. The atomization phenomenon is much faster than that of diesel. Therefore, as discussed earlier somewhat reduced injection pressure is required for proper homogeneous mixing and utilization of

maximum surrounded oxygen all over chamber space when DME sprays in diesel engine.

#### **11.4.6 Sauter Mean Diameter (SMD)**

SMD is defined as the diameter of a sphere, assuming all of them have the same volume/surface area ratio. Under similar operating condition in diesel engine the overall Sauter mean diameter of DME is lesser as comparison with diesel and it further reduces continuously with the elapsed injection timing after start of injection (Roh and Lee 2017). The reason of lower SMD of DME is due to its smaller kinetic viscosity than diesel fuel that improves the fuel atomization under the same injection conditions (Suh et al. 2006). Sauter mean diameter of diesel fuel reduced in stages throughout the time lapsed after start of injection but in case of DME the rapid fall of SDM is observed at 0.3 ms after start of injection.

### **11.5 Optimization of Fuel Injection Strategies**

Optimization of fuel system is important, mainly, to resist vapor lock while fueling DME oil into diesel engine. To achieve this, fuel storage tank is needed to pressurize over 0.5 MPa and fuel delivery pressure is precisely maintained in between 1.2 to 3 MPa. In addition, vapor blockage also interrupts frequent flow of fuel for attaining proper injection conditions, which may occur for DME. This problem, by large can be solved by placing the backup pressure over 0.8 MPa on-road condition to maintain injection procedures free from vapor blockage (Arcoumanis et al. 2008). Lower viscosity of DME fuel may leads to lower lubricity in fuel system and leakage during injection procedure. To avoid leakage, better products with high sealing mechanism are required and Teflon coated O-rings or polytetrafluoroethylene based high-tension inert sealing are preferred. To cope with poor lubrication and to eliminate this wear in fuel system for DME operation; up to 2000 ppm of lubricity additive is required to be mixed with fuel (Arcoumanis et al. 2008).

To attain the peak pressure after the TDC in the engine, advancement in fuel injection is employed. However, an over advanced injection timing may result in occurrence of maximum peak pressure before the piston reaches at TDC which opposes the upward piston motion and decreases the engine power. This requires optimization of injection timing for maximum engine efficiency. It was shown earlier that engine peak thermal efficiency can be achieved for DME by advancing the fuel delivery at 19 °CA BTDC at high engine rpm of 2300 and 15 CA BTDC at low engine rpm of 1400. These values of fuel delivery angle are lesser than those of the diesel fueled engine due to shorter ignition delay (Zhang et al. 2008; Wang et al. 2000).

Spray tip penetration and spray distribution for DME are much lower than that in diesel injection, so spray droplets are not able to utilize much portion of cylinder air for active air–fuel mixing. It is desirable to achieve longer penetration for DME spray to attain increased homogeneity all over the cylinder. However, increase in penetration after certain limit may result in wall wetting that may lead to increased emissions and deteriorates the engine efficacy. Hence, it is concluded that by increasing the injection duration by 0.1 ms the spray distribution and tip penetration of DME spray become identical to diesel spray with same time delay for under same engine operations. In DME fueled engine, to overcome the problems like large injection duration, atomization and lower power output, the increase in nozzle orifice diameter and plunger diameter are the solutions for acquiring better results. By doing this, more fuel is allowed to enter inside the combustion chamber per cycle which is required for efficient operation of DME due to its lower calorific value. Hence, these parameters are optimized in the range of 8.5–9.5 mm for plunger diameter and 0.32–0.42 mm for nozzle orifice diameter (Zhang et al. 2008).

Number of holes has great influence on injection strategies. The fuel injection by 3 and 7 nozzle holes provide different results in terms of the parameters like emissions, performance and efficiency and extreme tradeoff of these factors are observed in between. 7-hole nozzle configuration has shown much improved fuel consumption at high loads due to superior fuel distribution in engine cylinder, but the  $\text{NO}_x$  emissions and combustion noises are quite higher. On the other hand, in 3-hole nozzle configuration, lower  $\text{NO}_x$  emissions and higher fuel consumption are observed. Therefore, a balance between both configurations is important and that is provided by optimization of nozzle hole configuration, which authenticate better performance of 5-hole nozzle for DME fueled engine (Arcoumanis et al. 2008). Protruding distance for diesel operated engine cylinder is 3 mm, however, in case of DME, higher protruding distance is required due to high atomization and vaporizing rate of fuel. To fulfill this necessity, protruding distance is optimized to 5 mm for DME operation (Wang et al. 2000). Increase of injection pressure is responsible for instant vaporization of fuel spray that accumulates majority of DME droplets near to injector. So, reduced injection pressure is required for DME operation, however, lowering injection pressure below certain limit may lead to steep rise in injection duration. Hence, to create balance between vaporization characteristics and injection duration parameters, DME is optimized at the injection pressure of 15 MPa instead of 18 MPa at which diesel fuel is injected in same combustion chamber (Zhang et al. 2008).

## 11.6 Conclusion

The present chapter focuses on studying Dimethyl Ether as a substitute to conventional diesel. Even though DME has various advantages over diesel in terms of combustion, performance, and low emissions, yet it cannot be used straightaway in

the diesel engines for its optimum performance without undergoing some modifications in engine operating parameters. This chapter discusses all those injection parameters which are inevitable to obtain complete combustion, high power delivery and less emission while using DME as a diesel engine fuels. The suitable changes required in the fuel injection strategies to enhance the performance and emission characteristics of DMEs fuelled engine have also been discussed.

The following major conclusions may be drawn:

- The factors that affect fuel injection properties are vapour lock, injection pressure, needle lift behaviour, plunger diameter, nozzle diameter and number of nozzles and fuel properties have lot of impact on the performance parameters using DME. Lower viscosity of DME fuel can increase the chance of wear in moving parts of fuel system. To get rid from high frequent wearing in fuel system components, extra lubricant additives up to 2000 ppm is mixed with fuel.
- The probability of vapor lock phenomenon in DME fuelled engine is extremely high. Thus, it is imperative to store DME in the liquid form. In addition, retaining higher pressure inside the fuel system assist in avoiding vapour lock formation.
- The ignition delay for DME is reported to be less than that of diesel which can be attributed to characteristics like higher cetane number, better atomization and low auto-ignition temperature. Hence, optimisation of injection timing can be adopted to ameliorate the effects of shorter ignition delay. It has been shown that the maximum thermal efficiency for DME can be achieve by advancing in fuel delivery timing to 19 °CA BTDC for high engine speed (2300 rpm) and 15 °CA BTDC for low engine speed (1400 rpm).
- Longer injection duration is required for DME fuelled engine compared to that of diesel to mitigate the effects of shorter spray length which occurs due to higher vaporisation rate of DME spray. An identical spray penetration as diesel spray can be achieve by increasing injection duration by 0.1 ms under same operating circumstances.
- Breakdown of DME spray molecules are executed in its very early stage after SOI. This demands higher protruding distance of 5 mm for DME operation in comparison to 3 mm protruding distance for diesel fuelled engine.
- To cover entire chamber space and achieving better spray quality for enhancing homogeneity in cylinder, 5-hole nozzle configuration with reduced injection pressure as compare to diesel operation will serve best results for DME operation.

## References

- Alam M, Kajitani S (2001) DME as an alternative fuel for direct injection diesel engine. In: 4th International conference on mechanical engineering in Dhaka Bangladesh, 26–28 Dec 2001, pp III 87–92
- Arcoumanis C, Bae C, Crookes R, Kinoshita E (2008) The potential of di-methyl ether (DME) as an alternative fuel for compression-ignition engines: a review. *Fuel* 87:1014–1030

- Egnell R (2001) Comparison of heat release and NO<sub>x</sub> formation in a DI diesel engine running on DME and diesel fuel. SAE Technical Paper Series. SAE International
- Fleisch T, McCarthy C, Basu A, Udovich C, Charbonneau P, Slodowski W et al (1995) A new clean diesel technology: demonstration of ULEV emissions on a navistar diesel engine fueled with dimethyl ether. SAE Technical Paper Series. SAE International
- Glensvig M, Soreson SC, Abata DL (1997) High pressure injection of dimethyl ether. Department of Energy Engineering, Energy Conversion
- Huang Z, Qiao X, Zhang W, Wu J, Zhang J (2009) Dimethyl ether as alternative fuel for CI engine and vehicle. *Front Energy Power Eng Chin* 3:99–108
- Iliuta I, Larachi F, Fongarland P (2010) Dimethyl ether synthesis with in situ H<sub>2</sub>O removal in fixed-bed membrane reactor: model and simulations. *Ind Eng Chem Res* 49:6870–6877
- Kajitani S, Oguma M and Mori T (2000) DME fuel blends for lowemission direct-injection diesel engines, SAE Paper 2000-01-2004
- Kamil M, Nazzal IT (2016) Performance evaluation of spark ignited engine fueled with gasoline-ethanol-methanol blends. *J Energy Power Eng* 10
- Khunaphan S, Hartley UW, Theinnoi K (2013) Characterization and potential of dimethyl ether (DME) as dual fuel combustion in a compression ignition engine. *Int J Eng Sci Innov Technol*
- Kim MY, Bang SH, Lee CS (2007) Experimental investigation of spray and combustion characteristics of dimethyl ether in a common-rail diesel engine. *Energy Fuels* 21:793–800
- Kim HJ, Park SH, Lee CS (2010) A study on the macroscopic spray behavior and atomization characteristics of biodiesel and dimethyl ether sprays under increased ambient pressure. *Fuel Process Technol* 91:354–363
- Kumar N (2019) Study of oxygenated ecofuel applications in CI engine, gas turbine, and jet engine. In: *Advanced biofuels*. Elsevier, pp 405–441.
- Lee JH, Cho S, Lee SY, Bae C (2002) Bouncing of the diesel injector needle at the closing stage. *Proc Inst Mech Eng Part D J Automob Eng* 216:691–700
- Li GB (2010) Dimethyl ether (DME): a new alternative fuel for diesel vehicle. *Adv Mater Res* 156–157:1014–1018
- Liuzzi D, Peinado C, Peña MA, Kampen JV, Boon J, Rojas S (2020) Increasing dimethyl ether production from biomass-derived syngas via sorption enhanced dimethyl ether synthesis. *Sustain Energy Fuels*, Article
- Longbao Z, Hewu W, Deming J, Zuohua H (1999) Study of performance and combustion characteristics of a DME-fueled light-duty direct-injection diesel engine. SAE Technical Paper Series, 1999-01-3669
- Makoś P, Ślupek E, Sobczak J, Zabrocki D, Hupka J, Rogala A (2019) Dimethyl ether (DM) as potential environmental friendly fuel. In: Sayegh MA, Danielewicz J, Jouhara H, Kaźmierczak B, Kutylowska M, Piekarska K (eds) *E3S web of conferences*, vol 116, p 00048
- Nautiyal H, Shree V, Khurana S, Kumar N, Varun (2015) Recycling potential of building materials: a review. In: *Environmental implications of recycling and recycled products*. Springer Singapore, pp 31–50
- Park SH, Chang SL (2014) Applicability of dimethyl ether (DME) in a compression ignition engine as an alternative fuel. *Energy Convers Manage* 86:848–863
- Park SH, Kim HJ, Lee CS (2010) Macroscopic spray characteristics and breakup performance of dimethyl ether (DME) fuel at high fuel temperatures and ambient conditions. *Fuel* 89:3001–3011
- Peral E, Martín M (2015) Optimal production of dimethyl ether from switchgrass-based syngas via direct synthesis. *Ind Eng Chem Res* 54:7465–7475
- Perathoner S, Centi G (2014) CO<sub>2</sub> recycling: a key strategy to introduce green energy in the chemical production chain. *Chemsuschem* 7:1274–1282
- Pontzen F, Liebner W, Gronemann V, Rothaemel M, Ahlers B (2011) CO<sub>2</sub>-based methanol and DME—efficient technologies for industrial scale production. *Catal Today* 171:242–250
- Rakopoulos CD, Rakopoulos DC, Giakoumis EG, Kyritsis DC (2011) The combustion of n-butanol/diesel fuel blends and its cyclic variability in a direct injection diesel engine. *Proc Inst Mech Eng Part A J Power Energy* 225:289–308



- Rao YV, Voleti RS, Hariharan VS, Raju AV, Redd PN (2009) Use of Jatropha oil methyl ester and its blends as an alternative fuel in diesel engine. *J Braz Soc Mech Sci Eng* 31:253–260
- Roh HG, Lee CS (2017) Fuel properties and emission characteristics of dimethyl ether in a diesel engine. In: *Locomotives and rail road transportation*. Springer Singapore, pp 113–128
- Sato Y, Noda A, Jun L (2001) Effects of fuel injection characteristics on heat release and emissions in a DI diesel engine operated on DME. *SAE Technical Paper Series*. SAE International
- Sato Y, Nozaki S, Noda T (2004) The performance of a diesel engine for light duty truck using a jerk type in-line DME injection system. *SAE Tech Paper*. 2004-01-1862
- Saxena V, Kumar N, Saxena VK (2021) Combustion, performance and emissions of Acacia concinna biodiesel blends in a diesel engine with variable specific heat ratio. *J Therm Anal Calorimet*
- Song R, Li K, Feng Y, Liu S (2009) Performance and emission characteristics of DME engine with high ratio of EGR. *Energy Fuels* 23:5460–5466
- Sorenson SC, Mikkelsen SE (1995) Performance and emissions of a 0.273 liter direct injection diesel engine fueled with neat dimethyl ether. *SAE Paper* 950964
- Sorenson SC, Glensvig M, Abata DL (1998) Dimethyl ether in diesel fuel injection systems. *SAE Technical Paper Series*. SAE International
- Suh HK, Park SW, Lee CS (2006) Atomization characteristics of dimethyl ether fuel as an alternative fuel injected through a common-rail injection system. *Energy Fuels* 20:1471–1481
- Teng H, Mccandless JC (2005) Comparative study of characteristics of diesel-fuel and dimethyl-ether sprays in the engine. *SAE Technical Paper Series*. SAE International
- Thomas G, Feng B, Veeraragavan A, Cleary MJ, Drinnan N (2014) Emissions from DME combustion in diesel engines and their implications on meeting future emission norms: a review. *Fuel Process Technol* 119:286–304
- Wakai K, Nishida K, Yoshizaki T, Hiroyasu H (1999) Ignition delays of DME and diesel fuel sprays injected by a D.I. diesel injector. *SAE Technical Paper Series*. SAE International
- Wang HW, Zhou LB, Jiang DM, Huang ZH (2000) Study on the performance and emissions of a compression ignition engine fuelled with dimethyl ether. *Proc Inst Mech Eng Part D J Automob Eng* 214:101–106
- Wattanavichien K (2009) Implementation of DME in a small direct injection diesel engine. *Int J Renew Energy* 2(4)
- Wu S, Bao J, Wang Z, Zhang H, Xiao R (2021) The regulated emissions and PAH emissions of bio-based long-chain ethers in a diesel engine. *Fuel Process Technol* 214:106724
- Xinling L, Zhen H (2009) Emission reduction potential of using gas-to-liquid and dimethyl ether fuels on a turbocharged diesel engine. *Sci Total Environ* 407:2234–2244
- Ying W, Genbao L, Wei Z, Longbao Z (2008) Study on the application of DME/diesel blends in a diesel engine. *Fuel Process Technol* 89:1272–1280
- Zhang Y, Yu J, Mo C, Zhou S (2008) A study on combustion and emission characteristics of small DI diesel engine fuelled with dimethyl ether. *SAE Technical Paper Series*. SAE International
- Zhu Z, Li DK, Liu J, Wei YJ, Liu SH (2012) Investigation on the regulated and unregulated emissions of a DME engine under different injection timing. *Appl Therm Eng* 35:9–14

**Part IV**  
**Application of Methanol and Ammonia**  
**as an E-Fuel**

# Chapter 12

## ECU Calibration for Methanol Fuelled Spark Ignition Engines



Omkar Yadav, Hardikk Valera , and Avinash Kumar Agarwal 

**Abstract** Energy demand for the transport sector is continuously increasing along with the implementation of stricter emission norms. It is necessary to find alternatives for conventional petroleum fuels. Methanol has emerged as a promising replacement for conventional petroleum fuels in the transport sector. It can be produced using renewable and non-renewable feedstocks. Also, it is considered an E-fuel as it can be produced using renewable electricity. The physicochemical properties of methanol are more suitable for its use in spark-ignition engines. Out of all the technologies, port fuel injection technology is one of the best ways for methanol utilization in existing electronic fuel injection (EFI) engines with minimal structural changes in the engine. The typical properties of methanol like lower calorific value, higher latent heat of vaporization, low volatility, higher laminar flame speed and higher octane number warrants modifications in the injection and ignition strategies in the conventional gasoline engines. For better performance, these strategies must be optimized for corresponding engine operating conditions. The combustion of EFI engines is primarily governed by Electronic Control Unit (ECU), which contains pre-calibrated maps to decide optimum injection and ignition strategy. ECU calibration is the process of determining the optimal calibration tables for an engine. In this chapter, the methodology of ECU calibration for methanol-fueled SI engine equipped vehicles is discussed at length.

**Keywords** Methanol · EFI · Calibration · Ignition maps · ECU

### 12.1 Introduction

In recent years with growing industrialization, the energy demand has been continuously increasing. According to BP statistical review of world energy 2020, despite a reduction in the growth rate in 2019, the overall global energy consumption rose at an

---

O. Yadav · H. Valera · A. K. Agarwal (✉)  
Engine Research Laboratory, Department of Mechanical Engineering,  
Indian Institute of Technology Kanpur, Kanpur 208016, India  
e-mail: [akag@iitk.ac.in](mailto:akag@iitk.ac.in)

© The Author(s), under exclusive license to Springer Nature Singapore Pte Ltd. 2022  
A. K. Agarwal and H. Valera (eds.), *Greener and Scalable E-fuels for Decarbonization of Transport*, Energy, Environment, and Sustainability,  
[https://doi.org/10.1007/978-981-16-8344-2\\_12](https://doi.org/10.1007/978-981-16-8344-2_12)

317

average rate of 1.6% per year in the last ten years. It can be observed that renewables and natural gas drove the energy consumption growth in recent years; however, oil continued to hold the largest share of the energy mix (33.1%) (Fig. 12.1).

Despite the reduced energy demand in 2020–21, the global energy demand is expected to rise shortly. International Energy Agency predicted global future energy demands in the view of the pandemic, as shown in Fig. 12.2. The future energy demand is anticipated for three scenarios: (i) pre-crisis, (ii) stated policies, and (iii) delayed recovery.

Energy is the oxygen of the economy for any country. Economic development depends on the cost-effectiveness and environment-friendliness of the energy sources. In developing countries, reliable and affordable energy is vital for supporting their economic and social progress to improve their quality of life. Countries having higher GDP consume higher per capita energy. Efforts are being made to reduce energy poverty by searching for sustainable energy resources to boost the country’s economy. There is a need to search for sustainable alternative fuels to satisfy the increased future energy demand while ensuring low emissions. The transport sector is the foundation of any economy, ensuring the smooth movement of passengers and goods.

Moreover, it maintains balanced socio-economic development in different regions of any country. The use of affordable, efficient, and sustainable energy sources is the key to develop the transport sector and, ultimately, the national economy. Currently, coal, natural gas, and oil are the three primary energy sources.

The contribution of various energy sources to the global energy demand is shown in Fig. 12.3. Coal is the most significant contributor to energy. Moreover, there are

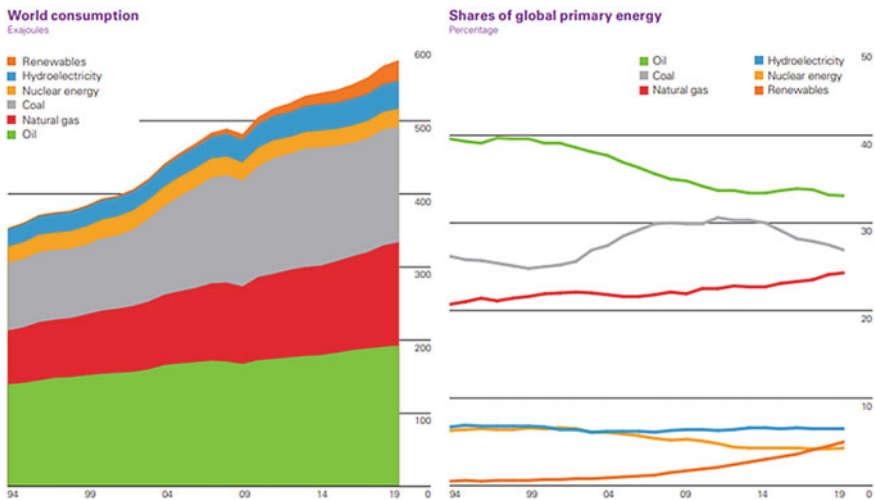


**Fig. 12.1** BP Statistical review of global energy scenario 2020 (Statistical Review of World Energy 2020)

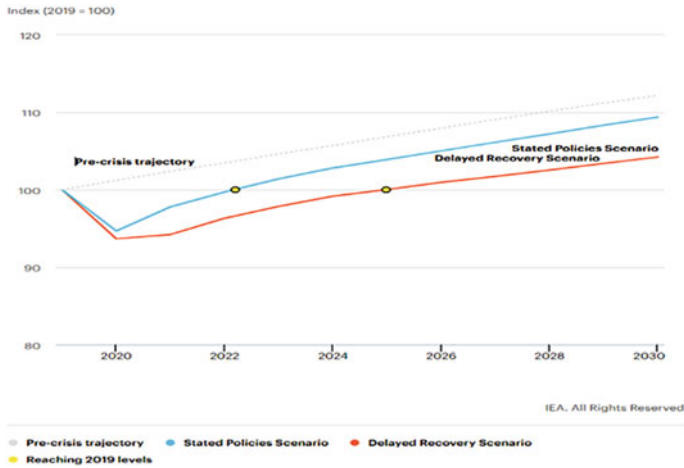
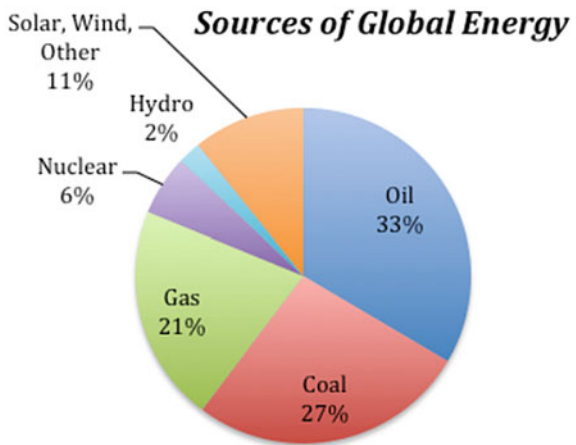


Fig. 12.2 Global primary energy demand growth (2019–30), IEA (World Energy Outlook 2019)

Fig. 12.3 Energy source data (World Energy Balances 2021)



surplus quantities of high ash content coal, which is not useful for electricity generation, steel making, or other industrial applications. This coal with high ash content, however, can be utilized to produce methanol. Along with availability and environmental impact, there is one more vital factor to consider while selecting energy sources, e.g., energy cost. The fuel cost includes the cost associated with energy production (extraction, refinement, and conversion), current supply and demand, and the tax levied by the government. There is a need to search for sustainable alternative fuels catering to rising energy demand and ensuring low emissions simultaneously to cater to constantly increasing energy demand. The majority of energy demand is satisfied by fossil fuels; however, their reserves are limited. With the same consumption rate, oil reserves would run out in ~53 years. Consumption of fossil fuels leads

to greenhouse gas (GHG) emissions as well. With continuously increasing energy demand for transport energy and stringent emission norms, it becomes essential to find alternatives for conventional petroleum fuels, fulfilling these needs. The basic requirement for global acceptance of any fuel is its availability at an affordable cost. They should also comply with the existing and future emission norms without major hardware changes in existing engines.

Primary alcohols can be an alternative fuel against conventional gasoline fuel. These alcohols can be produced from non-petroleum feedstocks such as coal, biomass, municipal solid waste (MSW), biogas, waste CO<sub>2</sub> (Valera and Agarwal 2019). Their octane number is high, which ensures smoother combustion even in higher compression ratio engines. Methanol fueled vehicles produce fewer emissions than conventional petroleum-fueled vehicles (Zhen and Wang 2015). The well-to-wheel (WTW) emissions during coal-to-methanol production compared to gasoline production are higher. However, it should be noted that methanol emissions from coal can be reduced to a greater extent if cogeneration plants are operated for electricity generation. Moreover, for other feedstocks except coal, the well-to-wheel emissions from methanol-fueled vehicles are lower than conventionally fueled vehicles.

## 12.2 Methanol as Engine Fuel

Methanol is a colourless and tasteless liquid with a light odour. It is the simplest alcohol consisting of a single carbon atom. Methanol has comparable/similar physio-chemical properties to conventional fuels like gasoline and diesel (Agarwal et al. 2021). However, the benefits of the properties come with several challenges; both advantages and challenges are discussed in detail.

### *Advantages*

- Methanol possesses higher latent heat of vaporization and a lower stoichiometric air-fuel ratio than gasoline. This leads to a cooling effect on the intake charge, improving the volumetric efficiency of the engine.
- Due to the higher octane rating of methanol, it can be used in engines with higher compression ratios (Göktaş et al. 2021). This improves engine efficiency and reduces the possibility of knocking.
- Methanol has a high auto-ignition temperature compared to gasoline. It ensures smooth engine operation even at relatively high compression ratios, making the engine more efficient.
- Methanol's higher laminar flame speed decreases the combustion duration and improves the power output and engine efficiency (Verhelst et al. 2019).
- Inherent oxygen of methanol ensures complete combustion. CO is oxidized to CO<sub>2</sub>, unburned hydrocarbons from crevice volumes, and the lubricating oil layer is burned in the late expansion stroke. This ensures complete combustion during the expansion stroke. However, it leads to relatively high aldehyde emissions (Wei 2021; Valera et al. 2021).

- Methanol is a sulphur-free fuel, and it does not produce any sulphur oxide emissions.

### *Challenges*

- The energy density of methanol is very low compared to gasoline. Hence, methanol-fueled engines require almost double fuel quantity for producing the same power output. This can be achieved by upsizing the nozzle jet diameter of the existing carburettor in the case of carbureted SI engines (Valera et al. 2020). Similarly, in engines equipped with an electronic fuel injection (EFI) system, fuel injection quantity can be increased by increasing the pulse width of fuel injection.
- The low energy density of methanol reduces the mileage per fuel tank filling. The fuel tank capacity must be increased to address this issue.
- The methanol-fueled engines have poor cold startability. Higher energy is required for methanol vaporization to form a combustible charge.
- Methanol flames are invisible. The lower flame luminosity creates challenges for its use as automotive fuel from a safety perspective.
- Methanol is corrosive; hence brass and copper-containing components cannot be used in methanol-fueled engines. Even some plastics get easily dissolved in methanol. This creates material compatibility issues for methanol adaptation in IC engines. However, synthetic rubber components, seals, and gaskets made of Neoprene and Buna-N can be used. Careful material selection is required during manufacturing engine parts to make them compatible with methanol.

China is currently leading for commercial production and use of methanol-fueled engines. They have implemented M15 (15% methanol and 85% gasoline) standards in dozens of Chinese provinces, having octane number requirements of 95 and 97 (Methanol Fuels » Demonstration Projects 2021). Also, drivers had tested methanol-fueled cars for more than 200 million miles. The Chinese government had launched demonstration programs of M85 and M100 fueled vehicles in Shaanxi, Shanghai, and Shanxi. The Israeli government also launched a demonstration program of M15 fueled vehicles to show its potential. Other than these two countries, India (IS: 17076: 2019), Australia, and European countries are implementing methanol usage as fuel for SI and CI engines.

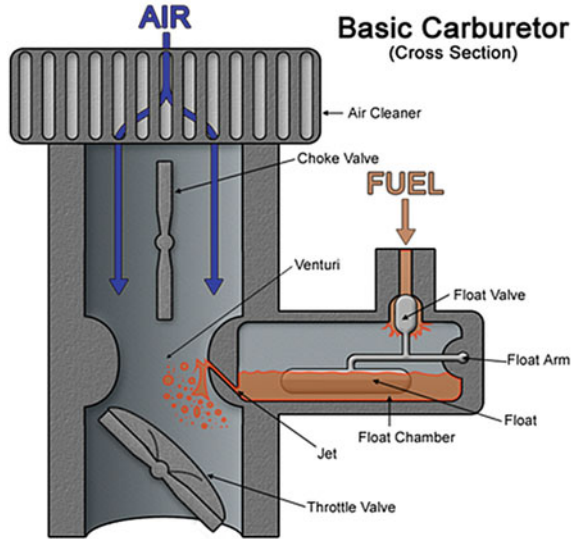
## ***12.2.1 Methanol Utilization Strategies***

Currently, the fuel injection strategies used: (a) carburettor assisted fuel injection and (b) modern electronic fuel injection (EFI) systems. These strategies are discussed in the next sub-sections.

### *Conventional Carbureted Fuel Supply*

A carburettor is a mechanical device used to prepare a suitable charge by premixing air and fuel in the required ratio before inducting it into the combustion chamber. In a

**Fig. 12.4** Schematic of Carburetor



carburettor, air flows through a venturi, which is a converging-diverging nozzle. The pressure difference is created between the inlet and throat of the venturi, depending upon the throttle opening and current engine operating condition. This pressure difference causes the airflow from the intake manifold in the venturi. The fast-moving air reduces the static pressure in the throat, which leads to the fuel flow into the intake air stream from the float chamber. The photographic images of various parts used for meeting the engine requirements are shown in Fig. 12.4. Fuel is injected into the throttle body, and it evaporates in the air stream to form a suitable charge. Although Modern carburetors provide few compensations and adjustments in the air-fuel ratio with changing operating conditions, they still have many limitations. These limitations include dynamic AFR adjustments, injection timing adjustments, acceleration and deceleration compensations, altitude, temperature-based compensations, etc. Hence, close control over the fuel flow is not possible, and it adversely affects the engine efficiency and emissions. Moreover, poor cold-starting characteristics and lower calorific value of methanol offer challenges in adapting higher methanol blends in conventional carbureted vehicles. Another promising technology for methanol utilization in the two-wheelers is the electronic fuel injection (EFI) system, discussed in the following sub-section.

#### *Modern Electronic Fuel Injection*

The modern EFI system is equipped with an Electronic Control Unit (ECU), sensors, and actuators. An ECU ensures optimal engine performance by reading the input values related to engine operating conditions from various sensors and calculates the injection and ignition parameters with the help of pre-installed maps. Output signals are then sent to actuators such as the fuel injectors, ignition coil, and fuel pumps. The EFI system allows air-fuel ratio and injection timing to be precisely



and separately adjusted, unlike carbureted fuel injection systems. The quantities of fuel and air in the EFI system can be adjusted independently. Hence, using either a lean or rich air-fuel ratio is possible by optimizing the engine performance. Injection timing can be varied, which significantly improves the acceleration characteristics of the vehicle. With real-time data monitoring using sensors, the EFI system can adjust engine operation even in changing environmental conditions such as ambient pressure and temperature changes due to a change in altitude. A comparative analysis of both these fuel injection systems reveals the following:

- An EFI system can dynamically adjust the AFR based on engine operating conditions, whereas carbureted system generally runs with fuel-rich mixtures at all engine loads. AFR optimization is challenging in the carbureted systems.
- With close control over the AFR in an EFI system, reducing emissions and improving engine efficiency is possible compared to the carbureted system.
- An EFI system can account for altitude compensations and environmental variables with continuous data monitoring using sensors, unlike in the carbureted system.
- EFI system allows altering fuel injection timings, which improve fuel evaporation at all speeds. Moreover, with acceleration compensation and deceleration fuel cutoffs, the throttle response can be improved. Due to continuous fuel injection in the carbureted system, control over the injection timings is not possible.

Carbureted system is a mechanical system, warrants periodic adjustments. On the other hand, the EFI system is more reliable and continuously adjusts itself by using feedback control. Few more techniques can be utilized for methanol utilization in SI engines. The methanol direct injection technique can be used in the existing GDI engines. Another promising technique for utilizing different blends of methanol is the flex fuel technique, which uses a flex-fuel sensor in the fuel tank to sense the methanol-gasoline blend ratio. Accordingly, ECU decides fuel injection and ignition strategy. However, these techniques have certain challenges and warrants major modifications in the existing SI engines. In this chapter, the methanol utilization strategy using EFI technology is discussed elaborately. The EFI system is equipped with an engine management system (EMS) that controls overall engine operation. EMS consists of an electronic control unit, sensors, actuators, and a power module. ECU continuously receives signals from various input sensors. Based on these inputs, it determines fuel injection quantity and ignition timing. The output signals are then sent to the actuators. Figure 12.5 shows the ECU operation in brief.

The primary task of the EFI system is to determine the amount of fuel mass to be injected and the duration of pulse width required for injection in each cycle. The mass of air inducted in every cycle depends on the engine load. Based upon the engine load and the desired AFR, the fuel injection quantity is calculated. Different methods are used to determine engine load by OEMs based upon the application and sensor. These methods use either mass airflow sensor (MAF) sensor, manifold absolute pressure (MAP) sensor, Throttle position sensor (TPS) sensor, or a combination of these sensors. MAF sensor directly provides a mass flow rate of air as input information to the ECU.

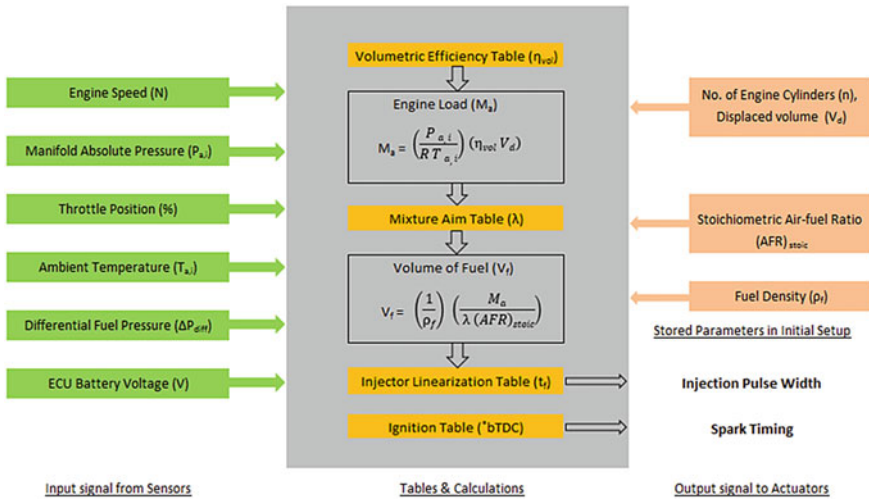


Fig. 12.5 Working of the EMS system

On the other hand, MAP and TPS sensors provide absolute pressure and throttle opening angles, respectively, as input signals to the ECU. This information is further processed using an algorithm. The algorithm uses an ideal gas equation to evaluate the engine load. Let’s understand in detail how the ECU works on MAP-based algorithms to determine the injection pulse width.

$$Air\ mass\ (m_a) = \frac{P \times V_{rel}}{RT} \quad (\text{From Ideal gas law}) \quad (12.1)$$

Here, Air mass = mass of air inducted during the suction stroke  
 P = Manifold absolute pressure in KPa  
 $V_{rel}$  = Relative volume =  $V_{cyl} \times$  Volumetric efficiency ( $\eta_{vol}$ )

$$\eta_{vol} = \frac{\text{Actual volume of intake air drawn into cylinder}}{\text{Theoretical volume of cylinder}}$$

R = Universal gas constant = 0.287 J/kg K for air  
 T = Ambient temperature in K.

The volumetric efficiency is the variable that depends upon relative cylinder filling, and it affects the engine load. It is a direct function of manifold pressure and the throttle position. As the pressure in the intake manifold increases, more air is inducted into the cylinder. The volumetric efficiency should be carefully selected at each engine operating condition to meet the desired AFR. This is known as volumetric efficiency tuning and is discussed at length in the ECU calibration process.

For an engine with n number of cylinders and total capacity  $V_{engine}$ , the individual cylinder volume is calculated by,

$$V_{cyl} = \frac{V_{engine}}{\text{number of cylinders } (n)}$$

Using this relation in Eq. 12.1,

$$\text{Air mass (g/cyl)} = \frac{V_{engine(l)} \times \eta_{vol} \times P(KPa)}{0.287 \times T(K) \times \text{number of cylinders } (n)} \quad (12.2)$$

Now, for an engine operating with N RPM, suction stroke occurs once in every two revolutions. Mass of air inducted (g/s) for an engine operating at N RPM is given by,

$$\text{Air mass (g/s)} = \frac{V_{engine(l)} \times \eta_{vol} \times P(KPa) \times N(RPM)}{0.287 \times 60 \times 2 \times T(K) \times \text{number of cylinders } (n)} \quad (12.3)$$

Once the air mass or engine load is calculated, ECU determines the fuel injection quantity based on the desired air-fuel ratio (AFR) from the aim lambda table. The AFR is given by,

$$\text{AFR} = \lambda \times (\text{AFR})_{\text{stoich}}$$

Using this relationship, fuel rate is calculated as,

$$\text{Fuel flow (g/s)} = \frac{\text{Airflow} \left( \frac{\text{g}}{\text{s}} \right)}{\text{AFR}} \quad (12.4)$$

Fuel flow (g/s)

$$= \frac{V_{engine(l)} \times \eta_{vol} \times P(KPa) \times N(RPM)}{0.287 \times 60 \times 2 \times T(K) \times \text{number of cylinders } (n) \times \lambda \times (\text{AFR})_{\text{stoich}}} \quad (12.5)$$

Fuel mass (g/cyl)

$$= \frac{V_{engine(l)} \times \eta_{vol} \times P(KPa)}{0.287 \times T(K) \times \text{number of cylinders } (n) \times \lambda \times (\text{AFR})_{\text{stoich}}} \quad (12.6)$$

With the pre-installed value of the density of fuel and taking into account the temperature coefficient for change in density, the volume of fuel to be injected in each cylinder is calculated by Eq. 12.7:

$$V_f = \frac{1}{\rho_f} \times \frac{V_{engine(l)} \times \eta_{vol} \times P(KPa)}{0.287 \times T(K) \times \text{number of cylinders } (n) \times \lambda \times (\text{AFR})_{\text{stoich}}} \quad (12.7)$$

ECU determines the injector pulse width and injection timing depending upon the number of injectors and engine speed. Injector pulse width is the injector open time for the required fuel delivery.

In the Alpha-N algorithm, throttle opening angle ( $\alpha$ ) and engine speed (N) determine the fuel quantity to be injected. Throttle opening is also directly related to the engine load and varies almost linearly with the manifold absolute pressure except at low load and WOT conditions. Hence it is very convenient to use throttle opening as an indicator of engine load. Throttle opening varies from 0% at no load and 0 kPa to 100% at WOT and 101.325 kPa manifold absolute pressure with linear scale in-between. In this algorithm, the throttle opening value from TPS is used to replace the manifold pressure (P); subsequently, the ECU follows the same algorithm as used in the MAP-based method. In the MAF-based approach, the MAF sensor directly provides the mass flow rate of air. Hence, initial steps for engine load calculation are not required, and the algorithm follows a similar estimate from Eq. 12.4 onwards.

All the three MAP, TPS, or MAF-based methods have their advantages and limitations. MAF-based methods have good accuracy and faster response except at low loads. So, this method ensures close control over the AFR and ensures lower emissions. But as the MAF sensor is mounted in the intake manifold, it obstructs the airflow and reduces the cylinder filling. Moreover, MAF sensors work well with the factory settings, but they need to be replaced or recalibrated while tuning using standalone ECU. MAP sensors show fluctuating output responses at higher loads. MAP and MAF-based methods are often used together to have their advantages. Although TPS based approach has the least accuracy, it is simpler in construction and operation. In this study, TPS based Alpha-N method was used for engine load calculations. Ignition timing is directly determined from the pre-installed ignition maps. The ignition map contains ignition timing advance in  $^{\circ}\text{CA}$  before the TDC for all engine speeds and throttle-based loads. The detailed procedure of ECU calibration for both injection and ignition strategies are explained in the next section.

## 12.3 Instruments Used in the Calibration Setup

### 12.3.1 Engine Dynamometer Setup

The engine dynamometer setup is used to calibrate ECU in the steady-state operating conditions consists of a test engine and dynamometer assembly, ECU calibration setup, combustion, and emissions analysis system. ECU was first calibrated under steady-state operating conditions. Engine exhaust emissions are monitored using an emission analyzer. A combustion analyzer is used to measure combustion parameters such as in-cylinder pressure versus  $^{\circ}\text{CA}$  history, HRR versus  $^{\circ}\text{CA}$ , and other dependent quantities. An electrical spark plug is replaced with a spark plug pressure transducer to monitor in-cylinder pressure. The engine crankshaft is extended out to install a precision angle encoder for measuring the engine rotation. Figure 12.6 shows the schematic of an engine dynamometer experimental setup.

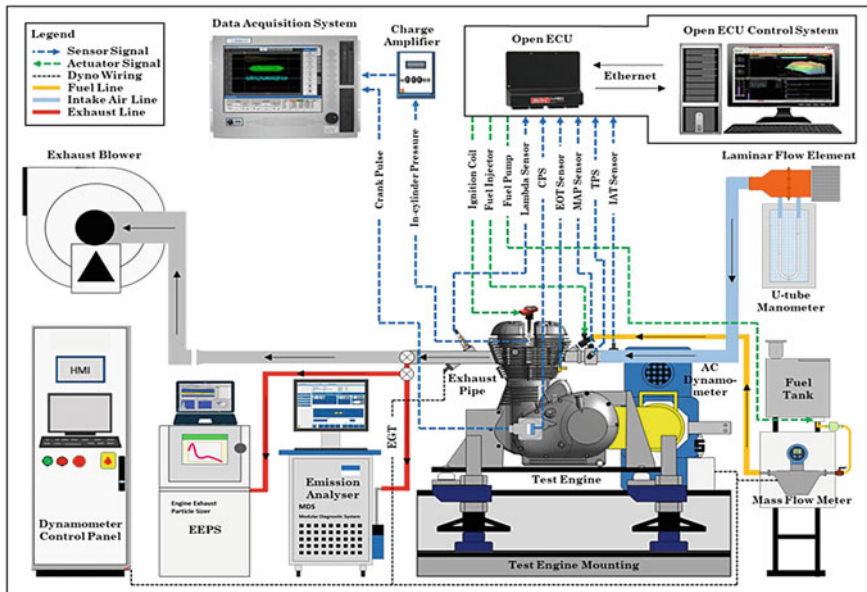


Fig. 12.6 Schematic of engine dynamometer test setup

### 12.3.2 Chassis Dynamometer Setup

A chassis dynamometer setup is used to calibrate ECU in transient operating conditions and evaluate the vehicle’s transient performance. The overall setup can be divided into three sections: dynamometer room, dynamometer & ECU controller room, and underground pit covered by checkered plates. The vehicle’s rear wheel is mounted on the chassis roller, whereas the front wheel was clamped pneumatically to the testbed. A driver aid panel is provided to display important test parameters such as current vehicle operating condition, drive-cycle, etc. A heavy-duty blower with variable frequency drive is fixed in the vehicle’s front to simulate road-load conditions. The blower speed was synchronized with the vehicle speed. ECU of the vehicle was connected to the controller computer system using an Ethernet cable. Figure 12.7 shows the schematic of a chassis dynamometer experimental setup.

### 12.3.3 Combustion Data Acquisition System

The combustion data acquisition system monitors the in-cylinder pressure for controlling the combustion events in the engine cylinder. The combustion-related parameters such as combustion duration, combustion phasing, RoPR, mass fraction burned, HRR, etc., are important since they affect engine emissions and performance.

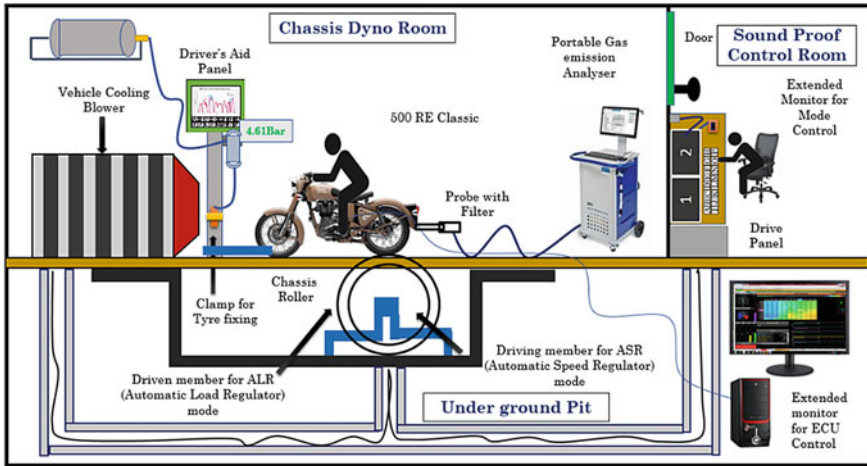


Fig. 12.7 Schematic of the chassis dynamometer experimental setup

Figure 12.8 shows the schematic of the combustion data acquisition system used in this study. The system consists of a spark plug pressure transducer, precision shaft encoder, charge amplifier, and high-speed combustion data acquisition system. The spark plug pressure transducer generates dynamic pressure signals, which are then

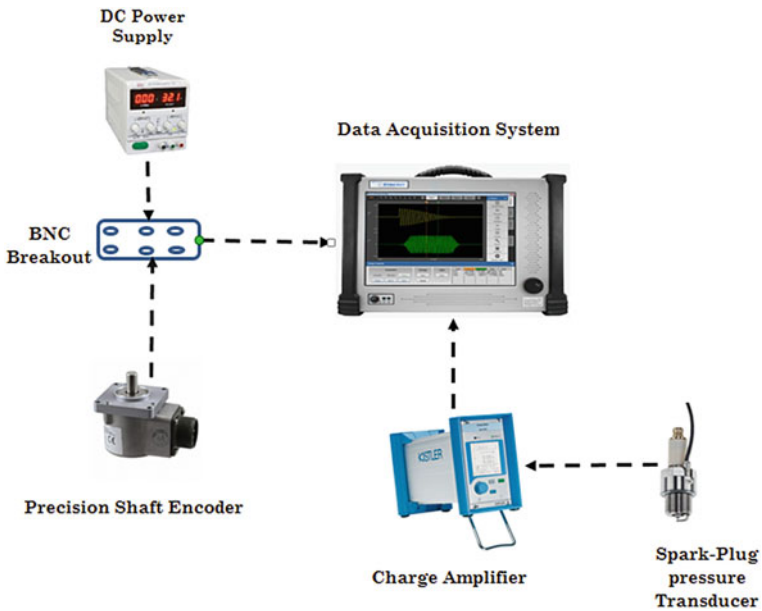


Fig. 12.8 Schematic of the combustion DAQ System

amplified by a charge amplifier. These signals are then post-processed by the DAQ system. The output pulse from the precision shaft encoder is synchronized with the actual °CA position in the engine cycle. Based on the in-cylinder pressure data, other combustion-related parameters are evaluated.

### ***12.3.4 Emissions Analysis System***

Emission measurement and analysis are vital during the development of engines since exhaust emissions constitute a significant source of air pollution. These emissions from IC engines can be broadly categorized into (i) regulated and (ii) non-regulated emissions. CO, THC (total hydrocarbons), NO<sub>x</sub>, and particulate matter (PM) are classified into regulated emissions, whereas the rest of the emissions, such as aldehydes, benzene, toluene, etc., are unregulated emissions. A probe is inserted into the engine tailpipe through a diversion pipe, extended from the engine exhaust. The analyzer uses non-dispersive infrared (NDIR) spectroscopy to measure CO, CO<sub>2</sub>, and total hydrocarbons (THC) and electrochemical sensing to measure the oxides of Nitrogen (NO<sub>x</sub>).

### ***12.3.5 Engine Management System***

Engines nowadays are equipped with an engine management system (EMS) that controls various operating parameters to optimize their performance. The number of electronic components in vehicles is increasing day by day. More than 80% of the innovations in the automotive sector are electronic. Today, the total electronics cost in the vehicle is almost 35–40% of vehicle cost. It is further expected to increase to 50% of the entire vehicle cost by 2050. Although electronics cost is comparatively lower in two-wheelers, it is also rising fast recently with the replacement of carburettor technology by electronic fuel injection technology. The EMS is a crucial component in modern-day vehicles. It can be described as the brain of a vehicle that controls engine operations, e.g., fuel injection system, ignition system, air handling system, thermal management system, and after-treatment system. A variety of onboard sensors are provided in the engine and the vehicle. The engine control unit (ECU) continuously receives inputs from various sensors such as throttle position, manifold air pressure, engine speed, engine temperature, exhaust oxygen feedback. Based on these inputs, ECU optimizes the fuel injection quantity and ignition timings based on pre-installed fuel and ignition maps in the ECU and maintains the desired AFR and optimum ignition timing for efficient vehicle operations in the entire operating envelope. The schematic of various components used in the EMS is given in Fig. 12.9. The role of each of them is explained in the following sub-sections.

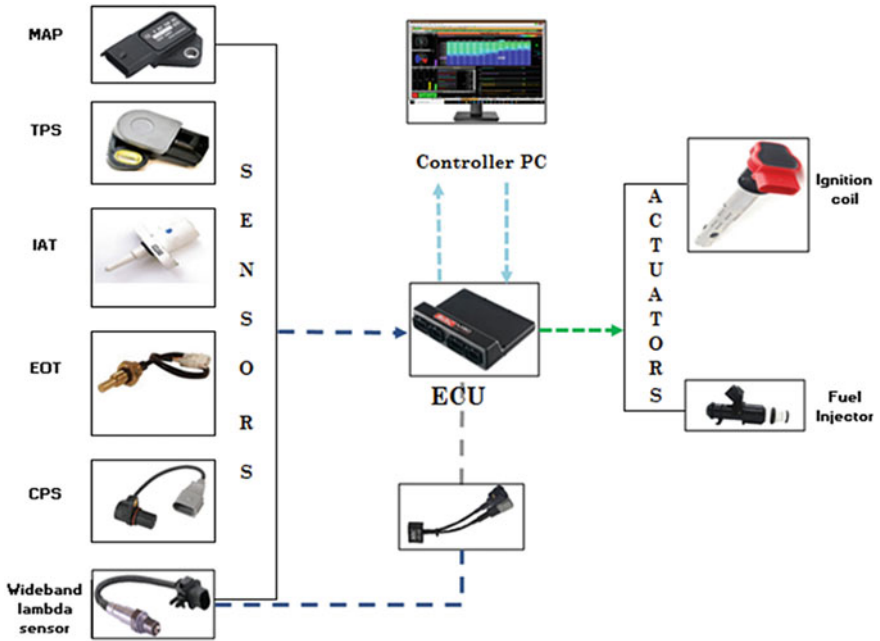


Fig. 12.9 Schematic and components used in the engine management system

*Open ECU*

An open ECU is used in calibration or research studies to optimize various parameters for engine operation. It is a programmable ECU that allows altering maps and other engine operating parameters, unlike stock ECU, which does not permit any modification once the data is encrypted in the ECU memory (Fig. 12.10).

Fig. 12.10 Open ECU





It can perform various primary functions such as fuel injection quantity and timing calculations, ignition timing determination, closed-loop lambda control, and advanced functions such as switchable fuel, ignition, boost trimming, knock control.

### *Manifold Absolute Pressure (MAP) Sensor*

The MAP sensor provides instantaneous intake manifold pressure values to the ECU. The ECU uses these values to determine the air density and calculates the air mass flow rate entering the engine cylinder. Depending on the mass flow rate, the fuel quantity to be injected is determined by the ECU, based on lambda ( $\lambda$ ) value derived from the pre-installed AFR maps. The MAP sensor consists of a diaphragm that separates two chambers. One chamber is air sealed at 1 atm or vented to the atmosphere used as a reference chamber. The other chamber is connected to the intake manifold. The voltage output is generated in the range of 1–5 V, proportional to the diaphragm movement when intake air flows through the manifold (Fig. 12.11).

### *Crank Position Sensor (CPS)*

The CPS is used as a reference sensor to monitor the current crankshaft position and the engine operating speed. It is directly attached to the engine crankshaft. It consists of a gear wheel with one or two missing teeth. For example, in 18-1 magneto wheel configuration, there are 18 equally spaced teeth and one missing tooth. The working of CPS is explained below in the figure, along with its picture (Fig. 12.12).

It is a variable reluctance passive sensor that does not require an external power supply for its operation. The output voltage is produced, which is proportional to the varying magnetic flux around it. The magnetic flux produced by a permanent magnet is varied by using a toothed wheel made of ferrous material. When the ferrous teeth pass in front of the tip, the magnetic flux through the sensor changes, and a voltage is induced. Therefore for 18-1 configuration, 17 AC waves are generated from the sensor for every crankshaft rotation. One missing wave will be used to determine the TDC position by synchronizing it with the motoring curve on the pressure crank angle diagram.

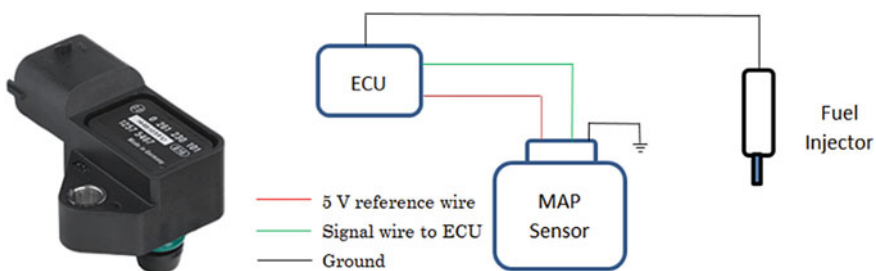


**Fig. 12.11** Manifold absolute pressure (MAP) sensor (example)

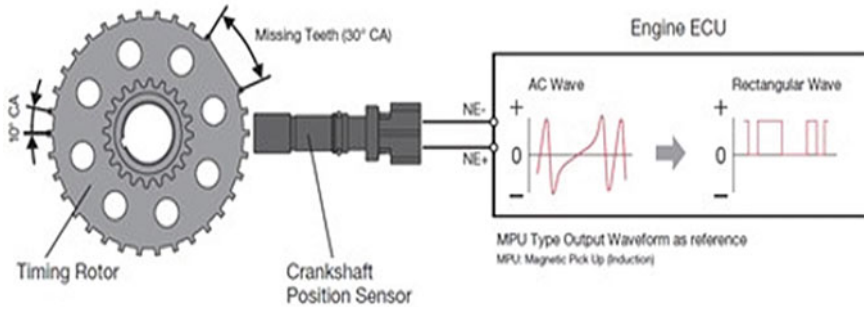


Fig. 12.12 Working of crank position sensor (CPS)

*Throttle Position Sensor (TPS)*

The vehicle's power output in SI engines is controlled by the air entering into the engine cylinder. The throttle position sensor continuously monitors the fluid flow in the engine. It is mounted in a throttle body. It constantly monitors the angular position of the spindle of the throttle valve and transmits the signal to the ECU. The throttle position sensor is essentially a three-wire potentiometer, consisting of wire with a 5 V reference signal from ECU. Another is the ground signal from ECU, and the third wire is the wiper. The sliding contact resistance changes by varying the wiper position, resulting in a proportional voltage input signal to the ECU. This voltage varies between 1 and 5 V, following the pre-installed map voltage versus angular position of the throttle valve. Depending upon the rate of acceleration and deceleration, the angular position of the throttle valve varies, and fuel enrichment is provided accordingly to ensure a smooth driving experience. The throttle position sensor is shown in Fig. 12.13.

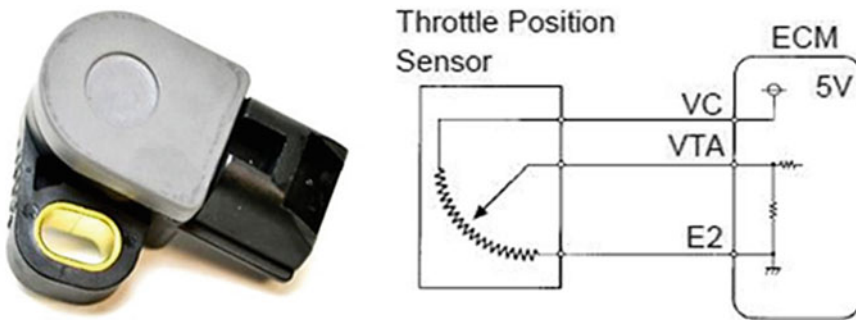


Fig. 12.13 Throttle Position Sensor (TPS)

### *Inlet Air Temperature (IAT) Sensor*

The IAT sensor records the ambient temperature and feeds it to the ECU. ECU uses this information to determine ambient air density using the pre-installed temperature versus density curve, which is then used to calculate the mass of air being inducted into the engine. The IAT sensor used in this setup is a thermistor of negative temperature coefficient (NTC) type, which implies that its resistance decreases with an increasing temperature. It has two connections: a reference ground signal from the ECU, and the other is voltage output back to the ECU.

### *Engine Oil Temperature (EOT) Sensor*

The EOT sensor measures the temperature of the lubricating oil in the engine. Similar to the IAT sensor, this sensor is also an NTC thermistor. It is used for temperature-based fuel and spark compensations and cold start compensations. In the event of a lower temperature than the average operating temperature, extra fuel is injected. The spark timing is retarded to compensate for the low evaporation rate of the fuel. Additionally, it also ensures engine operation within specified temperature limits to avoid overheating. The EOT sensor is shown in Fig. 12.14.

### *Wideband Lambda Sensor*

The AFR significantly affects engine/vehicle performance, brake-specific fuel consumption, and emissions. Hence it is essential to continuously monitor the AFR and provide feedback information to ECU accordingly. Lambda ( $\lambda$ ) is defined as the ratio of actual AFR to the stoichiometric AFR. It indicates whether the fuel-air mixture is rich or lean. The value  $\lambda = 1$  denotes stoichiometric mixture, whereas  $\lambda > 1$  and  $\lambda < 1$  represent lean and rich fuel-air mixtures. The wideband oxygen sensor measures oxygen in the engine exhaust to determine the  $\lambda$  value. ECU compares this actual  $\lambda$  value and the pre-installed aimed  $\lambda$  value from the engine maps. Accordingly, a suitable AFR correction is calculated, and the mass of fuel to be injected is adjusted. In this study, the stock narrowband oxygen sensor was replaced by a wideband oxygen sensor for ECU calibration purposes.

The narrowband lambda sensor is a binary sensor that only determines whether the mixture is rich or lean. On the contrary, a wideband oxygen sensor senses the exact lambda value. The function of both these sensors is based on an electrochemical cell called a Nernst cell, made of zirconium dioxide, which can conduct oxygen ions, a reference cell containing ambient air, and a thin coating of platinum on both sides, which act as an electrode. The one side of the Zirconia element is exposed to the exhaust gas. While the other side is in contact with the reference air, and the oxygen

**Fig. 12.14** Engine Oil Temperature (EOT) sensor



ions pass through these elements and deposit the charge on the electrodes to generate a voltage signal. A rich or lean AFR is determined by a narrowband sensor based on the voltage it produces. In rich AFR, the high signal voltage is generated across the electrodes due to the difference in oxygen concentration across the two sides of the zirconium element. In lean AFR, there will be a slight difference in oxygen concentration between the exhaust gas and the reference air inside the sensor; hence low voltage signal would be generated. The working of the wideband oxygen sensor is shown in Fig. 12.15.

The wideband oxygen sensor contains an additional ceramic cell. The exhaust gas enters this cell through a diffusion barrier. The AFR in the cell is measured by the Nernst cell. Depending on rich or lean AFR, the voltage is applied to the electrodes of the pump cell. Oxygen ions move from the inner side to the outer side of the electrode to make the AFR in the chamber stoichiometric. The diffusion of these ions sets up an electric current, which is converted into an equivalent voltage signal. The lambda sensor is shown in Fig. 12.16.

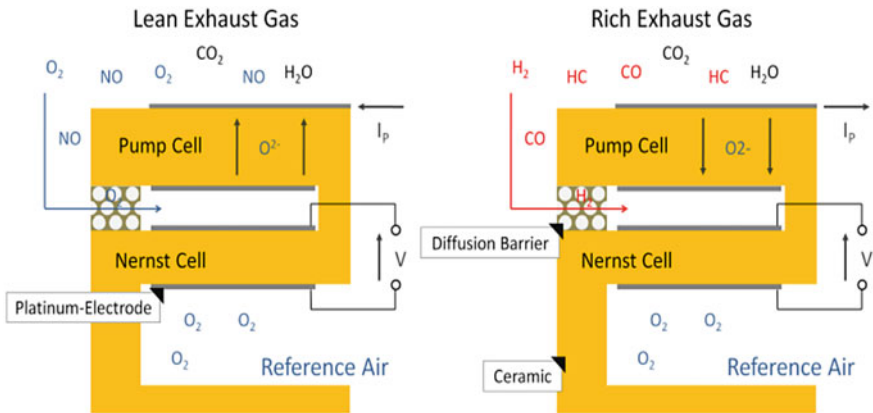


**Fig. 12.15** Working of wideband oxygen Lambda sensor (Electronics and Laboratory: Oxygen Sensors 2021)



**Fig. 12.16** Wideband Lambda sensor and Lambda module

**Fig. 12.17** Fuel pump assembly



### *Fuel Pump*

The fuel pump is an actuator that supplies liquid fuel to the injector by maintaining a positive pressure in the fuel supply line. It contains an integrated micro fuel filter to separate the impurities and ensure clean fuel reaches the fuel injector. The fuel pump is completely submerged in the fuel tank at its base to avoid running dry and protect it against accidental ignition by an electrical spark. The pump unit has two wire connections, one for battery positive triggered through the relay circuit and the other connected to the battery negative. The fuel pump unit is shown in Fig. 12.17.

### *Fuel Injector*

The fuel injector sprays the fuel at high pressure in the engine combustion chamber through the nozzle holes. Depending on the engine load and speed, ECU calculates the volume of fuel to be injected. The injection pulse width is calculated by the pre-installed linearization table in the engine map for a particular injector, considering the current battery voltage and fuel injection pressure. The solenoid valve in the injector is then energized for the calculated pulse width duration to inject the required fuel quantity into the engine combustion chamber. In this setup, the injector is mounted after the throttle body in the intake manifold at an optimum angle to minimize the wall wetting and maximize the fuel spray into the air from the throttle body. The injector has two pins, one connected to the battery positive and the other to the ground signal from the ECU. The injector used is shown in Fig. 12.18.

### *Ignition Coil*

The ignition coil is an actuator used to transform the low battery voltage (12 V) to high voltage (in the range of 25 kV) to produce an electric spark. The working principle of the ignition coil is similar to an electrical transformer. It consists of primary and secondary windings. The low induced voltage in the primary winding is transformed into high voltage in the secondary winding, in the same ratio as the number of turns.

**Fig. 12.18** Fuel injector

This extremely high voltage is supplied to the spark plug, which ionizes the charge in the gap between the electrodes and produces an electrical spark to ignite the fuel-air mixture in the combustion chamber. The ignition coil used in this experiment is a coil-on-plug (COP) type ignition coil, consisting of an internal power transistor, and it can be installed directly on the spark plug. It has four pins: battery positive, chassis earth, the output signal from ECU, and the engine block earth. The ignition coil is shown in Fig. 12.19.

#### *Wiring Harness*

A wiring harness is an organized set of wires, pins, and connectors that run throughout the vehicle to transfer the signals between various sensors, ECU, various actuators, and the battery. The stock wiring harness is replaced with a customized wiring loom. The wires from various sensors and actuators to the open ECU were connected into connectors at appropriate PINs. The circuit that didn't involve these sensors and actuators in open ECU operation was left unaltered to continue its functioning. For example, circuits involving alternator, rollover sensor, clutch switch, and kill switch, were connected in the stock wiring harness. The essential sensors such as CPS, TPS, MAP sensor, EOT sensor, and IAT sensors were connected directly into the designated PIN of the connector. The existing ignition coil with stock ECU was replaced with a 4-pin ignition coil having an internal power transistor. The fuel pump was driven using a relay, in which a low current circuit (typically ~40 mA) through the open ECU was used to trigger the high current circuit (0.8–1.2 A) of the fuel pump. A Wideband lambda sensor is connected to the open ECU Lambda-To-CAN

**Fig. 12.19** Ignition coil

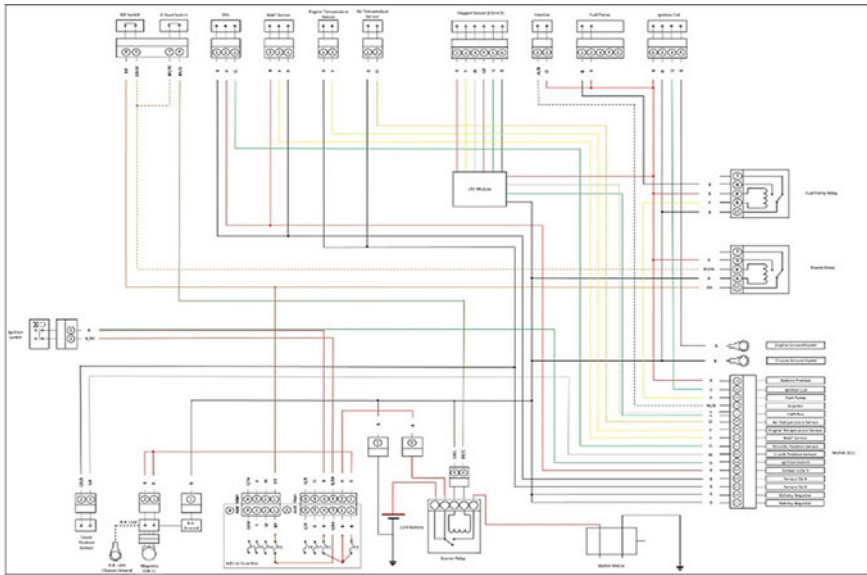


**Fig. 12.20** Wiring circuit diagram

(LTC) module via the CAN bus. Open ECU is connected to a computer via a high-speed Ethernet port to access live engine operation in the engine tuning software. After making the connections, the circuit is checked for connectivity, short-circuit, and input and output signals to ensure a safe connection. The wiring circuit diagram is shown in Fig. 12.20.

Automotive manufacturers use a stock engine management system (EMS), which does not allow any modifications once encrypted and locked. In contrast, open EMS is generally used for research, and it allows access to various tunable parameters to optimize overall engine/vehicle performance. Once the calibration setup is ready, the engine is operated at various engine operating conditions and the parameters are tuned to optimize engine performance. ECU calibration is the process of determining the optimal calibration tables and maps of volumetric efficiency, ignition timing and AFR for an engine to optimize the engine or vehicle performance as desired. In the following section, the ECU calibration procedure is explained in detail.

## 12.4 Engine Tuning and Recalibration

ECU continuously receives signals from various sensors. Based on these signals, it determines the fuel injection quantity and ignition timing. The output signals are then sent to the actuators. For a particular engine operation, we need to tune and calibrate the ECU. The details related to engine specifications, fuel properties, sensors

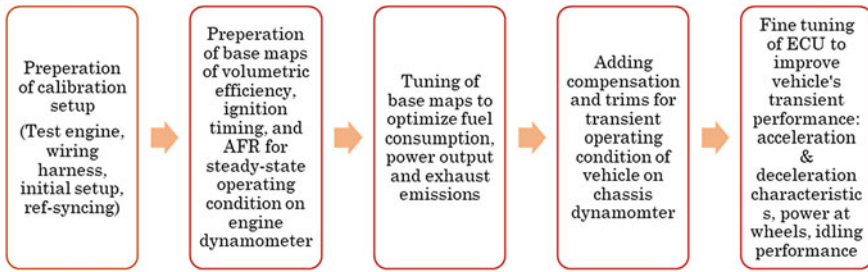


**Fig. 12.21** Flow procedure for calibration

and actuators, tuning maps, and other essential parameters related to fuel trims and enrichments were given as inputs to the software. In this section, the engine setup and tuning process are discussed in detail. Figure 12.21 shows the overall steps followed during ECU calibration.

Any particular package in tuning software consists of different worksheets, namely, tuning, initial setup, vehicle, diagnostics, and advanced race functions. These worksheets further consist of tabs for fine-tuning and calibration. E.g., the Tuning worksheet consists of tabs like fuel, ignition, fuel mixture aim, ignition trims, etc. Each worksheet and corresponding tabs are discussed below.

### 12.4.1 Initial Setup

The details related to engine specifications are provided as input information to the ECU. It includes engine displacement, engine run threshold rpm, operating modes, and fuel properties such as stoichiometric ratio, density, and coefficient of thermal expansion. The engine run threshold rpm was set to some lower value, such as 300 rpm, which is considered the minimum speed after the engine is assumed to be running. Generally, ambient air density is used to calculate the engine's volumetric efficiency, representing how effectively the cylinder fills the air with the current ambient air density. The engine load normalized mode represents the actual engine load compared to the estimated engine load under standard air pressure (101.3 kPa) and temperature (298 k) conditions.

As discussed earlier, there are different modes like MAP based, throttle based (alpha-N), and MAF based modes that can be used for engine load calculation. Alpha represents the throttle position angle (throttle opening %), and N represents the engine speed. Estimating mode is preferred since inlet manifold pressure has a linear relationship with the throttle position, and large fluctuations were observed in the inlet manifold absolute pressure. This mode estimates inlet manifold pressure from its linear relationship with the throttle position.



### *Ref. Sync.*

ECU determines the injection and ignition timing based on TDC position in the engine cycle. For this, the crank position must be synchronized with the cam position to determine an accurate engine piston position in the stroke. The ref sync worksheet is used to calibrate the crank trigger system for engine position and speed. In this case, a crank trigger wheel is used where the falling edge was selected as the engine speed active edge. In the absence of a cam sensor, an output from the MAP sensor was used for synchronization. The intake manifold pressure drops during suction stroke, and the corresponding signal is taken as a reference. The engine speed reference offset is determined. Once the synchronization is established, engine synchronization mode is ignored for engine speeds above 1200 rpm due to increased fluctuations.

### *ECU I/O*

This worksheet aids in the setup of inputs and outputs to and from the ECU. The pins are allocated for each sensor, actuator, relay, and other necessary equipment (e.g., wideband lambda sensor) connected to ECU via the wiring harness. The type of pin was decided by the corresponding current and voltage rating of the sensor and actuator.

### *Sensors, Critical and Optional*

In this worksheet, the critical and optional sensors are set up. ECU uses IAT, MAP, and TPS sensors for engine load calculations. The low and high voltage signal values are selected for the corresponding sensors, depending on the operating voltage of the sensor. Inlet manifold pressure mode is chosen as an estimate since throttle position values estimate the manifold pressure.

### *Ignition Configuration*

In this worksheet, parameters related to ignition were configured. Ignition coil with known configuration (pre-installed map) is selected. From a safety perspective, the ignition timing limit advance can be set to a value, for example, 60° BTDC.

### *Injectors*

The injector is configured in this worksheet. An injector is placed near the throttle body. The injector with a known configuration is selected.

### *Engine Outputs*

In this tab, setups related to outputs from the engine such as fuel pump, coolant pump, the ignition coil are done. The fuel pump is operated through the relay, where a high current fuel pump circuit is activated when a low current circuit is closed. When the current fall below this low current value when the output is driven.

### *Lambda Bank*

In this worksheet, CAN bus details of the LTC (Lambda-To-CAN) module are configured. LTC module is required to input wideband lambda sensor values to the ECU.

The overall lambda channel is called exhaust lambda and is used for functions such as quick lambda.

### 12.4.2 Tuning Process

Before starting the tuning process, it is necessary to understand the combustion events in the engine cylinder and the spark sweep test. The combustion event in the engine cylinder is divided into four phases: (i) Ignition, (ii) Flame development, (iii) Flame propagation, and (iv) Flame quenching.

The occurrence of combustion event must be precise relative to the TDC to obtain the maximum brake power. The flame development and propagation together occur between 30 to 90 °CA. Combustion is initiated by spark, a few °CA degrees before the TDC near the end of the compression stroke. It continues in the early expansion stroke, where peak cylinder pressure occurs and ends with the flame quenching near the walls. The ignition timing affects the location of peak cylinder pressure and hence the brake torque. The optimum ignition timing, which results in maximum brake torque, is called maximum brake torque (MBT) timing.

The MBT timing ensures the location of peak cylinder pressure around 10° aTDC. Suppose the timing is advanced before MBT timing, the compression work transfer increases. Also, knocking may take place because of the pre-ignition. On the other hand, delayed ignition timing causes peak cylinder pressure to occur later in the expansion stroke, which reduces its magnitude because of increased volume due to the downward movement of the piston. Determining the MBT timing for a particular speed and load condition is called a spark sweep test.

#### *Base Map Tuning*

After completing the initial setup in the separate worksheets, the engine is motored to check the cycle lock. Cycle lock ensures synchronization between the crankshaft and cam timing. The MAP sensor can be used in place of the cam position sensor. When the intake valve opens, the pressure in the intake manifold drops. This signal is synchronized with the crank position sensor to achieve the cycle lock. Initially, the volumetric efficiency table is populated with a random value, e.g., 60%, and the ignition table with 10° bTDC. The engine is operated at the desired speed and load condition, starting from low speed and load region to higher speed and load region. The wideband sensor records the actual lambda value, which is then compared with the aimed lambda value. The volumetric efficiency is then corrected according to aimed-lambda using the quick-lambda function available in the tuning software. Corrected volumetric efficiency can be calculated as,

$$(\text{VE})_{\text{corr}} = \text{VE} \times \frac{\lambda_{\text{actual}}}{\lambda_{\text{aim}}}$$

For example, consider a case where the engine is fired with an initial volumetric efficiency of 60%. It is desired to operate an engine with  $\lambda = 0.9$ , whereas the wideband lambda sensor measures an actual  $\lambda$  value of 0.7, showing that the engine runs with a richer AFR than required. So, in this case, to achieve the desired  $\lambda$ , the fuel quantity injected must be reduced. As one doesn't directly control the amount of fuel being injected, this is achieved by reducing the volumetric efficiency to 46.67%. By doing so, one makes the ECU understand that lesser air is being inducted. ECU then recalculates the corrected engine load and quantity of fuel to be injected, although, in reality, the amount of air inducted remains the same. Once the volumetric efficiency is tuned, ignition timing is either advanced or retarded to target the MBT timing. The interface of tuning software contains current engine operating conditions such as engine speed, inlet manifold pressure, engine oil temperature, actual and aim lambda value, fuel injection quantity, compensations, fuel pressure, and battery voltage. The fuel and ignition tables contain volumetric efficiency and spark timings tuned to optimize engine performance.

The AFR greatly affects the performance and emissions from spark-ignition engines. So, it is crucial to choose an aimed lambda to optimize the engine operation. Volumetric efficiency and ignition timing can be tuned accordingly once the aimed lambda is fixed for all engine operating conditions. A set of preliminary experiments are conducted to evaluate the effect of lambda on engine performance and emissions. Engine performance and emissions are then assessed for different lambda values.

- Peak power at the rich AFR was obtained for  $\lambda$  between 0.84 and 0.90.
- The best economy was obtained for a slightly lean AFR.
- Optimal CO & HC emissions were obtained at a slightly lean AFR.
- NO<sub>x</sub> emissions are higher for a slightly lean AFR.

#### *Example for Tuning of Methanol-Fueled Vehicles*

The tuning strategy for volumetric efficiency to achieve aimed lambda is discussed using the following points (Fig. 12.22).

- To ensure a quick cold start of the engine considering the lower evaporation rate of methanol, a rich AFR ( $\lambda \sim 0.92$ ) is generally assigned. Methanol is less volatile compared to gasoline, and more fuel is required to have a combustible mixture in the combustion chamber. Along with a rich fuel-air mixture, additional starting compensation is also provided. Similarly, a rich mixture is preferred in the idling range to cater to exhaust gas dilution. During idling, exhaust gases cannot escape smoothly compared to normal operating conditions, which causes a leaning effect, and hence richer mixture is required to compensate for this.
- The engine generally spends maximum time in the cruising zone. An optimum lean AFR ( $\lambda \sim 1.04$ ) is assigned to maximize the engine efficiency and minimize the exhaust emissions in this zone. Maximum engine efficiency is obtained for  $\lambda = 1.1$ . Also, the cooling effect caused by the higher latent heat of methanol allows a slightly leaner mixture than gasoline. However, there are limitations to operate the engine at such a lean AFR. The availability of excess oxygen along with higher

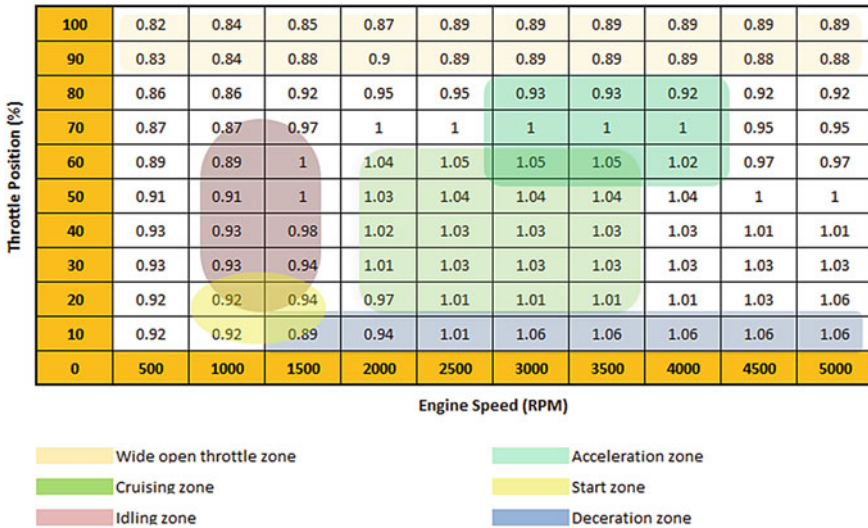


Fig. 12.22 Tuning table for methanol-fueled vehicles (example)

in-cylinder temperature increases NO<sub>x</sub> emissions. Also, the lean AFR results in lower power output. Moreover, in the event of an increased air density (engine operating in cold weather), the mass of air inducted per cycle also increases for constant throttle opening. Hence, the probability of misfiring increases when the fuel-air mixture becomes leaner than the combustion limit

- A slightly richer AFR ( $\lambda \sim 0.95$ ) is selected to target better acceleration characteristics in the acceleration zone. The vehicle usually spends very little time in this zone. The output torque is higher for a slightly richer AFR. Hence, accordingly, lambda is selected targeting higher torque output rather than engine efficiency and emissions.
- In the wide-open throttle zone, the rider demands maximum power output. In this zone, the engine operates at high speed and high load. A rich AFR is assigned to target maximum power output. Moreover, while running at such a high engine speed, the in-cylinder temperature remained very high due to higher friction losses and elevated in-cylinder pressure. A richer AFR ( $\lambda \sim 0.88$ ) is selected to absorb this excess heat in the engine cylinder. The extra fuel absorbs heat as LHV to reduce the in-cylinder temperature. This also helps in reducing NO<sub>x</sub> emissions, usually higher at high loads.
- In the deceleration zone, the power output is not a concern. Hence, a lean AFR ( $\lambda \sim 1.06$ ) is assigned to optimize the engine efficiency and exhaust emissions.
- In this way, the aimed lambda values are assigned to important engine operation cells. These values were then interpolated linearly for the rest of the table.

Once the aimed lambda table is ready, the engine is operated at the desired speed and load condition using a dynamometer. Volumetric efficiency is tuned to achieve

aimed lambda, as explained earlier. Once the actual lambda value is matched with the aimed lambda value, the volumetric efficiency value is kept fixed for that particular speed and load condition. Now to tune ignition timing, a spark sweep test is performed. The strategies used to tune ignition timing are discussed using the following points.

- In both start and idling zones, ignition timing is retarded from the MBT timing. During idling, the torque produced is barely enough to maintain constant idle speed against the friction, pumping losses, transmission losses, and operation of other auxiliary systems. When a sudden load is applied by pulling the vehicle into gear, the engine speed should not drop, and stalling must be avoided. By retarding the ignition timing, ECU will have additional torque to cater to a sudden increase in load demand.
- In the cruising zone, ignition timing is set to MBT timing to maximize engine efficiency. The engine operates at part load, and the knocking chances are low. So, it is safe to run the engine at MBT or slightly retarded timing than MBT.
- More spark advance (almost up to  $40^\circ$ ) is needed during engine operation at higher speeds to ensure complete combustion within required  $^\circ\text{CA}$  degrees. The in-cylinder pressure versus  $^\circ\text{CA}$  curve is monitored continuously to see if any fluctuations occur in the pressure, indicating knock. If knock appears, ignition advance is retarded, and fuel-air mixture lambda value is made slightly rich.
- As the in-cylinder temperature and pressure are higher in the WOT zone due to increased cylinder filling, the ignition advance is retarded to avoid knocking.
- As the lean AFR is used in the deceleration zone, the laminar flame speed is lower. Hence to achieve complete combustion, ignition is advanced slightly closer to the MBT timing.
- ECU is tuned meticulously at the maximum number of speed-load combinations, and the values are interpolated for the rest of the cells.

Following the above strategies, volumetric efficiency and ignition timings are tuned, starting with random values of 60% and  $10^\circ$ , respectively. Emissions data from the same engine fueled with baseline gasoline can be used as the reference. If the exhaust emissions deviated from the reference value, the ignition timing and lambda aimed values are adjusted accordingly to improve the new fuel's engine performance.

#### *Tuning for Acceleration and Deceleration Conditions*

The volumetric efficiency map denotes the pumping efficiency of the engine in steady-state conditions. ECU calculates the fuel quantity to be injected, depending on the air-mass intake. However, in transient conditions, the fuel calculations need to be modified as per instantaneous throttle response. A sudden change in throttle position causes a slight change in the fuel delivery. This occurs because of the formation of fuel film in the intake manifold before the valves. The fuel film also contributes to the desired AFR in the engine cylinder in transient conditions such as acceleration and deceleration. ECU controls the fuel injector, but there is no direct control over the fuel film on the intake port walls. For example, consider an acceleration event.

During acceleration, the airflow through the port rapidly increases. The increased airflow tends to evaporate the wall film on the port walls. Due to a faster evaporation rate during acceleration owing to higher air velocity, the overall contribution by the fuel film to the cylinder filling reduces. This results in a leaner fuel-air mixture being delivered to the engine cylinder. On the contrary, the fuel film contribution makes the AFR richer than expected during the deceleration event.

As discussed earlier, the leaner AFR would cause a reduction in output torque, resulting in poor drivability, which is not desirable during acceleration. Some extra fuel quantities must be injected to avoid lean fuel-air mixture due to temporary wall film reduction. It is achieved by providing fuel film compensations. ECU detects the change in throttle position during acceleration and enables fuel film mode to inject higher fuel quantity. The actual fuel quantity for compensation needs to be calibrated. It is important to note that it is necessary to complete a volumetric efficiency tuning for acceleration enrichments. For fuel film primary main calibration, engine rpm can be fixed to a lower speed of 2000 rpm since fuel film has a higher effect on the lower speeds. The throttle position is then changed suddenly from 40 to 50%. An instantaneous deviation from the desired lambda value is observed. The fuel volume added as compensation to maintain the desired lambda is calculated. This quantity is then added to all the values bigger than 40 kPa.

Similarly, compensation is added for the rest of the throttle responses. During deceleration, the fuel trims are provided to account for the effect of fuel film during sudden throttle reduction. A similar operation is performed for few other throttle position changes, and compensations are added to the fuel film secondary main table. Fuel film time constant denotes the time within which these compensations are applied. A fast time constant of 1 s with a 60% primary scale is selected, indicating 60% of the compensation fuel quantity supplied within 1 s.

## 12.5 Compensations Required for Tuning

### *Altitude Compensation*

The volumetric efficiency table is a 3-dimensional table consisting of a 3<sub>rd</sub> axis denoting the ambient pressure. With the change in altitude, the ambient pressure and density of air change, and hence altitude compensation must be added to cater to the difference in the cylinder filling. Accordingly, volumetric efficiency can be tuned to different values of ambient pressures, and the values can be interpolated in the entire range of pressure.

### *Speed Compensation*

At higher engine speeds, the velocity of inlet air is higher, increasing the evaporation rate of the fuel film. This reduces the thickness of fuel film on the port walls. A negative compensation called fuel film primary trim engine speed (%) is provided, which considers the effect of higher engine speed on fuel film thickness.

### *Compensation for Cooling Oil Temperature*

When the engine operates at a higher temperature, the evaporation rate of fuel film increases, reducing the film thickness. A negative compensation called fuel film primary film temperature is provided to account for this. The engine operating temperature is directly related to the engine oil temperature; hence a signal from the engine oil temperature sensor is given as an input. Up to 90 °C engine oil temperature, a positive compensation is provided to assist lower evaporation rate at lower engine operating temperature, whereas negative compensation is provided for engine oil temperature beyond 120 °C.

### *Cranking Compensation*

A cranking compensation is provided, in which extra fuel is injected for the initial 20 engine crank cycles to facilitate smooth cold starting. 200% of the actual fuel injection quantity is injected for the first crank rotation, which is then gradually reduced for the next 20 engine crank cycles.

### *Post-start Compensation*

During the initial few seconds of engine operation after cranking, as the temperature in the intake port is low, the rate of fuel evaporation is low. An extra fuel quantity is provided for initial 10 s to compensate for this.

### *Inlet Air Temperature Compensation*

With changing ambient air temperature, the density of inlet air also changes. This affects the volumetric efficiency. Hence variations in the inlet air temperature must be considered.

## **12.6 Summary**

ECU calibration is a vital step in vehicle development. In the present chapter, a detailed procedure of ECU calibration for methanol adaptation in port-fuel injected SI engines is discussed. The main objective of this chapter is to establish the process of tuning to improve overall engine performance, fuel economy, vehicle drivability and reduce emission characteristics. In the first section of this chapter, the advantages and challenges encountered during methanol utilization strategies: (i) conventional carbureted fuel supply and (ii) modern electronic fuel injection are discussed. Working of fuel model and engine management system (EMS) consisting of open ECU, a set of sensors and actuators, and wiring harness is covered. ECU calibration process at steady-state conditions on an engine dynamometer and transient conditions using chassis dynamometer is discussed. An example lambda table is formulated for tuning, which denotes the target air-fuel ratio for optimized performance with methanol as fuel. A detailed procedure for calibrating volumetric efficiency and ignition table is given. Finally, a strategy of adding various compensations and trims for

improving vehicle drivability in road load simulation conditions and varying weather conditions is discussed. This detailed calibration procedure would help automakers in calibrating the methanol-fueled vehicles.

## References

- Agarwal AK, Valera H, Pexa M, Čedík J (2021) Introduction of methanol: a sustainable transport fuel for SI engines. In: Agarwal AK, Valera H, Pexa M, Čedík J (eds) Methanol: a sustainable transport fuel for SI engines. Energy, environment, and sustainability. Springer, Singapore, pp 3–7. [https://doi.org/10.1007/978-981-16-1224-4\\_1](https://doi.org/10.1007/978-981-16-1224-4_1)
- Clemson Vehicular Electronics Laboratory: Oxygen Sensors n.d. <https://cecas.clemson.edu/cvel/auto/sensors/oxygen.html>. Accessed 15 Sept 2021
- Göktaş M, Kemal Balki M, Sayin C, Canakci M (2021) An evaluation of the use of alcohol fuels in SI engines in terms of performance, emission and combustion characteristics: a review. Fuel 286. <https://doi.org/10.1016/j.fuel.2020.119425>
- M15 fuel - Admixture of anhydrous methanol and motor gasoline as fuel for spark ignited engines - Specification IS 17076: 2019. [https://www.services.bis.gov.in:8071/php/BIS/bisconnect/pow/is\\_details?IDS=MjM3NTI%3D](https://www.services.bis.gov.in:8071/php/BIS/bisconnect/pow/is_details?IDS=MjM3NTI%3D) (accessed May 20, 2021)
- Methanol Fuels » Demonstration Project <https://methanolfuels.org/on-the-road/demonstration-projects/>. Accessed 15 Sept 2021
- Physical-Chemical Properties. <https://www.mandieselturbo.com/docs/default-source/shopware-documents/using-methanol-fuel-in-the-man-b-w-me-lgi-series.pdf>
- Statistical Review of World Energy 2020 | 69<sup>th</sup> edition. <https://www.bp.com/content/dam/bp/business-sites/en/global/corporate/pdfs/energy-economics/statistical-review/bp-stats-review-2020-full-report.pdf>
- Valera H, Agarwal AK (2019) Methanol as an alternative fuel for diesel engines. In: Agarwal A, Gautam A, Sharma N, Singh A (eds) Methanol and the alternate fuel economy. Energy, environment, and sustainability. Springer, Singapore, pp 9–33. [https://doi.org/10.1007/978-981-13-3287-6\\_2](https://doi.org/10.1007/978-981-13-3287-6_2)
- Valera H, Singh AP, Agarwal AK (2020) Prospects of methanol-fuelled carburetted two wheelers in developing countries. In: Singh A, Sharma N, Agarwal R, Agarwal A (eds) Advanced combustion techniques and engine technologies for the automotive sector. Energy, environment, and sustainability. Springer, Singapore, pp 53–73. [https://doi.org/10.1007/978-981-15-0368-9\\_4](https://doi.org/10.1007/978-981-15-0368-9_4)
- Valera H, Čedík J, Pexa M, Agarwal AK (2021) Regulated and unregulated emissions from methanol fuelled engines. In: Agarwal AK, Valera H, Pexa M, Čedík J (eds) Methanol: a sustainable transport fuel for SI engines. Energy, environment, and sustainability. Springer, Singapore, pp 161–89. [https://doi.org/10.1007/978-981-16-1224-4\\_7](https://doi.org/10.1007/978-981-16-1224-4_7)
- Verhelst S, Turner JW, Sileghem L, Vancoillie J (2019) Methanol as a fuel for internal combustion engines. Prog Energy Combust Sci 70:43–88. <https://doi.org/10.1016/j.pecs.2018.10.001>
- Wei Y (2021) Measurement, mechanism and characteristics of formaldehyde emission from methanol/gasoline blends fueled engine BT—methanol: a sustainable transport fuel for SI engines. In: Agarwal AK, Valera H, Pexa M, Čedík J (eds) Springer, Singapore, pp 243–63. [https://doi.org/10.1007/978-981-16-1224-4\\_10](https://doi.org/10.1007/978-981-16-1224-4_10)
- World Energy Balances – Analysis - IEA <https://www.iea.org/reports/world-energy-balances-overview>. Accessed 15 Sept 2021
- World Energy Outlook 2019 – Analysis - IEA <https://www.iea.org/reports/world-energy-outlook-2019>. Accessed 15 Sept 2021
- Zhen X, Wang Y (2015) An overview of methanol as an internal combustion engine fuel. Renew Sustain Energy Rev 52:477–493. <https://doi.org/10.1016/j.rser.2015.07.083>



# Chapter 13

## A Novel DoE Perspective for Robust Multi-objective Optimization in the Performance-Emission-Stability Response Realms of Methanol Induced RCCI Profiles of an Existing Diesel Engine



Dipankar Kakati , Srijit Biswas , and Rahul Banerjee 

**Abstract** To exploit the potential benefits of reactivity controlled combustion (RCCI) of methanol induced diesel dual fuel operation under split injection strategy, the present study has adopted data driven surrogate modelling technique in contrast to the computationally expensive computational fluid dynamics (CFD) platform. For the partial replacement of conventional diesel fuel, port premixed methanol has been introduced in this study as a renewable alternative energy resource considering its renewability and sustainability perspectives [E-fuel]. To explore the challenges and opportunities of RCCI operation the response parameters of nitrogen oxides ( $\text{NO}_x$ ), soot, unburned hydrocarbon (UHC), carbon-dioxide ( $\text{CO}_2$ ), exergy efficiency and co-efficient of variation of indicated mean effective pressure ( $\text{COV}_{\text{IMEP}}$ ) have been studied considering pilot (PIA) and main injection timings (MIA), overall reactivity (R0) and pilot injection mass percentage (PIM) of diesel fuel as the control parameters. A constrained optimization study has been carried out in this investigation based on the response surface methodology under the respective constraints of emission elements as per the EPA Tier-4 emission mandates and operational stability. The study also incorporated a novel customized design of experiment (DoE) for the multi-variate exploration of design space followed by a thorough analysis of the robustness of design space, which has been characterized through the measures of fraction of design space (FDS) metric, D-optimality criteria, G-efficiency and condition number (CoN). Further, desirability based multi-criteria decision making approach has been undertaken wherein, the highest desirability was observed as 0.832. Subsequently the optimization results revealed that the footprints of  $\text{NO}_x$ , soot, UHC,  $\text{CO}_2$  and  $\text{COV}_{\text{IMEP}}$  were improved by 3.59%, 96.2%, 49.3%, 2.5% and 15.95% respectively compared to the experimental investigation. Besides, with respect to the limits for emission elements specified in the EPA Tier 4 norms, the study yielded 77 and 73.33% lower footprint of NHC and PM compared to the limits specified as constraints. The

---

D. Kakati (✉) · S. Biswas · R. Banerjee  
Department of Mechanical Engineering, NIT Agartala, Jirania, Tripura 799046, India

study further revealed that the CO<sub>2</sub> emission is 42.3% less than the amount of CO<sub>2</sub> consumed in the process of methanol production, which eventually displays the potential of such RCCI operational regime in addressing the carbon emissions crisis.

**Keywords** Methanol-diesel RCCI combustion · Exergy efficiency · Split injections · Carbon negative footprint · Robustness of design space · Multiobjective RSM optimization

## Abbreviations

CO <sub>2</sub>	Carbon-di-oxide
COV <sub>IMEP</sub>	Coefficient of variance of indicated mean effective pressure
CRDI	Common rail direct injection
EXG	Exergy
MCDM	Multi criteria decision making
MIA	Main injection angle
NO <sub>x</sub>	Nitrogen oxides
PIA	Pilot injection angle
PIM	Pilot injection mass percentage
PM	Particulate matter
RCCI	Reactivity controlled compression ignition
R <sub>O</sub>	Overall reactivity
RSM	Response surface methodology
UHC	Unburnt hydrocarbon

## 13.1 Introduction

Considerations of the present day insecurities of conventional fossil fuel based energy resources, air pollution, and climate change are collectively calling into question the fundamental sustainability of the current fossil fuel based energy system. Standing at the cross-roads of the contemporary frontiers of engine research, the rationale of utilizing sustainable bio-resources in new or existing engines have been envisaged distinctly in the National Biofuel Policies. Such objectives are poised to herald a new chapter in engine research dominated by optimal combustion phasing which is firmly believed to address simultaneously the omnipresent challenges of the ever increasing National fuel import bill, pollution control and establishment of a sustained rural bio-resource economy without the necessity to switch to radically new technological paradigms from existing conventional diesel engines of the day. In this context of utilizing alternative energy resources, the interests in biofuel based renewable alternative fuels have grown in the recent years to resolve the issues of pollution control

as well as to reduce the dependency on fossil fuels simultaneously (Zou et al. 2016; Udayakumar et al. 2004; Valera and Agarwal 2019).

The rural areas in India wherein the grid extension is not economically viable, primarily rely on the diesel engines in electricity generation for rural electrification (Palit et al. 2017). Under the domain of the “Decentralized distributed generation of power” which is typically dedicated for energy supply in the rural areas, the diesel engines have been performing as a major source for electricity generation as well as for agricultural purposes, but the operations of such engines under conventional strategies yielded significant amount of carbon-di-oxide ( $\text{CO}_2$ ) emissions along with other major environment deteriorating pollutants. From the perspectives of future energy security and reductions of  $\text{CO}_2$  emissions, however various environment friendly and renewable alternative resources can be employed as partial or full replacement of diesel fuel in the process of localized power generation.

To this end, especially methanol as a diesel substitute when injected through an additional system of port fuel injection has shown promising results in reducing the emissions due to its lean combustion characteristics and high latent heat of vaporization (Li et al. 2014). Moreover, methanol is an easy source of renewable and environment friendly alternative fuel, which is quite cheap and locally available and can be utilized as a reliable alternative source of energy to curb the environmental pollutions. The introduction of renewable methanol (E-fuel) will further enhance the National sustainability perspectives on energy harnessing and contribute to rural upliftment. It is evident in many studies (Dempsey et al. 2013a) that the traditional  $\text{NO}_x$ -soot trade-off setback of diesel engine operation can be exempted with the methanol-diesel dual fuel operational tactic. As an alternative energy carrier, methanol possesses a significantly pertinent advantage to the global environmental health, as it consumes carbon-di-oxide ( $\text{CO}_2$ ), the foremost contributor to the global warming while it is considered as a chemical feedstock for methanol production. To this effect, Matzen et al. (2015) in their study revealed that as a chemical feedstock, 0.85 kg of  $\text{CO}_2$  was consumed for per kg of methanol production while, only 0.53 kg of  $\text{CO}_2$  was released to the environment for per kg of methanol combustion, which eventually resulted in the negative carbon footprint in the environment. Thus, the renewable methanol can contribute greatly to the cause of tackling the challenges of climate change due to global warming. Besides, there are various feed stocks available for the production of E-methanol, such as hydrogen electrolysis, carbon capture, coal gasification, natural gas, biomass conversion and many more (Agarwal et al. 2019). Along with the power generation for electrification, the renewable and environment friendly E-methanol have posed significant potential in the contemporary energy sector as a climate neutral solution for the automobile sector. Due to the compatibility of E-methanol with the present day IC engine configuration, it can be used to power the ships, cars, aircrafts and other transportation vehicles, which is extensively environment friendly compared to the traditional fuels. The E-methanol was initially used in the IC engine regime as an additive to the conventional fuels and then gradually increased the energy share with the development of innovative techniques and finally substitutes the conventional fuels partially or completely with the E-methanol fuel as a climate-friendly alternative to the traditional fuels.

It is pertinent to note that the National Policy on Biofuels-2018 (National Policy on Biofuels 2018) essentially targets the rationale of utilizing a maximum of 15% of methanol in SI engine which essentially caters to the personnel transportation sector. However, the present study attempts to explore and establish a feasibility of bio-resource based energy share significantly higher (more than 50%) than the set targets that can readily be exploited on the significantly large diesel engine sectors as being explored internationally under the advanced combustion modes of reactivity controlled dual fuel operation, thereby motivates a paradigm shift in the perspectives of bio-resource based energy carriers in the future chapters of the National policies on the diesel engine sector.

The recent developments in utilizing methanol in existing diesel engines have revealed an advanced low temperature combustion regime of reactivity controlled combustion strategy (RCCI) with reactivity gradient, the studies of which have demonstrated a more promising strategy than the conventional dual fuel tactics of external blending strategy in the contemporary diesel engine research in view of its superior emissions reduction capability on one hand with higher fuel efficiency on the other hand. In the conventional dual fuel blending technique, the energy share of methanol is limited to 10–15% only due to the miscibility problem with diesel, which has hindered to obtain full potential of methanol. Whereas, the port injected methanol RCCI system eradicates such issues and enhances the methanol energy share significantly in the dual fuel LTC operation. The RCCI strategy basically utilizes low reactive fuel as the primary fuel which is injected through the inlet port during the suction stroke, while the high reactive fuel is injected directly into the combustion chamber, which acts as an energy deposit necessary for the ignition of primary fuel since the autoignition of low reactive fuel is difficult. The RCCI profiles offer better thermal efficiency compared to the conventional diesel operations owing to the reduction in heat transfer losses (Reitz and Duraisamy 2015). Furthermore, Wei et al. (2016) observed in their study of methanol-diesel dual fuel operation that  $\text{NO}_x$ , soot and ringing intensity decreased significantly with the increase in methanol energy share in RCCI operation, while the UHC emissions decreased with retarded diesel injection timing. Dempsey et al. (2013b) studied the effects of cetane improver on emissions and combustion characteristics of premixed methanol (port injected) as well as methanol blend with diesel operated on a RCCI engine. They observed that the methanol injection rate in premixed mode and the diesel injection timing were the core parameters, on which the ignition timing of RCCI operation depends. With proper tuning of diesel injection timing, the heat release shape can be accurately controlled to achieve a desirable combustion phasing. However, several researchers also observed operational instability of such advanced dual fuel LTC operation which further impacts on the overall performance of the engine operation. In this context, Yasin et al. (2017) studied the cyclic variations of cylinder pressure operating with biodiesel-alcohol blends evaluated for 200 consecutive combustion cycles. They observed that the alcohols contribute significantly to the higher cyclic variability of the combustion parameters. Similarly, Wang et al. (2015) investigated the cycle-to-cycle variation in the combustion parameters over 100 consecutive cycles operated in a diesel engine with dimethyl ether (DME) as premixing fuel. They found that the

induction of large quantity of DME increases the variations in IMEP indicated by higher  $COV_{IMEP}$ , which eventually limited the range of LTC operation. Thus, a trade-off relation was apparent in the RCCI operation amongst the response parameters with respect to the increasing participations of methanol in dual fuel operation, while very few studies have been observed to address such trade-off issues appropriately.

On the other hand, the reactivity gradients greatly rely on the premixing characteristics of high reactive fuel, wherein the pilot injection plays a vital role to this end. By attaining various reactivity gradients, better controllability in tuning of combustion phasing can be achieved. Implementation of such strategy hence further enhances the scope of the RCCI operation to achieve better operational stability at higher methanol energy share with lower emissions and higher efficiency profiles. To this end, the evolvement of common rail direct injection (CRDI) in the contemporary research of diesel engine has further enhanced the potential of such advanced dual fuel operation in its better exploring capability and controllability in fuel injection pressure, fuel injection timing and the amount of pilot injection mass in splitting of diesel fuel. The splitting of diesel under multiple injection strategy as observed in the Partially Premixed combustion (PPCI) regime of LTC operation further provides the opportunity of varying pilot and main injection timings along with the pilot mass percentage, which increases the flexibility in the area of operation with increasing control parameters. Hence, the present study has attempted to utilize the potential of split injection strategy to enhance the scope of premixed methanol with diesel based RCCI operation through an optimization study, wherein the best compromised trade-off solutions have been unearthed to observe the synergistic benefits of higher efficiency and lower emissions under the constraints of 5% variability in the combustion cycles. It is also pertinent to mention that the previous optimization studies have not targeted to achieve the emission limits as specified in the emission regulations, whereas the present optimization study has been strictly carried out to satisfy the relevant emissions regulations of EPA Tier 4 along with improving the operational stability and exergy efficiency of the dual fuel LTC operation.

However, the implementation of such advanced dual fuel reactivity controlled combustion strategy in an existing conventional diesel engine increases the operational complexity due to critical tuning of increased actuating variables, which necessitates a robust engine management system (Isermann et al. 1998). The enhanced parametric degrees of freedom in such combustion technologies have to be addressed to avail the maximum advantages by optimizing the control variables. For parametric exploration and optimization studies, various techniques were employed in IC engine domain, wherein Response Surface Methodology (RSM) was one of the most extensively used techniques for attaining the maximum performance and minimum emission profiles. The efficacy of RSM technique is evident in the vast ranges of literatures. Fang et al. (2015) investigated the hydrous ethanol injected RCCI operation with diesel for studying its emissions characteristics and employed Design of Experiments (DoE) based RSM technique to optimize the parameters for achieving the desired objectives. They observed a reduction of 79% and 72% in  $NO_x$  and 50% and 27% in soot at low and high load conditions respectively. Kim et al. (2012) used DoE based RSM optimization technique for designing the experiments and carrying

out the statistical analysis in which they observed  $\text{NO}_x$  and PM reduction of 57% and 39% respectively in PCCI mode of combustion on a diesel engine. Pandian et al. (2011) used the desirability approach in RSM technique for optimizing the injection pressure, injection timing and nozzle tip protrusion. They found a high desirability of 0.98 at the optimum injection parameters of 225 bar FIP,  $21^\circ$  BTDC injection timing and 2.5 mm of nozzle tip protrusion. Lee and Reitz (2003) found that RSM based optimization of EGR and other system parameters showed a simultaneous reduction of  $\text{NO}_x$  and PM without decreasing fuel efficiency on a HSDI engine. RSM helped to reach a modulated kinetics (MK) combustion zone or simply LTC zone and premixed combustion zone. Ricaud and Lavoisier (2004) explored the effects of injection topology, injection pressure, EGR rate and start of injection using a dedicated CRDI system. They used RSM approach for optimizing the multiple injection topology for getting superior performance and lower emission mandate. Ileri et al. (2013) designed the experiments using a second order full quadratic RSM models which developed an empirical relationship for predicting performance and emissions in a diesel engine fuelled with canola oil methyl ester. The prediction of brake power, brake torque, BMEP, BSFC,  $\text{CO}_2$ ,  $\text{O}_2$ , EGT, BTE,  $\text{NO}_x$  and CO with higher accuracy by the mathematical modelling proved the effectiveness of RSM in IC engine application.

Therefore, in consideration to the significant reliability of RSM platform in IC engine applications as observed in the numerous relevant literatures, the present study has attempted to optimize the response parameters to attain the optimum reactivity in RCCI operation coupled with the multiple injection strategy through the Design of Experiment (DoE) based multi-objective RSM optimization technique. Besides, the present study demonstrates the relevance of robustness assessment of design space for estimating the variability of the response parameters of interest corresponding to the variation in the decision variables in order to calibrate the engine system behavior, wherein the design space robustness characterization has been perused under an innovative foray of FDS metric along with the typically employed set of comprehensive measures. The study further displays the potential of such advanced mode of RCCI operation coupled with split injection strategy in satisfying the respective emission mandates of EPA Tier 4 as well as achieving the carbon negative footprint towards the global environmental crisis.

### ***13.1.1 Motivation and Novel Viewpoint of the Present Study***

The rsm intervention in the field of dual fuel operation is very common. However, the contemporary development of reactivity controlled combustion technique based port injected premixed methanol/diesel dual fuel operations have been primarily studied on computational fluid dynamics (CFD) platform as evident in the literatures (Li et al. 2013, 2014). Wherein, the complex physical and chemical processes of combustion phenomena are analyzed by emulating the gas exchange, intricate heat transfer processes, multi-phase flows, turbulence-gas dynamics and different species

reaction chemistry (Valera and Agarwal 2019) through the implementation of high fidelity multi-physics based code. However, such effort involves a significant cost in chemistry solution times which reduces its relevance as an efficient vector in detailed engine response characterization and rapid calibration based multi-objective optimization solution requirements of the day. On the other hand, the data-driven surrogate model based characterization of engine responses has been evolved as an efficient alternative to the CFD regime owing to the considerable improvement in computational pace and therefore significantly reduced solution time cycles in calibration and decision-making strategies.

However, the superiority of data-driven based model development are subjective to the expanse of experimental observations in the designated parametric space and posed with distinct challenges of reliability and robustness under the present notions of restricted test bench recourses. This is basically due to the absence of adequate system information on the unknown degrees of non-linearity that may exist in the experimentally unmapped zones. Subsequently, it is apparent from the fundamental conception of Response Surface methodology technique that the success of RSM simulation and optimization regime is pivotally and intrinsically related to the quality of the parametric design space being mapped under the experimental regime which is performed through a design of experiment strategy. Therefore, it becomes critically important to analyze the robustness of the design space developed by the Design of Experiment in the optimization study. But none of those studies as apparent in Table 13.1 have relegated to the cause of the development of a robust Design of Experiment (DoE). The design of experiment is the only way possible to explore the continuous space such that the system is represented in all its facets and described by the parameters chosen. Hence in this regard, to address such research gap, the present study has undertaken a dedicated effort in analyzing the robustness of design space to ensure the precision of RSM endeavor (Mathematical expression) in emulating the experimentally unmapped design space with commendable accuracy. To this effect, the present study has engaged a comprehensive set of measures to quantify the quality of the design space employed in the experimental design. The metrics of Condition number of the correlation matrix (CoN), scaled D-optimality criteria, G-efficiency and Fraction of Design Space (FDS) have been incorporated in this regard to evaluate and analyze the design space offered in each design of experiment in this study. Furthermore, it is evident in the literatures as shown in Table 13.1 that most of the relevant studies employed CCD or Box-Behnken designs in DoE strategy, while implementation of such designs in a reactivity controlled combustion of dual fuel LTC operation may not be efficient enough due to its incompetency in adding multi-linear constraints as well as in providing higher order model and different designs for the same factors and model information. In this context, the present study has employed a novel customized design of experiment which offers different designs for the same factors with an incremental design points. Thus, the present study endeavors a unique optimization case study integrated with a novel design of experiment strategy to satisfy multiple objectives of premixed methanol with diesel RCCI operation.

**Table 13.1** Literature studies of design of experiment based RSM optimization

Studies carried out by	Design of experiment used	Robustness evaluation of design space				Year	References
		Condition no. (CoN) assessment	G-efficiency analysis	D-Optimality analysis	FDS analysis		
Liang et al.	Box Behnken	Not done	Not done	Not done	Not done	2021	Liang et al. (2021)
Samet Uslu	Central composite design	Not done	Not done	Not done	Not done	2020	Uslu (2020)
Hariharan et al.	Factorial design	Not done	Not done	Not done	Not done	2020	Hariharan (2020)
Subramani et al.	Taguchi orthogonal array	Not done	Not done	Not done	Not done	2020	Subramani et al. (2020)
Krishnamoorthi et al.	Factorial design	Not done	Not done	Not done	Not done	2017	Krishnamoorthi et al. (2018)
Chen et al.	Face-centered composite design	Not done	Not done	Not done	Not done	2017	Chen et al. (2017)
Ganji et al.	Box Behnken	Not done	Not done	Not done	Not done	2016	Ganji et al. (2017)
Klos et al.	Full factorial	Not done	Not done	Not done	Not done	2016	Klos and Kokjohn (2016)
Fang et al.	Fractional factorial design and Central composite design	Not done	Not done	Not done	Not done	2015	Fang et al. (2015)
Dhole et al.	Factorial design	Not done	Not done	Not done	Not done	2014	Dhole et al. (2014)



## 13.2 Materials and Methods

Figure 13.1 (Kakati et al. 2021) demonstrates the schematic diagram of the complete engine test set up arrangement used in this study. In this investigation, the existing diesel engine test set up was upgraded for adaptation of the dual fuel operational strategy. The synchronization of the methanol injection mechanism with the existing diesel engine operation was done through synchronization of the crank angle sensing unit. The controlling and monitoring of the methanol injection system was performed through the control unit of “Performance electronics USA model PE3-SP000”. The methanol participation in dual fuel operation was quantified and controlled in terms of duration (ms), while pilot and main injection mass of diesel in split injection strategy was quantified in terms of percentage of the total mass of diesel required to keep the engine run at constant speed of 1500 rpm. Figure 13.2 demonstrates the calibration curve between the methanol injection durations (ms) and the methanol mass flow rates (kg/h).

The data acquisition for all the cases of split injections was only performed after achieving the steady state condition, as verified from the engine operational sound and vibration. Initially the engine was operated on diesel only mode and then slowly methanol was injected. The duration of methanol injection was gradually increased from 4 ms to the highest possible duration of 10 ms in consideration of the stability of the operation. As the engine used in this study was a constant speed engine, the energy required to develop the same brake power is constant, thereby the participation of

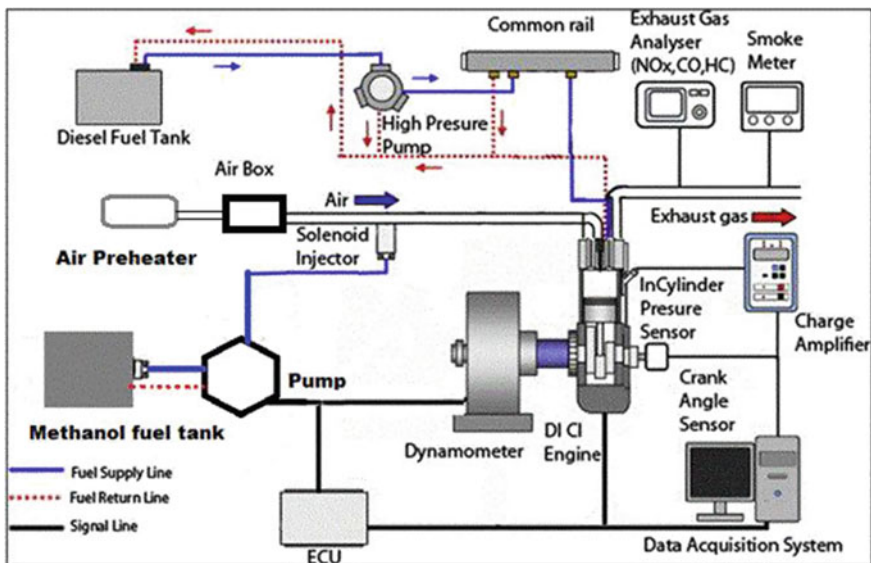
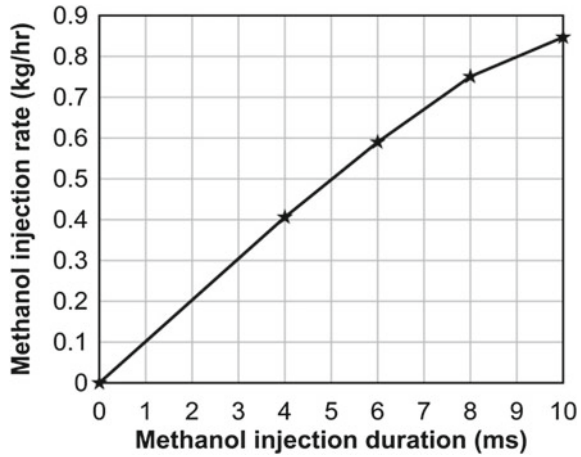


Fig. 13.1 Schematic diagram of the experimental setup

**Fig. 13.2** Calibration curve between methanol injection duration (ms) and flow rate (kg/h)



methanol in dual fuel operation resulted in reduction of the amount of diesel required to develop the same power.

In the preliminary investigation of split injection strategy, the parametric variations of split injection timing and pilot mass percentage of diesel was carried out to identify the range of operation for optimization study considering the stability of the operation. The necessary instruments used in this study to measure all the input and output variables of interest, along with the sensitivity and make model of individual instruments and the associated uncertainties have been comprehensively demonstrated in the previous work of the authors (Kakati et al. 2019). The sampling and computational uncertainties incurred in the process of data analysis have also been demonstrated and explained in detail in the previous work (Kakati et al. 2019).

The estimation of overall cetane number (Eq. 13.1) for the RCCI operation demonstrating the overall reactivity of the dual fuel strategy with different reactivity has been carried out by following the work of Sadabadi et al. (2016).

$$CN_{overall} = \frac{(CN_{FLR} \times \Phi_{FLR})/AFR_{st,FLR} + (CN_{FHR} \times \Phi_{FHR})/AFR_{st,FHR}}{(\Phi_{FLR}/AFR_{st,FLR}) + (\Phi_{FHR}/AFR_{st,FHR})} \quad (13.1)$$

where,  $m_{FLR}$  and  $m_{FHR}$  are the mass flow rate,  $CN_{FLR}$  and  $CN_{FHR}$  are the cetane numbers,  $\Phi_{FLR}$  and  $\Phi_{FHR}$  are the equivalence ratio of low reactivity fuel (methanol) and high reactivity fuel (diesel) respectively. Equations (Eqs. 13.2, 13.2a and 13.2b) demonstrate the calculation of coefficient of variation of indicated mean effective pressure,  $COV_{IMEP}$  (Maurya 2017).

$$COV_V = \frac{\sigma_V}{V_{mean}} \times 100 \quad (13.2)$$

$$\sigma_V = \sqrt{\sum_{i=1}^n (V_i - V_{mean})^2 / (n - 1)} \quad (13.2a)$$

$$V_{mean} = \sum_{i=1}^n V_i / n \quad (13.2b)$$

where,  $\sigma_V$  is the standard deviation,  $V_{mean}$  is the mean of the variable,  $n$  is the number of data points. While, the calculation of exergy efficiency has been carried out by following the work of Morsy et al. (2015). The sustainability characteristic of the methanol based RCCI operation is encapsulated by the sustainability index (STI), which is related to the exergy efficiency of the operation through the following equation (Eq. 13.3).

$$STI = \frac{1}{1 - \text{exg. eff.}} \quad (13.3)$$

The emission elements of  $\text{NO}_x$ , UHC and  $\text{CO}_2$  were measured using a 5 gas analyzer (AVL Digas-444), while smoke was measured using a smokemeter (AVL 437 smokemeter). Since, all the emission elements were expressed in terms of g/kWhr unit in the emissions regulations, the units of  $\text{NO}_x$  and UHC have been converted from ppm to g/kWh by following the procedure mentioned in the work of Mohan et al. (2014).

The conversion formulae are as follows (Eqs. 13.4a and 13.4b)

$$\text{NO}_x(\text{g/kWh}) = C_1 \times \text{NO}_x(\text{ppm}) \times C_{\text{NO}_x} \times BP \times \dot{m}_{ex} \quad (13.4a)$$

$$\text{UHC}(\text{g/kWh}) = C_2 \times \text{UHC}(\text{ppm}) \times BP \times \dot{m}_{ex} \quad (13.4b)$$

where,  $C_1$  and  $C_2$  are constants whose values were considered as per the study of Mohan et al. (2014),  $\dot{m}_{ex}$  is the exhaust gas mass flow rate (Eq. 13.4c)

$$\dot{m}_{ex} = \dot{m}_d + \dot{m}_a + \dot{m}_m \quad (13.4c)$$

where,  $\dot{m}_d$ ,  $\dot{m}_a$  and  $\dot{m}_m$  are respectively the mass flow rates of diesel, air and methanol.  $C_{\text{NO}_x}$  is the  $\text{NO}_x$  correction factor as demonstrated by Fritz and Dodge (2003). Furthermore, the conversion of smoke or opacity (%) into soot (g/kWh) has been shown in the following equations (Eqs. 13.5a–13.5c) (Benajes et al. 2016).

$$\text{Smoke}(\%) = 0.12 \times \text{FSN}^3 + 0.62 \times \text{FSN}^2 + 3.96 \times \text{FSN} \quad (13.5a)$$

$$\text{Soot}(\text{mg/m}^3) = \frac{4.95 \times \text{FSN}}{0.405} \times e^{(0.38 \times \text{FSN})} \quad (13.5b)$$

$$Soot(g/kWh) = \frac{Soot(mg/m^3)}{1000} \times \frac{(m_{air} \times m_{fuel}) \times 3.6}{1.165 \times BP} \quad (13.5c)$$

### 13.3 Design of Experiment

The conventional experimental investigation is generally carried out by varying one factor at a time, which may result in a very large number of experimental runs depending on the range of operation and the number of control variables. For determining the optimal set of control variables corresponding to the desired objectives in a typical optimization case, the acquisition of information regarding the interactions between the decision and response variables are of great importance, especially in such cases where non-linearity in the relationships is quite evident. To this end, the design of experiment (DoE), a statistical approach stands as a necessary tool in investigating the design space with the multivariate exploration capability, offering in-depth and diverse information from the minimum number of experiments.

In a typical multi-objective optimization case, the quest of finding the optimal solutions satisfying all the objectives is largely dependent on the engagement of the proper DoE. The pilot experimental study in this present case of investigation has experienced several physical limitations during its operation, which defines the range of operation with respect to each decision variable. Moreover, some additional limitations are also present in this current investigation apart from the range of operation, which must be included in the DoE as constraints to reduce the computational time in the pursuit of attaining the optimal solutions for the response variables. To this effect, a constrained design of experiment strategy has been employed in this present case of optimization study. The design constraints and the limits imposed in the DoE for exploring the design space in this case of investigation have been expressed in the following equations (Eqs. 13.6–13.10).

$$35 < PIA < 55 \quad (13.6)$$

$$5 < MIA < 25 \quad (13.7)$$

$$10 \leq PIA - MIA \leq 30 \quad (13.8)$$

$$10 < PIM\% < 50 \quad (13.9)$$

$$15 < CN_{mix} < 36 \quad (13.10)$$

The present study has incorporated the injection timings of pilot and main injection of diesel fuel as the control parameters to investigate the effects of injection timings under split injection strategy on the operation of such RCCI kind. The limits of injection timing for both pilot and main injection were determined in the preliminary investigation on the basis of stability of the operation. Besides, the dwell time between these two injections has been incorporated in this study as constraint to avoid the chance of overlapping of these two consecutive injections. For investigating the effects of premixed ratio of diesel fuel under split injections, the fraction of diesel fuel injected in the pilot injection has been considered in this study as an another control parameter, which was constrained in between 10 and 50% in consideration to the stability concerns of the operation. However, the fraction of the diesel fuel injected during the main injection is just the consequence of the preceding event of pilot injection and thereby excluded in this optimization study. The effect of methanol injection rate in this reactivity controlled combustion regime has been studied through the overall reactivity,  $R_O$  (or  $CN_O$ ) of the dual fuel operation, the calculation of which has been shown in the previous section (Sect. 13.2). The lower and upper limit of reactivity was evaluated corresponding to the maximum and minimum energy share of methanol in this dual fuel operation with diesel as shown in Fig. 13.3. For maximum energy share of methanol, the lowest overall reactivity was observed as 15.4; while for minimum energy share, the highest overall reactivity was observed as 35.8 in the preliminary investigation. Thus, the range of  $R_O$  in this case of optimization study has been determined as 15–36.

The present study considers  $NO_x$ , soot, UHC,  $CO_2$  emissions as the response parameters along with  $COV_{IMEP}$  as a measure of combustion stability and exergy efficiency for mapping the sustainability characteristics of RCCI operation. The respective constraints applicable to each response parameters have been illustrated in the following section (Sect. 13.4.1.1).

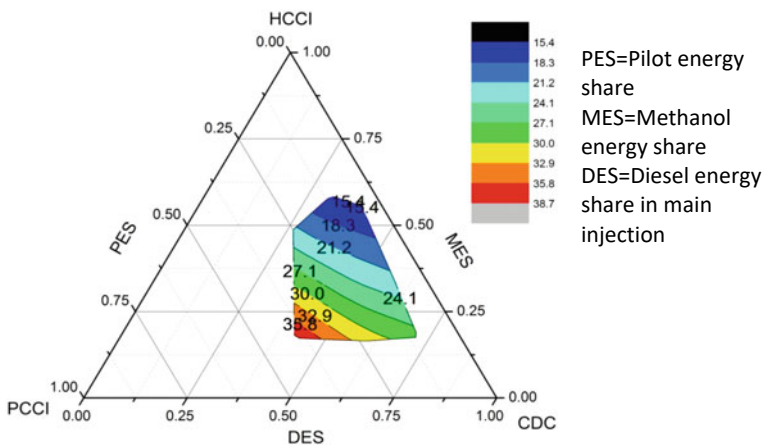


Fig. 13.3 Reactivity variation at different energy share

In typical optimization case of studies (Bose et al. 2017; Shirmeshan et al. 2016), the most prevalently response surface designs have been employed, wherein the emphasis is given on the fitted surface. But how well the surface follows the actual characteristics of the system is very crucial and hence the necessity of evaluating the design suitability. The evaluation criteria for the design matrix have been comprehensively demonstrated in the succeeding section of Sect. 3.1.

### 13.3.1 Evaluation of Design Space: Quality Metrics

As per the deliberations attributed in the previous section (Sect. 13.3), the quest of achieving the optimal zone of operation is significantly reliant on the employment of proper experimental design. Accordingly, the extensive evaluation of the design space is critically important for ensuring the deployment of appropriate experimental design for a particular optimization case of study. The present optimization study to this effect has engaged a comprehensive set of measures to quantify the quality of the design space employed in the experimental design. The literature to this context indicates that for the assessment of the employed designs, the most of the studies (Lucas 1976; Dette and Wong 1995; Borkowski and Valeroso 2001; Ye and Zhou 2013) incorporated the measures of Co-efficient of determination ( $R^2$ ), Condition number of matrix, scaled D-optimality criteria and G-efficiency.

The “Condition number of correlation matrix” as a metric to measure the multi-collinearity in the design matrix has been employed in this study. The condition number of score one indicates that the design matrix is orthogonal and no collinearity exists amongst the model terms in the design. In case of comparing the performance of a design with different numbers of run, the present study has employed the scaled D-optimality criterion, which aims for the maximization of the determinant of the information matrix  $I'$  of the design. The optimal number of experimental runs out of all the possible runs in the design matrices can be opted through the measure of D-optimality criterion. The mathematical expression for choosing the optimal design matrix  $I_0$  is expressed in the equation (Eq. 13.11).

$$|I'_0 I_0| = \max(|I'I|) \quad (13.11)$$

Another metric for choosing from the several equivalent designs, G-efficiency has been employed in this study, which expresses the average prediction variance in terms of the percentage of highest prediction variance. The G-efficiency can be defined as the expression demonstrated in the equation (Eq. 13.12).

$$G - eff. = \left( \frac{n_m}{n_d \times V_{\max}(I)} \right) \quad (13.12)$$

where,  $n_m$  and  $n_d$  are the number of model terms and the number of design runs,  $V_{\max}$  is the highest variance of prediction existent in the design matrix I.

In the preliminary stages of experimentation, for screening and characterization purposes, the factorial designs are mostly preferred, wherein the emphasis is given on the main and interaction effects between the model terms only. In such situations estimation of power metric is ideal for selecting the suitable design matrix. But in case of an optimization study such as response surface designs, the evaluation of power metric is inappropriate to use, instead a prediction based metric of Fraction of Design Space (FDS) statistics can be employed for estimating the design suitability. Fraction of Design Space (FDS) technique is basically utilized to determine the maximum possible fraction of volume of design space that can be used under the threshold limit of prediction variance. Zahran et al. (2018) mentioned in their study that for attaining the comprehensive idea of the performance of a design matrix, the volume of design space must be considered. The FDS plot encapsulates the distribution of mean standard error at different volume fraction of design space. The standard error at each fraction of volume can be estimated through the following equation (Eq. 13.13). For comparing the design with different number of runs, the present study has estimated the standard error at 80% of volume or 0.8 volume fraction of the design space, which is the minimum FDS score for optimization case of study.

$$Std. E_{FDS} = \frac{(d/t_{\alpha/2,df})}{s} \quad (13.13)$$

where,  $d$  is the acceptable error limit or interval half-width and  $s$  is the anticipated standard deviation.

### 13.3.2 Model Evaluation Metric

The subsequent metamodels developed under RSM iterative platform for each response variables must be examined across a comprehensive set of metrics to evaluate the model accuracy in predicting the response parameters along with the reliability in estimation and the model uncertainty before approving it as a robust system characterization platform of high precision. The study incorporates the correlation metric of coefficient of determination  $R^2$  (Chakraborty et al. 2016; Castelli et al. 2013) (Eq. 13.14) and Nash–Sutcliffe efficiency NSCE (Yassin et al. 2016) (Eq. 13.15) as the common benchmark for the model assessment. The Nash–Sutcliffe efficiency improves upon the limitations of  $R^2$  by including a measure which is sensitive to the differences in the model estimated mean and variance of the observed and model estimated values. The study further employs the Symmetric mean absolute percentage error, SMAPE (Eq. 13.16) for estimating the absolute error in the prediction of response values (Armstrong 1985). Besides, for the estimation of model performance independent to dimensional bias, the present study has employed a relative

error metric of Root relative square error, RRSE (Eq. 13.17) that allows a comparative venture of examining estimation quality of different meta-modelling mechanisms simultaneously across all response categories being modeled (Ebrahizade et al. 2018).

$$R^2 = 1 - \left( \frac{\sum_{i=1}^n (\text{exp}_i - \text{pred}_i)^2}{\sum_{i=1}^n (\text{exp}_i)^2} \right) \quad (13.14)$$

$$NSCE = 1 - \left\{ \frac{\sum_{i=1}^n (\text{exp}_i - \text{pred}_i)^2}{\sum_{i=1}^n (\text{exp}_i - \text{exp}_{av})^2} \right\} \quad (13.15)$$

$$SMAPE = \frac{1}{n} \sum_{i=1}^n \frac{2 \times |\text{exp}_i - \text{pred}_i|}{|\text{exp}_i| + |\text{pred}_i|} \quad (13.16)$$

$$RRSE = \sqrt{\frac{\sum_{i=1}^n (\text{pred}_i - \text{exp}_i)^2}{\sum_{i=1}^n (\text{exp}_i - \text{exp}_{av})^2}} \quad (13.17)$$

where,  $n$  denotes the number of samplings and  $\text{exp}_i$ ,  $\text{pred}_i$  and  $\text{exp}_{av}$  are the experimental, predicted and average of experimental values respectively.

The above deliberations mainly focused on the attempt of evaluating the forecasting capability of the model evolved from the RSM platform. The present study has further adopted the Theil uncertainty,  $U(\text{II})$  estimation (Eq. 13.18) in line with the work of Bliemel (1973) to enumerate the uncertainty in prediction, existent in the developed metamodels of respective response categories.

$$\text{Thiel } U(\text{II}) = \frac{\sqrt{\left[ \sum_{i=1}^n (\text{exp}_i - \text{pred}_i)^2 \right]}}{\sqrt{\left[ \sum_{i=1}^n (\text{exp}_i)^2 \right]}} \quad (13.18)$$

### 13.4 Multi-objective Optimization (MOOP) Endeavors

The optimization regime in any engineering field is fundamentally devoted in the task of finding the optimal set of control variables which offer the maximum or minimum values of the objective functions defined in the respective optimization study. The objective functions are basically the mathematical expressions of the physical problem, emulating the responses of the output variables. But, the real world optimization problems primarily pose multiple yet contradictory criteria to be addressed simultaneously (Deb 2001). Optimization under such paradigms, characteristically induce challenges in that, the computed solutions need to satisfy the



conditions of optimality as set by the decision maker (DM) for all the involved objectives simultaneously (Osyczka 1985). As the included objectives being contradictory in their nature, efforts to optimize an objective would inherently cause a penalty in the path of attaining optimality of the other. Formulation or selection of a global objective function for optimization recourse to a given problem under such contradicting individualities is the pivotal step in the entire optimization endeavour. The objective function in such cases should effectively embody the desired indices of the problem at hand without compromising the underlying physics of the problem through appropriate system identification techniques.

Optimization of multiple conflicting objectives in a multi-dimensional design space is difficult; as such multi-objective optimization yields multiple optimal solutions instead of a desirable single optimum as seen in typical single objective optimization (SOOP) domains, due to the inherent contradictory nature of the objectives that need to be satisfied simultaneously. Instead, a set of compromising solutions, generally known as the Pareto optimal (Ehrgott 2012) solutions are obtained which signify the best trade-off between the conflicting requirements. The essence of such multi-objective optimization is characterized by the concepts of Pareto optimality (Pareto et al. 1896), named after the contributions of *Vilfredo Federico Damaso Pareto*, the Italian economist. The Pareto optimal solutions are the non-dominant solutions in which none of the optimal solutions are dominant or superior to any other solutions to the objectives in the search space. These Pareto optimal solutions provide the best possible trade-off scenario in the conflicting objectives, wherein the non dominated solutions deny any chance of obtaining a better solution which may improve one objective without compromising the others. To this end, the preliminary task in a typical MOOP endeavor is to search for non-dominant optimal solutions as many as possible in the entire design space, which eventually visualize all the trade-off relations between the objectives that exist in the design space of multiobjective optimization recourse.

### 13.4.1 Methodology

The comprehensive demonstration of the present study has been presented in the work flow depicted in Fig. 13.4. The optimization iterations in this present study have been carried out in the Design Expert environment. The exploration of the design space in search of the solutions satisfying the multiple objectives was initiated subsequent to the development and critical evaluation of the metamodels corresponding to each response parameters of interest. The objective functions and the design constraints invoked in the optimization routine applicable to the present investigation have been enumerated in the following Sect. 13.4.1.1. However, such search routine delivers a multitude of non-dominated trade-off solutions, out of which identifying the best compromised solution is quite complicated for the decision makers. The non dominated solutions are a group of Pareto solutions signifying the best negotiation amongst the contradictory objectives set in an optimization study. Thus, selection of the best

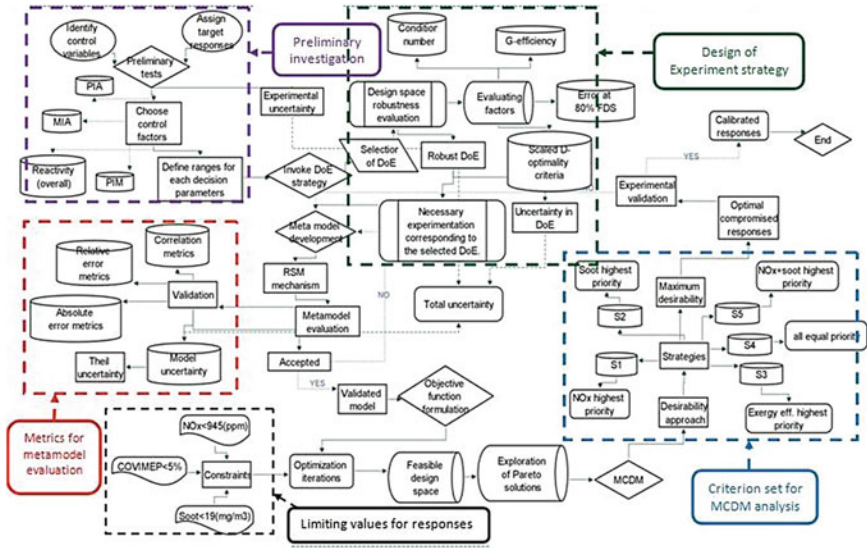


Fig. 13.4 The workflow of the entire optimization study

compromised solution amongst the numerous non dominated solutions evolved in an optimization study often becomes a challenging task for the designer. To this end, multi criteria decision making analysis was undertaken to determine the optimal choice of the control parameters which yields the best compromised response values. The study further engaged desirability approach in the MCDM endeavor to locate the optimal Pareto set, wherein the maximum score of overall desirability denotes the optimal Pareto solution for the given set of investigation.

13.4.1.1 Design Constraints

Equations 13.19 and 13.20 represent the objective functions of the present multi-objective optimization study, wherein Eq. 13.19 represent the minimization problem of NO<sub>x</sub>, soot, UHC, CO<sub>2</sub> and COV<sub>IMEP</sub> and Eq. 13.20 represent the maximization of exergy efficiency respectively.

$$Minimize \left\{ \begin{matrix} NO_x \\ Soot \\ UHC \\ CO_2 \\ COV_{IMEP} \end{matrix} \right\} = f_{RSM} [\Psi(R_0, PIM, PIA, MIA)] \quad (13.19)$$

$$Maximize \{ [Exgeff] \} = f_{RSM} [\Psi(R_0, PIM, PIA, MIA)] \quad (13.20)$$

Apart from the operational limitations identified and quantified as the limits of decision parameters as deliberated in the preceding section (Sect. 13.3), the present study invokes the pertinent design constraints of emissions regulations as well as the stability indicator in the optimization iterations for finding the non-dominated solutions. Equations (13.21a–13.21e) demonstrate the constraints invoked for each response parameters in optimization iterations in this study.

$$0 < \text{NO}_x < 945, \quad \text{NO}_x \text{ (ppm)} \quad (13.21a)$$

$$0 < \text{Soot} < 19, \quad \text{Soot (mg/m}^3\text{)} \quad (13.21b)$$

$$\text{CO}_2 > 0, \quad \text{CO}_2 \text{ (%) } \quad (13.21c)$$

$$0 < \text{COV}_{\text{IMEP}} \leq 5, \quad \text{COV}_{\text{IMEP}} \text{ (%) } \quad (13.21d)$$

$$\text{Exergy eff.} > 0, \quad \text{Exergy eff. (%) } \quad (13.21e)$$

The respective constraints of  $\text{NO}_x$  in ppm (Eq. 13.21a) and soot in  $\text{mg/m}^3$  (Eq. 13.21b) corresponding to EPA Tier 4 norms was estimated at the baseline single injection operation by following the work of Benajes et al. (2016). However, the constraints corresponding to EPA Tier 4 emissions regulations are set for NHC and PM as shown in Eqs. 13.22a and 13.22b.

$$\text{NHC} < 7.5 \text{ (g/kWh)} \quad (13.22a)$$

$$\text{PM} < 0.3 \text{ (g/kWh)} \quad (13.22b)$$

#### 13.4.1.2 Multi Criteria Decision Making (MCDM)

The quest of obtaining the optimal solution in the multi-objective optimization endeavor frequently experience the multitude of non-dominated solutions, out of which estimating the optimal one is a task of great hurdles, in which a careful practice of systematic diagnosis is required in the decision making. Such practice of multi criteria decision making regime often employs the desirability approach as evident in many literatures of multi-objective optimization studies (Kumar et al. 2016; Odu and Charles-Owaba 2013). To this effect, the present study has incorporated the desirability method in MCDM strategy to find the optimal set of Pareto solution which can provide the optimal responses of desired level. In this scope of optimization study,

**Table 13.2** Different criteria set for multi-criteria decision making

Criteria	Highest priority	Weightage given					
		NO <sub>x</sub>	Soot	UHC	Exergy efficiency	CO <sub>2</sub>	COV <sub>IMEP</sub>
S1	NO <sub>x</sub>	5	1	1	1	1	1
S2	Soot	1	5	1	1	1	1
S3	Exergy efficiency	1	1	1	5	1	1
S4	All equal	1	1	1	1	1	1
S5	NO <sub>x</sub> + soot	5	5	1	1	1	1

five different criteria has been set according to the objectives of this study as demonstrated in Table 13.2, each of these criteria poses different emphasis on the response parameters. The highest priority was given to NO<sub>x</sub> in the set criteria of S1, while S2 corresponds to the highest priority in soot. Similarly, the highest emphasis on exergy efficiency was given to the criteria of S3. While, S5 criterion poses equal emphasis on each of the response parameters, S6 gives the highest priority to NO<sub>x</sub> and soot simultaneously. This criteria as depicted in Table 13.2 has been utilized for both the experimental as well as Pareto solutions obtained from the optimization iterations to estimate the desirability score and thus compare the optimal results obtained from the optimization study with the experimentally observed best results. The set of Pareto solution scoring the highest desirability is considered as the best compromised set of solution for the entire scope of investigation satisfying all the desired objectives of this study.

Deployment of desirability function in the regime of multi-objective optimization problem is evident in extensive literatures, however it was first proposed by Harington (1965) and later modified by Derringer and Suich (1980) and Kim and Lin (2000). The method investigates the decision parameters which provide the best desirability for the respective response variables. In this method, the objective functions for each response variables are converted into scale free desirability scores ( $d_i$ ) (Eq. 13.23 and 13.24), which are further aggregated into a single global desirability index ( $D$ ) through weighted geometric mean as shown in the equation (Eq. 13.25), in order to unearth the global optimal operating condition. This desirability value  $d_i$  ranges from 0 to 1, wherein 0 indicates that the response is completely unacceptable while, 1 represents the ideal score for the response to be accepted.

$$[d_i]_{\text{maximize}} = \left[ \frac{g_i - g_{i \text{ min}}}{g_{i \text{ max}} - g_{i \text{ min}}} \right]^{t_i}, \quad g_{i \text{ min}} \leq g_i \leq g_{i \text{ max}} \tag{13.23}$$

$i = 1, 2, \dots, n$ ; while  $n$  denotes the number of objectives. Whereas,  $g_{i \text{ max}}$  and  $g_{i \text{ min}}$  are the maximum and minimum scores of  $g_i$  respectively. For the condition of  $g_i < g_{i \text{ min}}$ , the  $[d_i]_{\text{maximize}}$  becomes 0, while for  $g_i > g_{i \text{ min}}$  the  $[d_i]_{\text{maximize}}$  becomes 1.

$$[d_i]_{\text{minimize}} = \left[ \frac{g_{i \max} - g_i}{g_{i \max} - g_{i \min}} \right]^{t_i}, \quad g_{i \min} \leq g_i \leq g_{i \max} \quad (13.24)$$

In case of minimization objective, for the condition of  $g_i < g_{i \min}$ , the  $[d_i]_{\text{minimize}}$  becomes 1, while for  $g_i > g_{i \min}$  the  $[d_i]_{\text{minimize}}$  becomes 0.

$$D = \left( \prod_{i=1}^n d_i^{w_i} \right)^{\frac{1}{\sum_{i=1}^n w_i}} \quad (13.25)$$

where,  $Des$  is the overall desirability and  $w_i$  is the relative importance or weightage given to  $i^{\text{th}}$  objective.

Depending on the nature of objective function, the goal of the response parameters can be set as maximize, minimize or set as target. The methodologies for estimation of desirability of each response variables contingent to the goal of objectives have been shown in the equations (Eqs. 13.23 and 13.24) in line with the study of Odu and Charles-Owaba (2013).

The overall desirability function ( $D$ ) (Eq. 13.25), is a measure of finding the best global trade-off solution amongst the competing objectives in a multiobjective optimization problem. However, the capability of discovering the best solution is dependent upon the proper optimizer specification (min, max, and target) and the selection of appropriate desirability objectives (weightage). In this case, the objectives set for each response variable were allocated weightage depending on their relative importance wherein, the weightage value ranges from 1 to 5. The minimum importance is denoted by 1 while, the greatest importance is signified by 5. The set of input factors which attains the optimal trade-off solutions are generally identified by the highest overall desirability score,  $D_{\max}$ .

## 13.5 Results and Discussion

### 13.5.1 DoE Evaluation and Selection

The quest of achieving the optimal zone of operation corresponding to the desired objectives of the study is significantly reliant on the precision of the RSM metamodelling in mapping the responses of output variables of interest, which further immutably and irrevocably depends on the quality of the design of experiment proposed by the designer. Especially the situation of complex engineering problems, wherein system non-linearity due to the interactions among the control variables are prevalent, pose distinct challenges in gathering the necessary information about the system behaviors or the characteristics of the response parameters. The quality of the information gathered through experimentation eventually depends on the quality of the proposed design, which necessitates the relevant evaluation of the design matrix. To this effect,

**Table 13.3** Ranges of control parameters employed in design

Factor	Name	Type	Minimum	Maximum	Coded low	Coded high	Mean	Std. dev.
A	Reactivity	Numeric	15.00	36.00	-1 ↔ 15.00	+1 ↔ 36.00	25.40	8.05
B	PIM	Numeric	10.00	50.00	-1 ↔ 10.00	+1 ↔ 50.00	30.57	15.62
C	PIA	Numeric	35.00	55.00	-1 ↔ 35.00	+1 ↔ 55.00	41.48	6.76
D	MIA	Numeric	5.00	25.00	-1 ↔ 5.00	+1 ↔ 25.00	18.52	6.95

**Table 13.4** Particulars of the design of experiment

File version	12.0.1.0			
Study type	Response surface		Subtype	Randomized
Design type	I-optimal	Coordinate exchange	Runs	35
Design model	Quadratic		Blocks	No blocks
Build time (ms)	2804.00			

the present case of optimization study has employed a comprehensive set of evaluation measures to quantify the robustness of the design space employed in this study as deliberated in the previous section (Sect. 3.1). The proposed DoE in this study has been developed considering four factors and six response parameters under the relevant constraints of the control parameters defined in the preliminary investigation. Tables 13.3 and 13.4 demonstrate the details of the design of experiment undertaken in this present case of optimization study.

The proposed design matrix initially offers 25 number of design points, however to enhance the robustness of the design space, additional design points have been incorporated in the design space with a regular increment of 5 extra random points. The subsequent deliberation to this effect highlights the enhancement of the robustness of the design space with the increasing design points. Figure 13.5 encapsulates the scores of different evaluation measures for estimating the performance of the designs. The D-optimality criteria as evident in Fig. 13.5 shows a decreasing trend with the increasing number of design points, wherein the design (D35) with 35 number of design points exhibit the lowest score of D-optimality as 3.8. Similarly, the condition number demonstrates the decreasing trend till the D35 design, wherein the lowest score was observed as 38.02. Furthermore, the mean standard error calculated at 80% fraction of design space follows the similar trend, wherein the minimum score of the mean standard error was also found at D35 design. The FDS analysis of D35 design has been demonstrated in Fig. 13.6. However, the G-efficiency registered its highest score of 48.3% at D40 design, which shows an increasing trend with the design points. The pertinent design D35 to this end exhibits moderate G-efficiency as observed in Fig. 13.5.

From the analysis of the performance of designs based on the evaluation measures as deliberated above, D35 design undoubtedly exhibits the best overall characteristics

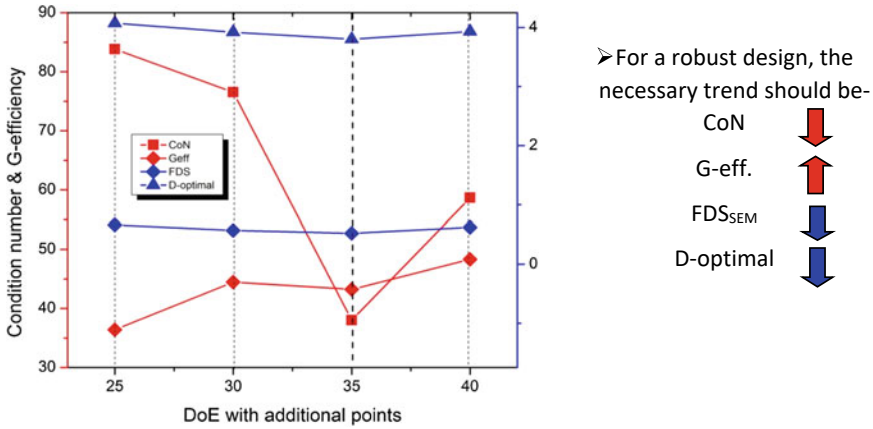


Fig. 13.5 Robustness evaluation of different designs

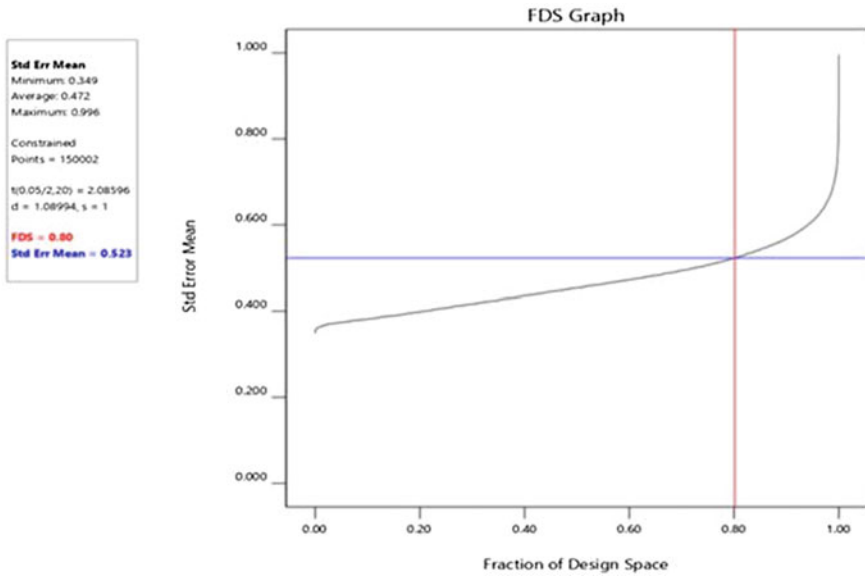


Fig. 13.6 Standard error mean at 80% FDS for D35 design

compared to the other equivalent designs and hence, the present study adopts the D35 design for carrying out the necessary experimental investigations.

### 13.5.2 ANOVA Analysis

The ANOVA findings dictate how each response model is to be built. Basically, it's an approach that involves trial and error, and it's distinct for each data type. To ensure the model passes fitting diagnostic, the procedure sequence and points selected must be well-tuned. Table 13.5 summarizes the ANOVA results for the different response models. Every response model has importance in terms of F-values and P-values, which show how each model influences the response. If the model terms are significant, then the P-values shouldn't be greater than 0.1. The total significance of the response models was calculated using the greater F-value and the lower P-value (<0.05). A smaller model may enhance the resilience of the model when it includes a large number of unimportant model terms. 'Adequate Precision' is the label for the particular model's signal-to-noise ratio. It is preferred to have a value higher than 4, and the final model will help you traverse the design space. An equation derived from the collected data may be used to assess the effect of each variable in detail, with different quantities being tested. It is important to state the levels of the factors in their order of appearance. Due to the coefficients being scaled to work with different units, and the intercept not being in the heart of the design space, the equation cannot be used to quantify each factor's influence. The following Table 13.5 displays the P-values and F-values of the ANOVA analysis, wherein the respective scores of  $R^2$ , adjusted  $R^2$  and predicted  $R^2$  for each response parameter were also displayed for model evaluation. Besides, Figs. 13.7, 13.8, 13.9, 13.10, 13.11 and 13.12 encapsulate the experimental versus predicted scores of the response parameters, which demonstrate the competency of the developed models in emulating the engine responses.

The subsequent mathematical expressions evolved from the developed meta-models for each response parameters have been enumerated in the following equations (Eqs. 13.26–13.31).

$$\begin{aligned}
 NO_x = & 4699.7 - 113.69 \times R_o + 9.8 \times PIM - 156.2 \times PIA - 16.09 \times MIA \\
 & + 0.013 \times R_o \times PIM + 1.75 \times R_o \times PIA - 0.52 \times R_o \times MIA \\
 & - 0.43 \times PIM \times PIA - 0.149 \times PIM \times MIA + 1.95 \times PIA \times MIA \\
 & + 1.34 \times R_o^2 + 0.21 \times PIM^2 + 1.2 \times PIA^2 - 0.98 \times MIA^2 \quad (13.26)
 \end{aligned}$$

$$\begin{aligned}
 UHC = & (5630 - 264 \times R_o + 18.18 \times PIM - 120.7 \times PIA + 133.88 \times MIA \\
 & - 0.34 \times R_o \times PIM - 2.69 \times R_o \times PIA + 0.397 \times R_o \times MIA \\
 & + 0.483 \times PIM \times PIA - 0.5 \times PIM \times MIA - 3.1 \times PIA \times MIA \\
 & + 5.8 \times R_o^2 - 0.33 \times PIM^2 + 3.2 \times PIA^2 - 0.67 \times MIA^2)^{(1/1.38)} \quad (13.27)
 \end{aligned}$$



**Table 13.5** P-values and F-values of the model terms of ANOVA analysis

Model	NO <sub>x</sub>	UHC	Soot	CO <sub>2</sub>	COVIMEP	Exg. eff.
R <sup>2</sup>	0.939	0.977	0.967	0.953	0.985	0.979
Adjusted R <sup>2</sup>	0.924	0.968	0.961	0.944	0.951	0.964
Predicted R <sup>2</sup>	0.905	0.918	0.917	0.909	0.910	0.901
Adequate precision	3896	33.97	39.29	61.21	92.65	42.31
Source	F-value	P-value	F-value	P-value	F-value	P-value
Model	442,859.6	<0.0001	92.52	<0.0001	269.00	<0.0001
A-Reactivity	13,115.7	<0.0001	243.26	<0.0001	54.35	<0.0001
B-PIM	3479.794	<0.0001	118.21	<0.0001	96.53	<0.0001
C-PIA	5119.3	<0.0001	30.58	<0.0001	23.14	<0.0001
D-MIA	33,457.63	<0.0001	137.83	<0.0001	20.11	<0.0001
AB	48,039.06	<0.0001	39.38	<0.0001	16.99	<0.0001
AC	4969.137	<0.0001	46.78	<0.0001	22.84	<0.0001
AD	8221.652	<0.0001	76.73	<0.0001	53.37	<0.0001
BC	20,001.43	<0.0001	30.98	<0.0001	27.63	<0.0001
BD	18,647.42	<0.0001	44.02	<0.0001	18.79	<0.0001
CD	70,029.21	<0.0001	32.57	<0.0001	15.24	<0.0001
A <sup>2</sup>	99,190.78	<0.0001	16.94	<0.0001	206.60	<0.0001
B <sup>2</sup>	3715.599	<0.0001	15.07	<0.0001	13.02	<0.0001
C <sup>2</sup>	7474.562	<0.0001	15.97	<0.0001	12.44	<0.0001
D <sup>2</sup>	28,911.64	<0.0001	41.48	<0.0001	18.61	<0.0001

**Fig. 13.7** Predicted versus experimental NO<sub>x</sub>

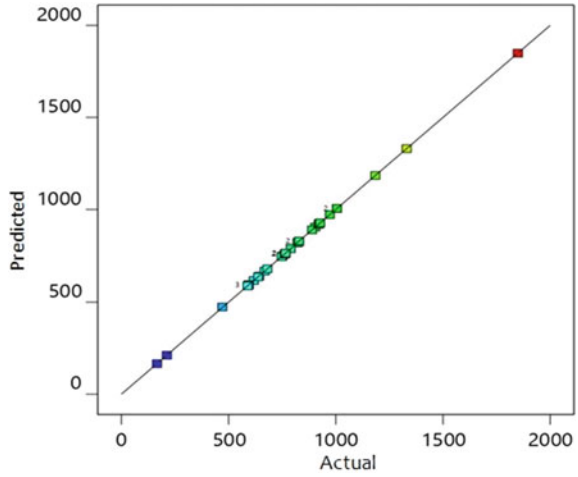
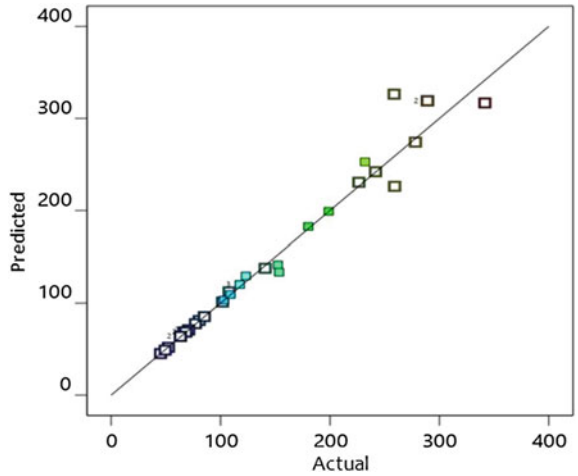


**Fig. 13.8** Predicted versus experimental UHC



$$\begin{aligned}
 Soot = & (0.394 + 0.014 \times R_o - 0.079 \times PIM + 0.14 \times PIA \\
 & - 0.133 \times MIA - 0.0008 \times R_o \times PIM + 0.002 \times R_o \times PIA \\
 & - 0.005 \times R_o \times MIA + 0.0005 \times PIM \times PIA + 0.0003 \times PIM \times MIA \\
 & - 0.0005 \times PIA \times MIA + 0.001 \times R_o^2 + 0.0007 \times PIM^2 \\
 & - 0.002 \times PIA^2 + 0.005 \times MIA^2)^{(1/0.32)} \tag{13.28}
 \end{aligned}$$

**Fig. 13.9** Predicted versus experimental soot

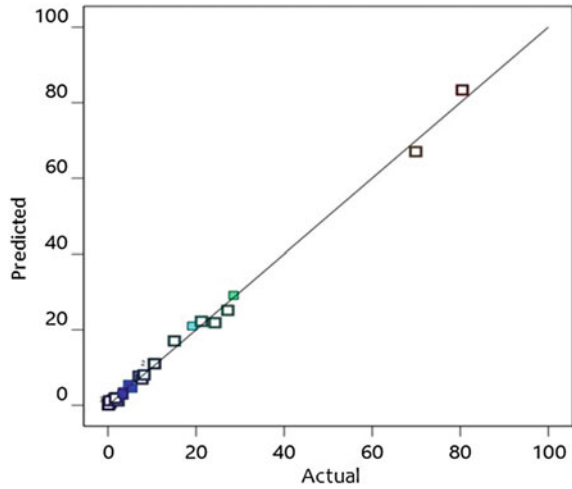
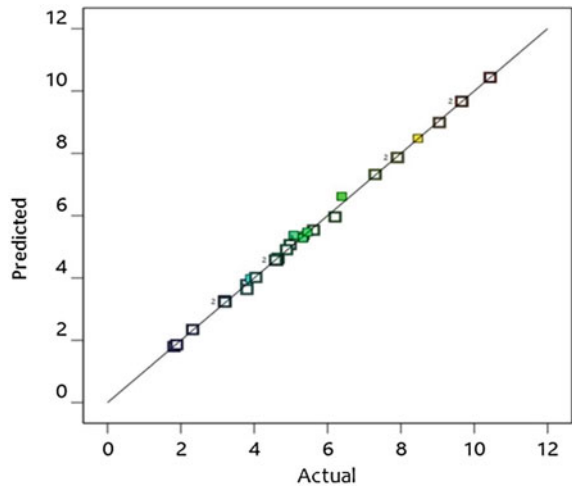


**Fig. 13.10** Predicted versus experimental CO<sub>2</sub>



$$\begin{aligned}
 CO_2 = & (-6.3 + 0.125 \times R_o - 0.002 \times PIM + 0.34 \times PIA - 0.01 \times MIA \\
 & + 0.0012 \times R_o \times PIM + 0.0004 \times R_o \times PIA + 0.003 \times R_o \times MIA \\
 & + 0.0002 \times PIM \times PIA + 0.0003 \times PIM \times MIA \\
 & + 0.0002 \times PIA \times MIA - 0.003 \times R_o^2 - 0.0001 \times PIM^2 \\
 & - 0.004 \times PIA^2 - 0.0009 \times MIA^2)^{(1/0.65)}
 \end{aligned}
 \tag{13.29}$$

**Fig. 13.11** Predicted versus experimental COVIMEP

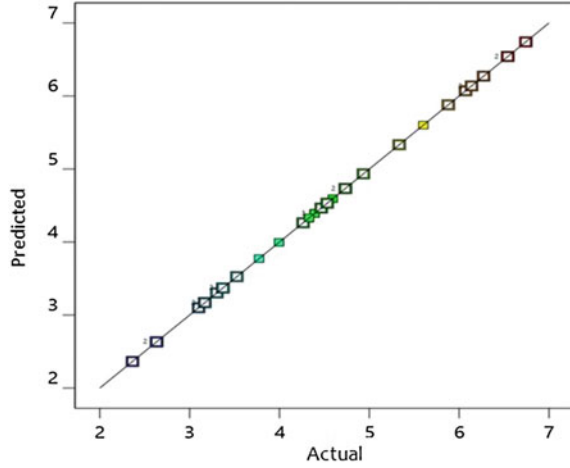
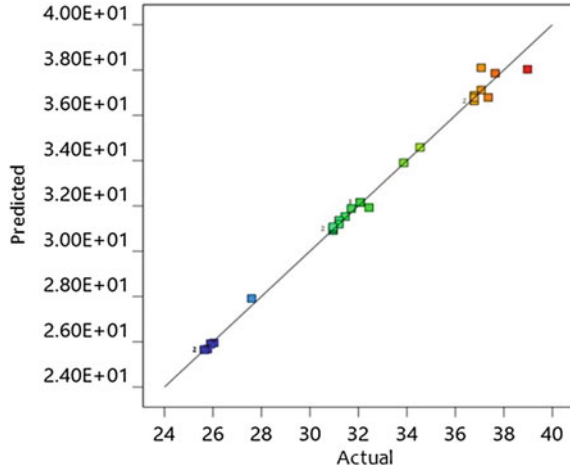


**Fig. 13.12** Predicted versus experimental exergy efficiency



$$\begin{aligned}
 COV_{IMEP} = & 6.98 - 0.22 \times R_o - 07.5 \times 10^{-8} \times PIM + 0.03 \times PIA \\
 & + 0.04 \times MIA + 5 \times 10^{-9} \times R_o \times PIM - 1.23 \times 10^{-8} \\
 & \times R_o \times PIA + 4.87 \times 10^{-9} \times R_o \times MIA - 2.7 \times 10^{-9} \\
 & \times PIM \times PIA + 1.8 \times 10^{-10} \times PIM \times MIA \\
 & - 3.9 \times 10^{-9} \times PIA \times MIA + 0.001 \times R_o^2 + 3.42 \times 10^{-10} \times PIM^2 \\
 & + 2 \times 10^{-7} \times PIA^2 + 2.99 \times 10^{-7} \times MIA^2 \qquad (13.30)
 \end{aligned}$$

$$\begin{aligned}
\text{Exg. eff.} = & 41.92 - 0.42 \times R_o - 3.16 \times 10^{-10} \times PIM - 2.75 \times 10^{-9} \times PIA \\
& - 2.5 \times 10^{-7} \times MIA + 2.42 \times 10^{-12} \times R_o \times PIM - 3.19 \times 10^{-11} \\
& \times R_o \times PIA + 5.15 \times 10^{-11} \times R_o \times MIA + 1.23 \times 10^{-11} \times PIM \times PIA \\
& - 1.44 \times 10^{-11} \times PIM \times MIA + 9.77 \times 10^{-11} \times PIA \times MIA \\
& + 1.79 \times 10^{-6} \times R_o^2 + 9.49 \times 10^{-13} \times PIM^2 + 8.22 \times 10^{-12} \times PIA^2 \\
& + 2.7 \times 10^{-11} \times MIA^2 \tag{13.31}
\end{aligned}$$

### 13.5.3 Model Evaluation

In this study, the metamodelling has been developed for each response variables based on the response surface methodology for emulating the characteristics of the responses for the entire scope of investigation. The prime motive of developing metamodelling in this study is to engage it as the objective function in the optimization iterations. However, the reliability of the developed metamodelling in emulating the behavior of the output variables must be evaluated comprehensively before the deployment in optimization study. Hence, the present study utilizes a set of comprehensive evaluation metric of correlation metrics, absolute and relative error metrics and the uncertainty posed by the metamodelling in predicting the responses considering the pertinences of each metric as deliberated in the previous section (Sect. 3.2) in this study. Subsequently, the analysis of  $\text{NO}_x$  metamodelling reveals the score of  $R^2$  as 0.939 and that of NSCE as 0.911 (Fig. 13.13), while the scores of SMAPE and RRSE were observed as 0.325 and 0.374 respectively (Fig. 13.14). Besides, the evaluation of model robustness under the metric of Theil uncertainty has yielded the subsequent score as 0.251, which demonstrates the greater reliability of the corresponding metamodelling in emulating the  $\text{NO}_x$  trends. Similarly, the assessment of UHC metamodelling demonstrates significant model adequacy owing to the higher scores of  $R^2$  and NSCE as 0.977 and 0.956 respectively (Fig. 13.13). The respective scores of SMAPE and RRSE for the UHC metamodelling were registered as 0.113 and 0.244 (Fig. 13.14), which establishes higher precision in emulating the UHC responses observable at different matrix of decision factors. The Theil uncertainty analysis for the corresponding metamodelling further reveals the greater robustness of the metamodelling in estimating the UHC scores (Fig. 13.15). The subsequent analysis of the soot metamodelling also yielded higher degree of  $R^2$  and NSCE scores of 0.967 and 0.952 respectively (Fig. 13.13). Besides, the SMAPE and RRSE scores of significantly lower level of 0.234 and 0.42 respectively as evident in the figure (Fig. 13.14) indicates the greater competence of the metamodelling in predicting the soot scores. Furthermore, the uncertainty analysis of the corresponding soot metamodelling reveals the superior model reliability on account of the significantly lower scores of Theil uncertainty as evident in Fig. 13.15. The subsequent evaluation of the  $\text{CO}_2$  metamodelling registered

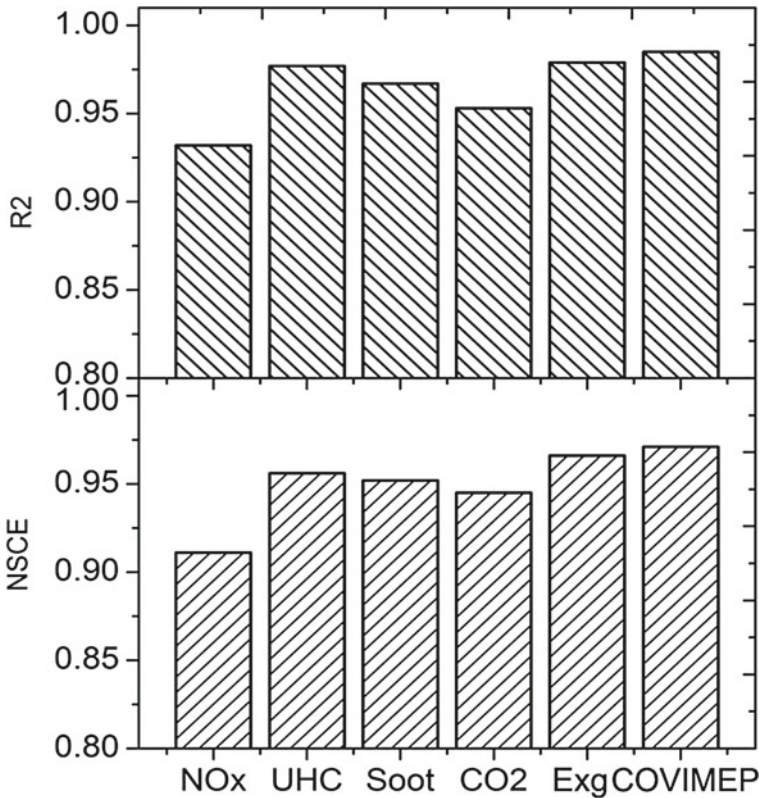


**Fig. 13.13** Correlation metrics for each response models

the scores of  $R^2$  and NSCE as 0.953 and 0.945 (Fig. 13.13) respectively and that of the error metrics of SMAPE and RRSE as 0.255 and 0.269, indicating the superior competency of the metamodel in forecasting the non-linear trends of CO<sub>2</sub> scores. The reliability of CO<sub>2</sub> metamodel was further fortified with the negligible scores of Thiel uncertainty of 0.25 (Fig. 13.15). The scores of  $R^2$  and NSCE observed in the succeeding analysis of the exergy efficiency profile demonstrates the better model adequacy attributing to the lower scores of 0.979 and 0.966 respectively as evident in Fig. 13.13. The lower scores of SMAPE and RRSE as evident in Fig. 13.14 further highlight the superior forecasting capability of the metamodel. The lower footprint of Thiel uncertainty estimated as 0.143 for the metamodel of exergy efficiency as evident in Fig. 13.15 approves the greater reliability in the prediction of respective scores of exergy efficiency. The assessment of the stability profile of COV<sub>IMEP</sub> has revealed the significantly higher scores of  $R^2$  and NSCE as 0.985 and 0.971 respectively (Fig. 13.13). The further evaluation of the COV<sub>IMEP</sub> metamodel against the error metrics of SMAPE and RRSE yielded significantly lower extent of 0.097 and 0.142 respectively, which demonstrates the significant competence of the metamodel

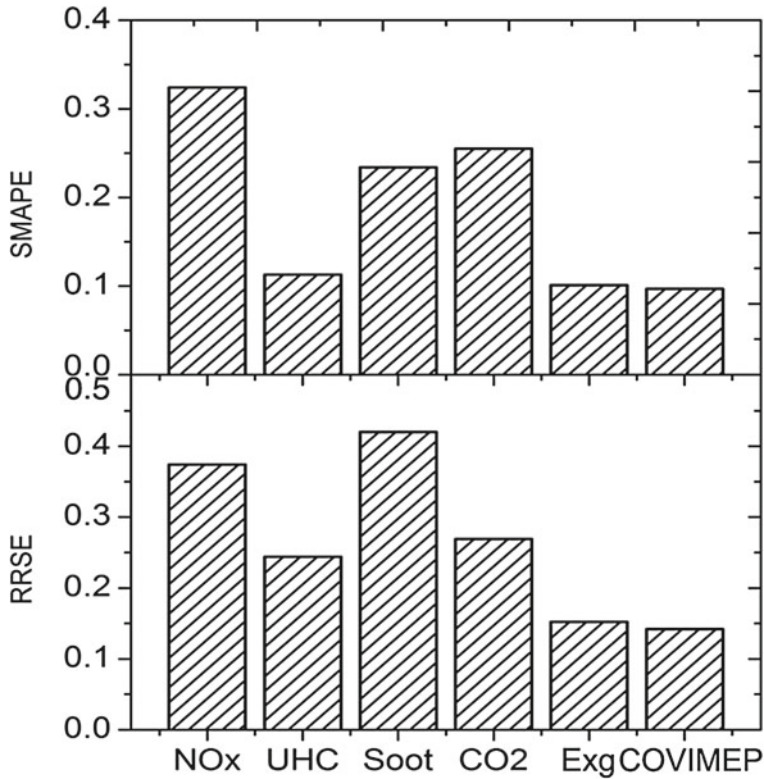


Fig. 13.14 Error metrics for each response models

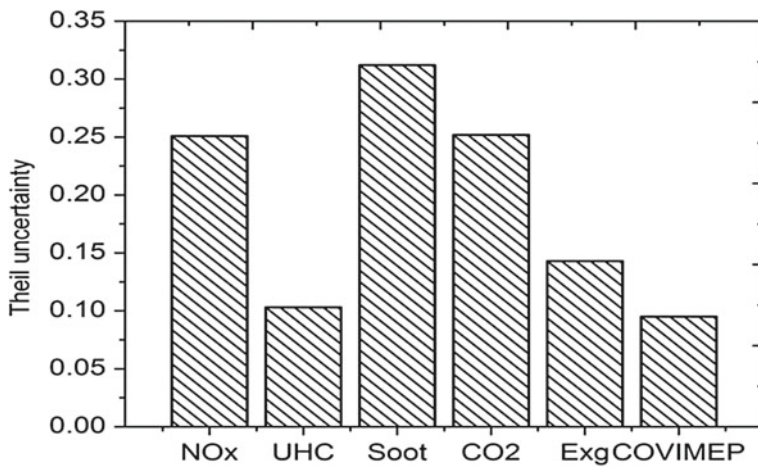


Fig. 13.15 Theil uncertainty for each response models

in emulating the characteristics of  $COV_{IMEP}$  and hence in predicting the respective scores accurately. Besides, the lower scores of Theil uncertainty (Fig. 13.15) observed as 0.095 in the assessment of the metamodel of  $COV_{IMEP}$  confirmed the greater reliability in predicting the scores of stability indicator of  $COV_{IMEP}$ .

### 13.5.4 Optimization Endeavor

#### 13.5.4.1 Effects of Injection Timing on the Operating Range of RCCI Regime

The present study undertakes a multi-objective investigation of the methanol premixed diesel RCCI operation considering the sustainability aspects of such LTC regime along with the obligatory emissions legislatives and the operational stability criteria. In consideration of multiple objectives, the ranges of the tuning parameters may differ for each response entities to satisfy the desired objectives in this study. Besides, the variation of individual tuning parameters changes the entire region of feasible operating zone as depicted in Figs. 13.16[a–d] and 13.17[a–d]. The primary goal of this optimization study is to obtain the maximum exergy efficiency and the operational stability and the minimum emissions under the preset constraints of

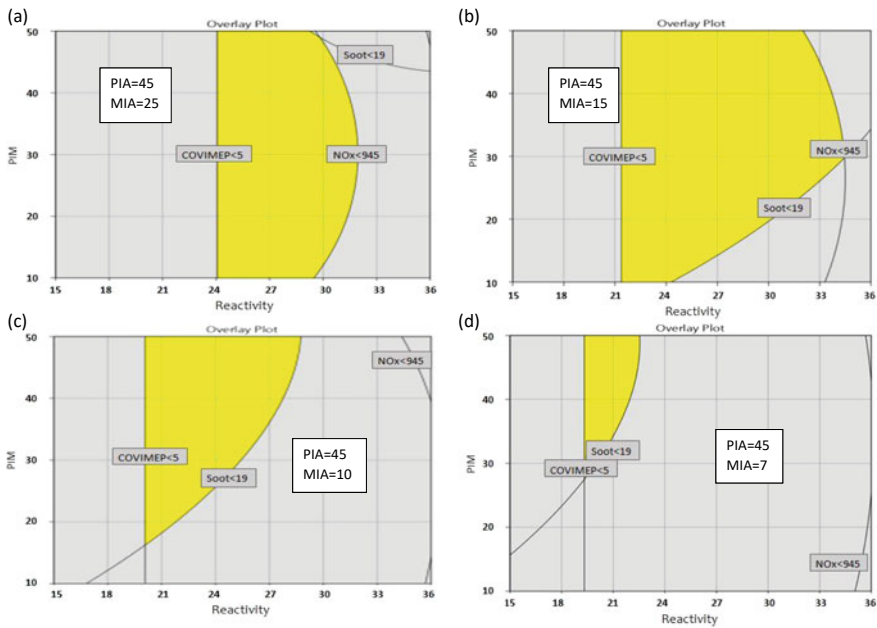


**Fig. 13.16** Effects of main injection timing on feasible operating zone for optimization search routine



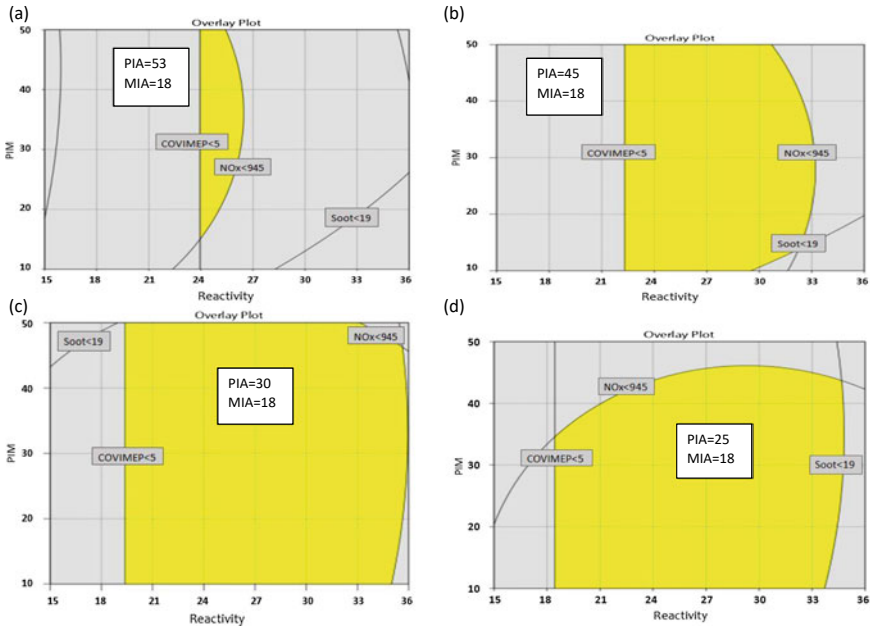


**Fig. 13.17** Effects of pilot injection timing on feasible operating zone for optimization search routine

coefficient of variations and the EPA Tier-4 emission legislations. The larger area of the feasible region of operation enhances the scope of the optimization study by increasing the search space for finding the optimal solution.

Figures 13.16[a–d] and 13.17[a–d] demonstrates the effects of injection timings of PIA and MIA with respect to the overall reactivity and the premixed ratio of diesel fuel on the feasible operating range of RCCI combustion constrained by the emissions mandate and the stability criteria. It is clearly observed in Fig. 13.16 that with the retardation of main injection timing, the stability indicator of  $COV_{IMEP}$  shifts towards the lower overall reactivity, which eventually indicates the potential of using higher methanol participation ratio under the stable operating condition. It is also evident in Fig. 13.16 that the slight retardation of the main injection timing resulted in the extension of the reactivity range; however the constraint of soot emissions allows the utilization of pilot injection mass percentage in the higher extent only. Further retardation of the main injection timing reduces the overall feasible area for the optimization study mainly due to the violation of the soot constraint. Similar trend can be seen in Fig. 13.17, wherein with the retardation of the pilot injection timing, the scope of RCCI operation increases due to the enlargement of the stable region of operation. The medium range of pilot injection timing is observed to be more suitable for achieving a broader feasible operational region as distinctly evident in Fig. 17c. Though, at the extremely retarded point of pilot injection timing, the feasible range is partially diminished due to the defiance of  $NO_x$  constraint, restricting the operation at

higher pilot injection mass percentage of diesel. Thus, it can be observed that during the delayed injection timings of pilot injections, the feasible zone of operation is more sensitive to the  $\text{NO}_x$  constraint, whereas during the retardation of the main injection timings, the feasible operating region is primarily affected by the soot constraint. Besides, both the pilot and main injections are effective in achieving stable operations in its delayed injections allowing further to lower the reactivity within the limits of feasible zone of operation or in other words higher methanol participation ratio can be utilized in the present RCCI domain.

#### 13.5.4.2 Analysis of Desirability Based MCDM Approach

As evident in Table 13.6, the analysis of the strategy S1 reveals that the maximum desirability of the optimization study is 0.8 which is 7.63% higher than that observed in the experimental study, which corresponds to the simultaneous improvements of 23.1%, 92%, 72% and 24.49% for  $\text{NO}_x$ , soot, UHC and  $\text{COV}_{\text{IMEP}}$  compared to the experimental investigation. However, the S1 strategy also incurs the penalties of 135% and 18.5% in  $\text{CO}_2$  and exergy efficiency respectively in this case of optimization study. Furthermore, upon experimental validation of the optimal solution observed in this strategy yielded an imperceptible deviation of 1.8%, 12%, -8.8%, 9.7%, -0.72% and -4.6% for  $\text{NO}_x$ , soot, UHC,  $\text{CO}_2$ , exergy efficiency and  $\text{COV}_{\text{IMEP}}$  respectively from the scores observed in the computational study. Similarly, the subsequent strategy of S2 resulted in the improvement of the highest desirability by 1.8% compared to the experimental counterpart in this case. The analysis revealed the reductions in the scores of  $\text{NO}_x$ , soot, UHC and  $\text{COV}_{\text{IMEP}}$  by 65.8%, 96%, 50% and 27.72% correspondingly, while the deterioration in  $\text{CO}_2$  emissions and exergy efficiency of 24.8% and 26.5% were also observed in this strategy with respect to the results obtained in the experimental investigation. The experimental validation shows strong agreement with the computationally observed results as very small variations are registered in the subsequent analysis. The analysis of Strategy S3 on the other hand registered a reduction by 19.5% in the maximum desirability score compared to the equivalent experimental regime, which corresponds to the improvements of 32.7%, 56%, 25.3% and 17.6% in the corresponding scores of  $\text{NO}_x$ , soot, UHC and  $\text{COV}_{\text{IMEP}}$  and the deterioration in the scores of  $\text{CO}_2$  emissions of 31.4% and exergy efficiency of 14.11% respectively. The experimental validation corresponding to the observed optimal solutions establishes the tremendous reliability of the RSM based optimization study owing to the significantly lower footprint of the corresponding variation of the scores. Similarly, the analysis of S4 strategy revealed a decrement in the desirability score by 0.997% compared to the experimental endeavor, which is due to the significant reduction of exergy efficiency by 27.76%. However, in case of other response elements of  $\text{NO}_x$ , soot, UHC,  $\text{CO}_2$  and  $\text{COV}_{\text{IMEP}}$ , improvements were registered instead as 65.39%, 37.1%, 38.2%, 15.2% and 26% respectively. The experimental validation of the obtained solutions indicates very little variations in

**Table 13.6** Maximum desirability profiles for different categories and their constituents

Category set	Input variables					Output variables					Max. desirability	
	PIA	MIA	R <sub>0</sub>	PIM	NO <sub>x</sub>	Soot	UHC	CO <sub>2</sub>	Exg. eff.	COV <sub>IMEP</sub>	Dmax	
S1-NO <sub>x</sub> (Highest priority)	RSM	35	22.88	32.124	10.115	166	2.5	45	4.697	27.9	3.536	0.8
	Validated	35	23	32	10	163	2.2	49	4.24	28.1	3.7	0.79
	EXP	35	5	17	10	212	28	180	1.8	34.5	4.9	0.734
% deviation of the validated responses from the RSM results for S1 (%)												
% improvement of the optimization results for S1 (%)												
S2-Soot (Highest priority)	RSM	35	21.03	31.6	20.277	165	0.11	73	6.12	28.22	3.535	0.795
	Validated	35	21	32	20	161	0.13	77	6.24	28.57	3.614	0.787
	EXP	42	18	24	23	471	3.5	154	5	38.9	5	0.773
% deviation of the validated responses from the RSM results for S2 (%)												
% improvement of the optimization results for S2 (%)												
S3-Exg eff. (Highest priority)	RSM	35	15.5	24.07	33.34	323	1.77	119	6.48	32.89	4.3	0.64
	Validated	35	15	24	33	317	1.54	115	6.57	33.41	4.12	0.651
	EXP	42	18	24	23	471	3.5	154	5	38.9	5	0.809
% deviation of the validated responses from the RSM results for S3 (%)												
% improvement of the optimization results for S3 (%)												
S4-All equal priority	RSM	35	22.85	32.133	10.156	166.44	2.5	45.2	4.7	27.92	3.533	0.689
	Validated	35	23	32	10	163	2.2	49	4.24	28.1	3.7	0.695
	EXP	42	18	24	23	471	3.5	154	5	38.9	5	0.702
% deviation of the validated responses from the RSM results for S4 (%)												
% improvement of the optimization results for S4 (%)												
											26	0.997

(continued)

**Table 13.6** (continued)

Category set	Input variables				Output variables						Max. desirability	
	PIA	MIA	R <sub>0</sub>	PIM	NO <sub>x</sub>	Soot	UHC	CO <sub>2</sub>	Exg. eff.	COV <sub>IMEP</sub>	Dmax	
S5-NO <sub>x</sub> + soot (Highest priority)	RSM	35	21.02	31.6	20.3	165	0.11	74	6.13	30.22	3.5	0.832
	Validated	35	21	32	20	161	0.13	77	6.24	29.57	3.614	0.821
	EXP	42	12	24	50	167	3.4	152	6.4	31.1	4.3	0.79
% deviation of the validated responses from the RSM results for S5 (%)												
% improvement of the optimization results for S5 (%)												
					2.42	-18	-4.05	-1.79	5.45	-3.26	1.3	
					3.59	96.2	49.3	2.5	2	15.95	-3.92	

the respective scores of the response elements as enumerated in Table 13.6. Furthermore, the analysis of the Pareto solutions of maximum desirability studied under the strategy of S5 yielded the highest score of 0.832 in the entire scope of investigation, which is 3.92% higher than the observed highest desirability in the experimental regime. In this strategy, no significant reductions in  $\text{NO}_x$  and  $\text{CO}_2$  emissions were observed, however the response elements of soot, UHC and  $\text{COV}_{\text{IMEP}}$  demonstrated the respective reductions of 96.2%, 49.3% and 15.95% and yet again in this case also, the exergy efficiency deteriorated slightly by 2% compared to the experimental recourse.

From the above deliberation, the highest desirability has been observed as 0.832 for the strategy S5 compared to the other criterion set in the MCDM technique, in which the highest priority was given to  $\text{NO}_x$  and soot emissions simultaneously. The corresponding solutions for  $\text{NO}_x$ , soot, UHC,  $\text{CO}_2$ , exergy efficiency and  $\text{COV}_{\text{IMEP}}$  were respectively observed as 165 ppm, 0.11  $\text{mg}/\text{m}^3$ , 74 ppm, 6.13%, 28.22% and 3.5%, which have been found as the best compromised solution for the entire scope of investigation. The optimal setting of the control variables for which the above solution is observed, has been noted in the analysis as the pilot injection timing of 35<sup>0</sup> CA, main injection timing of 21<sup>0</sup> CA, reactivity of 32 and pilot mass injection percentage of 20%. The Reactivity of 32 corresponds to the diesel fuel consumption of 0.717 kg/h and methanol fuel consumption of 0.5 kg/h.

### 13.5.4.3 Confirmatory Test and the Uncertainty Analysis

The study further performed a confirmatory test to confirm the prediction capability of the rsm metamodells for each response entities. The test has been performed under 95% confidence interval. In this test, a series of trials are recorded for the responses at the identical combination of setting points and checked whether the average of the measured scores of the sample lies within the prediction interval. If the mean of the recorded scores is within the prediction nodes (lower and higher) of the confirmatory experiment, then the model is confirmed to be reliable in prediction. In this present study, the optimal setting as suggested in the numerical investigation has been considered as the factor setting for the confirmatory test. Table 13.7 encapsulates the lower and higher prediction intervals for each response variables along with

**Table 13.7** Confirmatory test of the optimization results

Responses	Predicted mean	Standard dev.	95% PI low	Data mean	95% PI high
$\text{NO}_x$	164	1.44E-05	161	165	168
UHC	75	0.199	72	74	77
Soot	0.115	0.04	0.08	0.11	0.15
$\text{CO}_2$	6.05	0.13	5.6	6.13	6.5
Exg. eff.	28.53	0.027	27.89	28.22	29.17
$\text{COV}_{\text{IMEP}}$	3.53	3.7E-07	3.48	3.5	3.58

the average of the recorded samples. The observations of Table 13.8 confirms the prediction capability of the rsm metamodels as the average scores for all the response parameters are well within the prediction intervals in this confirmatory test.

The total uncertainty (TU) of the obtained optimal results consists of the uncertainties associated with the experimentation, preparation of design of experiment and the Theil uncertainty (modelling uncertainty) as displayed in Fig. 13.4 and discussed in their respective sections. Root mean square method has been implemented to compute the total uncertainty in this case of study as detailed in Table 13.8. The associated total uncertainties in each response entity have been expressed in the following equations (Eqs. 13.32a–13.32f). Furthermore, it is also pertinent to mention that the total uncertainty associated with the predicted response entities are well within the prediction interval mentioned in Table 13.7.

$$NO_x = 165 \pm (TU\%)_{NO_x} = 165 \pm 0.61\% \quad (13.32a)$$

$$UHC = 74 \pm (TU\%)_{UHC} = 74 \pm 0.54\% \quad (13.32b)$$

$$Soot = 0.11 \pm (TU\%)_{soot} = 0.11 \pm 1.17\% \quad (13.32c)$$

$$CO_2 = 6.13 \pm (TU\%)_{CO_2} = 6.13 \pm 0.6\% \quad (13.32d)$$

$$Exg. \text{ eff.} = 28.22 \pm (TU\%)_{Exg. \text{ eff.}} = 28.22 \pm 1.9\% \quad (1332e)$$

$$COV_{IMEP} = 3.5 \pm (TU\%)_{COV_{IMEP}} = 3.5 \pm 1.13\% \quad (13.32f)$$

### 13.5.5 Discussions

The emissions regulations of EPA Tier 4 have been expressed in terms of NHC and PM, which combine UHC with  $NO_x$  as well as with soot emissions in the respective constraints. The present study on the contrary considers the emission elements of  $NO_x$ , soot and UHC as the individual entity. Due to the involvement of two independent variables in the emissions mandates, it is not possible to estimate the constraints for each individual entity and impose the same. Hence, the present study allows UHC to evolve without constraint to reduce the complexity of the optimization study. Besides, the constraints of NHC and PM are expressed in g/kWh, necessitating the conversion of the unit of individual entities of  $NO_x$ , soot and UHC emissions observed in the optimization study, which has been carried out by following the work of Benajes et al. (2016) as discussed in the previous section (Sect. 13.4.1.1). To this end, the subsequent conversion of  $NO_x$ , soot and UHC scores observed as the best

**Table 13.8** Uncertainty analysis of each response parameters

Responses	$U_{\text{exp}}$ (Uncertainty in experimentation)	$U_{\text{DoE}}$ (Uncertainty in DoE)	$U_{\text{Theil}}$ (Theil uncertainty)	Calculation, $\sqrt{(U_{\text{exp}})^2 + (U_{\text{DoE}})^2 + (U_{\text{Theil}})^2}$	Total uncertainty, (TU) (%)
$\text{NO}_x$	0.2	0.523	0.251	$\sqrt{(0.2)^2 + (0.523)^2 + (0.251)^2}$	0.61
UHC	0.1	0.523	0.103	$\sqrt{(0.1)^2 + (0.523)^2 + (0.103)^2}$	0.54
Soot	1	0.523	0.312	$\sqrt{(1)^2 + (0.523)^2 + (0.312)^2}$	1.17
$\text{CO}_2$	0.15	0.523	0.252	$\sqrt{(0.15)^2 + (0.523)^2 + (0.252)^2}$	0.6
Exg. eff.	1.82	0.523	0.143	$\sqrt{(1.82)^2 + (0.523)^2 + (0.143)^2}$	1.9
$\text{COV}_{\text{IMEP}}$	1	0.523	0.095	$\sqrt{(1)^2 + (0.523)^2 + (0.095)^2}$	1.13

compromised solution in the optimization study and expressing it in NHC and PM (Greeves and Wang 1981) by following the equations (Eqs. 13.33 and 13.34) yielded as 1.73 g/kWh and 0.08 g/kWh respectively, which apparently satisfies the respective constraints of NHC and PM imposed by EPA Tier 4 regulations. Pertinently, the optimized RCCI operation in this study demonstrates 77% and 73.33% lower footprint of NHC and PM compared to the limits specified in the EPA Tier 4 norms as the constraints.

$$NHC = NO_x + UHC \quad (13.33)$$

$$PM = 1.024 \times soot + 0.277 \times UHC \quad (13.34)$$

Furthermore, the emission of CO<sub>2</sub> in the optimal solution was registered as 6.24%, which turned out to be 0.49 kg for per kg of methanol consumption for this particular case of RCCI operation. Thus, it is distinctly evident that for the complete cycle of methanol production to its consumption, the net release of CO<sub>2</sub> emission into the environment is 42.3% negative consequent to the consumption of 0.85 kg of CO<sub>2</sub> during methanol production (Matzen et al. 2015), which displays the potential of such RCCI operation in attaining the goal of carbon negative in the facet of global struggle against the carbon emissions. The conversion of CO<sub>2</sub> from percentage to kg/h has been carried out by following the equations (Eqs. 13.35 and 13.36).

$$CO_2(kg/h) = CO_2(\%) \times \frac{(m_a + m_f) \times 1.517}{1000} \quad (13.35)$$

$$m_f = m_d + m_m \left( \frac{LHV_m}{LHV_d} \right) \quad (13.36)$$

where,  $m_a$  and  $m_f$  are the mass of air and fuel in kg/h respectively, while  $m_d$  and  $m_m$  denotes the mass flow rate of diesel and methanol.

## 13.6 Conclusion

The present study demonstrates a Design of Experiment based multi-objective RSM optimization endeavor to calibrate and achieve the desired objectives set for the response parameters through the precise tuning of the control parameters of the methanol premixed diesel RCCI operation coupled with spilt injection strategy. In this study, an attempt has been made to implement the concept of RCCI operation in the conventional diesel engine by inducting low reactive fuel of methanol through port injection. However, an accurate tuning of the response parameters is pre-requisite to the proper implementation of such LTC operation in a conventional diesel engine



due to the existing non-linearity in the system behavior. The study establishes a technically more correct way of determining the design space for carrying out the necessary experimental investigations. The robustness of the design space was critically evaluated through the comprehensive metrics of D-optimality criteria, G-efficiency, condition number and the standard mean error at 80% of fraction of design space (FDS). The optimization endeavor in this study has been further entrusted with the respective emission mandates of EPA Tier 4, while maintaining or even improving the efficiency of the RCCI operation at the same time, that too under the constraints of stable engine operation. The Pareto solutions to this end, evolved from the RSM optimization search routine delivers the potential trade-off solutions, out of which to determine the best compromised solution, desirability approach has been employed in this multi-criteria decision making endeavor. The optimal setting of the control parameters to this end was observed in this study as the pilot injection timing of  $35^{\circ}$  CA, main injection timing of  $21^{\circ}$  CA, reactivity of 32 and pilot mass injection percentage of 20%, which yielded the scores of the corresponding response parameters of  $\text{NO}_x$ , soot, UHC,  $\text{CO}_2$ , exergy efficiency and  $\text{COV}_{\text{IMEP}}$  as 165 ppm, 0.11  $\text{mg}/\text{m}^3$ , 74 ppm, 6.13%, 28.22% and 3.5%. The best compromised solution observed in this optimization study exhibits the desirability score of 0.832, following the corresponding reductions of  $\text{NO}_x$ , soot, UHC,  $\text{CO}_2$  emissions by 3.59, 96.2, 49.3, 2.5% and the stability improvement of 15.95% indicated by  $\text{COV}_{\text{IMEP}}$ . Besides, in respect to the limits put by the EPA Tier 4 regulations, the present study reveals that while satisfying the limits, the respective scores of NHC and PM displays a significant 77 and 73.33% lower footprint in comparison to the constraints specified in the regulation. Furthermore, as envisaged in the present study, the  $\text{CO}_2$  emission for 1 kg of methanol combustion in this RCCI operation that released into the environment is observed to be 0.49 kg, which is 42.3% less than the amount of  $\text{CO}_2$  consumed in the process of methanol production, which eventually displays the potential benefits of such methanol premixed diesel RCCI operational regime in addressing the carbon emissions crisis. To this end, the present optimization study delivers a platform which can simultaneously address multiple objectives of lower emissions of NHC and PM satisfying the strident emission norms along with lower  $\text{CO}_2$  emission and the higher exergy efficiency under the strict restrictions of stable engine operation. Thus, under the prevailing challenges of global environmental concerns, the energy starved countries like India has the huge opportunity to employ methanol in the conventional diesel engine under the advanced LTC regime of RCCI operation.

Thus, the optimization results showed that the RCCI operation of premixed methanol with diesel under split injection strategy exhibit significant NHC and PM emissions reduction capability while maintaining high exergy efficiency at stable operating conditions. Through the design of experiment based RSM optimization study, the effects of different parameters have been studied under the respective constraints of EPA emission norms and stability markers. However as a future scope of this study, the customized design of experiment based RSM investigation could further be extended to premixed methanol with biodiesel RCCI operation, wherein the potential of biodiesel may be explored under the envelope of LTC regime. A comparative study between the diesel and biodiesel based RCCI operation coupled

with split injection strategy could further be carried out for assessing the relative advantage of the RCCI operation of these two kinds.

## References

- Agarwal AK et al (2019) Methanol and the alternate fuel economy. Springer
- Armstrong JS (1985) Long-range forecasting. Wiley, New York ETC
- Benajes J et al (2016) A RCCI operational limits assessment in a medium duty compression ignition engine using an adapted compression ratio. *Energy Convers Manage* 126:497–508
- Bliemel F (1973) Theil's forecast accuracy coefficient: a clarification. SAGE Publications Sage CA, Los Angeles, CA
- Borkowski JJ, Valeroso ES (2001) Comparison of design optimality criteria of reduced models for response surface designs in the hypercube. *Technometrics* 43(4):468–477
- Bose PK et al (2017) Response surface methodology based multi-objective optimization of the performance-emission profile of a CI engine running on ethanol in blends with diesel. *Biofuels*. Springer, pp 201–228
- Castelli M, Vanneschi L, Silva S (2013) Prediction of high performance concrete strength using genetic programming with geometric semantic genetic operators. *Expert Syst Appl* 40(17):6856–6862
- Chakraborty A, Roy S, Banerjee R (2016) An experimental based ANN approach in mapping performance-emission characteristics of a diesel engine operating in dual-fuel mode with LPG. *J Nat Gas Sci Eng* 28:15–30
- Chen L et al (2017) Sensitivity analysis of fuel types and operational parameters on the particulate matter emissions from an aviation piston engine burning heavy fuels. *Fuel* 202:520–528
- Deb K (2001) Multi-objective optimization using evolutionary algorithms, vol 16. Wiley & Sons
- Dempsey AB, Walker NR, Reitz RD (2013a) Effect of piston bowl geometry on dual fuel reactivity controlled compression ignition (RCCI) in a light-duty engine operated with gasoline/diesel and methanol/diesel. *SAE Int J Engines* 6(1):78–100
- Dempsey AB, Walker NR, Reitz R (2013b) Effect of cetane improvers on gasoline, ethanol, and methanol reactivity and the implications for RCCI combustion. *SAE Int J Fuels Lubr* 6(1):170–187
- Derringer G, Suich R (1980) Simultaneous optimization of several response variables. *J Qual Technol* 12(4):214–219
- Dette H, Wong WK (1995) On G-efficiency calculation for polynomial models. *Ann Stat* 23(6):2081–2101
- Dhole A et al (2014) Mathematical modeling for the performance and emission parameters of dual fuel diesel engine using hydrogen as secondary fuel. *Int J Hydrogen Energy* 39(24):12991–13001
- Dodge LG et al (2003) Humidity and temperature correction factors for  $\text{NO}_x$  emissions from diesel engines. Environ International Corporation
- Ebrahimzade H, Khayati GR, Schaffie M (2018) A novel predictive model for estimation of cobalt leaching from waste Li-ion batteries: application of genetic programming for design. *J Environ Chem Eng*
- Ehrgott M (2012) Vilfredo Pareto and multi-objective optimization. *Doc math*, pp 447–453
- Fang W, Kittelson DB, Northrop WF (2015) Optimization of reactivity-controlled compression ignition combustion fueled with diesel and hydrous ethanol using response surface methodology. *Fuel* 160:446–457
- Ganji PR et al (2017) Parametric study and optimization using RSM of DI diesel engine for lower emissions. *J Braz Soc Mech Sci Eng* 39(3):671–680
- Greeves G, Wang C (1981) Origins of diesel particulate mass emission. *SAE Trans*, pp 1161–1172

- Hariharan N et al (2020) Application of artificial neural network and response surface methodology for predicting and optimizing dual-fuel CI engine characteristics using hydrogen and bio fuel with water injection. *Fuel* 270:117576
- Harrington EC (1965) The desirability function. *Ind Qual Control* 21(10):494–498
- Ileri E, Karaoglan AD, Atmanli A (2013) Response surface methodology based prediction of engine performance and exhaust emissions of a diesel engine fuelled with canola oil methyl ester. *J Renew Sustain Energy* 5(3):033132
- Isermann R, Sinsel S, Schaffnit J (1998) Modeling and real-time simulation of diesel engines for control design. SAE Technical Paper
- Kakati D, Roy S, Banerjee R (2019) Development of an artificial neural network based virtual sensing platform for the simultaneous prediction of emission-performance-stability parameters of a diesel engine operating in dual fuel mode with port injected methanol. *Energy Convers Manage* 184:488–509
- Kakati D, Biswas S, Banerjee R (2021) Parametric sensitivity analysis of split injection coupled varying methanol induced reactivity strategies on the exergy efficiency enhancement and emission reductions objectives in a biodiesel fuelled CI engine. *Energy* 225:120204
- Khodadadi Sadabadi K et al (2016) Modeling of combustion phasing of a reactivity-controlled compression ignition engine for control applications. *Int J Engine Res* 17(4):421–435
- Kim KJ, Lin DK (2000) Simultaneous optimization of mechanical properties of steel by maximizing exponential desirability functions. *J Roy Stat Soc: Ser C (appl Stat)* 49(3):311–325
- Kim K, Kim H, Lee K (2012) Novel strategies and optimization techniques to reduce harmful diesel engine emissions. *Environ Eng Sci* 29(5):335–342
- Klos DT, Kokjohn SL (2016) Investigation of the effect of injection and control strategies on combustion instability in reactivity-controlled compression ignition engines. *J Eng Gas Turb Power* 138(1)
- Krishnamoorthi M, Malayalamurthi R, Shameer PM (2018) RSM based optimization of performance and emission characteristics of DI compression ignition engine fuelled with diesel/aegle marmelos oil/diethyl ether blends at varying compression ratio, injection pressure and injection timing. *Fuel* 221:283–297
- Kumar BR et al (2016) Combined effect of injection timing and exhaust gas recirculation (EGR) on performance and emissions of a DI diesel engine fuelled with next-generation advanced biofuel–diesel blends using response surface methodology. *Energy Convers Manage* 123:470–486
- Lee T, Reitz RD (2003) Response surface method optimization of a high-speed direct-injection diesel engine equipped with a common rail injection system. *J Eng Gas Turbines Power* 125(2):541–546
- Li Y et al (2013) Numerical study on the combustion and emission characteristics of a methanol/diesel reactivity controlled compression ignition (RCCI) engine. *Appl Energy* 106:184–197
- Li Y et al (2014) Parametric study and optimization of a RCCI (reactivity controlled compression ignition) engine fueled with methanol and diesel. *Energy* 65:319–332
- Liang X et al (2021) Application of response surface methodology for the joint optimization of performance and emission characteristics of a diesel engine. *Int J Green Energy* 18(7):697–707
- Lucas JM (1976) Which response surface design is best: a performance comparison of several types of quadratic response surface designs in symmetric regions. *Technometrics* 18(4):411–417
- Matzen MJ, Alhajji MH, Demirel Y (2015) Technoeconomics and sustainability of renewable methanol and ammonia productions using wind power-based hydrogen
- Maurya RK (2017) Characteristics and control of low temperature combustion engines: employing gasoline, ethanol and methanol. Springer
- Mohan B et al (2014) Optimization of biodiesel fueled engine to meet emission standards through varying nozzle opening pressure and static injection timing. *Appl Energy* 130:450–457
- Morsy M, El-Leathy A, Hepbasli A (2015) An experimental study on the performance and emission assessment of a hydrogen/diesel fueled engine. *Energy Sour Part A Recov Utilization Environ Effects* 37(3):254–264

- National Policy on Biofuels (2018) Government of India Ministry of Petroleum & Natural Gas, 16 May 2018 3:27PM by PIB Delhi
- Odu G, Charles-Owaba O (2013) Review of multi-criteria optimization methods—theory and applications. *IOSR J Eng (IOSRJEN)* 3(10):1–14
- Oszyczka A (1985) Multicriteria optimization for engineering design. *Design optimization*. Elsevier, pp 193–227
- Palit D, Malhotra R, Mande S (2017) Enhancing viability of biofuel-based decentralized power projects for rural electrification in India. *Environ Dev Sustain* 19(1):263–283
- Pandian M, Sivapirakasam S, Udayakumar M (2011) Investigation on the effect of injection system parameters on performance and emission characteristics of a twin cylinder compression ignition direct injection engine fuelled with pongamia biodiesel–diesel blend using response surface methodology. *Appl Energy* 88(8):2663–2676
- Pareto V, *Politique CDE* (1896) vol. I and II, F. Rouge, Lausanne
- Reitz RD, Duraisamy G (2015) Review of high efficiency and clean reactivity controlled compression ignition (RCCI) combustion in internal combustion engines. *Prog Energy Combust Sci* 46:12–71
- Ricaud J, Lavoisier F (2004) Optimizing the multiple injection settings on an HSDI diesel engine. *Thermo-and fluid dynamic processes in diesel engines 2*. Springer, pp 199–234
- Shirmeshan A et al (2016) Response surface methodology (RSM) based optimization of biodiesel–diesel blends and investigation of their effects on diesel engine operating conditions and emission characteristics. *Environ Eng Manage J (EEMJ)* 15(12)
- Subramani S, Govindasamy R, Rao GLN (2020) Predictive correlations for NO<sub>x</sub> and smoke emission of DI CI engine fuelled with diesel–biodiesel–higher alcohol blends–response surface methodology approach. *Fuel* 269:117304
- Udayakumar R, Sundaram S, Sivakumar K (2004) Engine performance and exhaust characteristics of dual fuel operation in DI diesel engine with methanol. *SAE Technical Paper*
- Uslu S (2020) Optimization of diesel engine operating parameters fueled with palm oil–diesel blend: Comparative evaluation between response surface methodology (RSM) and artificial neural network (ANN). *Fuel* 276:117990
- Valera H, Agarwal AK (2019) Methanol as an alternative fuel for diesel engines. *Methanol and the alternate fuel economy*. Springer, pp 9–33
- Wang Y et al (2015) Study on cycle-by-cycle variations in a diesel engine with dimethyl ether as port premixing fuel. *Appl Energy* 143:58–70
- Wei L et al (2016) Effects of methanol to diesel ratio and diesel injection timing on combustion, performance and emissions of a methanol port premixed diesel engine. *Energy* 95:223–232
- Yasin MHM et al (2017) Cylinder pressure cyclic variations in a diesel engine operating with biodiesel–alcohol blends. *Energy Procedia* 142:303–308
- Yassin MA, Alazba AA, Mattar MA (2016) Artificial neural networks versus gene expression programming for estimating reference evapotranspiration in arid climate. *Agric Water Manag* 163:110–124
- Ye JJ, Zhou J (2013) Minimizing the condition number to construct design points for polynomial regression models. *SIAM J Optim* 23(1):666–686
- Zahran A, Anderson-Cook CM, Myers RH (2018) Fraction of Design Space to Assess Prediction Capability of Response Surface Designs. *J Qual Technol* 35(4):377–386
- Zou X et al (2016) Numerical study of the RCCI combustion processes fuelled with methanol, ethanol, n-butanol and diesel. In: *SAE Technical Paper Series*

# Chapter 14

## Scope and Limitations of Ammonia as Transport Fuel



Aaishi Ashirbad and Avinash Kumar Agarwal 

**Abstract** Fuel requirement for the transport sector is a function of population growth. Currently, the automotive industry is powered extensively by fossil fuels. Diesel and gasoline-powered vehicles contribute heavily to environmental pollution by emitting carbon dioxides (CO<sub>2</sub>) and other pollutant species. Greenhouse gas (GHG) emissions from fossil fuel combustion are significantly increasing since 1900. Fossil fuels depletion depends on discoveries of new petroleum reserves; however, the use of fossil fuels won't be feasible in the foreseeable future due to GHG emissions and other environmental concerns. To tackle these, several researchers have focused on developing alternative fuels. Although low carbon fuels (energy) are being explored for internal combustion engines (ICEs), nitrogen-based fuels are also beginning to attract researchers worldwide. Ammonia has potential as a low carbon fuel since it has a high-octane number and is carbon-free; therefore, it doesn't produce soot. Other nitrogen-based fuels are not viable low GHG alternatives for vehicles. Despite higher NO<sub>x</sub> emissions, ammonia has potential for heavy-duty power generation and the marine sector. This is because, in these applications, the implementation of exhaust gas after-treatment is feasible. Significant challenges that hinder ammonia's growth in the automotive sector as fuel are (i) narrow flammability limits, (ii) high ignition temperature, and (iii) low flame speed. Also, ammonia's higher heat of vaporization reduces the temperature when ammonia makes a phase transition from liquid to gas, reducing the in-cylinder temperature. Currently, vehicles are not operated using ammonia as fuel because its production involves extensive use of natural gas, which is not a zero-carbon fuel. Biogas is a sustainable carbon-free feedstock for producing ammonia, which uses a carbon-free path from well-to-tank (WTT). Ammonia can be produced from hydrogen, obtained from electrolysis of water and nitrogen obtained from air. Since, the electricity could be generated from renewable energy sources, ammonia can be considered as E-fuel. This chapter covers production methods, properties, environmental and health aspects, storage and transportation, and the potential of ammonia as a transport fuel in compression-ignition

---

A. Ashirbad · A. K. Agarwal (✉)  
Engine Research Laboratory, Department of Mechanical Engineering,  
Indian Institute of Technology Kanpur, Kanpur 208016, India  
e-mail: [akag@iitk.ac.in](mailto:akag@iitk.ac.in)

(CI) and spark-ignition (SI) engines. Pure Ammonia operation and dual-fuel modes are extensively discussed for both CI and SI engines. Hydrogen as a combustion improver is also covered towards the end of this chapter. However, for realizing the potential of ammonia as fuel, it is important to determine feasible Ammonia induction and combustion techniques applicable to ICEs, which would enhance engine performance in the entire operating range.

**Keywords** High octane number · Nitrogen-based fuels · Ammonia · Carbon-free fuel · Alternative fuels

## Abbreviations

AlN	Aluminum Nitride
ASU	Air Separation Unit
aTDC	After Top Dead Center
BSFC	Brake Specific Fuel Consumption
bTDC	Before Top Dead Center
BTE	Brake Thermal Efficiency
CFR	Cooperative Fuel Research
CI	Compression Ignition
CO	Carbon Monoxide
CO <sub>2</sub>	Carbon Dioxide
COV	Coefficient of Variation
DME	Dimethyl Ether
GHG	Greenhouse Gas
HAER	Hydrogen-Ammonia Energy Ratio
HC	Hydrocarbons
HCCI	Homogenous Charge Compression Ignition
HRR	Heat Release Rate
ICE	Internal Combustion Engine
IMEP	Indicated Mean Effective Pressure
LTC	Low Temperature Combustion
MBT	Maximum Brake Torque
NH <sub>3</sub>	Ammonia
NO <sub>x</sub>	Oxides of Nitrogen
ON	Octane Number
PM	Particulate Matter
RPM	Revolutions Per Minute
SCR	Selective Catalytic Reduction
SI	Spark Ignition
SMR	Steam Methane Reforming

SoI	Start of Injection
SSAS	Solid State Ammonia Synthesis
TDC	Top Dead Center
WOT	Wide Open Throttle

## 14.1 Introduction

Fossil fuels have emerged as the most suitable transport fuels because of their easier availability, ease of transportation, and high energy density. Globally, over 100 million barrels of petroleum products are used every day (<https://www.eia.gov/energyexplained/oil-and-petroleum-products/use-of-oil.php>), and their consumption is increasing day by day. However, the burning of fossil fuels contributes significantly to global warming because of the emission of CO<sub>2</sub>. Overall, CO<sub>2</sub> emissions have increased by ~90% since 1970, with the consumption of fossil fuels and industrial processes contributing ~78% of total greenhouse gas (GHG) emissions (<https://www.epa.gov/ghgemissions/global-greenhouse-gas-emissions-data>). There has been a significant increase (~70%) in global CO<sub>2</sub> emissions from 1990 to 2020 in the automotive sector due to the extensive use of fossil fuels (Fig. 14.1). The CO<sub>2</sub> emissions in the transport sector are estimated to increase by ~21% from 2020 to 2030.

The rise in GHG from the automotive industry has provoked many countries to put emission restrictions in place. President of the United States, Barack Obama, had set an upper limit on the CO<sub>2</sub> emission levels from vehicles as ~80 g/km for 2025 and 60 g/km for 2030 (<https://www.euractiv.com/section/transport/news/eu-gears-up-co2-car-targets-for-2025-2030/>).

Figure 14.2 shows how the earth's average temperature has increased in the past 170 years, starting the industrial revolution in 1850. The upper and lower curves represent the confidence intervals, whereas the middle red curve denotes the average annual earth temperature. There is a sharp increase of ~0.7 °C above the reference baseline (1961–1990). CO<sub>2</sub> and other GHG emissions are the primary drivers of such a temperature rise. Though a temperature rise of ~1 °C seems insignificant, it severely impacts climate change.

There are two possible ways to control the GHG emissions from transport, (a) electrification using carbon-free primary energy and (b) carbon-free alternative fuels. Although electrification reduces CO<sub>2</sub> emissions, most electricity is generated from non-renewable sources, indirectly contributing to CO<sub>2</sub> emissions. This leads to developing new alternative fuels to reduce our dependence on fossil fuels and reduce transport costs by their localized production from carbon-free primary energy. This is because the primary concern today is the CO<sub>2</sub> being emitted into the atmosphere. Several researchers investigated carbon-free alternative fuels, which can be handled without significant modifications in the current infrastructure and ICE design. This led to the idea of exploring alternative fuels in the natural nitrogen cycle instead of

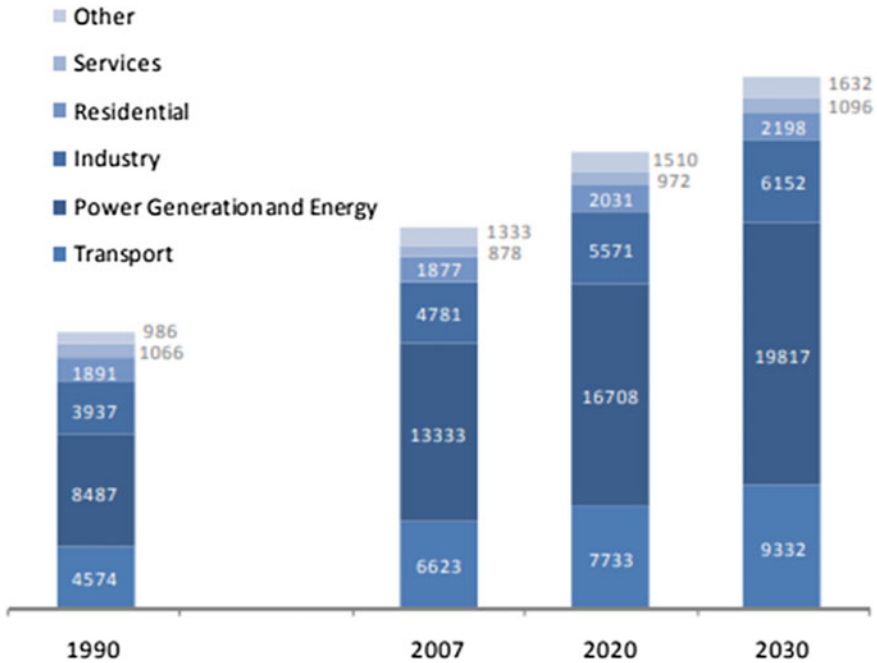


**Fig. 14.1** Estimated CO<sub>2</sub> emissions worldwide (In Million Metric Tons, MMT) (<https://iea.blob.core.windows.net/assets/ac80b701-bdfc-48cf-ac4c-00e60e1246a0/weo2009.pdf>)

the carbon cycle. Ammonia is a carbon-free fuel and has high hydrogen to nitrogen ratio. Anhydrous Ammonia can be pressurized to 10 bar and stored as a liquid at room temperature (Xiang 2004). Liquid ammonia has a volumetric energy density (22.5 MJ/kg), somewhat lower than methanol (22.7 MJ/kg) and DME (31.7 MJ/kg). The cost per unit of energy of conventionally produced ammonia is 9.9 US\$/GJ, significantly lower than 21.8 US\$/GJ of gasoline (Zamfirescu and Dincer 2009).

Furthermore, ammonia is widely used in applications such as the production of fertilizer, explosives, etc. Therefore, the methods of Ammonia production and distribution are already well established worldwide (Avery 1988). During the 1960s, the US Army implemented the ‘Energy Depot Concept’ scheme to incorporate fuel transportation issues for military purposes, and they explored ammonia as a fuel in combustion engines (Rosenthal 1965; Grimes 1965). The primary objective was safe handling of fuel supply to distant areas instead of discovering an alternate fuel for better and clean combustion. Recently, there has been an inclination towards exploring ammonia as a clean ICE fuel. The studies mainly include theoretical forecasts and experimental tests related to ammonia as fuel in CI and SI engines. The research results have shown the possibility of using ammonia as a fuel in ICE with minor modifications in the fuel injection system. However, comprehensive testing and analysis are essential to improve engine efficiency, operability, and NO<sub>x</sub> emissions.



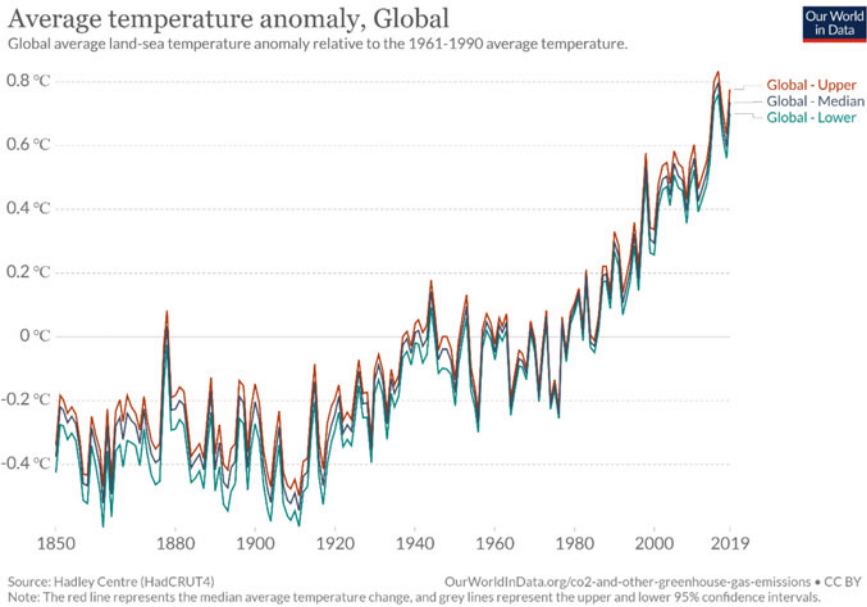


**Fig. 14.2** Earth's average temperature relative to 1961–90 average temperature (<https://ourworldindata.org/co2-and-other-greenhouse-gas-emissions>)

This chapter focuses on various production methods of ammonia, its effect on health and the environment, storage and transportation infrastructure requirements, and extensive exploratory studies in ICE.

## 14.2 Production Routes

### 14.2.1 Haber–Bosch Method

The main route for Ammonia synthesis is the Haber–Bosch process, where iron oxide acts as a catalyst combining reactants, hydrogen, and nitrogen. The operating temperature of the catalytic converter in the process is in the range of 380–500 °C (Bartels 2008).

A schematic of the Haber–Bosch method is shown in Fig. 14.3. It works by fixing nitrogen from the ambient air with hydrogen from the natural gas to produce ammonia. A high-pressure environment is required to overcome strong triple bonds of nitrogen. In this synthesis, natural gas acts as a hydrogen source and fuel.

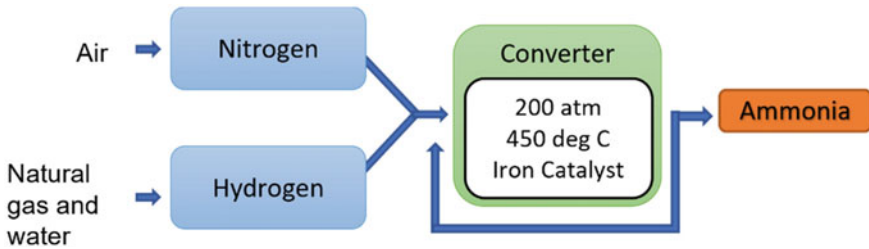


Fig. 14.3 Schematic of Haber–Bosch Method

### 14.2.2 Methods for Producing Hydrogen

Alternative methods for producing ammonia need to be found to attain a carbon-free Well-to-Wheel process. Some of these methods are discussed below. Figure 14.4 shows a general process flow diagram of different alternative methods.

#### 14.2.2.1 Steam Methane Reforming (SMR)

In Steam Methane Reforming (SMR), methane in the natural gas is heated with steam, and a catalyst is used to produce hydrogen, which is then used in the Haber–Bosch method to produce ammonia.

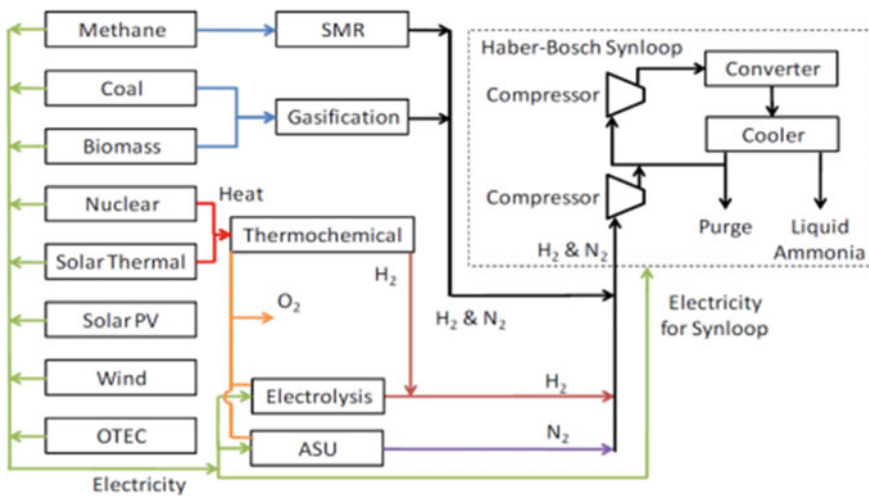
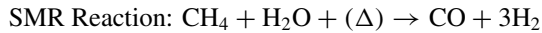


Fig. 14.4 Various ways of executing energy sources with Haber–Bosch synthesis (Bartels 2008)

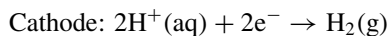
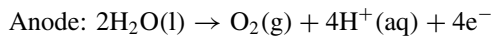


#### 14.2.2.2 Thermochemical Process

Thermochemical splitting of water to produce hydrogen require high temperature heat (500–2000 °C). Concentrated solar energy on reactors or waste heat from nuclear reactors are used to achieve this high temperature for producing hydrogen. Then hydrogen is used along with nitrogen in the Haber–Bosch method to produce ammonia (<https://www.energy.gov/eere/fuelcells/hydrogen-production-the-thermochemical-water-splitting>).

#### 14.2.2.3 Electrolysis

Ammonia synthesized from water as the sole hydrogen source can be reasonable when employing electrolysis. Electricity can be obtained from renewable sources or by burning fossil fuels. The hydrogen produced by the electrolysis can be used in the Haber–Bosch method (Bartels 2008). At anode, oxidation occurs producing O<sub>2</sub> and electrons whereas at cathode, reduction takes place providing electrons to hydrogen cations to form hydrogen gas.



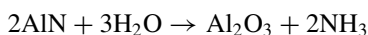
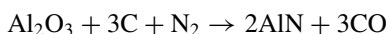
#### 14.2.2.4 Air Separation Unit

Air Separation Unit (ASU) is a popular process used to separate major constituents of atmospheric air. It is based on different physical properties (molecule sizes, diffusion rates, adsorption preference, boiling temperature etc.) of air constituents. It uses an electricity source for electrolysis that provides nitrogen and hydrogen to the Haber–Bosch Ammonia synthesis loop.

### 14.2.3 Alternative Methods

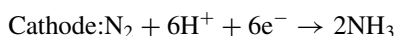
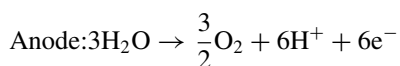
#### 14.2.3.1 Two-Step Al<sub>2</sub>O<sub>3</sub>/AlN Thermochemical Process

A novel cyclic process is demonstrated to produce ammonia in two stages. In the first endothermic stage, alumina is reduced to aluminum nitride (AlN) by carbon in a dense nitrogen atmosphere. In the second step, AlN is hydrolyzed to form Ammonia and Al<sub>2</sub>O<sub>3</sub>. The Al<sub>2</sub>O<sub>3</sub> can be used again in the first step, and the CO produced can be used for producing methanol. It is essential to use a carbon-free source for the reduction of Al<sub>2</sub>O<sub>3</sub> to AlN and CO to obtain a carbon-less source of methanol production.



#### 14.2.3.2 Solid State Ammonia Synthesis (SSAS)

In SSAS, water is decomposed at the anode, and hydrogen atoms adsorb the stripped-off electrons. Hydrogen operates through the proton-conducting ceramic electrolyte. At the cathode, the protons originate, regain electrons, and react with adsorbed (or dissociated) nitrogen atoms to form NH<sub>3</sub>. This process requires nitrogen, electricity, and water to produce ammonia. SSAS is adaptable to renewable sources. It consumes 7–8 MWh per ton of NH<sub>3</sub> production. In comparison, the Electrolysis and Haber–Bosch processes consume 12 MWh per ton of NH<sub>3</sub> production (Bartels 2008).



## 14.3 Physical and Chemical Properties of Ammonia

Dry ammonia is a colorless and flammable gas. It has a pungent smell and is lighter than air. It is soluble in water but ionizes partially in water to form weak alkali. Since it is alkaline, it can undergo neutralization with acids to form salts. Ammonia solution can react with metal ions to form metal hydroxide precipitate (<https://pubchem.ncbi.nlm.nih.gov/compound/Ammonia>; Busby et al. 1976). It is highly stable and decomposes in the presence of heated catalysts or electrical discharge. Therefore,

**Table 14.1** Comparison of fuel properties of Ammonia with diesel and gasoline (Hodgson 1973; <https://www.euratex.co.uk/110411020.pdf>; Mørch et al. 2011; Tillner-Roth and Baehr 1993)

Fuel/Properties	Gasoline	Diesel	Ammonia
Energy content (LHV) (MJ/kg)	44.34	44.11	18.6
Density (kg/m <sup>3</sup> )	697.6	745.7	626
Research octane number (RON)	100	<20	>130
Cetane Number	0–5	45–55	–
Flammability-limits (vol/%)	0.95–6	0.43–0.6	15–28
Flash point (°C)	–42.7	73.8	–33.4
Autoignition temperature (°C)	300	230	651
Flame velocity (m/s)	0.41	0.80	0.067
Minimum Ignition energy (mJ)	0.8	0.23	680

it is combustible in the air. Nitric oxide is obtained when the Ammonia-air mixture is passed over the platinum–rhodium catalyst at 800 °C (Busby et al. 1976). Ammonia readily donates one pair of electrons to other molecules. Hence, it is a strong Lewis base. On the other hand, due to OH<sup>−</sup> ions, the aqueous solution of ammonia acts as a weak base (Table 14.1).

Ammonia has lower energy content than conventional fuels, namely diesel, and gasoline. It has a lower cetane number and flame velocity, making it challenging to adapt as fuel in ICES.

## 14.4 Effect on the Health and Environment

According to the world health organization (WHO), continuous exposure to ~25 ppm of ammonia in the air does not affect the Ammonia levels in human blood. But exposure to ~400 ppm of ammonia irritates the throat, nose, and eyes (<https://www.tfi.org/sites/default/files/documents/HealthAmmoniaFINAL.pdf>). Ammonia is always present in the human body, and there are no long-term health effects from inhaling air with a low Ammonia level. However, ammonia is dangerous if inhaled above the maximum acceptable level. Ammonia may cause lung injury, and the liquefied ammonia can cause frostbite and damage to the eyes and skin. People who are hyperreactive to respiratory nuisances or asthmatic are more prone to issues with high Ammonia levels (Table 14.2).

Ammonia negatively affects biodiversity (<https://www.rand.org/randeurope/research/projects/impact-ofAmmonia-emissions-on-biodiversity.html>). Some of the major effects of excess ammonia are toxic damaging of leaves, altering the vulnerability of plants to pathogens, drought and frost. Accumulation of excess nitrogen has a significant effect on plant species diversity and composition. In addition, the Haber Bosch process leads to eutrophication, which promotes abnormal growth of algae that covers the water surface, preventing sunlight. As a result, it leads to biodiversity

**Table 14.2** exposure guidance according to the National Fire Protection Association (Valera-Medina et al. 2018)

Effect	Ammonia in air (by volume) (ppm)
Readily detectable odor	20–50
No harm on health over long exposure	50–100
Severe irritation to eyes, nose and throats	400–700
Dangerous, half-hour exposure may be severe	2000–3000
Serious edema, strangulation, asphyxia, rapidly fatal	5000–10,000

loss because submerged species cannot get enough sunlight for the photosynthesis process. Also, Ammonia production consumes a significant fraction of natural gas produced. Vapours of ammonia are harmful to swine, dairy and poultry livestock. Also ammonia vapours react with air moisture to form ammonium and ultimately return to ground in rainfall. Ammonium combine with negative soil clays and organic matter which otherwise cause the accumulation of contaminants.

## 14.5 Storage and Transportation

Even if all ammonia in a factory is used up to control the interruptions in operation, it is common to have storage facilities for at least 15 days. Hence large Ammonia storage would be required for Industrial installations if operated on ammonia. Pressurized storage and semi-refrigerated storage are cost-effective for up to 2000 tons. The spherical semi-refrigerated tanks can be used for higher-pressure storage and cylindrical tanks with hemispherical ends for the lower pressure storage of ammonia. There are two types of Ammonia storage tanks. The first is a double-wall construction, kept at a slightly higher pressure than the atmosphere and filled with perlite insulation with dry air, nitrogen, or inert gas. The second is a single-wall construction with foam glass insulation. The maintenance costs are usually low for a double-wall tank, even though its upfront cost is higher than the single-wall tank (Hignett 1985). On the basis of different withstandable pressures, storage tanks are classified as pressurized (unrefrigerated), storage spheres and fully-refrigerated storage tanks. Unrefrigerated pressurized tanks operate at ambient temperature and can withstand pressure upto 18.25 bar. Storage sphere tanks operates from  $-1$  to  $+2$  °C and can withstand pressure in the range of 3.8–5.15 bar. Fully-refrigerated ones operate at  $-33$  °C and are designed for pressure of 1.117 bar. Pressurized tanks can store upto 270 t, storage spheres from 450 to 2750 t and fully refrigerated ones upto 45,000 t (Nielsen 1995).

Ships with well-covered tanks maintained over atmosphere pressure and temperature  $\sim 33$  °C are commonly used for overseas transportation of ammonia (Hignett 1985). The ships have cooling facilities, similar to a storage facility. For transportation of anhydrous ammonia, pipelines connected from manufacturing plants to the marine terminals for factories producing finished manure are used. There are

three major pipelines for ammonia transportation worldwide. One of these has a capacity to deliver 8000 t per day. Generally, rail transportation is preferred over pipeline transportation for shorter distances. Transportation of anhydrous Ammonia through trucks is the most expensive method. Therefore, it is used mainly for nearer locations (<150 km). Overall, transport of ammonia through pipeline appears to be considerably cheaper than rail, while truck transport is the most expensive. However, many distribution locations can be accessed by truck rather than the railroad. Ammonia transportation through the railroad is preferred over pipelines or waterways in most developed countries (Hignett 1985). Ships are required for transportation of ammonia and hydrogen as a part of upcoming FuelEU Maritime initiative (<https://www.offshore-energy.biz/industry-groups-tell-eu-to-incentivize-green-hydrogen-and-ammonia-as-fuels-of-the-future/>).

## 14.6 Ammonia for Compression Ignition Engines

### 14.6.1 Pure Ammonia as Primary Fuel

Pearsall et al. (1967) studied direct injection of ammonia in a Vee-Twin engine. According to this study, a compression ratio of 35:1 was required for the combustion of ammonia. However, combustion did not happen even at a high compression ratio of 30:1. Regular glow plugs failed to initiate Ammonia combustion. Hence, high-temperature glow coils were used, which were found suitable. Starkman et al. (1967) experimented with pure ammonia and diesel in a 606 cc Waukesha CFR engine. CR of the engine was varied from 10:1 to 34:1 by altering the plug movement back and forth in the ante-chamber. The engine was controlled such that it could easily switch to either diesel or ammonia without an interruption. They confirmed that Ammonia combustion was possible in a CI engine at a nominal CR using spark plugs. This was because of the high ignition temperature and high vaporization heat of ammonia. Persall et al. (1967a) observed no combustion despite solving the vaporization issues of ammonia by installing a heat exchanger and modifying the fuel injection system. When liquid ammonia was direct-injected with port-injected gaseous ammonia, combustion sustained up to 1200 rpm; however, the engine could not self-sustain at the engine speeds beyond 1200 rpm (Pearsall 1967a). There are limited studies available in the open literature on pure Ammonia operation because fuel properties are unsuitable for the CI engines. Hence, pure ammonia is challenging to implement due to high CR requirements.

### ***14.6.2 Port Injection of Ammonia Vapours with Diesel as Primary Fuel***

Retier and Kong (2010) introduced vapor Ammonia into the engine intake port with diesel as the primary direct-injected fuel to initiate combustion. Due to ammonia's high resistance to autoignition, the dual-fuel approach was investigated in this study. The study shows experimental results for constant Ammonia flow rates, where diesel fueling was adjusted to achieve desirable load.

The main objective was to determine ammonia's contribution to the engine output (torque) at a constant speed of 1400 rpm. Results showed continuous improvement in torque due to Ammonia combustion. At 20% engine load, diesel fueling rate was low, and ammonia replaced nearly half of the total energy. This study demonstrated that ammonia could be implemented in CI engines without significant changes in the existing design.

Experiments were performed for Ammonia implementation to compensate diesel energy to achieve peak torque regardless of diesel fuel flow rate (Reiter and Kong 2010). The engine only produced a certain fraction of peak torque by diesel fuel flow in the experiments. For a particular load on diesel, the Ammonia flow rate was monitored to generate the same torque (280 ft-lb) as 100% diesel. During the experiment (Reiter and Kong 2010), engine loads of 20, 40, 60, 80, and 100% were monitored by adjusting the diesel fuel flow rates. Engine torque constantly increased with increasing Ammonia flow rate. For a constant engine torque, at low diesel fueling, the Ammonia requirement was large, and there was a reduction in engine torque due to inadequate Ammonia supply. The engine setup could use higher energy content of nearly 95% from ammonia to attain peak torque (Reiter and Kong 2010).

The flow rate of ammonia was significantly higher than the diesel flow rate, particularly at low loads to provide enough energy. A higher Ammonia flow rate at 50% load was due to its low energy content on a mass basis. The brake specific fuel consumption (BSFC) of diesel was high at low diesel load due to the poor part-load efficiency of conventional diesel engines. At high diesel load (>60%), the quantity of ammonia introduced was small, and the premixed air-Ammonia mixture was too lean to burn effectively. Hence, lower combustion efficiency led to higher BSFC of Ammonia. Ammonia BSFC followed an opposite trend than diesel w.r.t. the engine load. For load under 15%, higher diesel BSFC accounted for weak part-load efficiency in a conventional diesel engine. However, when the load increased past ~70%, the Ammonia supply remained low, and the premixed Ammonia-air mixture was too lean. As a result, the combustion efficiency of ammonia was low, resulting in higher BSFC. Hence, operating an engine at extreme ends of Ammonia concentrations needs to be avoided to prevent lower efficiencies.

Bro and Pederson (1977) compared Ammonia gas in port injection with ethanol, methanol, and methane in dual fuel CI engines having diesel as the primary fuel. Ammonia was the least desirable fuel among all the gases tested due to its high unburned Ammonia emissions. Ammonia-fueled engine showed the highest ignition



delay and negligible improvement in the power output due to the slower combustion rate of ammonia (Pearsall and Garabedian 1967).

Pearsall et al. (1967) compared the performance of an Ammonia-diesel dual-fuel engine with baseline diesel. The indicated-thermal efficiency of ammonia was 51%, which was higher than diesel (45%). The variations of specific fuel consumption with indicated horsepower for various engine speeds. The lowest fuel consumption was found at the lowest speed of 1200 rpm, whereas the highest occurred at the highest speed of 2400 rpm (<https://www.rand.org/randeurope/research/projects/impact-of-ammonia-emissions-on-biodiversity.html>).

The reduction in NO<sub>x</sub> emissions was comparable to baseline diesel at the same torque (<https://www.offshore-energy.biz/industry-groups-tell-eu-to-incentivize-green-hydrogen-and-ammonia-as-fuels-of-the-future/>). There was a drop in combustion temperature due to ammonia; hence a reduction in NO<sub>x</sub> emission was observed. Hence, there was no serious concern about NO<sub>x</sub> emissions from the Ammonia combustion engines. This study indicated that lower NO<sub>x</sub> emissions could be achieved if Ammonia substitution on an energy basis does not exceed 70%. HC emissions showed an opposite trend to NO<sub>x</sub> emissions. Incomplete combustion due to lower combustion temperature produced higher HC emissions. Lower HC emissions were found for a larger energy substitution by ammonia. CO<sub>2</sub> emissions decreased steadily with diesel replacement by ammonia. It can be found that as diesel load reduced and Ammonia content increased, the CO<sub>2</sub> emissions significantly reduced compared to pure diesel (<https://www.offshore-energy.biz/industry-groups-tell-eu-to-incentivize-green-hydrogen-and-ammonia-as-fuels-of-the-future/>). CO<sub>2</sub> emission reduced drastically with Ammonia substitution. It reduced from 11 to 3% for 80% total energy replacement by ammonia. Due to lower combustion temperature, Ammonia-diesel combustion generated higher HC emissions, except at low diesel fueling conditions. Ammonia-diesel combustion resulted in relatively high unburned Ammonia and NO<sub>x</sub> emissions because of ammonia's nitrogen-rich nature. Hence, Ammonia implementation is feasible only in heavy engines, such as for marine transport, heavy-duty Gensets, etc., where enough space is available on the engine for installing after-treatment systems. Advanced injection strategies can be developed for ammonia to demonstrate superior engine performance and emission characteristics. In addition, efficient and compact after-treatment systems can be designed to reduce NO<sub>x</sub> emissions.

### 14.6.3 Direct Injection of Ammonia-DME Blends

Gross and Kong et al. (Gross and Kong 2012) investigated combustion characteristics of Ammonia-DME blends in a single-cylinder, DI compression ignition engine. A high-pressure mixing system was used to prepare blends of Ammonia and DME. Ammonia and DME have high cetane numbers and vapor pressures; hence both need to be pressurized to keep them in the liquid state.

Figure 14.5 shows that when ammonia was introduced, the operating range was

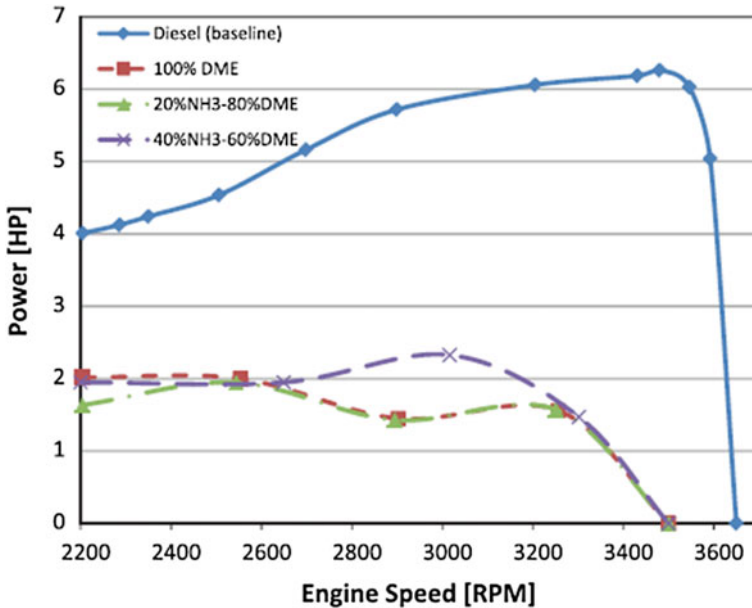


Fig. 14.5 Operating curves for different fuel blends (Gross and Kong 2012)

reduced. A higher quantity of ammonia was needed to achieve the same engine load due to ammonia's lower heating value compared to diesel. In addition, chemical reaction rates were slower due to ammonia's relatively higher latent heat of vaporization. Combustion further deteriorated because of the lower flame speed and peak combustion temperature of ammonia. Therefore, the engine's operating range was reduced due to the addition of ammonia in the DME. Also, reduced power and increased cyclic variations were observed compared to pure DME case.

Figures 14.6, 14.7, and 14.8 demonstrate a comparison of in-cylinder pressure and HRR of 60, 80, and 100% (w/w) DME, respectively, at different load conditions. Results showed that ammonia exhibited a longer ignition delay because of its higher resistance to autoignition. However, ammonia's presence did not influence the combustion. Among all fuel blends tested, the combination of 40%  $\text{NH}_3$ –60% DME exhibited the lowest in-cylinder pressure. The peaks of HRR increased with an increasing Ammonia content. From low load/ speed conditions (Fig. 14.6) to high load/ speed conditions (Fig. 14.8), the difference in the peak pressures between 40%  $\text{NH}_3$  and 60% DME w.r.t. other cases increased. Due to the short allowable time for combustion, the in-cylinder peak pressure decreased for higher speed conditions. The difference in ignition delays increased with an increasing Ammonia percentage. Also, the variations in ignition delay or peak pressure were substantially lower at low-speed conditions. According to a study (Ryu et al. 2014), the more was ammonia in the blend, the more retarded injection was required. For a blend of 60% (w/w) Ammonia, the injection was preferred in the range of  $340\text{--}90^\circ$  bTDC. The more

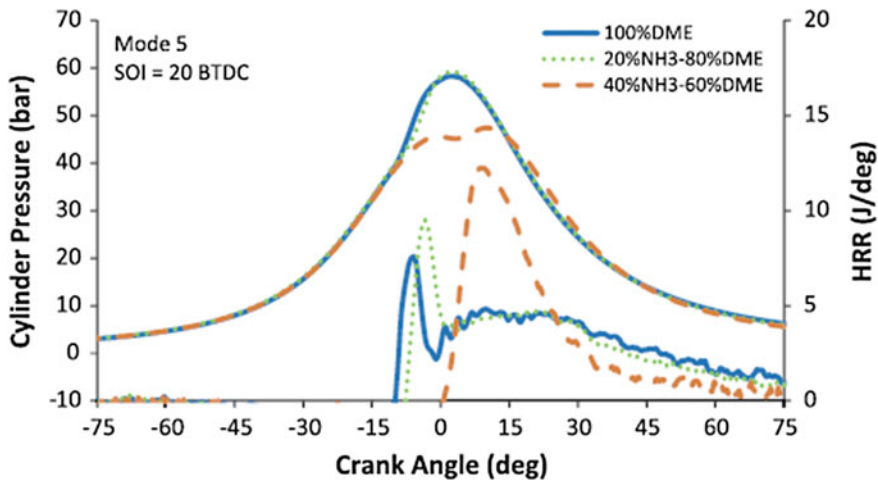


Fig. 14.6 In-cylinder pressure and HRR for low speed/ load conditions (Gross and Kong 2012)

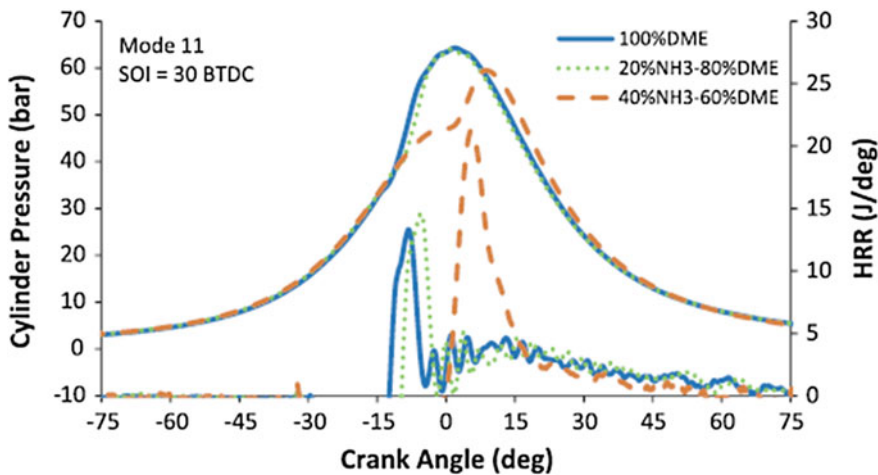


Fig. 14.7 In-cylinder pressure and HRR for medium speed/ load conditions (Gross and Kong 2012)

Ammonia present in the blend, the more HCCI like combustion characteristics were observed. Also, lower power and higher cyclic variations of 60% (w/w) ammonia compared to 100% DME were observed.

NOx emissions for 20% NH<sub>3</sub>–80% DME at low fueling conditions almost doubled the emissions produced by 100% DME at the same operating condition (Gross and Kong 2012). This increase in NOx emissions was possibly due to fuel NOx as the combustion temperature was low when ammonia was combusted. Low combustion temperature could also be justified by relatively lower in-cylinder pressures seen in

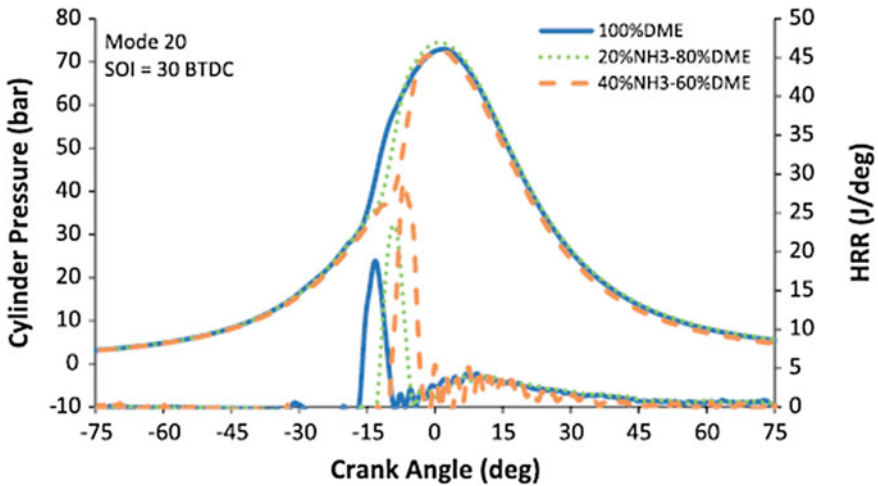


Fig. 14.8 In-cylinder pressure and HRR for high speed/ load conditions (Gross and Kong 2012)

previous figures. Ammonia emission levels increased with the addition of ammonia in the blend of Ammonia-DME at all engine speeds. Also, Ammonia emission levels increased with an increasing engine speed. For 20%  $\text{NH}_3$ -80% DME, soot emissions were well below 0.01 g/kWh. For 40%  $\text{NH}_3$ -60% DME, it is below 0.005 g/kWh, and for 100% DME, it is well below 0.02 g/kWh. Hence, soot emissions decreased with the addition of ammonia in the fuel mixture. Due to the carbon-free nature of ammonia, as ammonia increased, a lower amount of carbon atoms were available for soot formation. The overall CO and HC emissions for 20%  $\text{NH}_3$ -80% DME and 100% DME were similar. In contrast, these emissions were lower for 40%  $\text{NH}_3$ -60% DME due to high injection pressure that improved the combustion and fuel-air mixing (Gross and Kong 2012). According to a cost analysis report (Ryu et al. 2014), both Ammonia and DME mixture and diesel energy costs were comparable. In addition, the feasibility of Ammonia production from renewable sources of energy and its zero-carbon nature can further encourage Ammonia usage in practical applications. Hence, further growth in Ammonia engine expertise would enhance the potential of the use of Ammonia in ICEs.

## 14.7 Ammonia for Spark-Ignition Engines

### 14.7.1 Ammonia in Port Injection and Direct Injection

Mozafari-Varnuspadrani (1988) investigated ammonia as fuel without significant engine hardware modifications. The engine was operated at a constant speed of 2000 rpm, and ammonia was port-injected in the liquid phase. It was necessary to

warm up the engine by operating it on methanol, and then ammonia was gradually port-injected to achieve stable combustion. Finally, a complete transition from methanol to ammonia could be obtained. However, Ammonia combustion could only be sustained at a compression ratio of 15:1 and that too in a narrow range of equivalence ratio from 0.88 to 1.15. Still, the combustion remained erratic. It was possible to run the engine on 100% Ammonia for up to 90 min in a test. In other tests, the engine stopped after 10–15 min of operation. However, it emerged that the problem was possibly related to the ignition system since, after some time, it emerged that the spark plugs might have been damaged in the tests involving a high compression ratio. It was impossible to switch from methanol to 100% Ammonia in every test due to ammonia's narrow flammability limits. The highest BMEP and thermal efficiency were obtained at a slightly rich mixture at an equivalence ratio of 1.05, however, with a significantly lower BMEP and thermal efficiency than gasoline. At an equivalence ratio of 1.05 and 0.885, unburned Ammonia emissions of 11.8 and 23.2% were measured, respectively (Mozafari-Varnuspadran 1988).

To overcome ammonia's high resistance to autoignition, (i) stronger igniters, (ii) extended spark plugs, and (iii) compacted combustion chamber could be used that would enhance the combustion of Ammonia in SI-engines. The engine's volumetric efficiency could be maintained by direct injection of the fuel instead of conventional port fuel injection. However, some problems exist in implementing such an injection system. Traditional port injection systems use the storage pressure of the ammonia to sustain the injected fuel flow. On the contrary, direct injection uses higher pressure for delivering the fuel. There were several attempts to attain higher pressure for the gaseous ammonia (Zacharakis-Jutz 2013). The first attempt pressurized the ammonia using a liquid pump, then vaporized the fuel by passing it through a heating element just before the injection. However, the design of the pump and regulator was not feasible to implement this concept on the production-grade spark-ignition engines. In the second attempt, vapor pressure was increased by heating the tank directly, and then the gaseous ammonia was drawn off the top of the tank. It was evident that the second attempt was much better in handling a steady fuel injection pressure. According to a study (Zacharakis-Jutz 2013), the spark-ignition engine doesn't usually give a tolerable performance when operated on 100% Ammonia.

### ***14.7.2 Port Injection of Gaseous Ammonia***

Grannell et al. (2008) experimented with ammonia as a primary fuel and gasoline as a combustion promoter in a variable compression ratio (CR), single-cylinder Cooperative Fuel Research (CFR) engine. Gaseous Ammonia was port-injected, and gasoline was direct-injected. Study (Grannell et al. 2008) exhibited the fuel mix sweep running on the CFR engine at 8:1 CR with an intake pressure of 80 kPa. Ammonia was gradually introduced until maximum brake torque (MBT) spark timing was achieved without knock, and the upper limit occurred at 13% Ammonia and 87% gasoline on

an energy basis. Ammonia content was increased until excessive roughness in the engine was observed.

As we can see, the roughness ( $COV_{IMEP}$ ) increased rapidly when Ammonia quantity reached 63%. The lower limit was determined by the rough limit on gasoline proportion for a knock-free, smooth firing with MBT spark timing. Similarly, for the CR 12:1, 1600 rpm, and intake pressure of 50 kPa, the MBT knock limit was 58% gasoline and 42%  $NH_3$ , and the rough limit was 53% gasoline and 47%  $NH_3$  (Grannell et al. 2008).

This study shows that the rough limit is challenging to achieve when the allowed gasoline Ammonia substitution is high. The  $COV_{IMEP}$  curve did not cross ~2–3% with furthermore Ammonia substitution. This study shows the effect of retarded combustion timing for 100% gasoline since it was necessary to prevent knocking. The rough limit in-cylinder pressure–volume curves show an ideal shape that indicates MBT spark timing and combustion closer to the TDC.

There was a substantial efficiency gain for the above limits when the compression ratio was raised to 10:1 from 8:1 (Grannell et al. 2008). Net indicated efficiency curve for a compression ratio of 10:1 (rough limit), 12:1, and 14:1 (knock limit) coincide (Grannell et al. 2008). There was no visible improvement in efficiency beyond the compression ratio of 10:1. Caris and Nelson (1959) reported that the burn duration extended at high CRs and extended further as the CR was further increased. The maximum efficiency was achieved at a lower CR due to the higher heat loss caused by the pancake geometry of the CFR engine.

Experiments indicated that Ammonia/gasoline dual-fuel combustion could provide energy equivalent to gasoline-only operation. Pressure and heat curves showed that Ammonia/ gasoline combustion exhibited similar characteristics as a traditional SI engine. Since ammonia has a lower flame temperature and flame speed, the peak pressure was lower than baseline gasoline. However, higher knock resistance of ammonia allows the use of a higher CR and thereby higher peak pressures. As more Ammonia quantity is injected (longer injection duration), the combustion duration decreases. This denotes the extent to which Ammonia addition is limited. Ammonia does not increase the combustion rate to the extent same as gasoline. But the combustion duration between gasoline/Ammonia and pure gasoline is comparable. The higher the IMEP (load), the greater the proportion of gasoline that ammonia could replace. The higher the speed between 1000 and 1600 RPM, the smaller amount of ammonia could replace gasoline. For a higher CR, a higher Ammonia proportion is better. At the rough limits, the fuel has a strong dependence on load rather than the CR.

According to a research study, a larger proportion of gasoline could be replaced by Ammonia when IMEP >400 kPa (Grannell et al. 2008). There is no specific ratio of ammonia and gasoline for every load and speed condition. Still, a fuel mix map demonstrated the proportion of ammonia as a function of speed, compression ratio, and engine load. Due to ammonia's high knock resistance, the engine can operate at higher IMEPs than baseline gasoline. At a higher load, the efficiency of Ammonia-gasoline was higher due to maximum brake torque at higher IMEP. Therefore, in this study, a CR of 10:1 was suggested for a gasoline-Ammonia engine.

### 14.7.3 Direct Injection of Gaseous Ammonia

An engine having CR 10:1 was used to study the effect of direct-injected gaseous ammonia with port-injected gasoline (Ryu and George). There was an increase in engine power for the same injection duration since the Ammonia injection timing was advanced (Fig. 14.9). This was observed precisely between 270 and 320° bTDC. Furthermore, it was observed that despite identical injection duration, the retarded injection timings resulted in a lower Ammonia flow rate. This was because the pressure differences for gaseous Ammonia injection decreased with increased in-cylinder pressure for retarded ignition timings. Hence the Ammonia flow rate was reduced. At the far-right end, gasoline contributed 0.6 kW, whereas ammonia contributed to 2.1 kW to attain a 2.7 kW total power output i.e., ammonia contributed more energy than gasoline. In Fig. 14.10, for the 3 kW baseline gasoline engine, the early injection timings (370 and 320° bTDC) behaved similarly, whereas the late injection timing (270° bTDC) surpassed earlier injections (Fig. 14.10).

In Fig. 14.11, gasoline alone provided the baseline power, whereas ammonia was added to achieve the maximum power output under various conditions. As the initial gasoline quantity was increased, there was a reduction in power contribution from ammonia. It was unexpected as there would be a uniform contribution from ammonia in all baseline cases in a direct injection system. This was due to ammonia’s lower combustion temperature and flame speed, resulting in lower engine power output.

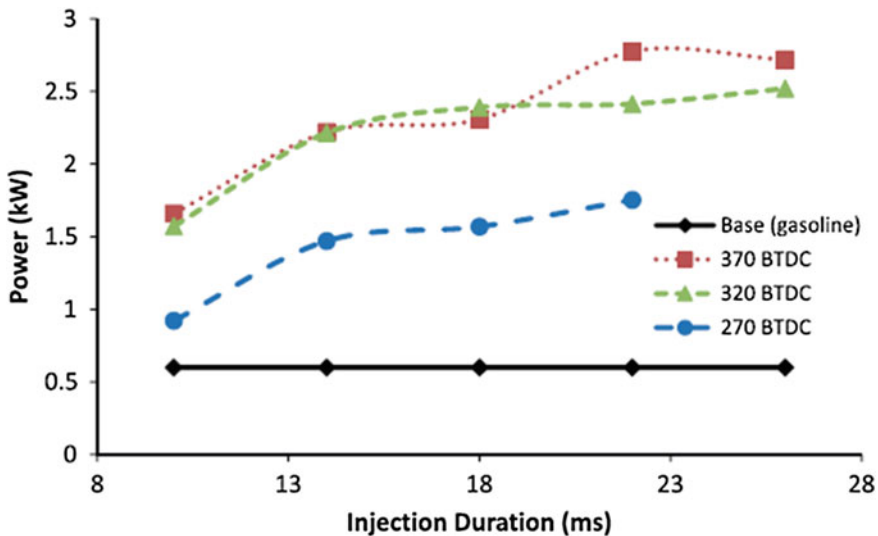


**Fig. 14.9** Engine power of different Injection duration of ammonia (gasoline contributes 0.6 kW baseline output) (Ryu et al.)

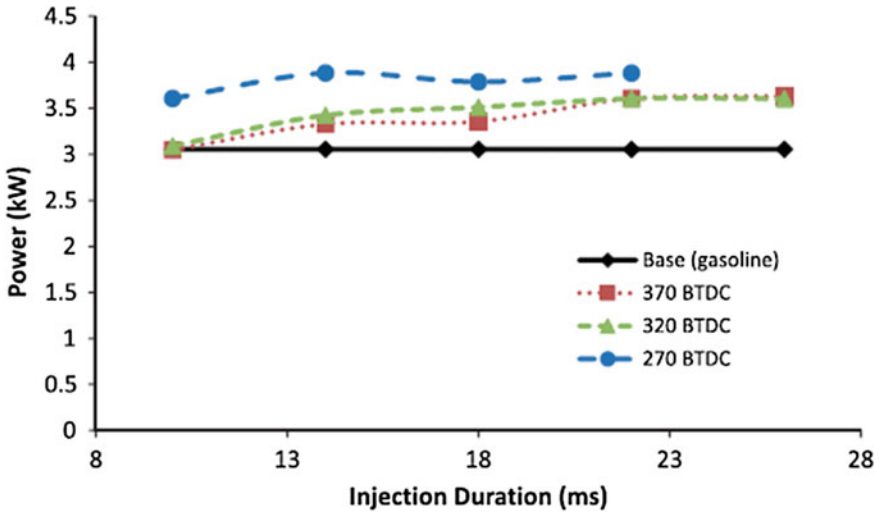


Fig. 14.10 Engine power of different injection timings (3 kW baseline output from gasoline) (Ryu et al.)

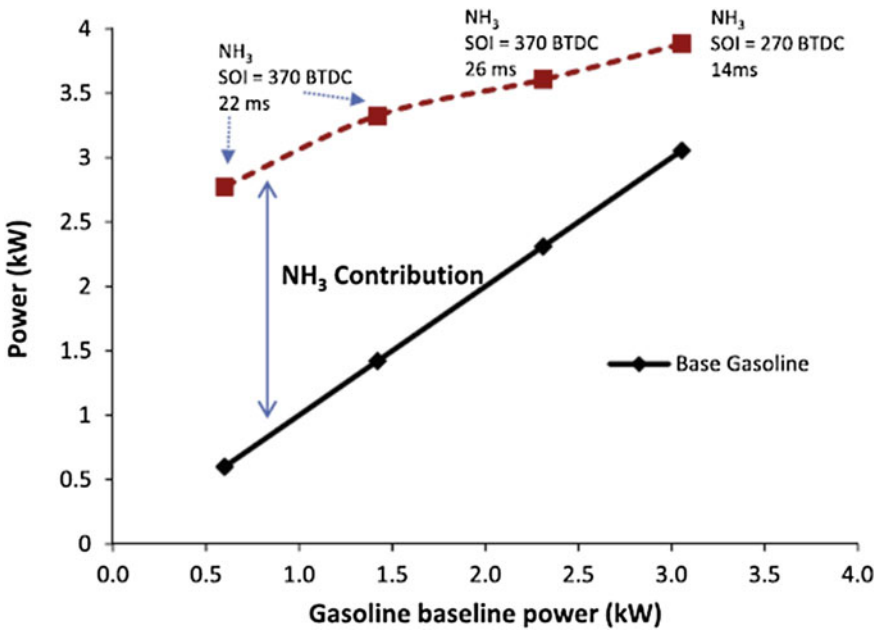


Fig. 14.11 Contributions of gasoline and Ammonia to the engine power output (Ryu et al.)



There was no difference in BSEC for baseline gasoline and gasoline-Ammonia dual-fuel mode. However, due to lower flame speed and combustion temperature, there was a slight reduction of the in-cylinder pressure while using ammonia.

In-cylinder pressure increased with an increasing engine load. However, it was observed that gasoline experienced a slightly higher in-cylinder pressure peak for specific performance modes (higher engine power) (Zacharakis-Jutz 2013). There was a greater reduction in combustion efficiency due to reduced peak pressure from gasoline-Ammonia compared to baseline gasoline. It was probably due to ammonia's slower flame speed, which increased the total combustion duration and reduced the thermal efficiency.

BSNO<sub>x</sub> concentration was substantially higher with the use of Ammonia/ gasoline than baseline gasoline. With an increase in Ammonia injection in the combustion chamber, NO<sub>x</sub> emissions in the exhaust increased because of fuel NO<sub>x</sub> and Ammonia slip. However, with an increasing engine load, both the BSNO<sub>x</sub> and BSNH<sub>3</sub> emissions decreased, indicating a superior fuel economy at higher load conditions even when ammonia was used (Ryu et al.). NO<sub>x</sub> emissions also increased with increasing engine load; however, the brake-specific NO<sub>x</sub> emissions decreased with increasing engine load. The BSNO<sub>x</sub> emissions were significantly higher than baseline gasoline combustion, possibly due to fuel-bound NO<sub>x</sub>. This was because the formation of thermal NO<sub>x</sub> was unlikely due to lower flame temperatures during Ammonia combustion.

There was an insignificant reduction in CO emissions. Due to ammonia's combustion inhibiting property, CO formation reduced, but the HC formation increased. Therefore, for gasoline-Ammonia, it was expected that CO<sub>2</sub> concentration would also reduce. However, due to the higher requirement of ammonia at full throttle condition of the CFR engine, the CO<sub>2</sub> levels didn't reduce by a significant amount compared to the CO<sub>2</sub> produced at idling.

#### ***14.7.4 Ammonia Dissolved in Gasoline***

Another approach to use ammonia with gasoline is using thermostated vapor-liquid equilibrium (VLE) in high-pressure cells, which can dissolve ammonia in the gasoline. For example, the experiments showed that 4.5% v/v Ammonia could be dissolved in gasoline at a pressure of 345 kPa and a temperature of 13.5 °C (Haputhanthri 2014). The use of ethanol or methanol as an emulsifier can enhance the solubility of ammonia in gasoline (Haputhanthri et al. 2015). Experiments showed that gasoline with 20% v/v ethanol and 12.9% v/v Ammonia was a preferable mixture for SI-engines using ECU-based controls. This mixture led to improved power at high speed and similar power at a lower speed than baseline gasoline. The use of Ammonia/ethanol/gasoline blends had a higher-octane rating; therefore, a higher compression ratio in SI-engines could be used (Haputhanthri 2014).

### 14.7.5 Ammonia-Hydrogen Blend

Many studies (Mørch et al. 2011; Haputhanthri et al. 2015; Starkman et al. 1966; Frigo and Gentili 2013; Pearsall 1967b) recommended hydrogen as a combustion improver in a SI engine fueled by Ammonia. Hydrogen’s combustion characteristics are preferable when combined with ammonia. If used in correct proportion, hydrogen can make up for ammonia’s slower flame speed and ignition requirements.

A SI engine was used for performing the experiments with hydrogen-Ammonia blends (Mørch et al. 2011). By analyzing Figs. 14.12 and 14.13, It was found that the highest efficiency was achieved at excess air ratio >1. The higher mean effective pressure was achieved at an excess air ratio <1. By increasing the CR, mixtures of Ammonia-hydrogen achieved similar mean effective pressure as baseline gasoline at the CR knock limit. An increase in CR from 7.12 to 11.64 led to significantly higher indicated thermal efficiency (ITE) for Ammonia-hydrogen than baseline gasoline. The same power output was achieved with hydrogen-Ammonia mixtures with higher efficiency. An increase in CR compensated for reduced airflow caused by intake air dilution from the port injection of ammonia and hydrogen. There was no increase in efficiency when CR was raised from 11.64 to 13.58, which led to effective pressure rise (Mørch et al. 2011).

The lowest indicated thermal efficiency and pressures were found for a higher proportion of hydrogen. This was due to an increase in the intake air dilution caused by hydrogen’s lower density. However, 5% hydrogen addition on a volume basis resulted in smoother engine operation, and 10% addition on a volume basis at stoichiometric conditions was optimal in terms of highest efficiency and brake mean

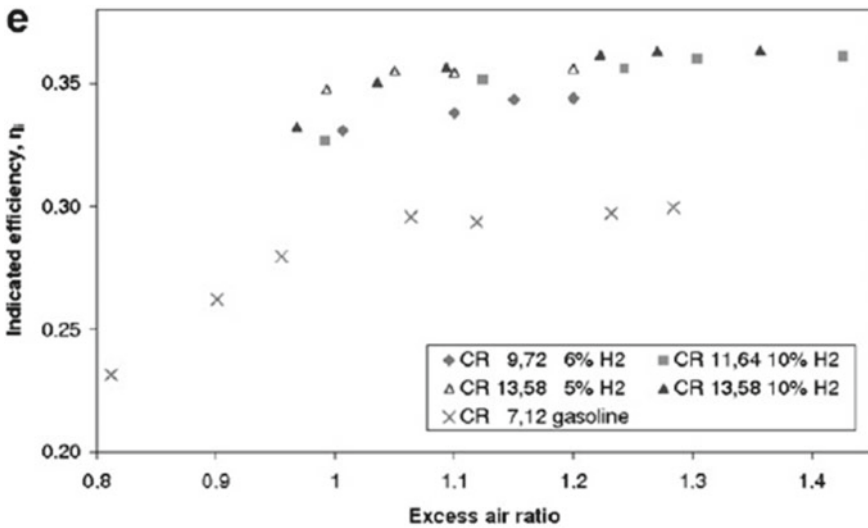


Fig. 14.12 Indicated efficiency for varying CR, 1200 rpm (Mørch et al. 2011)

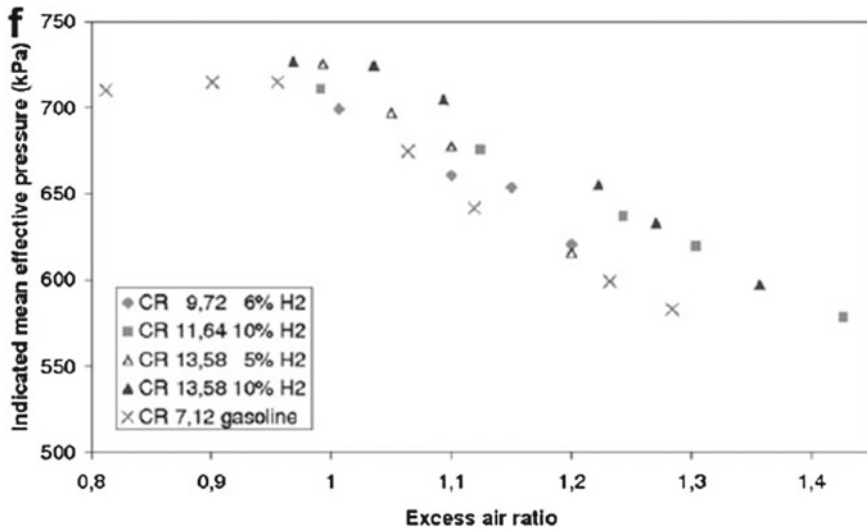


Fig. 14.13 IMEP (kPa), 1200 rpm, at varying CR (Mørch et al. 2011)

effective pressure (Fig. 14.13). Another study (Stefano Frigo\*, Roberto Gentili 2013) reported that 8% hydrogen addition on a volume basis (1% on a mass basis) was sufficient.

HAER is defined as the ratio of energy contributed by hydrogen to ammonia per cycle so that  $COV_{imep}$  was maintained  $<10\%$ . This was usually considered the expected maximum value of cyclic variations for appropriate engine behavior (Heywood 1988), even though modern engines hardly cross  $5\% COV_{imep}$ . From Fig. 14.14, it was noted that as the HAER dropped below 6%, the engine  $COV_{imep}$  quickly increased. The variations of HAER with rpm were significantly lower. Accordingly, it was necessary to speed up the combustion process by hydrogen addition to the Ammonia-air mixture, with more load-dependent ratios than the engine speed. The minimum HAER to obtain appropriate engine behavior (i.e.,  $COV_{imep}$  should be under 10%) was roughly 11% at half load and 7% at full load (Fig. 14.15).

Study (Comotti and Frigo 2015) showed that emission measurements revealed the most favorable operation at stoichiometric conditions and MBT timings in NO, NO<sub>2</sub>, and N<sub>2</sub>O. The NO content was lower than that in the gasoline exhaust at this condition. However, leaner conditions increased the formation of NO. The NO<sub>2</sub> share in the NO<sub>x</sub> emissions was higher than gasoline (3–4% for NH<sub>3</sub> and  $>2\%$  for gasoline). A slightly higher NO<sub>2</sub> share in the NO<sub>x</sub> than baseline gasoline was possibly due to a higher concentration of NO<sub>2</sub> in the flame zone when nitrogen was present in the fuel. Subsequently, the flame quenching led to its transformation to NO in the post-flame area. The Ammonia slip was in the range of 1000 ppm, which was higher than the allowable 0.01 ppm in EURO VI emission norms (Comotti and Frigo 2015). An exhaust gas after-treatment is necessary to comply with the legislative limits of NO<sub>x</sub> emissions. In addition, a larger hydrogen flow rate is required to facilitate

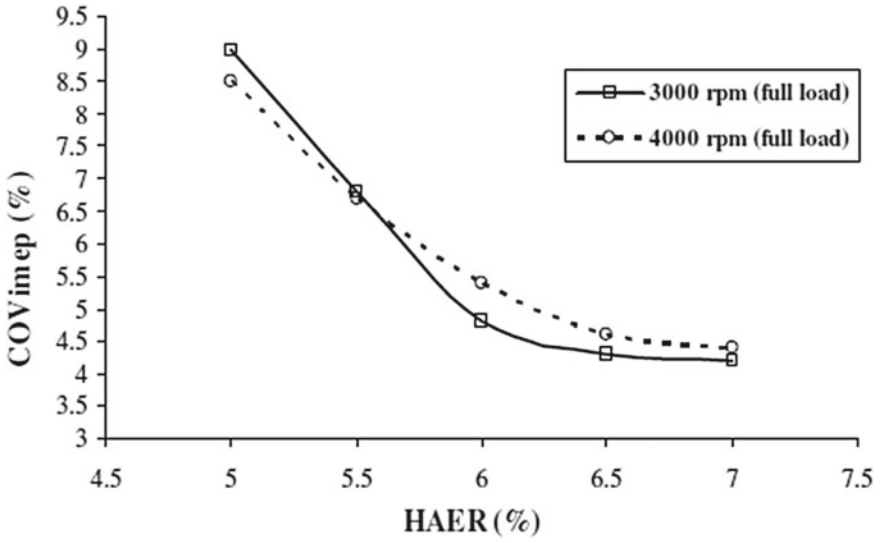


Fig. 14.14 COV<sub>imep</sub> versus HAER at 3000 and 4000 rpm, full load, lambda = 1 (Frigo et al. 2014)

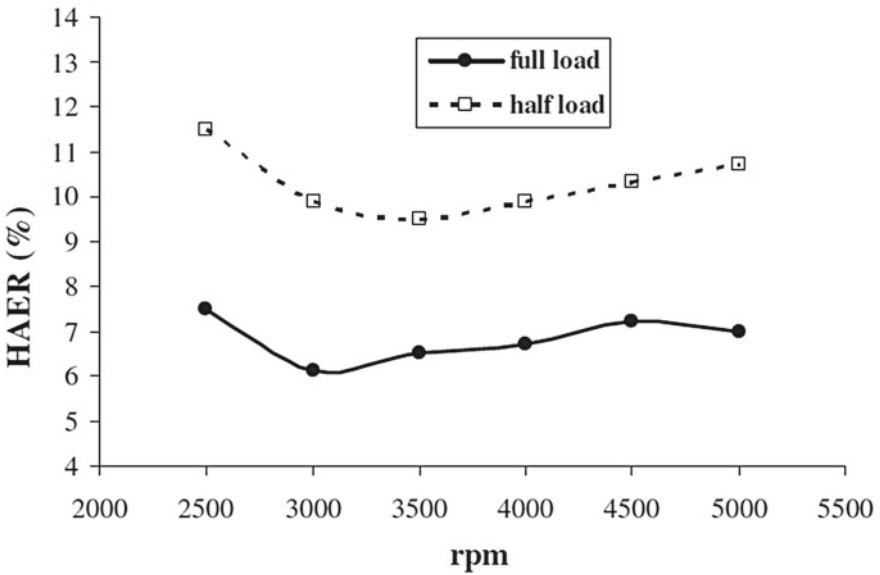


Fig. 14.15 HAER versus rpm at the half and the full load (Frigo et al. 2014)

combustion at lower speeds, including the cold-start conditions. A larger hydrogen storage tank use can be used to address the need for hydrogen. Another method could be electricity use and a larger heat exchanger, sufficient to produce an adequately large amount of hydrogen.

## 14.8 Summary

Using Ammonia in ICEs causes several difficulties due to its fuel properties. The drawbacks are (i) narrow flammability limits, (ii) low flame speed, and (iii) high ignition temperature. This chapter presents some possible ways to resolve some of these properties related challenges. Few issues of ammonia, such as high ignition temperature, can be overcome by implementing a new ignition system or using a dual-fuel mode in the ICEs. Lower flame speeds in the engine can be handled by adding a suitable combustion promoter. Hence engine operated by 100% Ammonia is not feasible. The possibilities of ammonia as the only fuel and in dual-fuel mode with diesel or DME in the CI engines are discussed. High compression ratios, high loads, and low speeds are preferable for ammonia fueled engines. Pure ammonia is not suitable for running a CI engine due to the requirement of high compression ratios, which may lead to excessive knocking. Ammonia is used with high cetane number secondary fuel to compensate its high ignition delays and low combustion efficiencies. The performance characteristics of the engine mainly depends on the secondary fuel. The use of multiple injections strategies can contribute to low NO<sub>x</sub> and unburned ammonia emissions and will enhance combustion performance. Ammonia as fuel and mixed with gasoline or hydrogen in the dual-fuel mode were also examined for spark-ignition engines. Ammonia as fuel was not tested at such levels to make it viable for the existing SI engines. The studies included in this chapter concentrated more on combustion rather than the compatibility with existing engine designs.

A highly recommended future study could be on the Ammonia-hydrogen use in the ICEs. The use of hydrogen as a combustion improver could significantly improve ignition. Because of the higher ON of the Ammonia-hydrogen mixture, a higher CR in the SI engines is possible for operating the engine. It promotes indicated thermal efficiency and power output from the engine. However, there might be a problem during cold-start due to the need for hot exhaust and a certain engine speed to decompose ammonia. This calls for a hydrogen storage tank that can be used during the engine start-up. A significant amount of research is being done for assessing the compatibility of ammonia with existing engine hardware. The prominent usage of the Ammonia-hydrogen mixture might become feasible in the foreseeable future.

## References

- Avery WH (1988) A role for ammonia in the hydrogen economy. *Int J Hydrogen Energy* 13(12):761–773. [https://doi.org/10.1016/0360-3199\(88\)90037-7](https://doi.org/10.1016/0360-3199(88)90037-7)
- Bartels JR (2008) A feasibility study of implementing an ammonia economy. IOWA State University, Digital Repository. <https://doi.org/10.31274/etd-180810-1374>
- Bro K, Pedersen PS (1977) Alternative diesel engine fuels: an experimental investigation of methanol, ethanol, methane, and ammonia in a DI. Diesel engine with pilot injection. In: Passenger car meeting & exposition; SAE Technical Paper No. 770794. <https://doi.org/10.4271/770794>
- Busby JA, Chem C, MRIC (1976) The activation and deactivation of platinum/rhodium catalysts for ammonia oxidation. Ph.D. thesis, Department of Chemical Engineering, Imperial College London. <http://hdl.handle.net/10044/1/22269>
- Caris DF, Nelson EE (1959) A new look at high compression ratio engines. SAE Technical Paper No. 590015:112–124. <https://doi.org/10.4271/590015>
- Christopher WG, Kong S-C (2012) Performance characteristics of a compression-ignition engine using direct-injection Ammonia–DME mixtures. In: *Fuel*, vol 103, Iowa State University. <https://doi.org/10.1016/j.fuel.2012.08.026>
- Comotti M, Frigo S (2015) Hydrogen generation system for ammonia hydrogen-fuelled internal combustion engines. *Int J Hydrogen Energy* 40(33):10673–10686. <https://doi.org/10.1016/j.ijhydene.2015.06.080>
- Frigo S, Gentili R (2013) Analysis of the behavior of a 4-stroke Si engine fuelled with ammonia and hydrogen, Department of Energy and System Engineering (DESE), Università di Pisa, Largo Lucio Lazzarino 2, 56122 Pisa, Italy. <https://doi.org/10.1016/j.ijhydene.2012.10.114>
- Frigo S, Gentili R, De Angelis F (2014) Further insight into the possibility to fuel a SI engine with ammonia plus hydrogen. SAE Technical Paper No. 2014-32-0082. <https://doi.org/10.4271/2014-32-0082>
- Grannell SM, Assanis DN, Bohac SV, Gillespie DE (2008) The fuel mix limits and efficiency of a stoichiometric, ammonia, and gasoline dual fueled spark ignition engine. *J Eng Gas Turbines Power* 130(4):042802. <https://doi.org/10.1115/1.2898837>
- Grimes PG (1965) Energy depot fuel production and utilization. SAE Technical Paper No. 650051. <https://doi.org/10.4271/650051>
- Haputhanthri S (2014) Ammonia gasoline fuel blends: feasibility study of commercially available emulsifiers and effects on stability and engine performance. SAE Technical Paper No. 2014-01-2759. <https://doi.org/10.4271/2014-01-2759>
- Haputhanthri S, Omantha M, Timothy T, Fleming J, Austin C (2015) Ammonia and gasoline fuel blends for spark ignited internal combustion engines. *ASME J Energy Res Technol* 137(6):062201. <https://doi.org/10.1115/1.4030443>
- Heywood JB (1988) *Internal combustion engine fundamentals*. McGraw-Hill
- Hignett TP (1985) Transportation and storage of ammonia. In: Hignett TP (eds) *Fertilizer manual*. Developments in plant and soil sciences, vol 15. Springer, Dordrecht. [https://doi.org/10.1007/978-94-017-1538-6\\_7](https://doi.org/10.1007/978-94-017-1538-6_7)
- Hodgson JW (1973) Is ammonia a transportation fuel for the future? In: *Proceedings of ASME conference, Denver*, Paper no. 73-ICT E65
- Mørch CS, Bjerre A, Gøttrup MP, Sorenson SC, Schramm J (2011) Ammonia/hydrogen mixtures in an SI-engine: engine performance and analysis of a proposed fuel system. *Fuel* 90(2):854–864. <https://doi.org/10.1016/j.fuel.2010.09.042>
- Mozafari-Varnuspadran A (1988) Predictions and measurements of spark-ignition engine characteristics using ammonia and other fuels. Ph.D. thesis, Mechanical Engineering, University of London. <http://qmro.qmul.ac.uk/xmlui/handle/123456789/1582>
- Nielsen A (1995) Ammonia storage and transportation-safety. In: Nielsen A (eds) *Ammonia*. Springer, Berlin, Heidelberg. [https://doi.org/10.1007/978-3-642-79197-0\\_7](https://doi.org/10.1007/978-3-642-79197-0_7)

- Pearsall TJ (1967) Ammonia application to reciprocating engines (Final Technical Report). Continental Aviation and Engineering Corp., Detroit, Michigan, Arsenal Contract. DA-20 113-AMC-05553(T)
- Pearsall TJ (1967) Ammonia application to reciprocating engines. Continental aviation and engineering corporation, Detroit, Michigan, CAE Report nr. 1054, vol I
- Pearsall TJ, Garabedian C (1967) Combustion of anhydrous ammonia in diesel engines. SAE Technical Paper No. 670947. <https://doi.org/10.4271/670947>
- Reiter AJ, Kong S (2010) Diesel engine operation using ammonia as a carbon-free fuel. In: Proceedings of the ASME 2010 internal combustion engine division fall technical conference. ASME 2010 internal combustion engine division fall technical conference. San Antonio, Texas, USA. September 12–15. pp. 111–117. ASME. <https://doi.org/10.1115/ICEF2010-35026>
- Rosenthal AB (1965) Energy depot—a concept for reducing the military supply burden. SAE Technical Paper No. 650050. <https://doi.org/10.4271/650050>
- Ryu K, Zacharakis-Jutz G, Kong S-C Effects of gaseous ammonia direct injection on performance characteristics of a spark-ignition engine. School of Mechanical and Automotive Engineering, Kunsan National University, South Korea, Department of Mechanical Engineering, Iowa State University, USA. <https://doi.org/10.1016/j.apenergy.2013.11.067>
- Ryu K, Zacharakis-Jutz G, Kong SC (2014) Performance characteristics of the compression-ignition engine using high concentration of ammonia mixed with dimethyl ether. Appl Energy 113:488–499. <https://doi.org/10.1016/j.apenergy.2013.07.065>
- Starkman E, Newhall H, Sutton R, Maguire T (1966) Ammonia as a spark ignition engine fuel: theory and application. SAE Technical Paper No. 660155. <https://doi.org/10.4271/660155>
- Starkman ES, James GE, Newhall HK (1967) Ammonia as a diesel engine fuel: theory and application. In: National fuels and lubricants, powerplants, transportation meetings; SAE Technical Paper No. 670946. <https://doi.org/10.4271/670946>
- Tillner-Roth, Harms-Watzenberg, Baehr (1993) A new fundamental equation of state for ammonia; Eine neue Fundamentalgleichung für Ammoniak, DKV-Tagungsbericht, vol 20, pp 167–181
- Valera-Medina A, Xiao H, Owen-Jones M, David WIF, Bowen PJ (2018) Ammonia for power. Prog Energy Combust Sci 69:63–102. <https://doi.org/10.1016/j.pecs.2018.07.001>
- Web source: [https://theict.org/sites/default/files/publications/ICCT\\_Euro6-VI\\_briefing\\_jun2016.pdf](https://theict.org/sites/default/files/publications/ICCT_Euro6-VI_briefing_jun2016.pdf). Accessed on 29th June 2021
- Web source: <https://ourworldindata.org/co2-and-other-greenhouse-gas-emissions>. Accessed on 26th June 2021
- Web source: <https://www.energy.gov/eere/fuelcells/hydrogen-production-thermochemical-water-splitting>. Accessed on 13th Sept 2021
- Web source: <https://pubchem.ncbi.nlm.nih.gov/compound/Ammonia>. Accessed on 26th June 2021
- Web source: <https://www.epa.gov/ghgemissions/global-greenhouse-gas-emissions-data>. Accessed on 29th June 2021
- Web source: <https://iea.blob.core.windows.net/assets/ac80b701-bdfc-48cf-ac4c-00e60e1246a0/weo2009.pdf>. Accessed on 29th Sept 2021
- Web source: <https://www.euractiv.com/section/transport/news/eu-gears-up-co2-car-targets-for-2025-2030/>. Accessed on 28th June 2021
- Web source: <https://www.offshore-energy.biz/industry-groups-tell-eu-to-incentivize-green-hydrogen-and-ammonia-as-fuels-of-the-future/> Accessed on 15th Sept 2021
- Web source: <https://www.eia.gov/energyexplained/oil-and-petroleum-products/use-of-oil.php>. Accessed on 29th June 2021
- Web source: <https://www.euratex.co.uk/110411020.pdf>. Accessed on 29th June 2021
- Web source: <https://www.rand.org/randeurope/research/projects/impact-of-ammonia-emissions-on-biodiversity.html>. Accessed on 28th June 2021
- Websource: <https://www.tfi.org/sites/default/files/documents/HealthAmmoniaFINAL.pdf>. Accessed on 28th June 2021

- Xiang HW (2004) Vapor pressures, critical parameters, boiling points, and triple points of ammonia and trideuteroammonia. *J Phys Chem Ref Data* 33(4):1005–1011. <https://doi.org/10.1063/1.1691451>
- Zacharakis-Jutz (2013) Performance characteristics of ammonia engines using direct injection strategies. Iowa State University. <https://doi.org/10.31274/etd-180810-3542>
- Zamfirescu C, Dincer I (2009) Ammonia as a green fuel and hydrogen source for vehicular applications. *Fuel Process Technol* 90(5):729. <https://doi.org/10.1016/j.fuproc.2009.02.004>